Copyright Warning & Restrictions

The copyright law of the United States (Title 17, United States Code) governs the making of photocopies or other reproductions of copyrighted material.

Under certain conditions specified in the law, libraries and archives are authorized to furnish a photocopy or other reproduction. One of these specified conditions is that the photocopy or reproduction is not to be "used for any purpose other than private study, scholarship, or research." If a, user makes a request for, or later uses, a photocopy or reproduction for purposes in excess of "fair use" that user may be liable for copyright infringement,

This institution reserves the right to refuse to accept a copying order if, in its judgment, fulfillment of the order would involve violation of copyright law.

Please Note: The author retains the copyright while the New Jersey Institute of Technology reserves the right to distribute this thesis or dissertation

Printing note: If you do not wish to print this page, then select "Pages from: first page # to: last page #" on the print dialog screen

FRACTURE ENERGY AND TENSILE BEHAVIOR OF CONCRETE

BY

WEN-JINN CHIOU

THESIS SUMITTED TO THE FACULTY OF THE GRADUATE SCHOOL OF THE NEW JERSEY INSTITUTE OF TECHNOLOGY IN PARTIAL FULFILLMENT OF THE REQUIREMENTS FOR THE DEGREE OF MASTER OF SCIENCE IN CIVIL ENGINEERING

1986

VITA

Name : Wen-Jinn Chiou

Degree and Date to be Conferred : Master of Science
Civil Engineering
1986

Secondary Education : Lo-Dong High School, June 1976

Collegiate Institute Attened	Date	Degree	Date of degree
New Jersey Institute of Technology	1984-86	M.S.C.E.	May, 1986
Feng Chia University	1976-80	B.S.C.E.	June, 1980

Major : Civil Engineering

Position Held : Jan. 1985- May, 86
Graduate Assistant
Department of Civil Engineering
Newark, New Jersey

ABSTRACT

Title of Thesis : Fracture Energy and Tensile Behavior of Concrete

Wen-Jinn Chiou , Master of Science , 1986

Thesis Directed by : Methi Wecharatana, Associate Professor
Civil Engineering Department

Fracture behavior of concrete has been a subject of investigation for the past two decades. The need of understanding the complete tensile response of concrete is absolutely essential for theoretical modelling as well as design application of plain concrete structures.

In this study, attempts were made to investigate the validity of two important fracture parameters , namely , the fracture energy and the critical crack tip opening displacement . Three types of test specimen , dog-bone shaped tension specimen , notched beam and compact tension specimen , were investigated . These tests were conducted using the closed-loop MTS 810 strain-controlled testing system . For the uniaxial tension specimen (dog-bone), monotonic and cyclic loadings were employed to observe the complete post-peak response of concrete . In

addition , fracture energy, critical crack opening displacement and the variation of post-peak elastic Young's Modulus , were studied . Four different mix-proportions of mortar and one mix of concrete were used to study the effect of matrix composition on the uniaxial tensile response of concrete . Three controlled grain sizes of sand were used to study the effects on maximum post-peak displacement , i.e., the critical crack opening displacement.

In addition to the direct tension test , the ASTM standard fracture specimens were also investigated . To study the size effect on fracture energy , three different sizes of compact tension specimen and one notched beam were used . Test results from the ASTM standard specimens were compared with those observed from the direct tension test.

The results of the above investigation reveal that fracture energy is a specimen size-dependent fracture parameter . It can be inferred from these results that the critical crack opening displacement is a material property influencing the fracture characteristics . From this study, a unique normalized post-peak stress-displacement relationship was found to exist. Such relationship is essential to most proposed theoretical models .

ACKNOWLEDGEMENTS

The author wishes to express his profound gratitude to his advisor , Professor Methi Wecharatana , for his valuable support , warmly encouragement and constructive supervision throughout the course of this study . The author would also like to thank Professor Dorairaja Raghu and Professor Paul C. Chan for serving as members of the advisory committee .

Thanks are also due to many friends and colleagues for their encouragement and friendship , particularly to Mr. James Petriville and Ms. Teresa Cintora . The author would also like to thank Ms. Susan Lee for her patience in calculating the tidious data .

Most of all, the author wishes to express his love to his family for their understanding, supporting and encouragement.

TABLE OF CONTENTS

LIST OF TABLES

LIST OF FIGURES

CHAPTER I

INTRODUCTION

1.1 GENERAL

In practical reinforced concrete design , it is a common practice to consider only the elastic stress-strain relationship of concrete in compression in which the tensile resistance of concrete is usually ignored . This is primarily due to the low tensile strength of concrete coupled with the difficulty in conducting the direct uniaxial tension test, particularly the observation of the post-peak response. Due to the brittle nature of concrete, it is very difficult , if not impossible , to obtain data regarding the descending branch of the stress-strain curve .

Post-peak uniaxial tensile response of concrete is vital when nonlinear finite element analysis is employed for complicated structural problems . Many theoretical models (Ref. 1-3) have been developed to study the fracture behavior of concrete in recent years . These models, in general , assumed a certain stress-strain or stress-displacement relationships of concrete under uniaxial tension . The validity of these models is questionable since information on the uniaxial post-peak tensile response of concrete is not available. Various fracture parameters

such as fracture energy and critical crack opening displacement have been widely used for predicting fracture behavior of concrete. These parameters have not been clearly verified as unique material properties . The ASTM standard test specimen such as notched beam and the compact tension were also used for fracture investigation . Recommendation for the standard testing method for fracture study in concrete has recently been proposed by the RILEM committee TC-50 in accordance with the fictitious. However, this recommendation has totally ignored the uniaxial tension test , crash model (Ref.1) and instead , proposed a standard notched beam test . This recommendation has generated criticism on the validity of the proposed standard testing method as well as its controlled parameter .

In this study , an attempt was made to verify the validity of two important fracture parameters , viz. , the fracture energy and the critical crack opening displacement. Effects of test specimens, mix-proportion as well as aggregate grain size on fracture parameters have been studied. It was observed that the fracture energy was a specimen size-depandent parameter and the critical crack opening displacement was a more promising material behavior for fracture studies . The normalized post-peak stress-displacement response in uniaxial tension was found to be a unique material property. The same behavior was also reported in fiber reinforced cement composites (Refs.14,15).

The present study was primarily an empirical investigation which was intended to support and verify the existing proposed theoretical models .

1.2 LITERATURE REVIEW

The application of linear elastic fracture mechanics to concrete has been found to be inaccurate . This was attributed to the existing large micro-crack zone in front of the crack tip as well as the extent of slow crack growth in concrete. Many non-linear fracture mechanics models have been proposed . These include the fictitious crack model by Hillerborg (Ref.1), the crack band model by Bazant (Ref.2) and the modified strain energy model by Wecharatana and Shah (Ref.3) . These proposed theoretical models all assumed certain post-peak uniaxial tensile response of concrete since crack tip process zone was assumed to fail under the direct tension failure (Mode I) usually ignored . The validity of these theoretical models is questionable since no information is available for the assumed post-peak tensile response of concrete . This is primarily due to the difficulty in conducting the direct tension test and in particular to obtain the post-peak response. Some of the difficulties arose from the brittle nature of concrete while some others were due to the limitation of the machine stiffness . As a result, only limited and often conflicting information is available in the literature.

Evans and Marathe (Ref. 4) increased the stiffness of testing machine by testing the concrete tension specimen parallel to 4 steel rods . They observed the post-peak tensile response using three different mix-proportions of concrete. Due to the limitation of the test setup , the post-peak response was measured down to approximately 100 psi after the peak (1/5 of the maximum strength) before abrupt failure occurred . Petersson (Ref. 5) also used the concept of increasing the stiffness of testing system by conducting a direct tension test using a heated aluminum rod. This process gradually increased the cross head displacement with a very slow rate of axial deformation. A better controlled post-peak response was then reported. However, his results presented a constant asymptotic stress value of approximately 60 psi , which was practically unrealistic . This problem was attributed to the limitation of his test setup rather than being the actual materials response . A large discrepancy of the post-peak uniaxial tensile response of concrete reported by Petersson's (Ref.5) and Evan et. al. (Ref.4) was presented in Ref.8.

Recently , more refined experimental programs have been conducted by Reinhardt (Ref. 6,7) and Gopalaratnum and Shah (Ref.8) , using a closed-loop strain-controlled testing system . Reinhardt developed a direct tension specimen with both ends glued to a steel plate by epoxy . Three different cyclic loading patterns were used . Gopalaratnum and Shah

used a plate specimen with two clamped plates at both ends. They tested specimens with two different plate thicknesses (3/4" and 3/2") . Seven mix-proportions were used to study the influence of aggregate size and water cement ratio on the post-peak response. Both of these two new types of tension specimen required special grip preparation which made the test tedious , time consuming and impractical . Furthermore, the clamped-end tension plate has a limited load carrying capacity . A thicker test specimen will generally cause slippage . The alignment in the epoxy-glued specimen is one of the most difficult setups . However , the same clamped-end tension specimen was also used to study the post-peak response in rocks (Ref.9,10). The post-peak tensile response of concrete has also been reported by a few other investigators who also used either the glued-end tension specimen or clamped-end plate (Ref.11,12,13).

With all the available post-peak uniaxial tensile responses of concrete, the reported stress-strain or stress-displacement relationships hardly presented a single complete curve which post-peak stress dropped to zero . An asymptotic stress value was generally presented as the remaining portion of the post-peak response was ignored . These results tend to be misleading since this leads one to believe that such a constant stress plateau exists. Furthermore since the fracture energy was normally obtained from the total area under the load-displacement curve , the

incomplete responses usually resulted into an inaccurate and inconsistent value of fracture energy which was further used in many proposed theoretical fracture models. The reported values of fracture energy vary from 0.104 lb/in. in direct tension specimen to 2.030 lb/in. in compact tension specimen.

1.3 OBJECTIVES

The objective of the research reported here was to obtain a reliable complete post-peak tensile response of concrete both in monotonic and cyclic loadings under a direct uniaxial tension test. Also studied were the effects of aggregate grain size , mix-proportions , and specimen size on the fracture energy , the critical crack opening displacement , and the change of elastic Young's modulus of cracked concrete . A unique normalized post-peak stress-displacement law , similar to what has been reported by Wecharatana and Shah (Ref. 14) and Visalvanich and Naaman (Ref. 15) , was also be verified in this study . Emphasis was given to the development of a simple direct tension specimen which can be used to obtain the post-peak tensile response of concrete.

CHAPTER II

EXPERIMENTAL PROGRAM

In this investigation , experimental programs were conducted for the purpose of studing the fracture energy and the critical crack opening displacement . Three different types of test specimen ,i.e., the direct tension , notched beam and the compact tension specimens , were used to study specimen size effects on the fracture energy . Effects of material composition on fracture behaviors of concrete were investigated by using five different mix-proportions and three different grain sizes of sand . Two loading patterns ,i.e., the monotonic and the cyclic loadings , were used to evaluate the variation of elastic Young's Modulus , the critical crack opening displacement and the fracture energy under different loading conditions . Details of specimen preparation and test setups were outlined as fellows :

2.1 SPECIMEN FABRICATION

Dog-Bone Specimen

A dog-bone shape specimen was made for the uniaxial

tension test . The dog-bone specimen is actually an extended briquette specimen with the straight portion of 7 inches in the middle and has a cross sectional area of 1 sq.in. (Fig.1). The purpose of having the extended straight portion was to avoid the stress concentration near the grips so that uniform stress distribution would cause the failure at the middle of the test specimen . In our dog-bone test, additional saw-cut notches of 0.1 inch were cut on both sides of the specimen to further assure the exact location of failure plane . This step is essential since feed back control signal should come from the fracture zone around the crack plane . Two extensometers were placed on both sides of the specimen for averaging feed back signals . If crack plane occured out side the range of extensometers, the test specimen was likely to fail abruptly . In the present study , 95% of the test specimens failed within the controlled range . The question of stress concentration around the notch-tip area has been verified to be negligible by both Reinhardt (Ref. 6,7) and Gopalaratnum and Shah (Ref. 8). This was because both mortar and concrete are notch insensitive while cement paste is notch sensitive.

The dog-bone specimen was normally cast in a plastic mold which was designed and fabricated in our concrete laboratory using plastic and hardener.

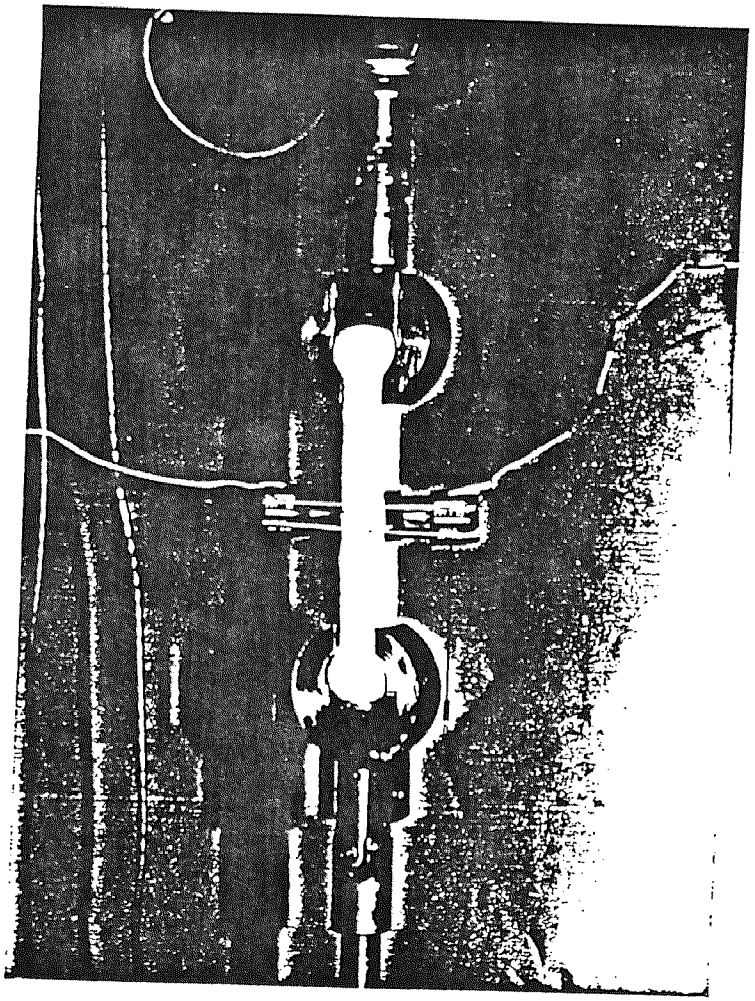

(a) Dog Bone Test Setup

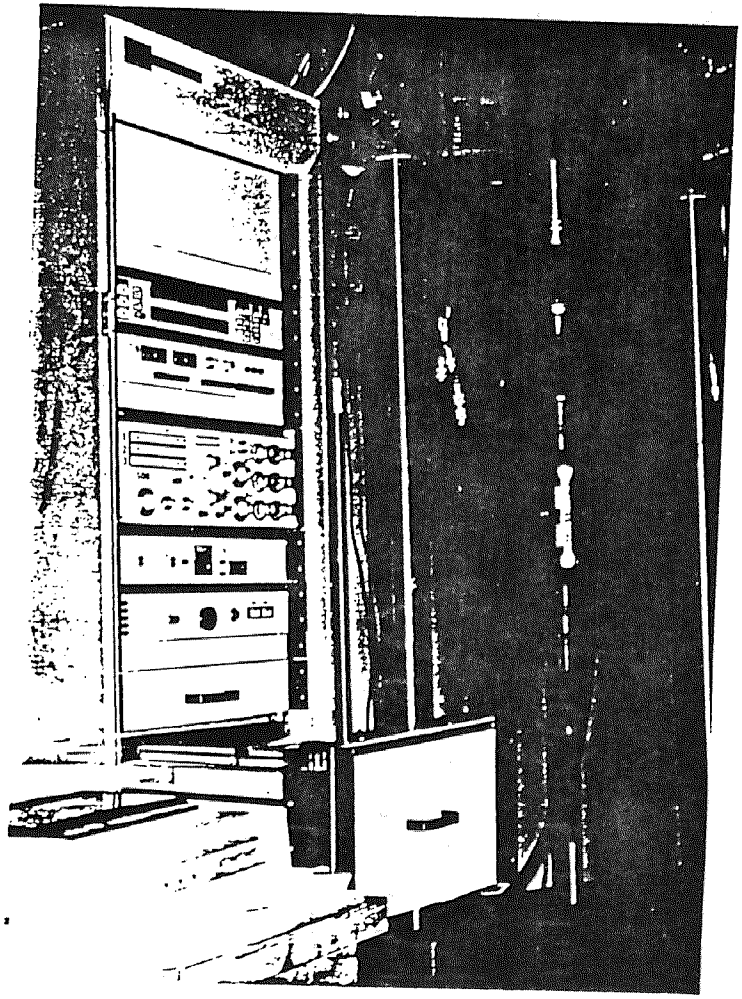

(b) Closed Loop Test Setup

FIG. 1 UNIAXIAL TENSION TEST SETUP

Notched Beam Specimen

The size of the notched beam specimen used in this study was in accordance with the ASTM Standard E-399 (Ref.22). The dimensions of the beam was 24 in. in length , 5 in. depth and 2 in. thickness . Three different notch depths of 1.0 in. , 2.0 in. and 3.0 in were either precast or saw-cut at the middle of the beam to simulate an actual crack. The notched beam was normally cast in a steel mold.

Compact Tension Specimen

Three different sizes of compact tension (CT) specimen were also used in this study. All three sizes of CT specimen had the same width of 12 in. and a thickness of 2 in.. Only the length of the specimen was varied as 10.5 in., 12.5 in. and 14.5 in.. A 4.5 in. notch was normally cast at the middle of the specimen to simulate an existing crack in the test specimen. The specimen was cast in a plexiglass mold made in our concrete laboratory. A more detailed listing of all specimen dimensions is given in the Table III.

2.2 MIX PROPORTION AND MATERIALS COMPOSITIONS

Ten different mix proportions were used in this study (see Table I) . The water cement ratio was varied from 0.4, 0.45, 0.5, and 0.55 . Three different controlled grain

TABLE I

MATERIALS COMPOSITIONS

Mix No.	Mix Proportion (by weight) C : S : A : W	Size of Sand
I	1 : 2 : 0 : 0.4	2 mm - 0.425 mm
II	1 : 2 : 0 : 0.45	2 mm - 0.425 mm
III	1 : 2 : 0 : 0.5	2 mm - 0.425 mm
IV	1 : 2 : 0 : 0.55	2 mm - 0.425 mm
V	1 : 2 : 0 : 0.5	0.425 mm - 0.212 mm
VI	1 : 2 : 0 : 0.45	< 0.212 mm
VII	1 : 2 : 0 : 0.5	< 0.212 mm
VIII	1 : 3 : 0 : 0.4	< 0.212 mm
IX	1 : 2 : 2 : 0.5	6 mm - 2 mm

Note: For uniaxial tension specimen, use Mix I to IX
For notched beam and compact tension, use Mix X

MATERIALS

Cement : Portland Cement Type III

Sand : Silicious Sand

Aggregate : Crushed Lime Stone with Maximum Size Between 1/4" to 3/8"

Note: Sieve # 10 (2 mm)

Sieve # 40 (0.425 mm)

Sieve # 70 (0.212 mm)

sizes of sand (passing from sieve #10, #40 and #70) were used to study the effects of grain size on both fracture energy and the critical crack opening displacement. The type of cement used in this investigation was Type III portland cement . Silicious sand and crushed limestone of size 1/4" to 3/8" was used to make the concrete mix.

Mortar and concrete were prepared by mixing all the materials in a mechanical mixer. After it was mixed thoroughly for 5 minutes, the mixture was then placed in oiled plastic or steel mold in layers. The mold was normally placed on the vibrating table in order to get rid of the excess air bubble. The vibrating process normally took less than 5 minutes to avoid breeding and aggregate segregation. The finished specimen was left to set in the mold for 24 hours and covering with plastic to reduce surface cracks due to shrinkage. The specimen was then removed from the mold and cured in the saturated limewater for twenty days, since all the specimen were planned to be tested at the age of 21 days . The specimen normally would be left to dry in the laboratory environment for 24 hours before being tested . For dog-bone specimen , the saw-cut notches would be cut with a thin diamond blade an hour before being tested .

For every mix-proportion of each type of test specimen at least 7 specimens were tested in order to obtain the average result .

2.3 EXPERIMENTAL PROCEDURE AND SETUP

Dog-Bone Specimen

Fig. 1 showed a dog-bone which specimen was slid into a pair of briquette grips. The two grips were connected to two universal joints which were intended to maintain the axial concentric load . A 5-kip load cell was connected in the axial direction of the test setup to measure the applied load . A steel bar with a turn buckle was added to the system to ease the setup process . Two 0.2-inch extensometers were placed on both sides of the test specimen over the saw-cut notches. Both extensometers have a gage length of 1 in.. Extensometers were tightened to the test specimen with two rubber bands , in which the normal force was controlled by two attached soft springs . The signals from both extensometers were averaged and fed back to the control circuit to re-adjust the hydraulic power actuator so that a constant strain rate could be maintained throughout the experiment . Observation of the post-peak tensile response of concrete , can be achieved only when the applied strain rate is constantly maintained .

The response of test specimen was recorded on an XY recorder where load and axial displacement or strain were monitored . In addition to the XY plot, MTS also provided a digital readout of two channels by which any of the three load, strain or stroke signals could be read.

The digital display also connected to a hard copy printer where six channels of output could be recorded as frequent as 5 seconds interval . In this study, load , strain and stroke were printed out at every 15 seconds . This information was later fed into the LOTUS-123 worksheet for computational and graphic purpose .

In most of the experiments in this investigation, two types of loading pattern ,viz., monotonic and cyclic, were used . Typical load-displacement curves under monotonic and cyclic loading were shown in Fig. 2. While monotonic loading condition is more common to pratical static loading situation , cyclic loading are normally encountered in earthquake and dynamic problems. Besides, cyclic loading response generally presents more information on materials and structural responses such as the actual elastic property of materials after cracking .

In conducting the monotonic loading , the specimen was initially loaded at the rate of 0.22 microstrain per second. This slow loading rate is normally required for maintaining stability in the peak region . This initial rate was slower than those used by Reinhardt (0.08 um/sec.-Ref. 6,7) and Gopalaratnum and Shah (1 um/sec.-Ref.8). After passing the peak and when the load dropped down to about 80% of the peak load, the strain rate could be increased without causing failure . In the present study, the strain rate was

gradually increased to 10 micro-strain/sec in order to shorten the total testing time . This process normally causes some slight changes in the load-displacement response due to the effect of strain rate. A single uniaxial tension test took between 2 to 8 hours to complete the whole post-peak response . The complete load-displacement curve was recorded by the XY recorder as well as in a computer printer which scanned every 15 seconds . The computer printer was also set to print out the response whenever the strain rate was increased to speed up the test .

For cyclic loading, once the load passed over the peak, the control unit was switched to have the strain return to zero . This process was a built-in system which the testing machine would unload automatically . Due to the torturous nature of the crack surface, crack tends to remain partially open . This phenomenon is known to be "aggregate interlocking". As a result, certain amount of permanent strain would be observed when the applied load reduced to zero . To reload the specimen, a load-switch was simply turned on. The same loading procedure was repeated whenever unloading and reloading were required . A typical cyclic load-displacement curve was shown in Fig.2 . The cyclic load-displacement relationship provided not only the actual elastic Young's Modulus of the test specimen in the post-peak region but also showed the extent of permanent deformation at any corresponding instance in the post-peak

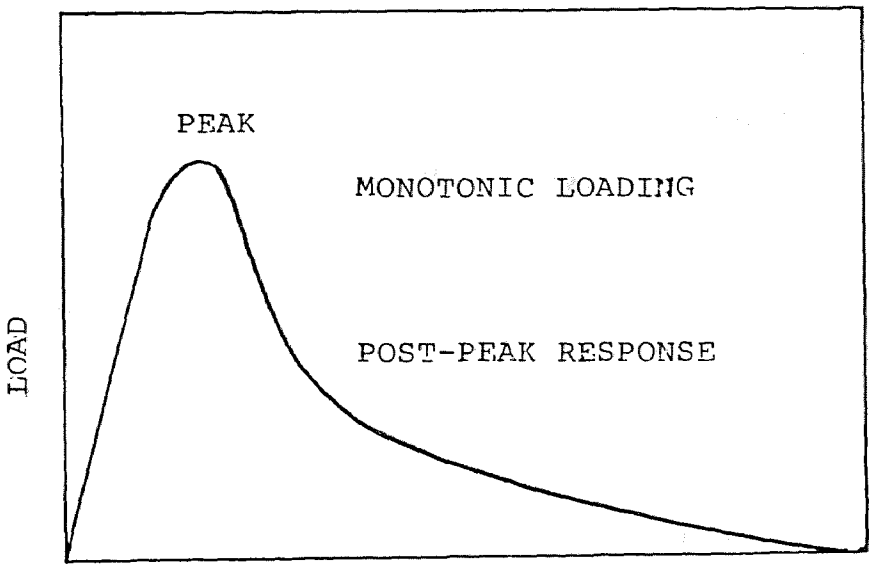

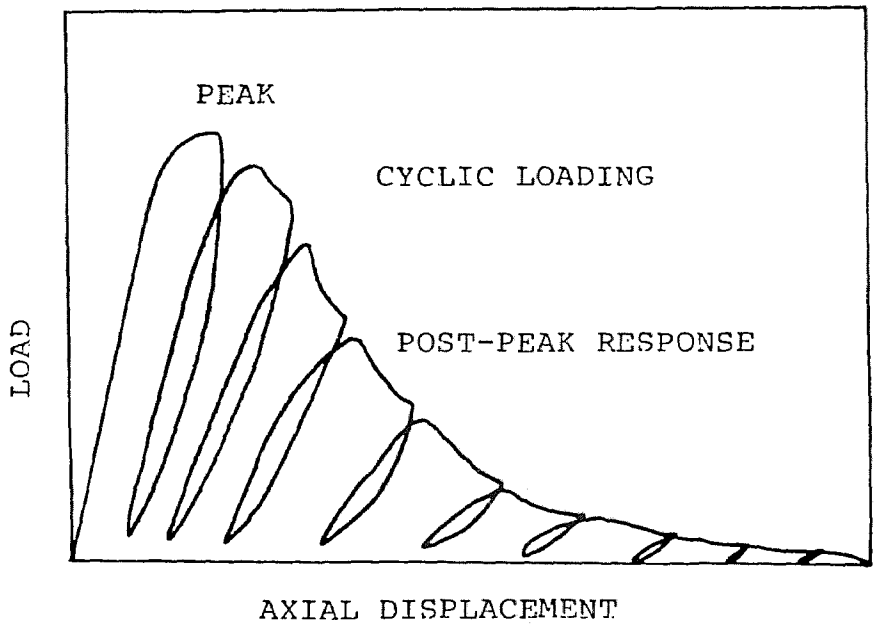

FIG. 2 -TYPICAL LOAD DISPLACEMENT CURVES UNDER MONOTONIC AND CYCLIC LOADING

zone . This information is crucial for the modified strain energy model proposed by Wecharatana and Shah (Ref. 16,17) as well as for the continuum damage theory used by Loland (Ref.18) and Janson and Hult (Ref. 19) .

Notched-Beam Specimen

General loading configuration of a standard notched beam specimen (Ref.22) can either be a four-point-bend or three-point-bent. In this study, a three-point-bend specimen (Fig.3a) was tested just for the purpose of studying the uniqueness of the fracture energy concept. A clip gage was placed over the notch to measure the crack mouth opening displacement . Vertical load-line deflection was measured by a linear Variable Differential Transformer (LVDT) with an accurate range of 0.5 in. The signal from the clip gage was used as a feed back control . The test was conducted under a constant rate of crack mouth opening displacement which made it possible to monitor the post-peak load-deformation response without abrupt failure even in plain concrete beam. The loading rate for testing the notched beam specimen was 33.3 micro-inch/sec. Output from the load cell, LVDT and the clip gage , were recorded in two XY recorders. Total area under the load-displacement curve was calculated to be the value of fracture energy. While most notched beam specimen were tested under monotonic loading, a few beams were also tested under cyclic load.

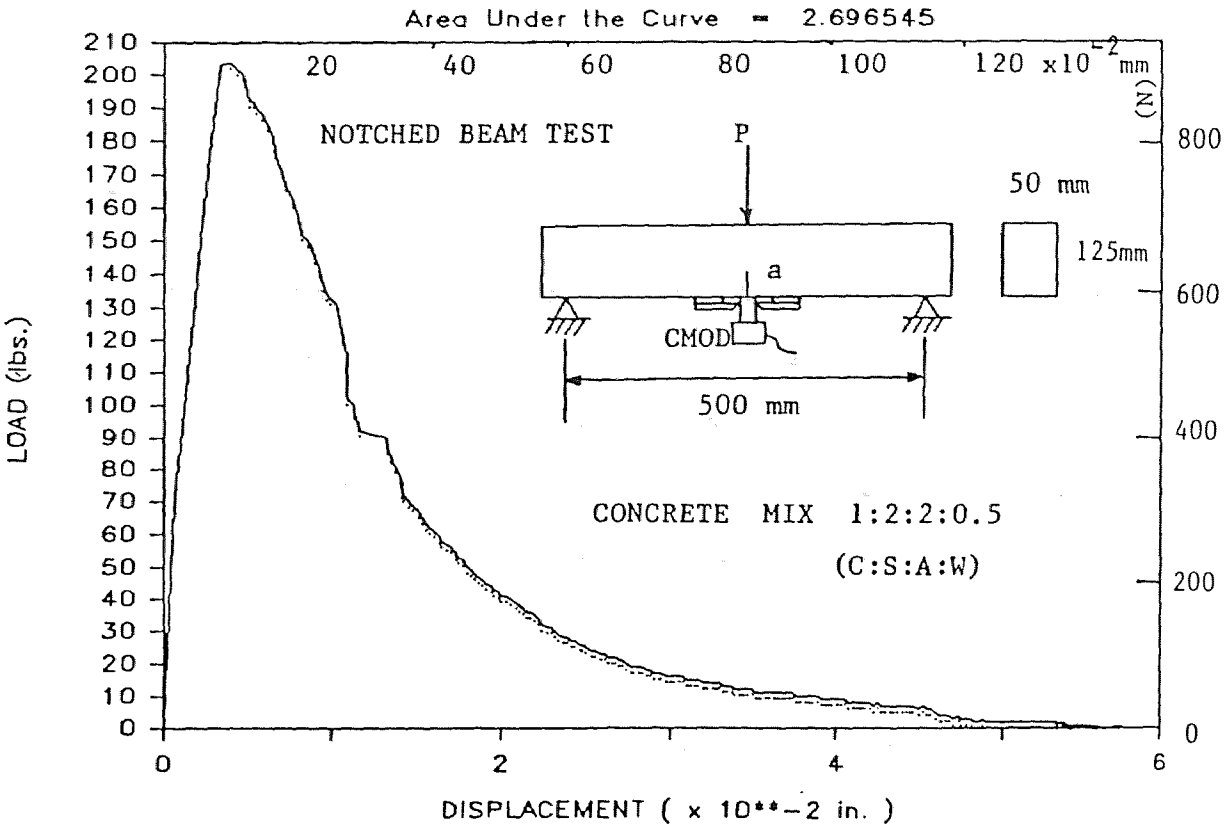

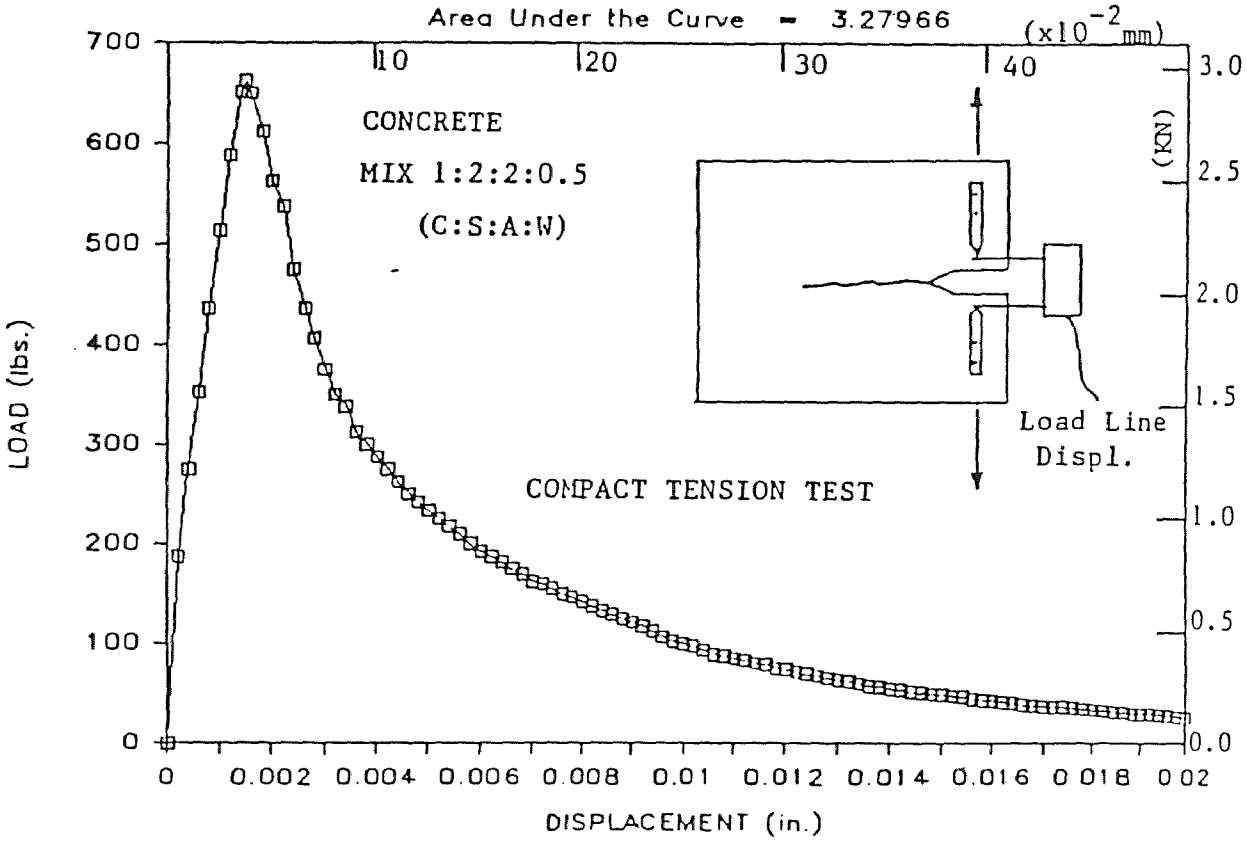

FIG. 3 TYPICAL LOAD DISPLACEMENT CURVES AND TEST SETUP OF
a) NOTCHED BEAM SPECIMEN
b) COMPACT TENSION SPECIMEN

Compact Tension Specimen

Another common test specimen recommended by Standard ASTM (Ref.22) is the compact tension specimen (Fig. 3b). Crack mouth opening displacement was again used as the feed back signal so the that post-peak response could be observed. A clip gage as well as an LVDT were placed between two knife edges which lied in the direction of the applied load. The test specimen was initially supported at the free end for test setup purpose. Once the applied load increased, the whole specimen was normally lifted from the support at the free end . Fracture energy was then calculated from the whole area under the load-displacement curve . Major differences between the notched beam and compact tension specimen were the size of the crack growth and the stress field around the crack tip. In notched beam specimen the crack propagates into the tension zone which is subsequently followed by a compression zone. While in compact tension, the tension zone in front of a crack tip covers the whole specimen except for a small area at the end of the specimen which is under compression.

Both notched beam and compact tension specimen practically have a mixed mode of direct pull-out combined with shear failure (Ref.1,2) . However , most theoretical models simply ignored the shear effect primarily just for simplicity. Nevertheless, even the uniaxial tensile response was rather difficult to obtain . In this thesis,

emphasis was mainly given to the experimental study of the complete uniaxial tensile response of mortar and concrete using a simple test specimen .

CHAPTER III

EXPERIMENTAL RESULTS AND DISCUSSIONS

Experimental study of the direct tension test was rather tedious and time consuming. The results obtained can be categorized into five series of post-peak relationships. These are :

1. Load-Displacement Relationship
2. Stress-Displacement Relationship
3. Normalized Post-Peak Stress-Displacement Relationship
4. Unloading Load-Displacement Relationship
5. Elastic Young's Modulus in Post-Peak Region

3.1 LOAD DISPLACEMENT RELATIONSHIPS

A typical load-displacement relationship is shown in Fig.4. It can be observed from the post-peak response that the stress gradually decreased from the ultimate tensile strength to zero. This observed response contradicts the constant-stress-plateau concept reported by other investigators (Refs.5-10) . The maximum post-peak displacement represents the pull-out distance where no traction

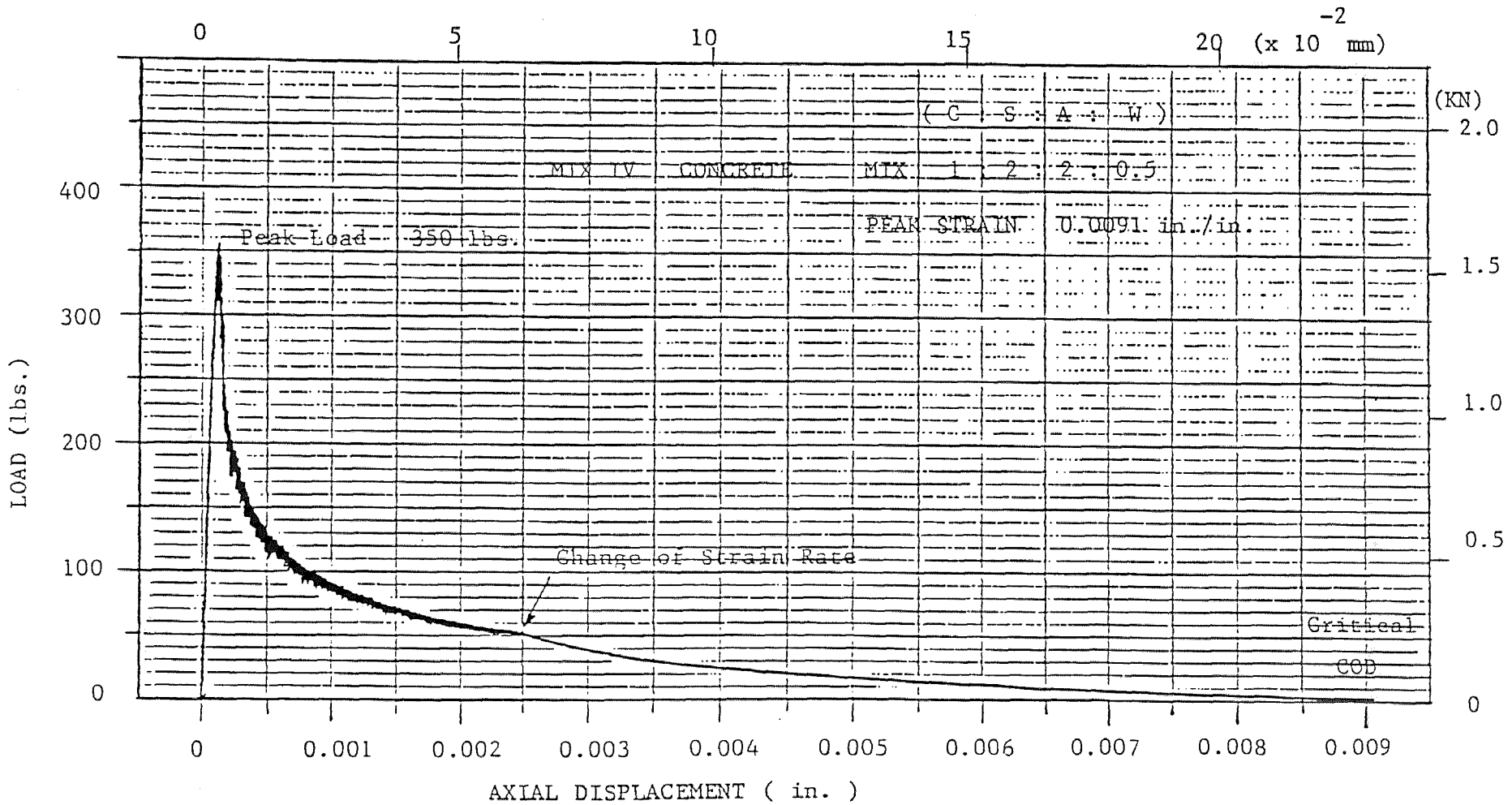

FIG. 4 -LOAD-DISPLACEMENT RELATIONSHIP OF CONCRETE IN DIRECT TENSION

remains across the crack plane or the fracture zone . This value is rather important since it represents the critical crack tip opening displacement . The ascending branch of the load-displacement curve is very close to linear. Enlarging the scale will generally show some nonlinearity around the peak region and also in part of the pre-peak zone. This is primarily due to the increase in internal micro-cracks. This nonlinear zone has been more clearly presented in Ref. 6,7,8 . The dark thick line area in Fig.4 was due to the effect of averaging signals between the two extensometers which led to loading and unloading within a small range so that stability in the post-peak zone could be maintained . The change in smoothness of the load-displacement curve was due to the change in strain rate . Practically , material response generally varies with the applied strain rate , however , no information has been reported on the effects of strain rate on the post-peak response of concrete . In this study , it was assumed that the strain rate had no significant effects in this experimental investigation . Since the loading strain rate required to maintain equilibrium stage in the post peak region was extremely slow in this study (.22 micron/sec) and to complete the whole post-peak response would take up to 20 hours ,the strain rate was therefore increased to shorten the testing time which consequently reduced the effect of creeping of the observed response . The typical curve in Fig.4 also showed that post-peak tensile response largely

varied as an exponential function . The comparison of area under the load-displacement curve clearly indicated that if conventional testing methods were used and no post-peak response was observed , the actual fracture energy would be under-estimated by as much as 10-20 times . This finding reinforces the significance of including softening effect in the nonlinear analysis .

Fracture phenomenon around the critical section was observed as follows : A crack always started from one side of the test specimen and gradually extended across the net section . This implies that the stress distribution across the critical section may not be uniform . Since concrete is a heterogeneous composite material, it is pratically impossible to have an even or uniform applied stress across the section . Discussions with Dr. Gopalaratnum concluded that the same behavior was inferred from available test data. Since two universal joints were placed on the top and the bottom of the test specimen to maintain concentric loading, although a crack may start from one side, the applied stress eventually will create additional crack on the other side to evenly balance the eccentricity . In addition , stress observation reported in Refs.(6,7,8) also showed a uniform stress distribution with slight variation in the early stage of the experiment . More work may be needed to thoroughly understand this existing problem . One possible approach is to conduct a tension test on a large

TABLE II

OVERALL OBSERVED PARAMETERS

Mix	Mix Proportion C : S : A : W	Grain Size (mm)	Compressive strength	Tensile strength (1)	Tensile strength (2)	Strain at Peak	E	COD	G
I	1 : 2 : 0 : 0.4	2	6571	430	330	0.993	3.32	60.06	0.287
II	1 : 2 : 0 : 0.45	2	5186	427	311	0.929	3.13	59.64	0.282
III	1 : 2 : 0 : 0.5	2	4697	341	335	0.997	3.36	55.47	0.227
IV	1 : 2 : 0 : 0.55	2	-	-	-	0.884	2.57	53.50	0.213
V	1 : 2 : 0 : 0.5	0.425	5539	337	381	1.009	3.78	50.35	0.218
VI	1 : 2 : 0 : 0.45	0.212	5179	382	224	0.771	2.91	53.86	0.247
VII	1 : 2 : 0 : 0.5	0.212	5690	-	346	1.265	2.74	38.43	0.206
VIII	1 : 3 : 0 : 0.4	0.212	-	-	89	1.020	0.87	41.84	0.109
IX	1 : 4 : 0 : 0.5	0.212	-	-	324	0.975	3.32	19.74	0.104
X	1 : 2 : 2 : 0.5	6	4654	-	538	1.378	3.90	86.44	0.385

Units:
- Compressive Strength (psi)
- Strain at Peak (x10 ** -4 in./in.)
- E -Young's Modulus (x10 ** 6 psi)
- COD (x10 ** -4 in.)
- G -Fracture Energy (lb./in.)

Note: (1) Split Tension in (psi)
(2) Direct Tension in (psi)

specimen which will clearly verify the problem of non-uniform stress distribution .

One of the important observed parameters was the critical crack opening displacement which corresponds to the maximum post-peak displacement in the descending branch . The observed critical COD values range between 0.005 in. to 0.008 in. (see Table II for more details) .

Since more than 70 specimens were tested , it is not possible to include all the results in this section . All load-displacement curves were presented in Appendix A . See Table IV for proper specimen numbering and its mix-proportion

3.2 STRESS DISPLACEMENT RELATIONSHIPS

Stress-displacement relationship has been commonly used as constitutive relationship in fracture mechanics of concrete . Since crack width induced discontinuity in the materials within the gage length , as a result , the definition of strain was no longer valid and stress-displacement was directly employed in most finite element analysis in the post-cracking zone . In the ascending region , the stress-strain relationship remains to be the constitutive law of materials. In this study , the gage length used was 1 in. , so the displacement and the strain have same magnitude . Fig.5 shows a typical comparison of stress-

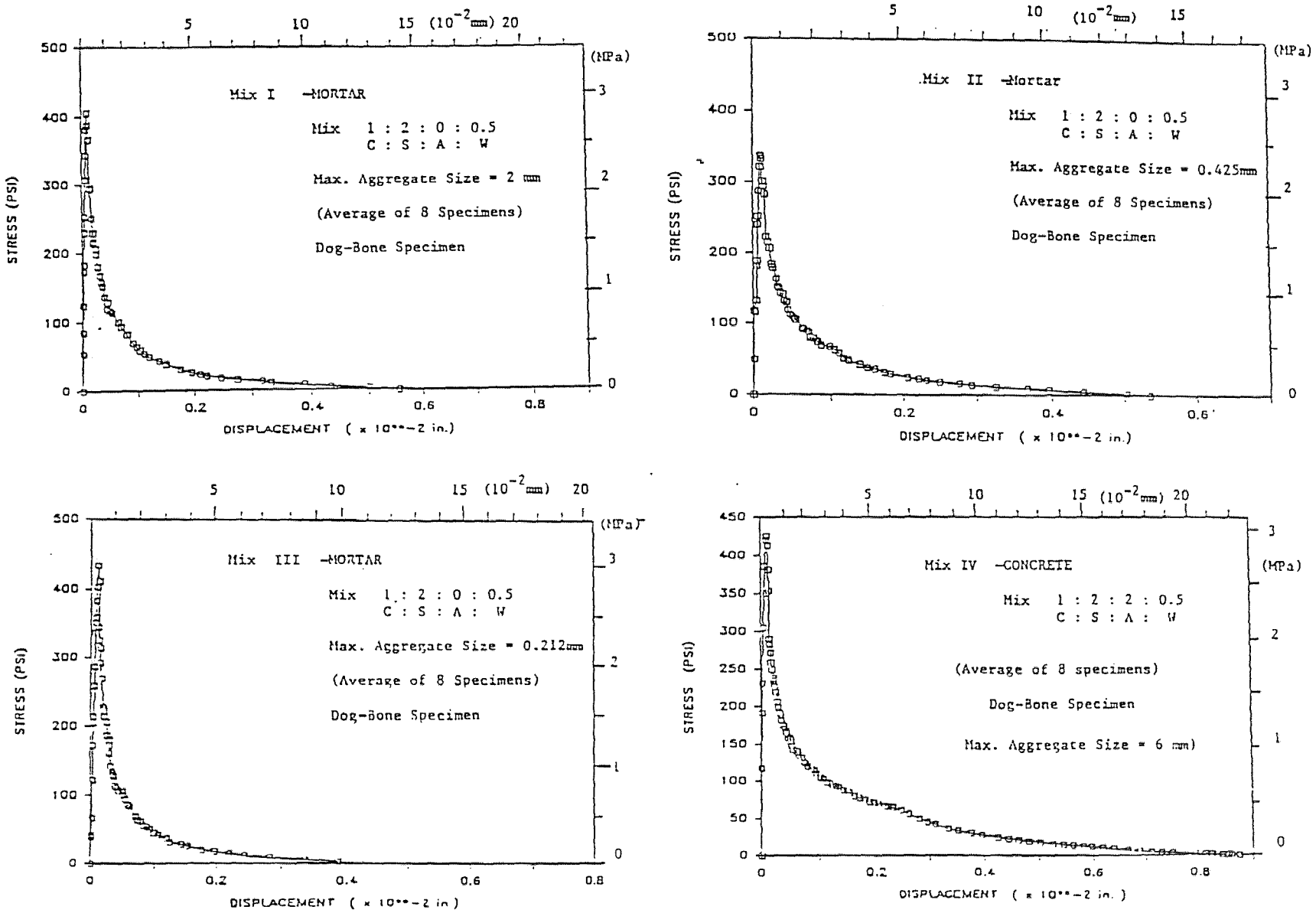

FIG.5 -STRESS-DISPLACEMENT RELATIONSHIPS OF MORTARS (I,II,III) and CONCRETE (IV) IN UNIAXIAL TENSION TEST (DOG-BONE SPECIMEN)

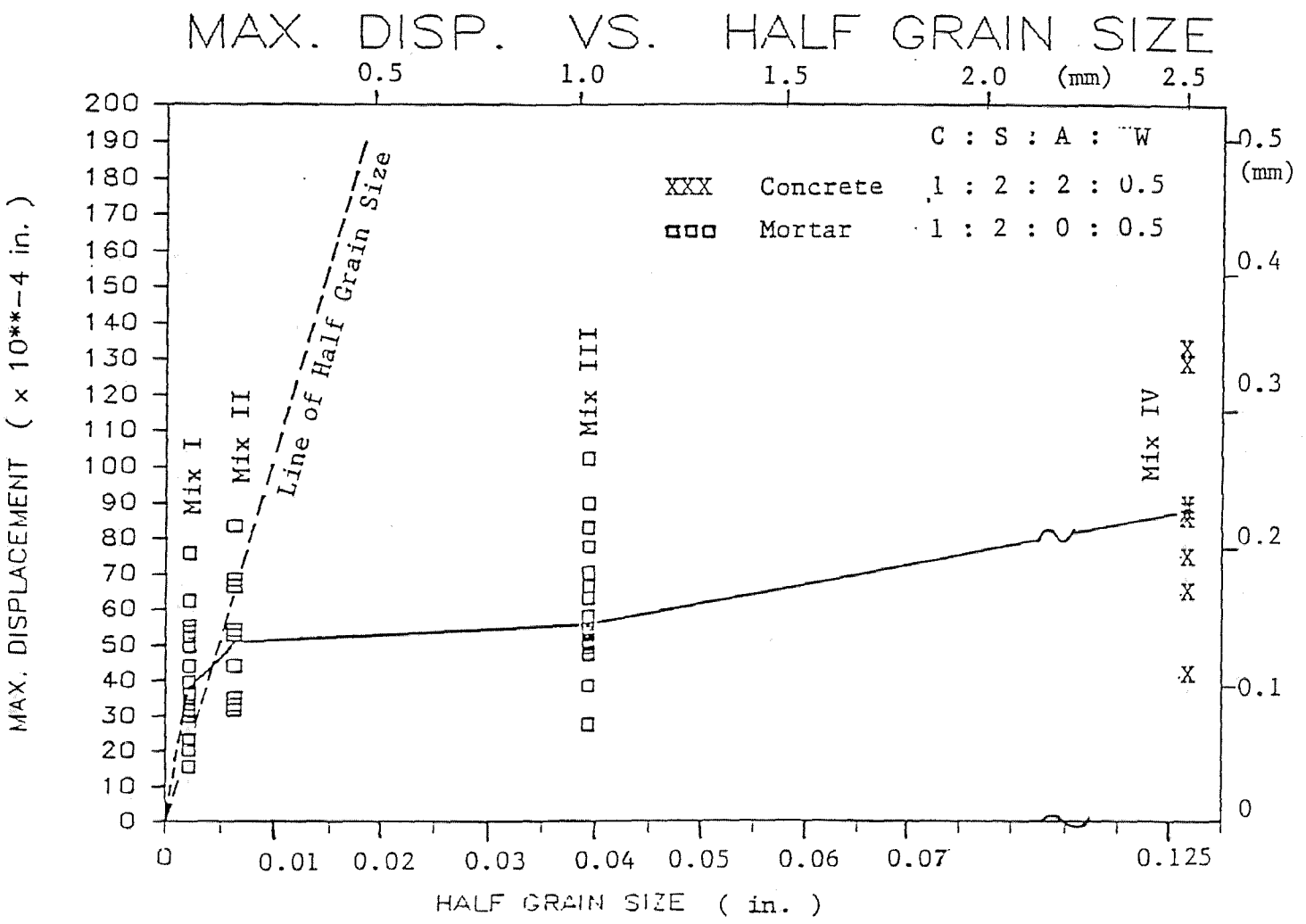

FIG. 6 -Relationship of Maximum Post-Peak Displacement and The Aggregate Grain Size

displacement relationships from four different mix-proportions with different grain sizes of sand . It can be observed that the larger aggregate grain size , larger is the observed maximum post-peak displacement . This can be explained by the fact that crack plane will be more torturous when aggregate grain size is bigger . Table II also indicated that larger the grain size, higher is the value of fracture energy . A similar trend was also observed in the change of maximum post-peak displacement or the critical crack opening displacement (COD) with aggregate grain size . Appendix B summarized all the tested stress-displacement relationships .

3.3 NORMALIZED POST-PEAK STRESS-DISPLACEMENT RELATIONSHIPS

It is postulated by the author that a typical load-displacement or stress-displacement relationship may be a specimen size-dependent relation . In order to verify this concept an attempt was made to propose a unique normalized relationship . In general , peak strength was used to normalize the stress , and therefore maximum post-peak displacement was a reasonable normalized factor for displacement . However, the value of maximum post-peak displacement was rather difficult to obtain unless certain aggregate grain size could be related to this critical value. A study of the maximum post-peak displacement and aggregate grain size indicated that the maximum pull out

displacement was not directly related to the maximum aggregate size of concrete . The value of maximum pull-out displacement varied from 0.005 in. to 0.008 in. even though a large maximum aggregate size of 1/4"-3/8" was used in concrete . For a smaller sand grain , the value of half the aggregate grain size was closely related to the maximum pull-out displacement . The maximum post-peak displacement was then used to normalize the post-peak stress-displacement relationship . Since stress-strain relationship remains a valid constitutive law in the ascending branch , only the post-peak region will be normalized . A typical post-cracking normalized stress-displacement relationship was presented in Fig. 7. The same trend was observed in both mortar and concrete in this study. Similar conclusions were reported for fiber reinforced concrete by Wecharatana and Shah (Ref.14) and Visalvanich and Naaman (Ref.15).

The unique relationship of the normalized post-peak stress-displacement for mortar and concrete was found in this study to be :

$$\frac{\sigma}{\sigma_{max}} = \left[1 - \frac{\eta}{\eta_{max}}\right]^{-m\left[\frac{\eta}{\eta_{max}}\right]^{n}}$$

where σ_{max} is the maximum post-cracking stress , η_{max} is the maximum pull-out displacement which is related to the grain size of sand , while m and n are constants .

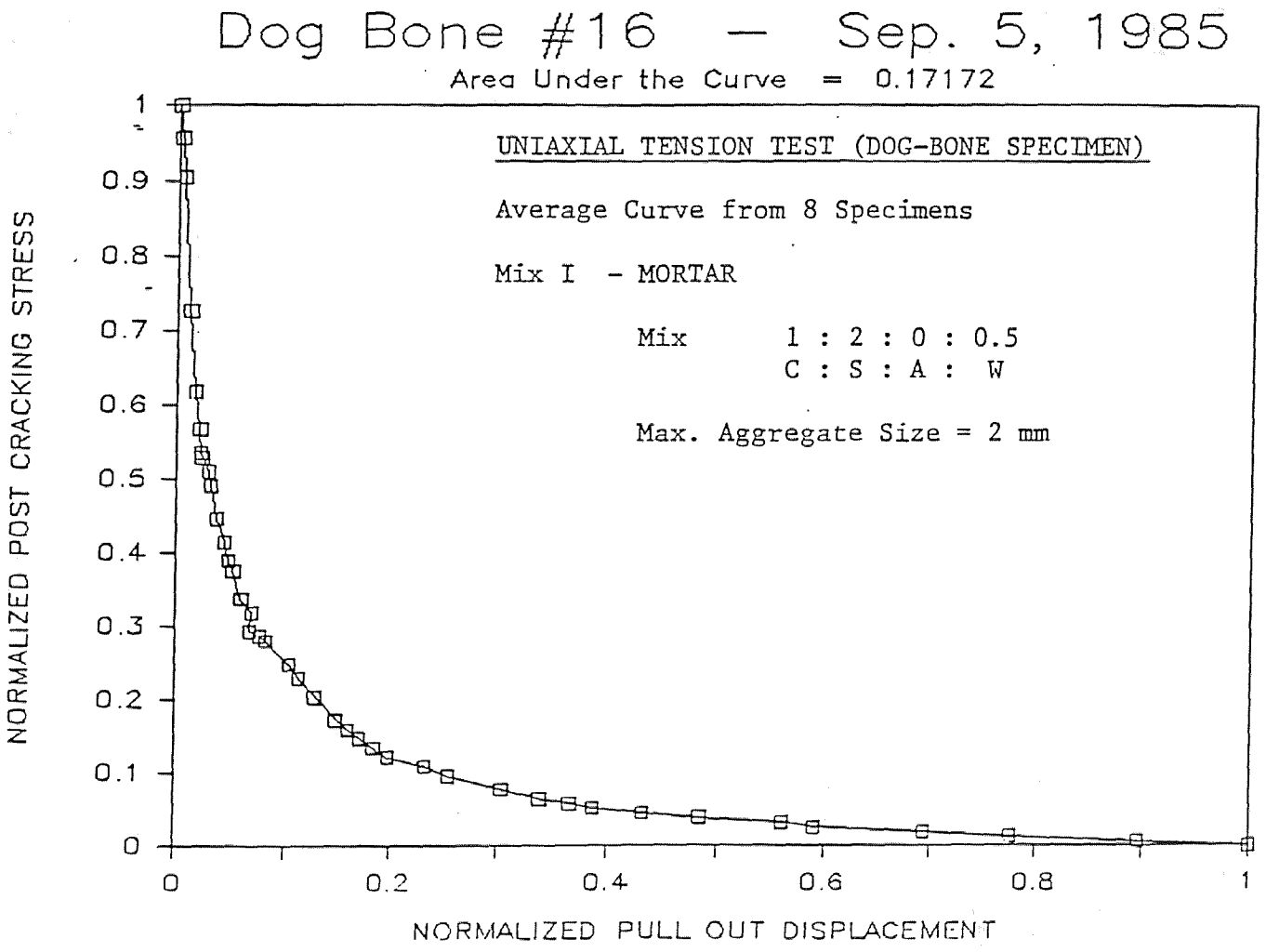

FIG. 7 -Normalized Post-Peak Stress-Displacement Relation

In this study , m was found to be 1.858 and n=0.319 . The plot of $\frac{\sigma}{\sigma_{max}}$ vs $\frac{\eta}{\eta_{max}}$ corresponds to the normalized curve. Knowing this unique relationship and the controlled grain size of sand used in a given mix-proportion of mortar or concrete , the post-peak response can easily be predicted from a single peak strength value . Appendix C presented all the observed normalized post-peak stress-displacement relationships.

3.4 CYCLIC LOAD-DISPLACEMENT RELATIONSHIP AND YOUNG'S MODULUS

A typical cyclic load-displacement relationship was presented in Fig.8 . It can be observed that the elastic Young's Modulus decreased as crack growth increased . Permanent deformation which resulted from aggregate interlocking also increased as the crack growth developed. The change in loading pattern from monotonic to cyclic loading did not significantly affect fracture energy nor the maximum post-peak displacement (critical COD) . A typical plot of elastic Young's Modulus versus pull-out displacement was presented in Fig. 9. The decrease of Young's Modulus was in good agreement with the change of compliance value reported by Swartz et. al (Ref.20).

Observed changes of the elastic modulus are essential information for several theoretical models such as the modified strain energy by Wecharatana and Shah (Ref.3), the

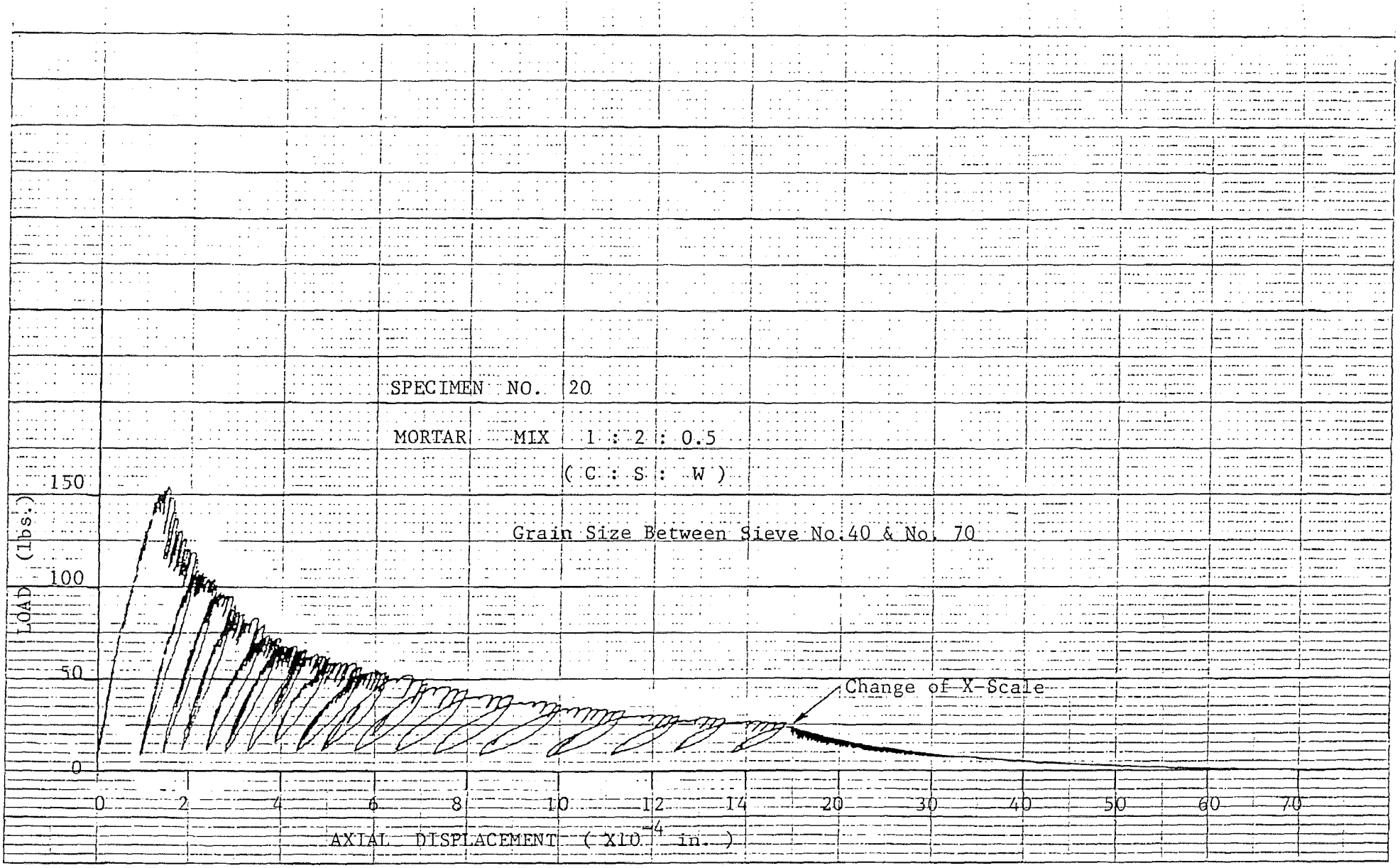

FIG. 8 -LOAD DISPLACEMENT RELATIONSHIP UNDER CYCLIC LOADING

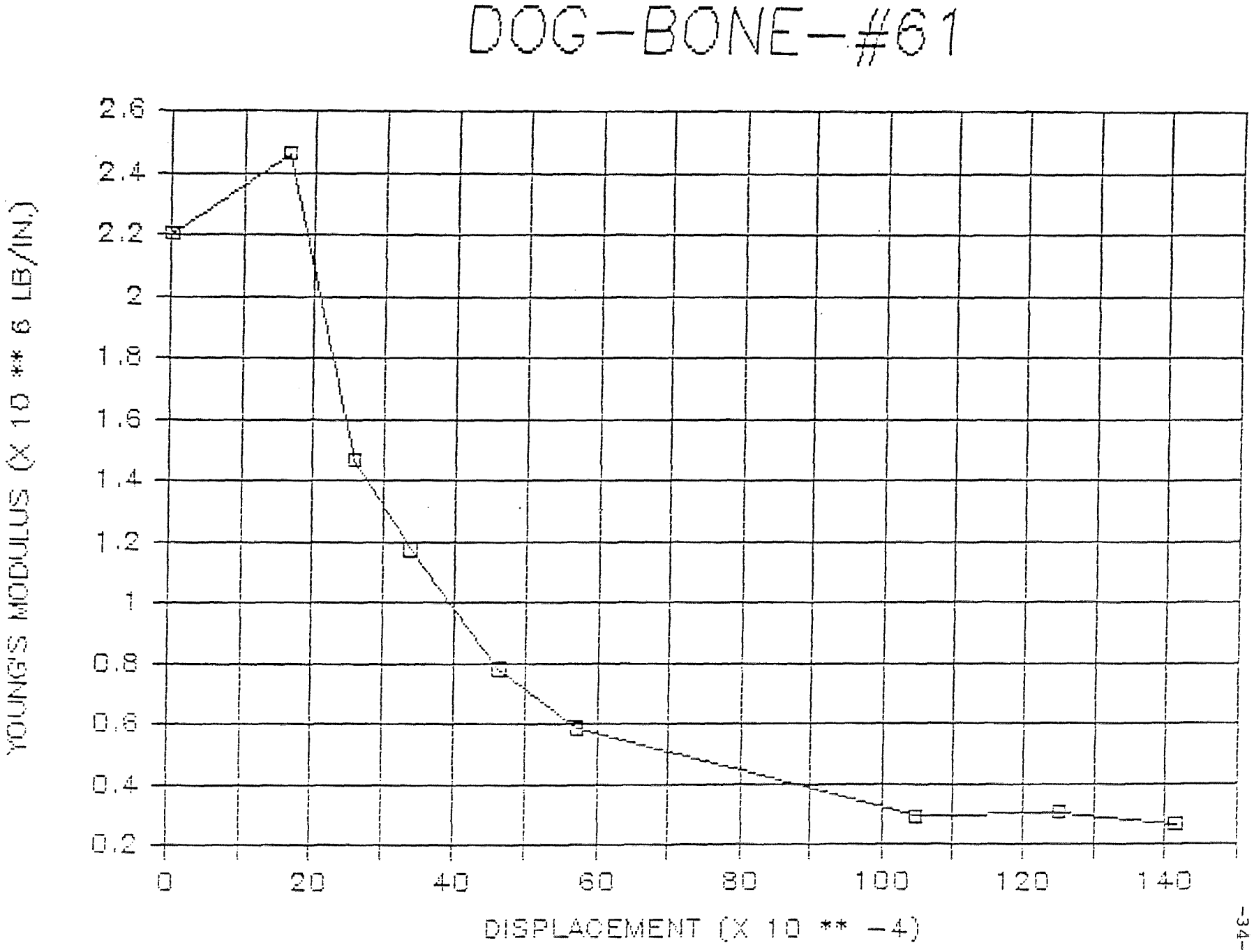

FIG. 9 -TYPICAL ELASTIC YOUNG'S MODULUS VERSUS PULL-OUT DISPLACEMENT RELATIONSHIP

band crack model by Bazant and Oh (Ref.2) etc.

The application of continuous damage mechanics to fracture of concrete proposed by Janson et. al (Ref.19) and Loland et. al (Ref.18,21) have shown the decrease of elastic Young's Modulus as a function of damage factor W_o where the descending portion can be predicted from :

$$E_i = E_n\ (1-W_o)$$

where

E_i= the slope of the unloading part of the curve

E_n= the initial Young's Modulus which corresponds to zero damage (W_o=0)

W_o= the ratio of the damage area to the total cross sectional area .

With the observed decrease of Young's Modulus , a better understanding of the damage parameter W_o can easily be studied . From the normalized post-peak stress-displacement, the damage parameter Wo should also be related to the aggregate grain size . The damage mechanics concept coupled with the observed normalized relationship can lead to a promising theoretical model for fracture study of concrete and other cementitious composites . Appendix D summaried all the observed unloading load-displacement relationship while Appendix E presented the observed elastic Young's Modulus of the unloading part of the cyclic load-displacement curves .

3.5 FRACTURE ENERGY

Table III summaried the values of fracture energy from three tension specimens , one notched beam and three compact tension specimens . This value varies from 0.104 lb/in. in tension specimen to 2.030 lb/in. in the compact tension specimen . It can be seen that fracture energy is clearly a specimen-dependent fracture parameter . The value of fracture energy was normally obtained from the total area under the load-displacement curve . Since some previous test results (Ref. 6,7,and 8) were not completed, the reported values may be errorneous . However, from the comparison of the three direct tension tests , fracture energy was not found to be a unique material property . Measuring the fracture energy from a notched beam as suggested by the RILEM recommendation is certainly an unreliable approach.

Form the present study ,the concept of critical crack opening displacement seems to be a more reliable concept . The value of critical crack opening displacement was found to vary within a small range of 0.005 in. to 0.008 in. even though large aggregate of 1/4 in. was used in the concrete mix. This implies that the value of critical crack opening displacement can be predicated if aggregate sizes of concrete or mortar are given . The concept of critical crack opening displacement was then concluded to be a more

promising concept for fracture study . The post-peak normalized relationship seems to be a material property and thus should be used in the theoretical modelling . More experimental and theoretical verification of the critical COD should be continued before a proper recommendation for standard testing method as well as proper theoretical model can be concluded .

TABLE III

FRACTURE ENERGY

Authors	Mix Proportion C : S : A : W	Type of Specimen	Maximum Post-Peak Displacement um (in.)	Fracture Energy N/m (lb/in)
Gopalaratnum & Shah (Ref. 8) (1 um/sec)	1 : 2 : 2 : 0.45	Plate Tension	61 (0.0024)	52.0 (0.297)
	1 : 2 : 2 : 0.60		61 (0.0024)	56.4 (0.322)
	1 : 2 : 0 : 0.50		61 (0.0024)	72.7 (0.415)
Reinhardt (Ref. 6,7) (0.08 um/sec)	1 : 3.38 : 0.5	Plate Tension	140 (0.0055)	135.0 (0.771)
Present Study (0.02 um/sec)		Dog Bone		
	1 : 2 : 0 : 0.4	2-0.425 mm	153 (0.0060)	50.3 (0.287)
	1 : 2 : 0 : 0.45	2-0.425 mm	150 (0.0059)	49.4 (0.282)
	1 : 2 : 0 : 0.5	2-0.425 mm	140 (0.0055)	40.0 (0.227)
	1 : 2 : 0 : 0.55	2-0.425 mm	137 (0.0054)	37.3 (0.213)
	1 : 2 : 0 : 0.5	0.425-0.212 mm	127 (0.0050)	38.2 (0.218)
	1 : 2 : 0 : 0.45	<0.212 mm	137 (0.0054)	43.3 (0.247)
	1 : 3 : 0 : 0.50	<0.212 mm	96.7 (0.0038)	36.1 (0.206)
	1 : 4 : 0 : 0.4	<0.212 mm	107 (0.0042)	19.1 (0.109)
	1 : 2 : 2 : 0.5	<0.212 mm	51 (0.0020)	18.2 (0.104)
	1 : 2 : 2 : 0.5	<2.0 mm	218 (0.0086)	67.4 (0.385)

TABLE III (continued)

FRACTURE ENERGY

Authors	Mix Proportion C : S : A : W	Type of Specimen	Maximum Post-Peak Displacement um (in.)	Fracture Energy N/m	Fracture Energy (lb/in)
Present Study					
	1 : 2 : 2 : 0.5	Notched Beam (50x125x600 mm.)		204.6	(1.168)
	1 : 2 : 2 : 0.5	Compact Tension			
		(50x300x300 mm)		212.3	(1.212)
		(50x300x400 mm)		263.0	(1.501)
		(50x300x500 mm)		355.8	(2.030)

TABLE IV

SPECIMEN NUMBERING AND ITS MIX-PROPORTION

Grain Size (mm)	Mix Proportion (C : S : A : W)	Specimen Number
	MORTAR	
2.0 - 0.425	1 : 2 : 0 : 0.4	*23, *38, *39, 45, 49
	1 : 2 : 0 : 0.45	22, *35, *36, 37, *59, *60
	1 : 2 : 0 : 0.5	*16, 17, 29, 30, *43, *44, 46, 47, 48
	1 : 2 : 0 : 0.55	*20, 21, 33, 34
0.425 - 0.212	1 : 2 : 0 : 0.45	*24, 25, 54, 55
	1 : 2 : 0 : 0.5	18, *19, 26, 27, 28, *40
< 0.212	1 : 2 : 0 : 0.4	50
	1 : 2 : 0 : 0.45	53, *57, *58
	1 : 2 : 0 : 0.5	31, 32, *41, *42, *61 62, 63
	1 : 3 : 0 : 0.4	51, 52, *56
	1 : 4 : 0 : 0.5	13, *14, 15
	CONCRETE	
< 6.0	1 : 2 : 2 : 0.5	2, 3, 9, 12, 68 69, 70, 71

REMARK: * refers to unloading

CHAPTER IV

CONCLUSIONS

From the results of this study , the following conclusions can be drawn :

1. Fracture energy is not a unique material property. Use of notched beam specimen as a standard testing method to measure fracture energy is unreliable since fracture energy is a specimen-dependent parameter .

2. The critical crack opening displacement was shown to be a more reliable approach for studying fracture behavior in cementitious composites .

3. The critical grain size of sand or fine aggregate which controls the maximum post-peak displacement or critical COD value is approximately the size of particle passing sieve no. 40 (0.425 mm) .

4. The uniqueness of normalized post-peak stress-

displacement relationship exists in mortar and concrete . The same normalized equation which has been proposed for fiber reinforced concrete is applicable to the mortar and concrete with constants m= 1.858 and n= 0.319 .

5. The decrease of elastic Young's Modulus in the post cracking region supports the the applicability of continuous damage theory to fracture of concrete. The damage constant-W_o for cementitious composite, may be related to aggregate grain size, and the unique normalized post-peak stress-displacement law.

6. A simple dog-bone tension specimen can be used to observe the post-peak uniaxial tensile response of concrete using a closed-loop strain controltesting system .

SELECTED BIBLIOGRAPHY

1. Hillerborg , A., Modeer , H. and Petersson , P.E. " Analysis of Crack formation and Crack Growth in Concrete by Means of Fracture Mechanics and Finite Elements" Cement and Concrete Reseach , Vol. 6, 1976, PP. 773-781
2. Bazant , Z.P., and Oh , B.H.," Crack Band Theory for Fracture of Concrete" Materiaux et Constructions , Vol. 16, No. 93 , 1983 , PP. 155-177
3. Wecharatana , M. and Shah, S.P. ," Predictions of Nonlinear Fracture Process Zone in Concrete", Journal of Engineering Mechanics Division , ASCE , Vol. 109 ,No. EMD5 , Oct. 1983, PP. 1231-1246
4. Evans, R.H. , and Marathe, M.S., "Microcracking and Stress-Strain Curves for Concrete in Tension" Materiaux et Constructions, No. 1, Jan.-Feb. 1968 , PP. 61-64
5. Petersson , P.E. ," Crack Growth and Development of Fracture Zones in Plain Concrete and Similar Materials" Report No. TVBM-1006 , Lund, Sweden
6. Reinhardt , H. W. , and Cornelissen , H.A.W.," Post-Peak Cyclic Behavior of Concrete in Uniaxial Tensile and Alternating Tensile and Compressive Loading" Cement and Concrete Research , Vol. 14 , PP. 263-270 , 1984
7. Reinhardt , H.W.," Crack Softening Zone in Plain Concrete under Static Loading " Cement and Concrete Research , Vol. 15,PP. 42-52, 1985

8. Gopalaratnum , V.S. ,and Shah , S.P. ,"Softening of Plain Concrete in Direct Tension" ACI Journal, V. 82, No.3 May-June 1985

9. Labuz ,J.F. , Shah , S.P., and Dowding , C.H.,"Experimental Analysis of Crack Propagation in Concrete " International Journal of Rock Mechnics and Mining Science , Vol.22, No.2, April, 1985 PP. 85-98

10. Lubuz, J.F. Shah, S.P., and Dowding, C.H., " Post-Peak Tensile Load-Displacement Response and the Fracture Process Zone in Rock" Proc. 24th U.S. Symp. on Rock Mechanics, PP. 421-428, College Station, Texas 1983

11. Willam, K.J., Bicanic, N., and Sture, S., " Constitutive and Computational Aspects of Strain Softening and Localization in Solids " Presented at the ASME-WAM 84 symposium on Constitutive Equations , New Orleans, December, 10-14, 1984

12. Willam ,K.J., and Sture, S.," A Composite Fracture Model for Localized Failure in Cementitious Materials" Proceedings of the second Symposium on " The Interaction of Non-Nuclear Munitions with Structures", Panama City Beach, Florida, April 15-18, 1985, PP. 272-277

13. Mazars,J., " Mechanical Damage Model and Fracture of Concrete Structures" Advances in Fracture Research , Vol.4, ICFS, Cannes, France , April 1981, PP. 1499-1506

14. Wecharatana , M., and Shah, S.P., " A Model for Predicting Fracture Resistance of Fiber Reinforced Concrete" Cement and Concrete Research, Vol. 13, PP.819-

829, 1983

15. Visalvanich, K., and Naaman,A.E., " Fracture Model for Fiber Reinforced Concrete" ACI Journal, Vol. 80, No.2, 1983, PP. 128-138
16. Wecharatana, M., and Shah, S.P. " Slow Crack Growth in Cement Composites " Proceedings of ASCE, Journal of Structural Division, Vol. 108, No.ST6, June 1982, PP. 1400-1413
17. Wecharatana, M., and Shah, S.P. ,"Double Torsion Tests for Studying Slow Crack Growth of Portland Cement Mortar" Cement and Concrete Research , Vol. 10, No.6, Nov. 1980
18. Loland, K.E., "Continuous Damage Model for Load Response Estimate of Concrete " Cement and Concrete Research , Vol. 10, 1980, PP. 395-402
19. Janson, J., and Hult, J., " Fracture Mechanics and Damage Mechanics : a Combined Approch" Journal de Mechaniquee, Vol. 1, No.1, 1977,PP. 69-84
20. Swartz, S.E., Hu, K.K., and Jones, G.L., " Compliance Monitoring of Crack Growth in Concrete" Proceedings of ASCE, Journal of Eng. Mech. Div., Vol. 104, No. EM4, August 1978, PP. 789-800
21. Loland, K.E., and Gjorv, O.E., " Ductility of Concrete and Tensile Behavior " presented at the ASCE Annual Convention , Hollywood , Florida , October 27-31, 1980
22. "Standard Method of Test for Plane-Strain Fracture

Toughness of Metallic Materials " ASTM Designation E-399 Part 10 , ASTM Annual Standard .

APPENDIX A

LOAD DISPLACEMENT CURVES

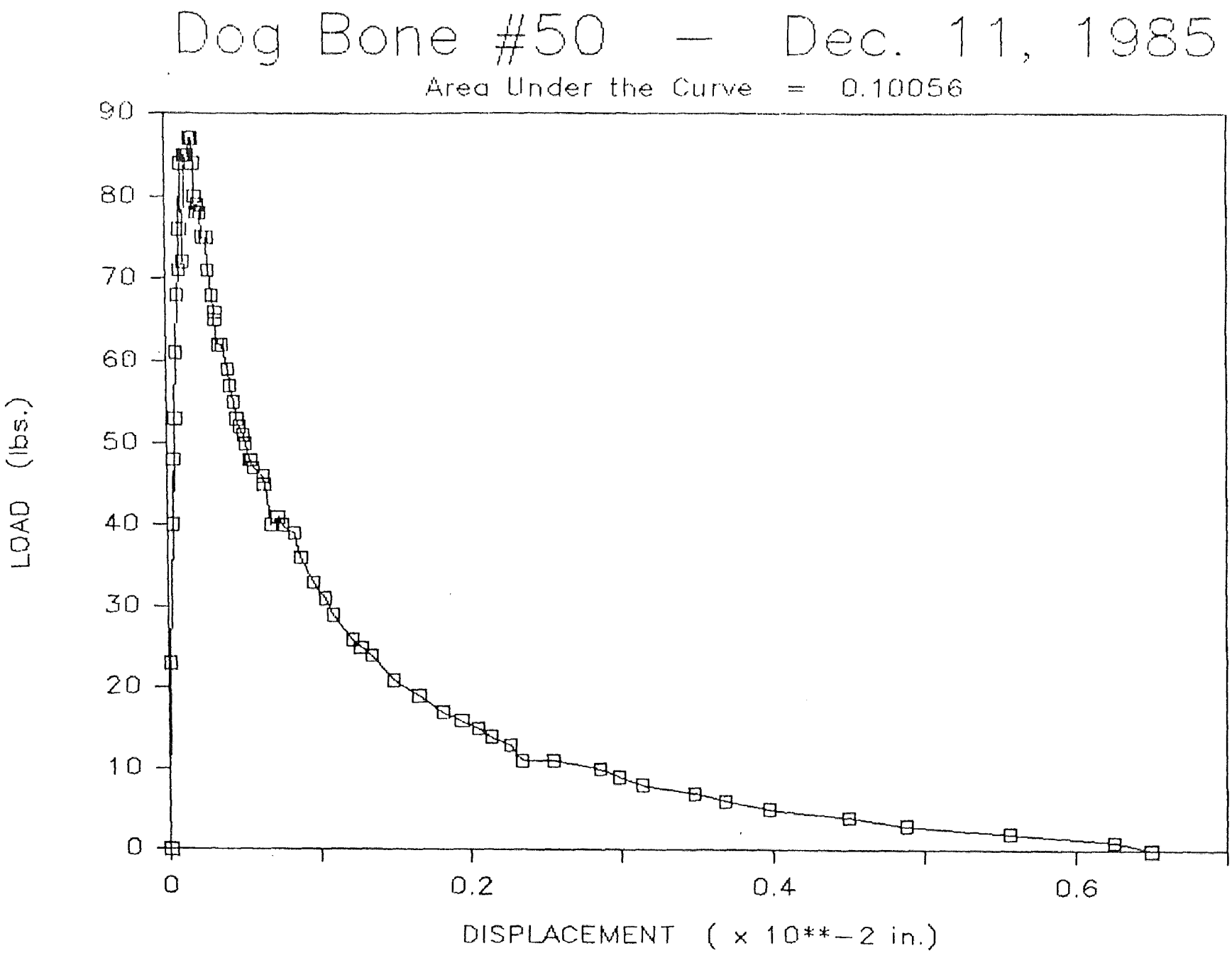
Dog Bone #50 — Dec. 11, 1985
Area Under the Curve = 0.10056
90
80
70
60
50
40
30
20
10
0
LOAD (lbs.)
0
0.2
0.4
0.6
DISPLACEMENT (x 10**-2 in.)

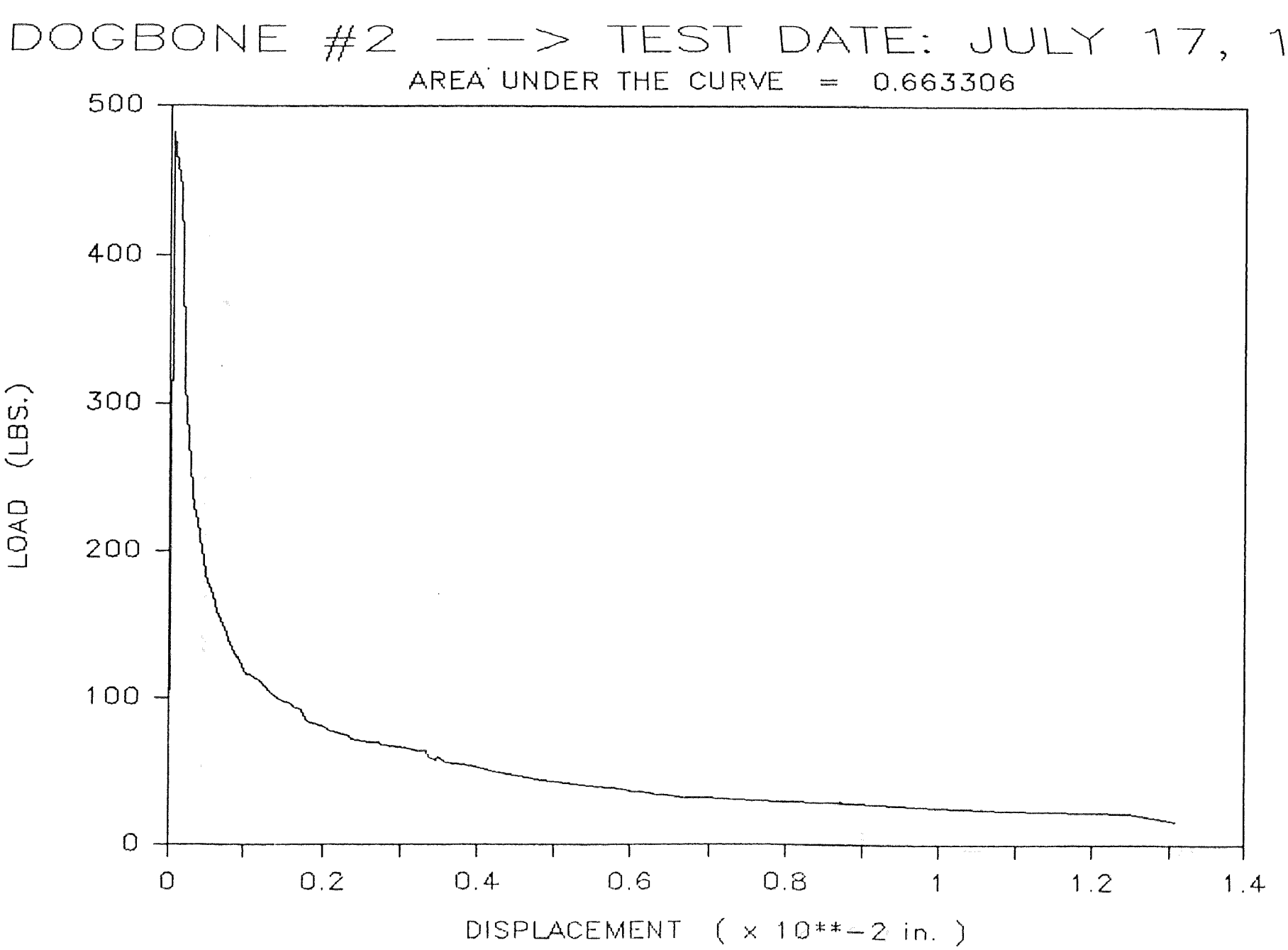
DOGBONE #2 ---> TEST DATE: JULY 17, 19
AREA UNDER THE CURVE = 0.663306
500
400
300
200
100
0
LOAD (LBS.)
0
0.2
0.4
0.6
0.8
1
1.2
1.4
DISPLACEMENT (x 10**-2 in.)

Dog Bone #9 — Aug. 19, 1985

Area Under the Curve = 0.330609

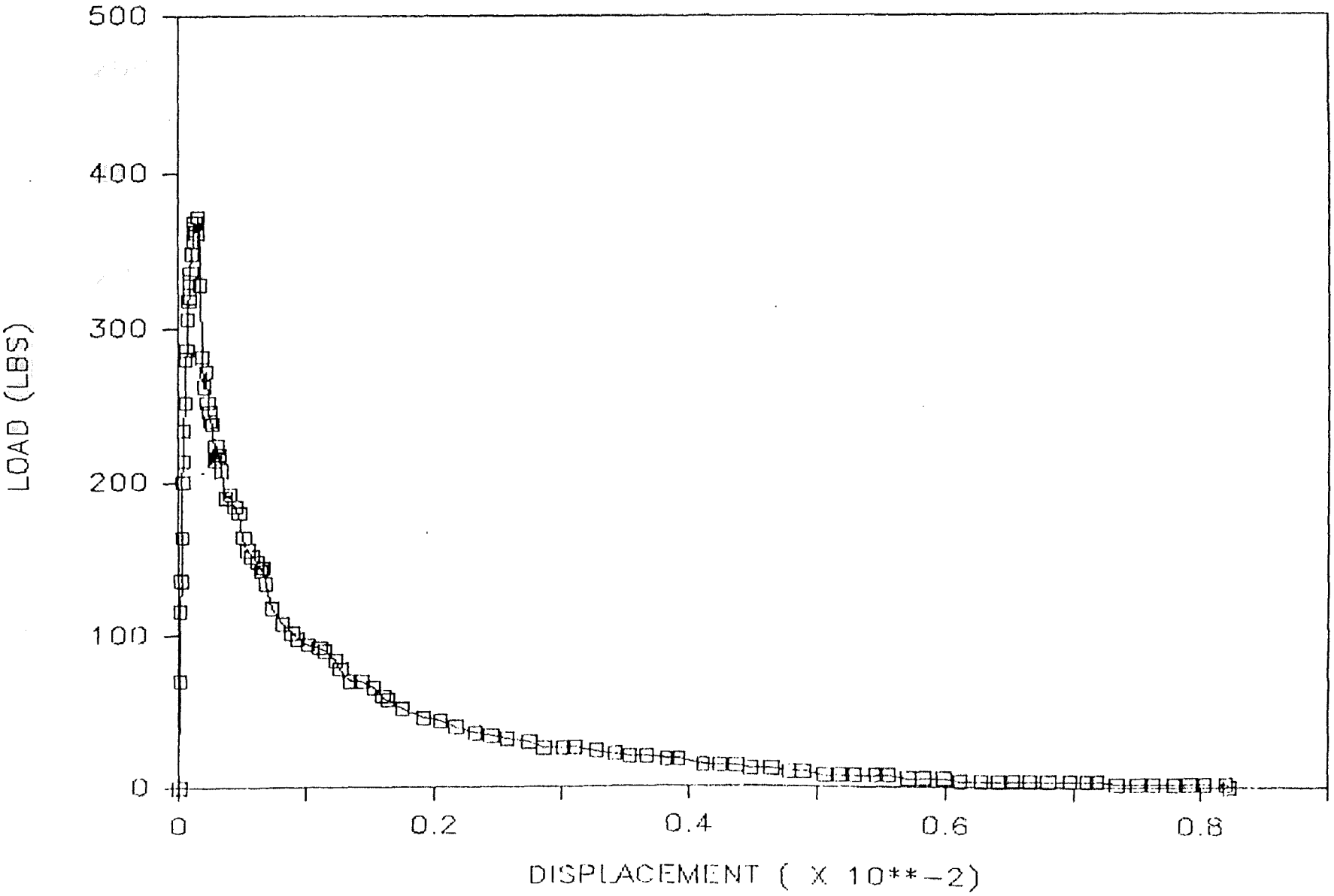

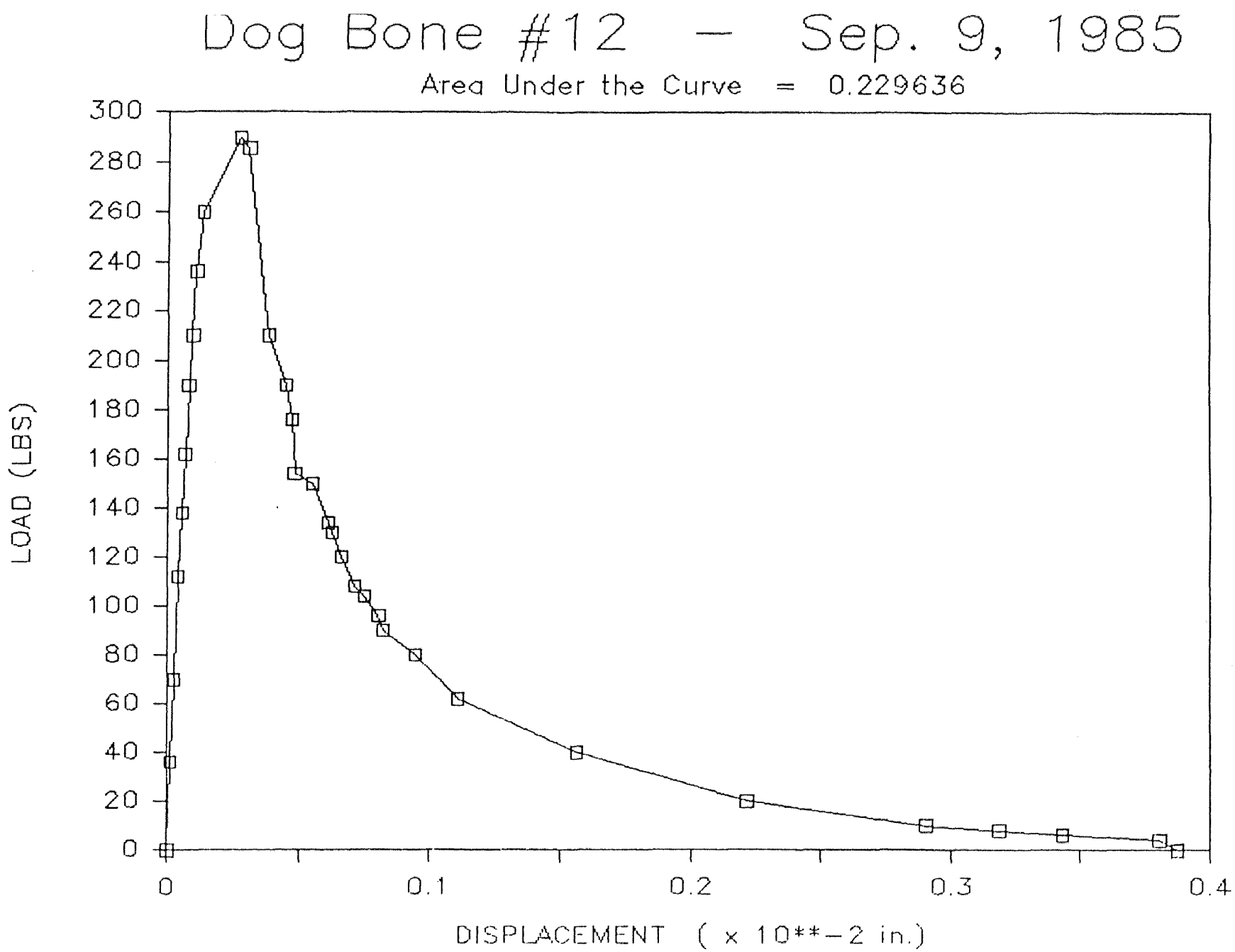
Dog Bone #12 — Sep. 9, 1985
Area Under the Curve = 0.229636
LOAD (LBS)
300
280
260
240
220
200
180
160
140
120
100
80
60
40
20
0
0
0.1
0.2
0.3
0.4
DISPLACEMENT (x 10**-2 in.)

Dogbone #68 ---> Test Date 3-4-86

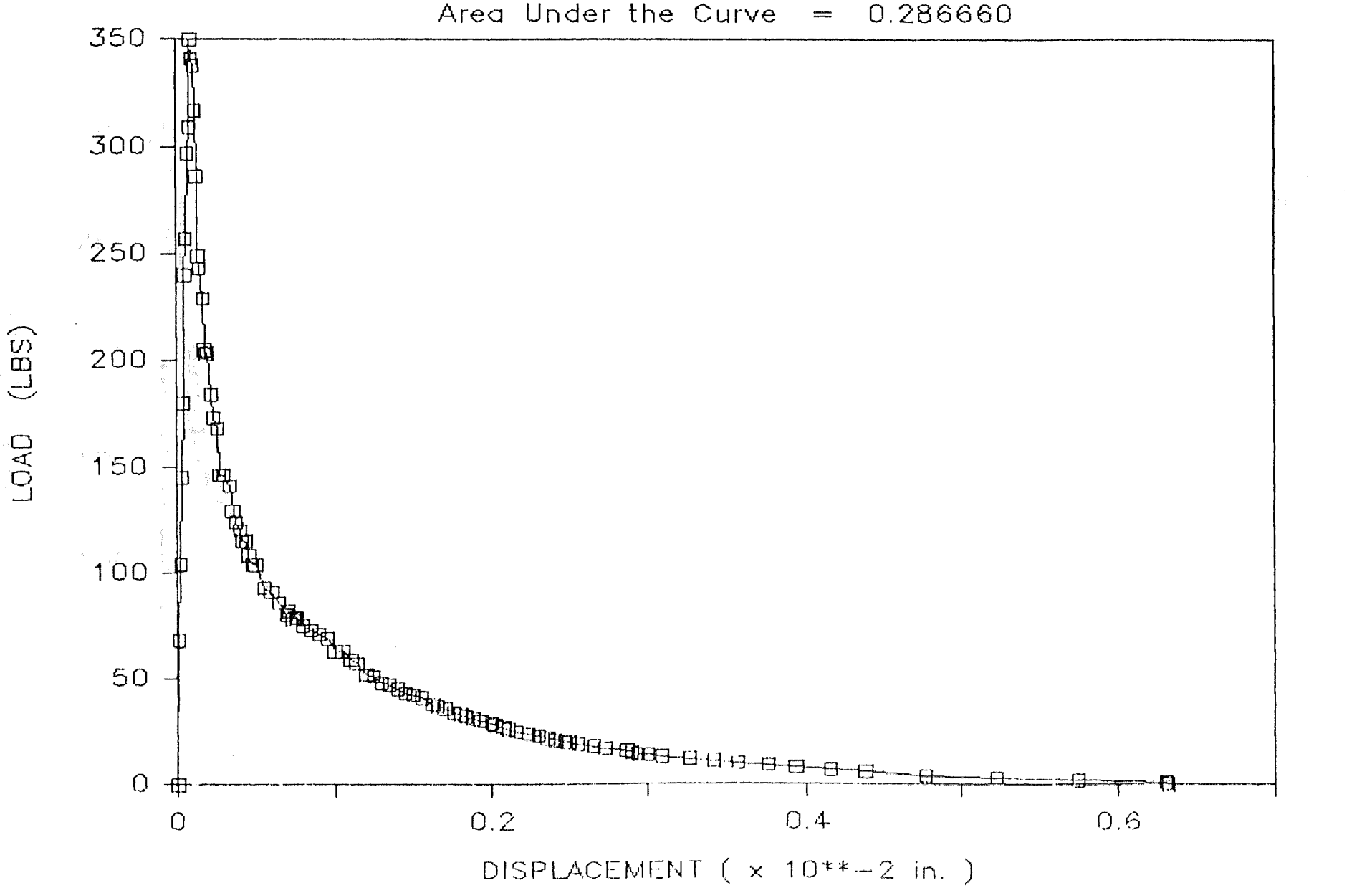

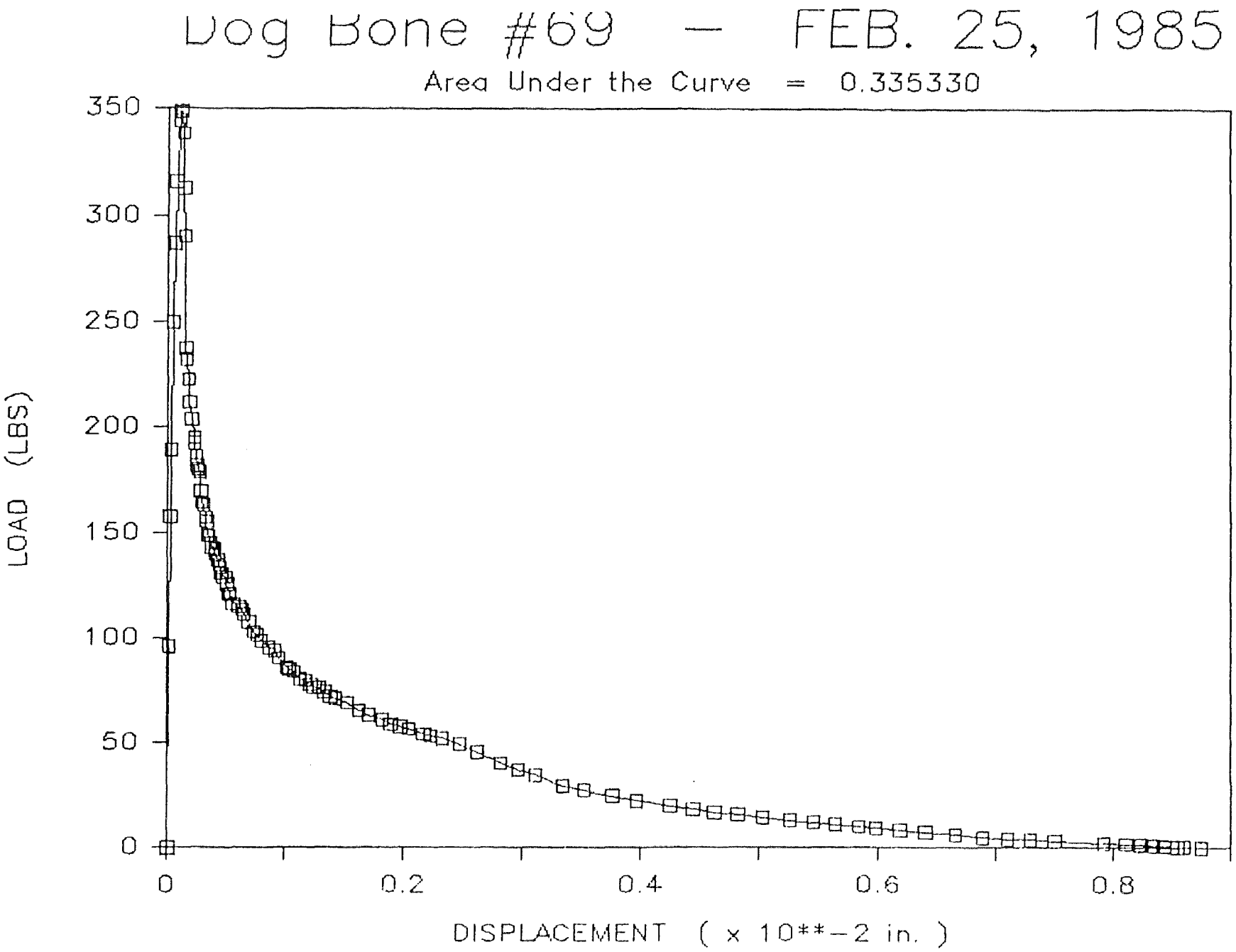
Dog Bone #69 — FEB. 25, 1985
Area Under the Curve = 0.335330
LOAD (LBS)
350
300
250
200
150
100
50
0
0
0.2
0.4
0.6
0.8
DISPLACEMENT (x 10**-2 in.)

Dogbone #70 --> Test Date: 3 - 26 - 8

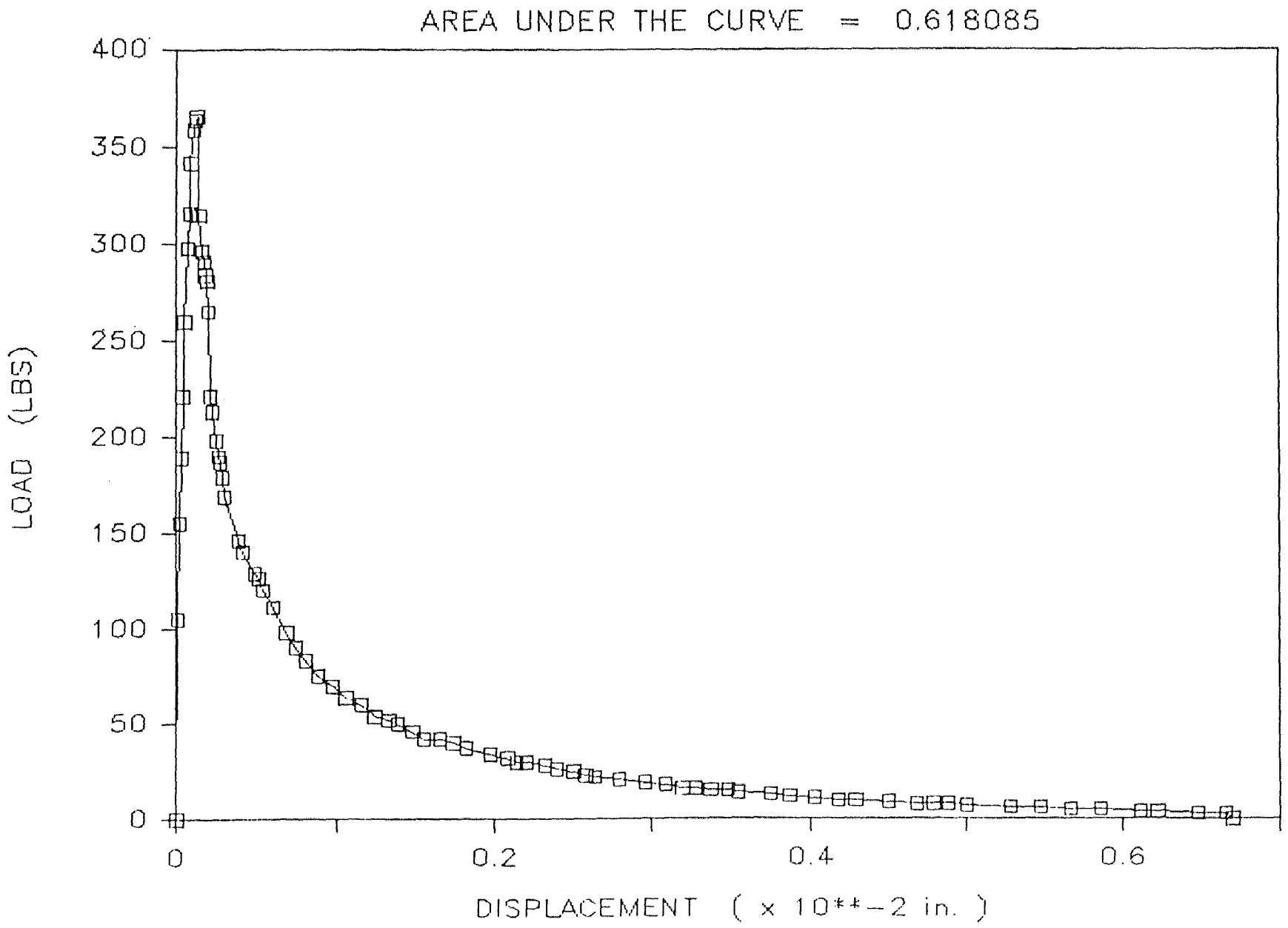

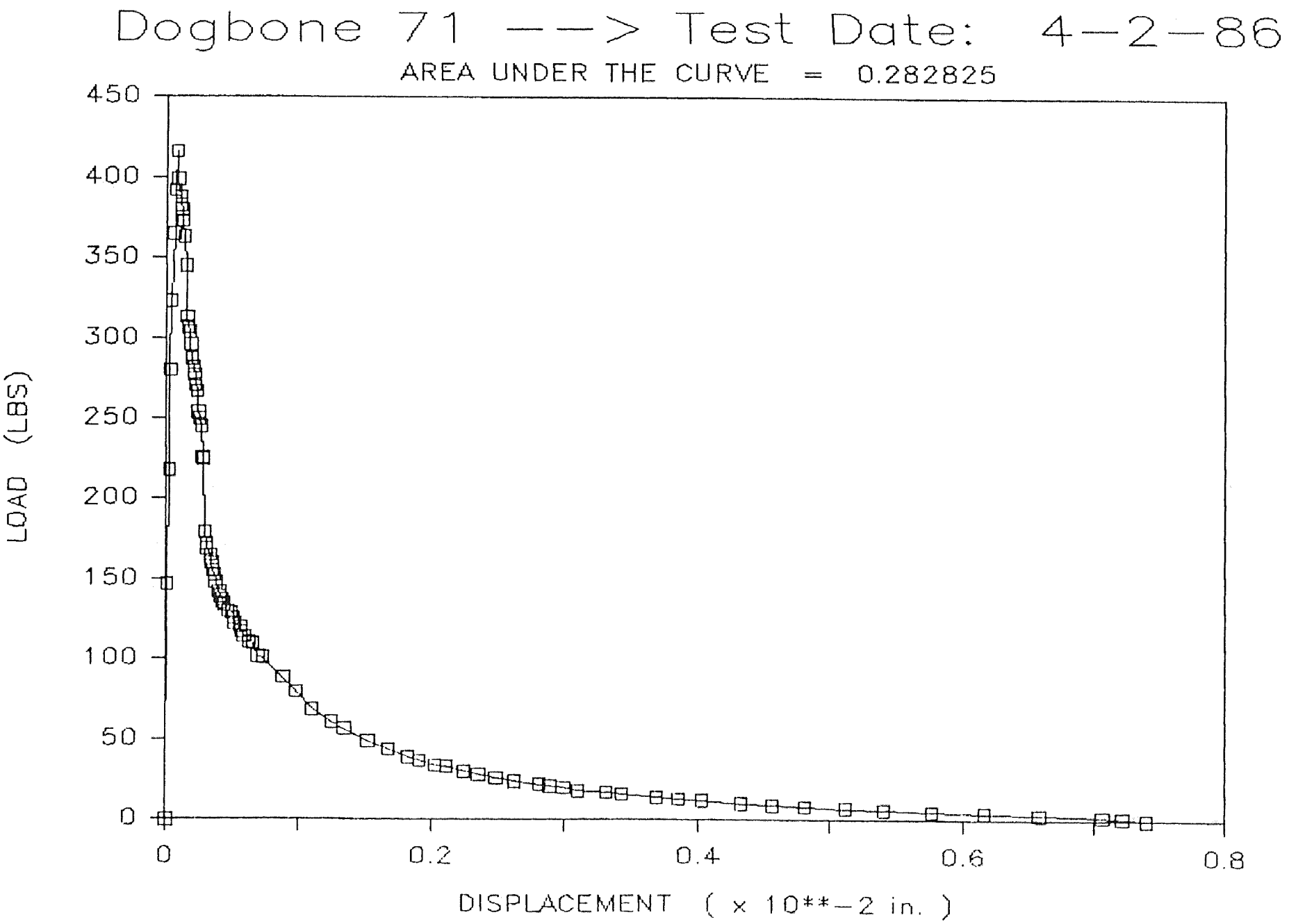
Dogbone 71 --> Test Date: 4-2-86
AREA UNDER THE CURVE = 0.282825
450
400
350
300
250
200
150
100
50
0
LOAD (LBS)
0
0.2
0.4
0.6
0.8
DISPLACEMENT (x 10**-2 in.)

Dog Bone #23 — Sep. 11, 1985

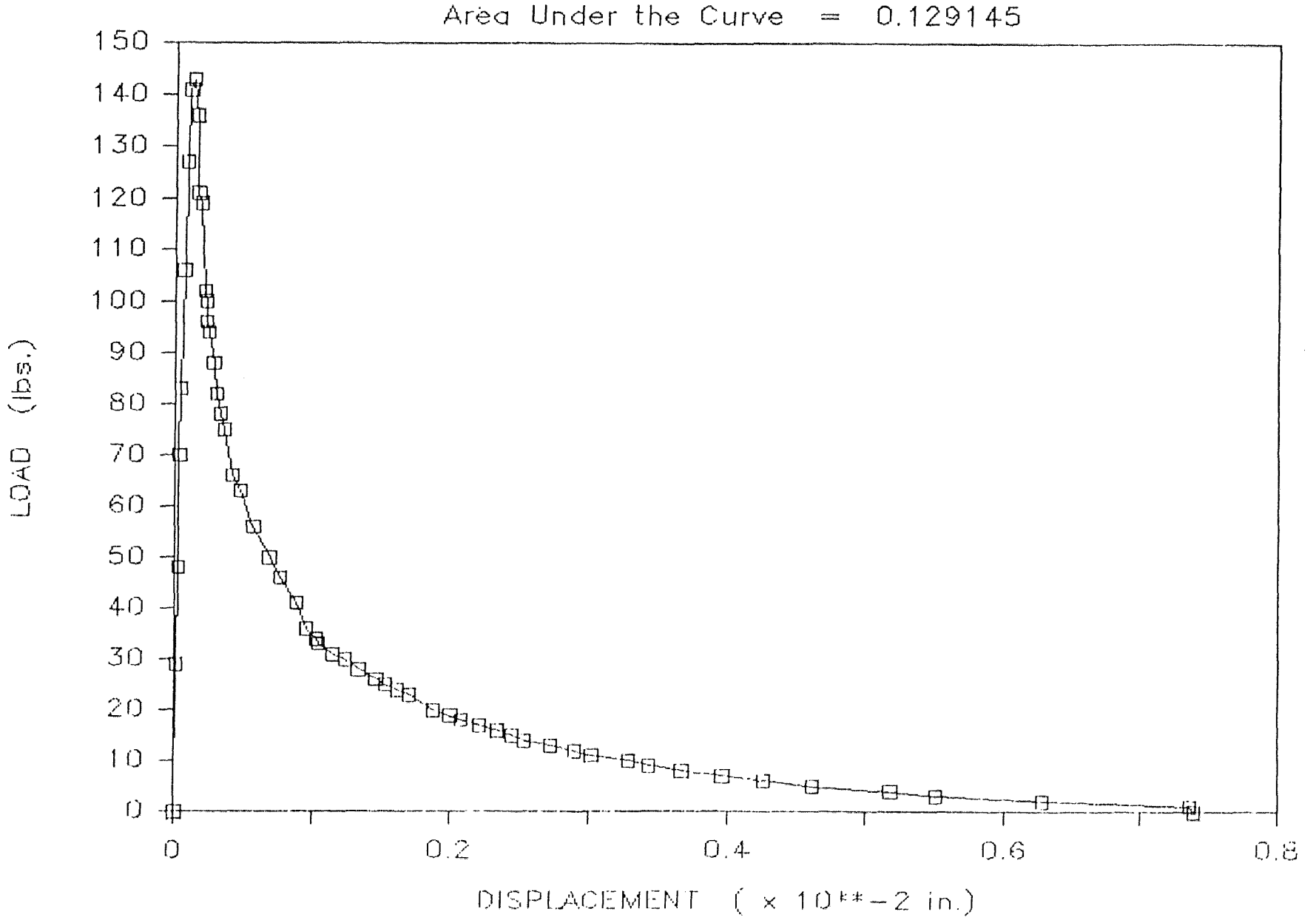

Dog Bone #38 — Oct. 15, 1985

Area Under the Curve = 0.179676

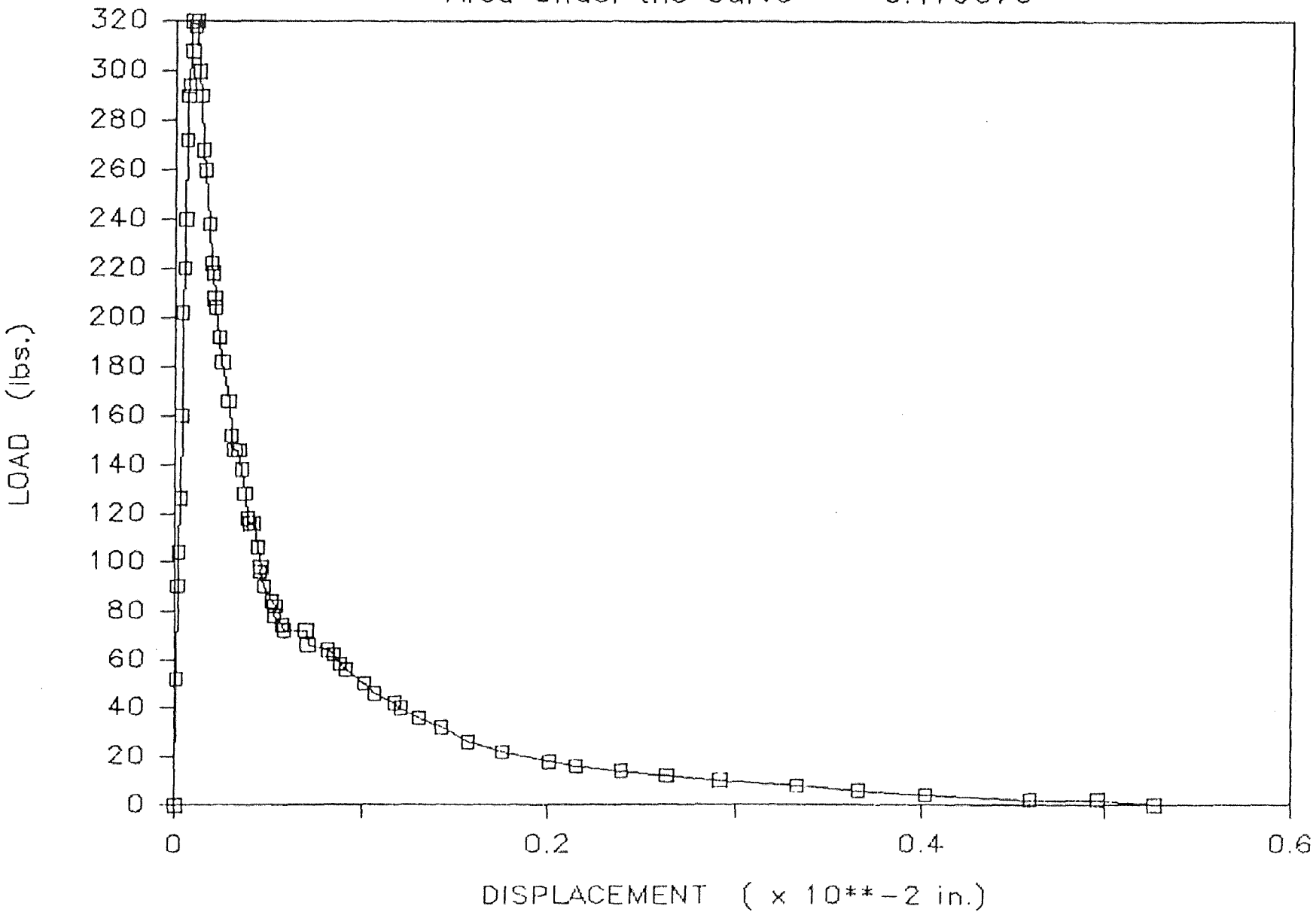

Dog Bone #39 — Oct. 15, 1985

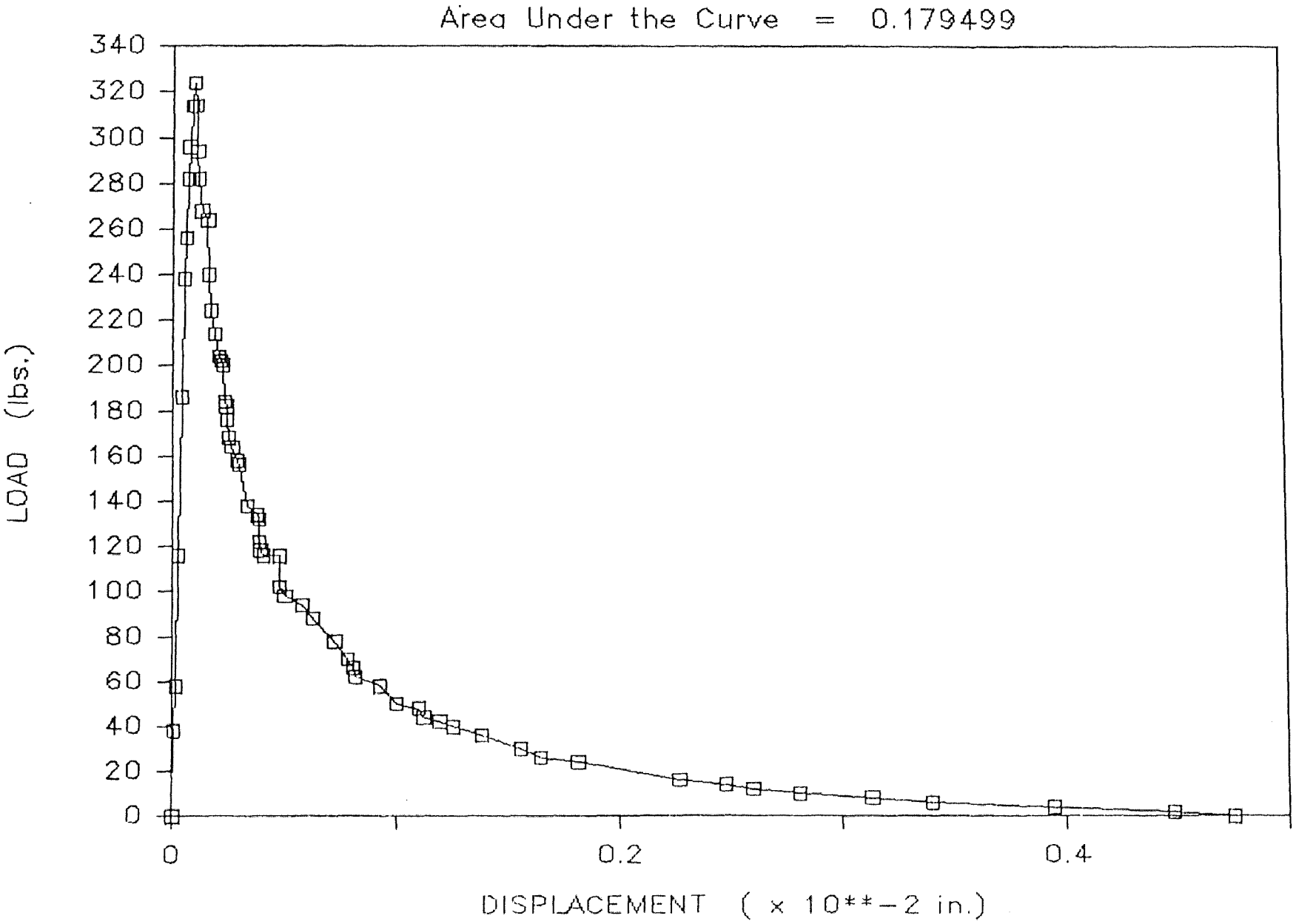

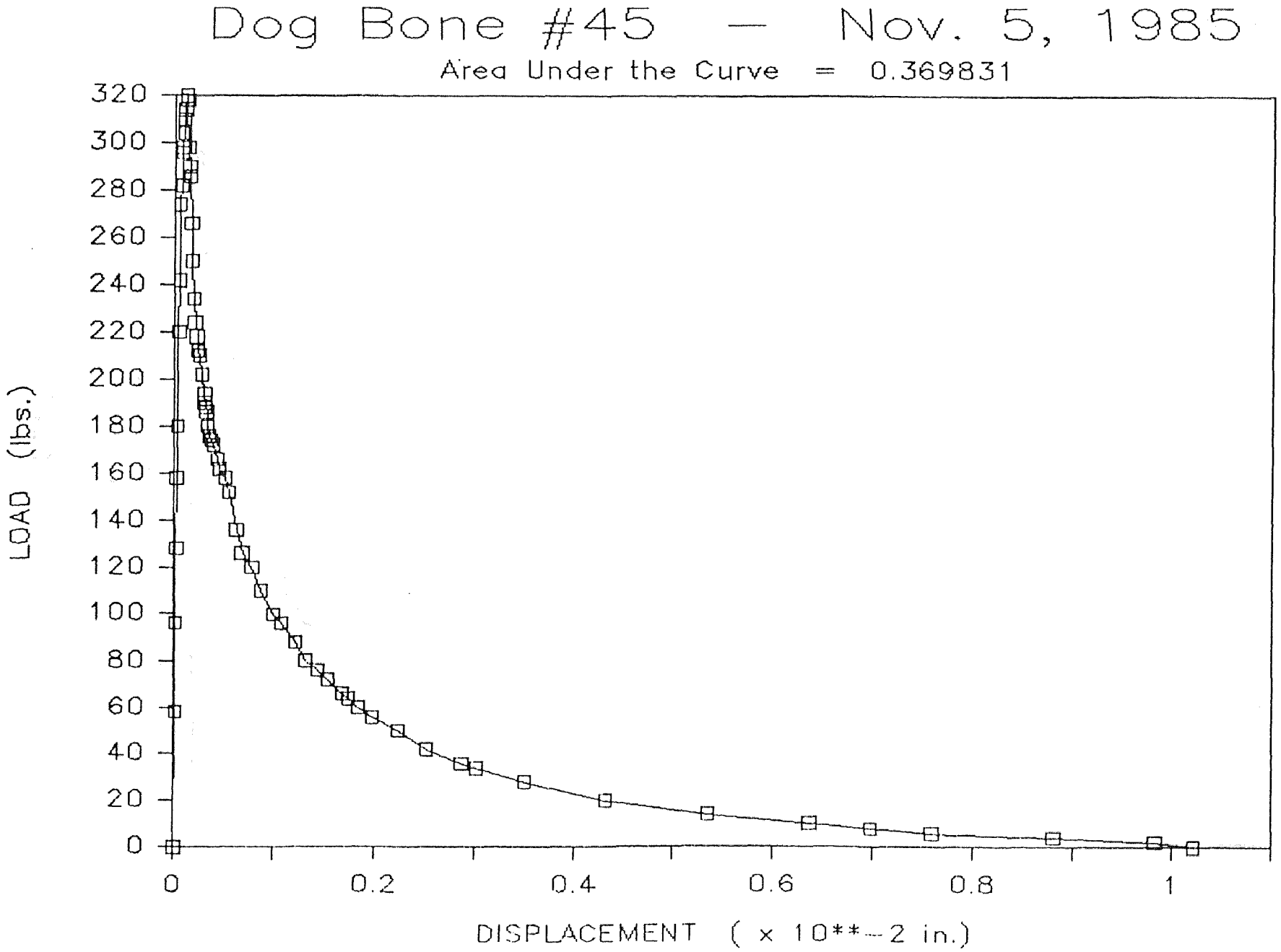
Dog Bone #45 — Nov. 5, 1985
Area Under the Curve = 0.369831
LOAD (lbs.)
320
300
280
260
240
220
200
180
160
140
120
100
80
60
40
20
0
0
0.2
0.4
0.6
0.8
1
DISPLACEMENT (x 10**-2 in.)

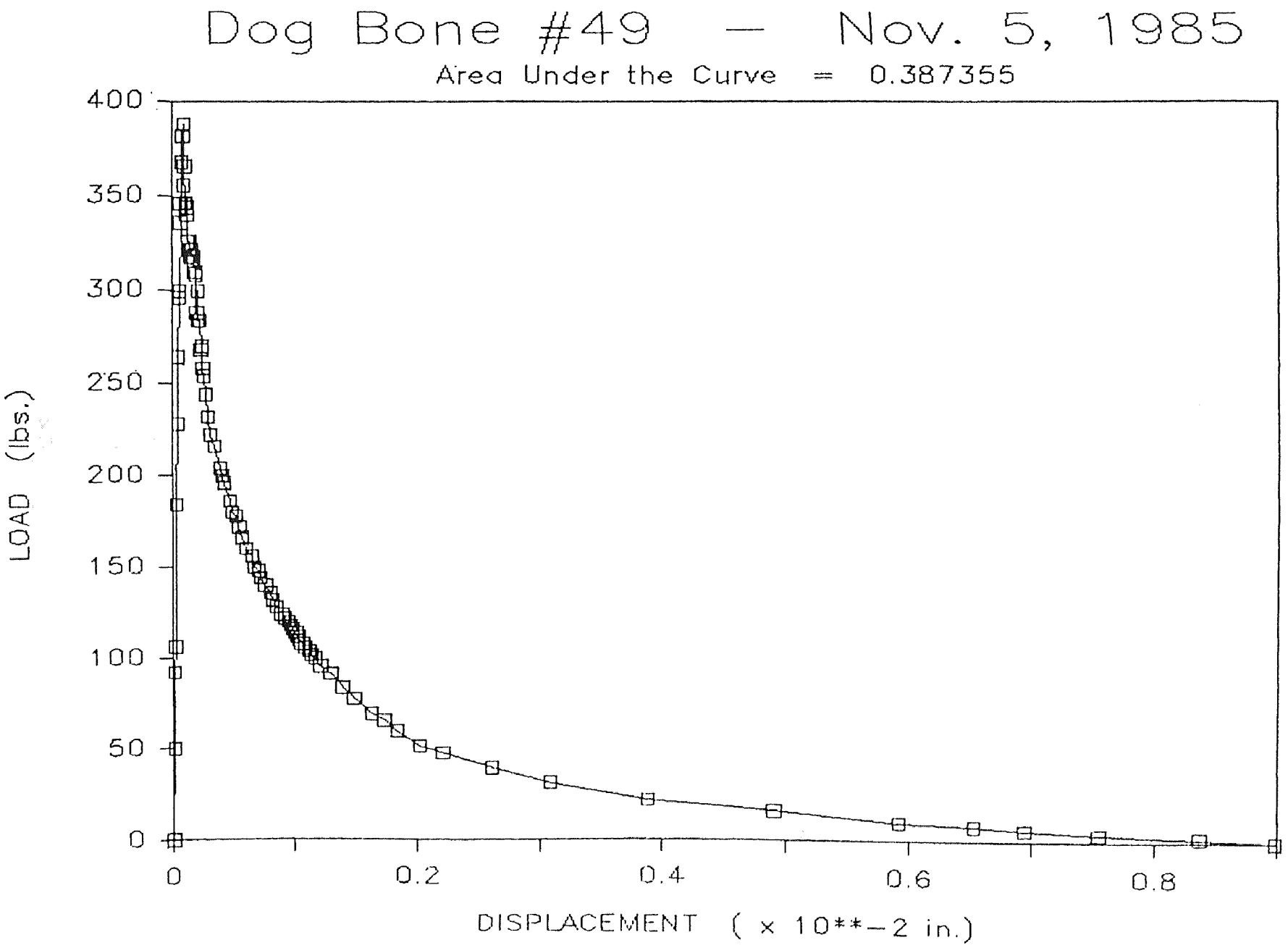
Dog Bone #49 — Nov. 5, 1985
Area Under the Curve = 0.387355
LOAD (lbs.)
400
350
300
250
200
150
100
50
0
0
0.2
0.4
0.6
0.8
DISPLACEMENT (x 10**-2 in.)

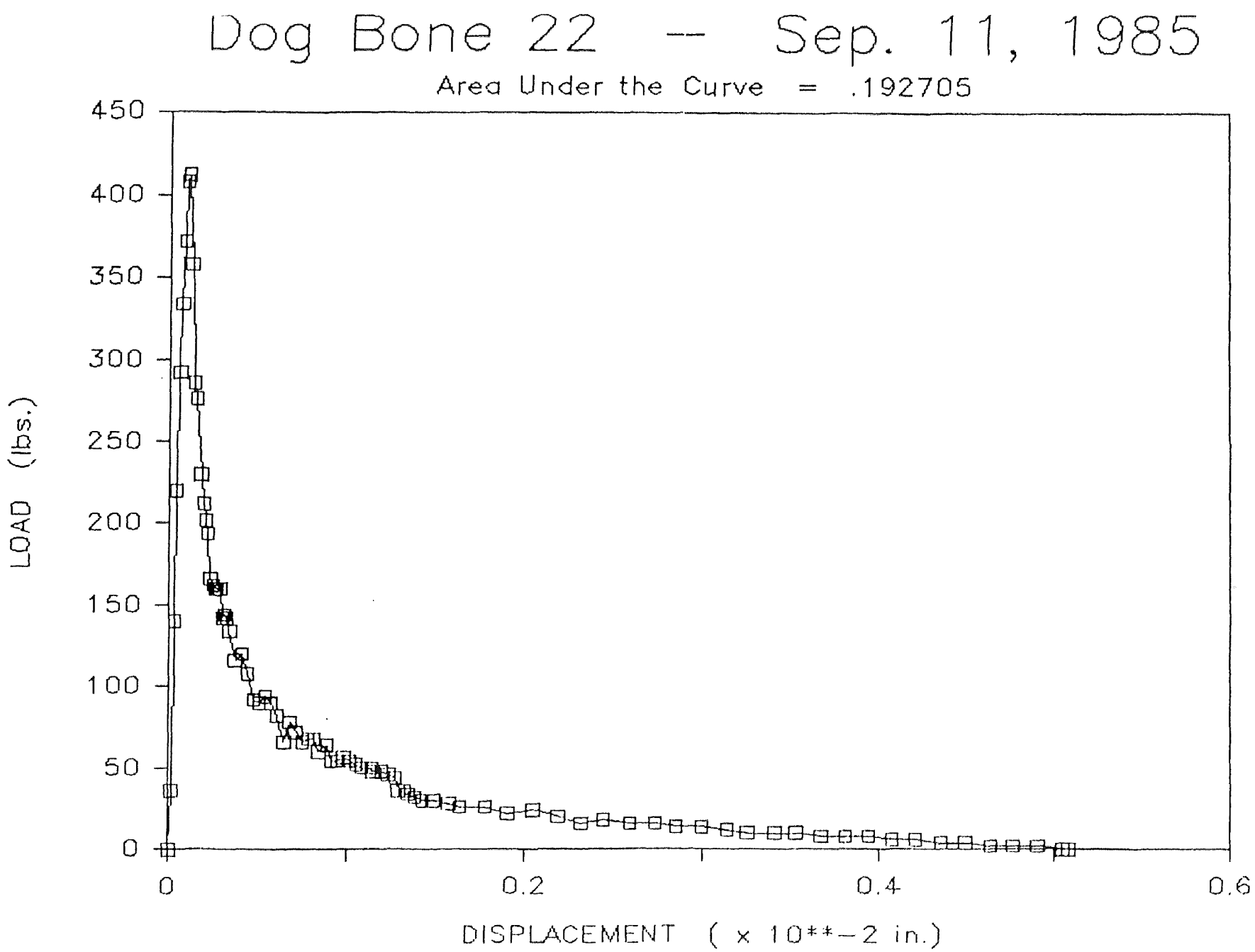
Dog Bone 22 -- Sep. 11, 1985
Area Under the Curve = .192705
LOAD (lbs.)
450
400
350
300
250
200
150
100
50
0
0
0.2
0.4
0.6
DISPLACEMENT (x 10**-2 in.)

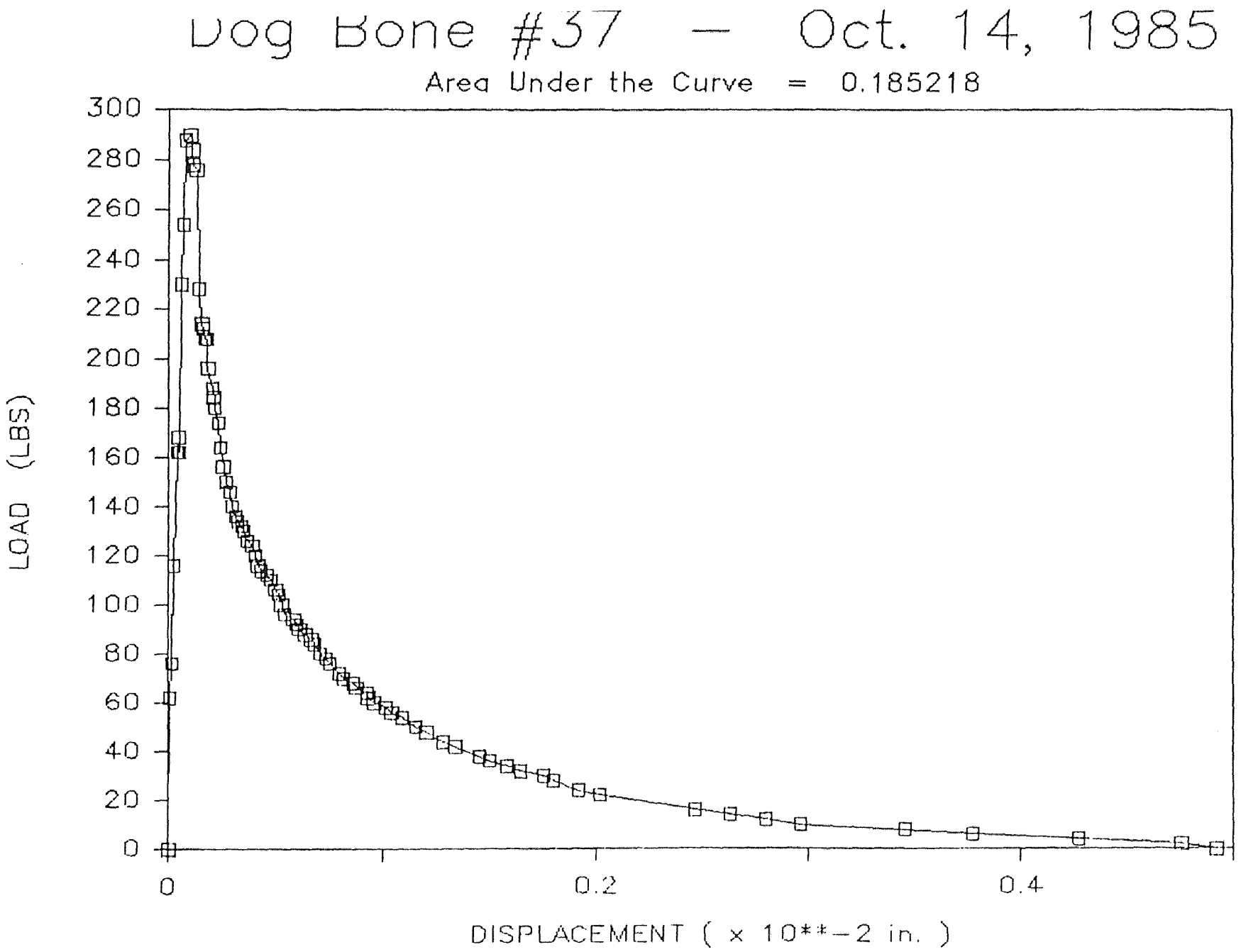
Dog Bone #37 — Oct. 14, 1985
Area Under the Curve = 0.185218
LOAD (LBS)
300
280
260
240
220
200
180
160
140
120
100
80
60
40
20
0
0
0.2
0.4
DISPLACEMENT (x 10**-2 in.)

Dog Bone #35 – Oct. 14, 1985

Area Under the Curve = 0.297051

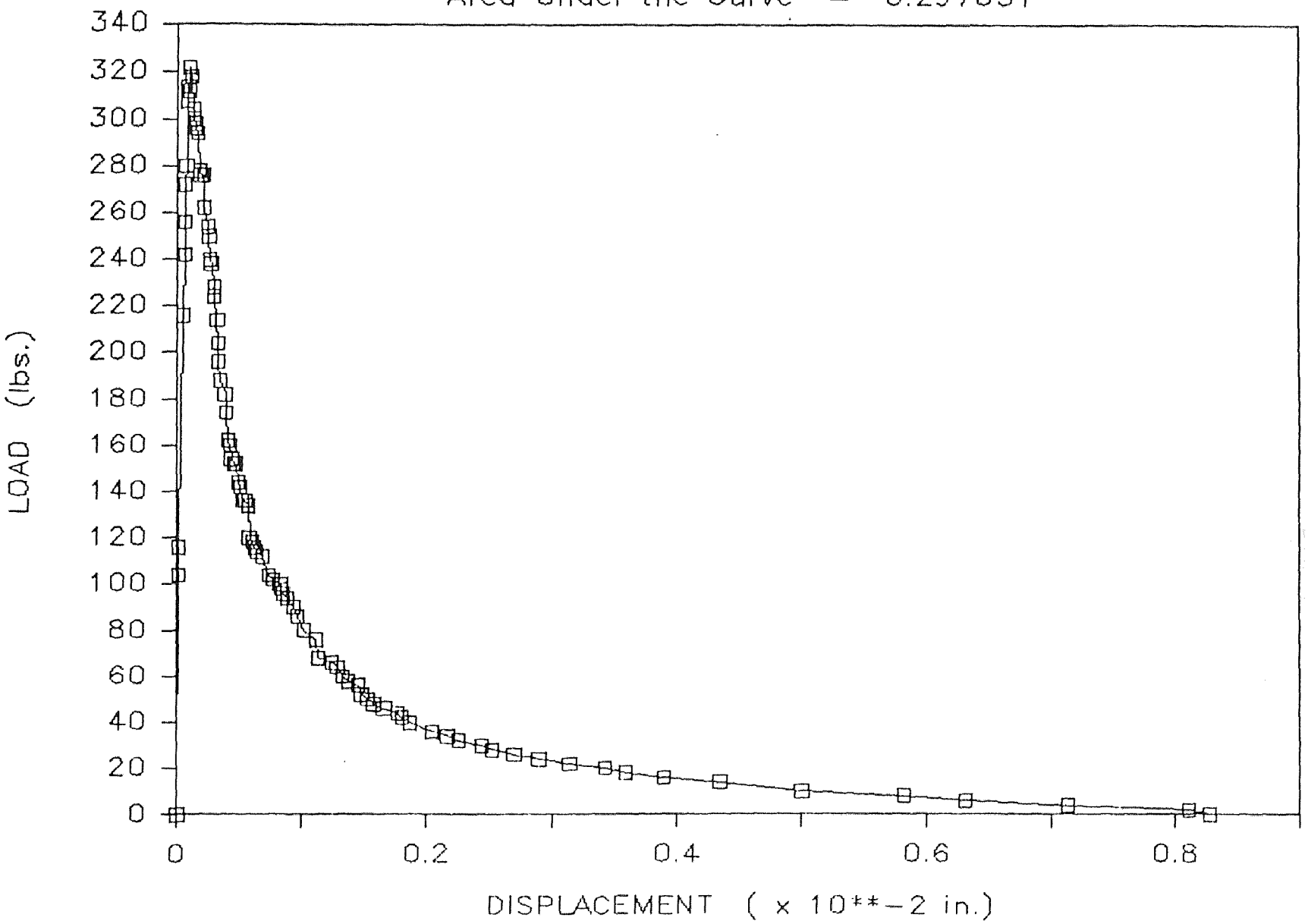

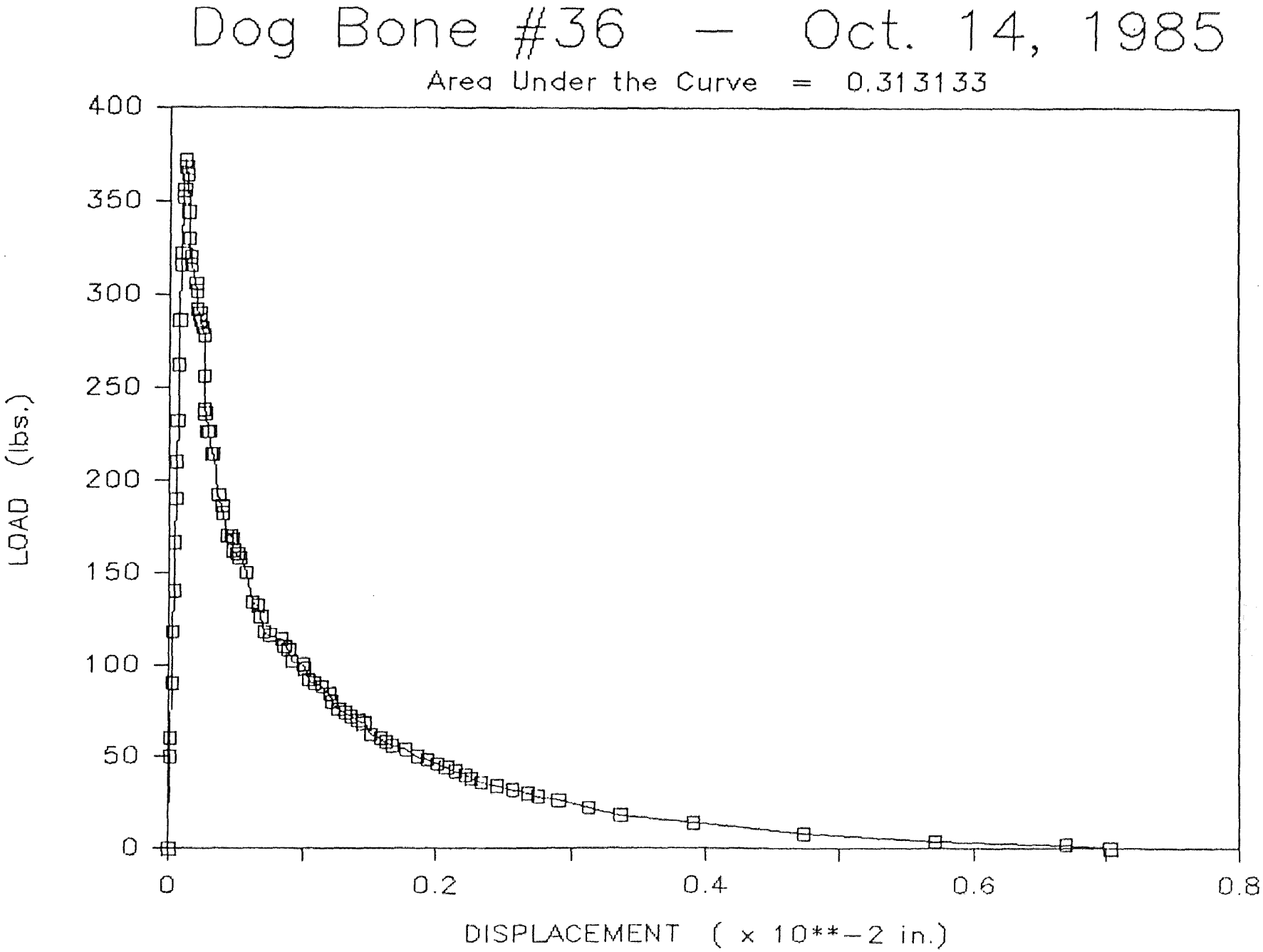
Dog Bone #36 — Oct. 14, 1985
Area Under the Curve = 0.313133
400
350
300
250
200
150
100
50
0
LOAD (lbs.)
0
0.2
0.4
0.6
0.8
DISPLACEMENT (x 10**-2 in.)

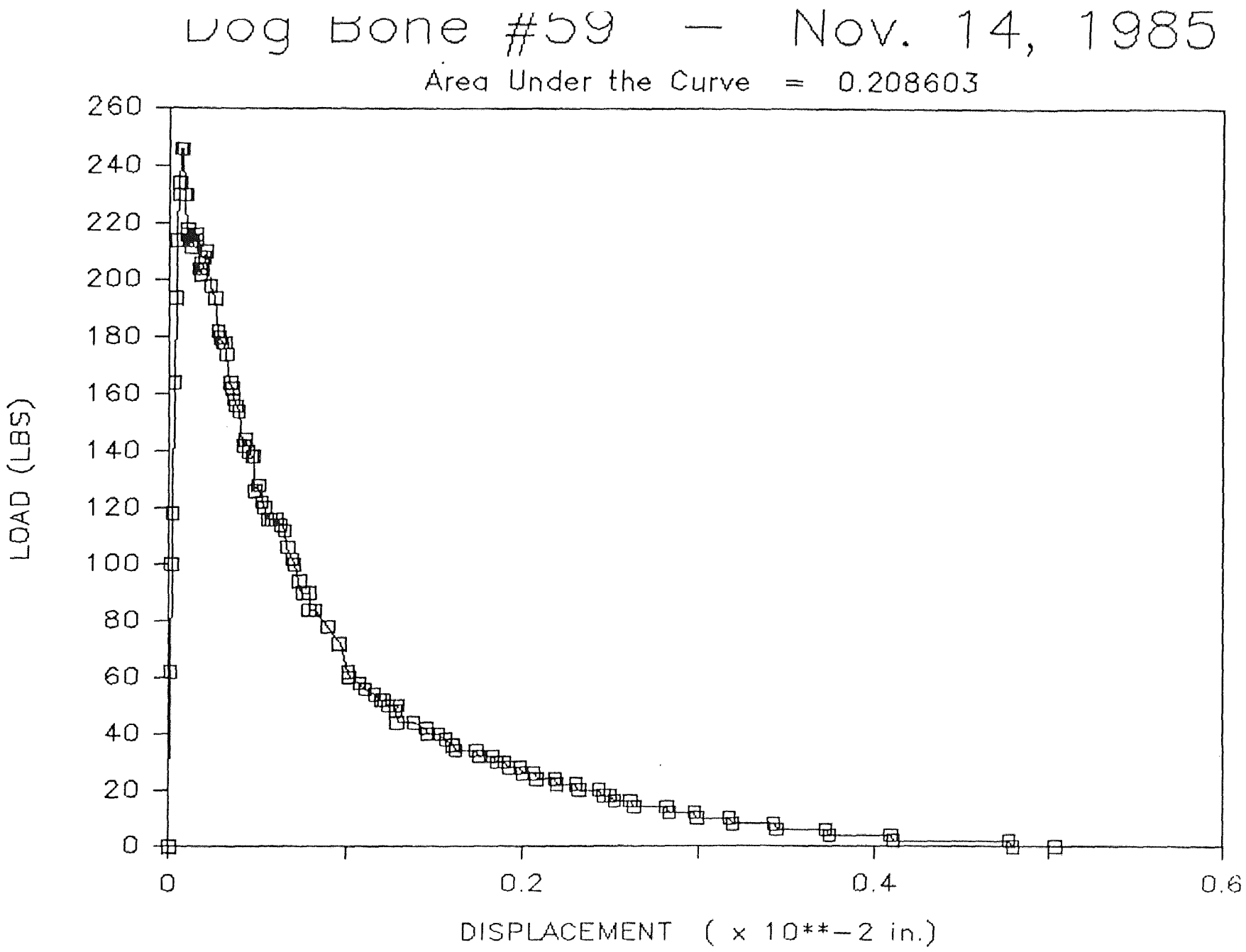
Dog Bone #59 — Nov. 14, 1985
Area Under the Curve = 0.208603
LOAD (LBS)
260
240
220
200
180
160
140
120
100
80
60
40
20
0
0
0.2
0.4
0.6
DISPLACEMENT (x 10**-2 in.)

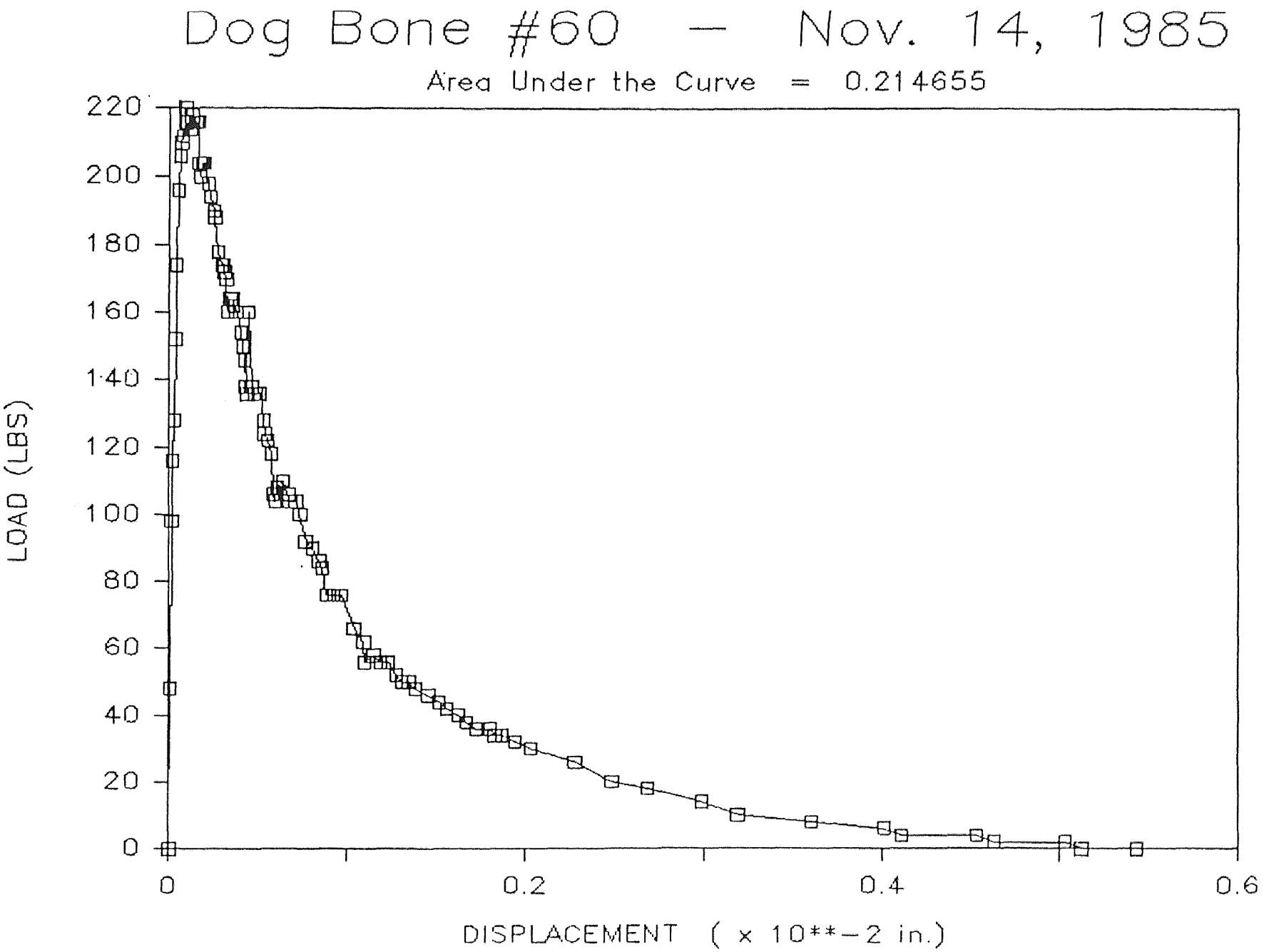
Dog Bone #60 — Nov. 14, 1985
Area Under the Curve = 0.214655
LOAD (LBS)
220
200
180
160
140
120
100
80
60
40
20
0
0
0.2
0.4
0.6
DISPLACEMENT (x 10**-2 in.)

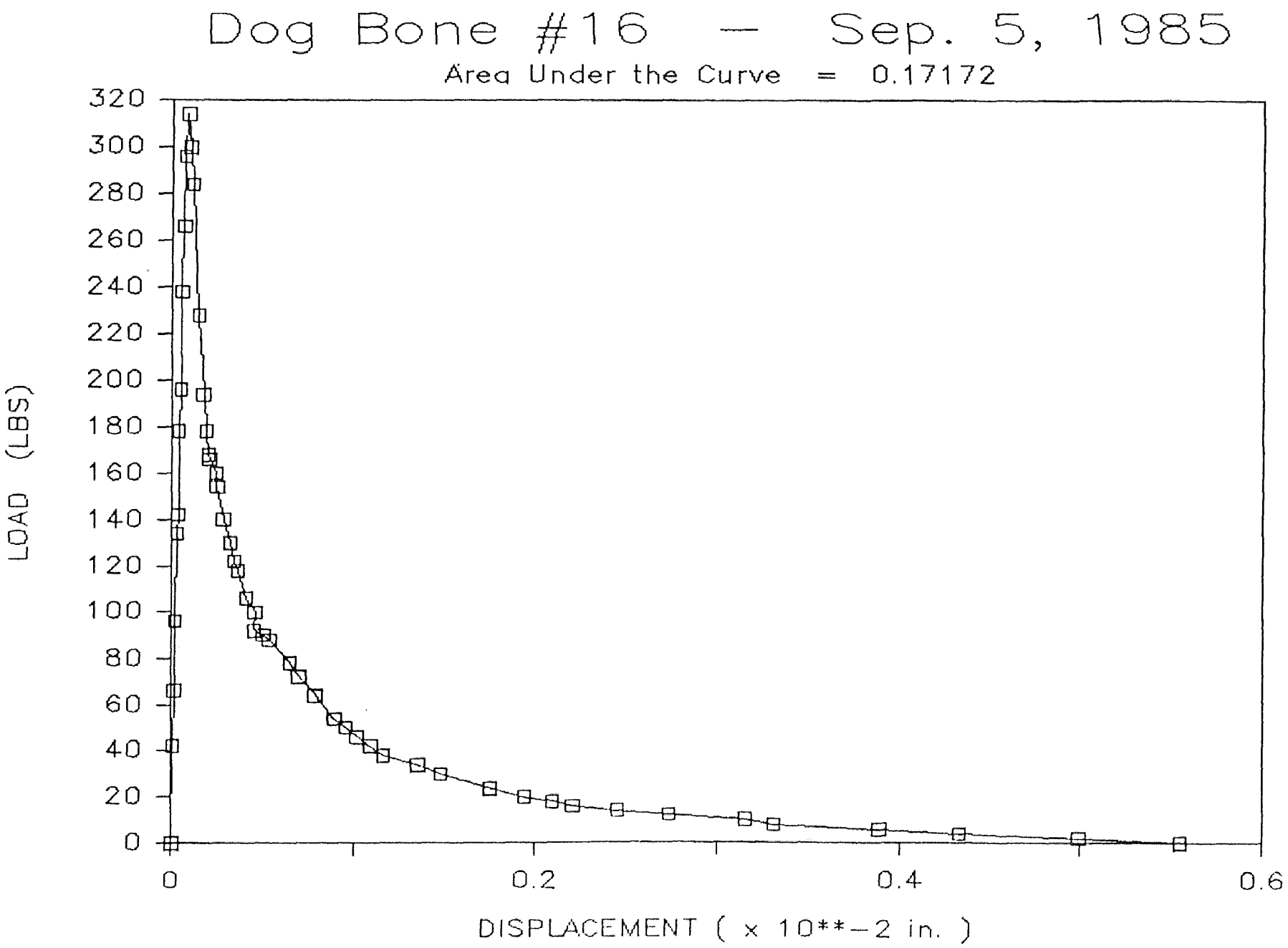
Dog Bone #16 — Sep. 5, 1985
Area Under the Curve = 0.17172
LOAD (LBS)
320
300
280
260
240
220
200
180
160
140
120
100
80
60
40
20
0
0
0.2
0.4
0.6
DISPLACEMENT (x 10**-2 in.)

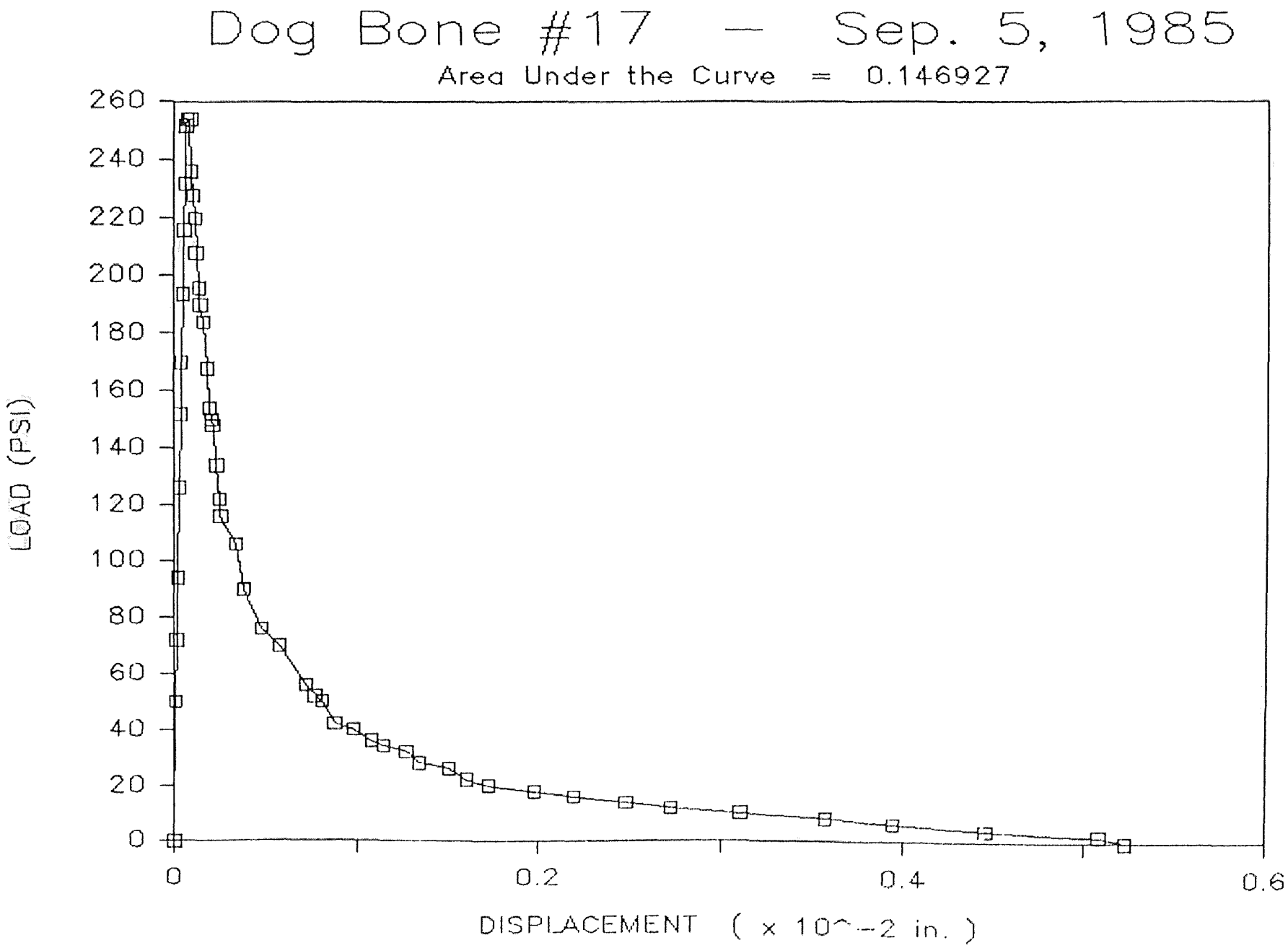
Dog Bone #17 — Sep. 5, 1985
Area Under the Curve = 0.146927
LOAD (PSI)
260
240
220
200
180
160
140
120
100
80
60
40
20
0
0
0.2
0.4
0.6
DISPLACEMENT (x 10^-2 in.)

Dog Bone #29 — Sep. 18, 1985

Area Under the Curve = 0.173753

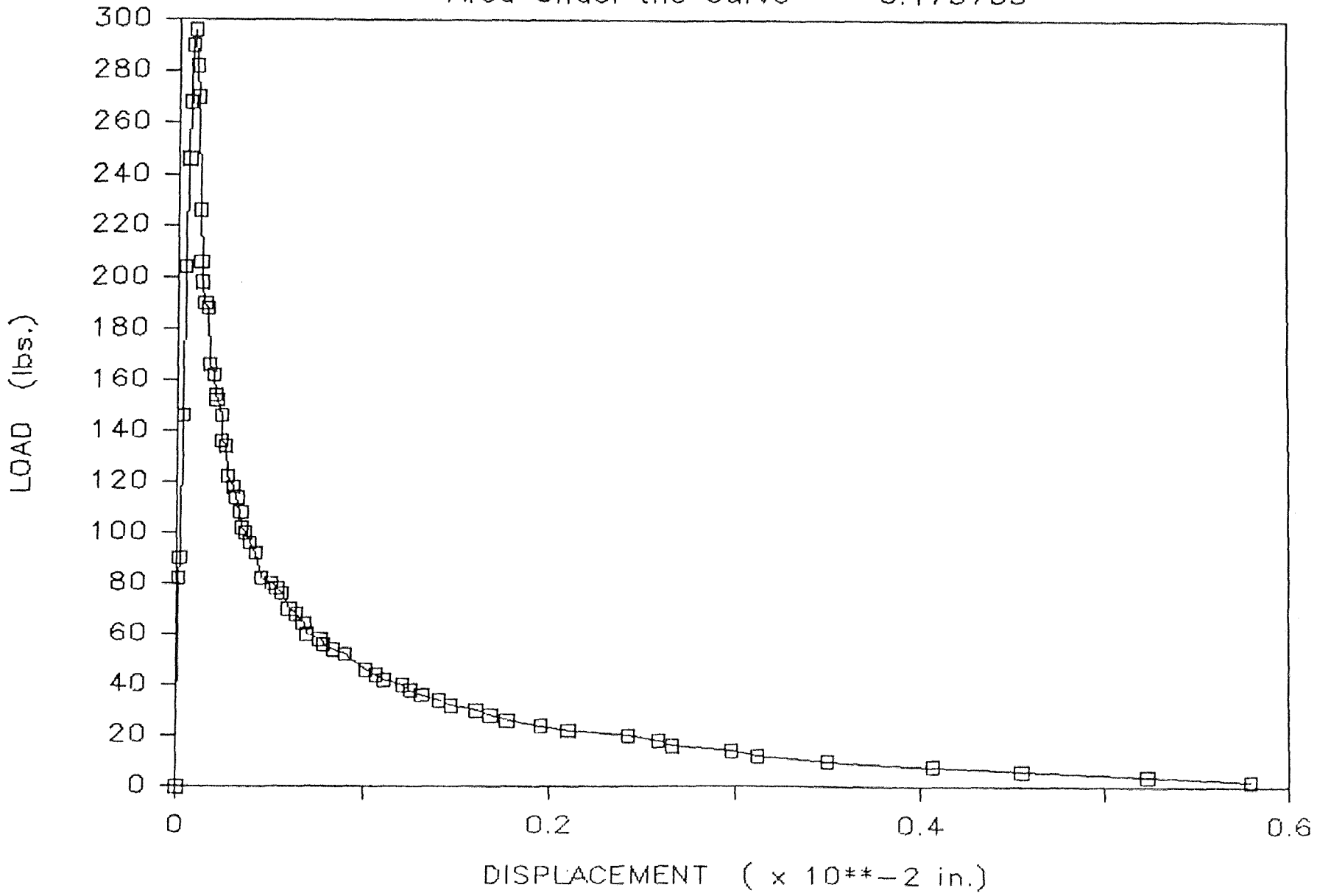

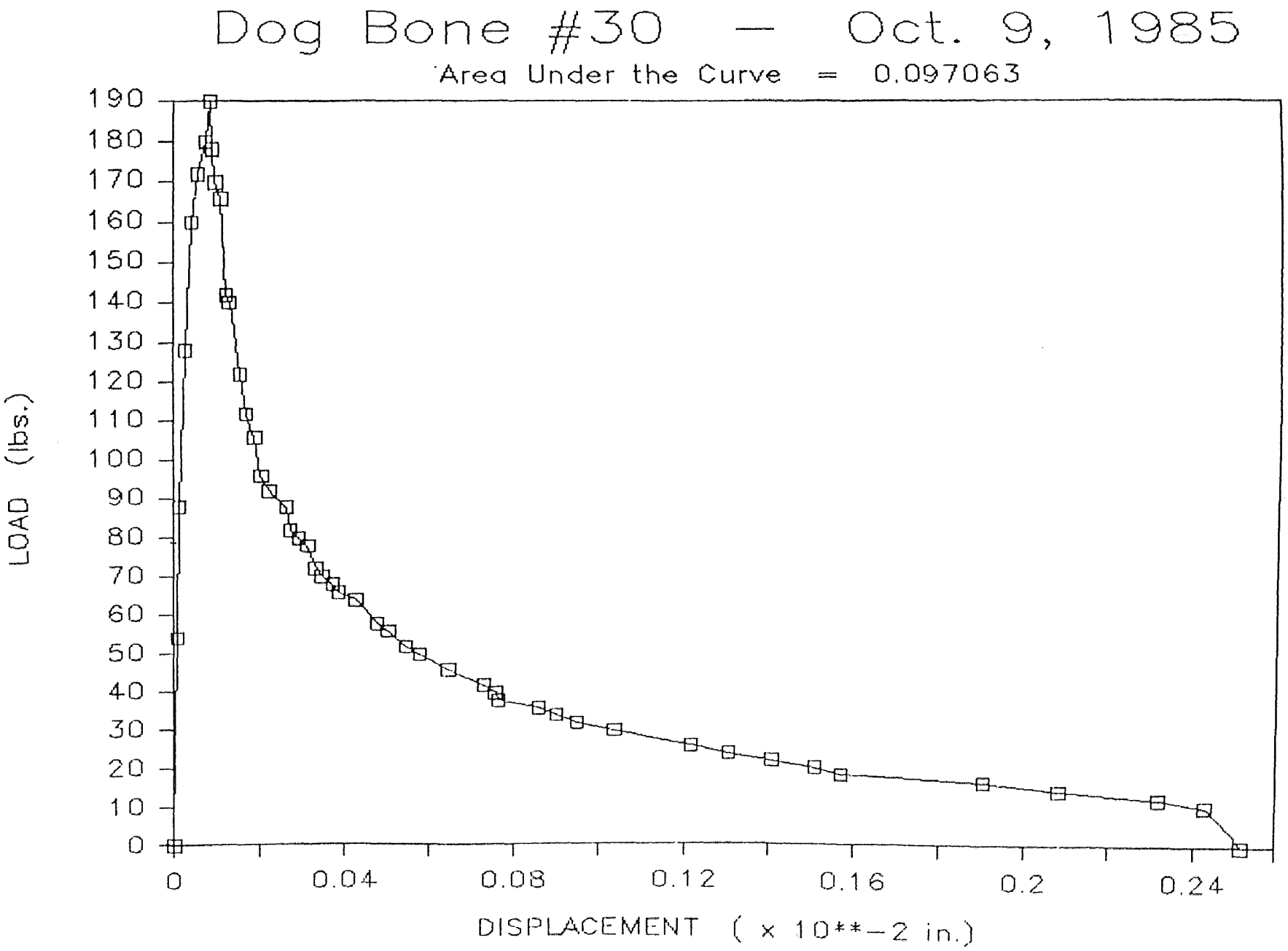
Dog Bone #30 — Oct. 9, 1985
Area Under the Curve = 0.097063
LOAD (lbs.)
190
180
170
160
150
140
130
120
110
100
90
80
70
60
50
40
30
20
10
0
0
0.04
0.08
0.12
0.16
0.2
0.24
DISPLACEMENT (x 10**-2 in.)

Dog Bone #43 — Nov. 14, 1985

Area Under the Curve = 0.166668

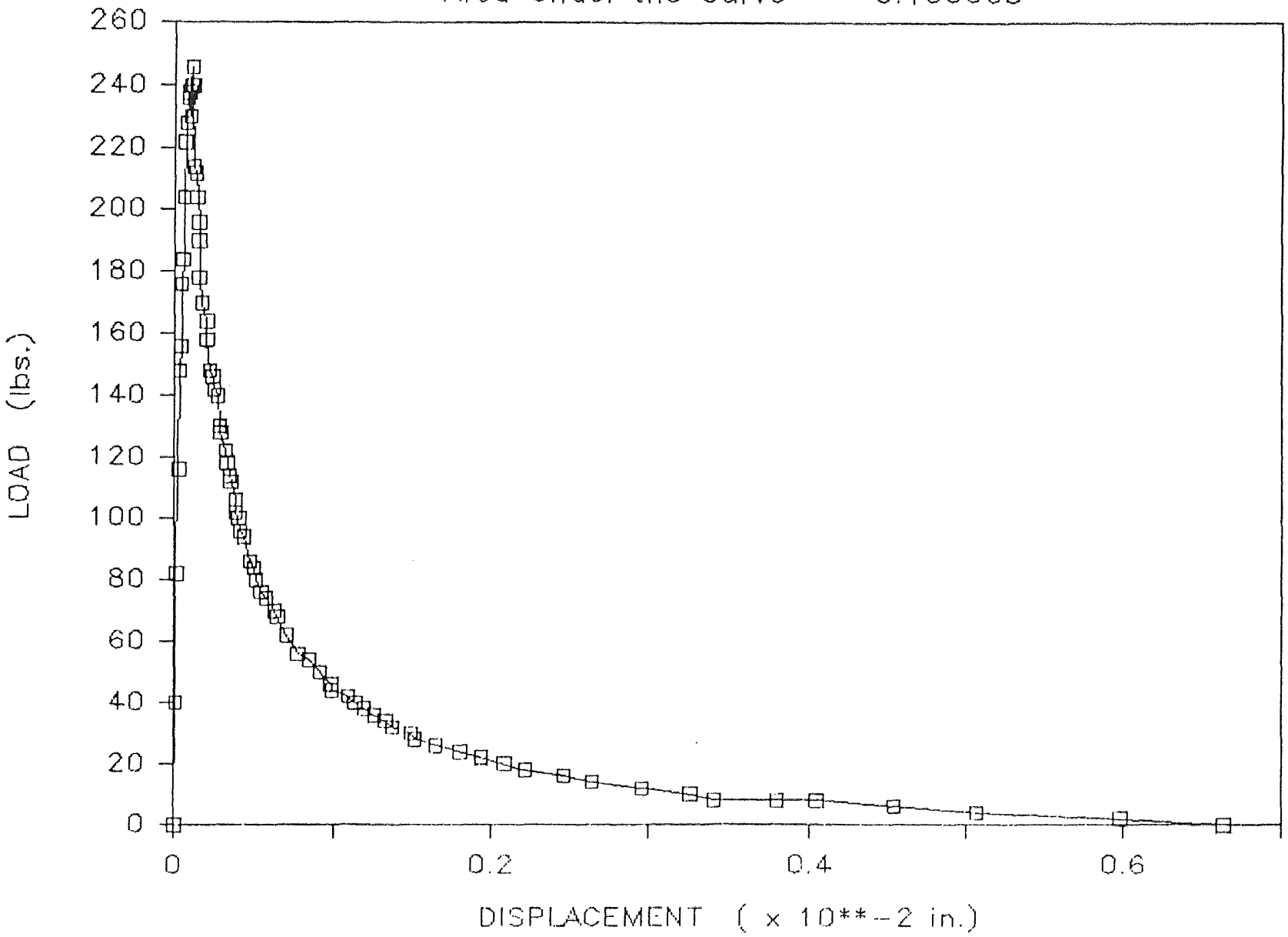

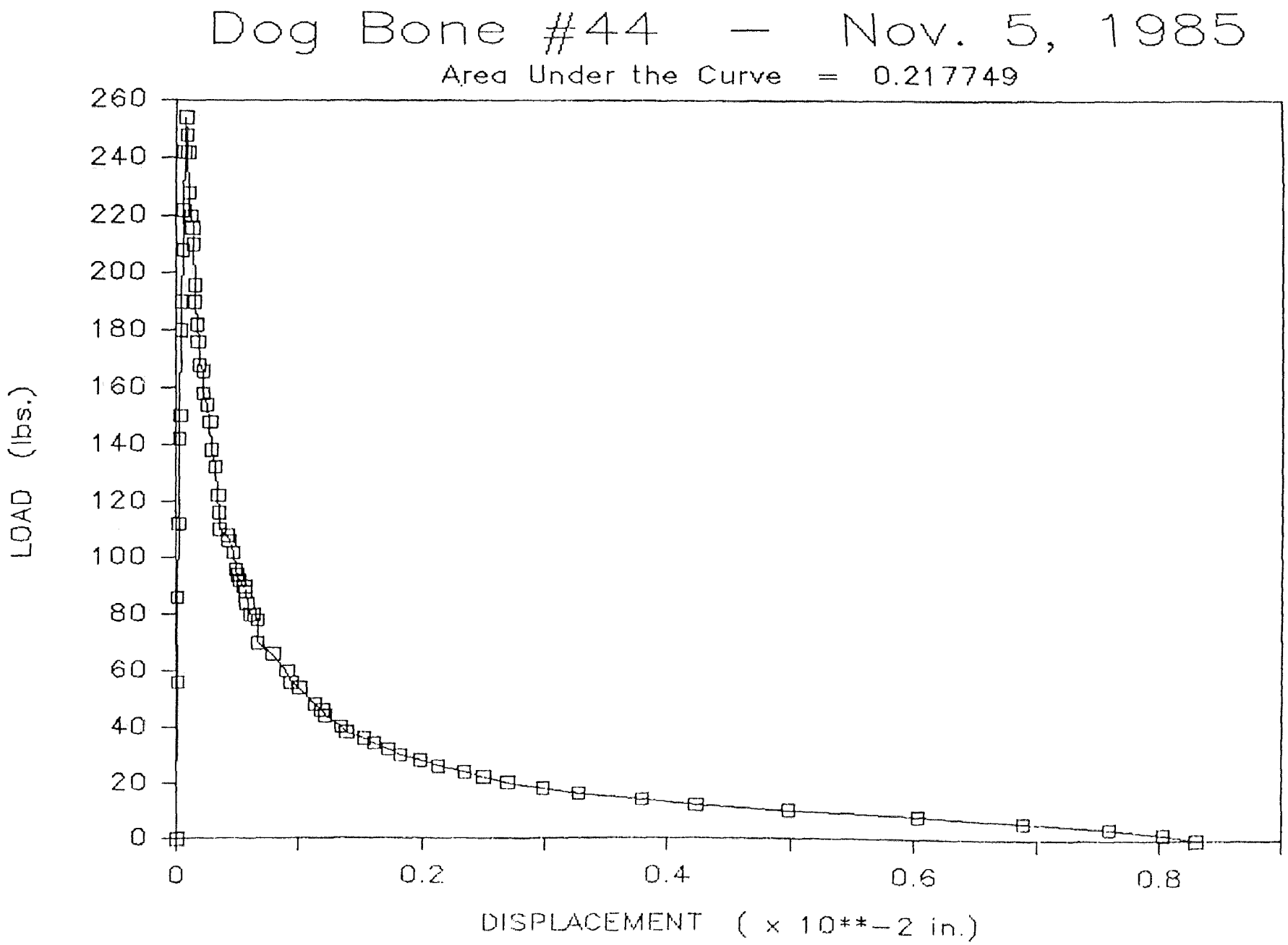
Dog Bone #44 — Nov. 5, 1985
Area Under the Curve = 0.217749
LOAD (lbs.)
260
240
220
200
180
160
140
120
100
80
60
40
20
0
0
0.2
0.4
0.6
0.8
DISPLACEMENT (x 10**-2 in.)

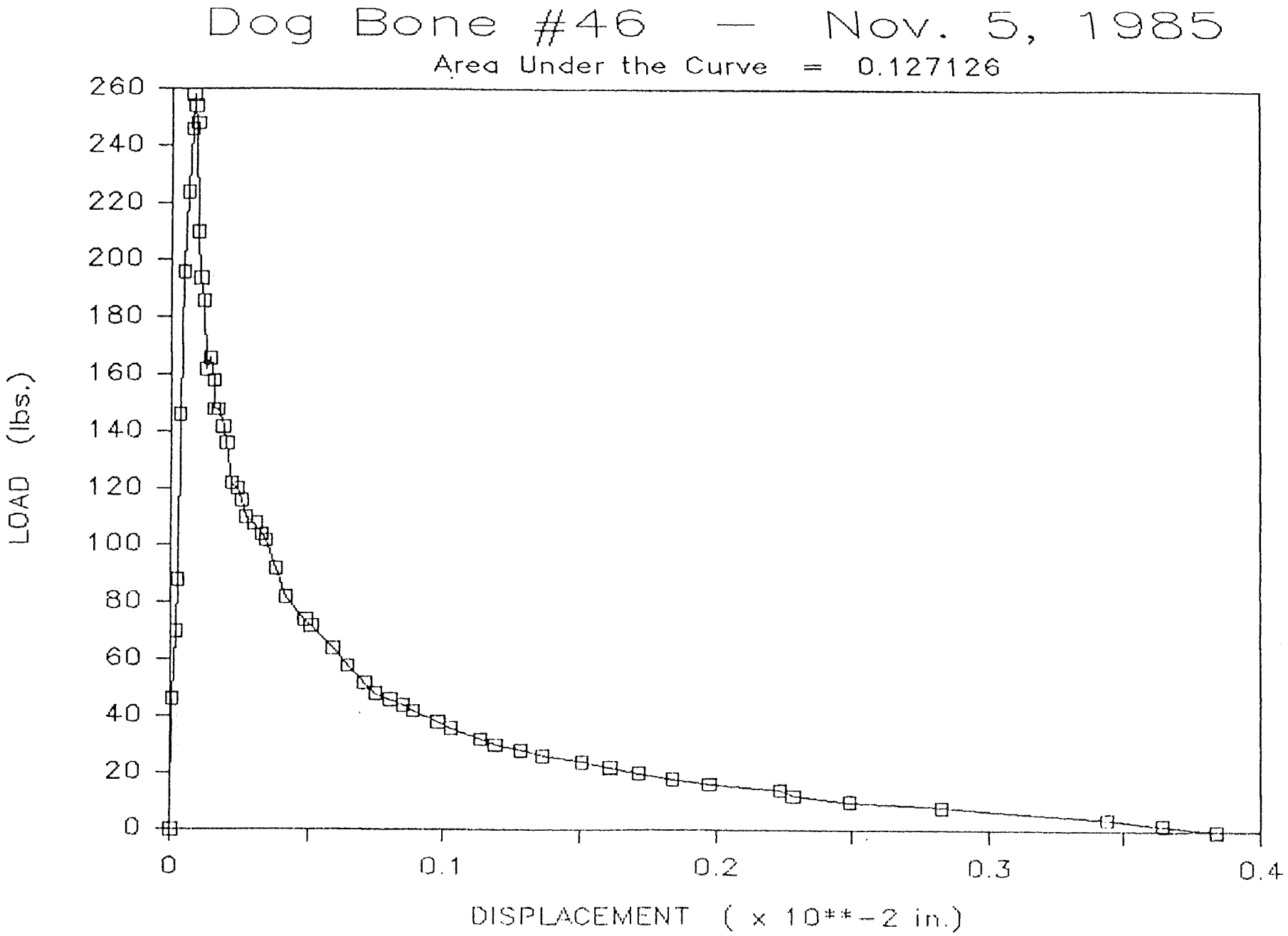
Dog Bone #46 — Nov. 5, 1985
Area Under the Curve = 0.127126
LOAD (lbs.)
260
240
220
200
180
160
140
120
100
80
60
40
20
0
0
0.1
0.2
0.3
0.4
DISPLACEMENT (x 10**-2 in.)

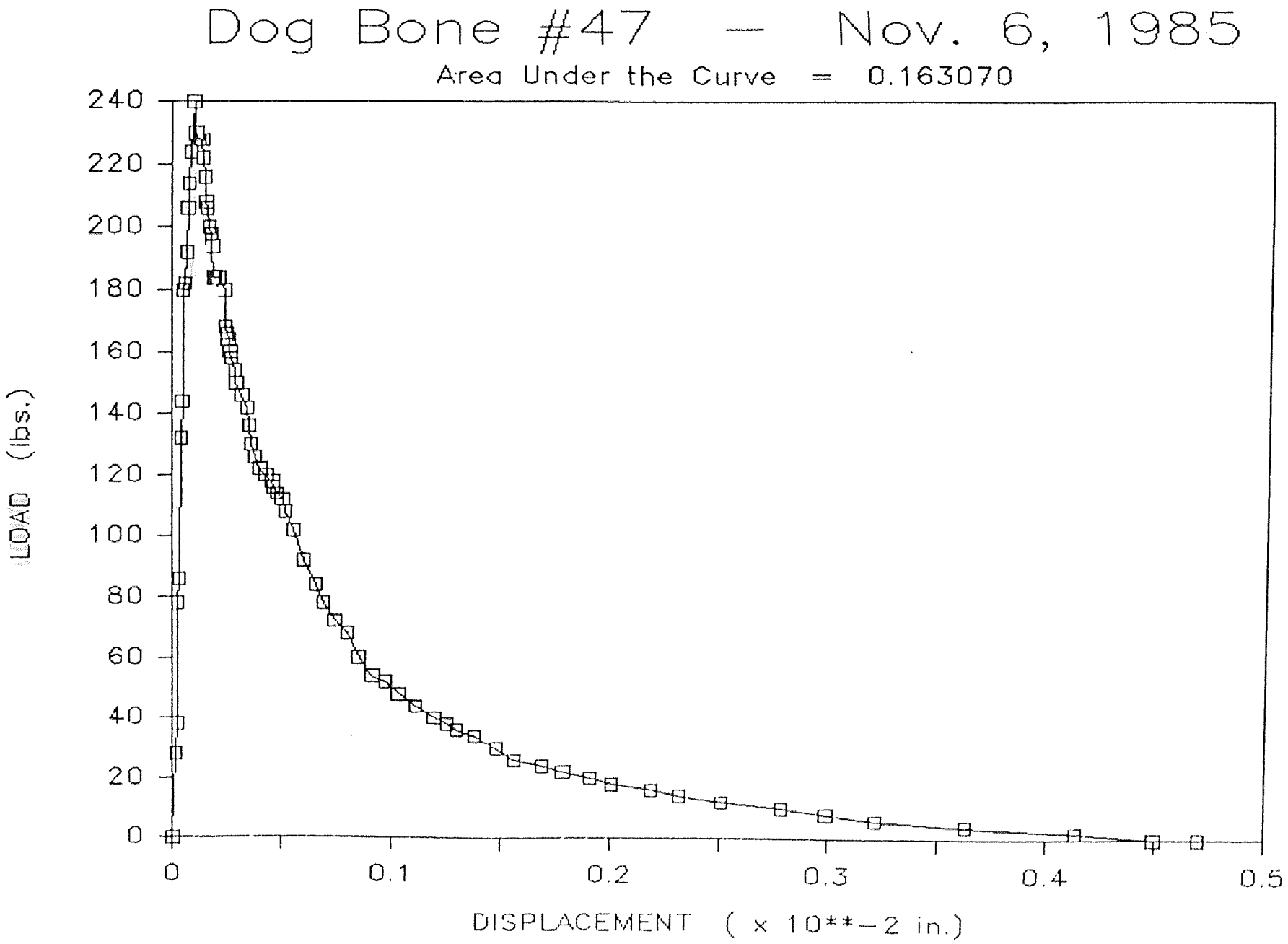
Dog Bone #47 — Nov. 6, 1985
Area Under the Curve = 0.163070
LOAD (lbs.)
240
220
200
180
160
140
120
100
80
60
40
20
0
0
0.1
0.2
0.3
0.4
0.5
DISPLACEMENT (x 10**-2 in.)

Dog Bone #48 — Nov. 15, 1985

Area Under the Curve = 0.297812

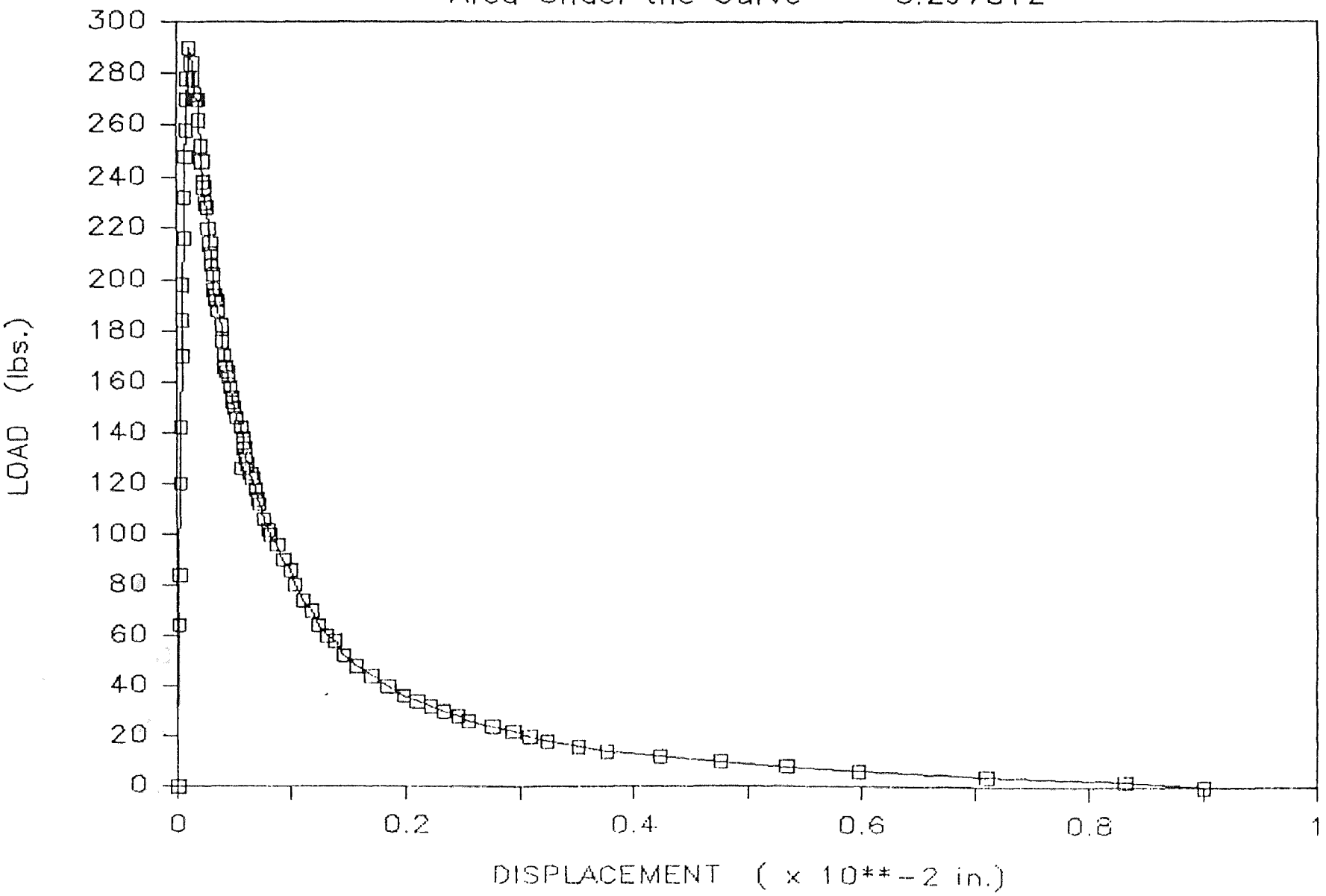

Dog Bone #21 — Sep. 9, 1985

Area Under the Curve = .164165

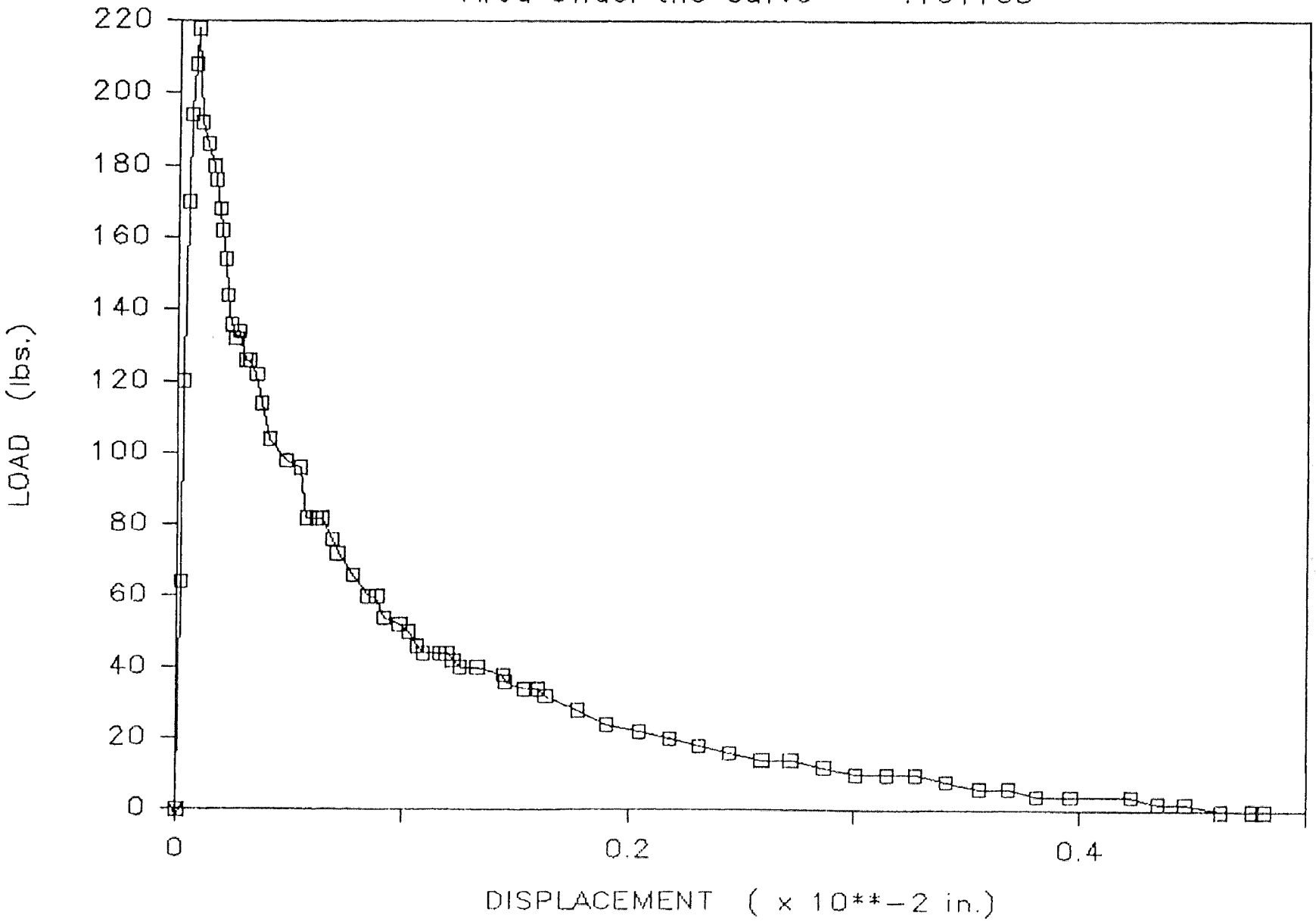

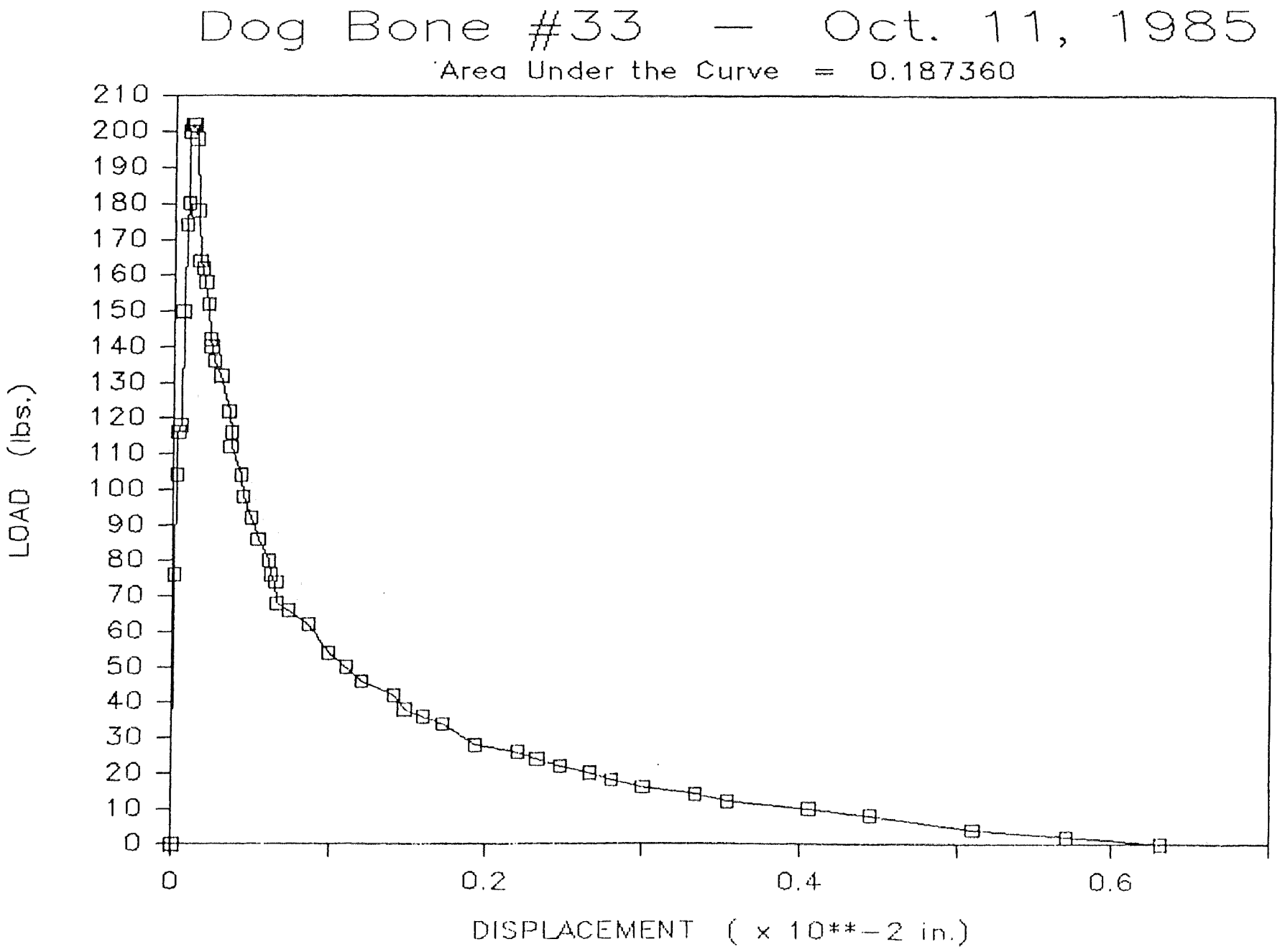
Dog Bone #33 — Oct. 11, 1985
Area Under the Curve = 0.187360
LOAD (lbs.)
210
200
190
180
170
160
150
140
130
120
110
100
90
80
70
60
50
40
30
20
10
0
0
0.2
0.4
0.6
DISPLACEMENT (x 10**-2 in.)

Dog Bone #34 — Oct. 11, 1985

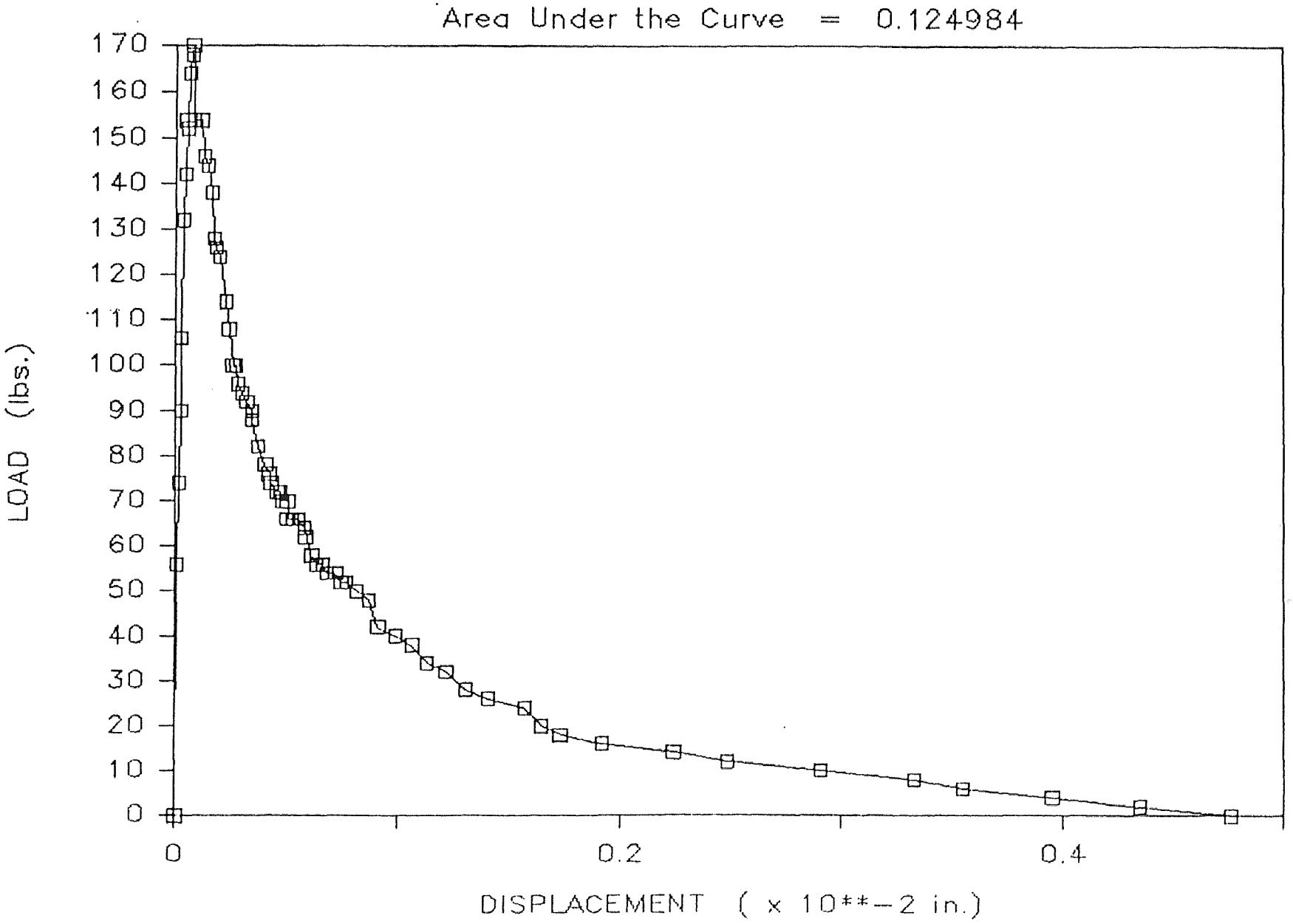

Dog Bone #20 — Sep. 9, 1985

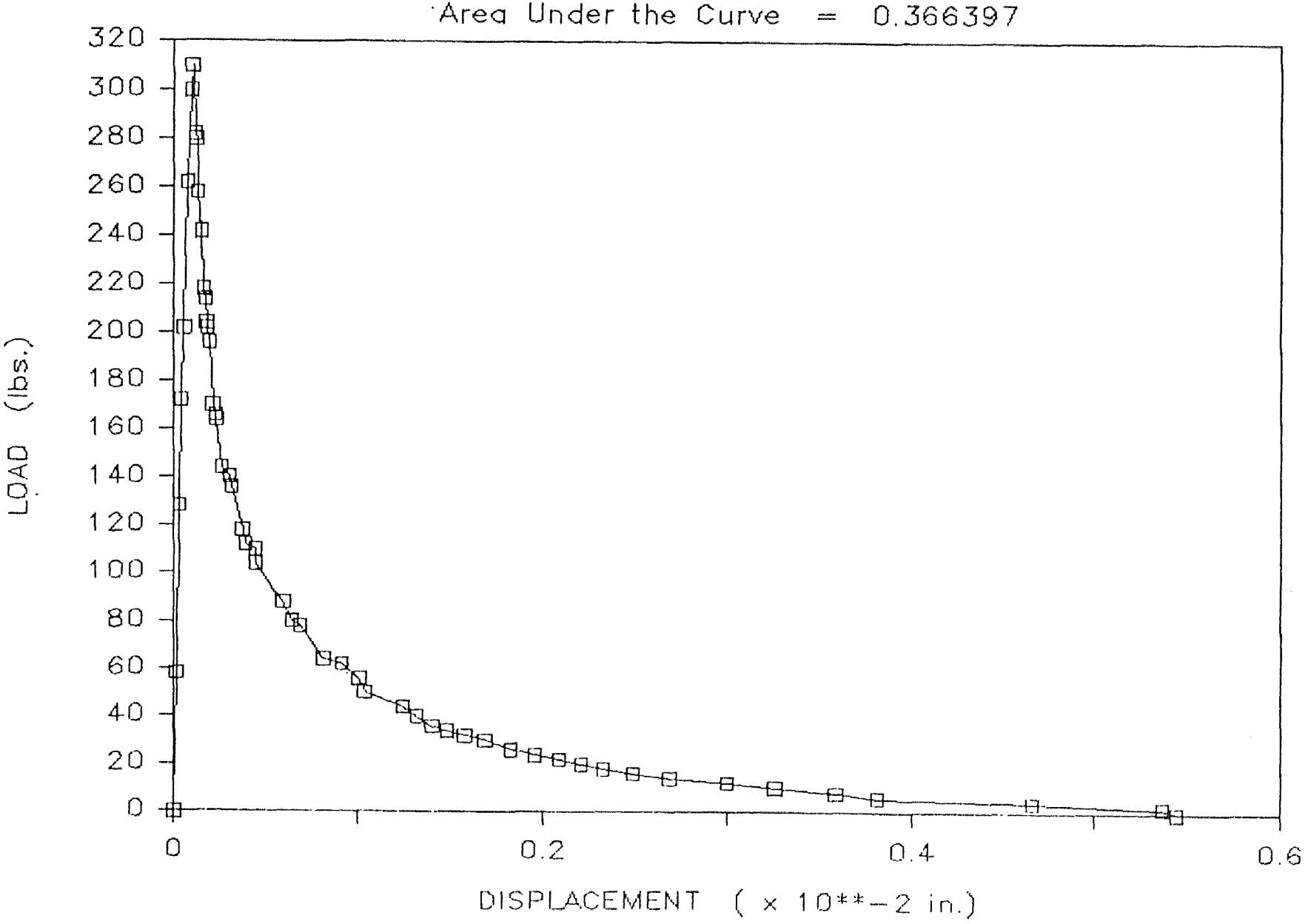

Dog Bone #25 — Sep. 11, 1985

Area Under the Curve = 0.066185

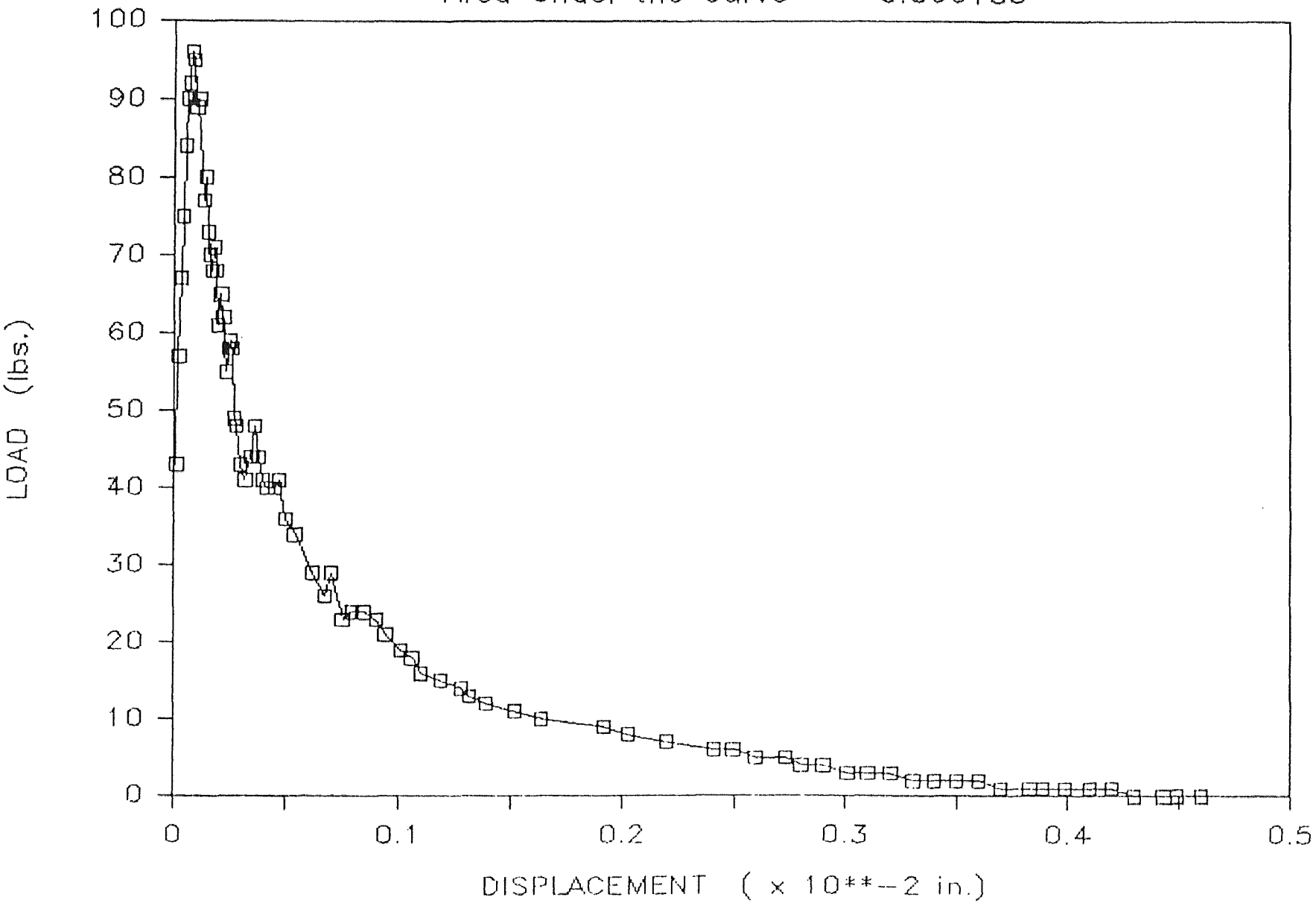

Dog Bone #54 — Dec. 11, 1985

Area Under the Curve = 0.404654

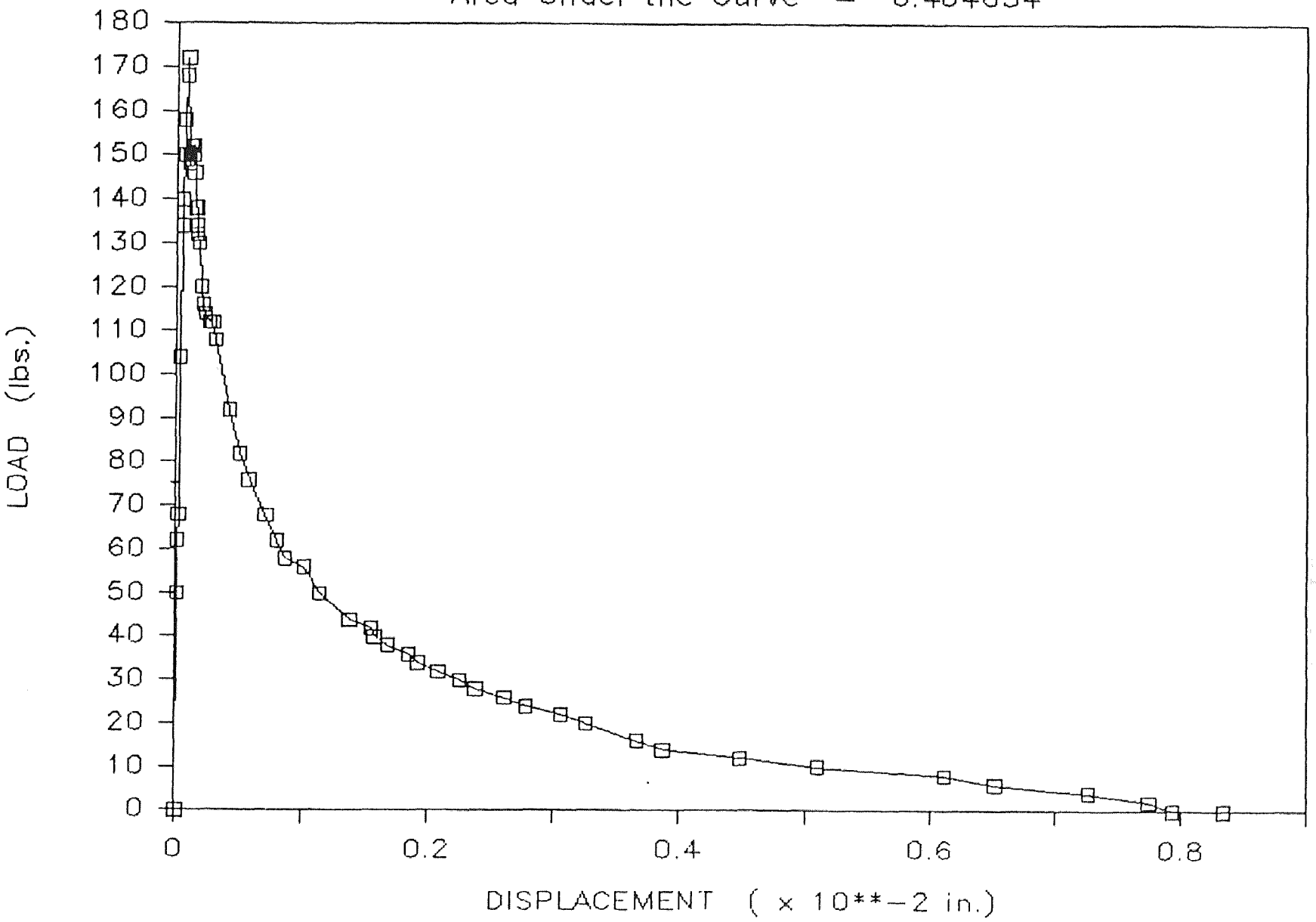

Dog Bone #55 — Dec. 11, 1985

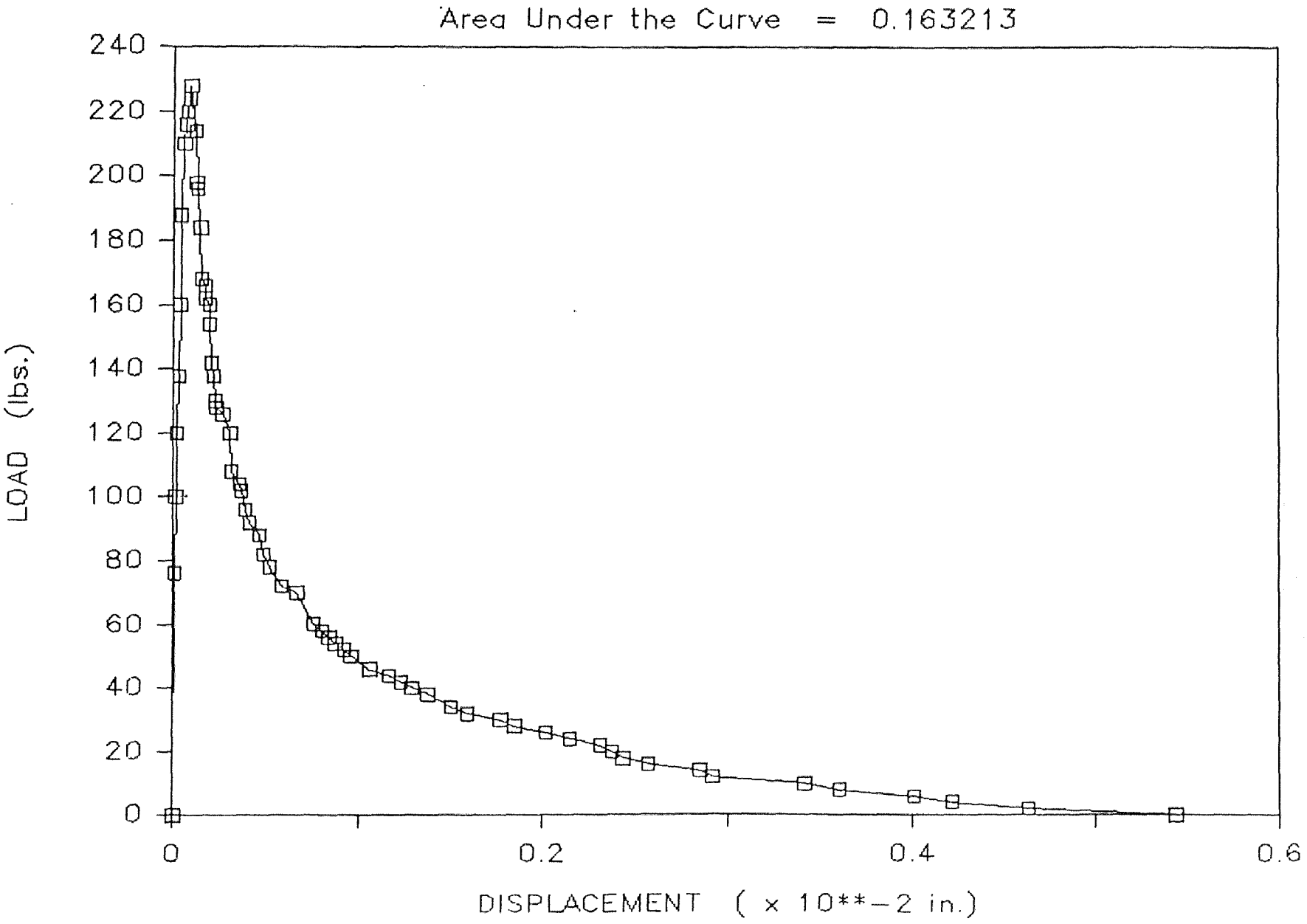

Dog Bone #24 — Sep.11, 1985

Area Under the Curve = 0.101175

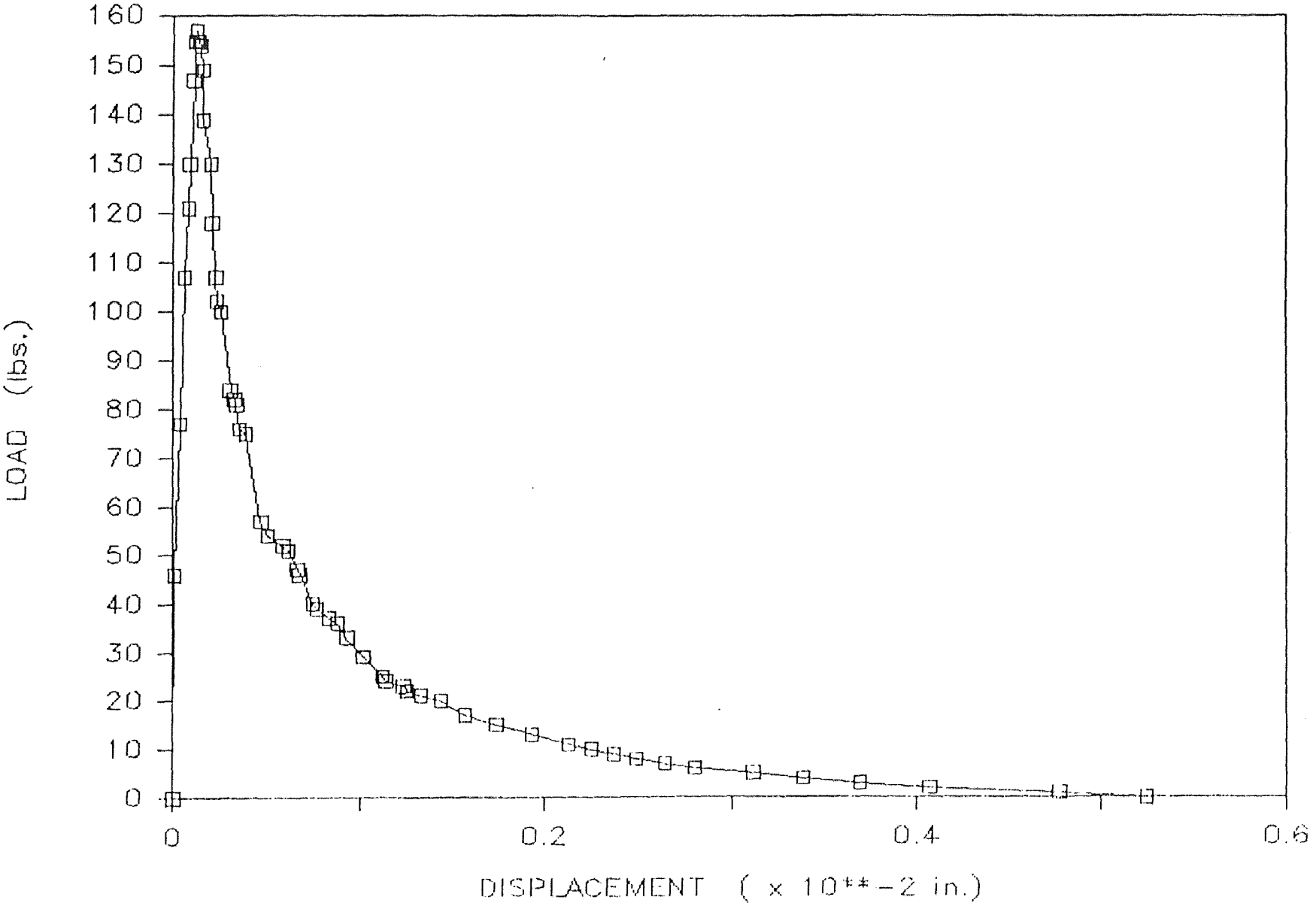

Dog Bone #18 --> Sep. 16, 1985

Area Under the Curve = .141202

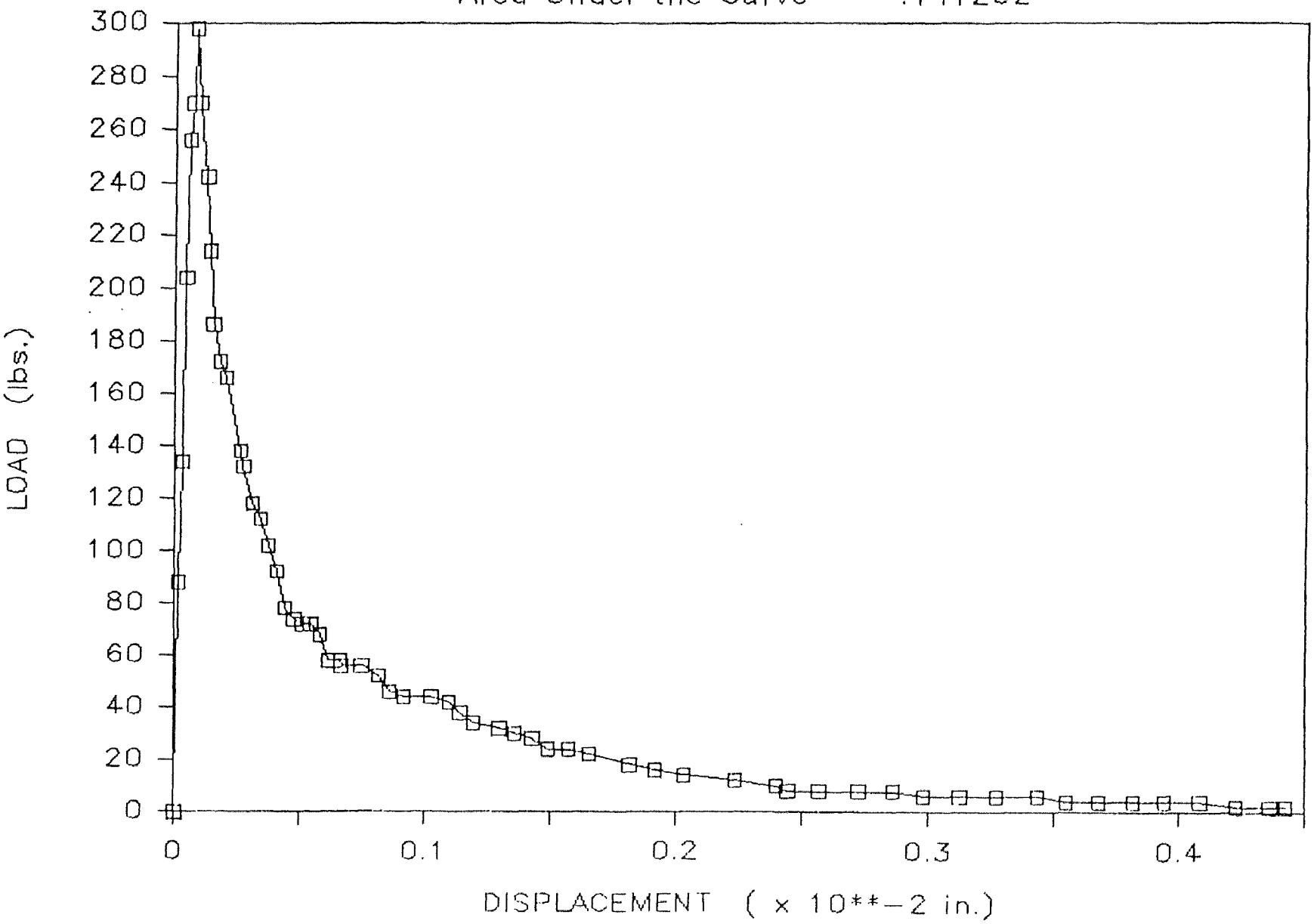

Dog Bone #19 — Sep. 6, 1985

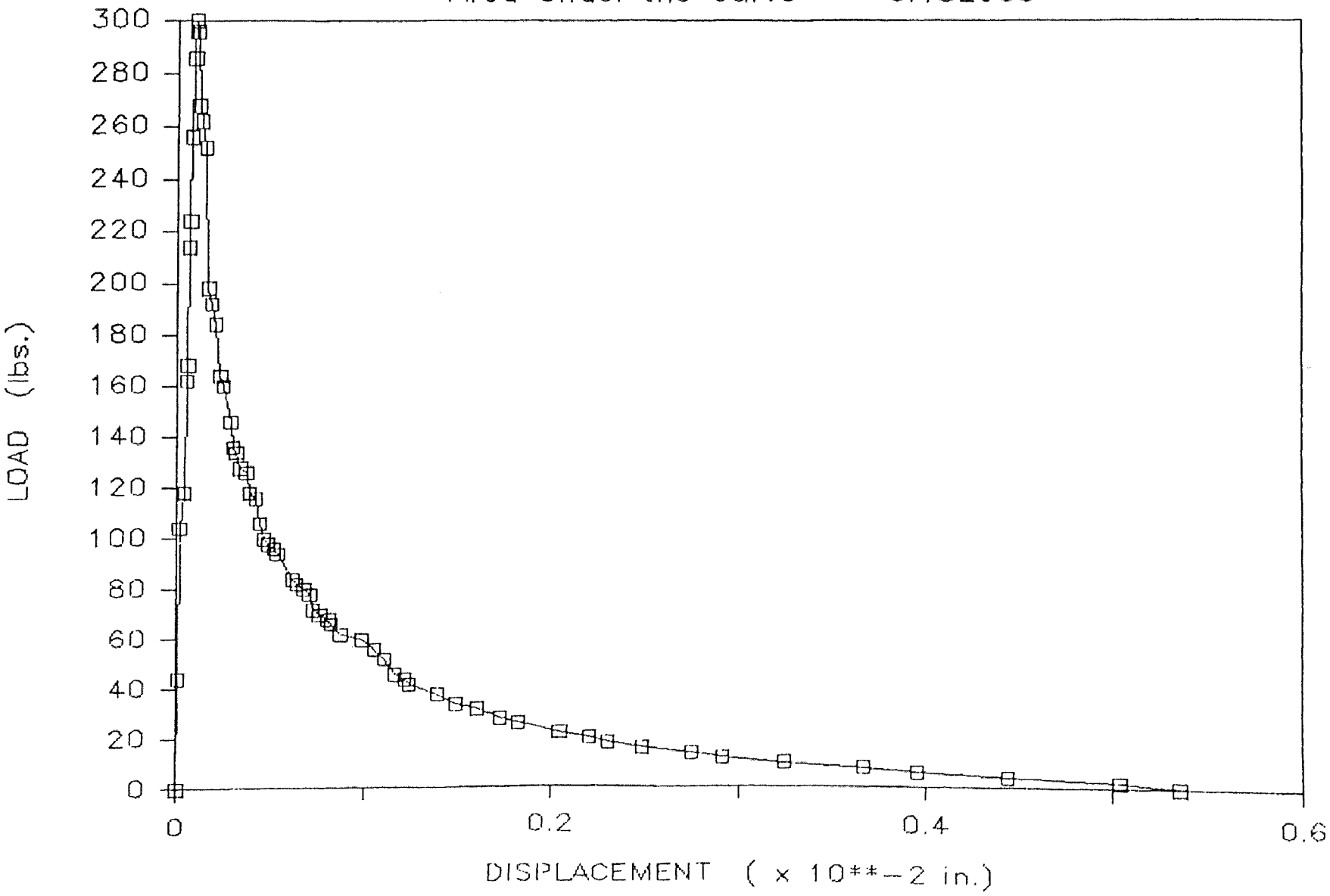

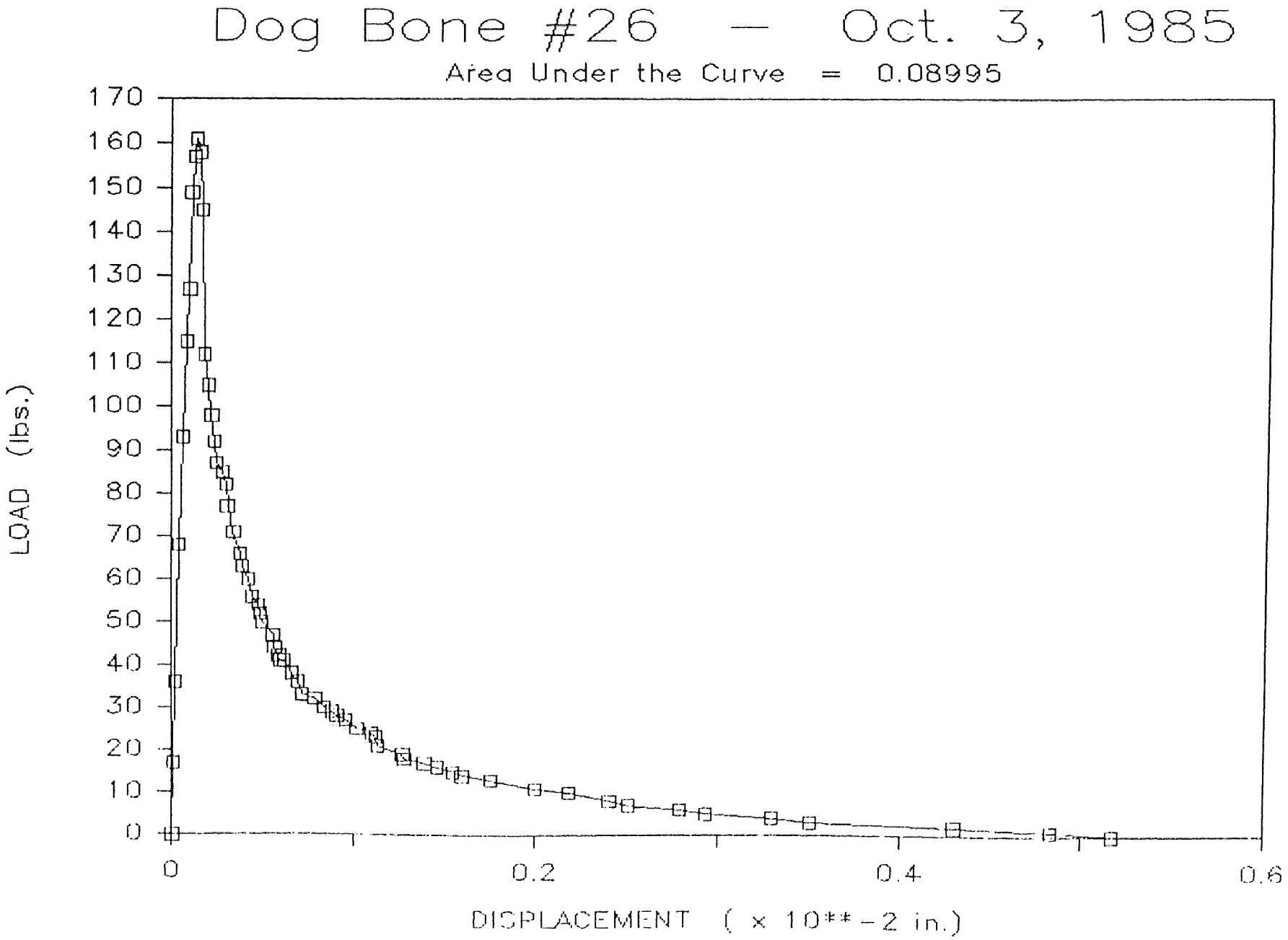
Dog Bone #26 — Oct. 3, 1985
Area Under the Curve = 0.08995
LOAD (lbs.)
170
160
150
140
130
120
110
100
90
80
70
60
50
40
30
20
10
0
0
0.2
0.4
0.6
DISPLACEMENT (x 10**-2 in.)

Dog Bone #27 — Sep. 17, 1985

Area Under the Curve = 0.079655

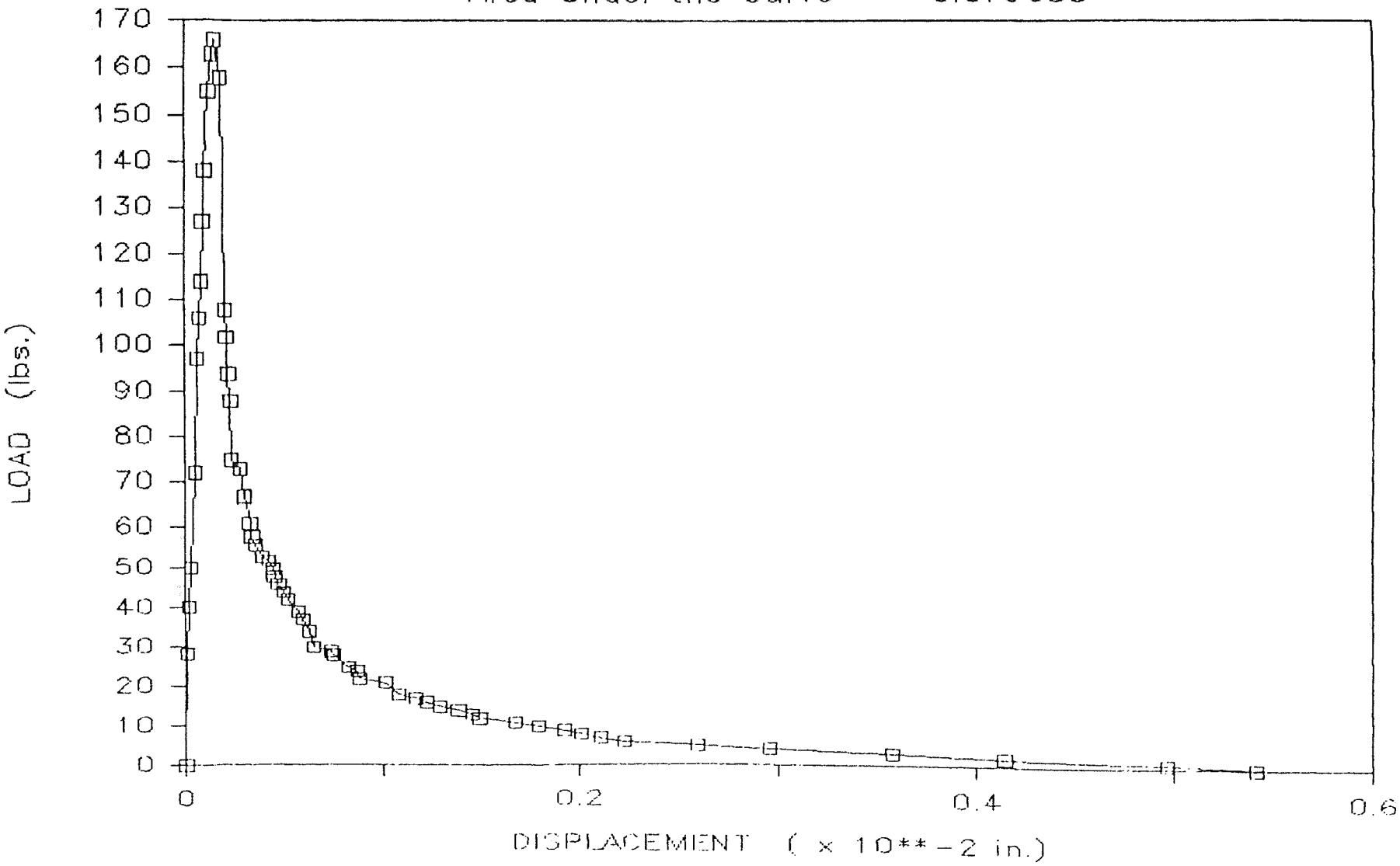

Dog Bone #28 — Sep. 17, 1985

Area Under the Curve = 0.15263

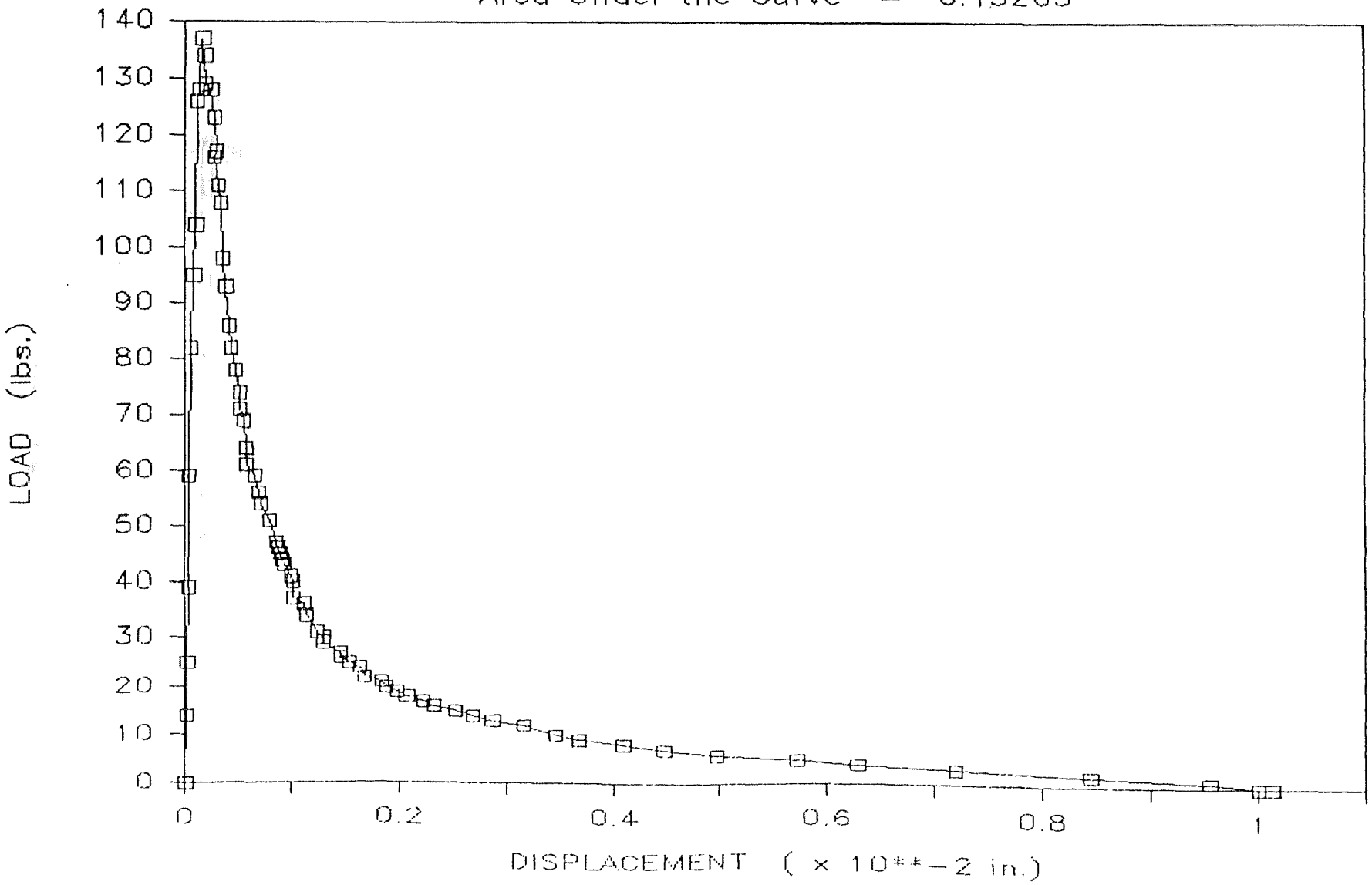

Dog Bone #40 — Oct. 10, 1985

Area Under the Curve = 0.251457

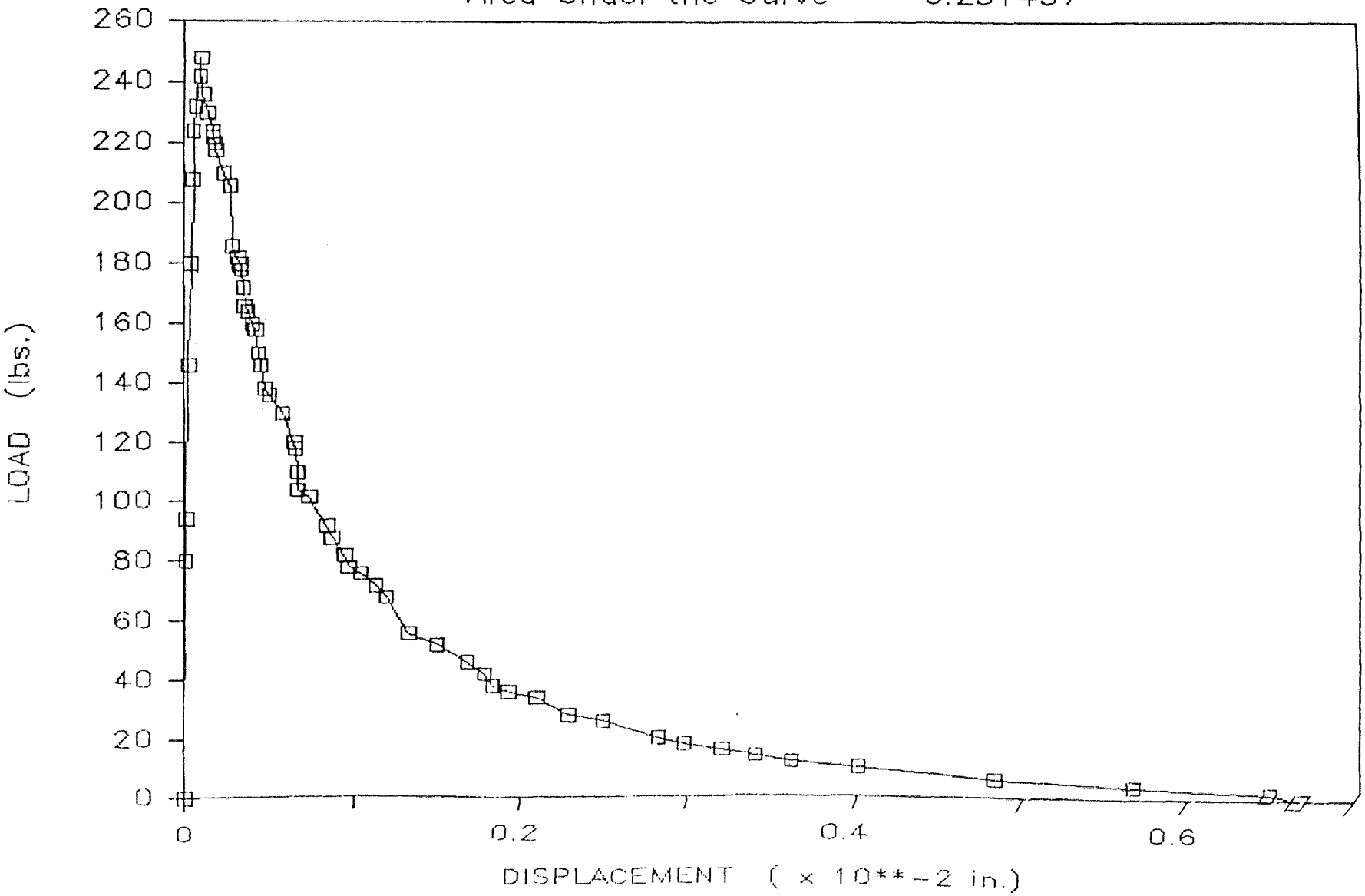

Dog Bone #50 — Dec. 11, 1985

Area Under the Curve = 0.136761

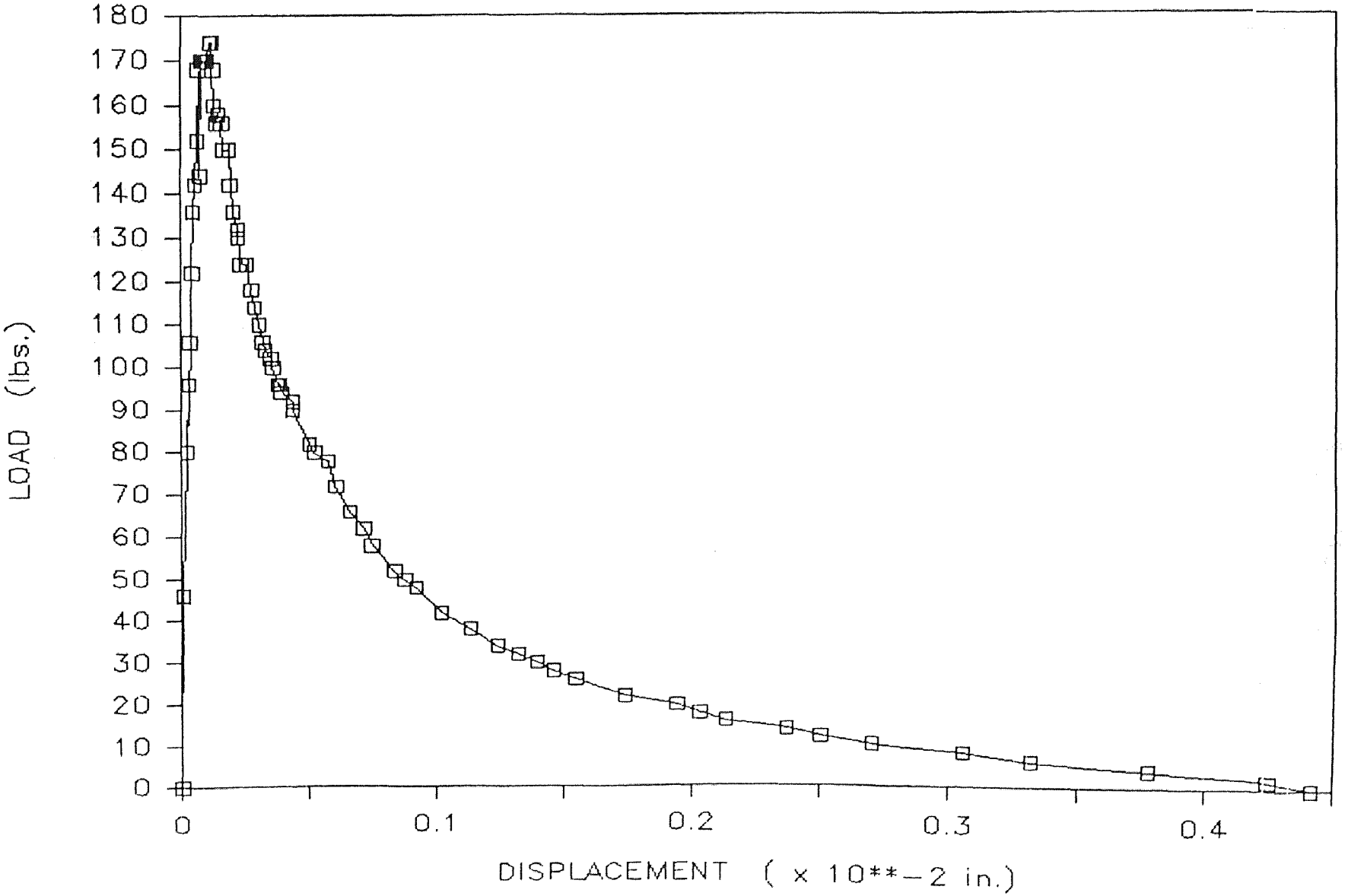

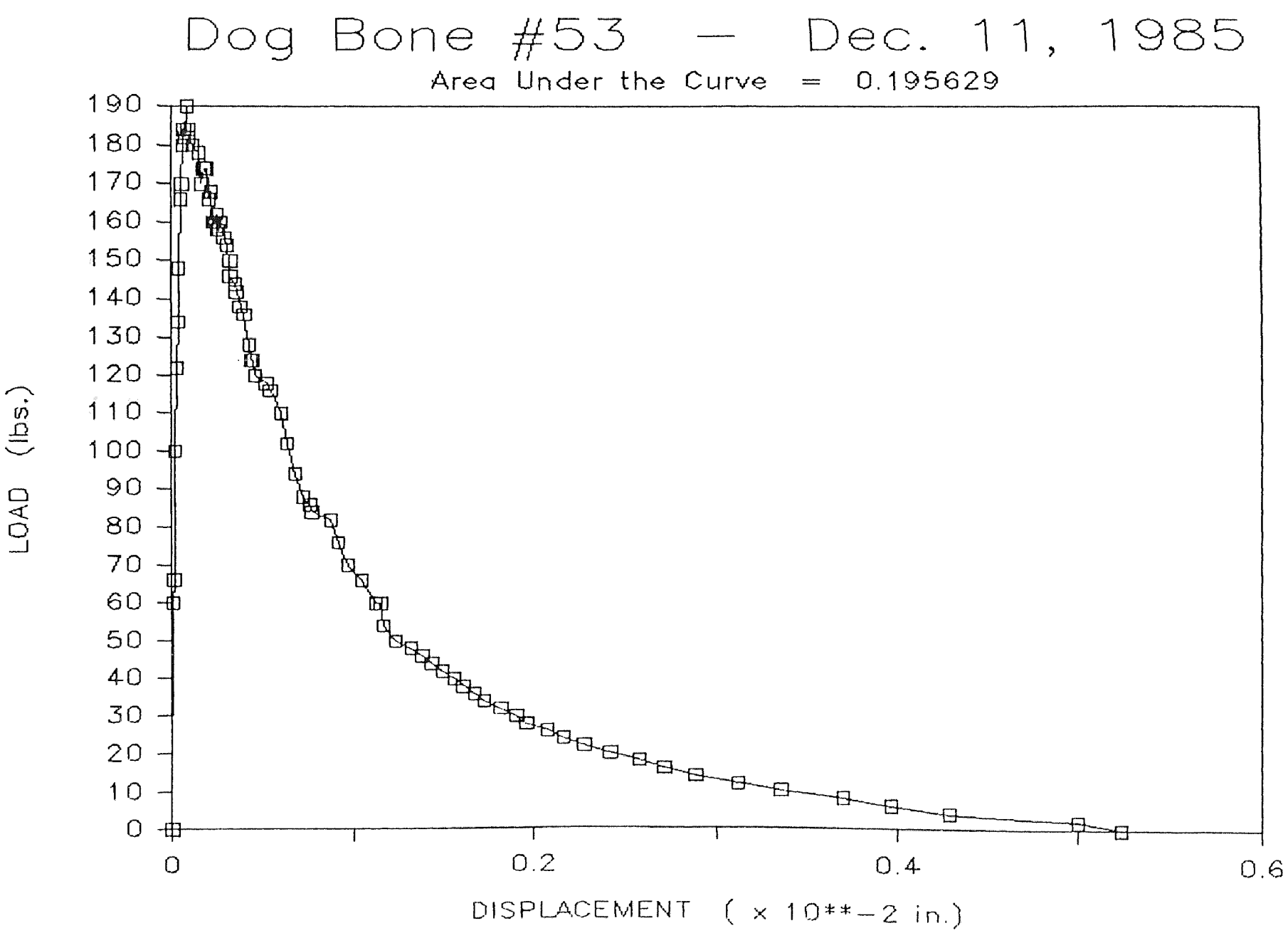
Dog Bone #53 — Dec. 11, 1985
Area Under the Curve = 0.195629
LOAD (lbs.)
190
180
170
160
150
140
130
120
110
100
90
80
70
60
50
40
30
20
10
0
0
0.2
0.4
0.6
DISPLACEMENT (x 10**-2 in.)

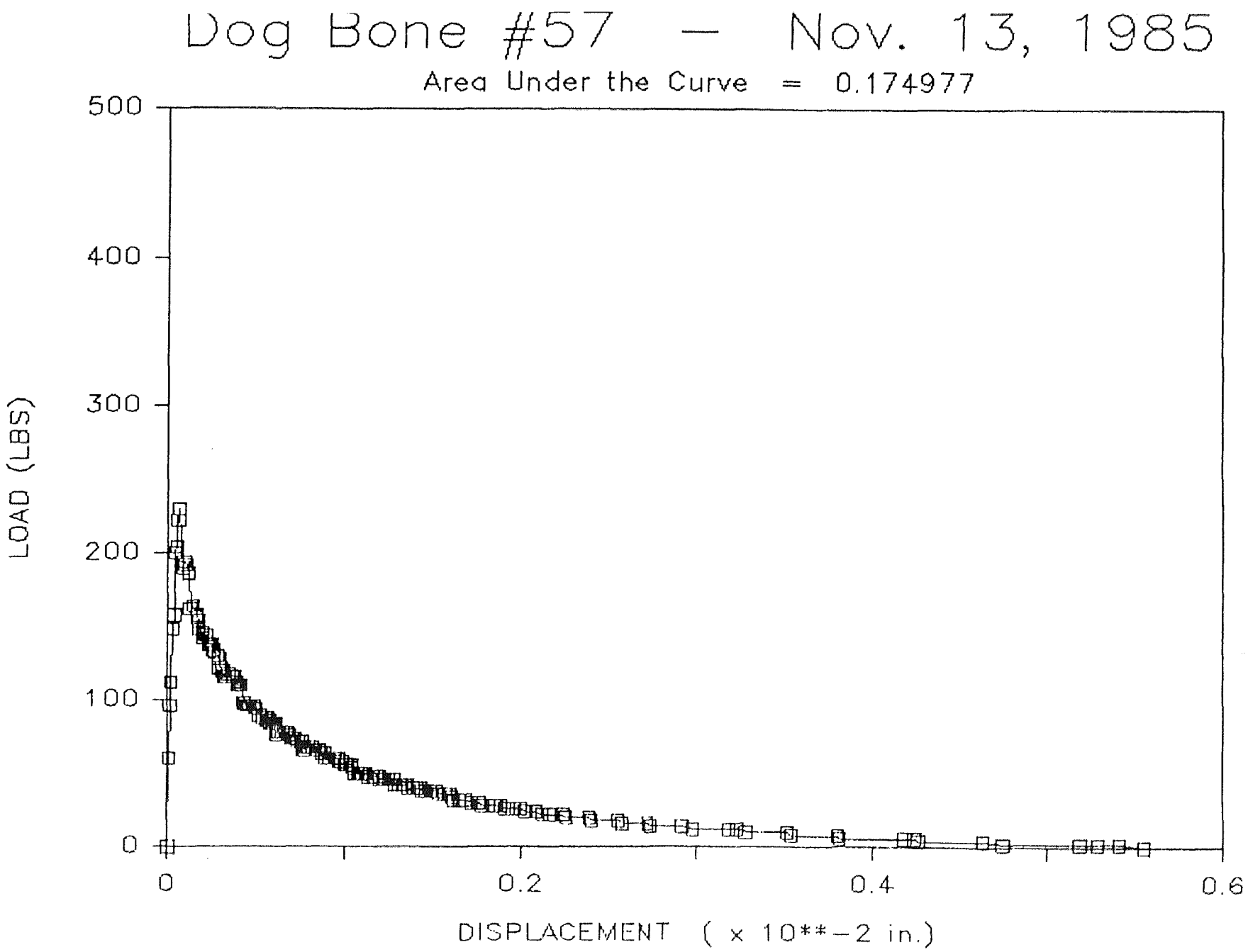
Dog Bone #57 — Nov. 13, 1985
Area Under the Curve = 0.174977
500
400
300
200
100
0
LOAD (LBS)
0
0.2
0.4
0.6
DISPLACEMENT (x 10**-2 in.)

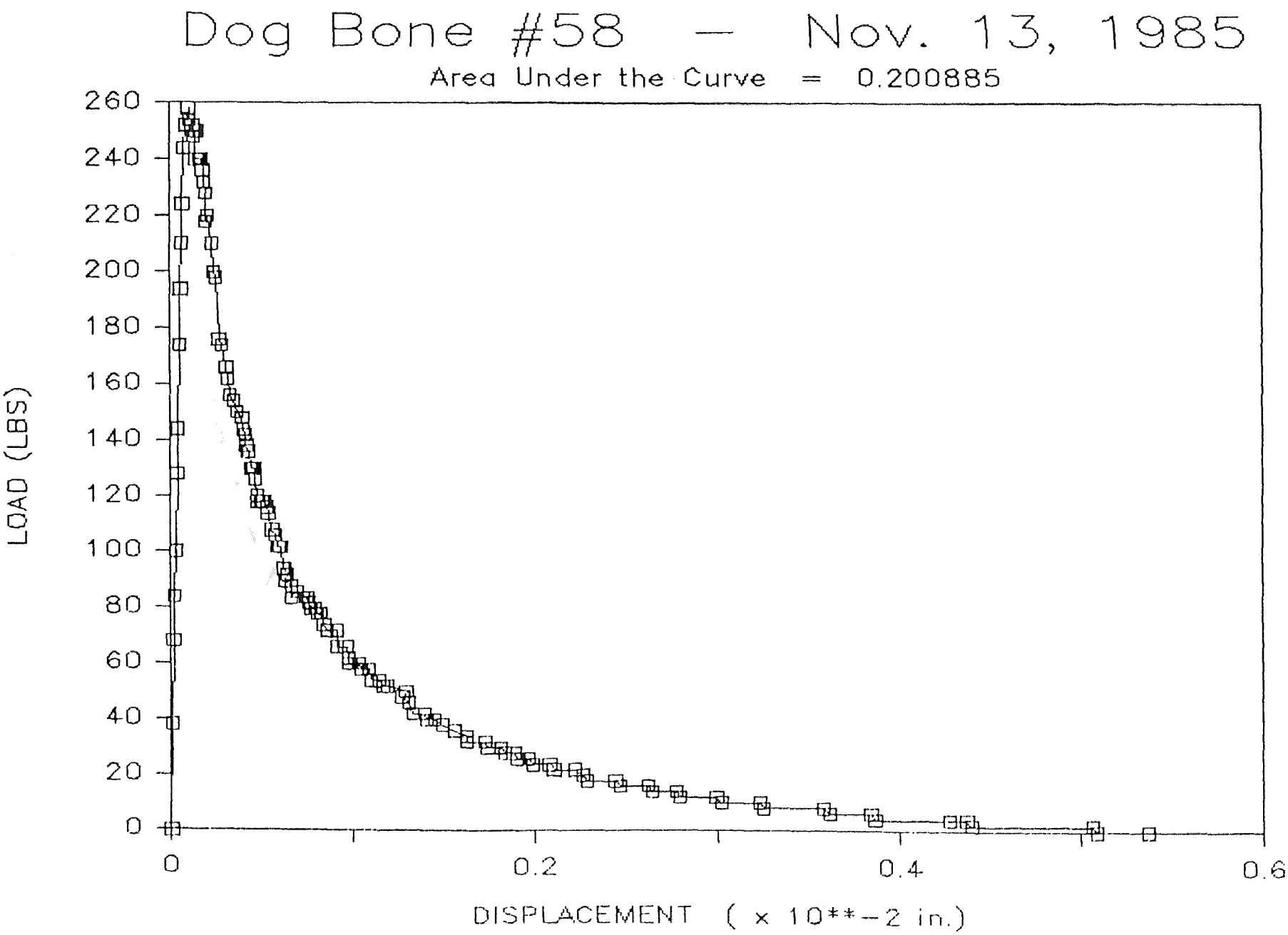
Dog Bone #58 — Nov. 13, 1985
Area Under the Curve = 0.200885
LOAD (LBS)
260
240
220
200
180
160
140
120
100
80
60
40
20
0
0
0.2
0.4
0.6
DISPLACEMENT (x 10**-2 in.)

Dog Bone #31 — Oct. 10, 1985

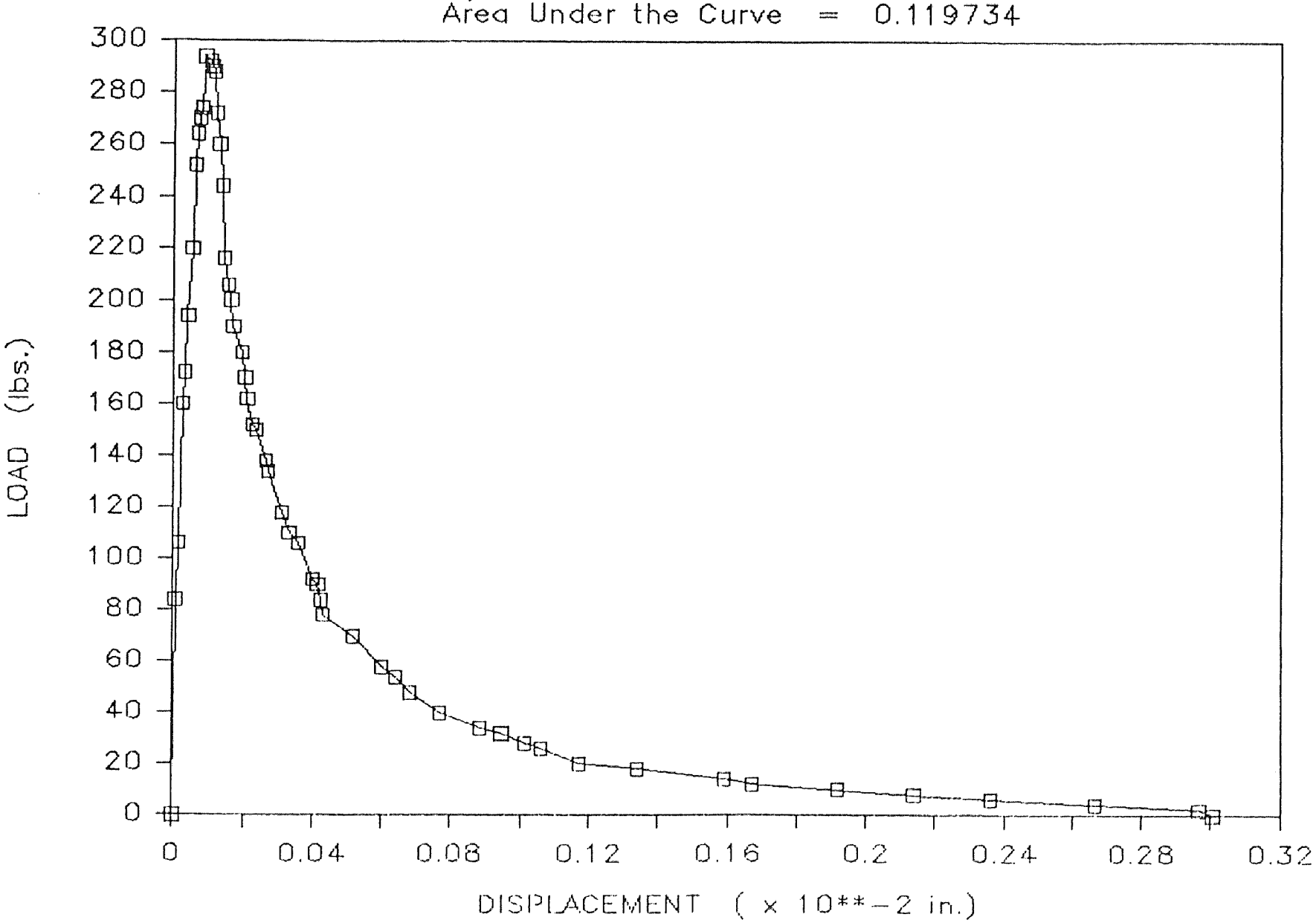

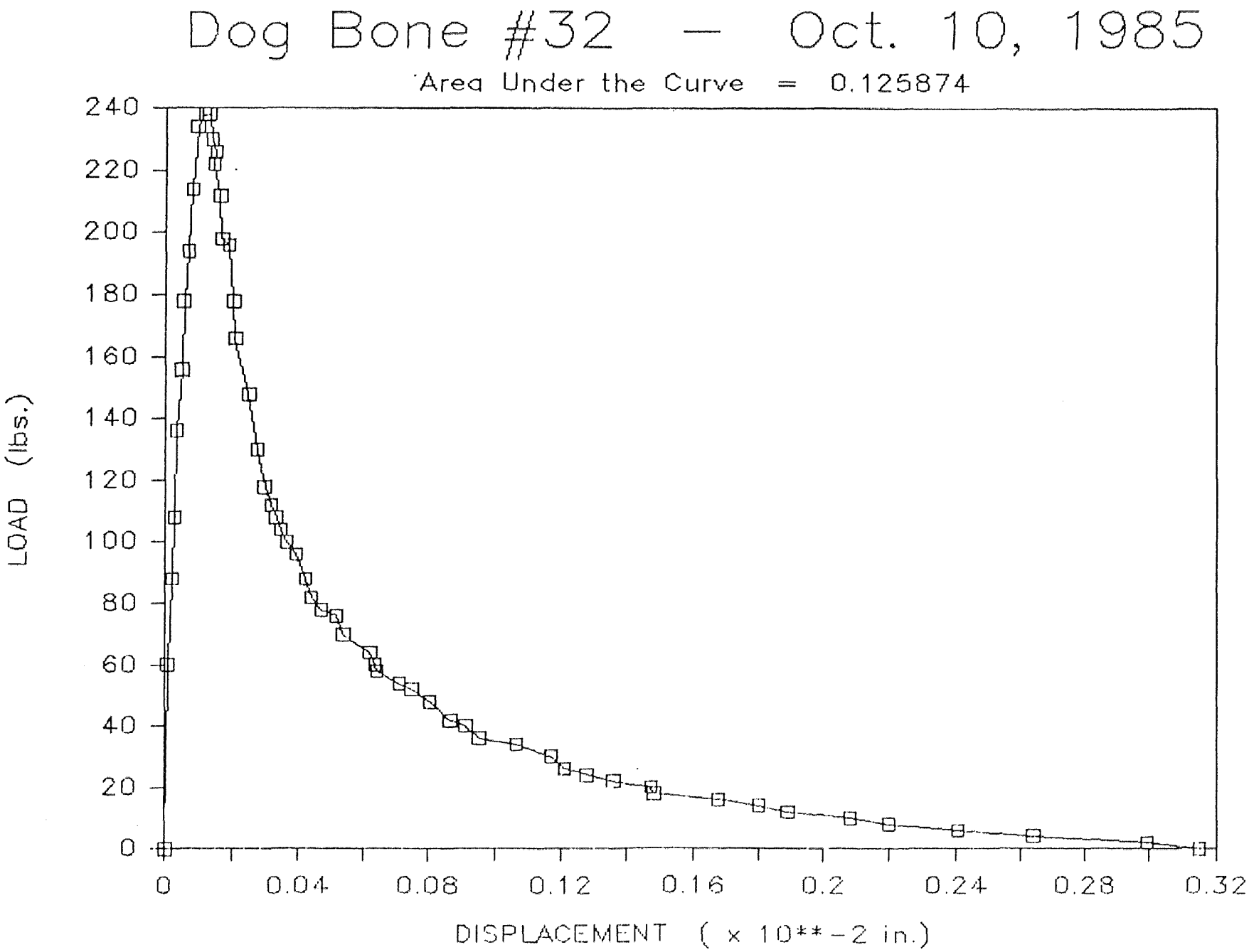
Dog Bone #32 — Oct. 10, 1985
Area Under the Curve = 0.125874
LOAD (lbs.)
240
220
200
180
160
140
120
100
80
60
40
20
0
0
0.04
0.08
0.12
0.16
0.2
0.24
0.28
0.32
DISPLACEMENT (x 10**-2 in.)

Dog Bone #41 — Nov. 10, 1985

Area Under the Curve = 0.13277

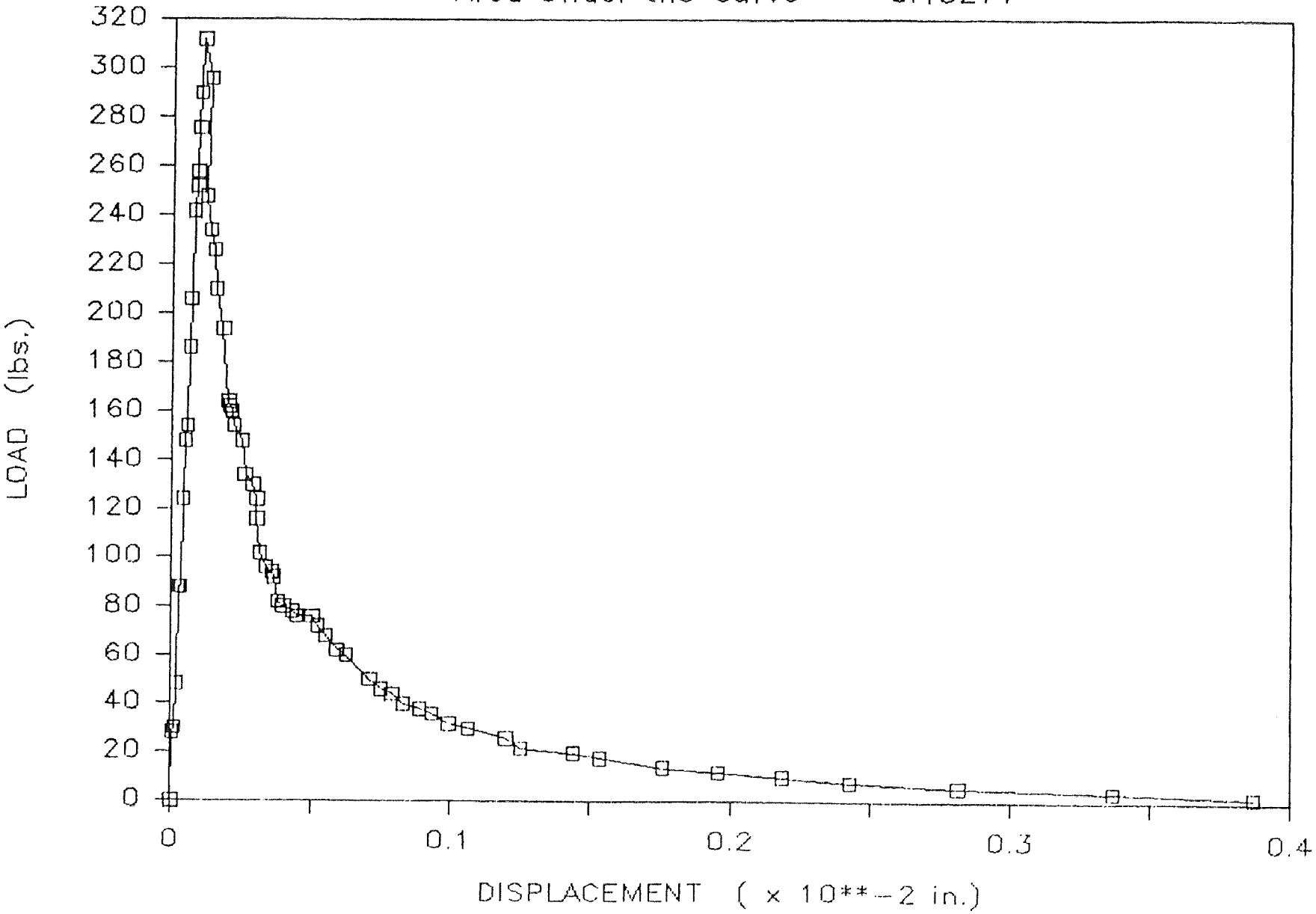

Dog Bone #42 — Nov. 10, 1985

Area Under the Curve = 0.106841

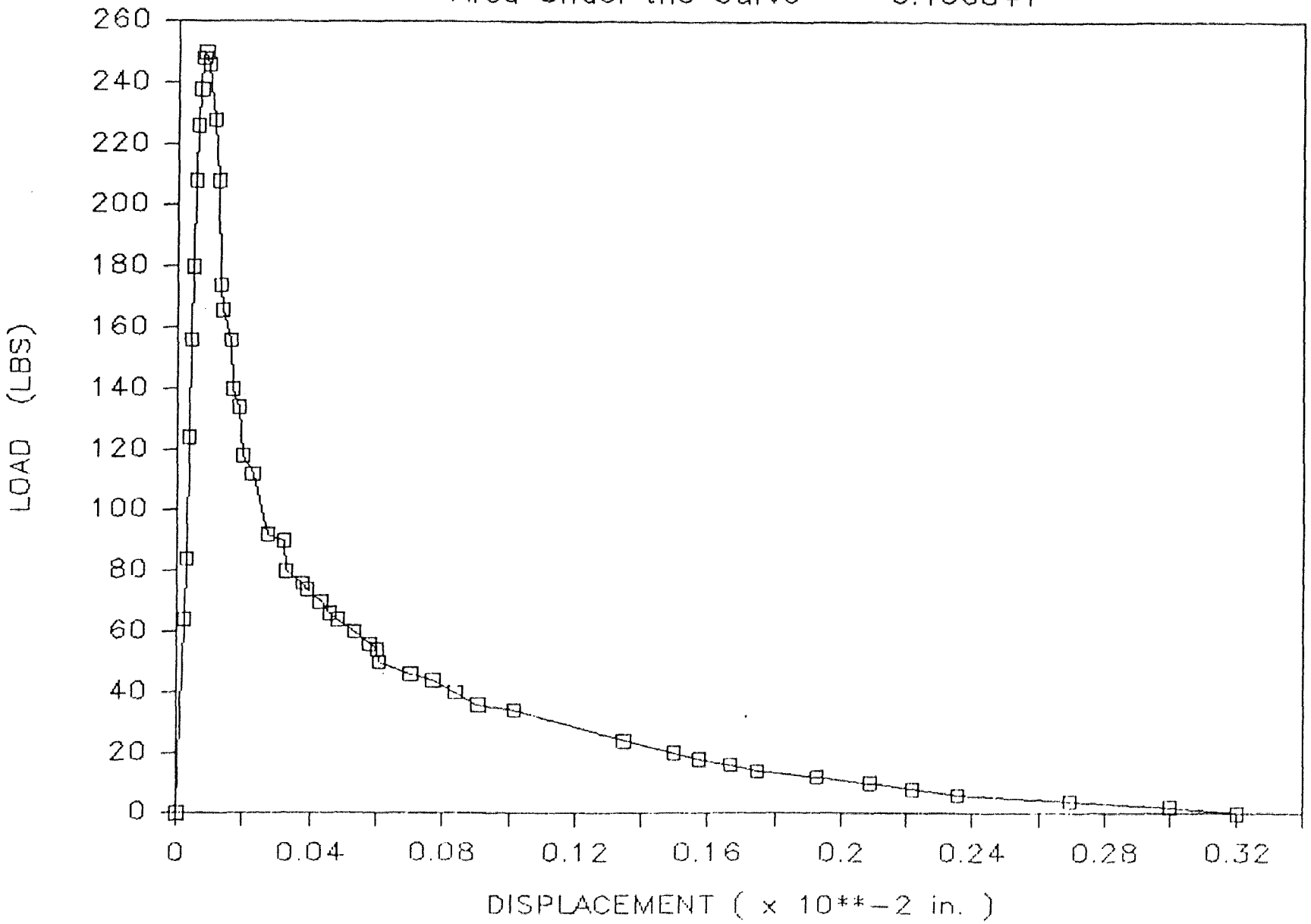

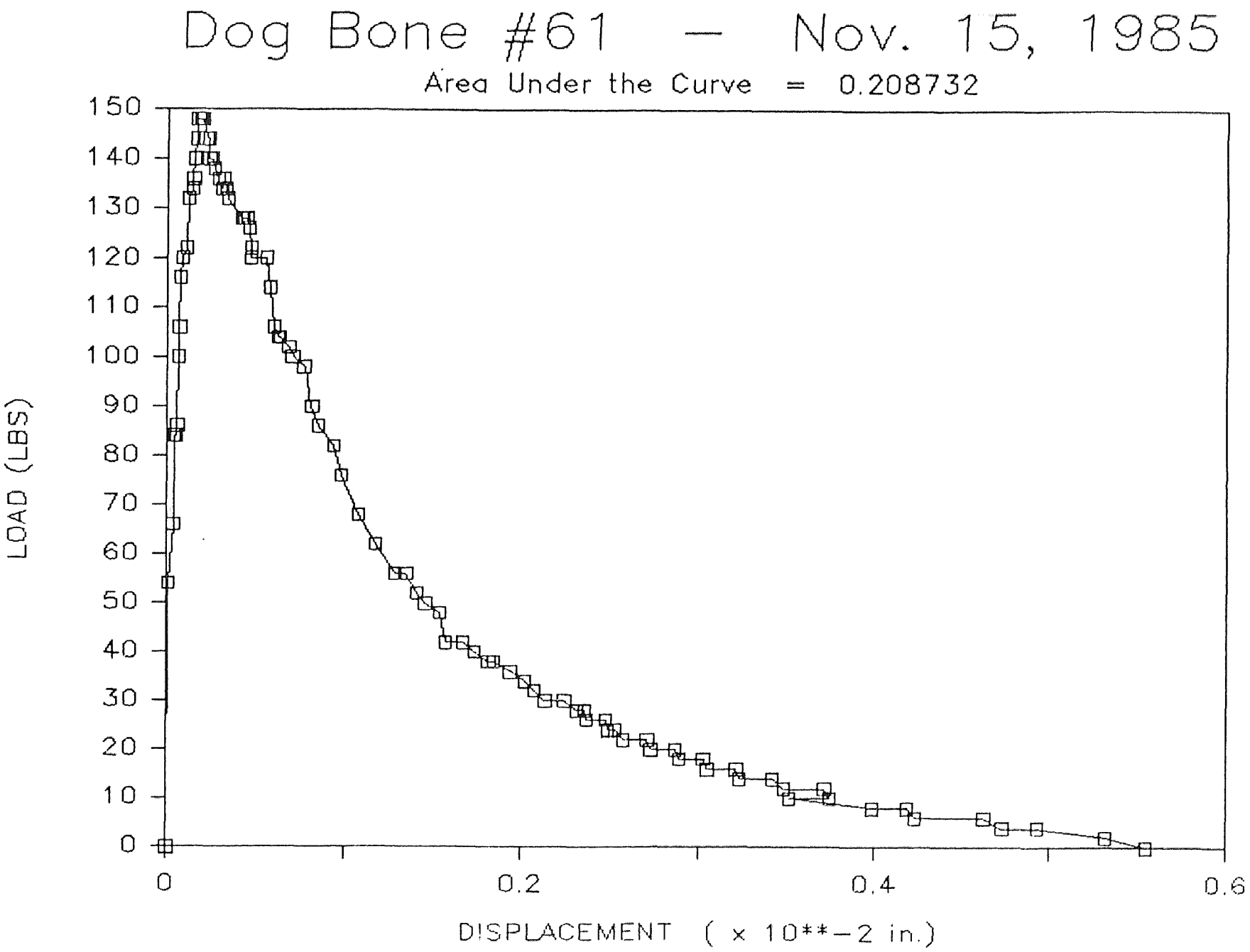
Dog Bone #61 — Nov. 15, 1985
Area Under the Curve = 0.208732
LOAD (LBS)
150
140
130
120
110
100
90
80
70
60
50
40
30
20
10
0
0
0.2
0.4
0.6
DISPLACEMENT (x 10**-2 in.)

Dog Bone #62 — Nov. 15, 1985

Area Under the Curve = 0.305864

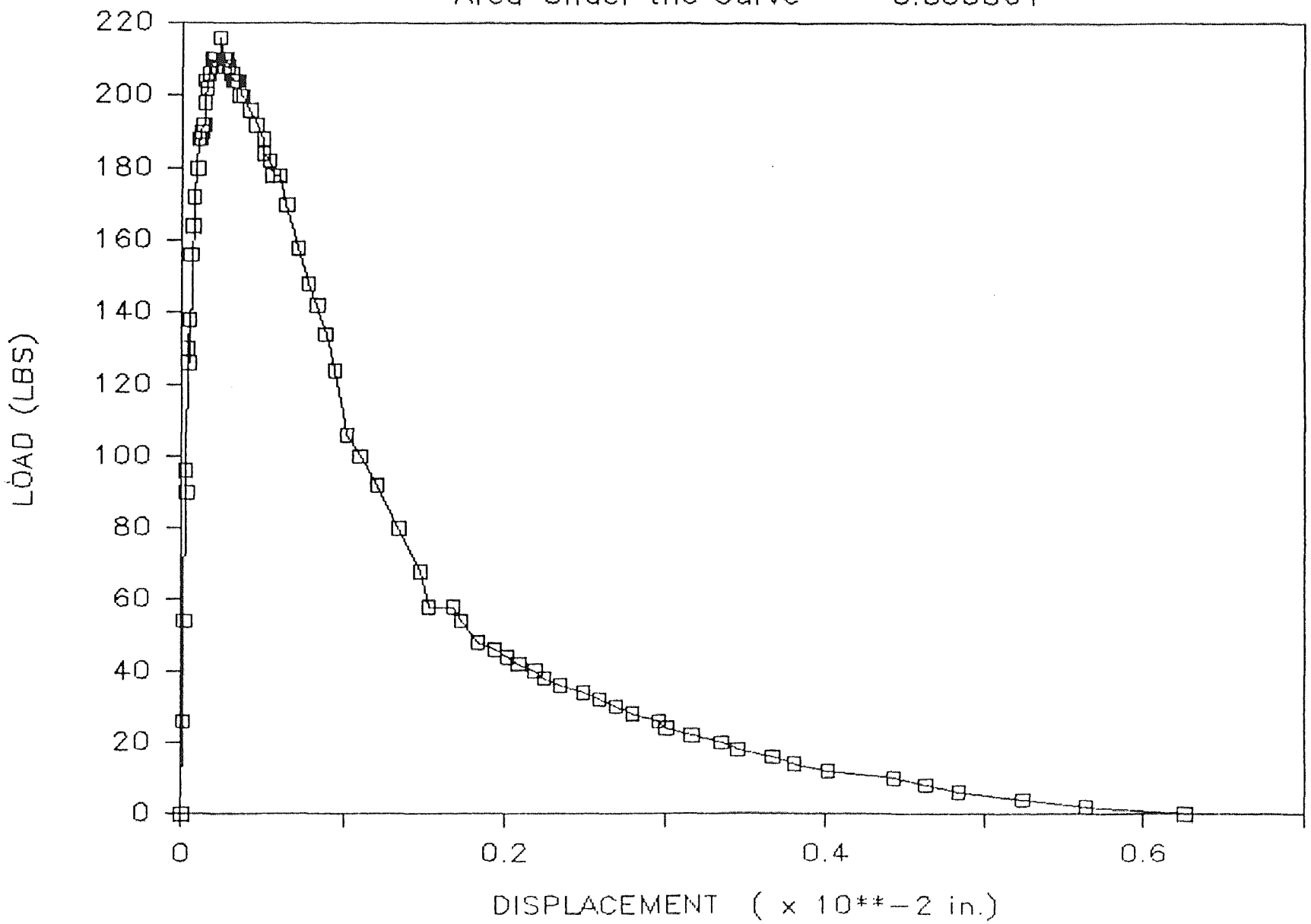

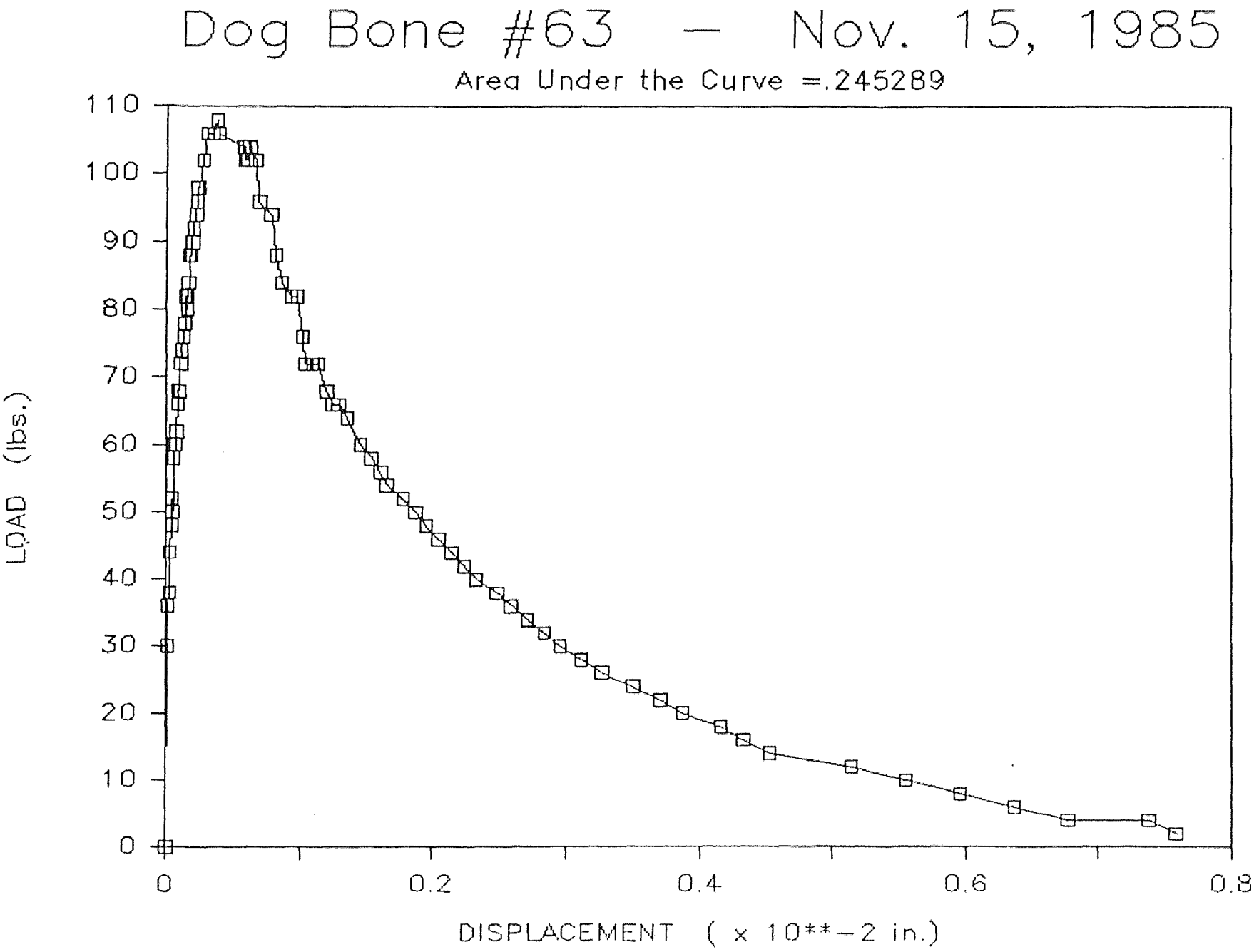
Dog Bone #63 — Nov. 15, 1985
Area Under the Curve =.245289
LOAD (lbs.)
110
100
90
80
70
60
50
40
30
20
10
0
0
0.2
0.4
0.6
0.8
DISPLACEMENT (x 10**-2 in.)

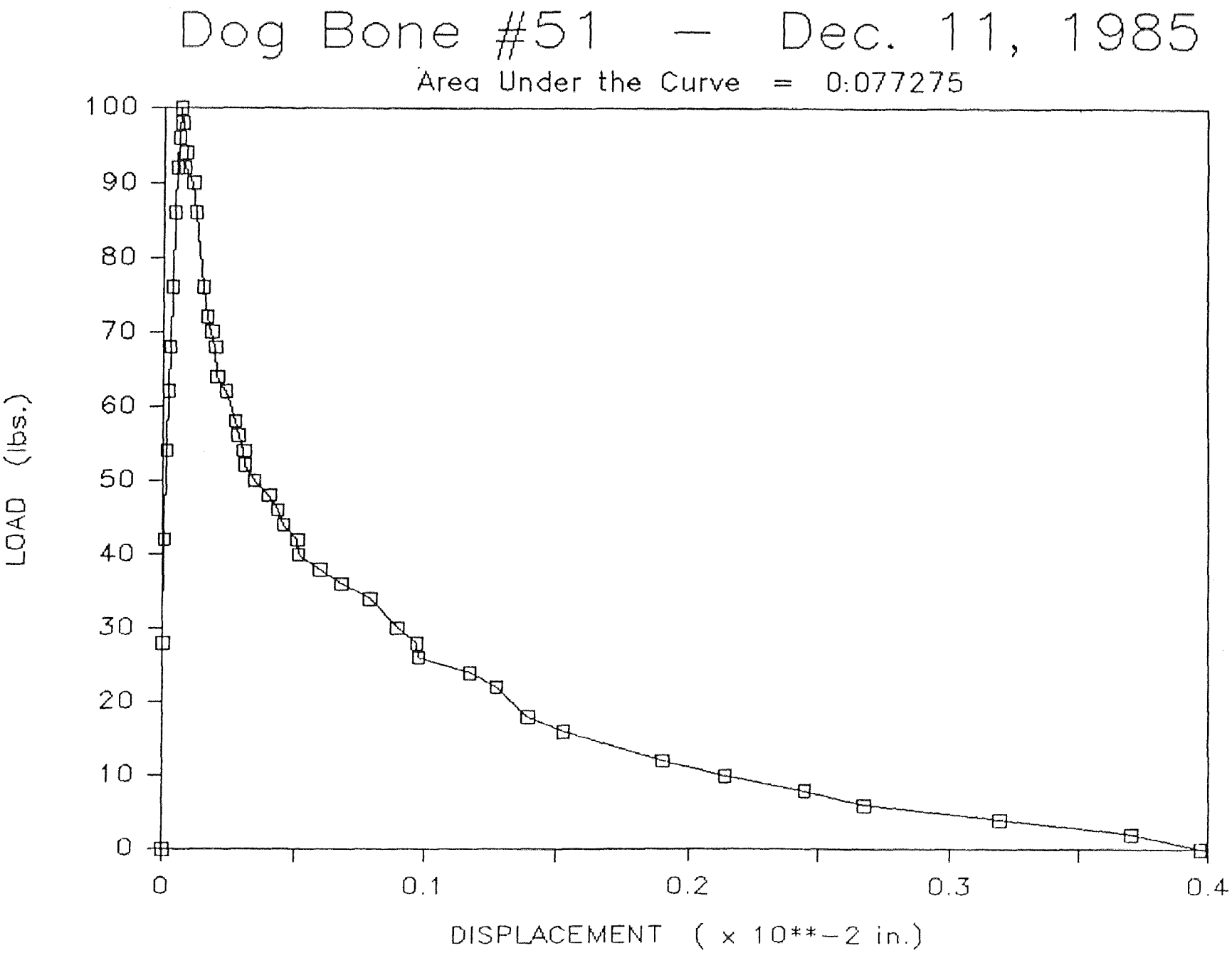
Dog Bone #51 — Dec. 11, 1985
Area Under the Curve = 0:077275
LOAD (lbs.)
100
90
80
70
60
50
40
30
20
10
0
0
0.1
0.2
0.3
0.4
DISPLACEMENT (x 10**-2 in.)

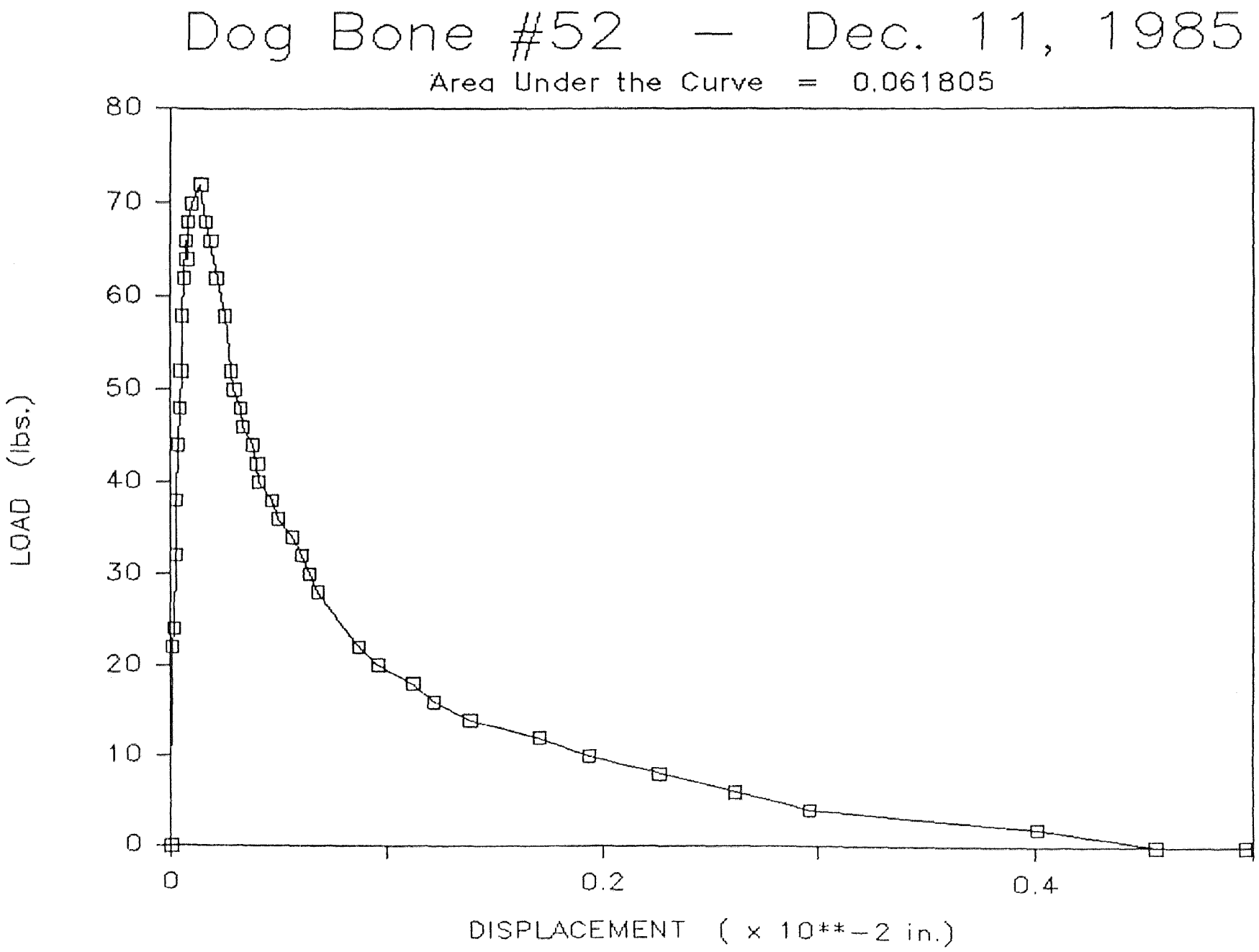
Dog Bone #52 — Dec. 11, 1985
Area Under the Curve = 0.061805
80
70
60
50
40
30
20
10
0
LOAD (lbs.)
0
0.2
0.4
DISPLACEMENT (x 10**-2 in.)

Dog Bone #56 — Dec. 11, 1985

Area Under the Curve = 0.115178

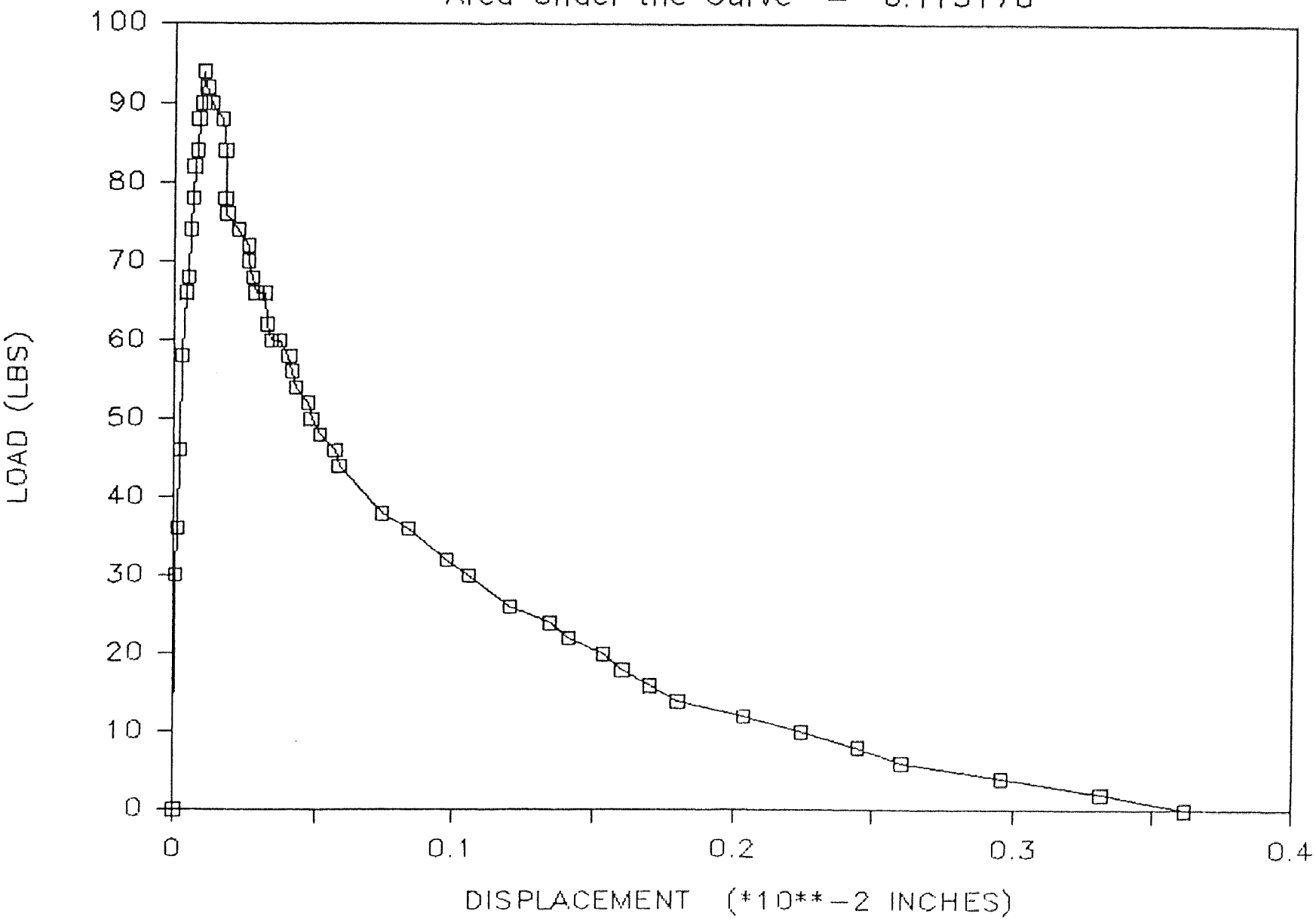

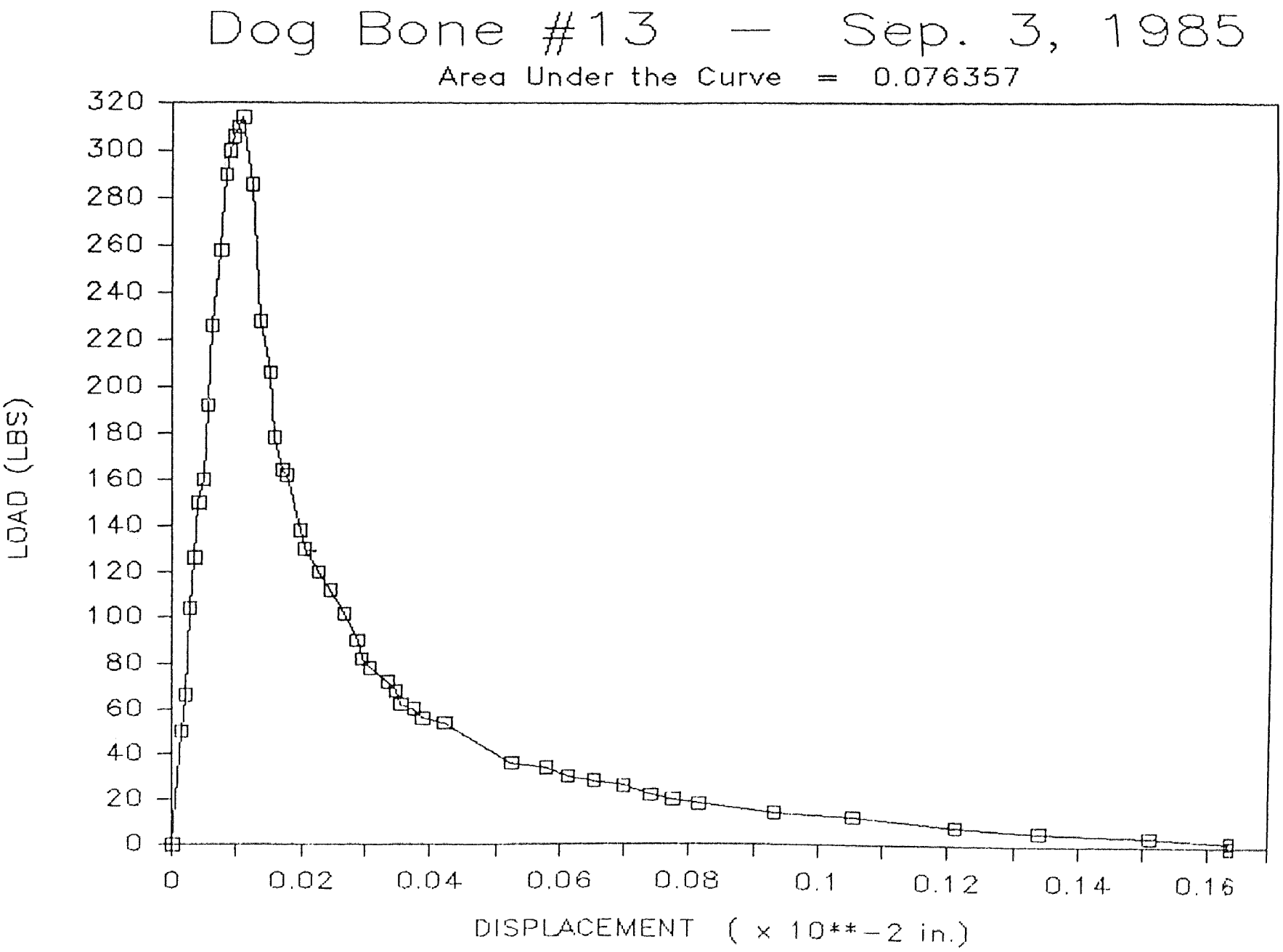
Dog Bone #13 — Sep. 3, 1985
Area Under the Curve = 0.076357
LOAD (LBS)
320
300
280
260
240
220
200
180
160
140
120
100
80
60
40
20
0
0
0.02
0.04
0.06
0.08
0.1
0.12
0.14
0.16
DISPLACEMENT (x 10**-2 in.)

Dog Bone #14 — Sep. 3, 1985

Area Under the curve = 0.085197

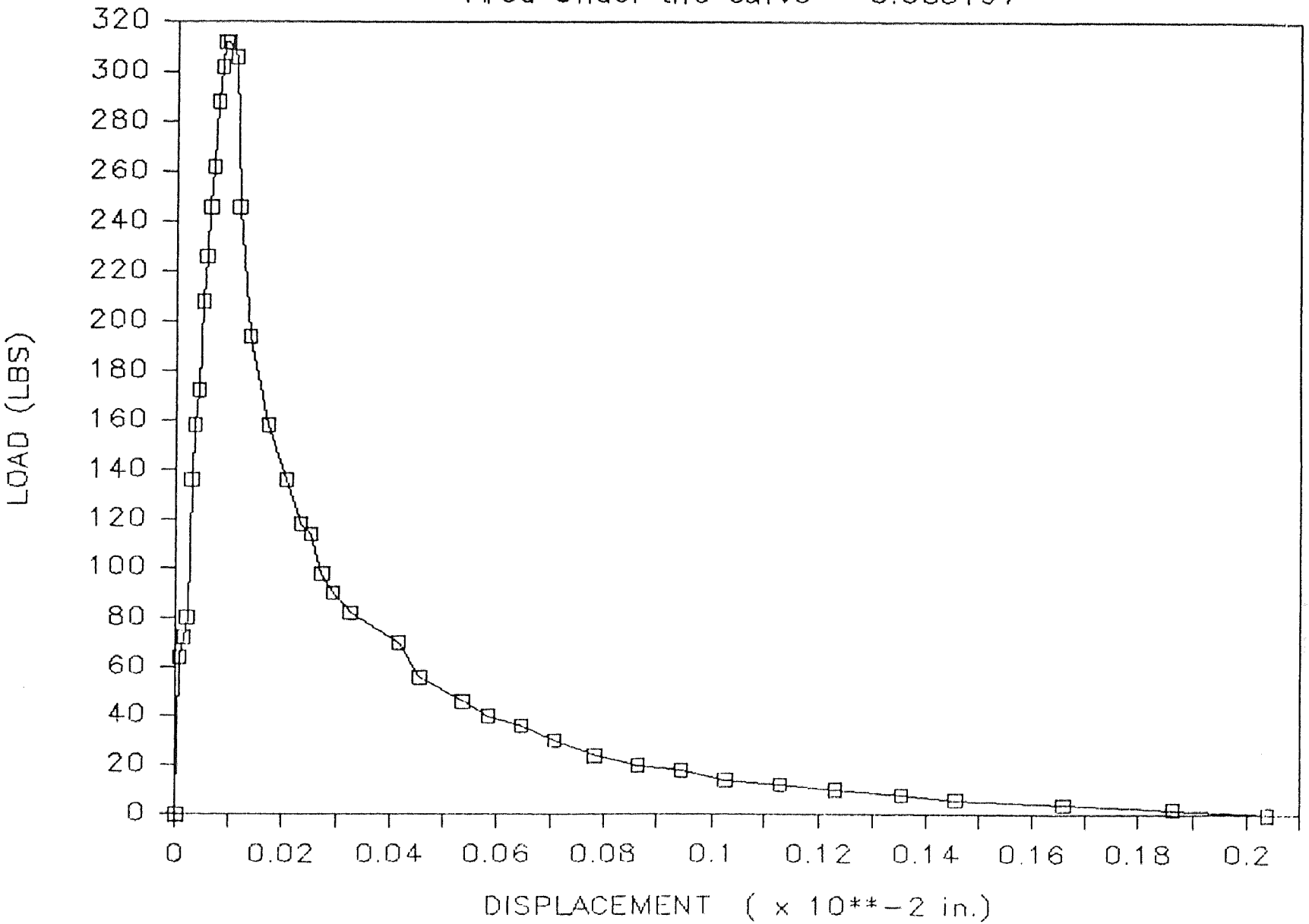

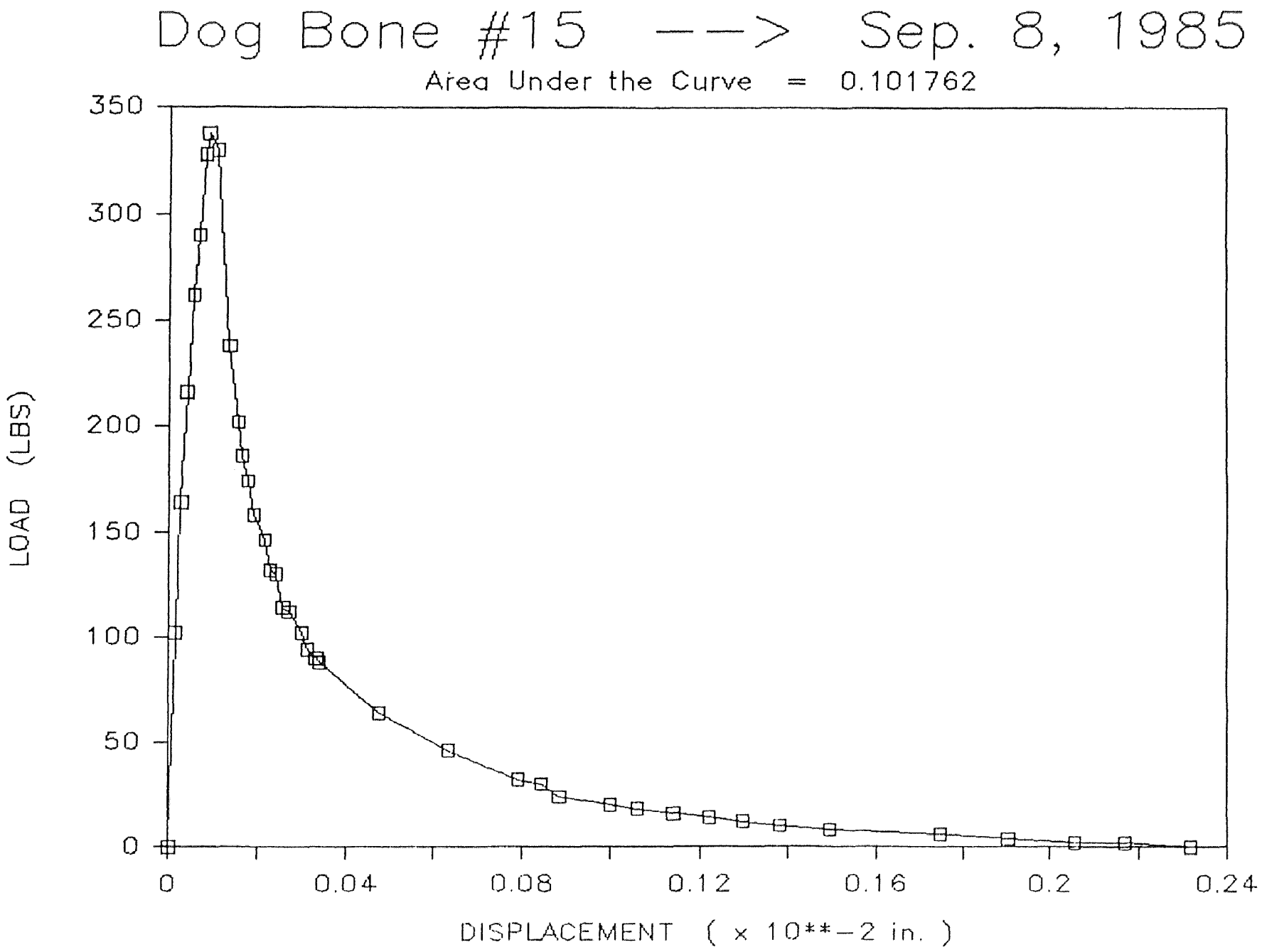
Dog Bone #15 --> Sep. 8, 1985
Area Under the Curve = 0.101762
350
300
250
200
150
100
50
0
LOAD (LBS)
0
0.04
0.08
0.12
0.16
0.2
0.24
DISPLACEMENT (x 10**-2 in.)

APPENDIX B

STRESS DISPLACEMENT RELATIONSHIPS

DOGBONE #2 --> TEST DATE: JULY 17, 19

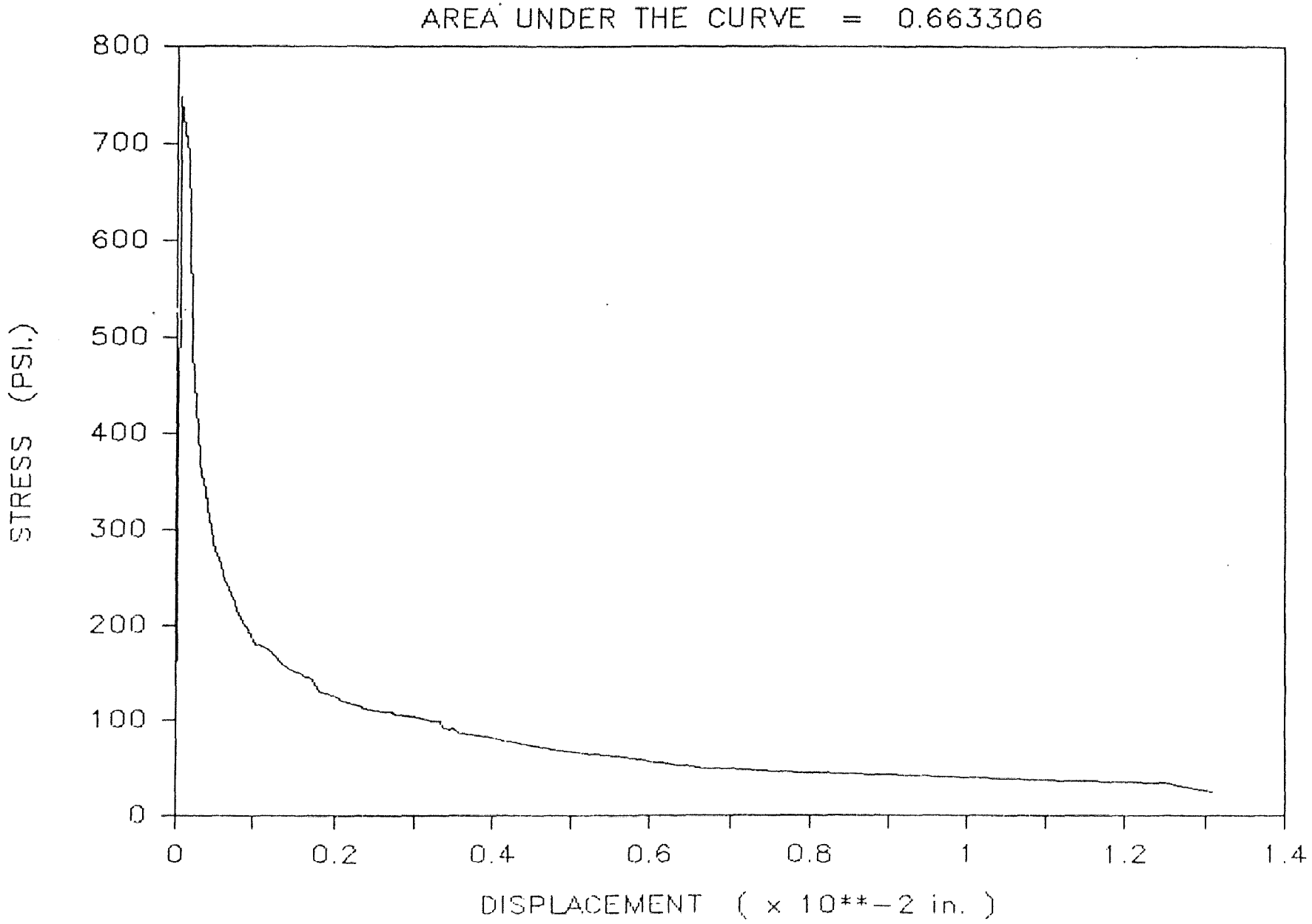

Dog Bone #9 — Aug. 19, 1985

Area Under the Curve = 0.330609

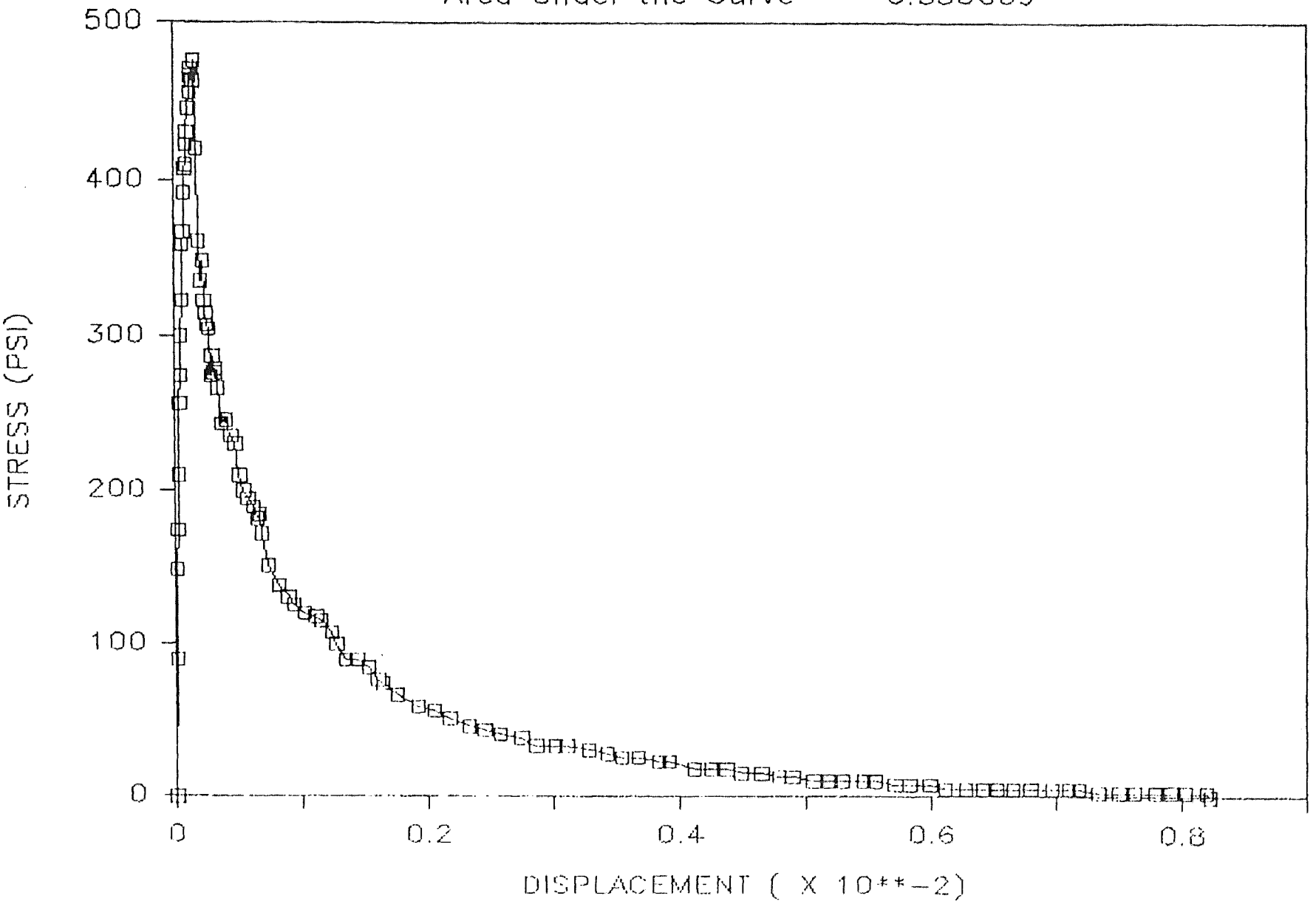

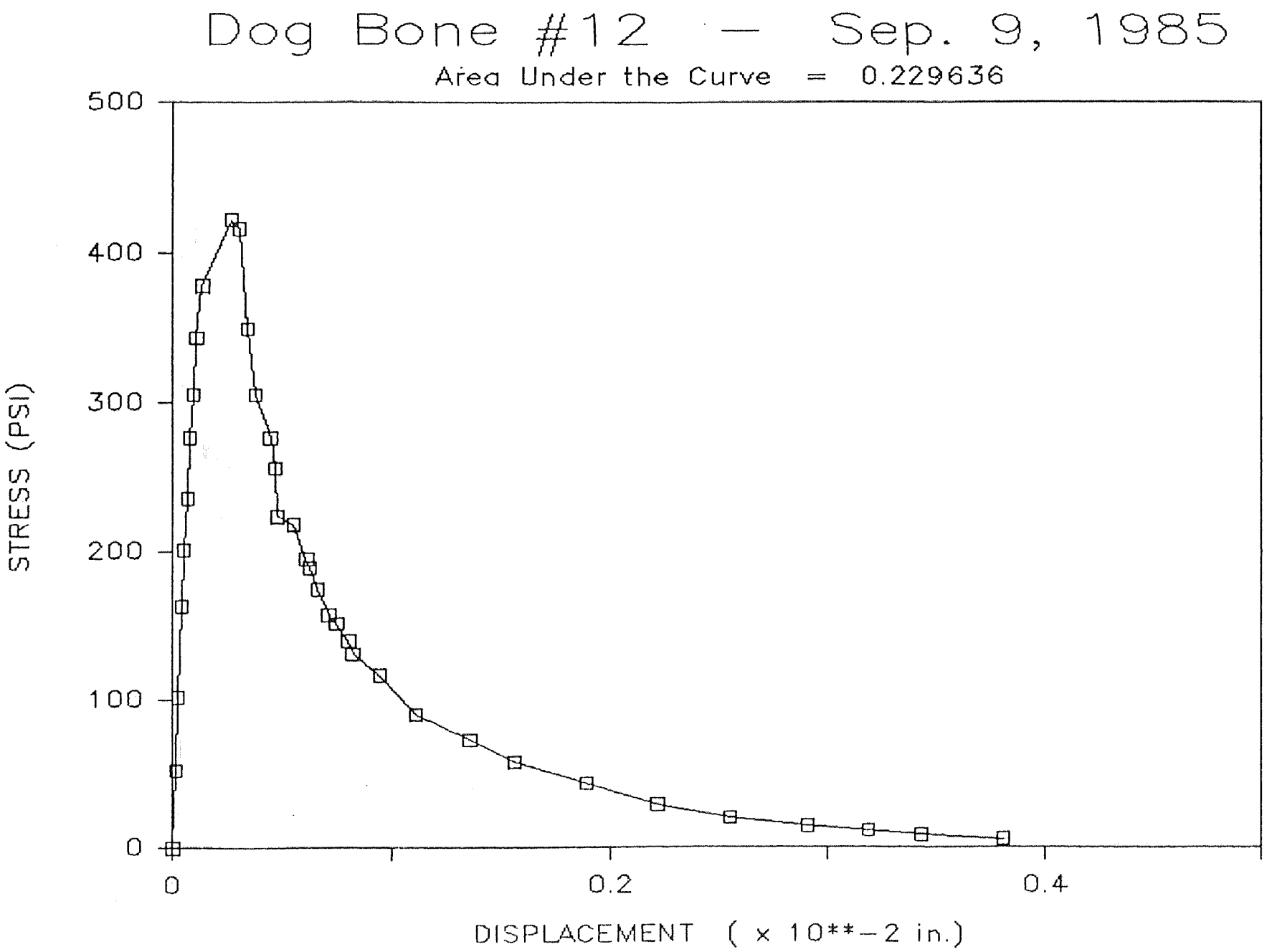
Dog Bone #12 — Sep. 9, 1985
Area Under the Curve = 0.229636
500
400
300
200
100
0
STRESS (PSI)
0
0.2
0.4
DISPLACEMENT (x 10**-2 in.)

DOGBONE 68 --> TEST DATE: 3-4-86

AREA UNDER THE CURVE = 0.21078

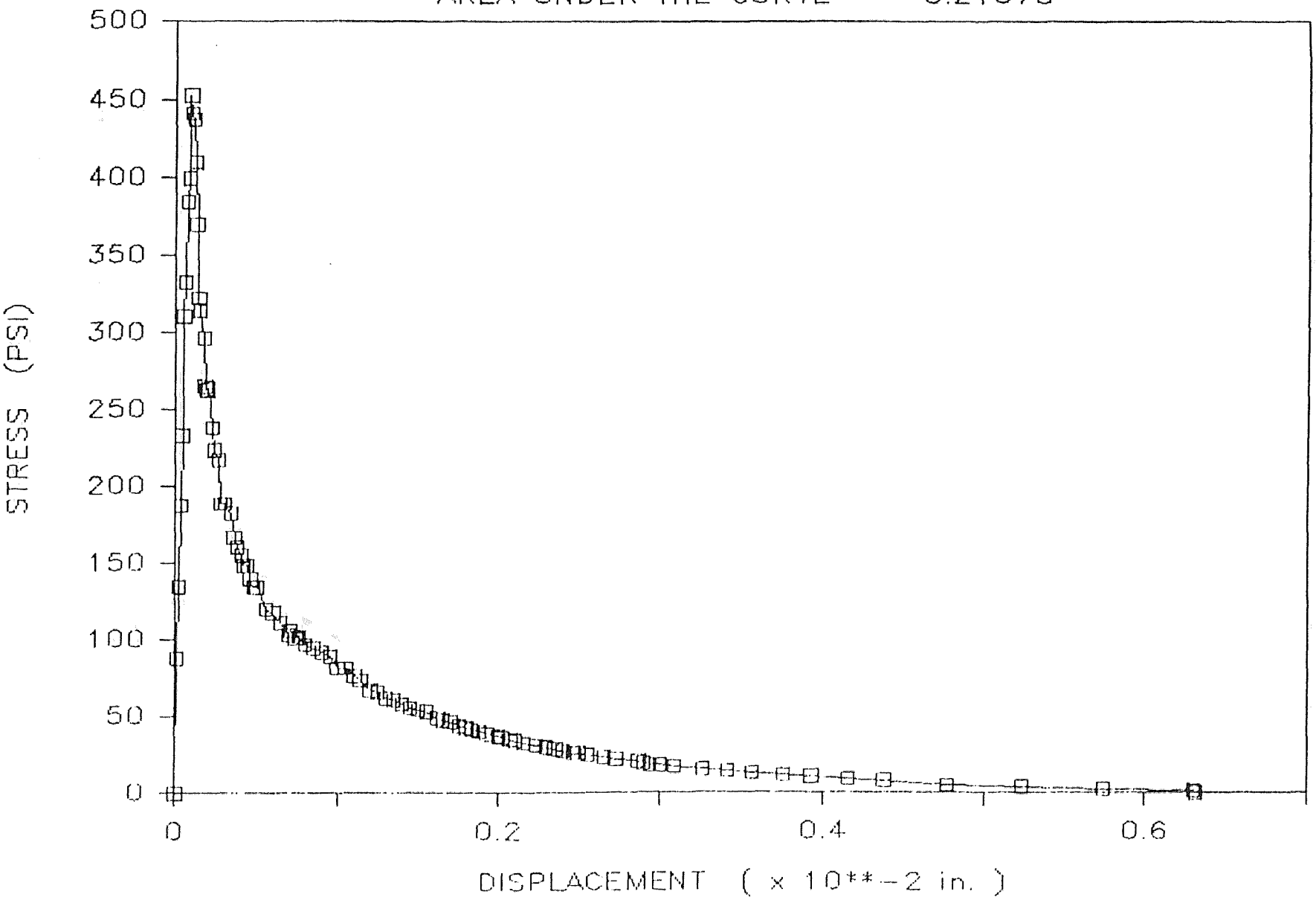

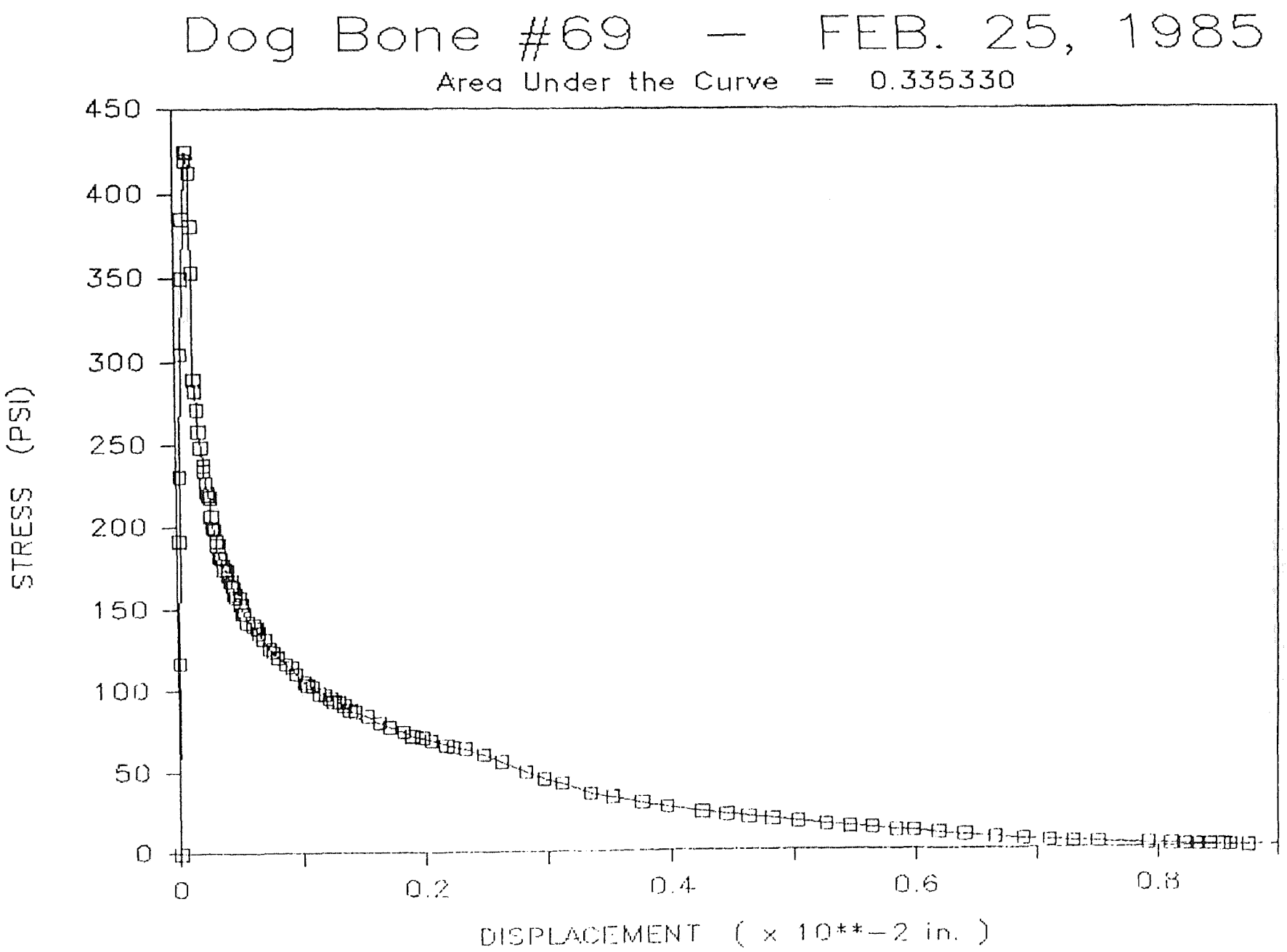
Dog Bone #69 — FEB. 25, 1985
Area Under the Curve = 0.335330
450
400
350
300
250
200
150
100
50
0
STRESS (PSI)
0
0.2
0.4
0.6
0.8
DISPLACEMENT (x 10**-2 in.)

Dogbone #70 --> Test Date: 3 - 26 - 8

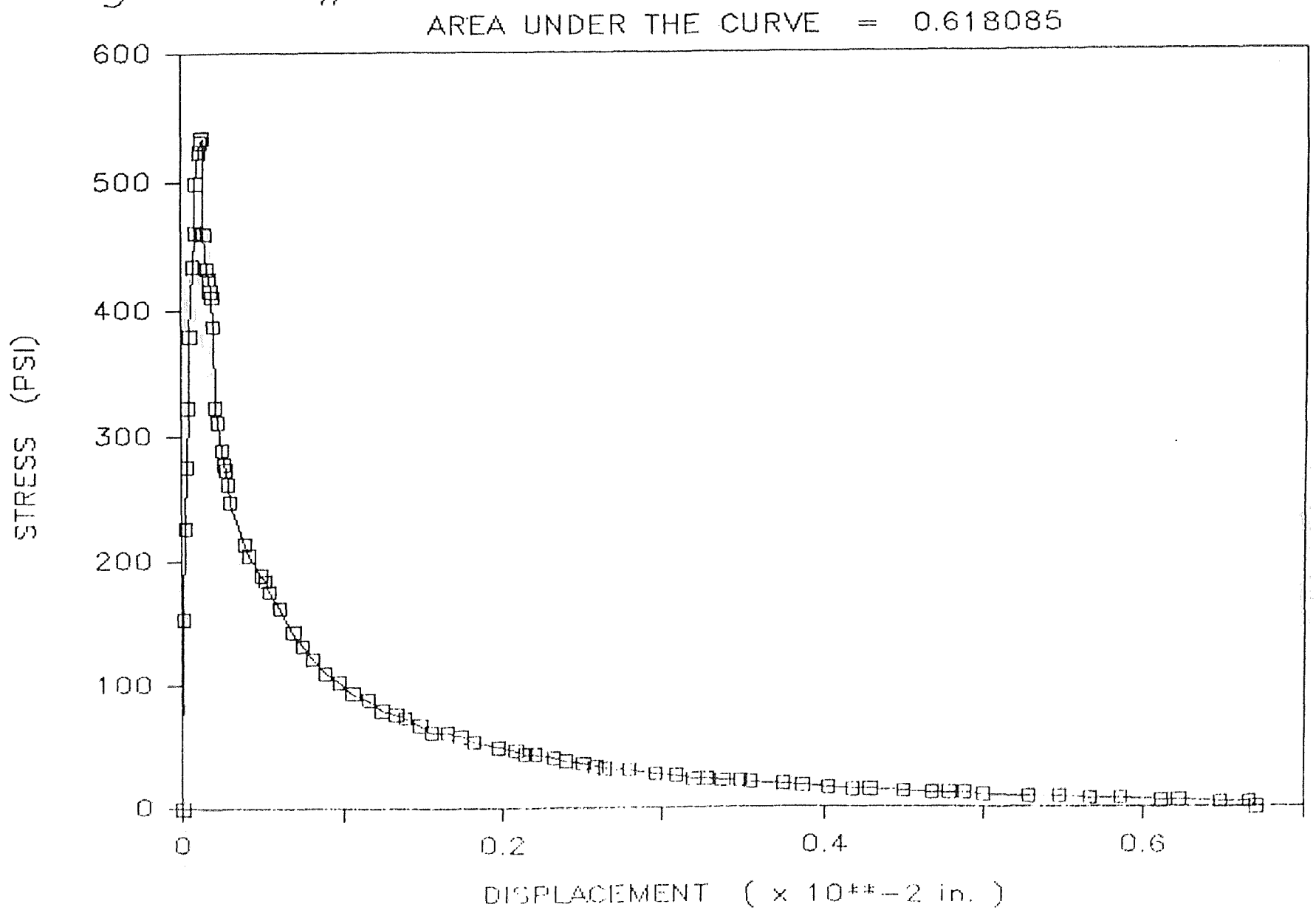

Dogbone 71 --> Test Date: 4-2-86

AREA UNDER THE CURVE = 0.282825

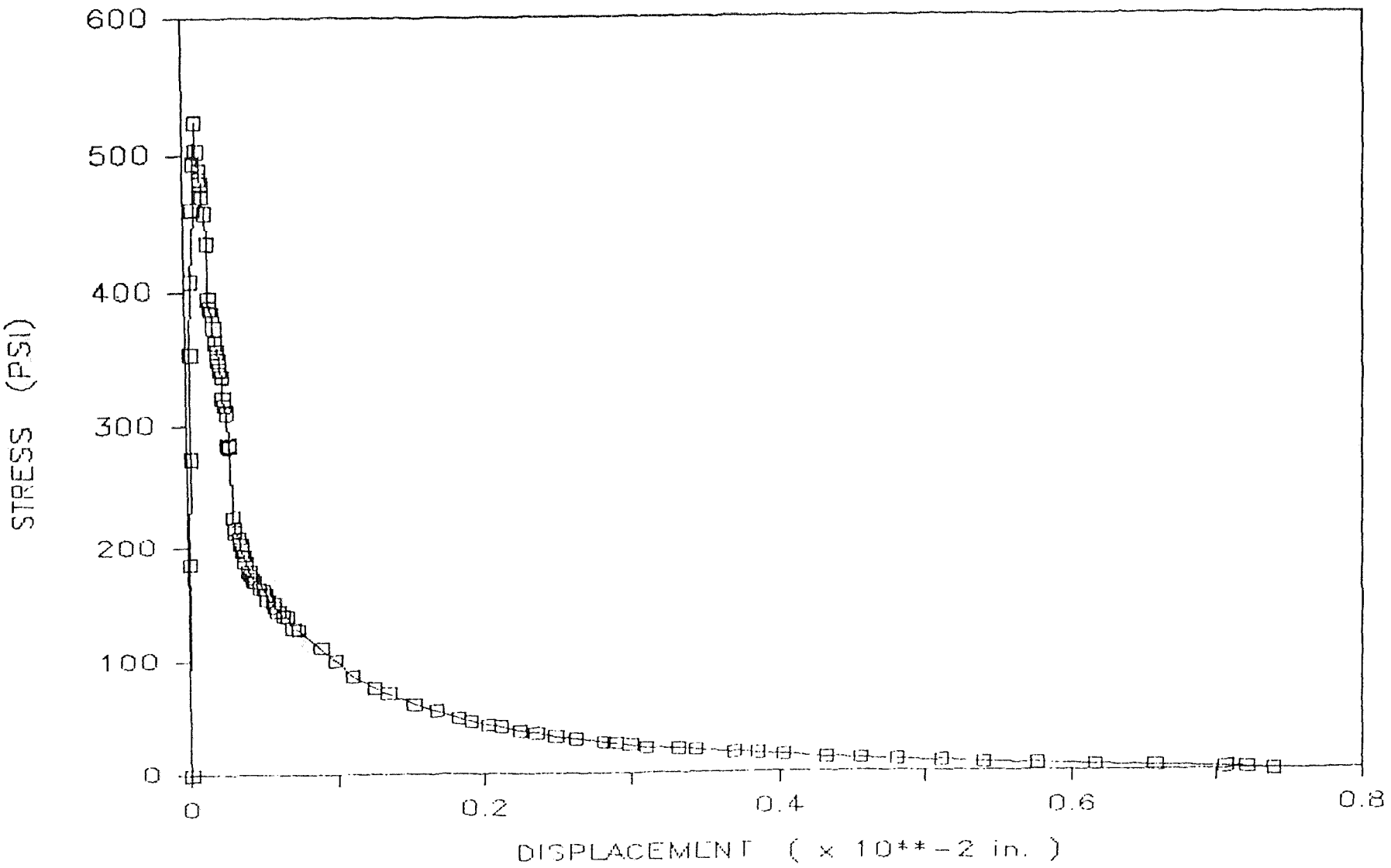

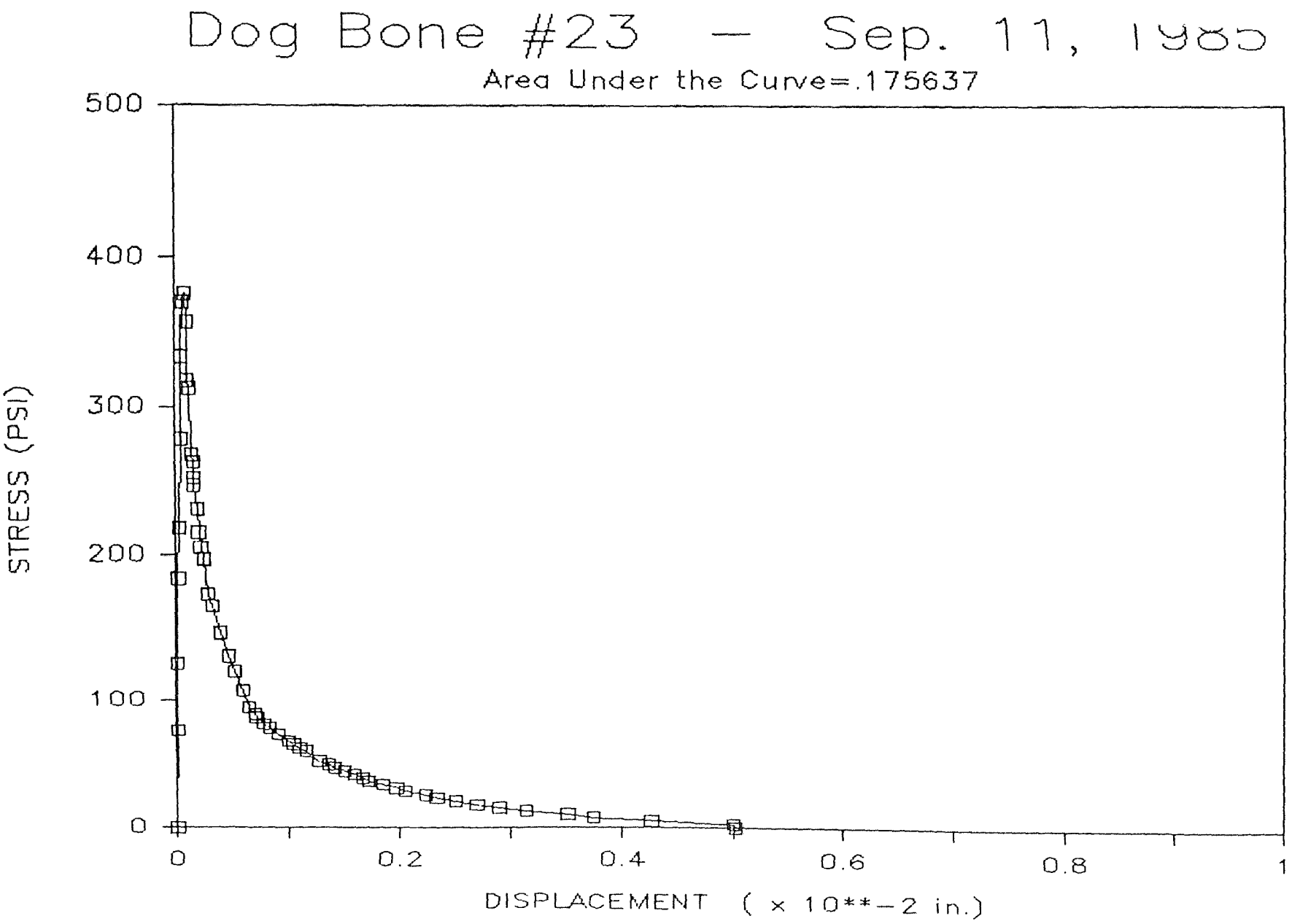
Dog Bone #23 — Sep. 11, 1985
Area Under the Curve=.175637
500
400
300
200
100
0
STRESS (PSI)
0
0.2
0.4
0.6
0.8
1
DISPLACEMENT (x 10**-2 in.)

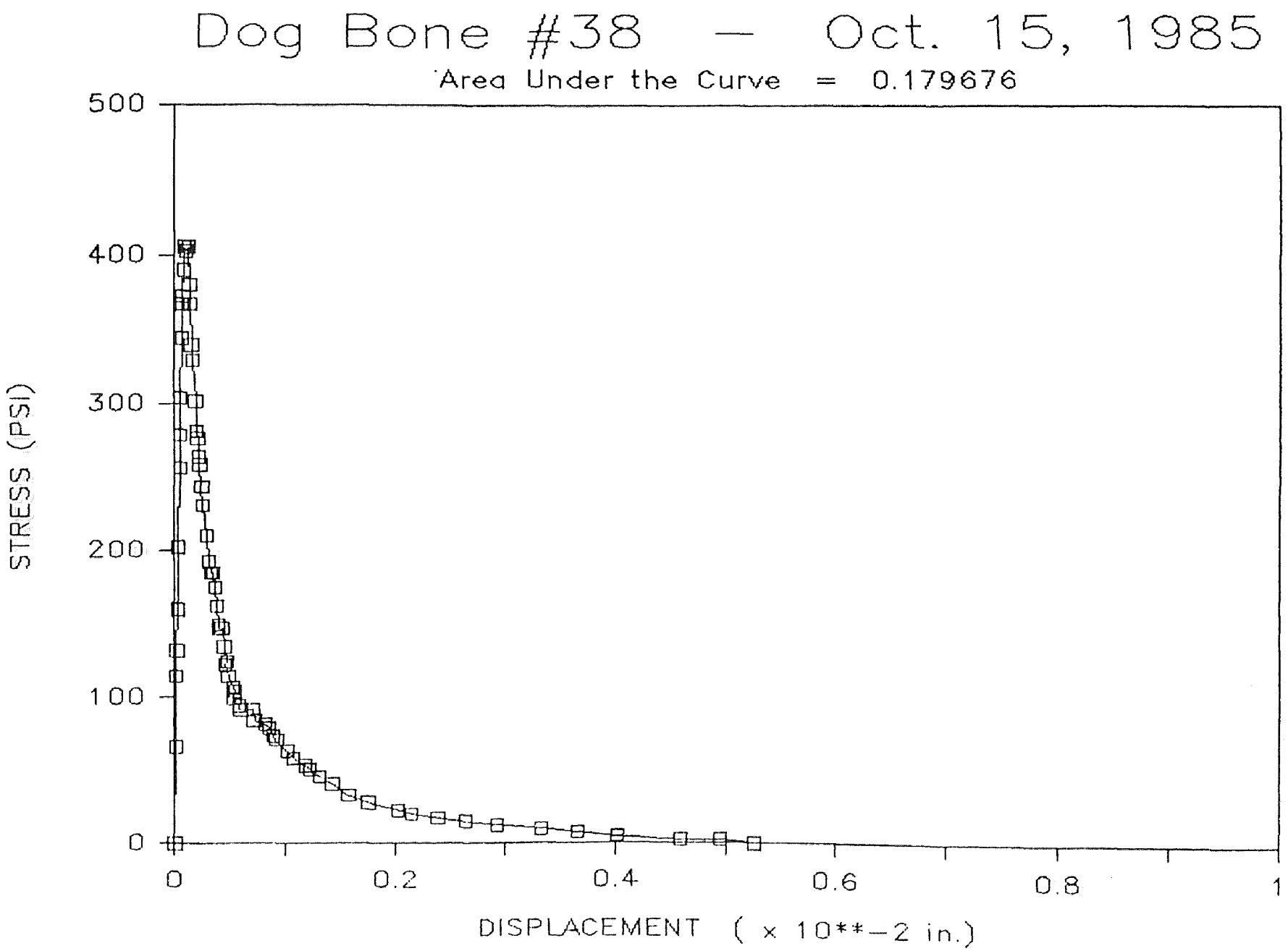
Dog Bone #38 — Oct. 15, 1985
Area Under the Curve = 0.179676
500
400
300
200
100
0
STRESS (PSI)
0
0.2
0.4
0.6
0.8
1
DISPLACEMENT (x 10**-2 in.)

Dog Bone #39 — Oct. 15, 1985

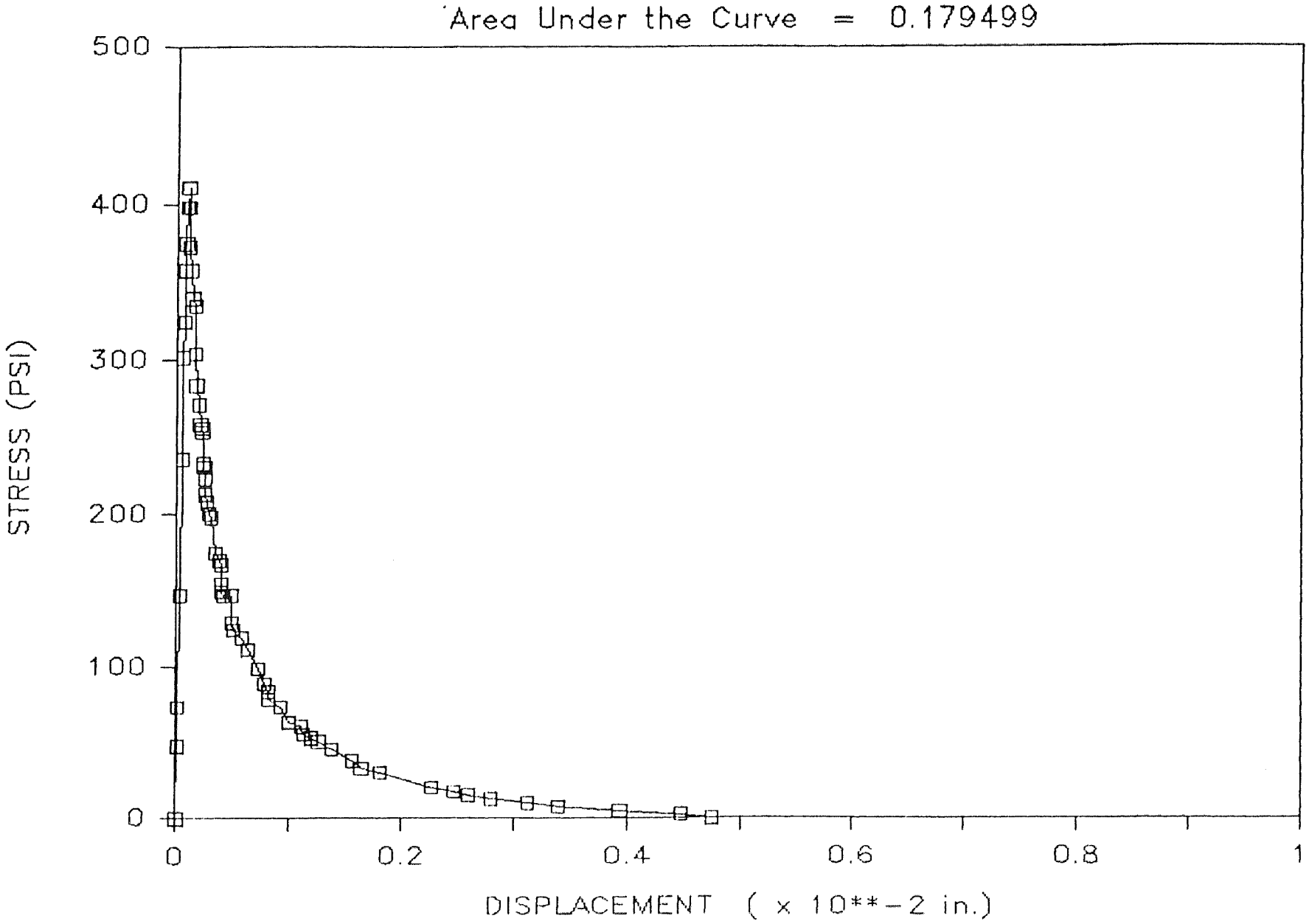

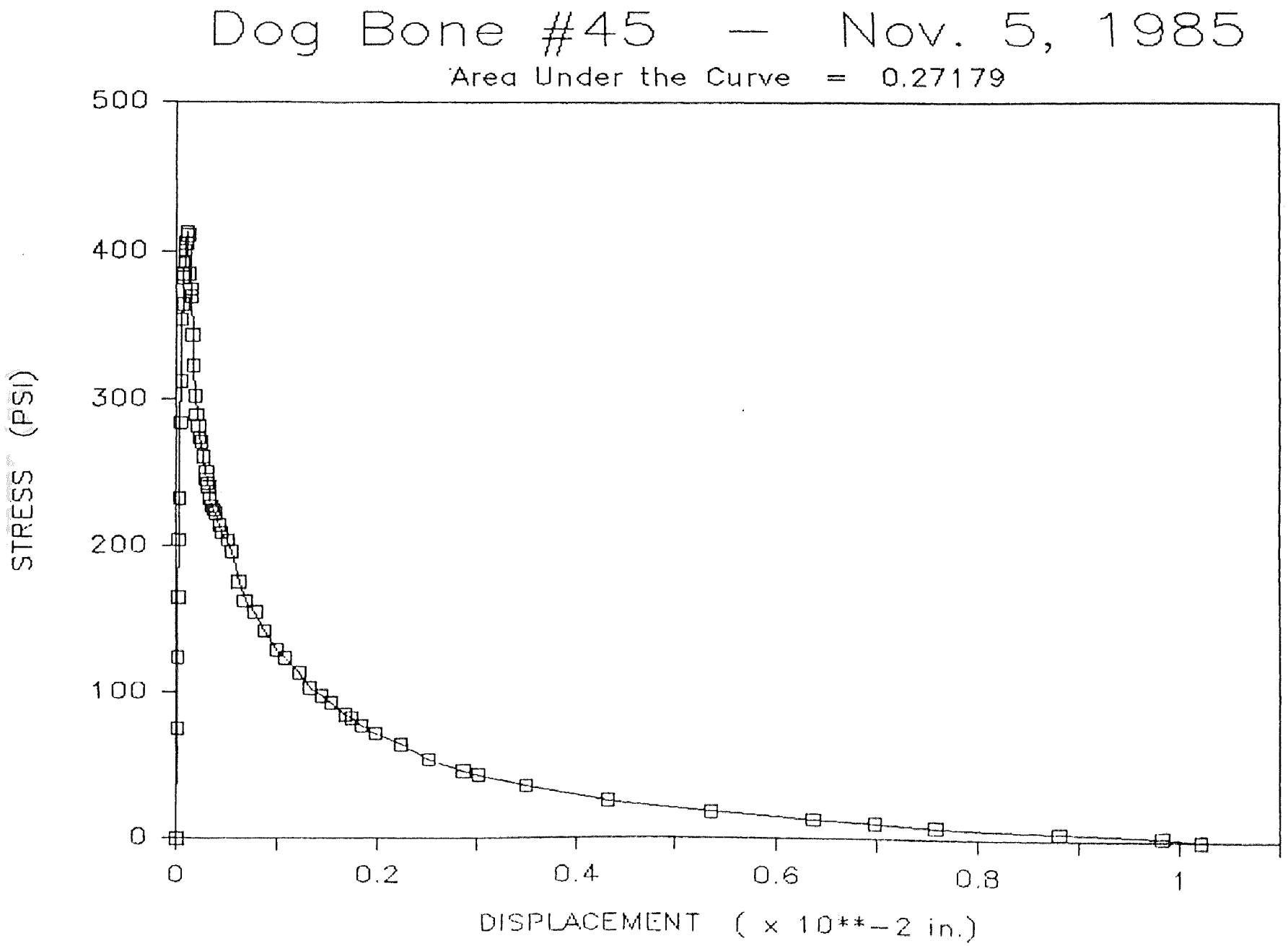
Dog Bone #45 — Nov. 5, 1985
Area Under the Curve = 0.27179
500
400
300
200
100
0
STRESS (PSI)
0
0.2
0.4
0.6
0.8
1
DISPLACEMENT (x 10**-2 in.)

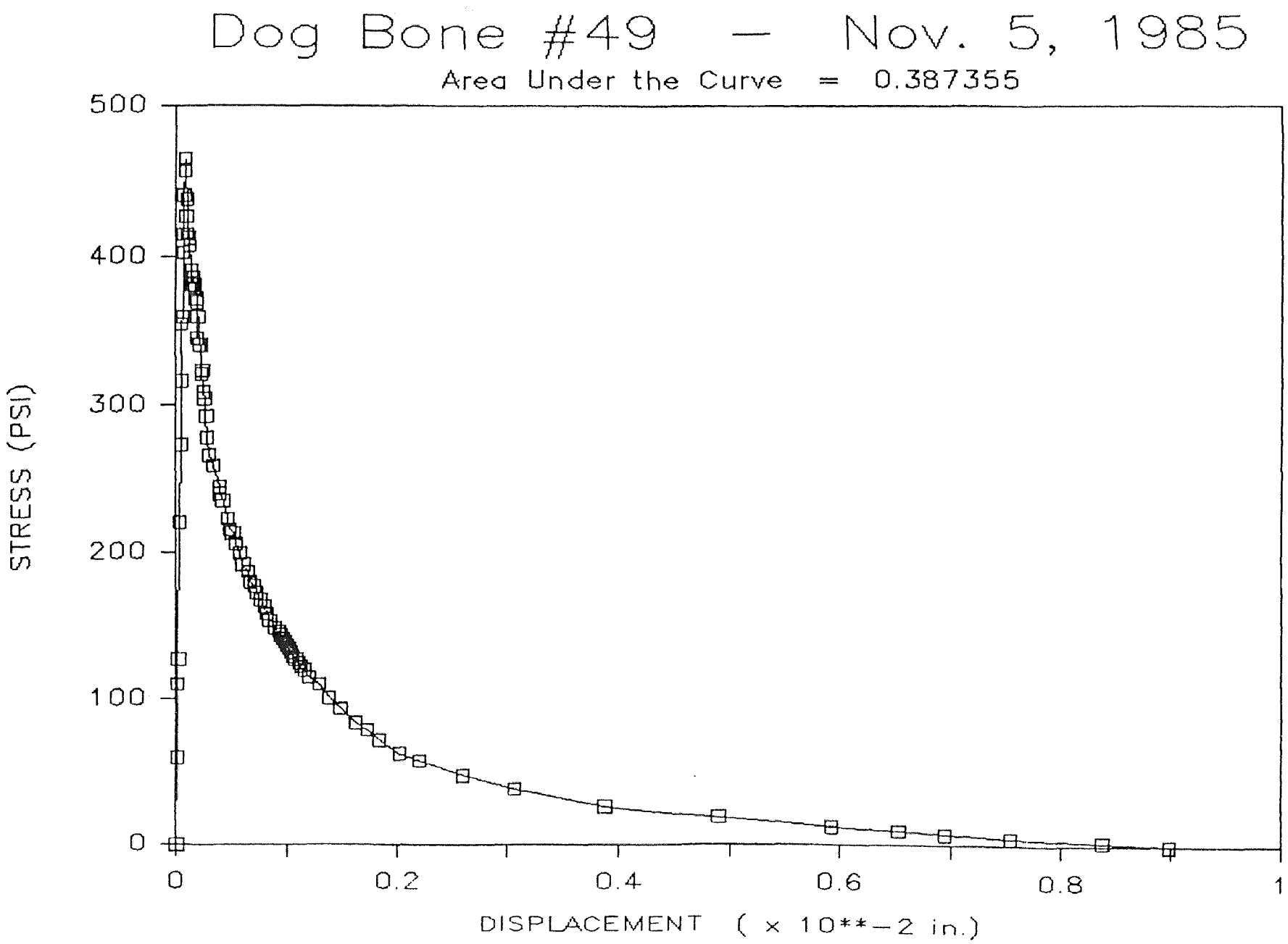
Dog Bone #49 — Nov. 5, 1985
Area Under the Curve = 0.387355
500
400
300
200
100
0
STRESS (PSI)
0
0.2
0.4
0.6
0.8
1
DISPLACEMENT (x 10**-2 in.)

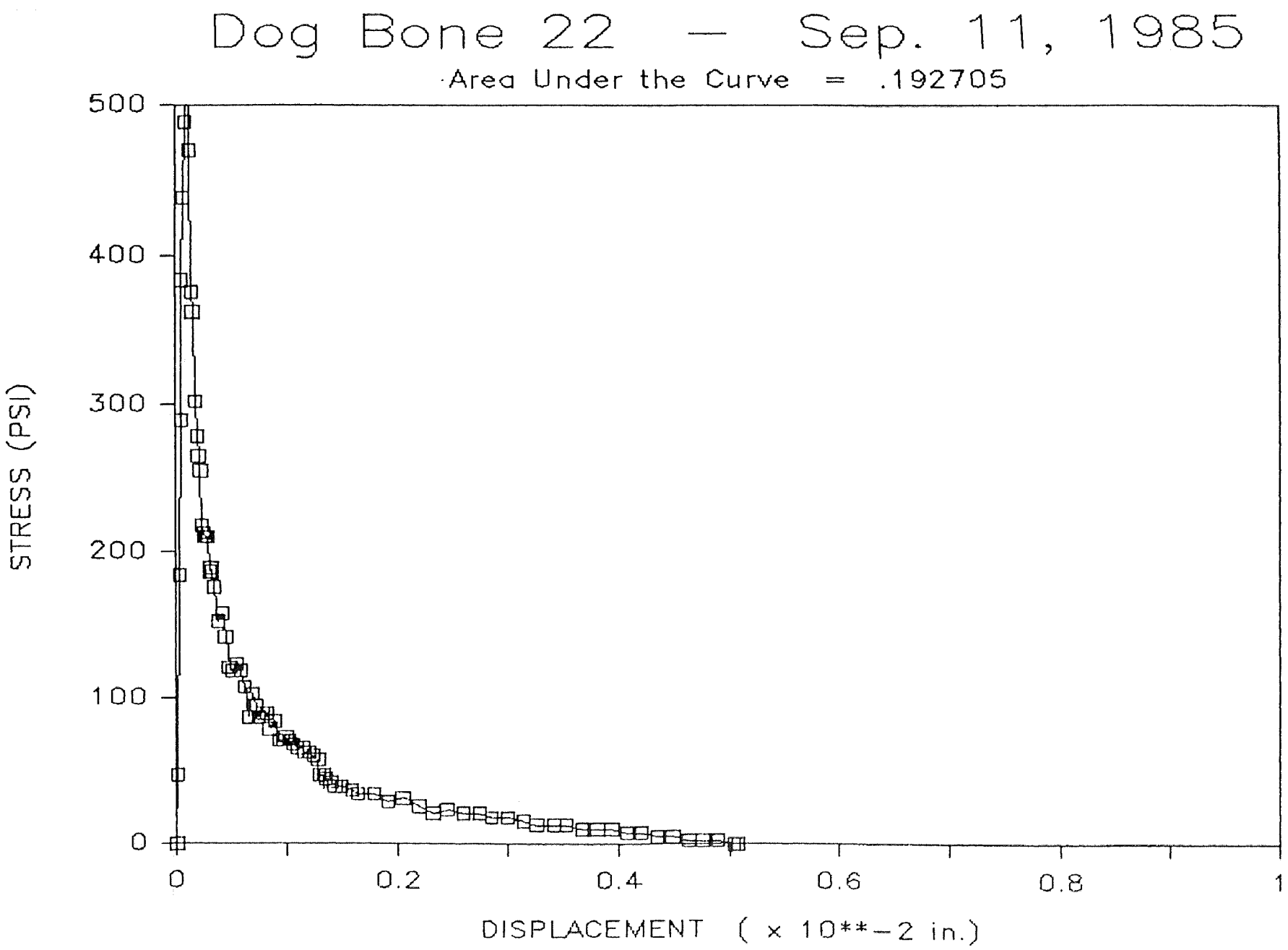
Dog Bone 22 — Sep. 11, 1985
Area Under the Curve = .192705
500
400
300
200
100
0
STRESS (PSI)
0
0.2
0.4
0.6
0.8
1
DISPLACEMENT (x 10**-2 in.)

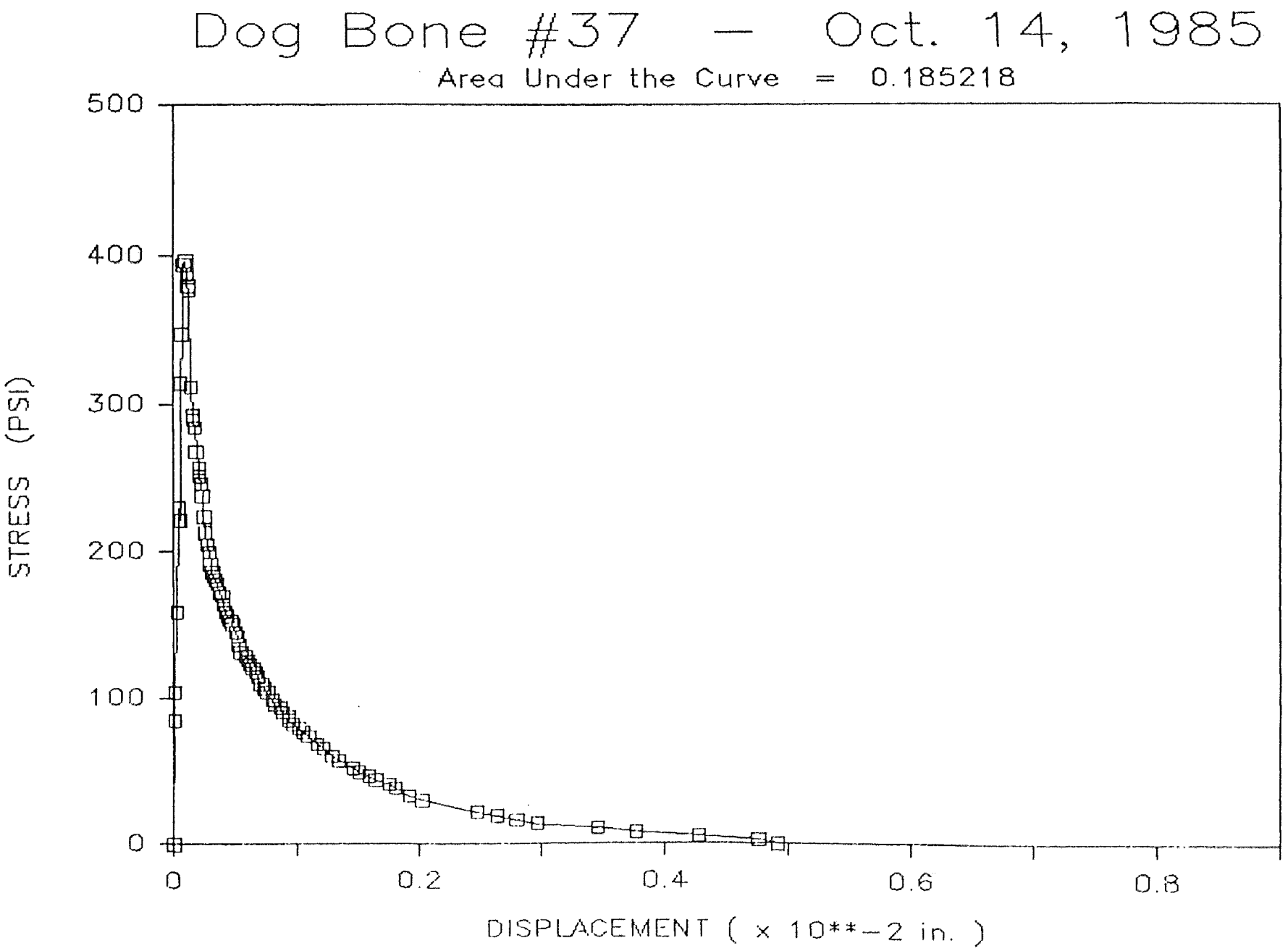
Dog Bone #37 — Oct. 14, 1985
Area Under the Curve = 0.185218
500
400
300
200
100
0
STRESS (PSI)
0
0.2
0.4
0.6
0.8
DISPLACEMENT (x 10**-2 in.)

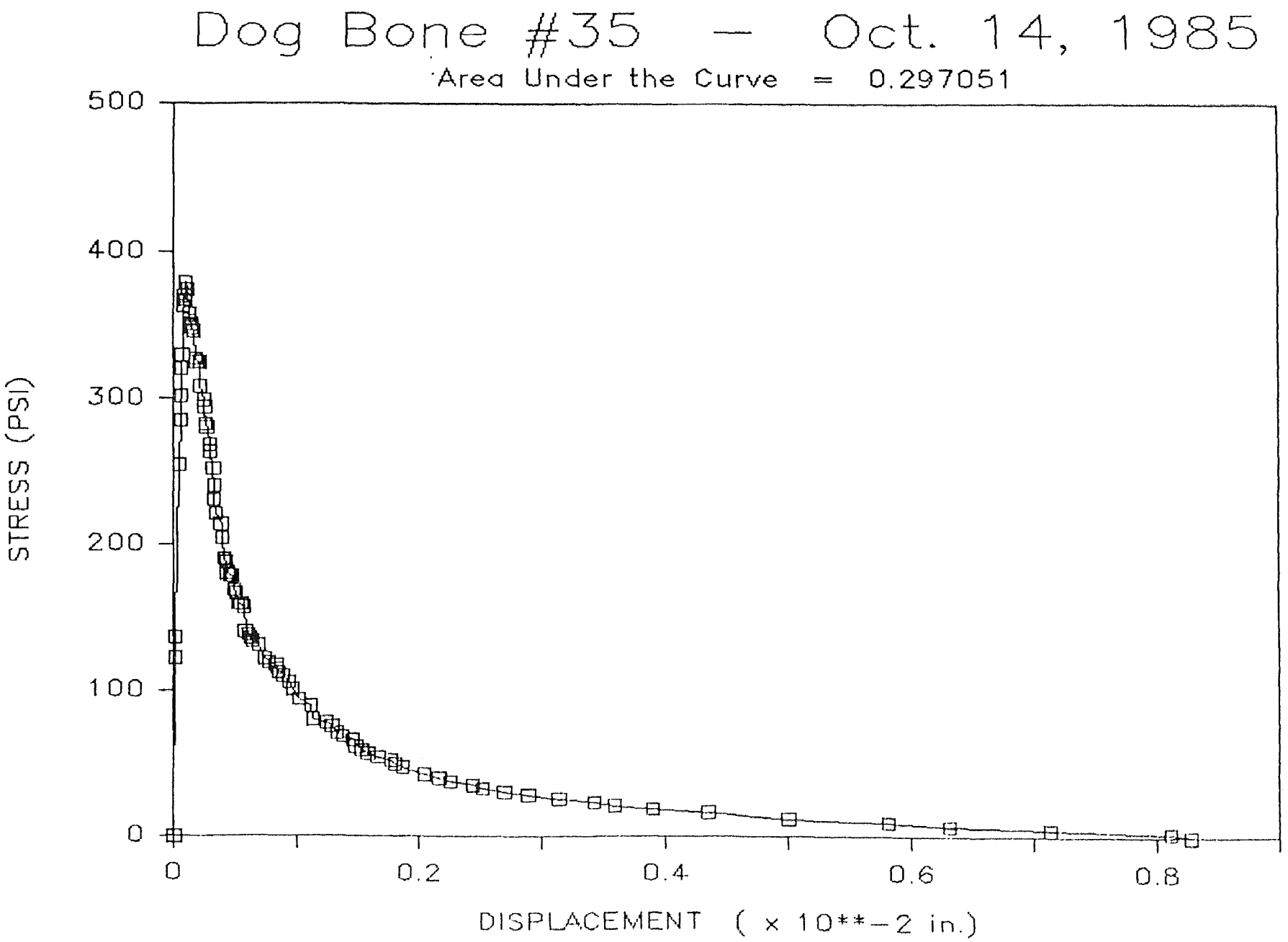
Dog Bone #35 — Oct. 14, 1985
Area Under the Curve = 0.297051
500
400
300
200
100
0
STRESS (PSI)
0
0.2
0.4
0.6
0.8
DISPLACEMENT (x 10**-2 in.)

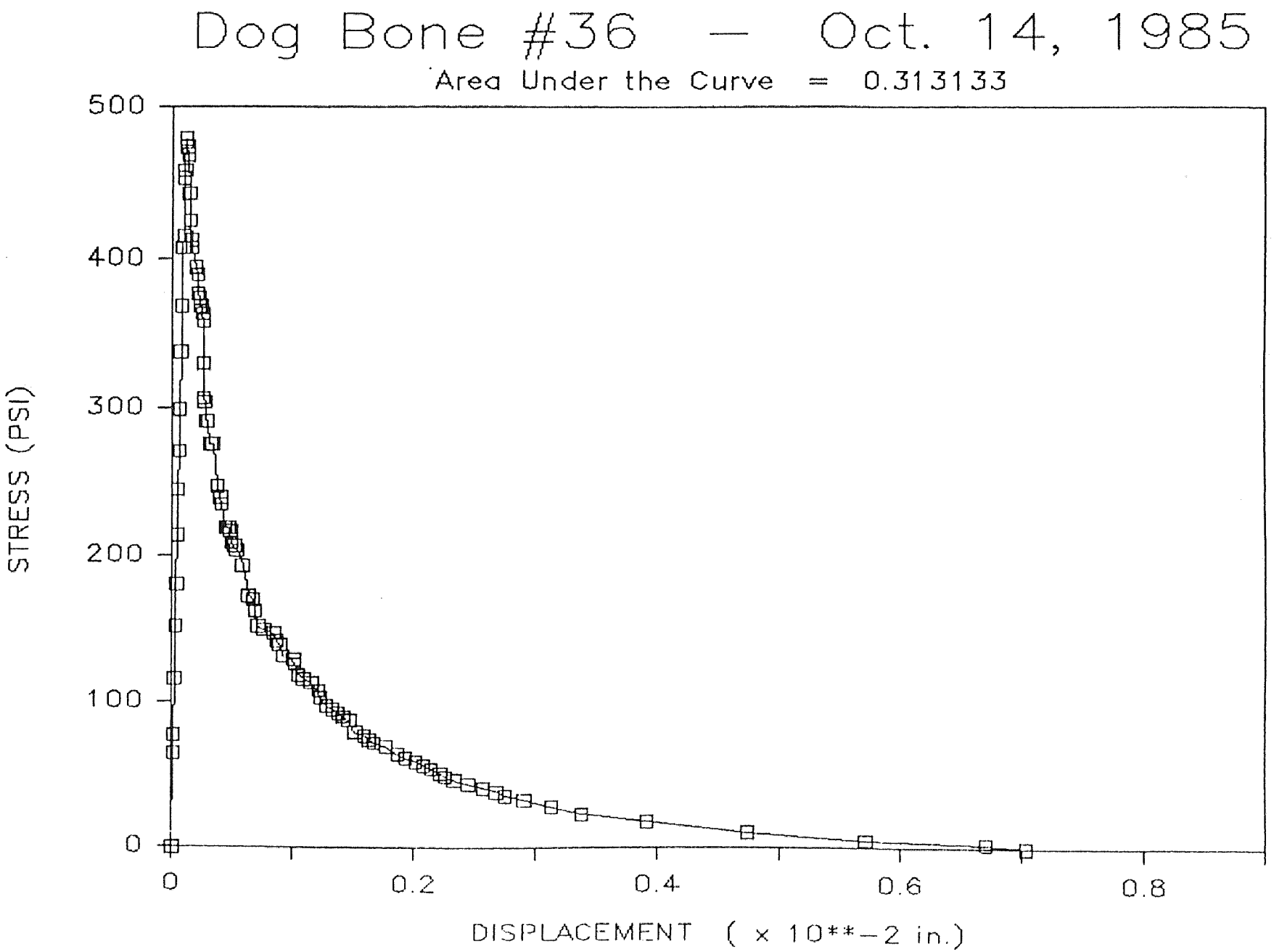
Dog Bone #36 — Oct. 14, 1985
Area Under the Curve = 0.313133
500
400
300
200
100
0
STRESS (PSI)
0
0.2
0.4
0.6
0.8
DISPLACEMENT (x 10**-2 in.)

Dog Bone #59 — Nov. 14, 1985

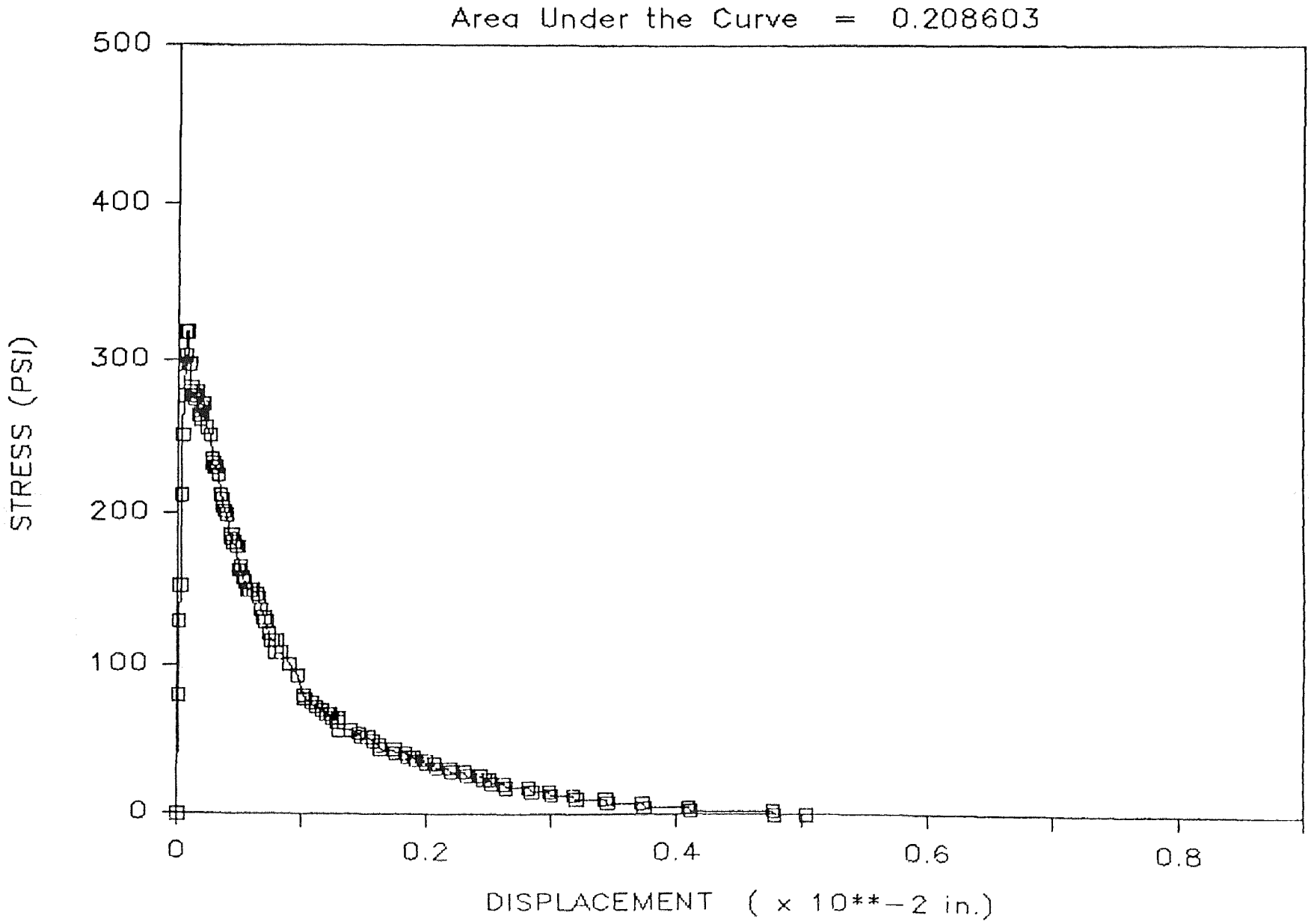

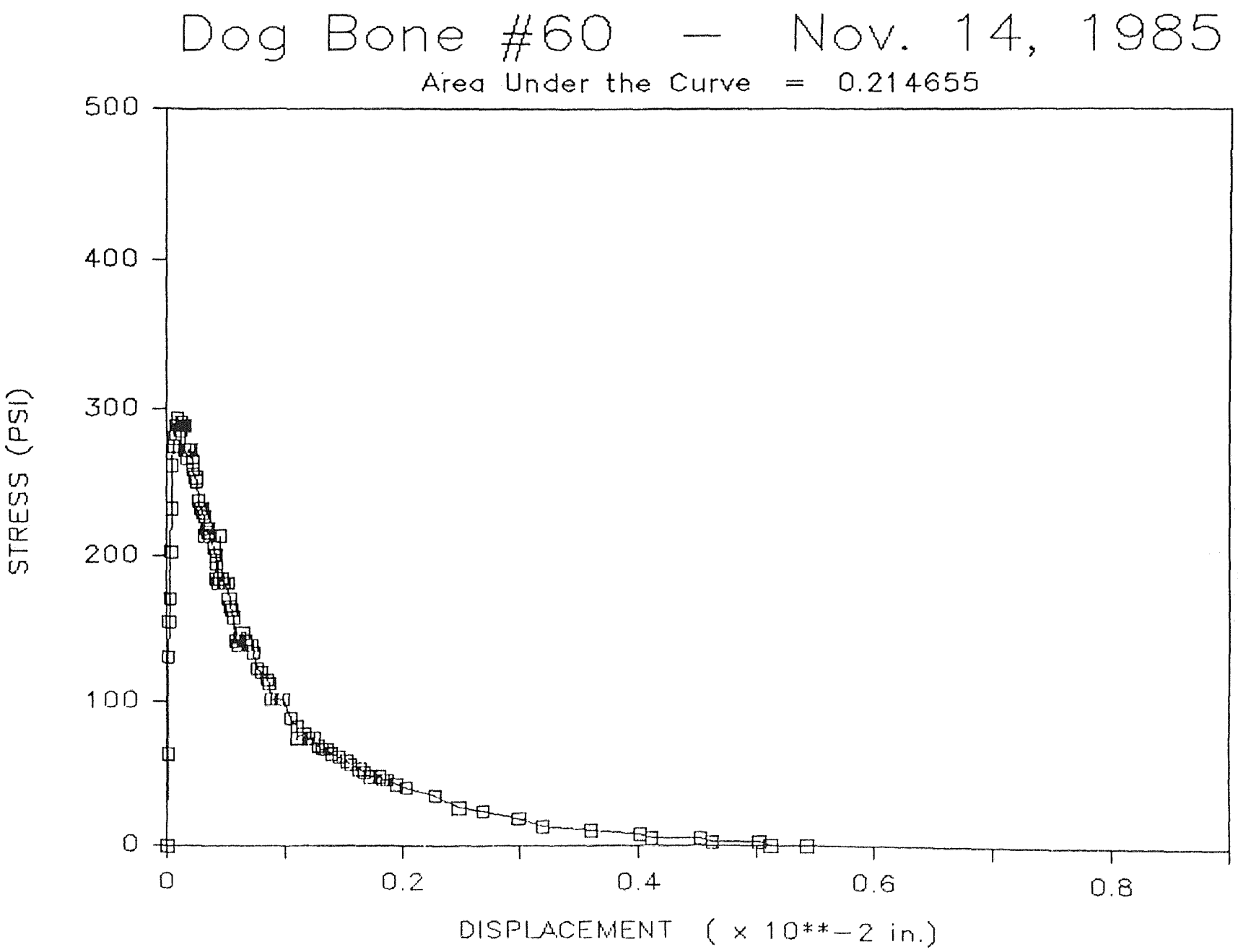
Dog Bone #60 — Nov. 14, 1985
Area Under the Curve = 0.214655
500
400
300
200
100
0
STRESS (PSI)
0
0.2
0.4
0.6
0.8
DISPLACEMENT (x 10**-2 in.)

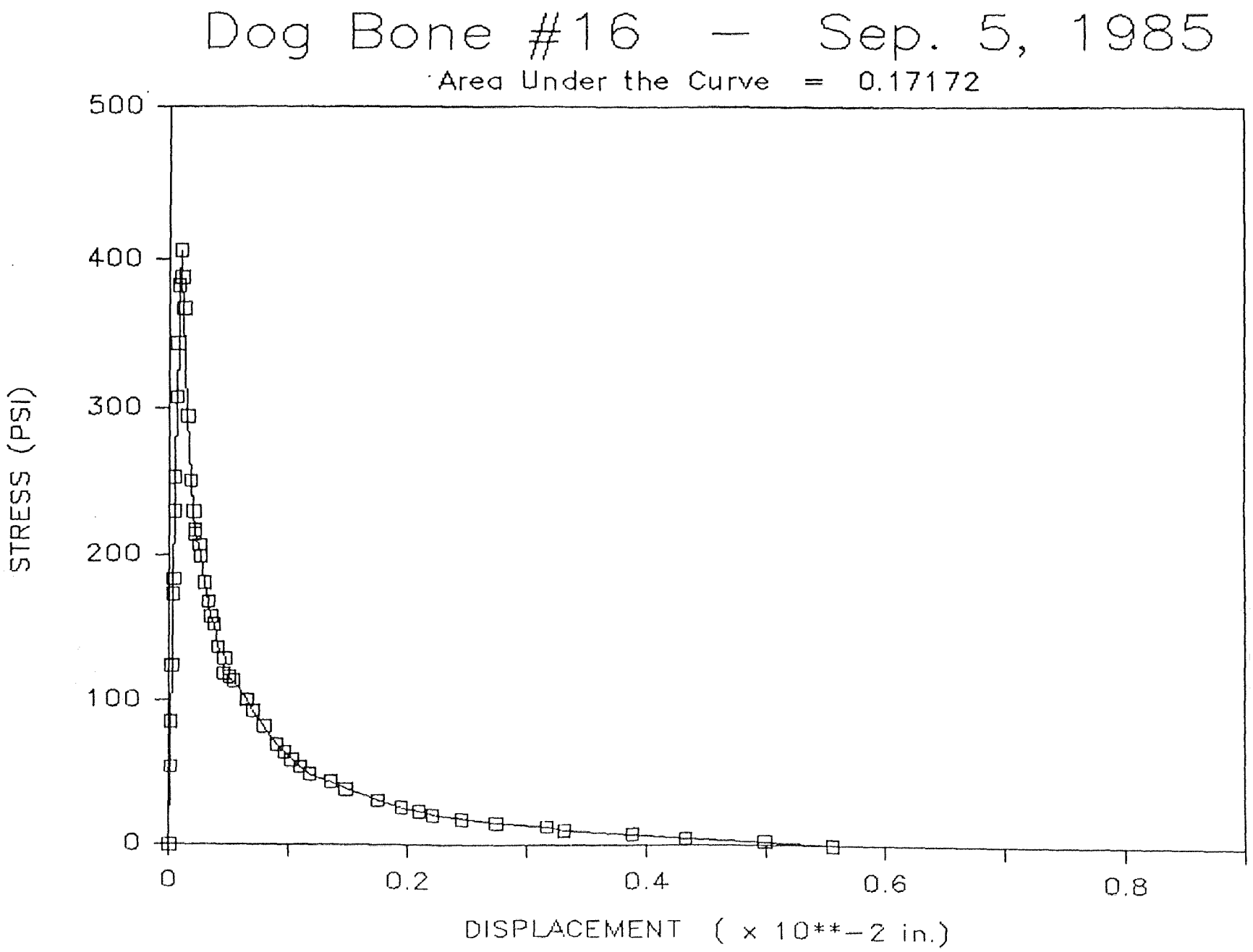
Dog Bone #16 — Sep. 5, 1985
Area Under the Curve = 0.17172
500
400
300
200
100
0
STRESS (PSI)
0
0.2
0.4
0.6
0.8
DISPLACEMENT (x 10**-2 in.)

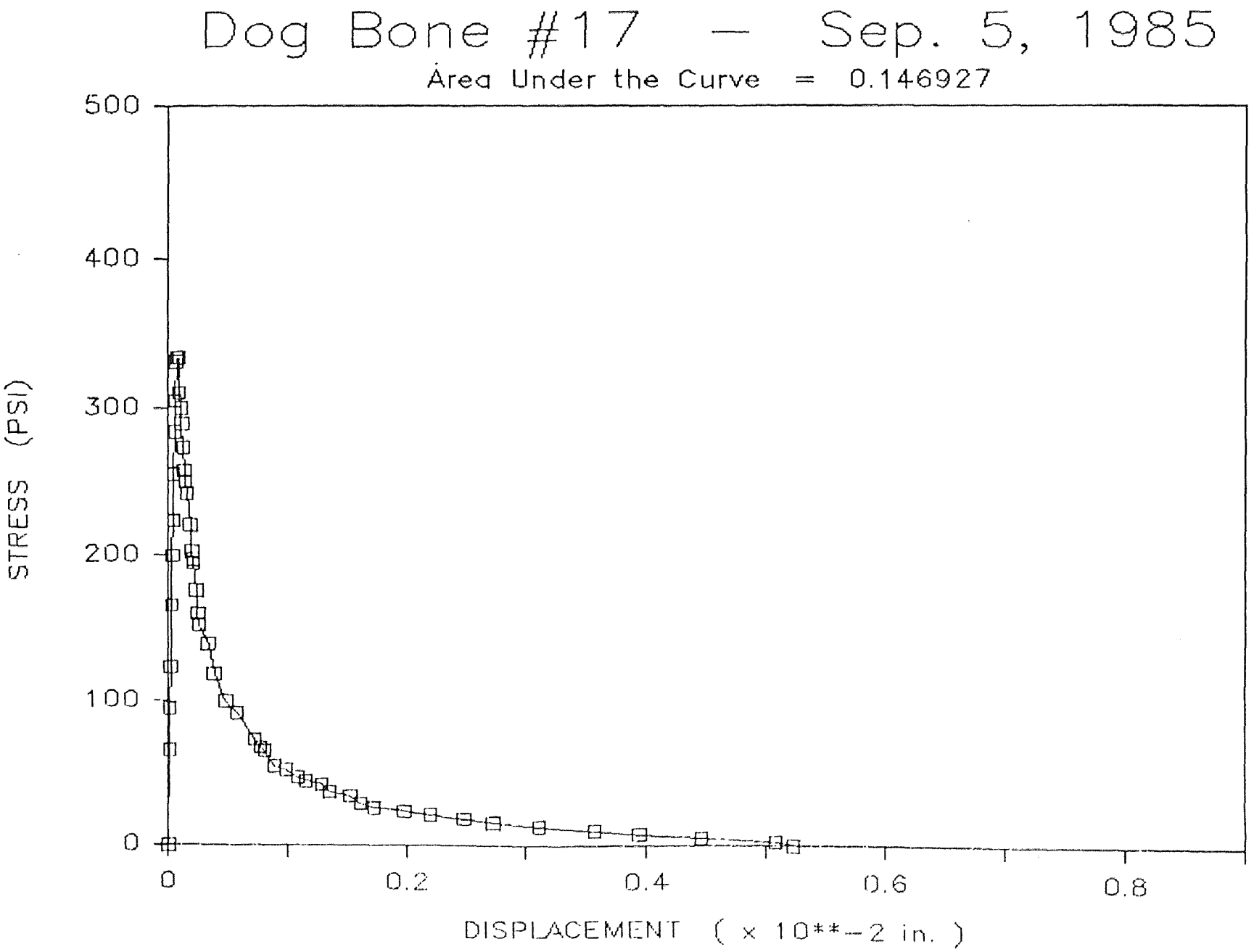
Dog Bone #17 — Sep. 5, 1985
Area Under the Curve = 0.146927
500
400
300
200
100
0
STRESS (PSI)
0
0.2
0.4
0.6
0.8
DISPLACEMENT (x 10**-2 in.)

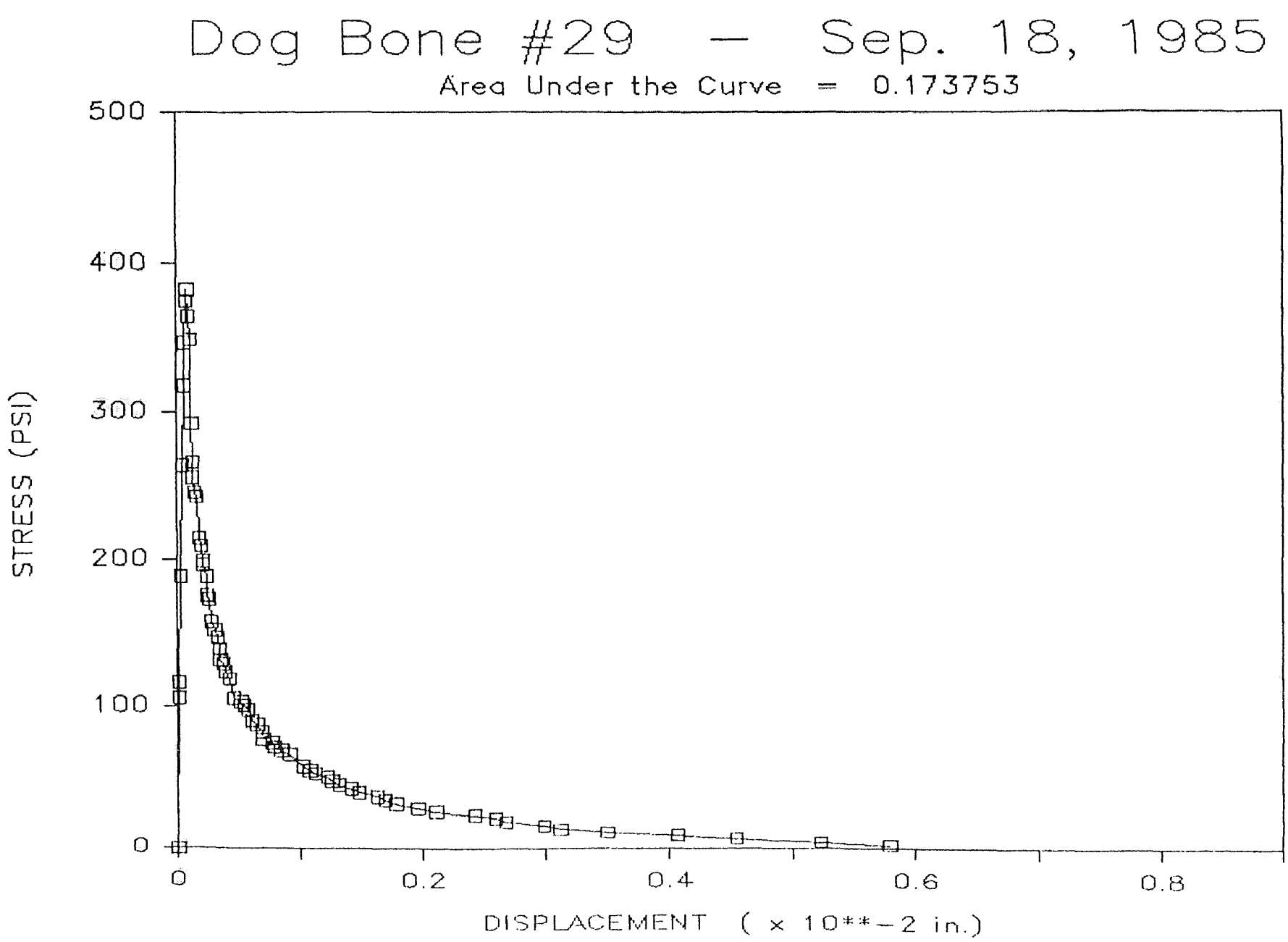
Dog Bone #29 — Sep. 18, 1985
Area Under the Curve = 0.173753
500
400
300
200
100
0
STRESS (PSI)
0
0.2
0.4
0.6
0.8
DISPLACEMENT (x 10**-2 in.)

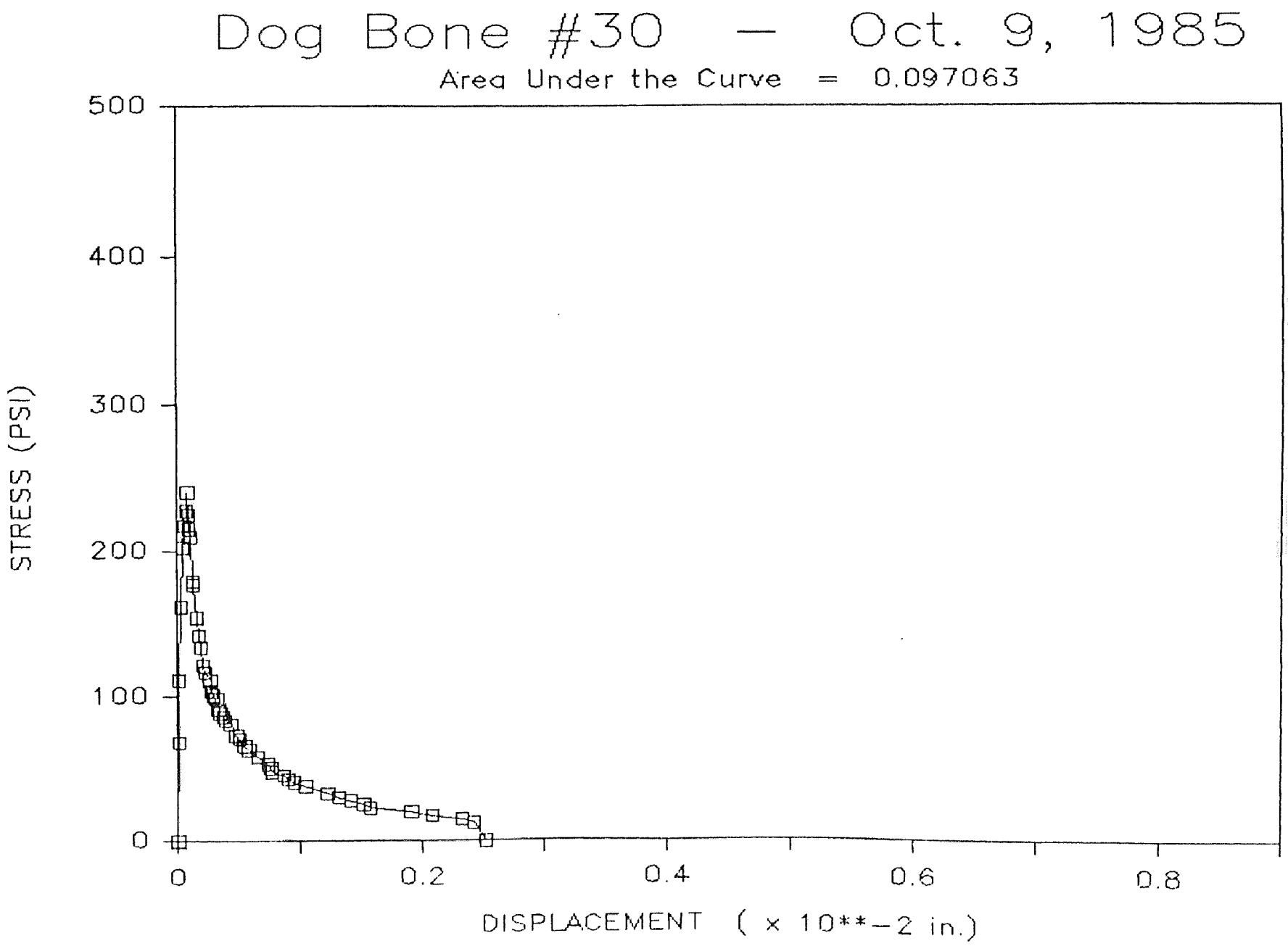
Dog Bone #30 — Oct. 9, 1985
Area Under the Curve = 0.097063
500
400
300
200
100
0
STRESS (PSI)
0
0.2
0.4
0.6
0.8
DISPLACEMENT (x 10**-2 in.)

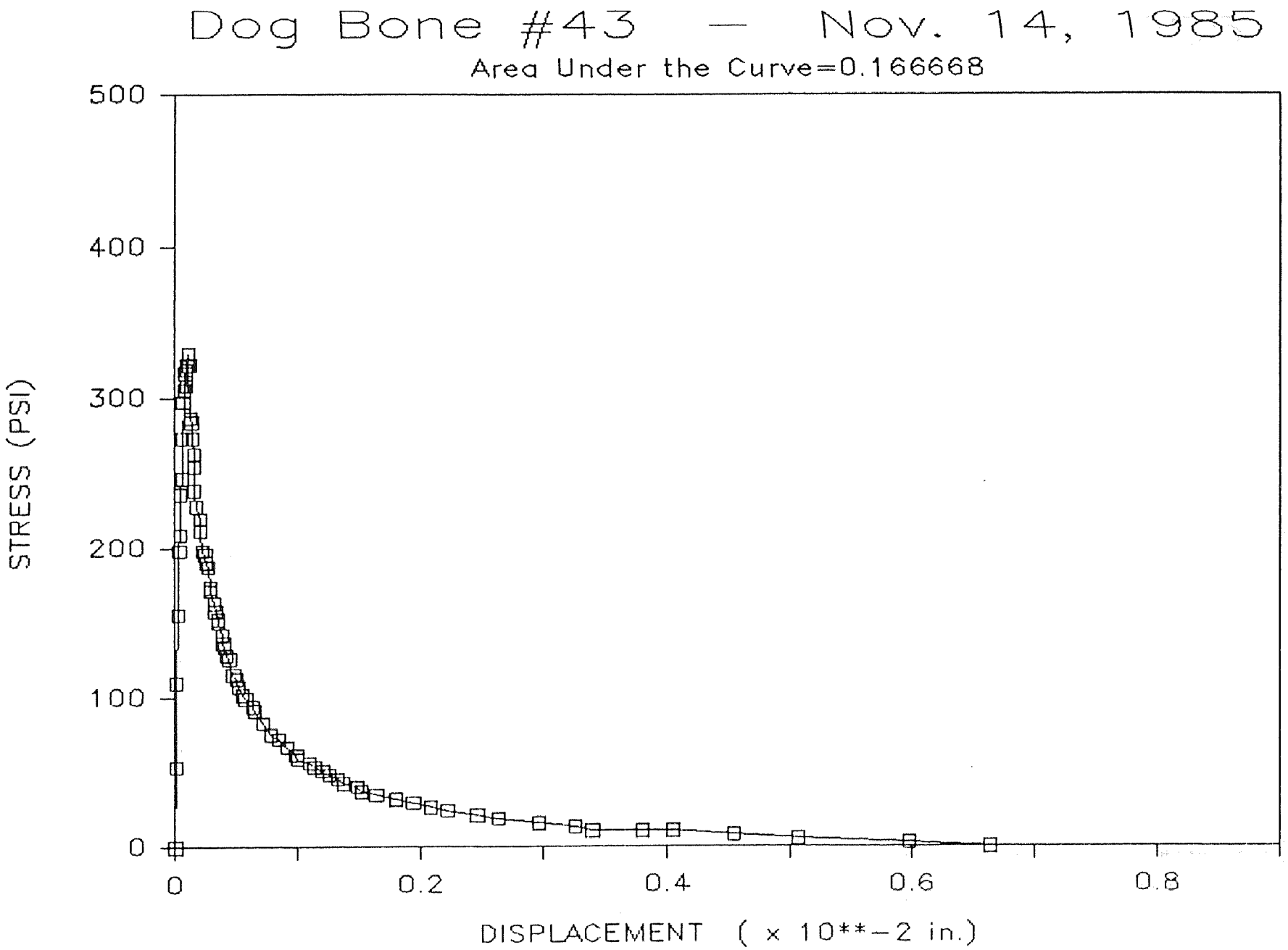
Dog Bone #43 — Nov. 14, 1985
Area Under the Curve=0.166668
500
400
300
200
100
0
STRESS (PSI)
0
0.2
0.4
0.6
0.8
DISPLACEMENT (x 10**-2 in.)

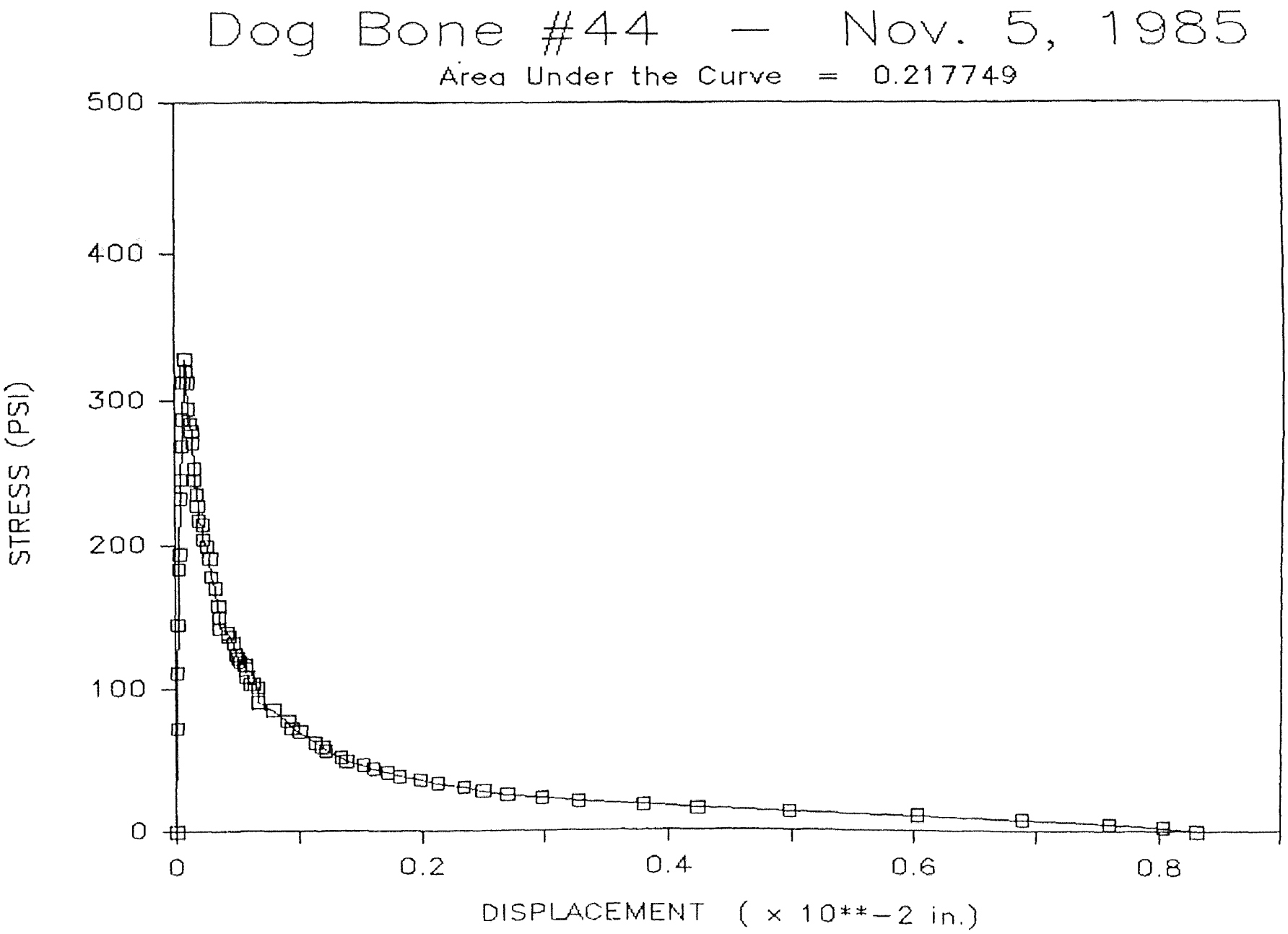
Dog Bone #44 — Nov. 5, 1985
Area Under the Curve = 0.217749
500
400
300
200
100
0
STRESS (PSI)
0
0.2
0.4
0.6
0.8
DISPLACEMENT (x 10**-2 in.)

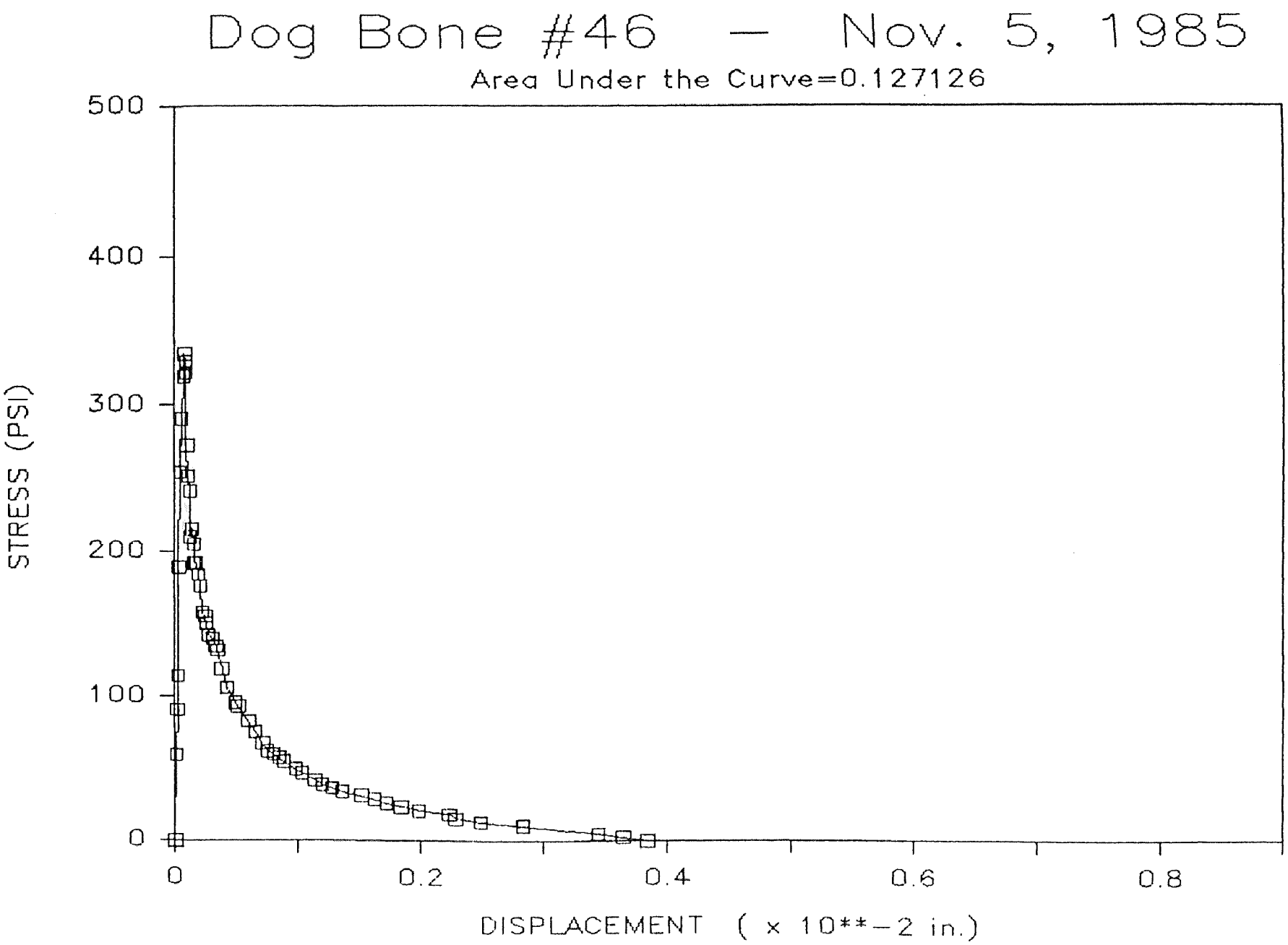
Dog Bone #46 — Nov. 5, 1985
Area Under the Curve=0.127126
500
400
300
200
100
0
STRESS (PSI)
0
0.2
0.4
0.6
0.8
DISPLACEMENT (x 10**-2 in.)

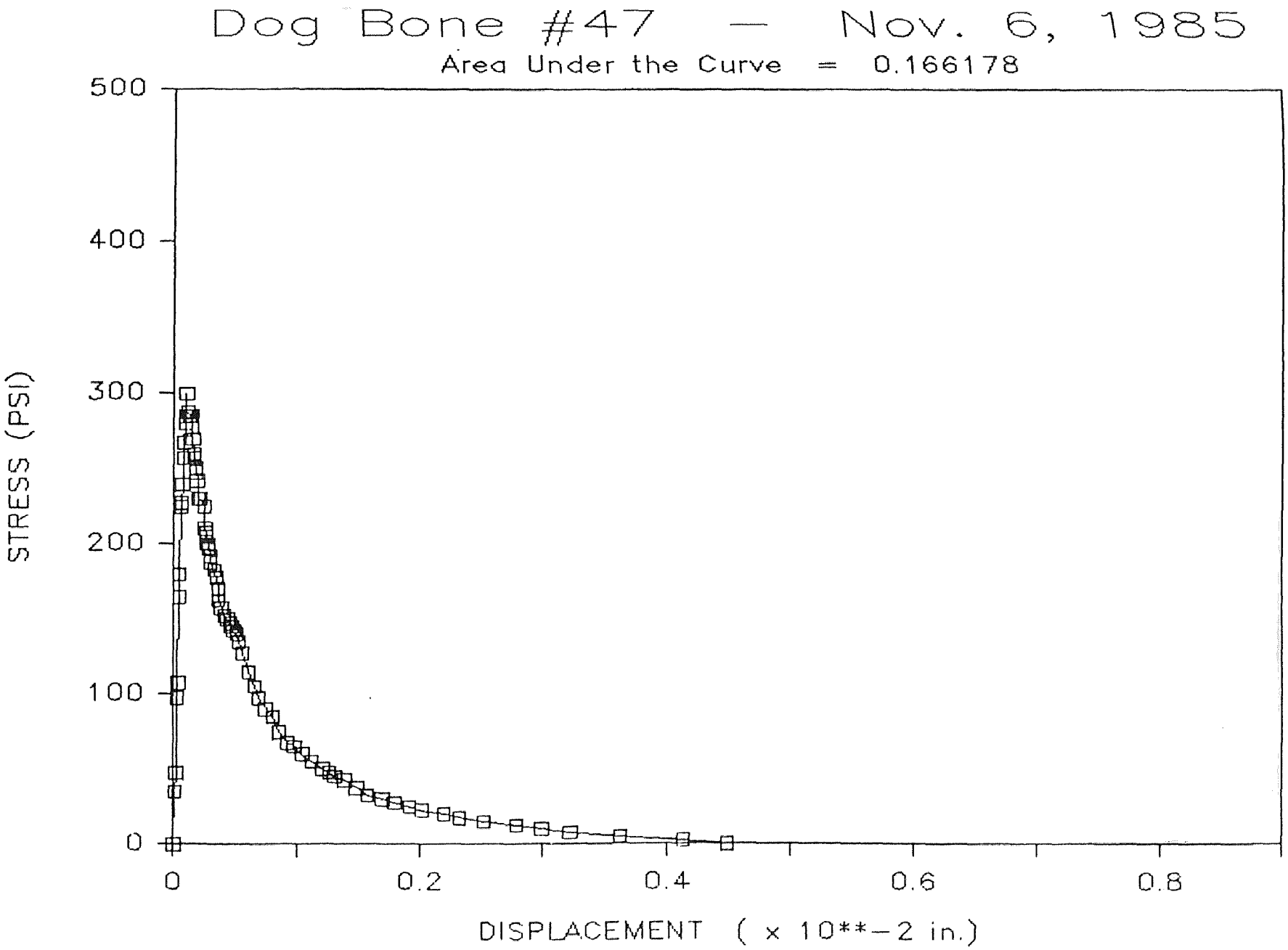
Dog Bone #47 — Nov. 6, 1985
Area Under the Curve = 0.166178
500
400
300
200
100
0
STRESS (PSI)
0
0.2
0.4
0.6
0.8
DISPLACEMENT (x 10**-2 in.)

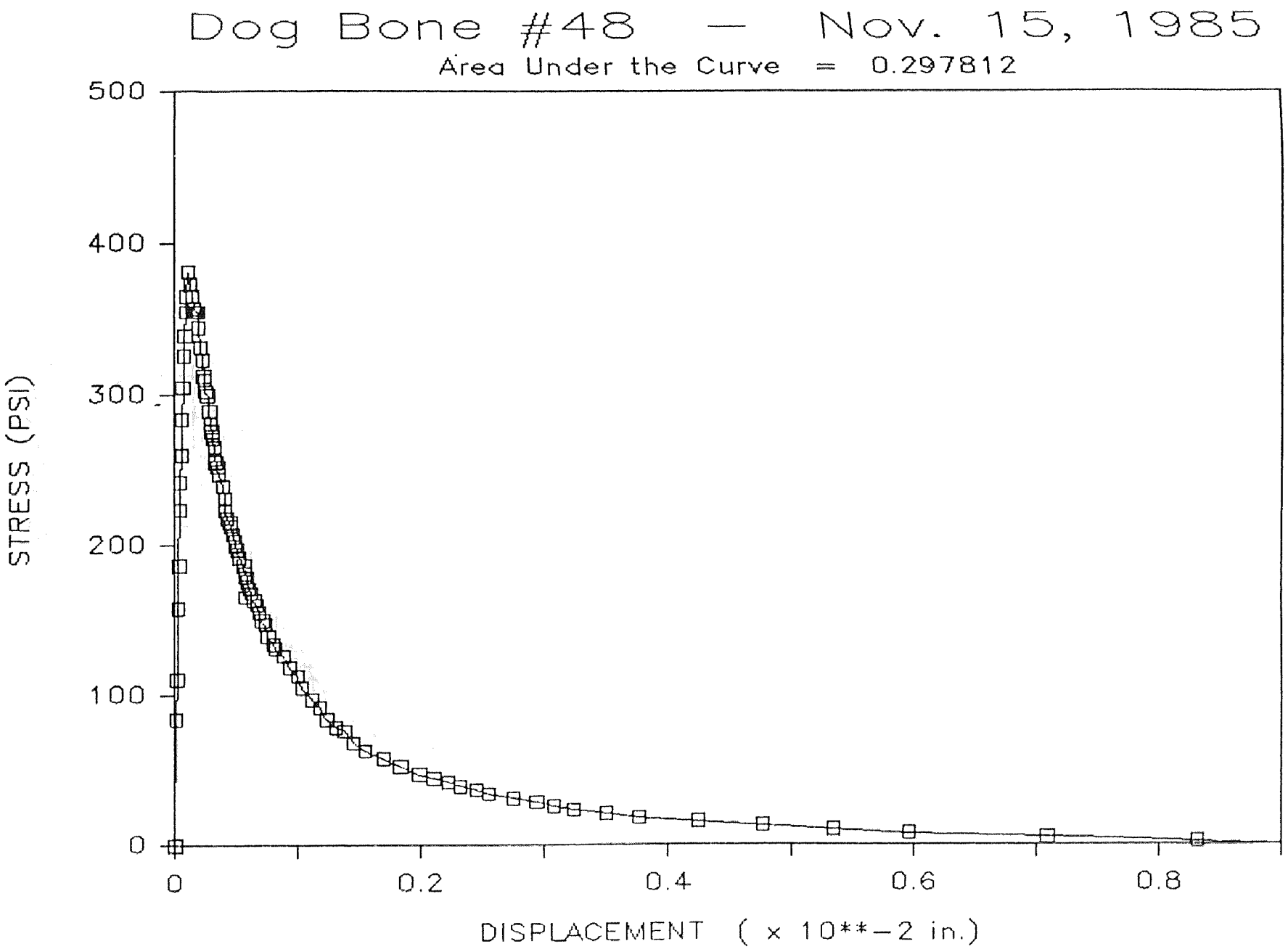
Dog Bone #48 — Nov. 15, 1985
Area Under the Curve = 0.297812
500
400
300
200
100
0
STRESS (PSI)
0
0.2
0.4
0.6
0.8
DISPLACEMENT (x 10**-2 in.)

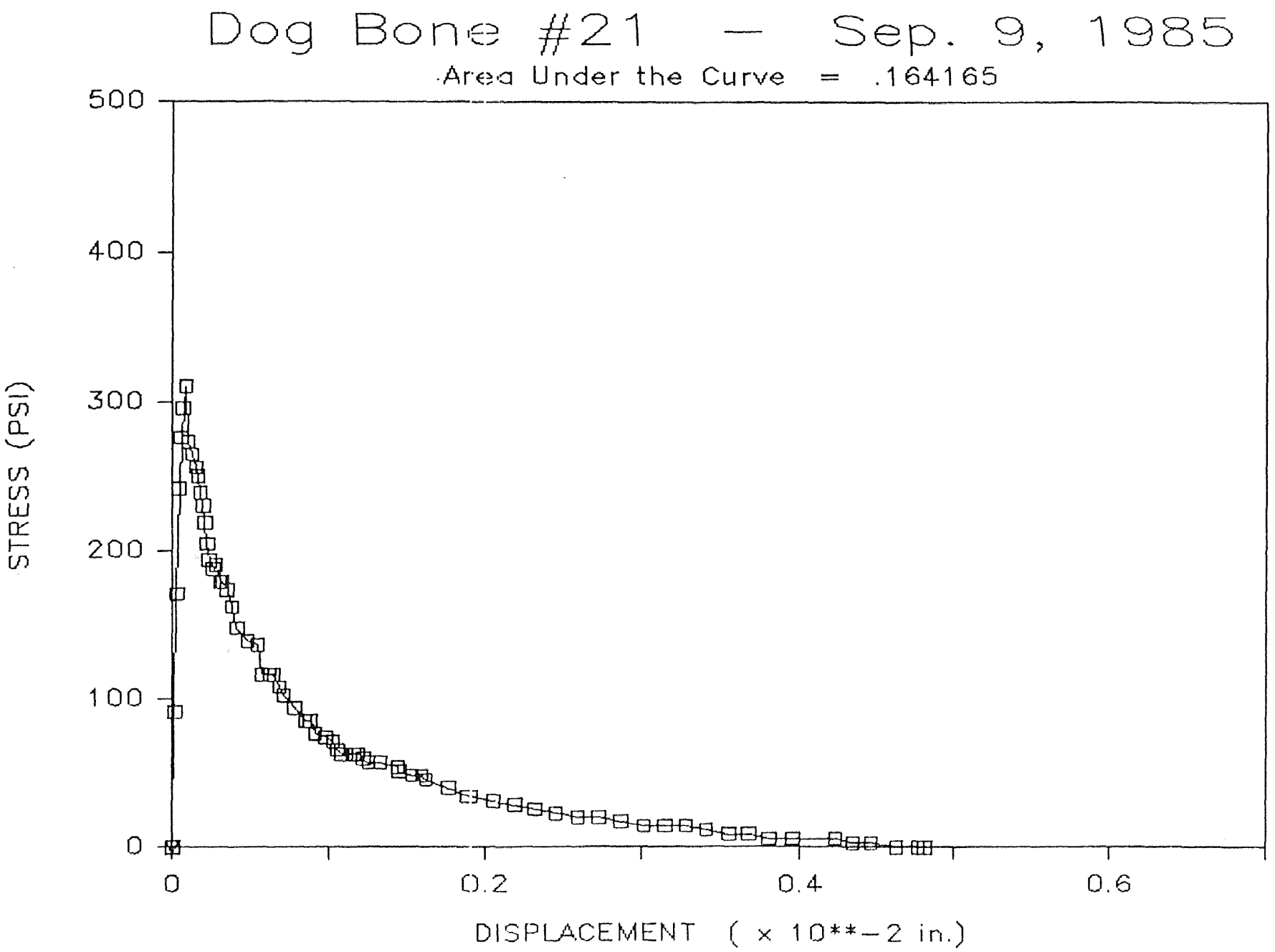
Dog Bone #21 — Sep. 9, 1985
Area Under the Curve = .164165
500
400
300
200
100
0
STRESS (PSI)
0
0.2
0.4
0.6
DISPLACEMENT (x 10**-2 in.)

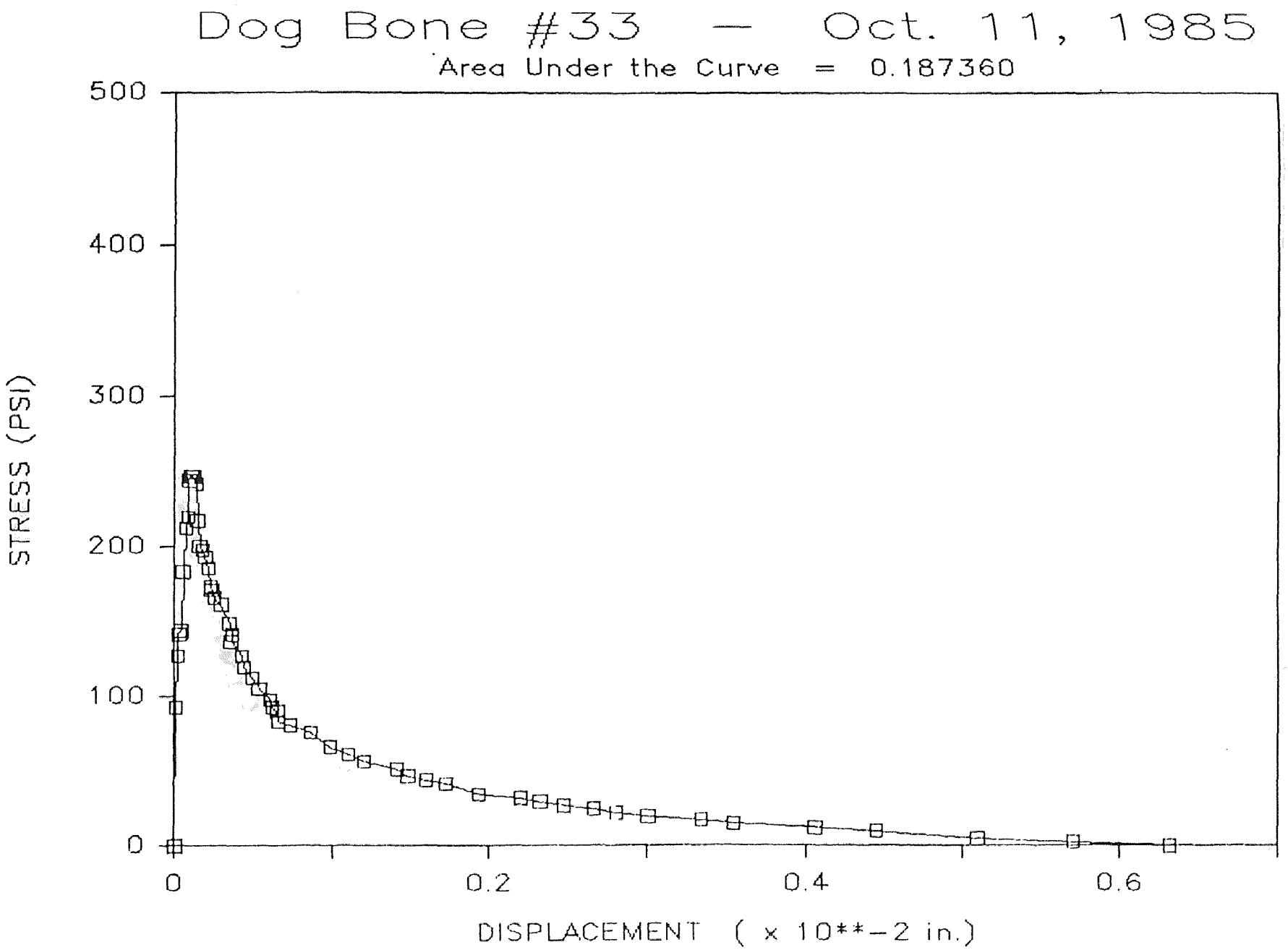
Dog Bone #33 — Oct. 11, 1985
Area Under the Curve = 0.187360
500
400
300
200
100
0
STRESS (PSI)
0
0.2
0.4
0.6
DISPLACEMENT (x 10**-2 in.)

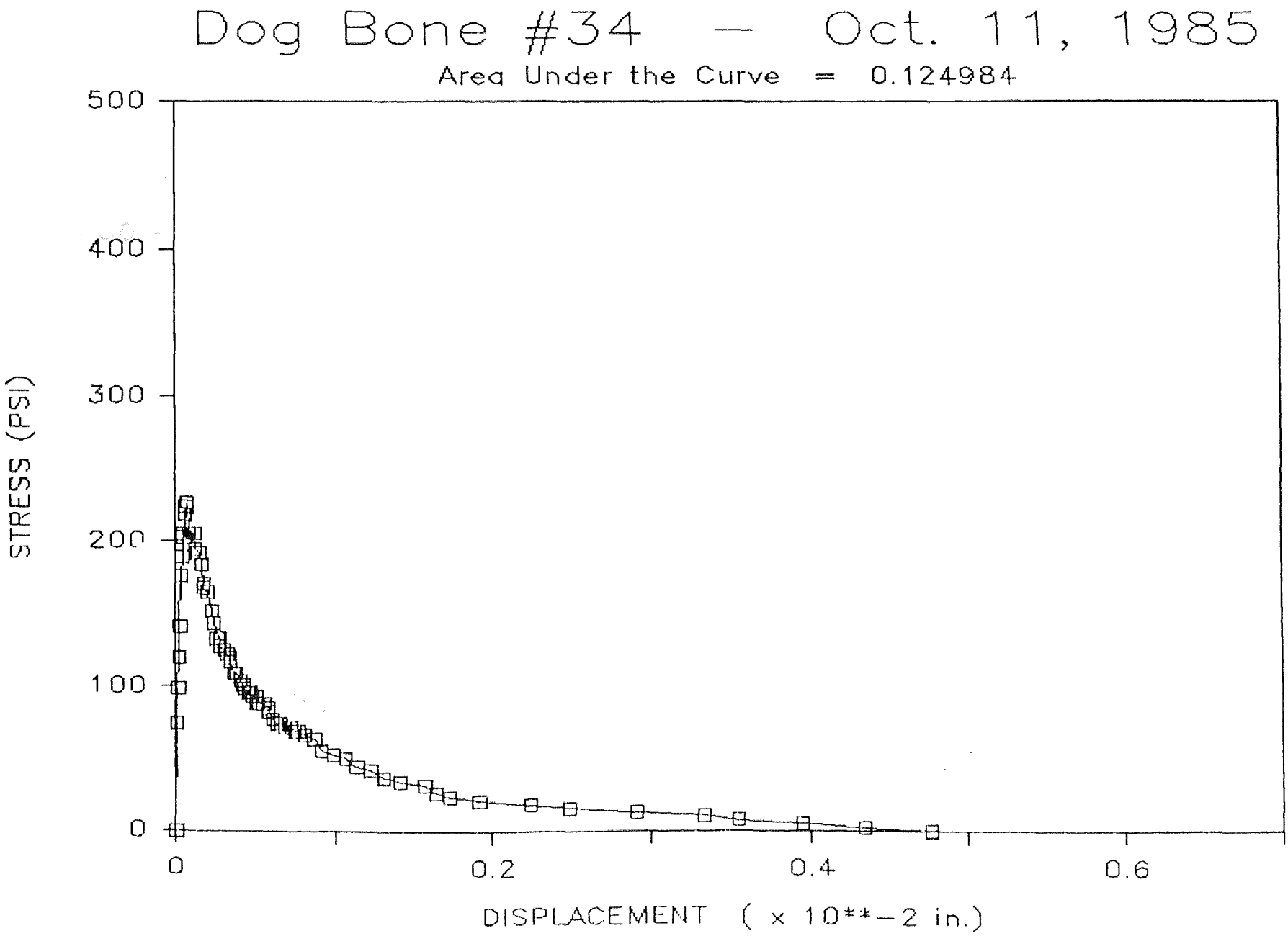
Dog Bone #34 — Oct. 11, 1985
Area Under the Curve = 0.124984
500
400
300
200
100
0
STRESS (PSI)
0
0.2
0.4
0.6
DISPLACEMENT (x 10**-2 in.)

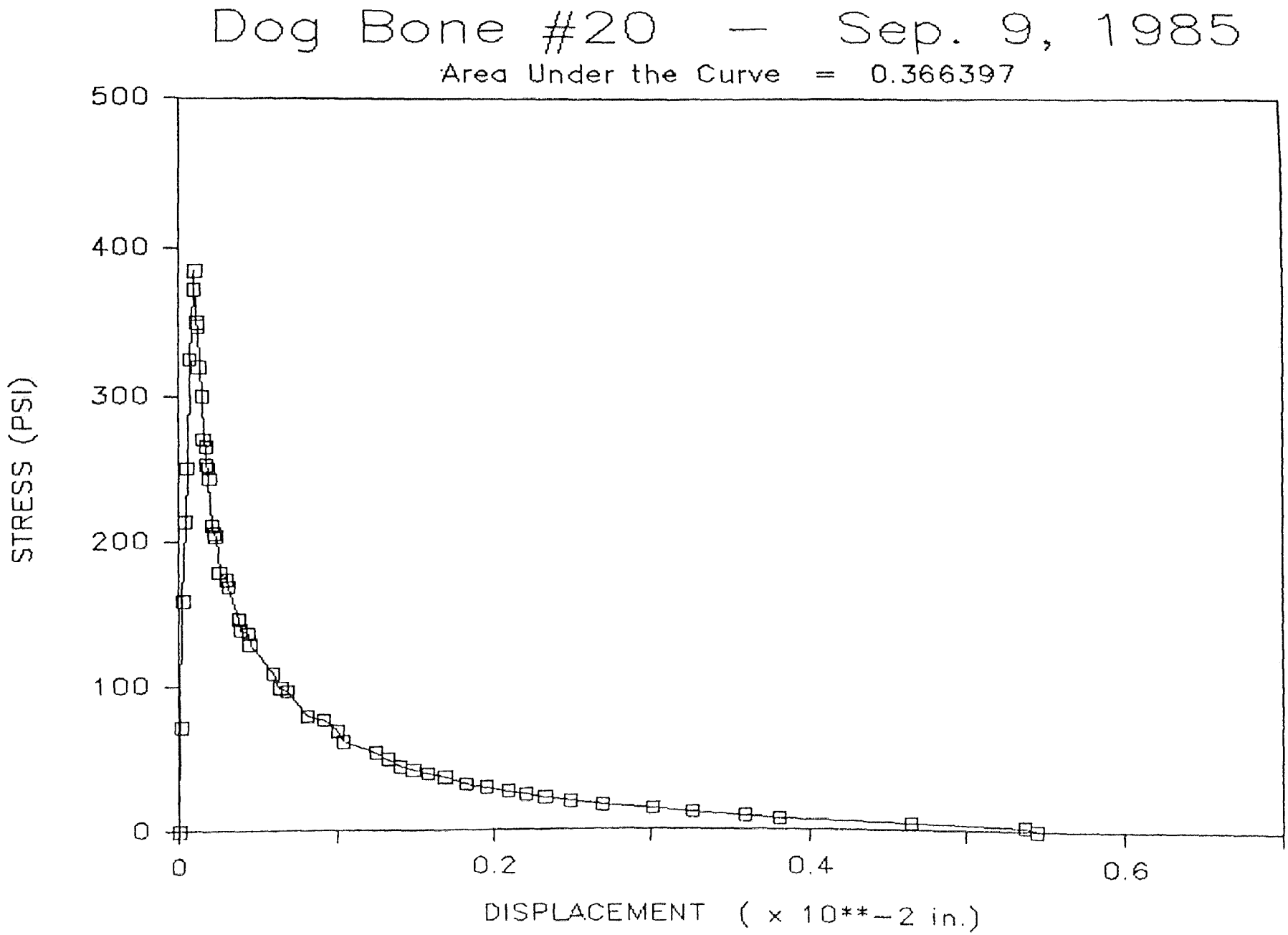
Dog Bone #20 — Sep. 9, 1985
Area Under the Curve = 0.366397
500
400
300
200
100
0
STRESS (PSI)
0
0.2
0.4
0.6
DISPLACEMENT (x 10**-2 in.)

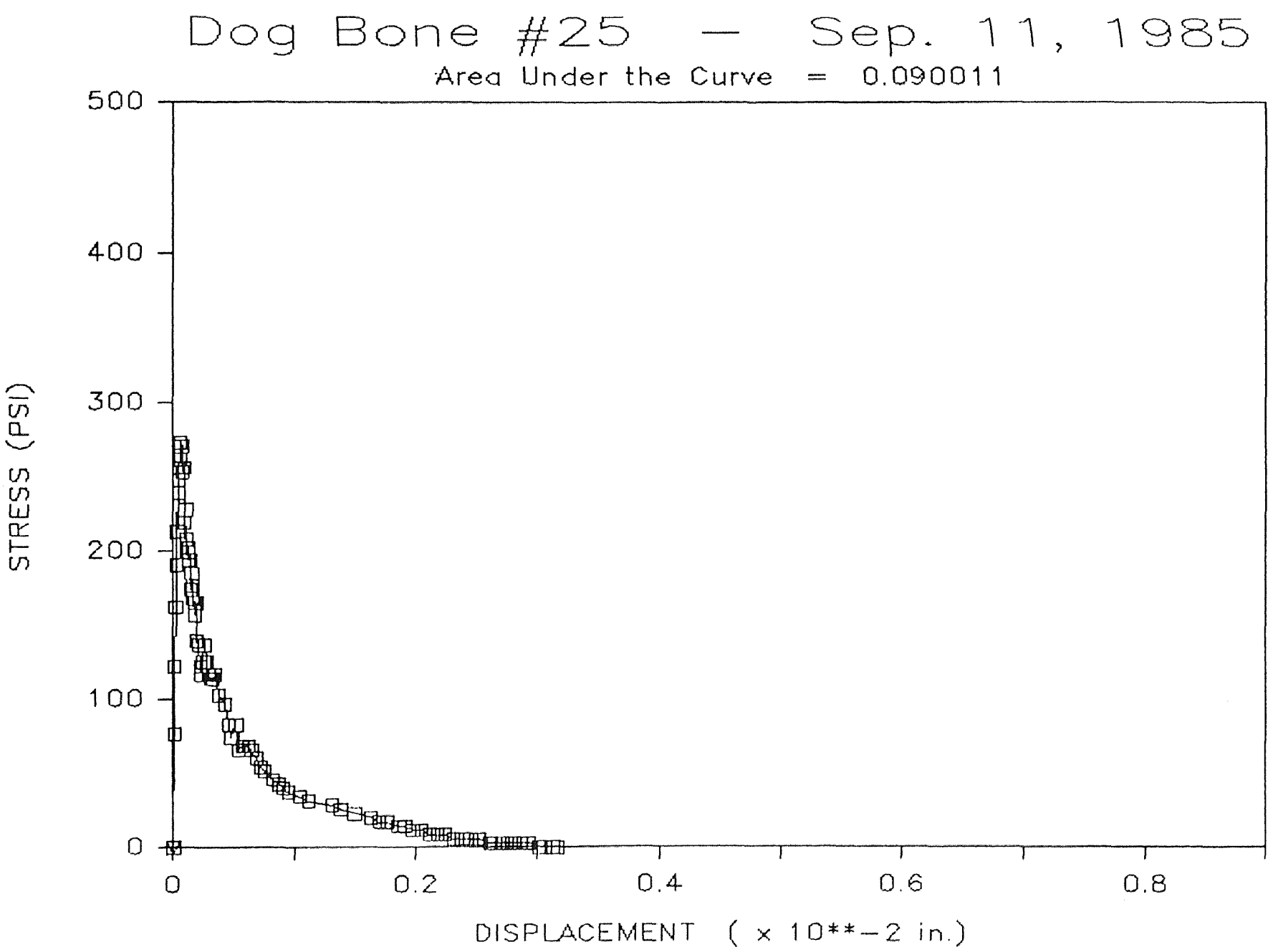
Dog Bone #25 — Sep. 11, 1985
Area Under the Curve = 0.090011
500
400
300
200
100
0
STRESS (PSI)
0
0.2
0.4
0.6
0.8
DISPLACEMENT (x 10**-2 in.)

Dog Bone #54 — Dec. 11, 1985

Area Under the Curve = 0.404654

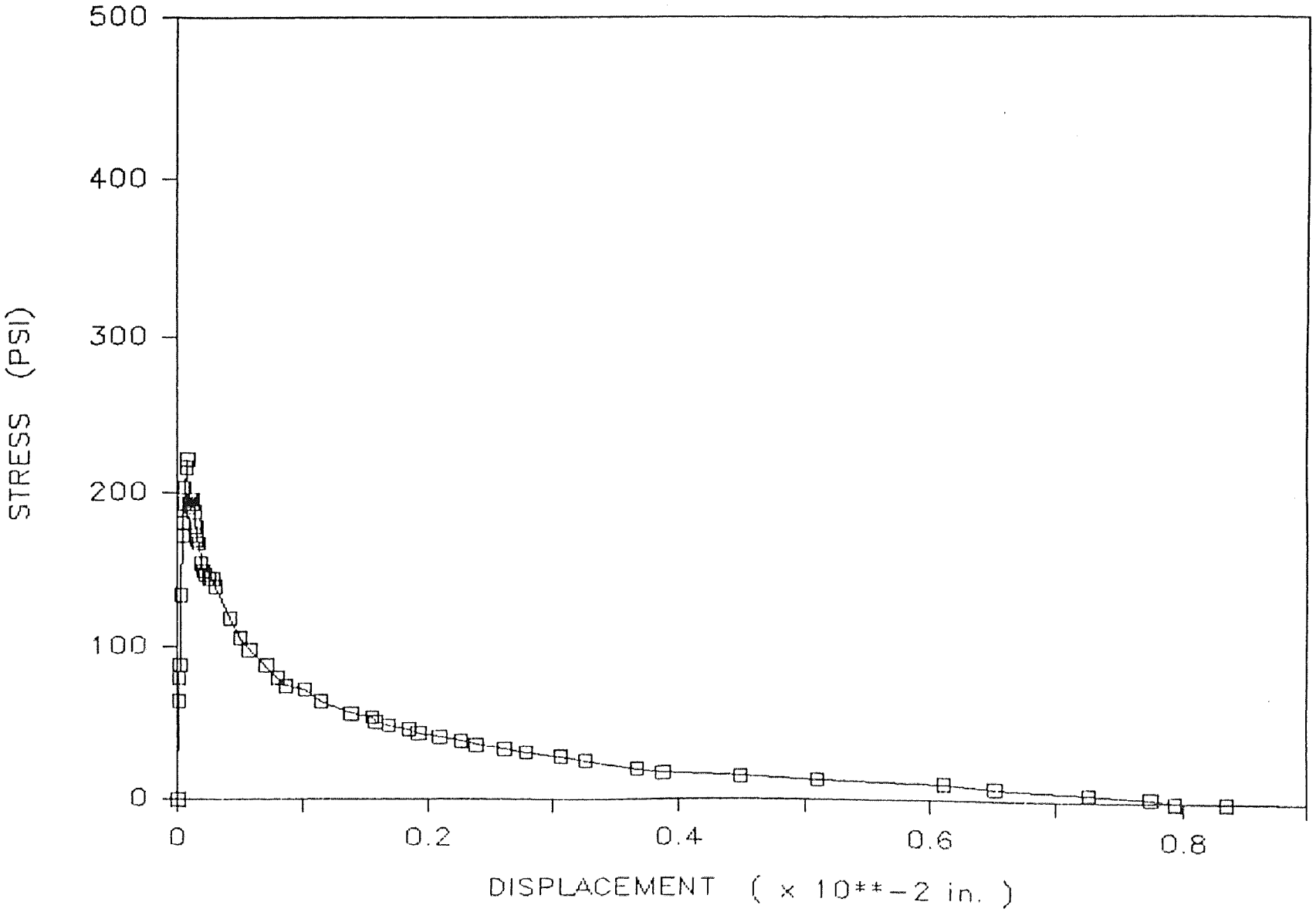

Dog Bone #55 — Dec. 11, 1985

Area Under the Curve = 0.163213

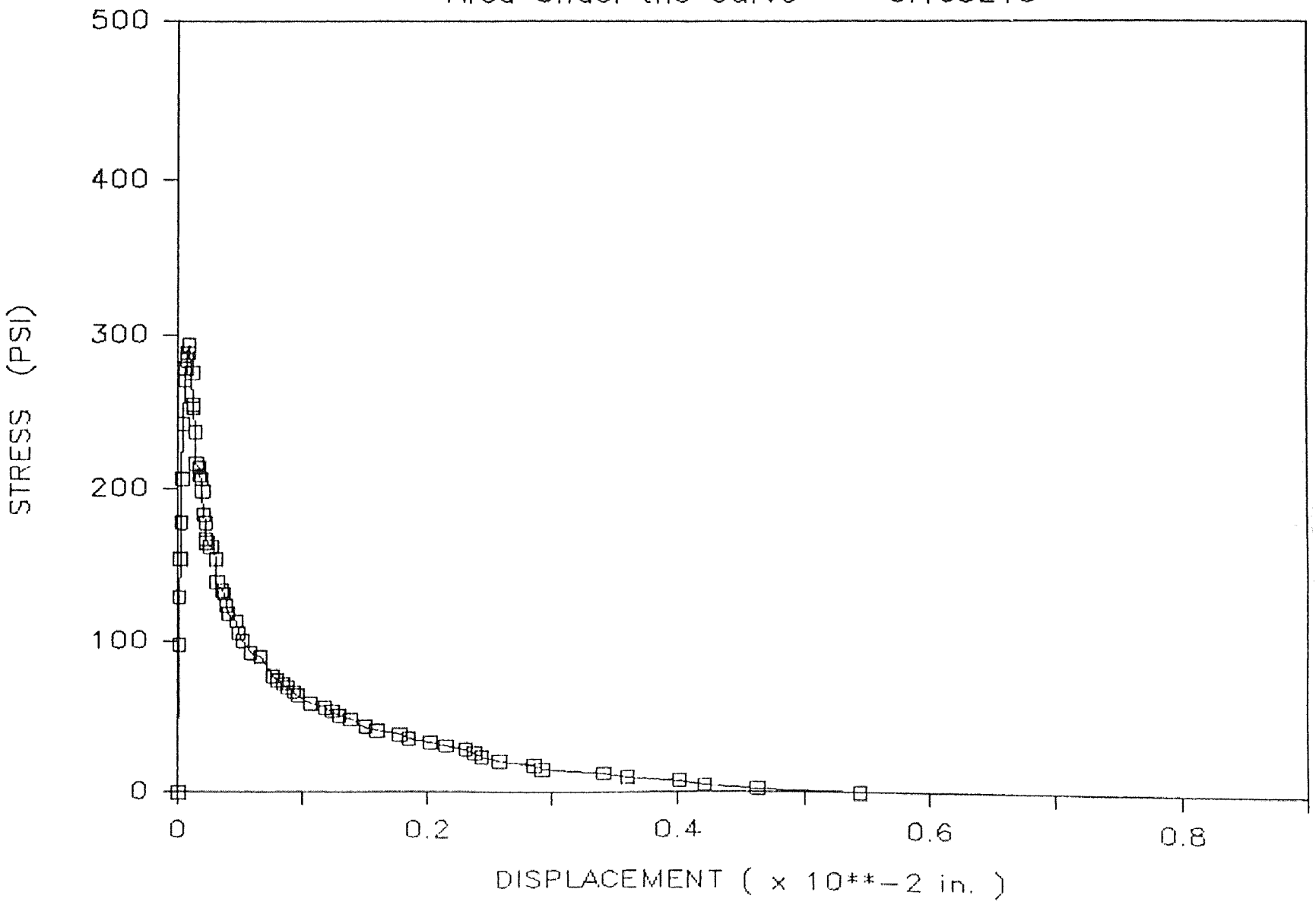

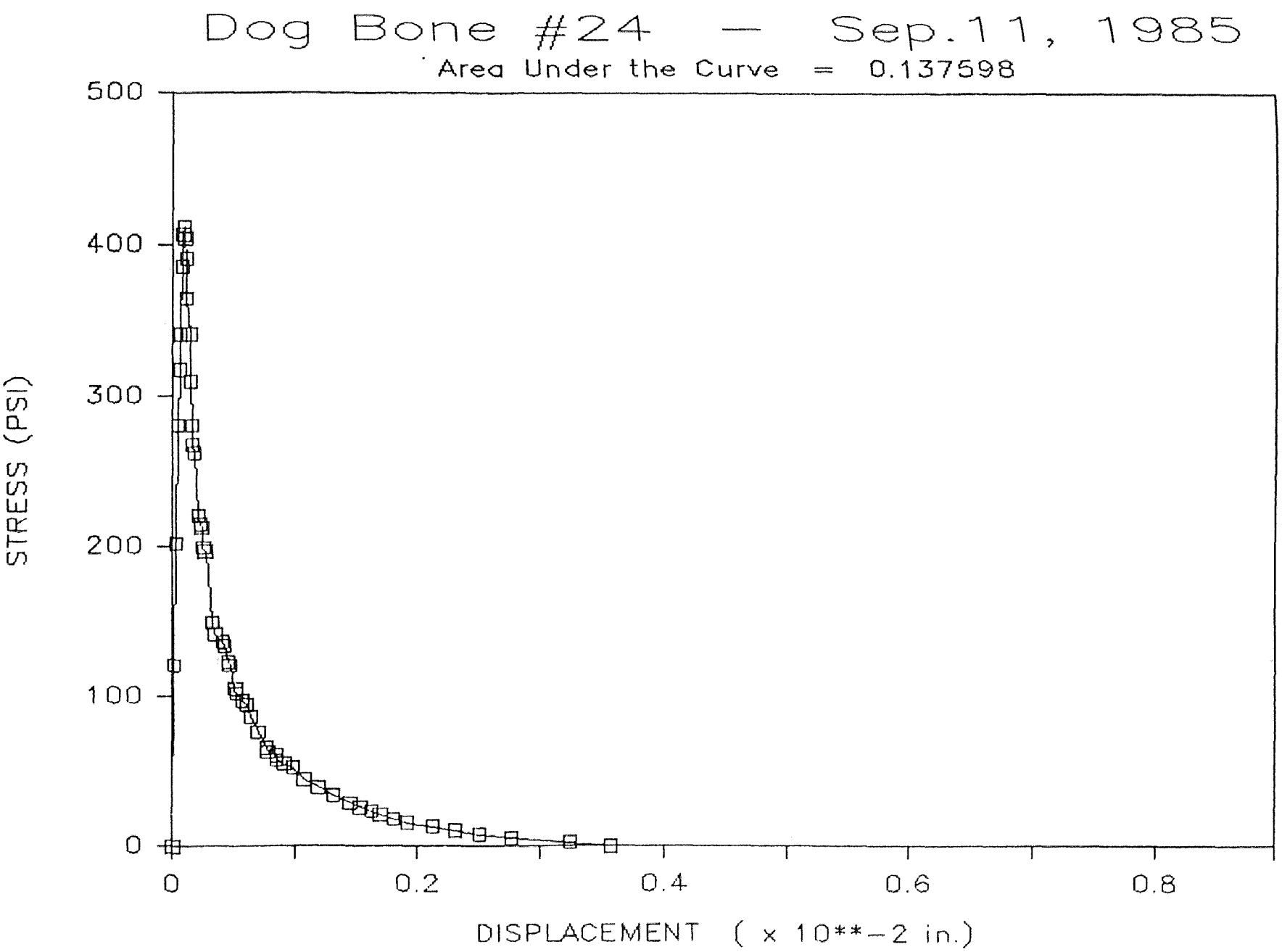
Dog Bone #24 — Sep.11, 1985
Area Under the Curve = 0.137598
500
400
300
200
100
0
STRESS (PSI)
0
0.2
0.4
0.6
0.8
DISPLACEMENT (x 10**-2 in.)

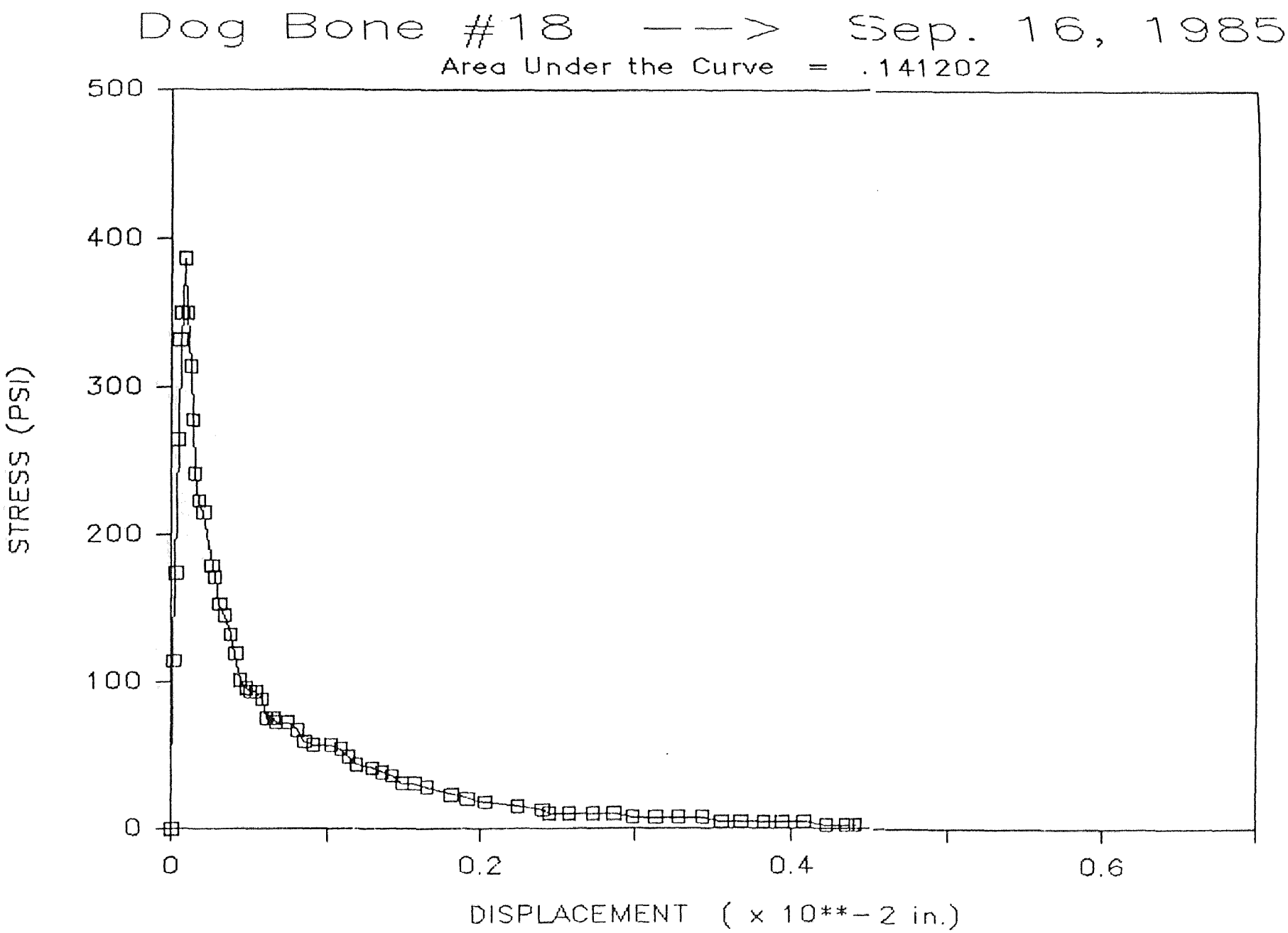
Dog Bone #18 ---> Sep. 16, 1985
Area Under the Curve = .141202
500
400
300
200
100
0
STRESS (PSI)
0
0.2
0.4
0.6
DISPLACEMENT (x 10**-2 in.)

Dog Bone #19 — Sep. 6, 1985

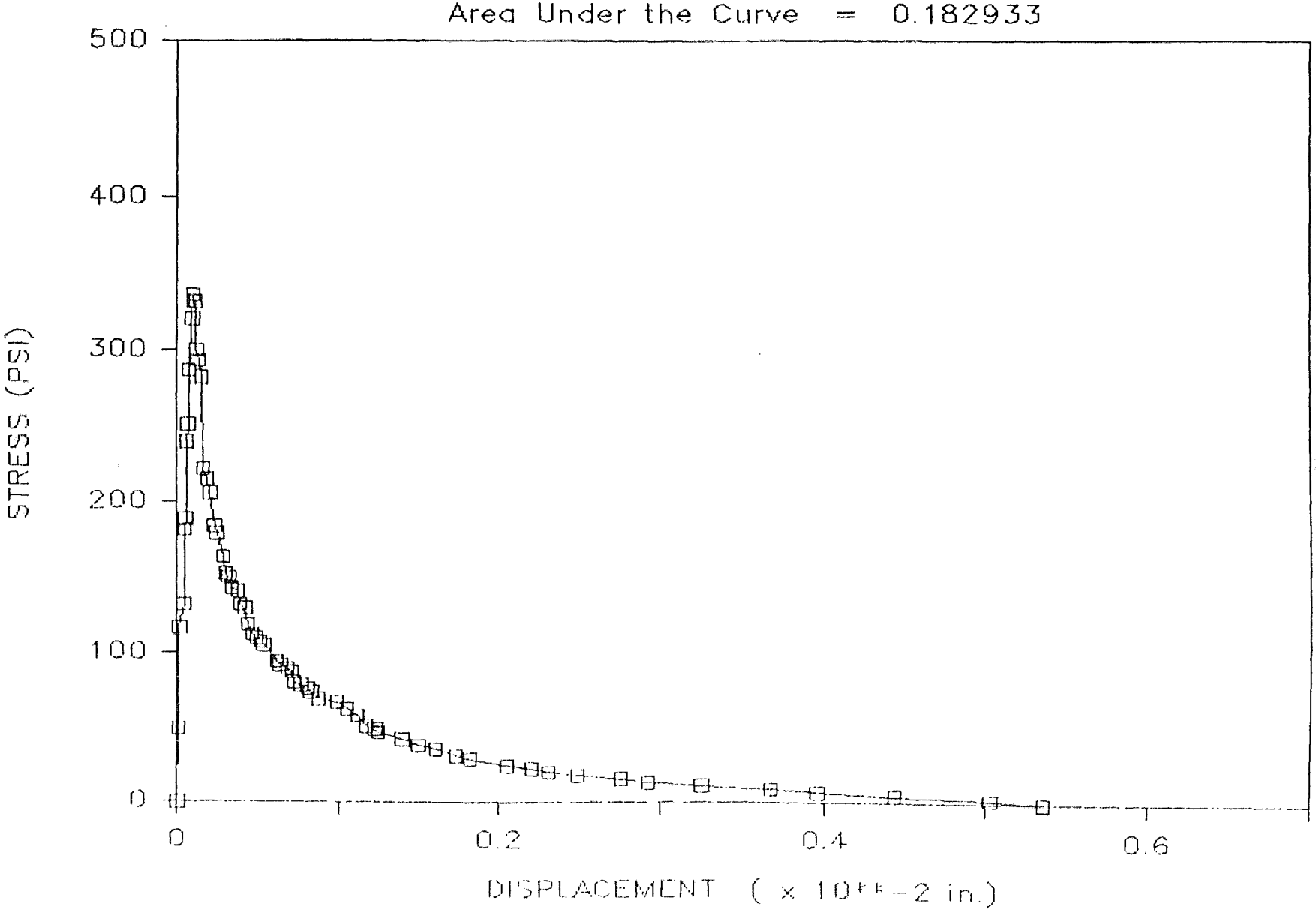

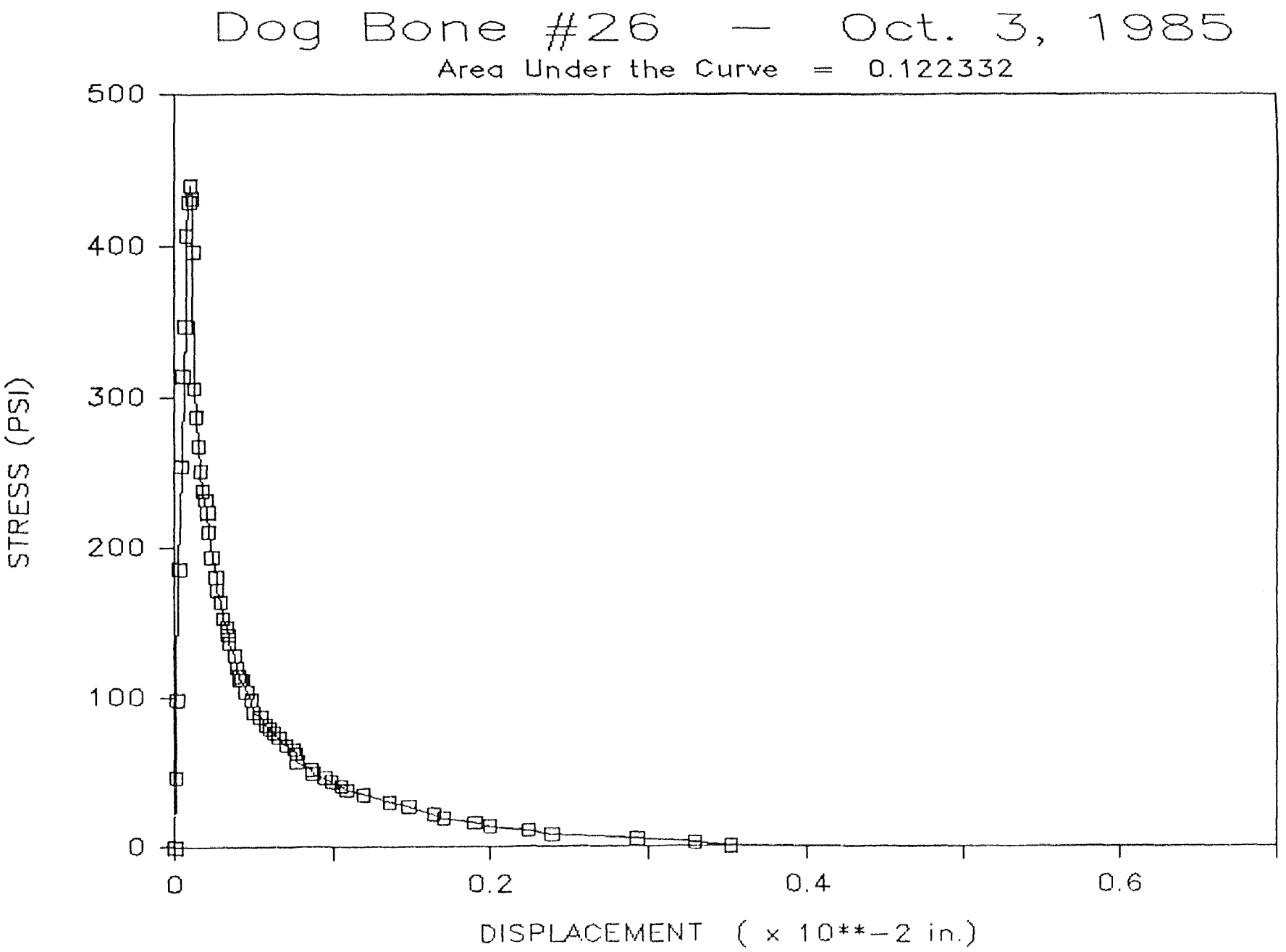
Dog Bone #26 — Oct. 3, 1985
Area Under the Curve = 0.122332
500
400
300
200
100
0
STRESS (PSI)
0
0.2
0.4
0.6
DISPLACEMENT (x 10**-2 in.)

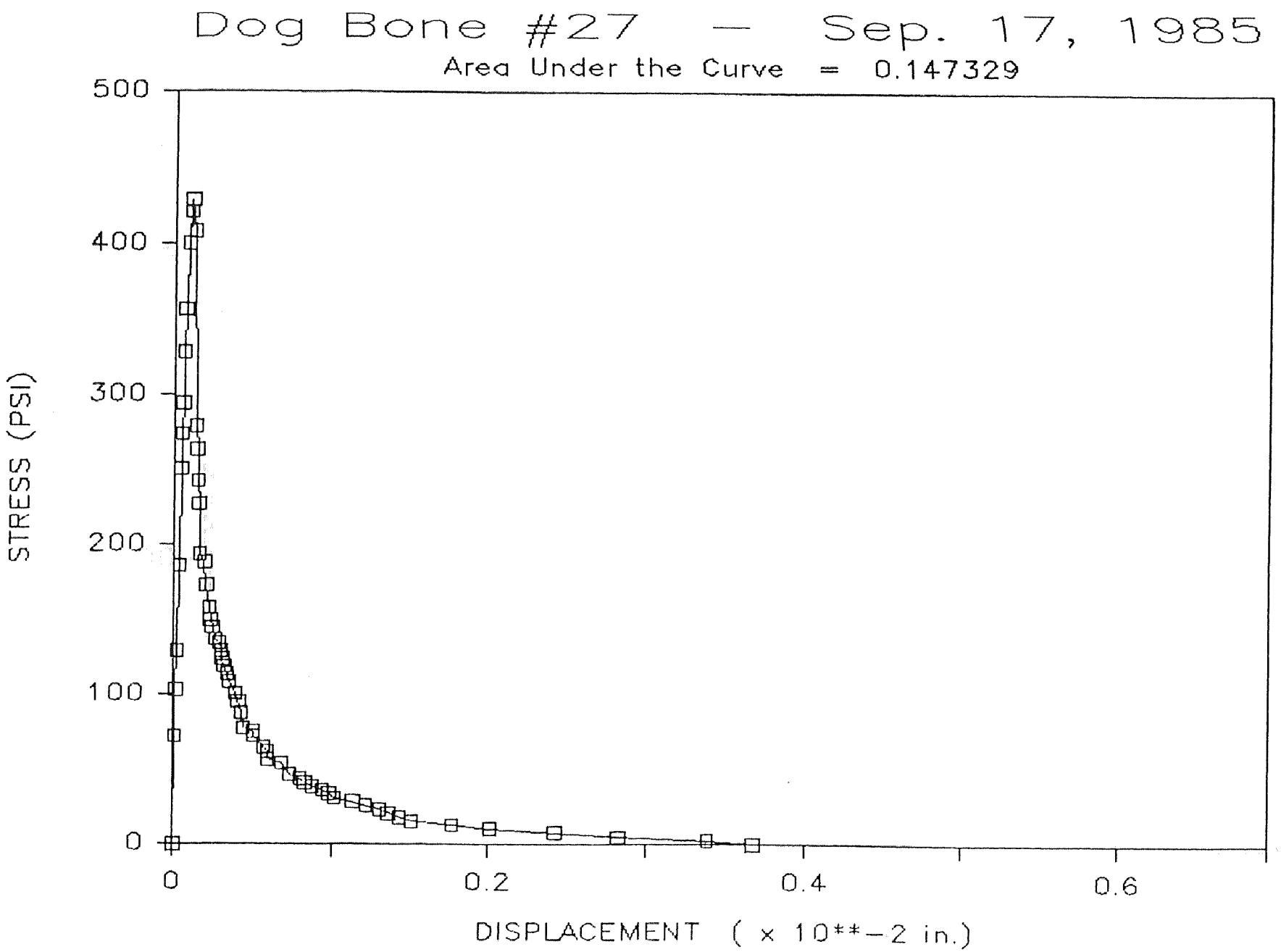
Dog Bone #27 — Sep. 17, 1985
Area Under the Curve = 0.147329
500
400
300
200
100
0
STRESS (PSI)
0
0.2
0.4
0.6
DISPLACEMENT (x 10**-2 in.)

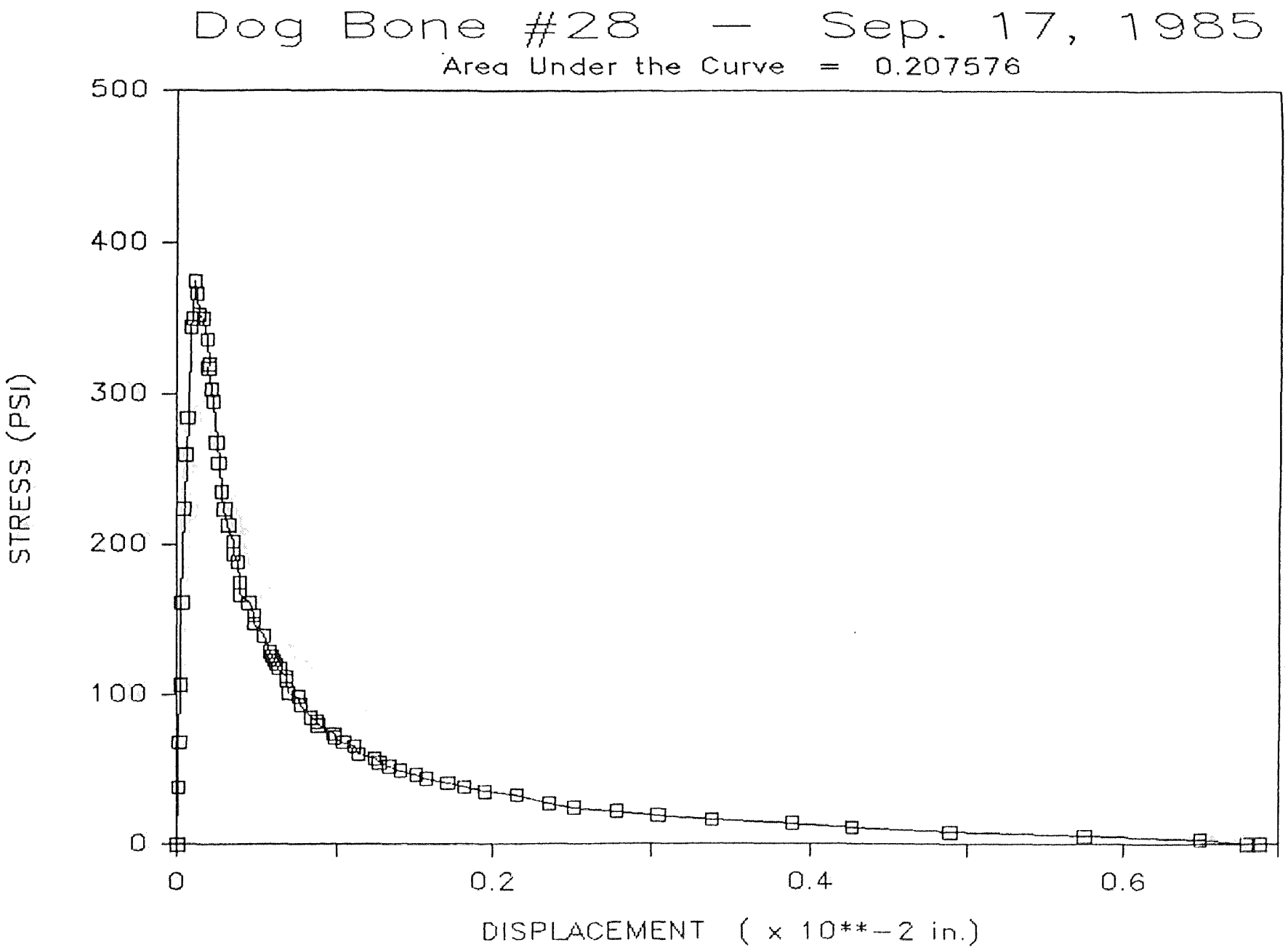
Dog Bone #28 — Sep. 17, 1985
Area Under the Curve = 0.207576
500
400
300
200
100
0
STRESS (PSI)
0
0.2
0.4
0.6
DISPLACEMENT (x 10**-2 in.)

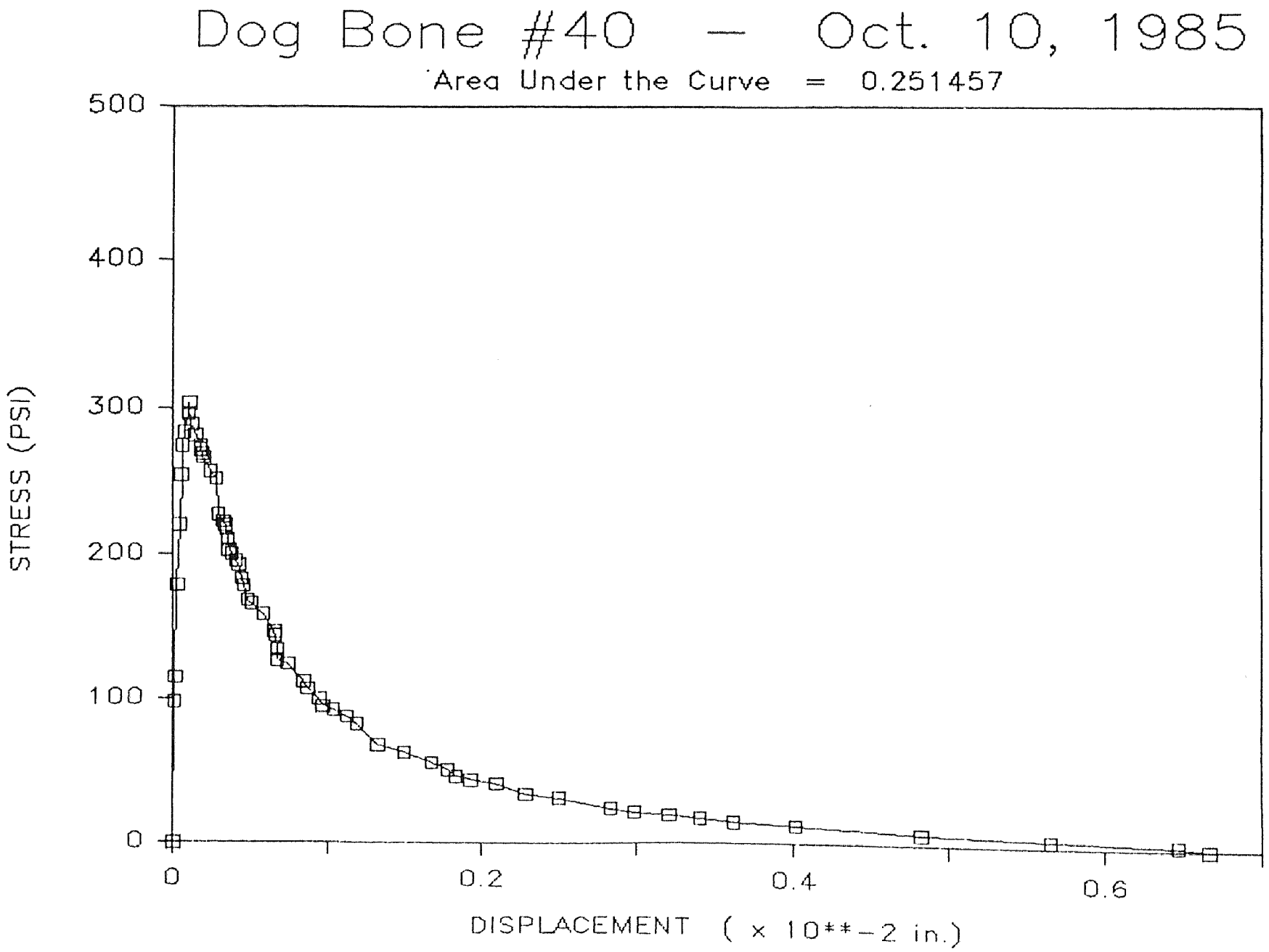
Dog Bone #40 — Oct. 10, 1985
Area Under the Curve = 0.251457
500
400
300
200
100
0
STRESS (PSI)
0
0.2
0.4
0.6
DISPLACEMENT (x 10**-2 in.)

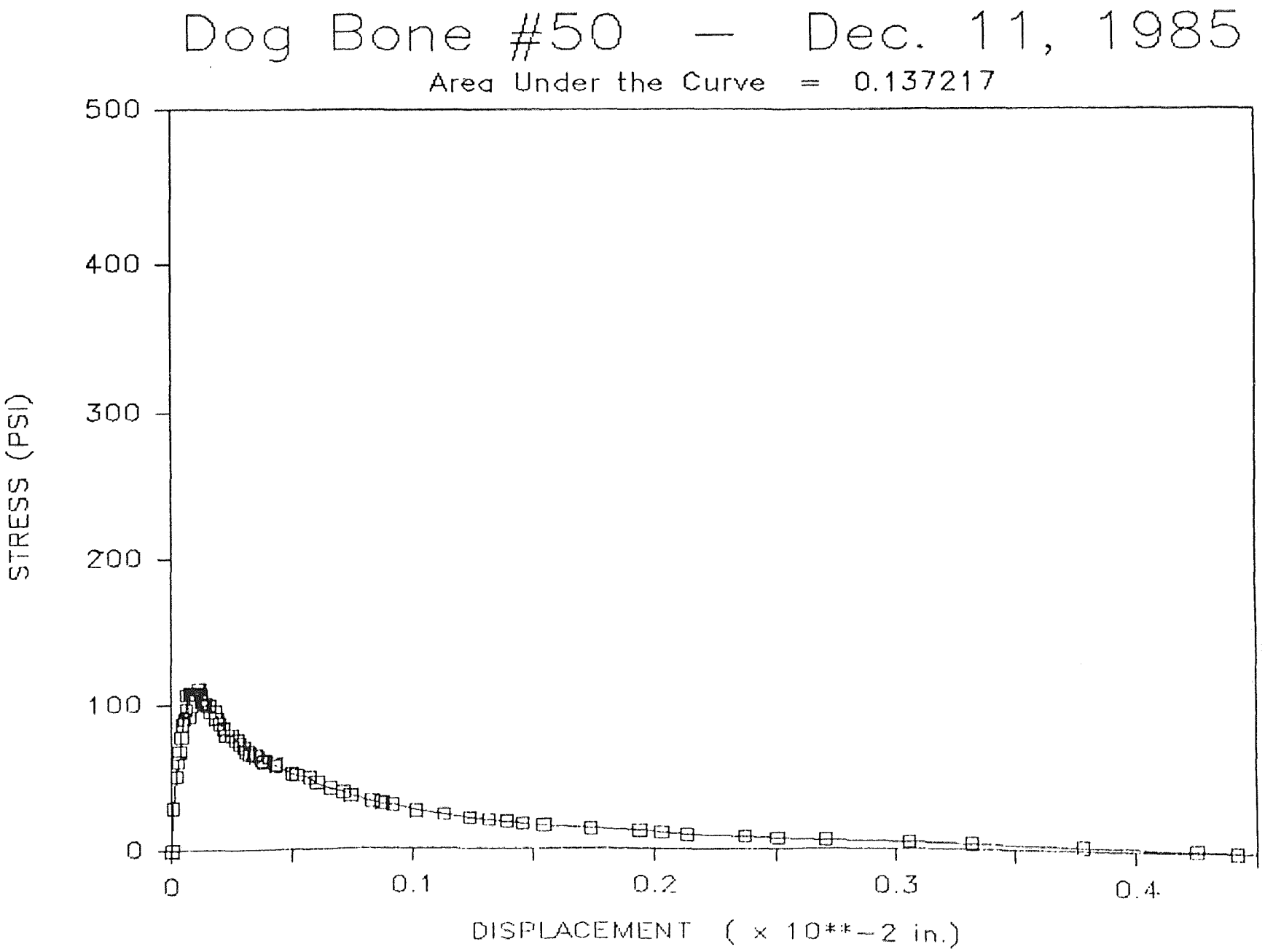
Dog Bone #50 — Dec. 11, 1985
Area Under the Curve = 0.137217
500
400
300
200
100
0
STRESS (PSI)
0
0.1
0.2
0.3
0.4
DISPLACEMENT (x 10**-2 in.)

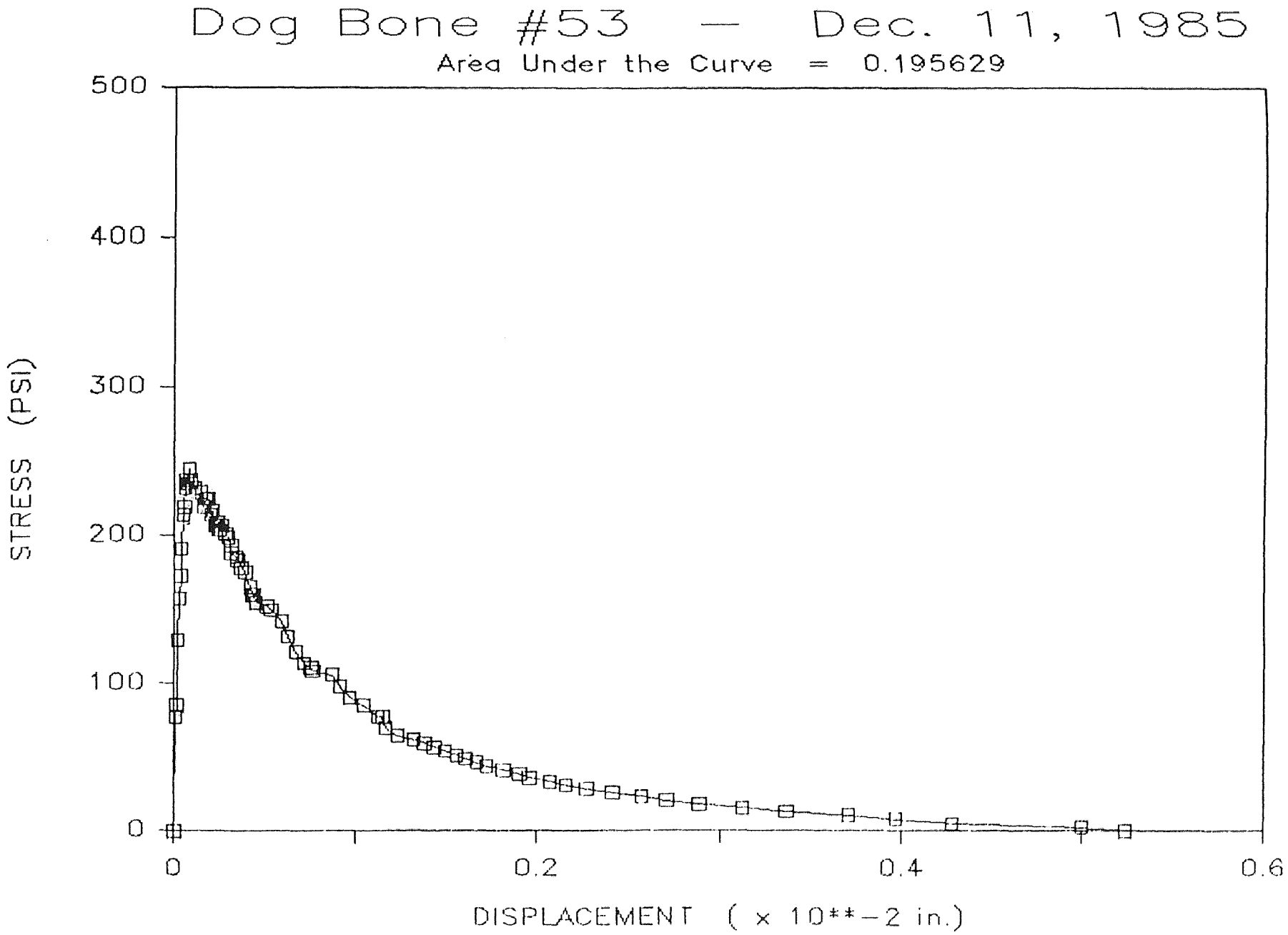
Dog Bone #53 — Dec. 11, 1985
Area Under the Curve = 0.195629
500
400
300
200
100
0
STRESS (PSI)
0
0.2
0.4
0.6
DISPLACEMENT (x 10**-2 in.)

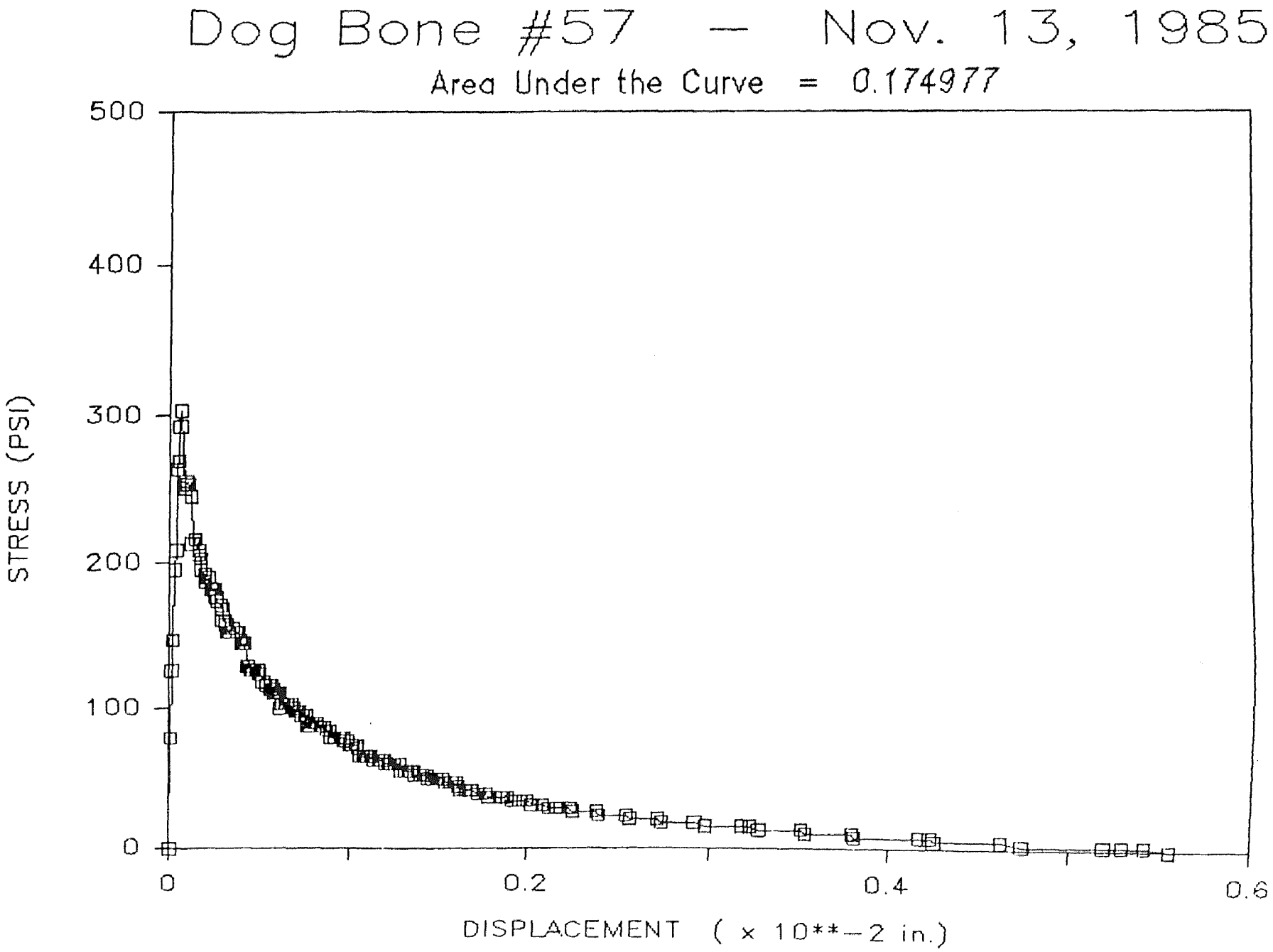
Dog Bone #57 — Nov. 13, 1985
Area Under the Curve = 0.174977
500
400
300
200
100
0
STRESS (PSI)
0
0.2
0.4
0.6
DISPLACEMENT (x 10**-2 in.)

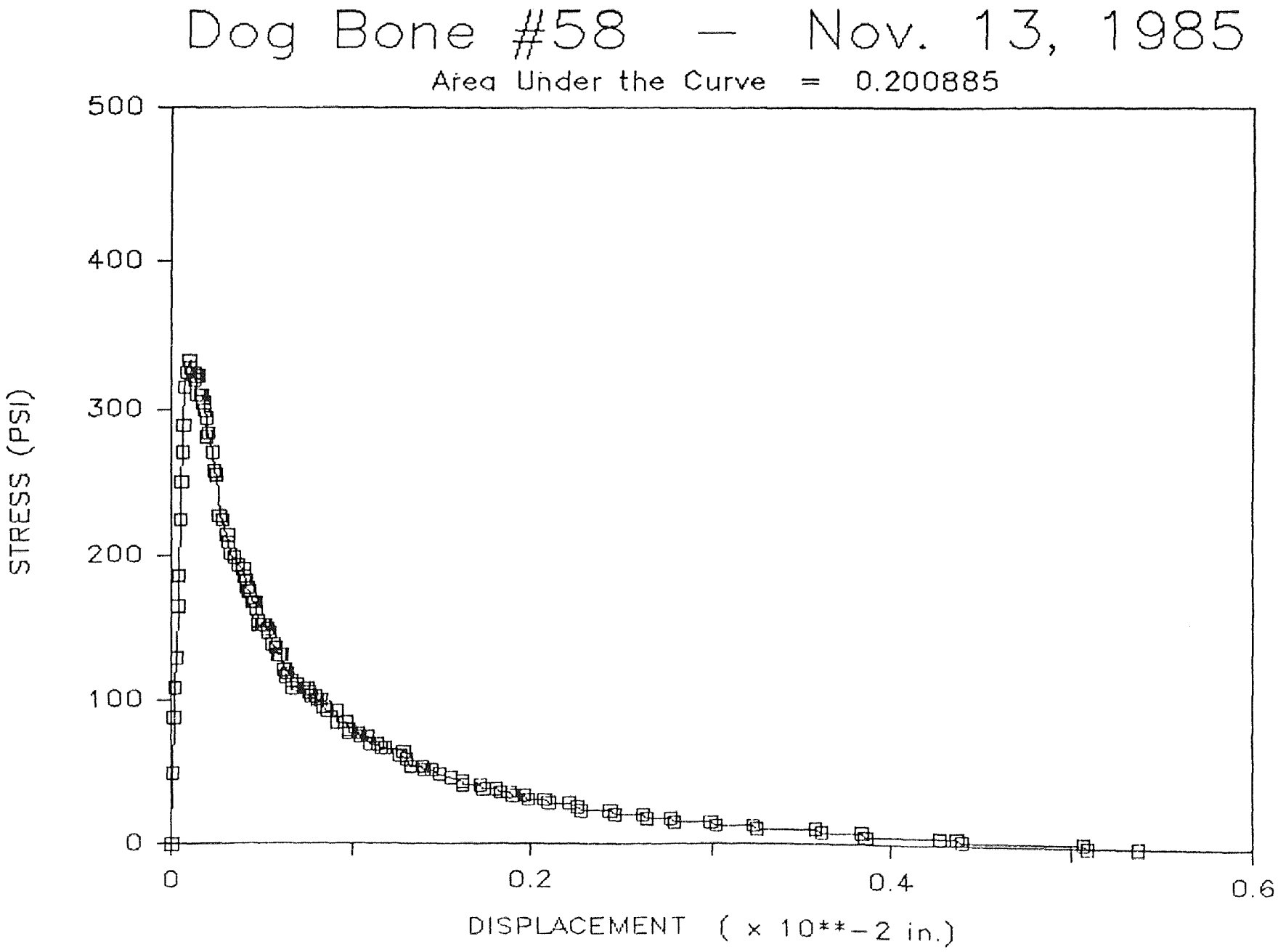
Dog Bone #58 — Nov. 13, 1985
Area Under the Curve = 0.200885
500
400
300
200
100
0
STRESS (PSI)
0
0.2
0.4
0.6
DISPLACEMENT (x 10**-2 in.)

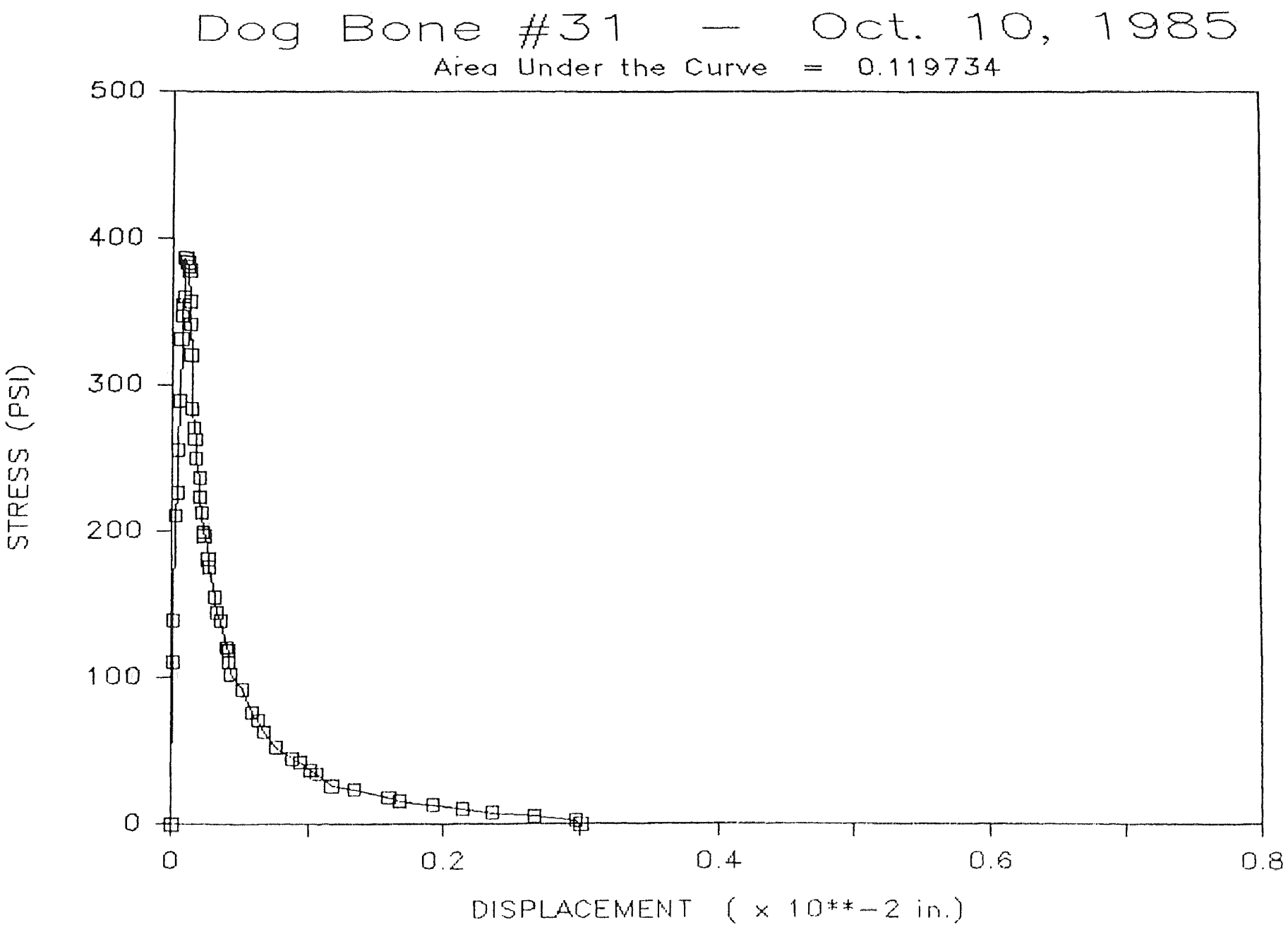
Dog Bone #31 — Oct. 10, 1985
Area Under the Curve = 0.119734
500
400
300
200
100
0
STRESS (PSI)
0
0.2
0.4
0.6
0.8
DISPLACEMENT (x 10**-2 in.)

Dog Bone #32 — Oct. 10, 1985

Area Under the Curve = 0.125874

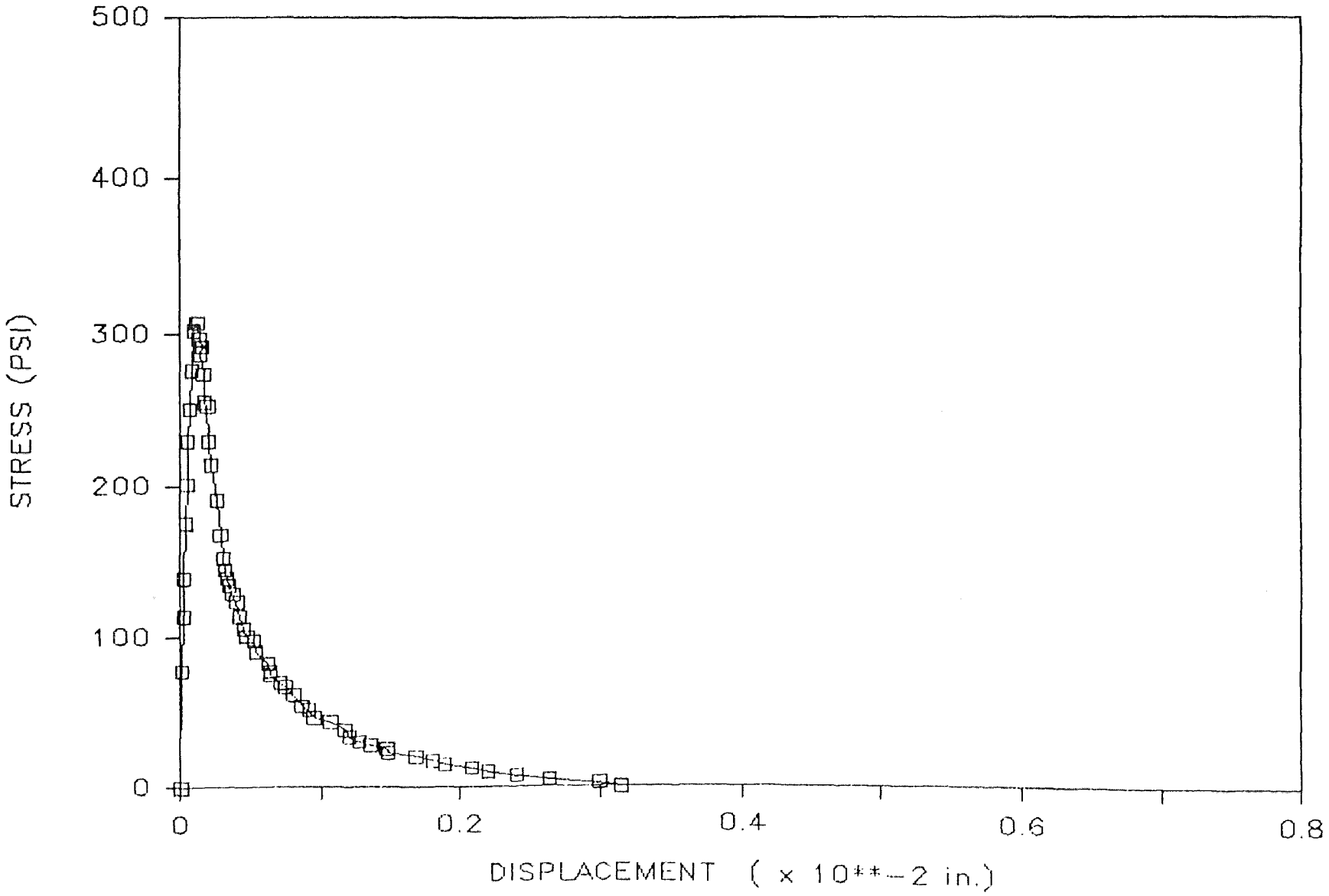

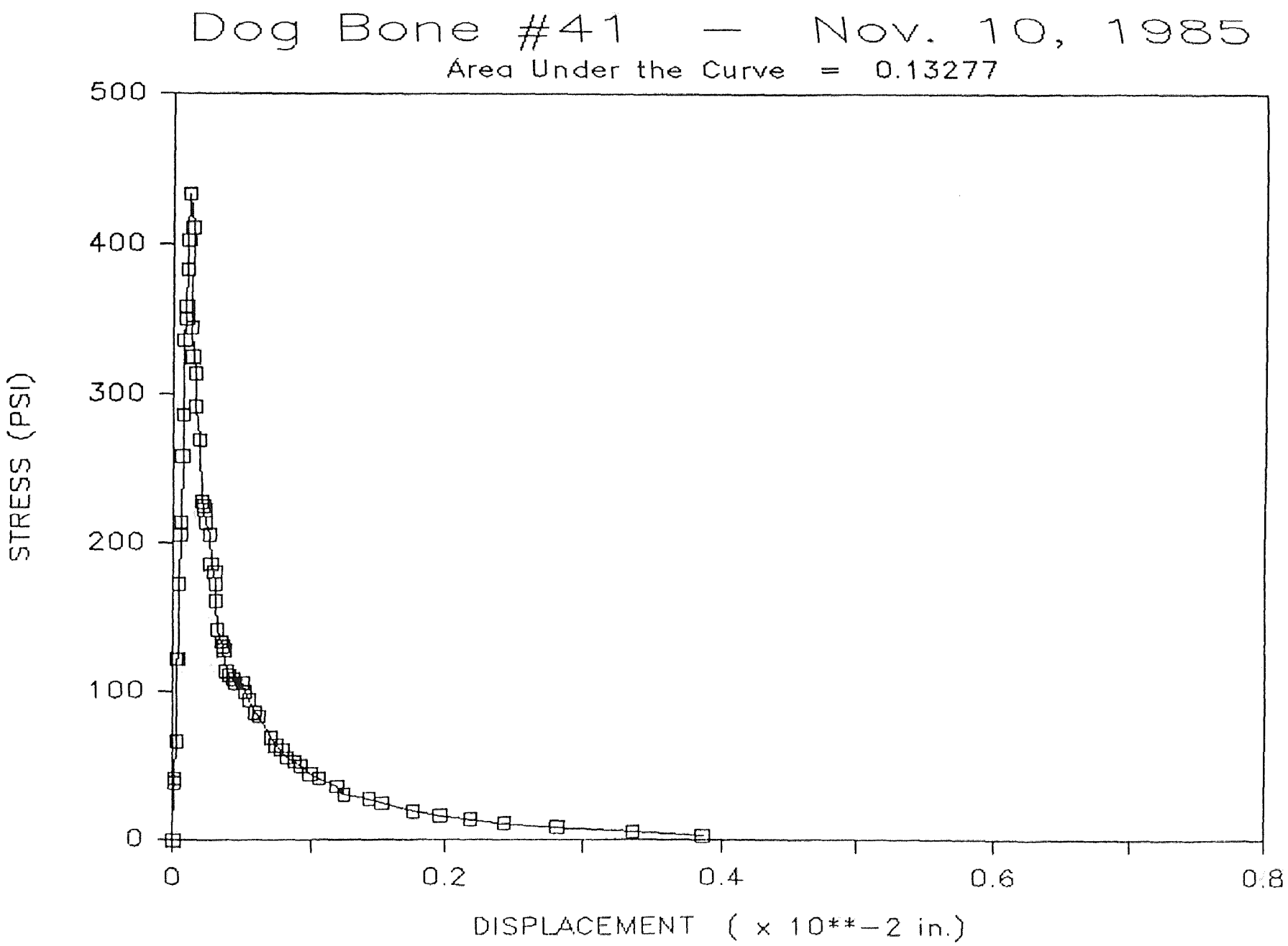
Dog Bone #41 — Nov. 10, 1985
Area Under the Curve = 0.13277
500
400
300
200
100
0
STRESS (PSI)
0
0.2
0.4
0.6
0.8
DISPLACEMENT (x 10**-2 in.)

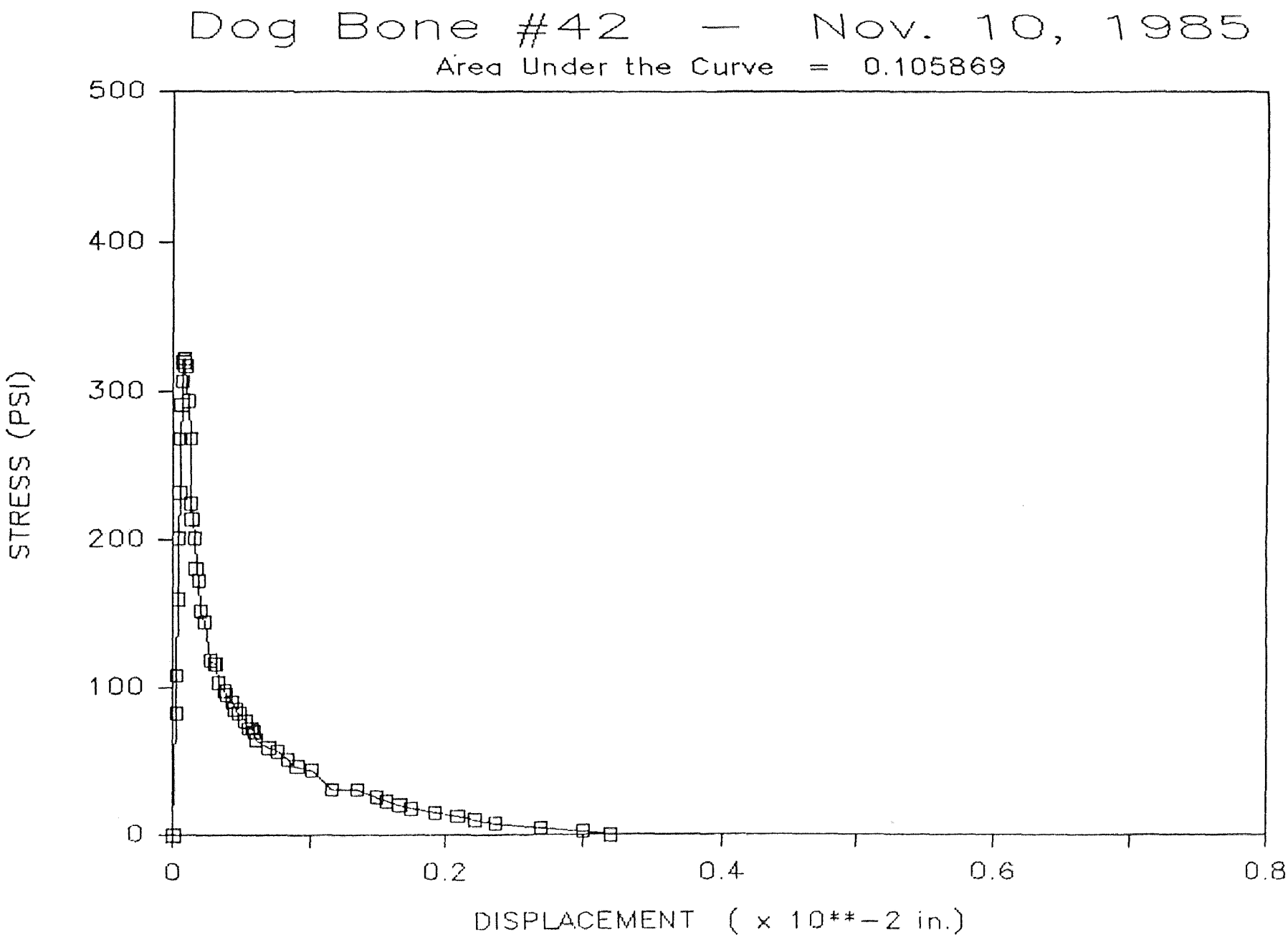
Dog Bone #42 — Nov. 10, 1985
Area Under the Curve = 0.105869
500
400
300
200
100
0
STRESS (PSI)
0
0.2
0.4
0.6
0.8
DISPLACEMENT (x 10**-2 in.)

Dog Bone #61 — Nov. 15, 1985

Area Under the Curve = 0.208732

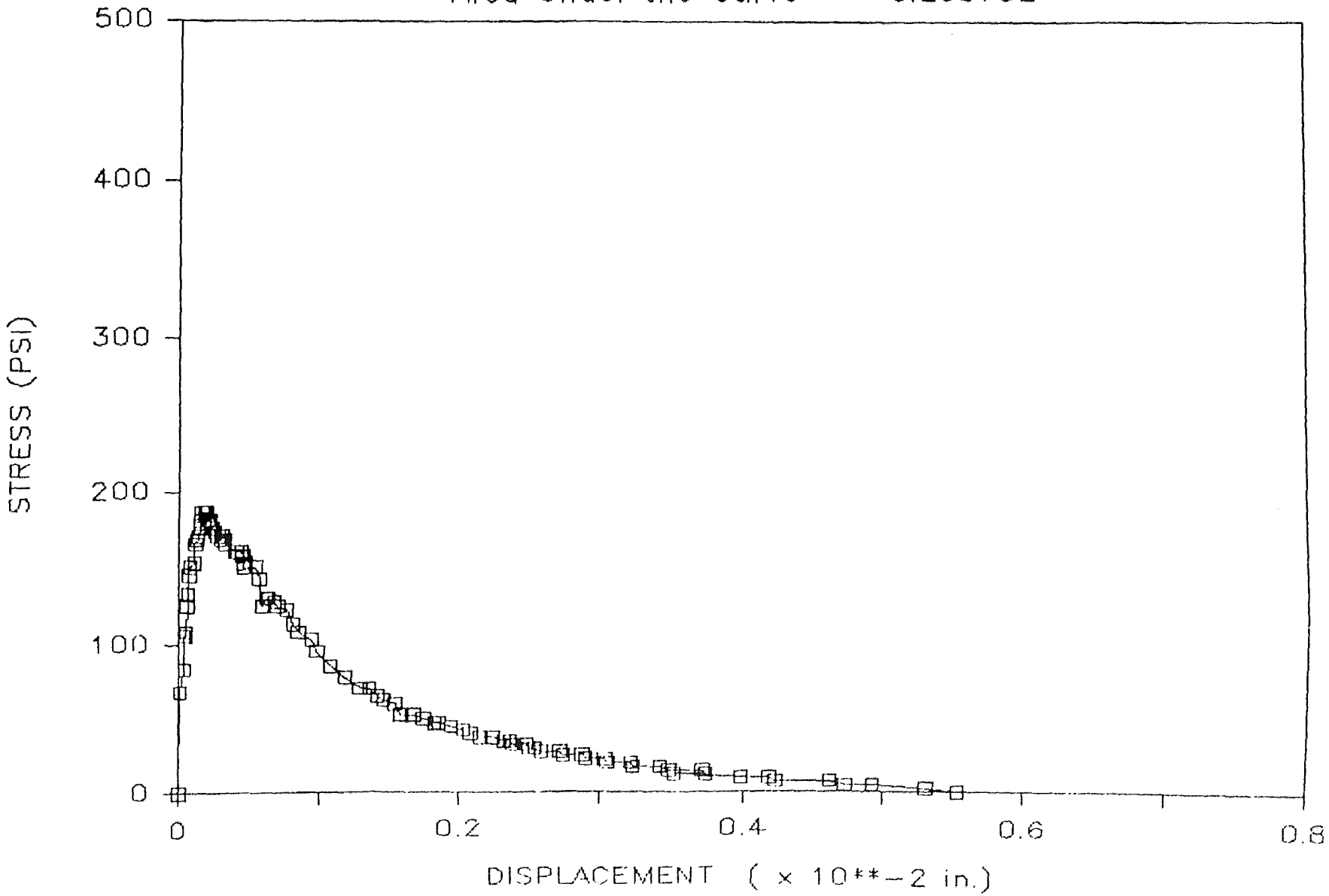

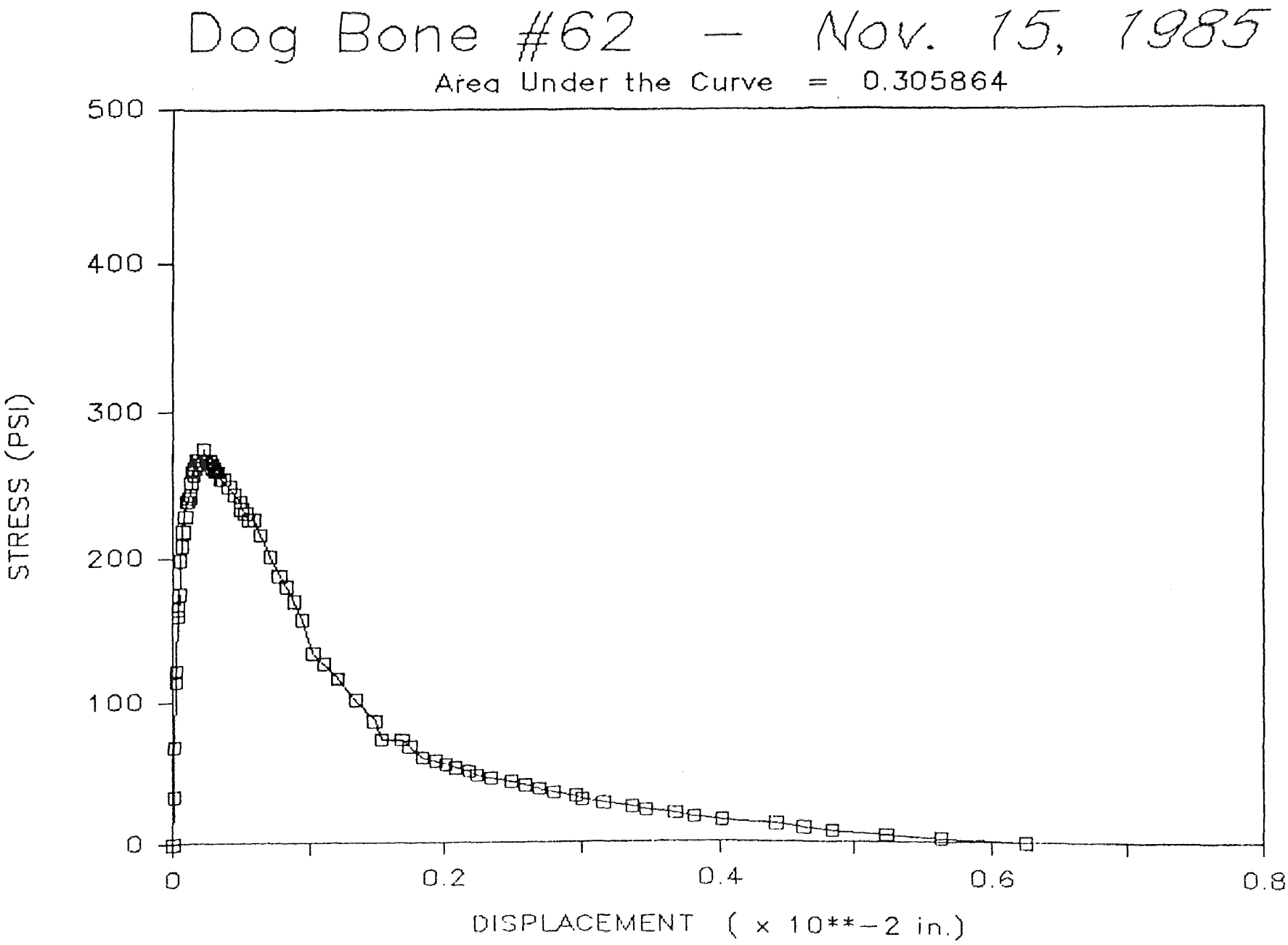
Dog Bone #62 — Nov. 15, 1985
Area Under the Curve = 0.305864
500
400
300
200
100
0
STRESS (PSI)
0
0.2
0.4
0.6
0.8
DISPLACEMENT (x 10**-2 in.)

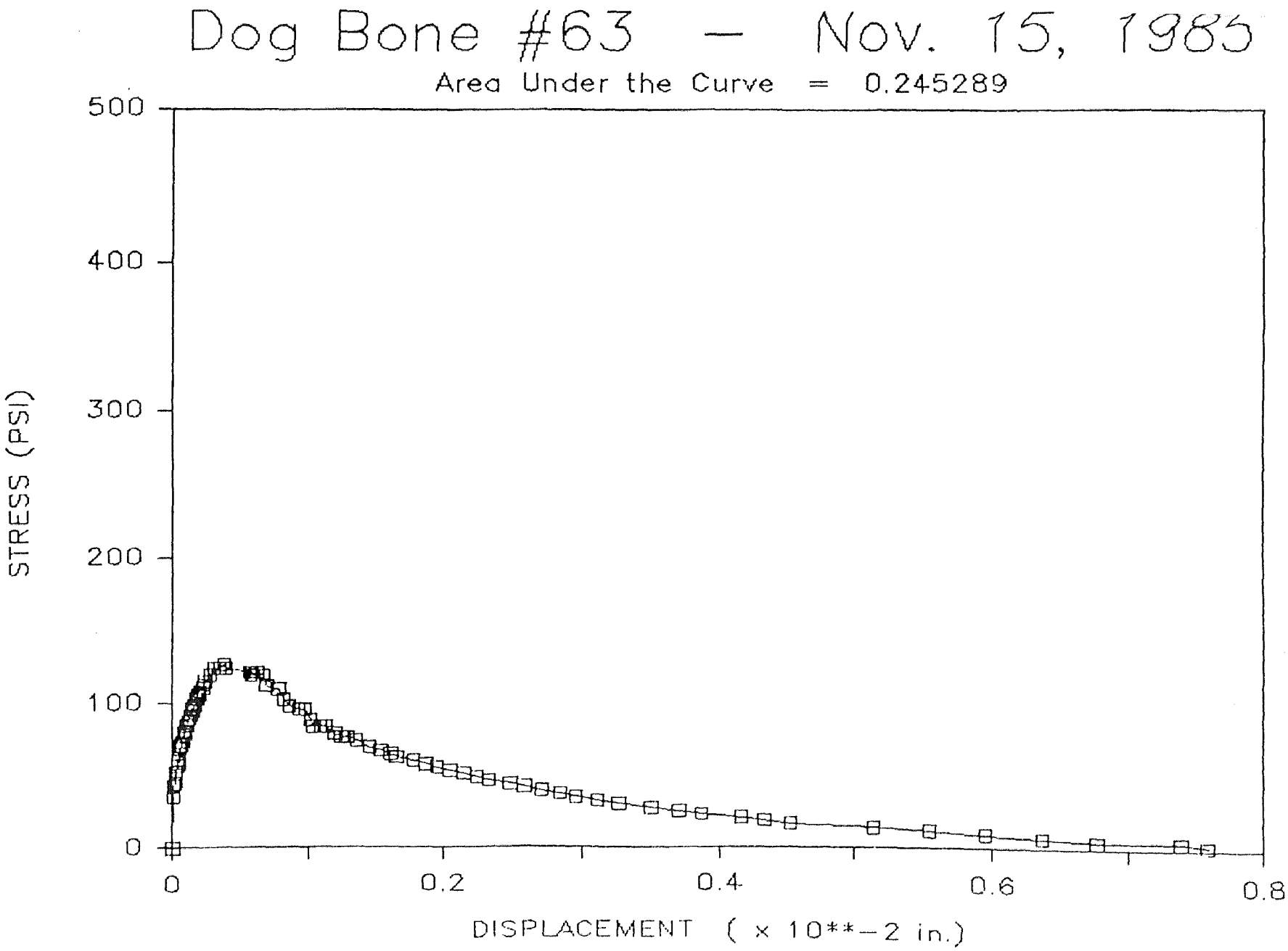
Dog Bone #63 — Nov. 15, 1985
Area Under the Curve = 0.245289
500
400
300
200
100
0
STRESS (PSI)
0
0.2
0.4
0.6
0.8
DISPLACEMENT (x 10**-2 in.)

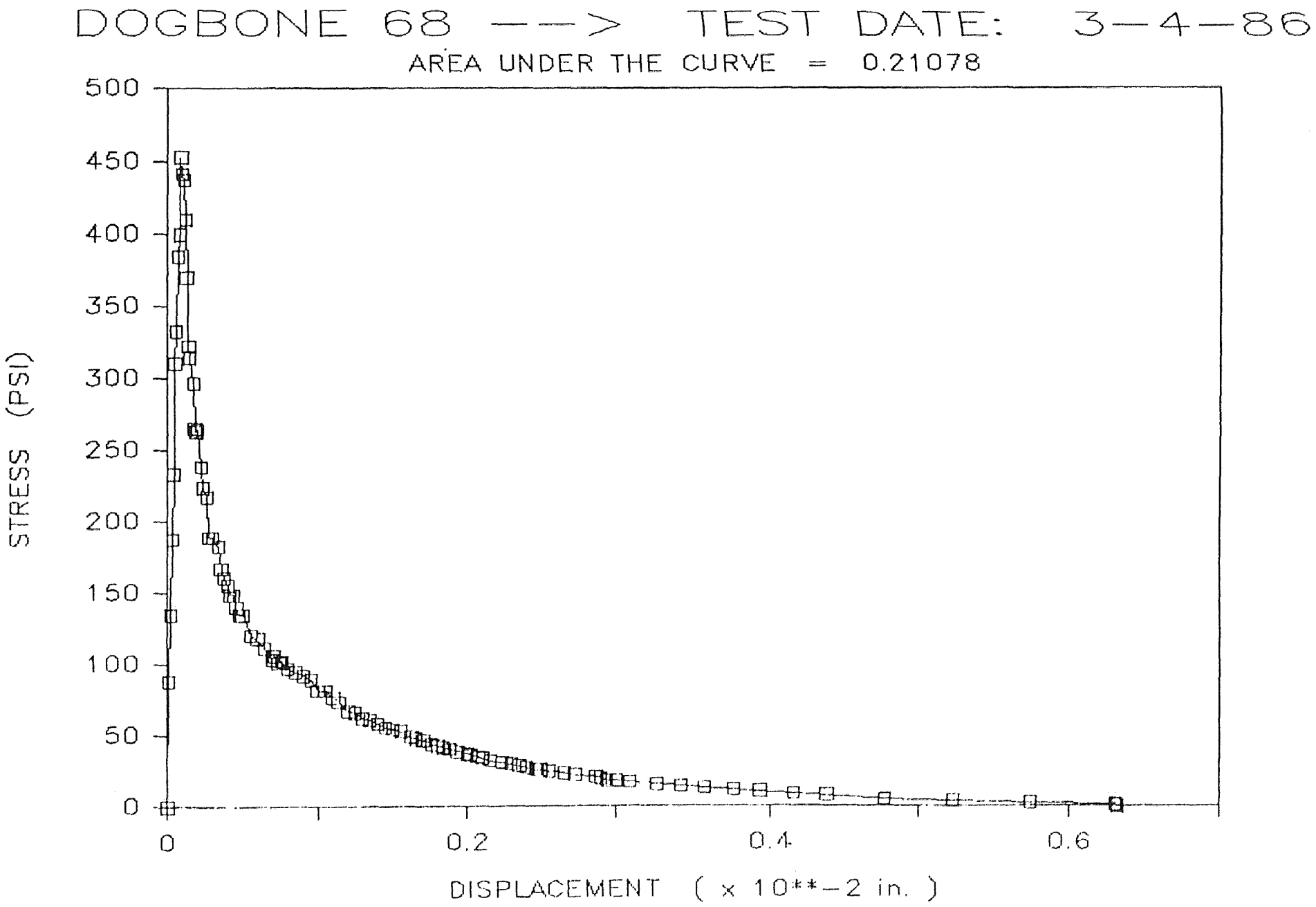
DOGBONE 68 --> TEST DATE: 3-4-86
AREA UNDER THE CURVE = 0.21078
500
450
400
350
300
250
200
150
100
50
0
STRESS (PSI)
0
0.2
0.4
0.6
DISPLACEMENT (x 10**-2 in.)

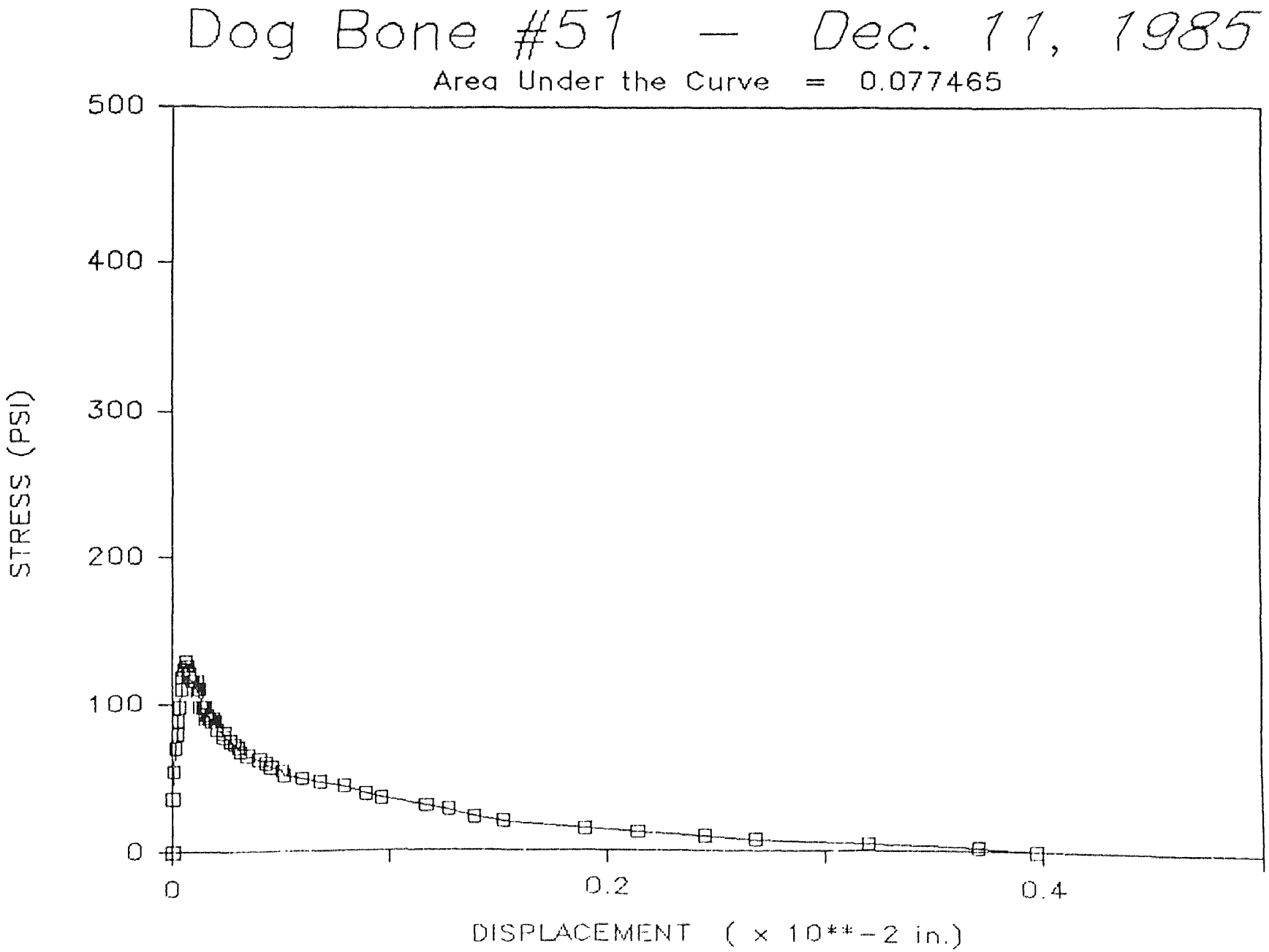
Dog Bone #51 — Dec. 11, 1985
Area Under the Curve = 0.077465
500
400
300
200
100
0
STRESS (PSI)
0
0.2
0.4
DISPLACEMENT (x 10**-2 in.)

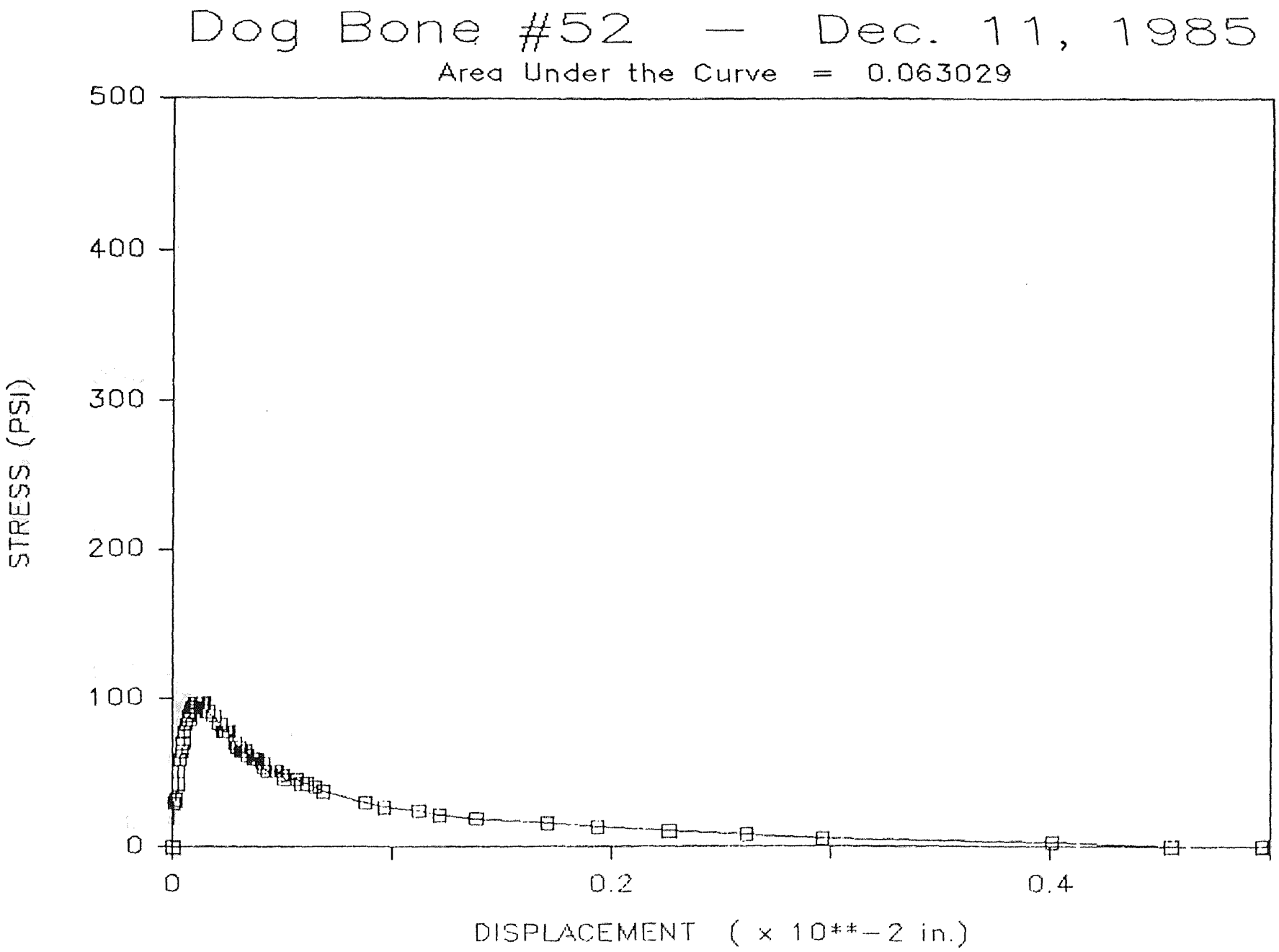
Dog Bone #52 — Dec. 11, 1985
Area Under the Curve = 0.063029
500
400
300
200
100
0
STRESS (PSI)
0
0.2
0.4
DISPLACEMENT (x 10**-2 in.)

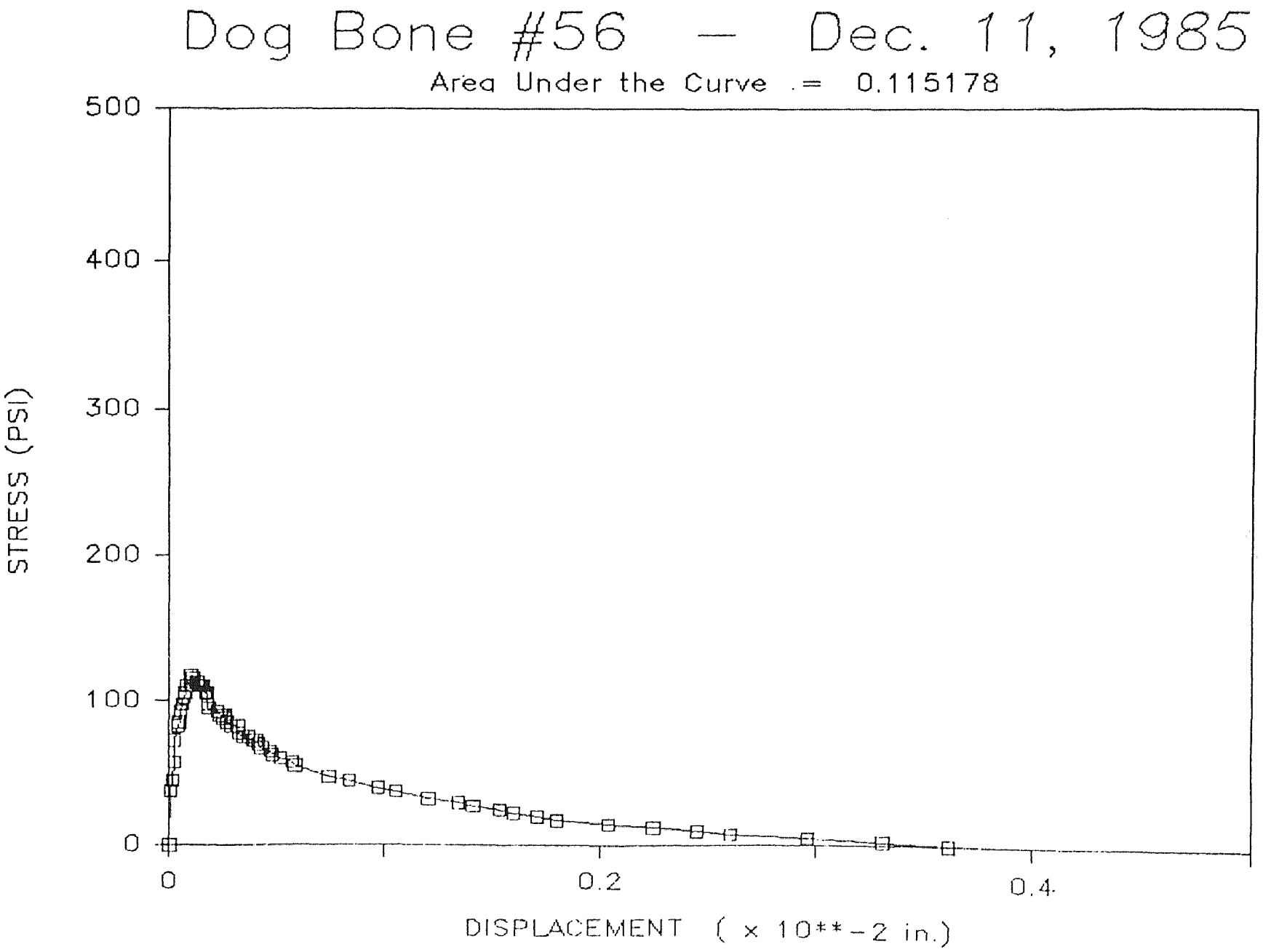
Dog Bone #56 — Dec. 11, 1985
Area Under the Curve .= 0.115178
500
400
300
200
100
0
STRESS (PSI)
0
0.2
0.4
DISPLACEMENT (x 10**-2 in.)

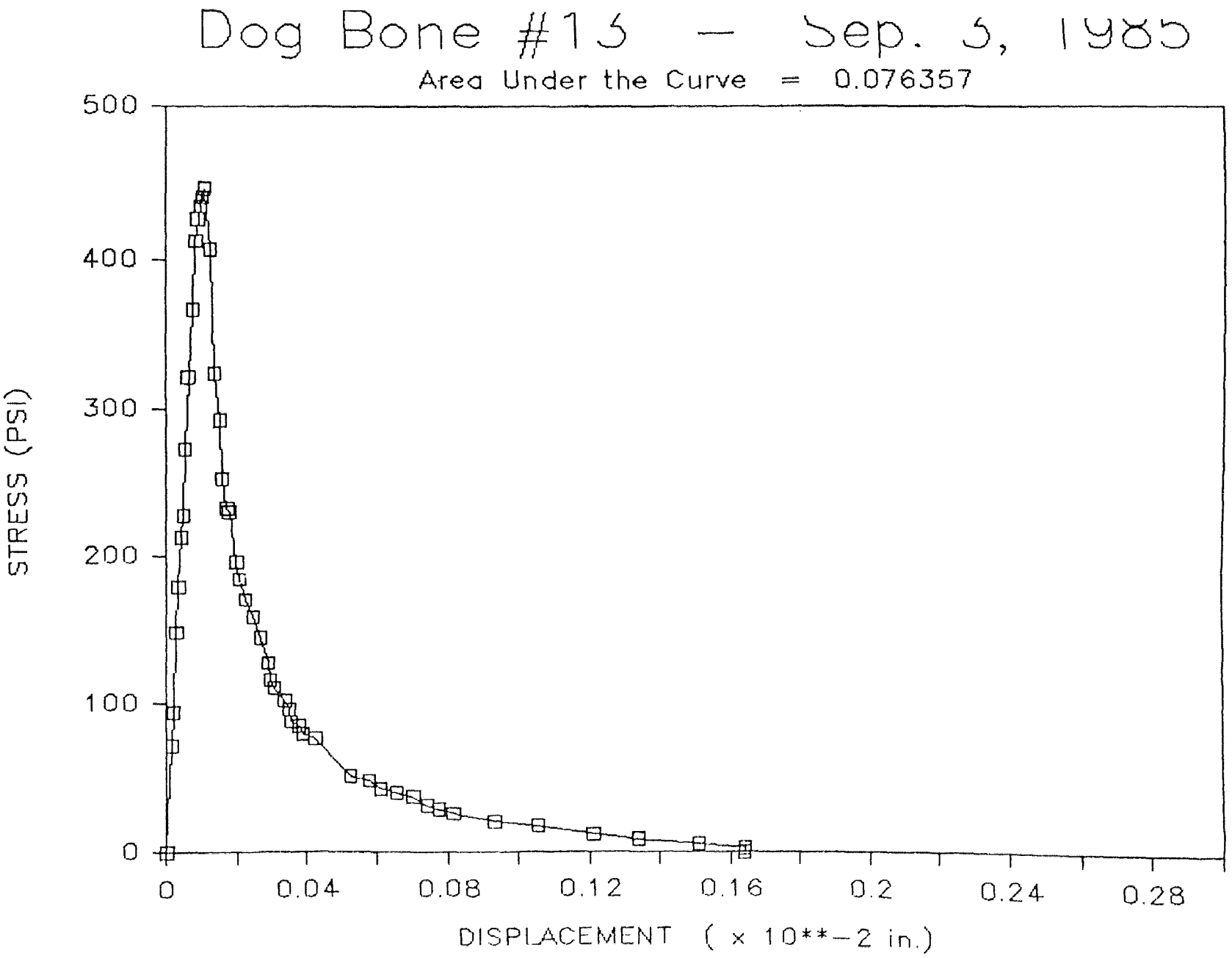
Dog Bone #13 — Sep. 3, 1985
Area Under the Curve = 0.076357
500
400
300
200
100
0
STRESS (PSI)
0
0.04
0.08
0.12
0.16
0.2
0.24
0.28
DISPLACEMENT (x 10**-2 in.)

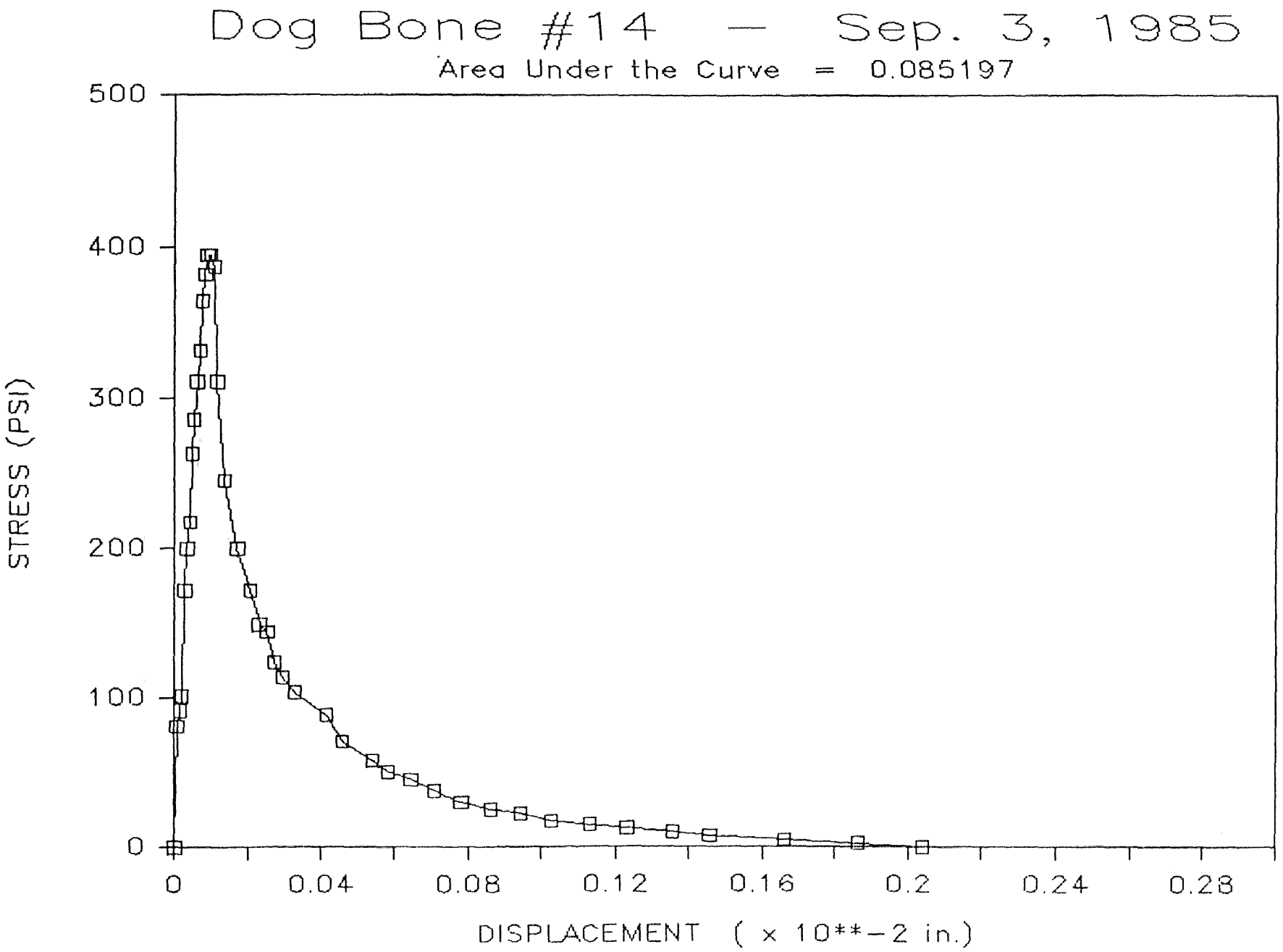
Dog Bone #14 — Sep. 3, 1985
Area Under the Curve = 0.085197
500
400
300
200
100
0
STRESS (PSI)
0
0.04
0.08
0.12
0.16
0.2
0.24
0.28
DISPLACEMENT (x 10**-2 in.)

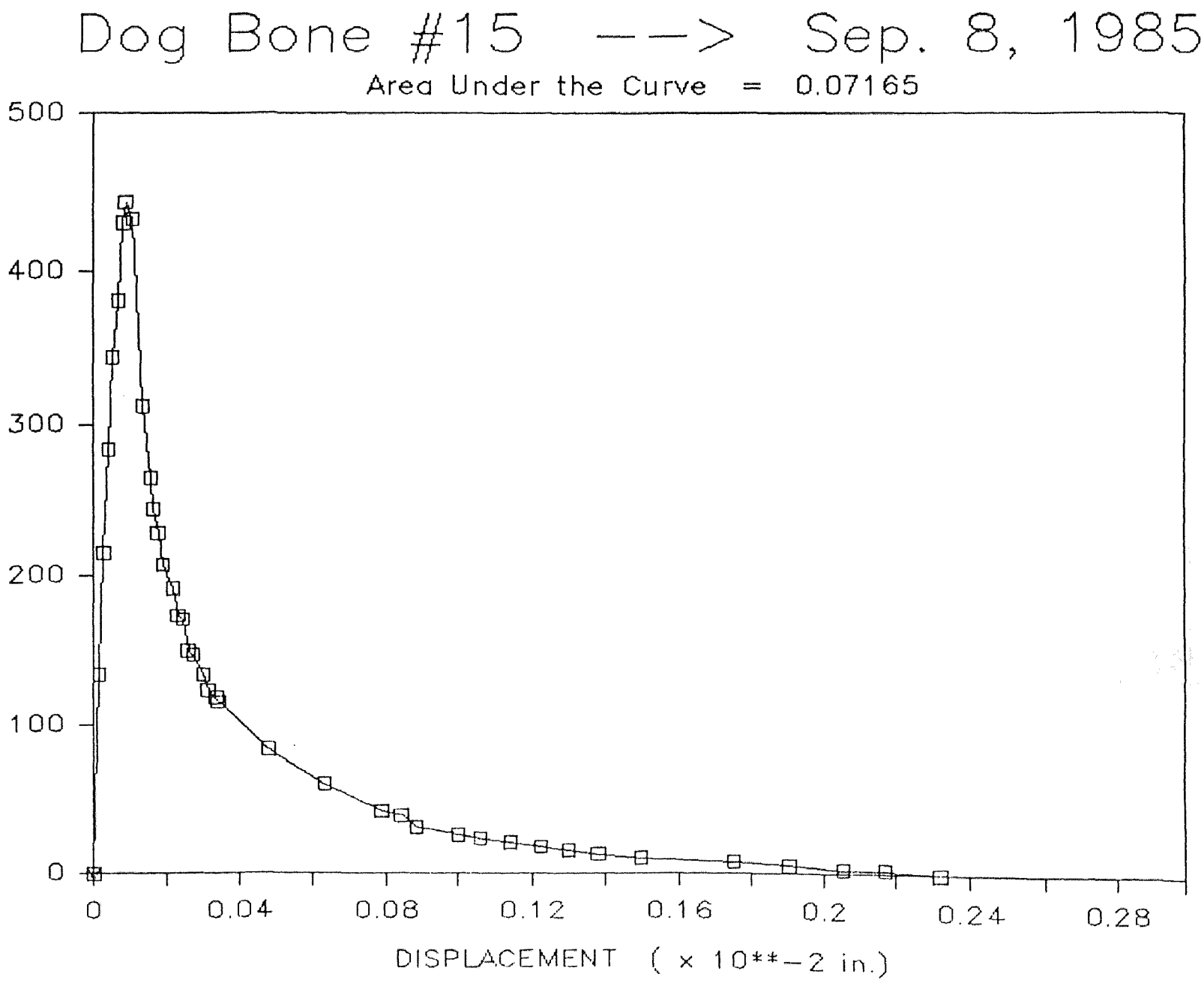
Dog Bone #15 --> Sep. 8, 1985
Area Under the Curve = 0.07165
500
400
300
200
100
0
0
0.04
0.08
0.12
0.16
0.2
0.24
0.28
DISPLACEMENT (x 10**-2 in.)

APPENDIX C

NORMALIZED POST-PEAK STRESS DISPLACEMENT RELATIONSHIPS

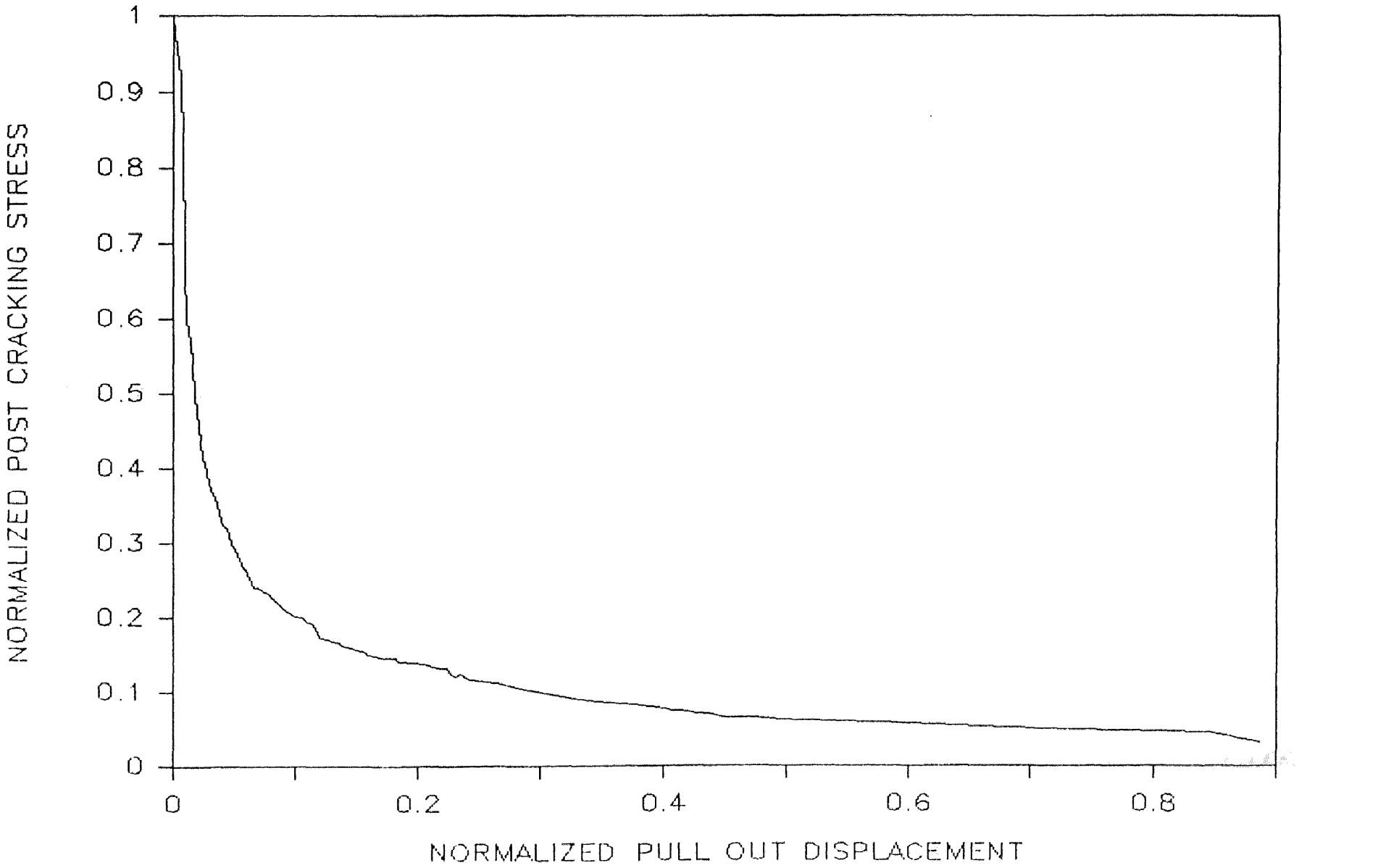
DOGBONE #2 ---> TEST DATE: JULY 17, 198
AREA UNDER THE CURVE = 0.663306
NORMALIZED POST CRACKING STRESS
1
0.9
0.8
0.7
0.6
0.5
0.4
0.3
0.2
0.1
0
0
0.2
0.4
0.6
0.8
NORMALIZED PULL OUT DISPLACEMENT

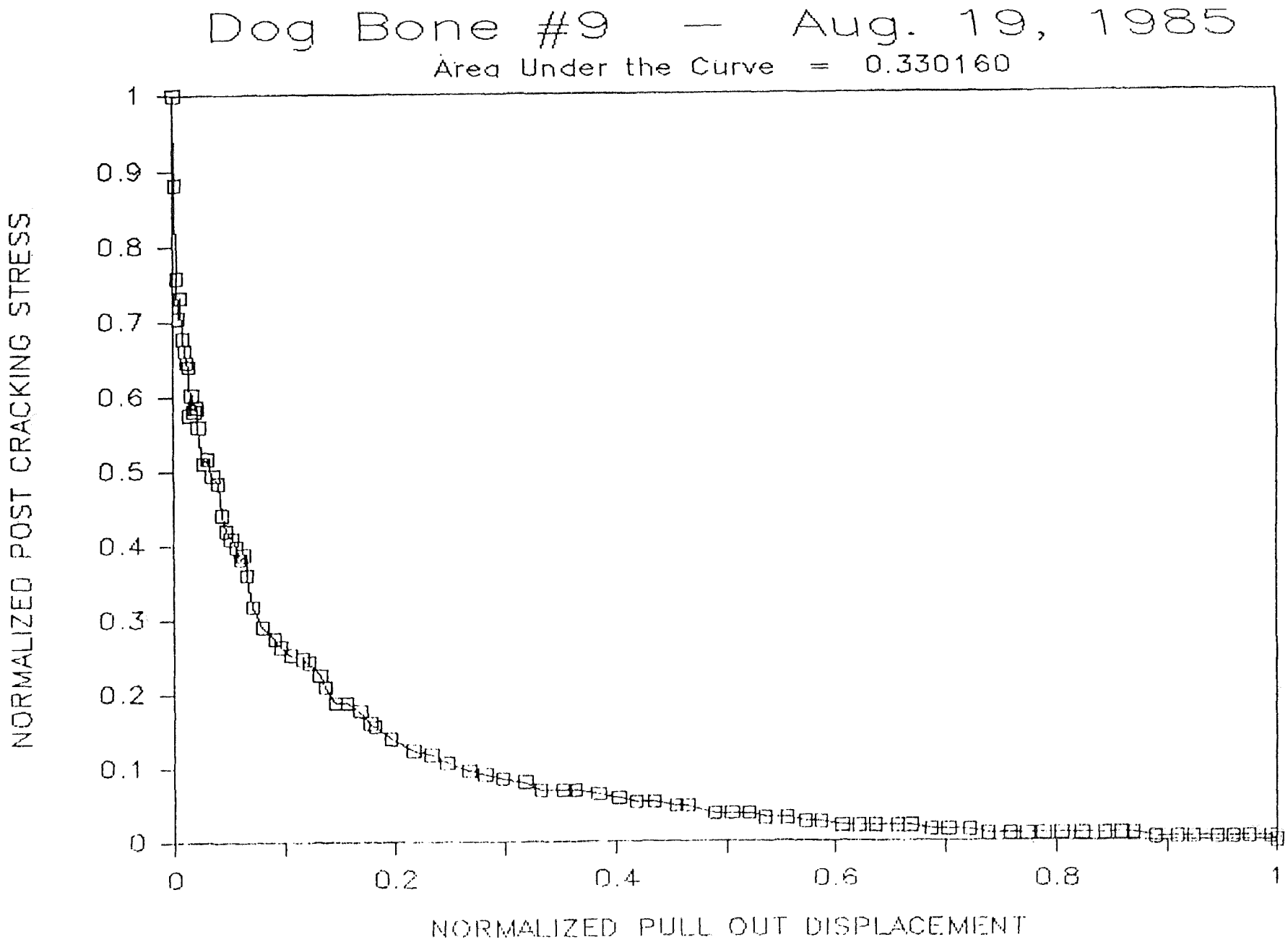
Dog Bone #9 — Aug. 19, 1985
Area Under the Curve = 0.330160
NORMALIZED POST CRACKING STRESS
1
0.9
0.8
0.7
0.6
0.5
0.4
0.3
0.2
0.1
0
0
0.2
0.4
0.6
0.8
1
NORMALIZED PULL OUT DISPLACEMENT

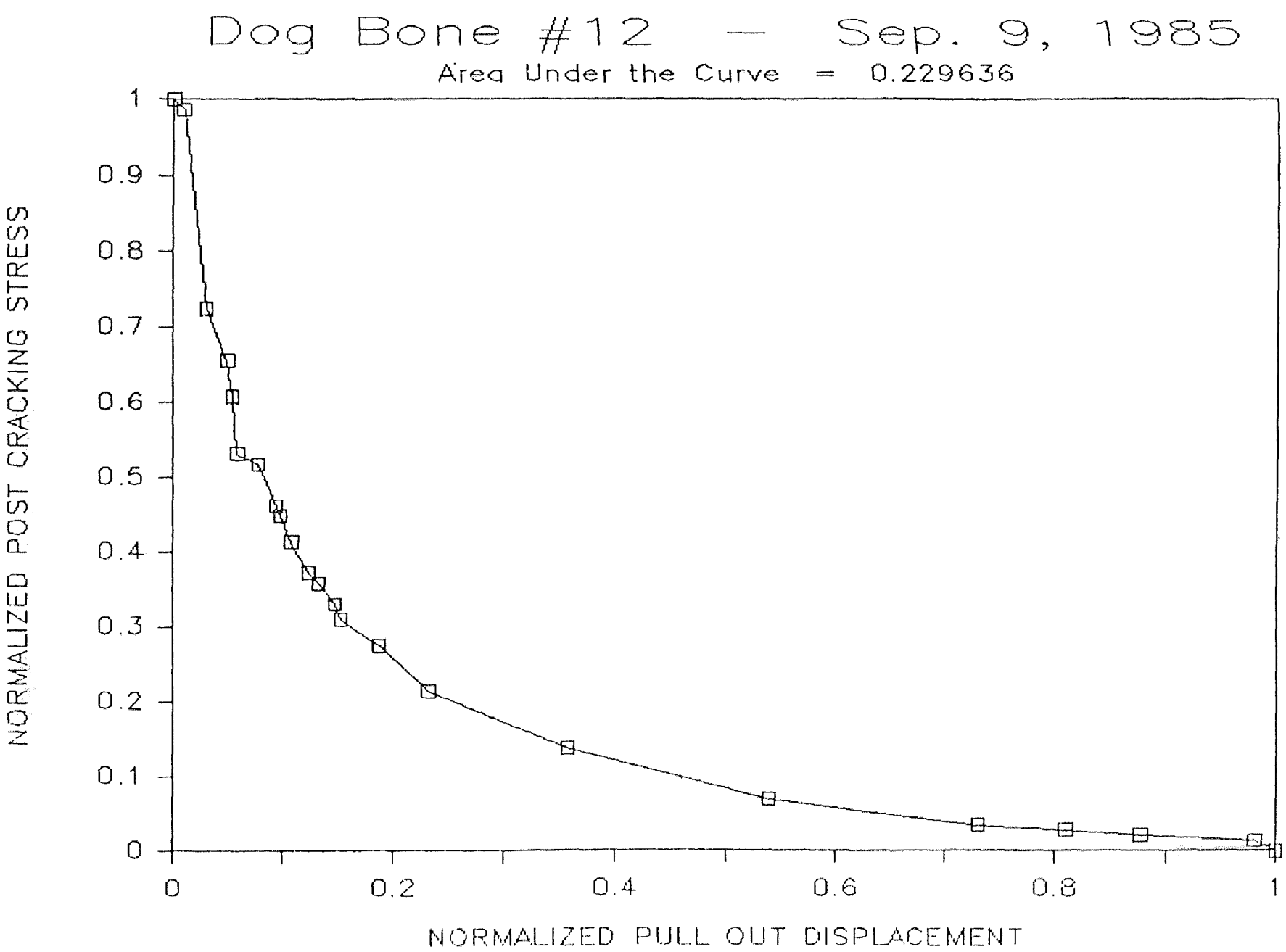
Dog Bone #12 — Sep. 9, 1985
Area Under the Curve = 0.229636
NORMALIZED POST CRACKING STRESS
NORMALIZED PULL OUT DISPLACEMENT
0
0.1
0.2
0.3
0.4
0.5
0.6
0.7
0.8
0.9
1
0
0.2
0.4
0.6
0.8
1

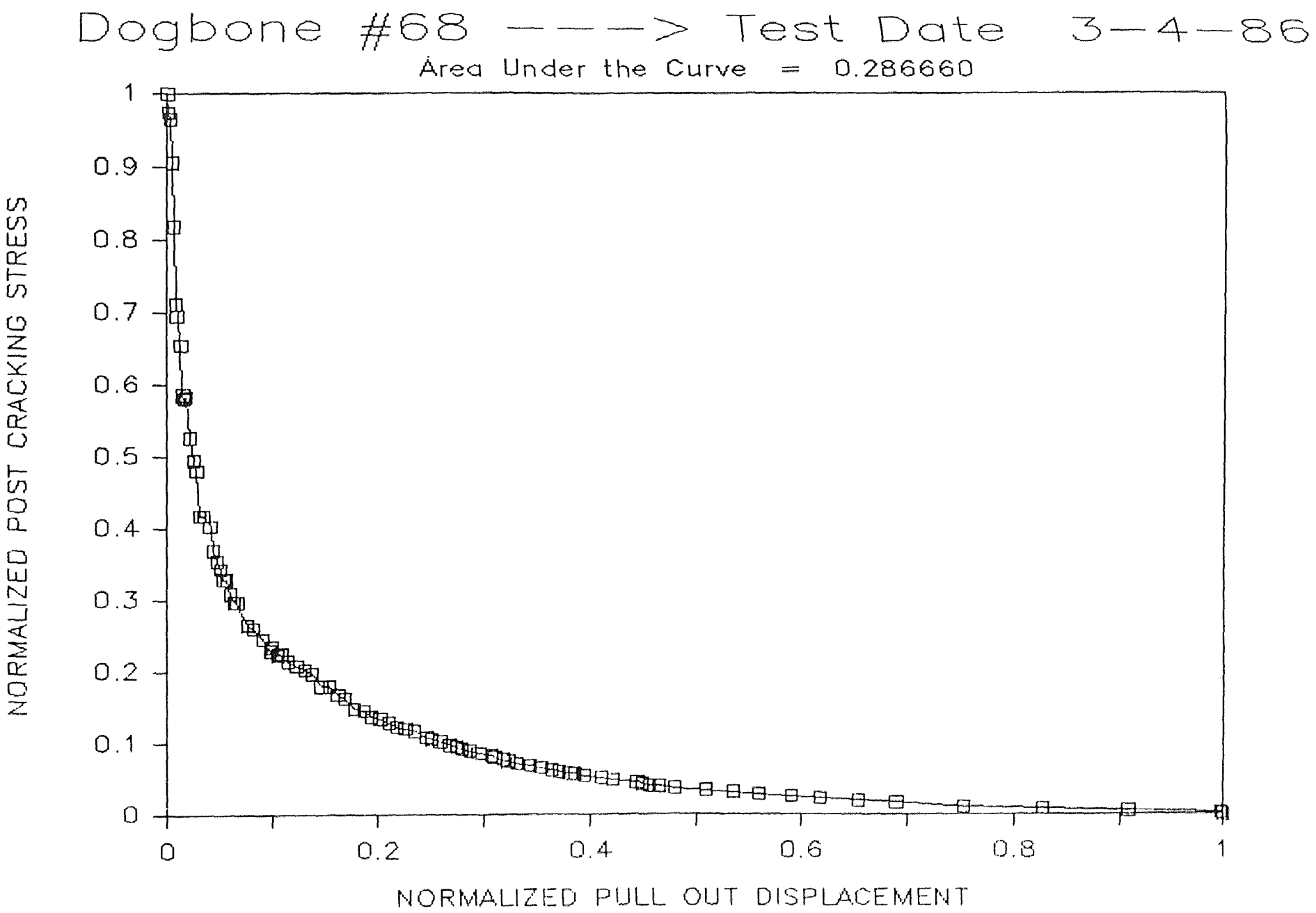
Dogbone #68 ---> Test Date 3-4-86
Area Under the Curve = 0.286660
NORMALIZED POST CRACKING STRESS
1
0.9
0.8
0.7
0.6
0.5
0.4
0.3
0.2
0.1
0
0
0.2
0.4
0.6
0.8
1
NORMALIZED PULL OUT DISPLACEMENT

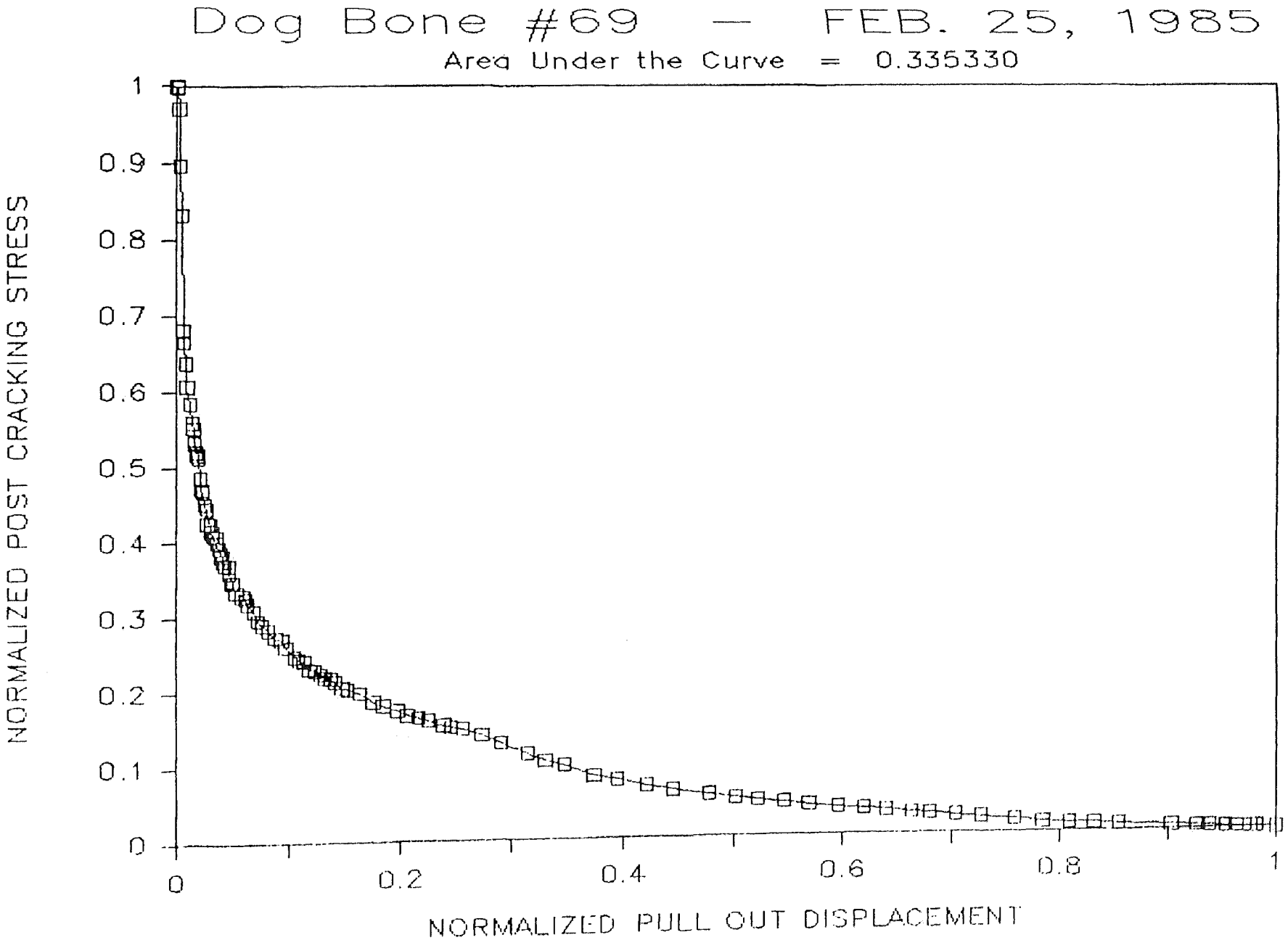
Dog Bone #69 — FEB. 25, 1985
Area Under the Curve = 0.335330
NORMALIZED POST CRACKING STRESS
NORMALIZED PULL OUT DISPLACEMENT
0
0.1
0.2
0.3
0.4
0.5
0.6
0.7
0.8
0.9
1
0
0.2
0.4
0.6
0.8
1

Dogbone #70 ---> Test Date: 3 — 26 — ε

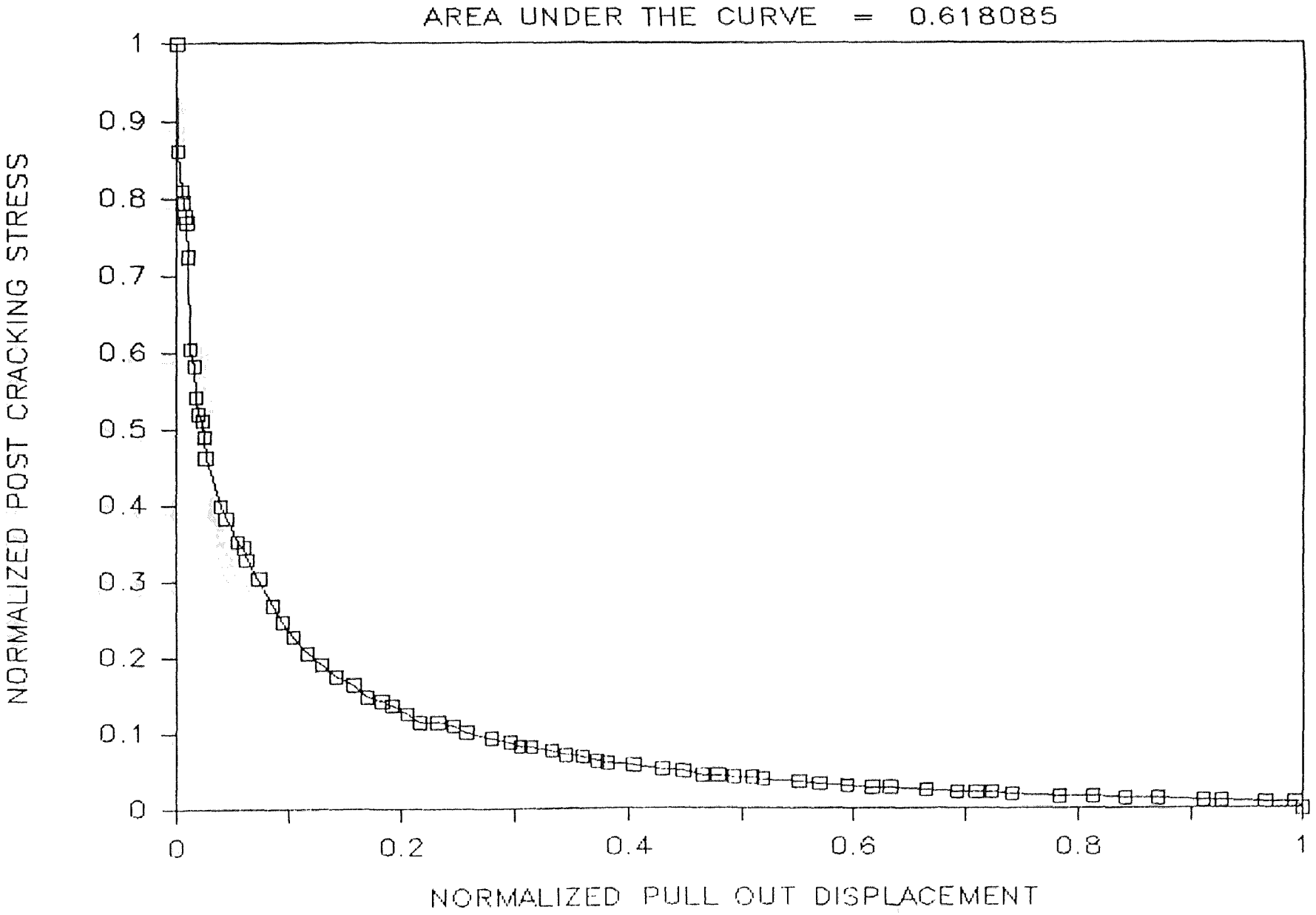

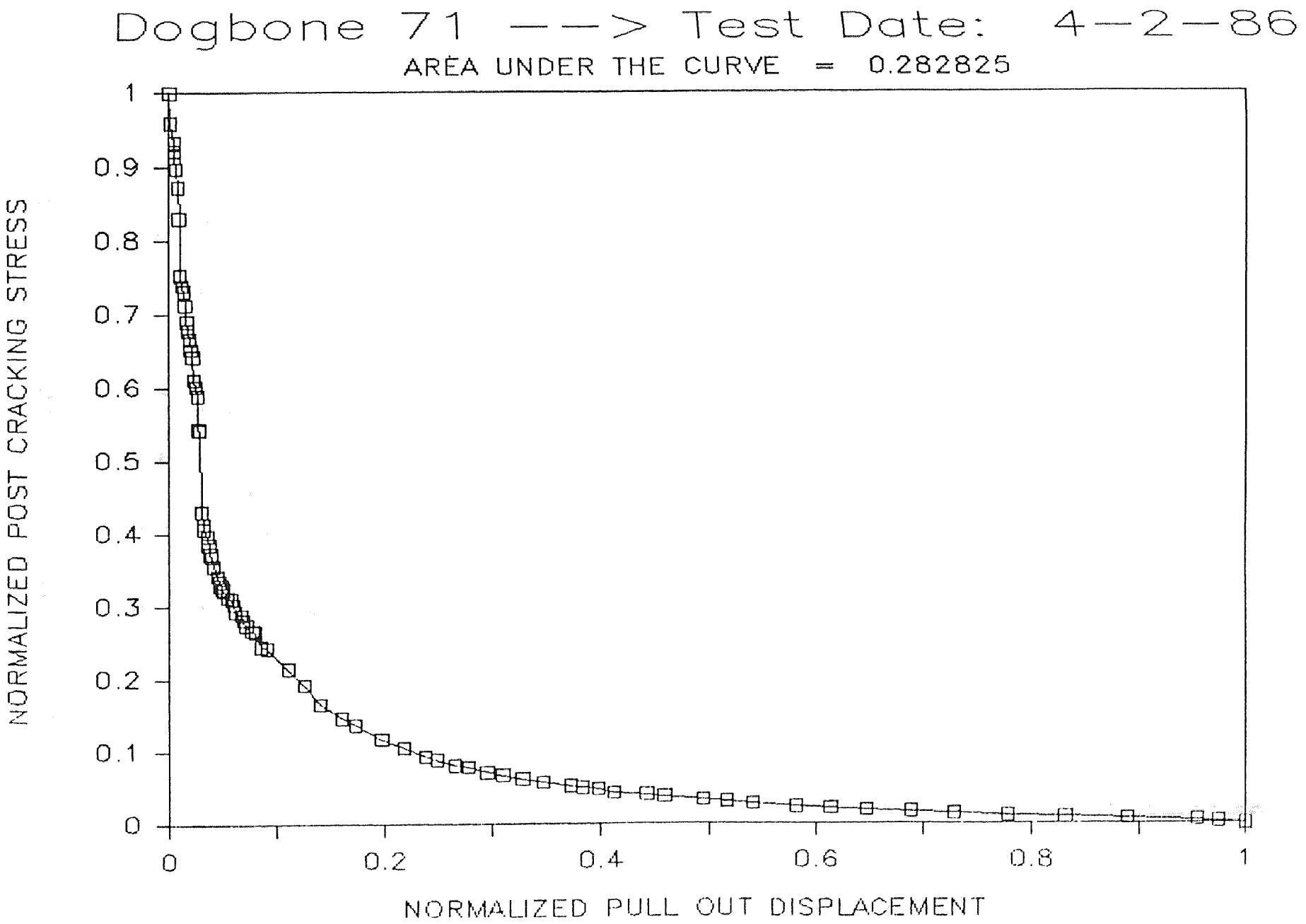
Dogbone 71 --> Test Date: 4-2-86
AREA UNDER THE CURVE = 0.282825
NORMALIZED POST CRACKING STRESS
NORMALIZED PULL OUT DISPLACEMENT
0
0.1
0.2
0.3
0.4
0.5
0.6
0.7
0.8
0.9
1
0
0.2
0.4
0.6
0.8
1

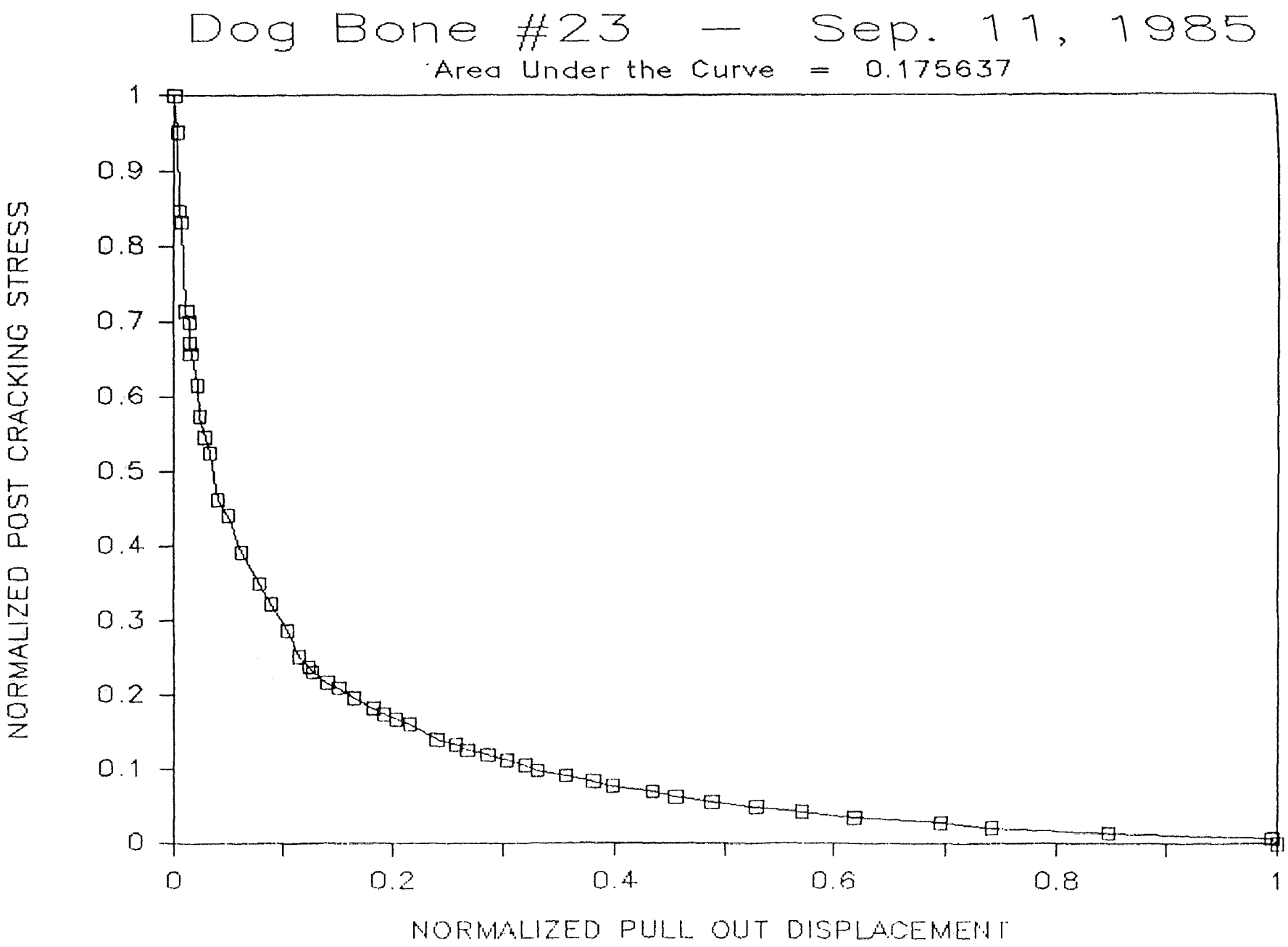
Dog Bone #23 — Sep. 11, 1985
Area Under the Curve = 0.175637
NORMALIZED POST CRACKING STRESS
NORMALIZED PULL OUT DISPLACEMENT
0
0.1
0.2
0.3
0.4
0.5
0.6
0.7
0.8
0.9
1
0
0.2
0.4
0.6
0.8
1

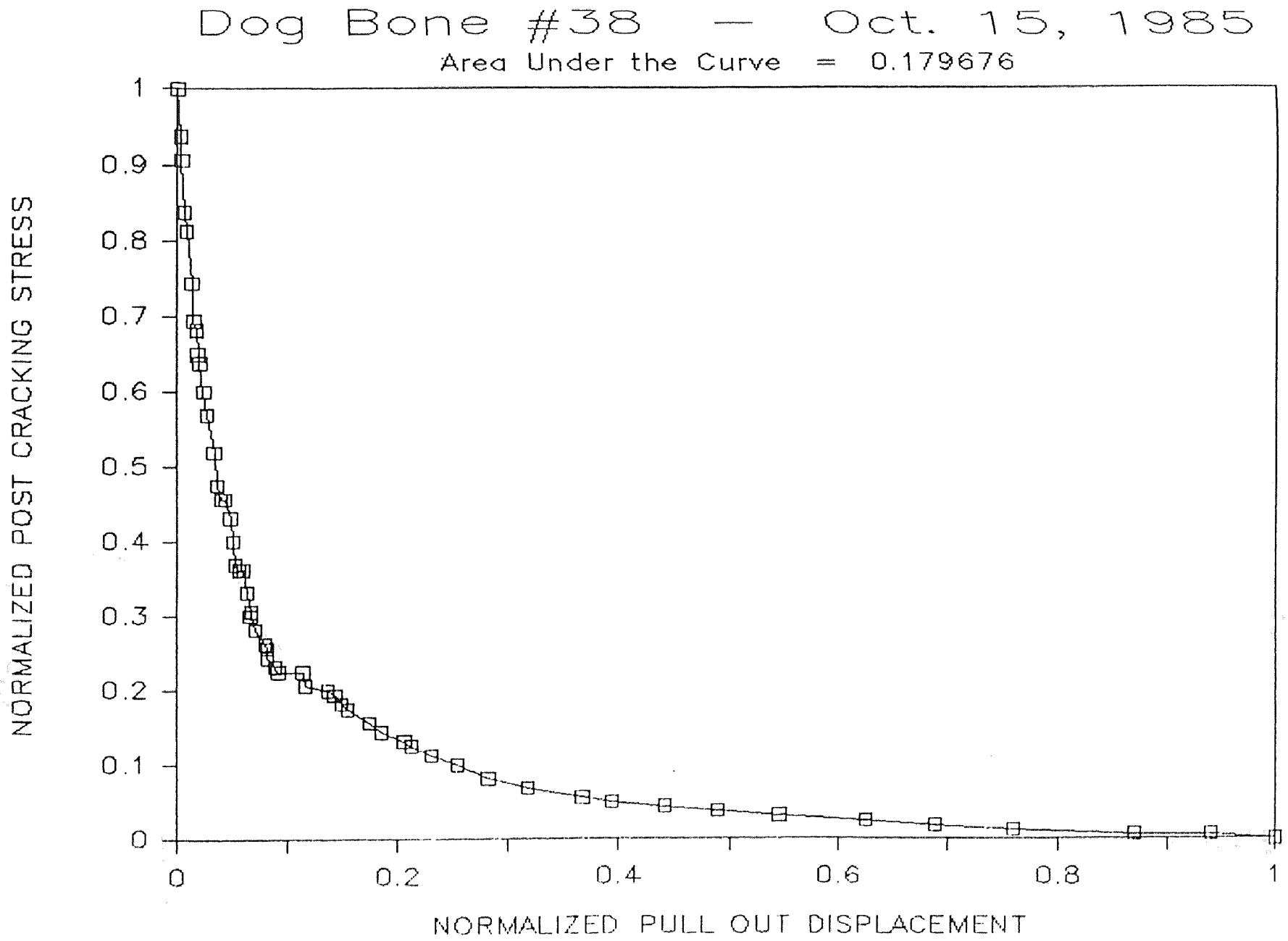
Dog Bone #38 — Oct. 15, 1985
Area Under the Curve = 0.179676
NORMALIZED POST CRACKING STRESS
1
0.9
0.8
0.7
0.6
0.5
0.4
0.3
0.2
0.1
0
0
0.2
0.4
0.6
0.8
1
NORMALIZED PULL OUT DISPLACEMENT

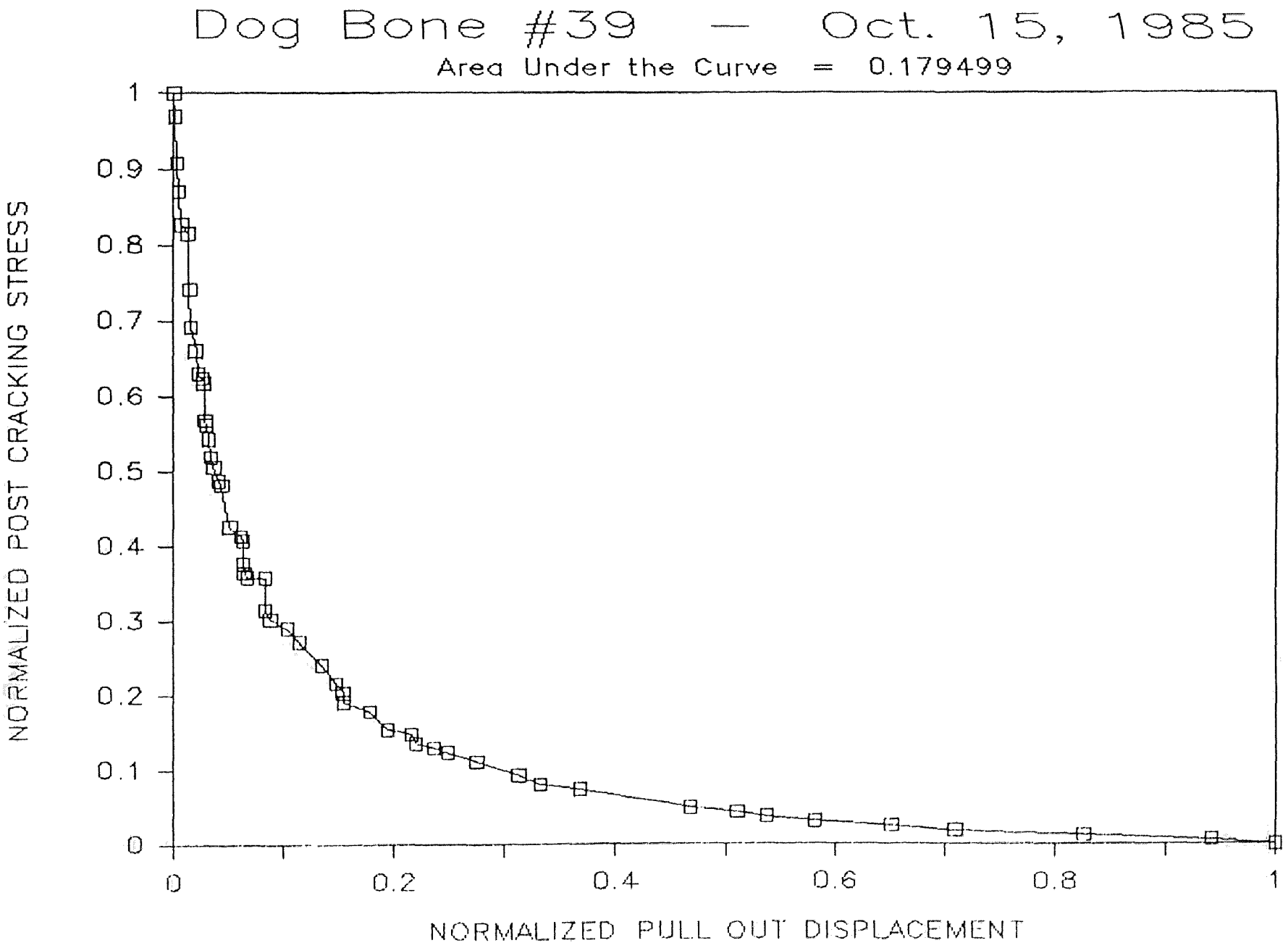
Dog Bone #39 — Oct. 15, 1985
Area Under the Curve = 0.179499
NORMALIZED POST CRACKING STRESS
1
0.9
0.8
0.7
0.6
0.5
0.4
0.3
0.2
0.1
0
0
0.2
0.4
0.6
0.8
1
NORMALIZED PULL OUT DISPLACEMENT

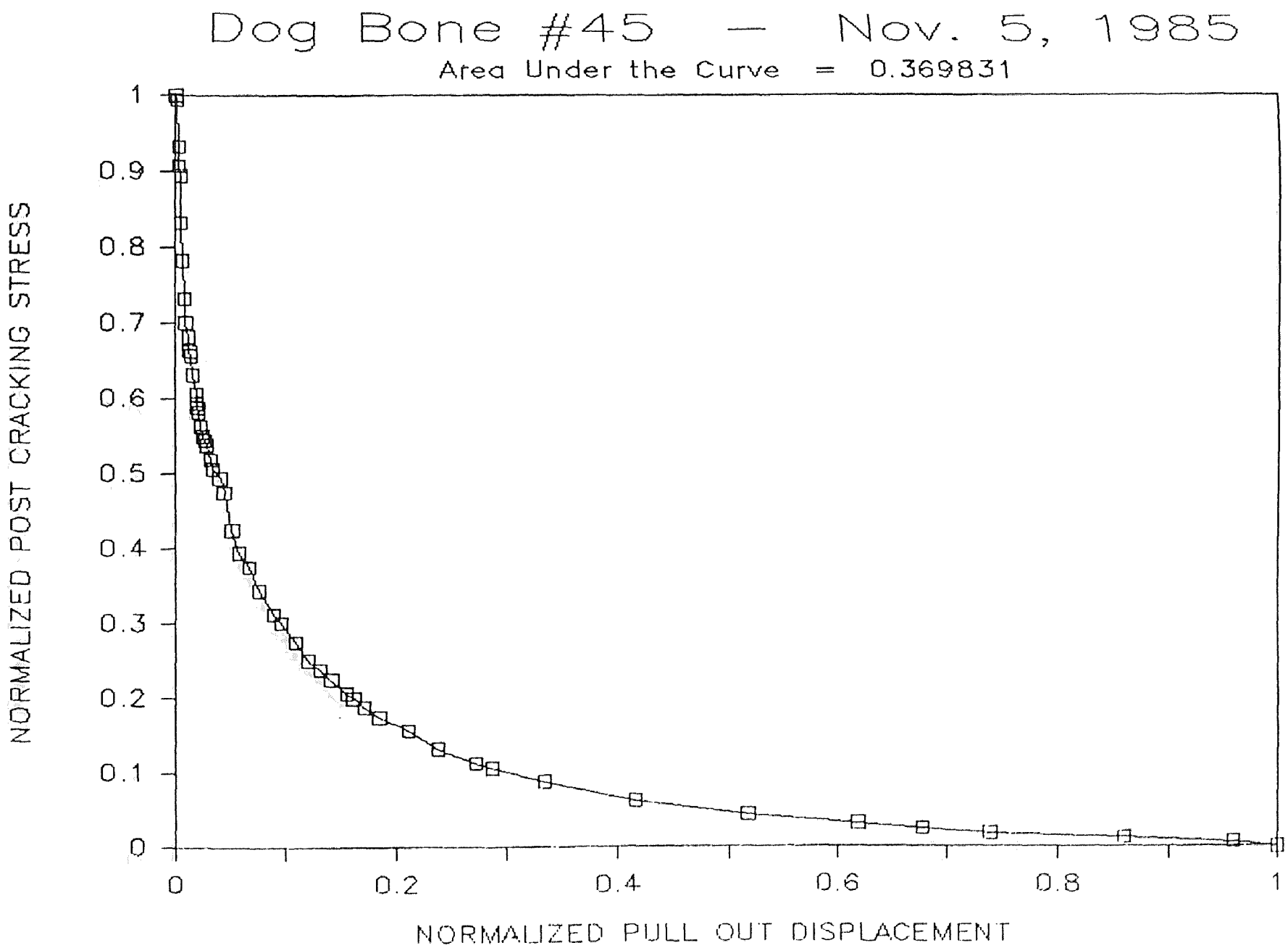
Dog Bone #45 — Nov. 5, 1985
Area Under the Curve = 0.369831
NORMALIZED POST CRACKING STRESS
NORMALIZED PULL OUT DISPLACEMENT
0
0.1
0.2
0.3
0.4
0.5
0.6
0.7
0.8
0.9
1
0
0.2
0.4
0.6
0.8
1

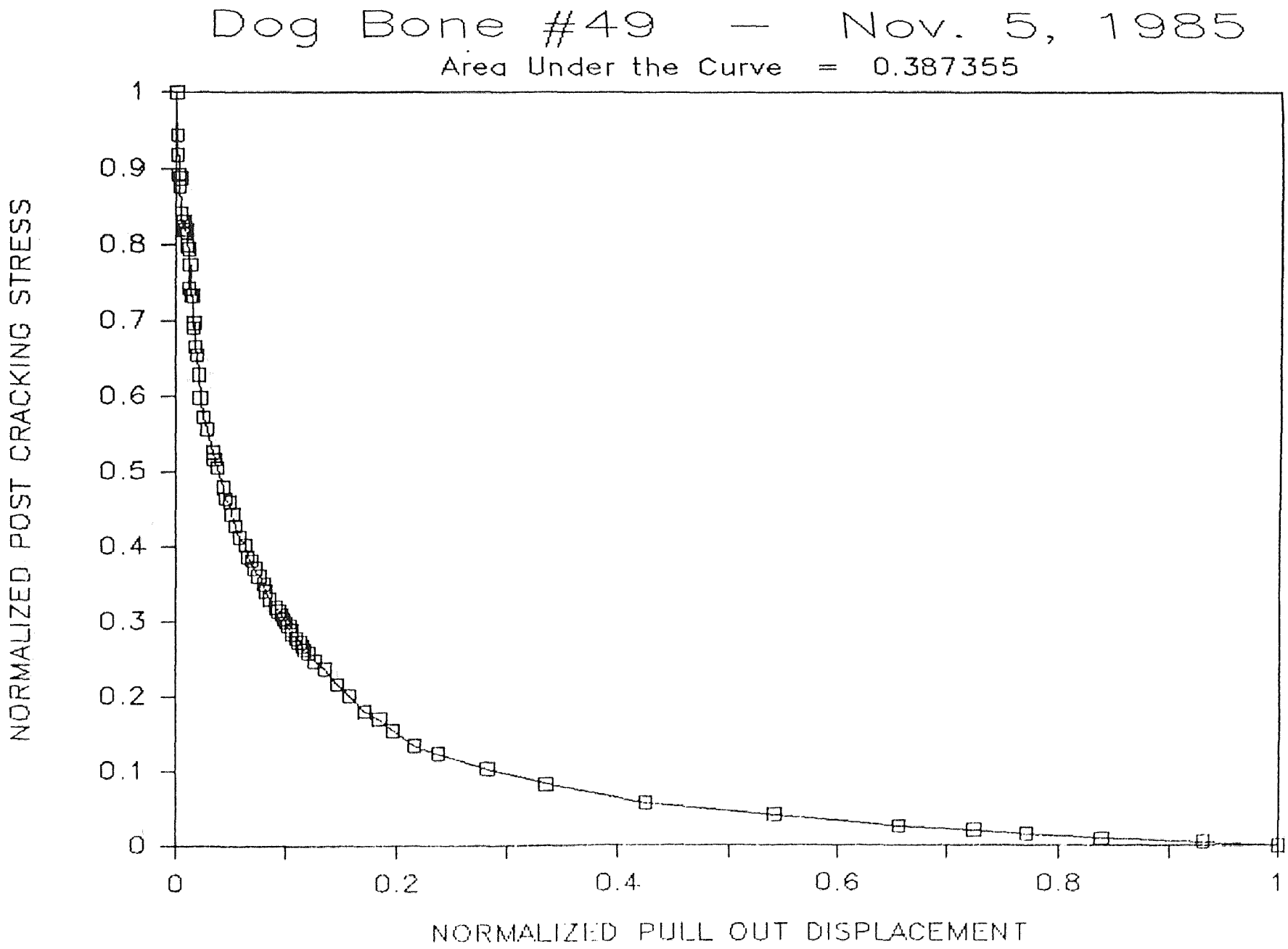
Dog Bone #49 — Nov. 5, 1985
Area Under the Curve = 0.387355
NORMALIZED POST CRACKING STRESS
NORMALIZED PULL OUT DISPLACEMENT
0
0.1
0.2
0.3
0.4
0.5
0.6
0.7
0.8
0.9
1
0
0.2
0.4
0.6
0.8
1

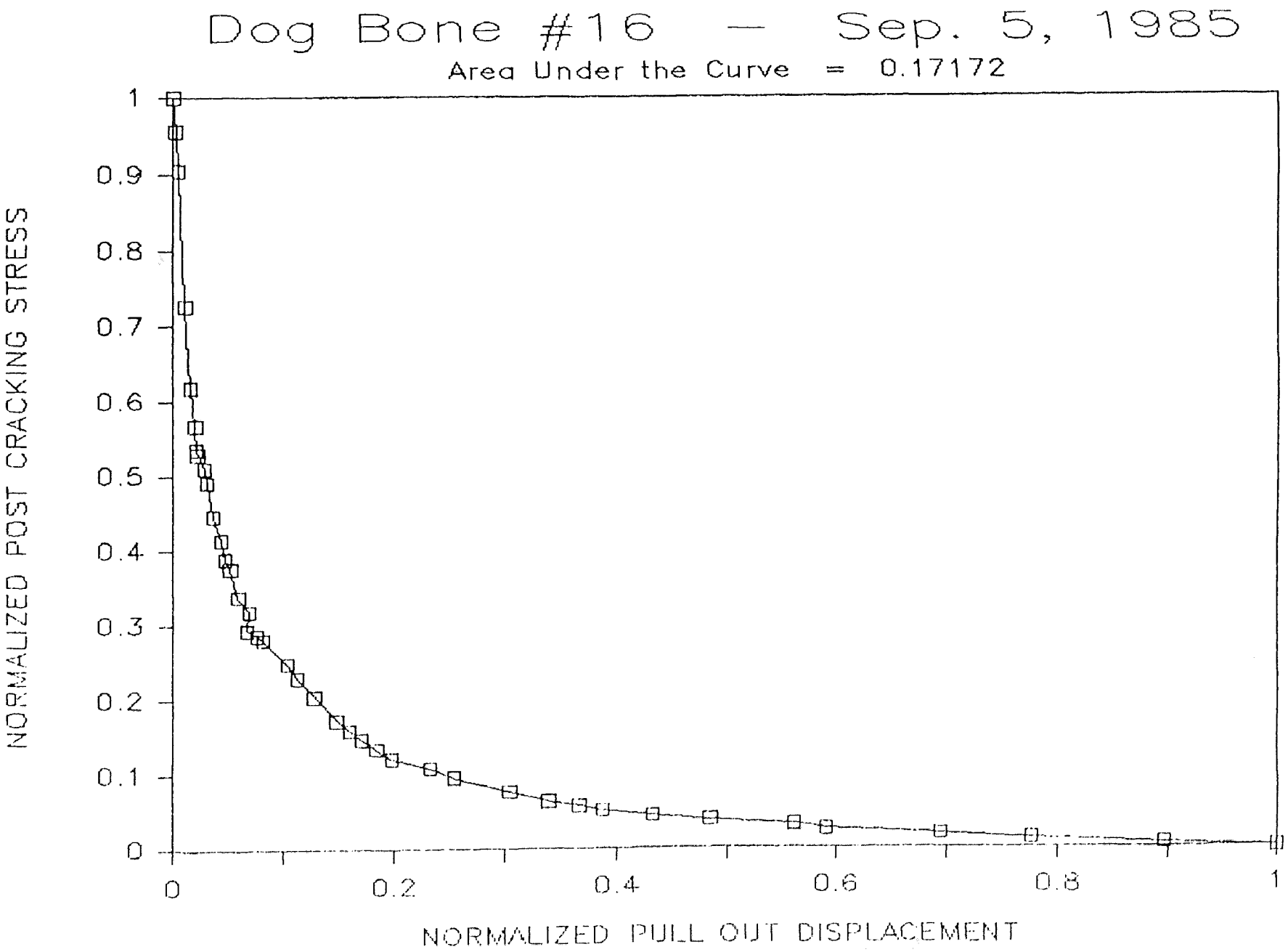
Dog Bone #16 — Sep. 5, 1985
Area Under the Curve = 0.17172
NORMALIZED POST CRACKING STRESS
1
0.9
0.8
0.7
0.6
0.5
0.4
0.3
0.2
0.1
0
0
0.2
0.4
0.6
0.8
1
NORMALIZED PULL OUT DISPLACEMENT

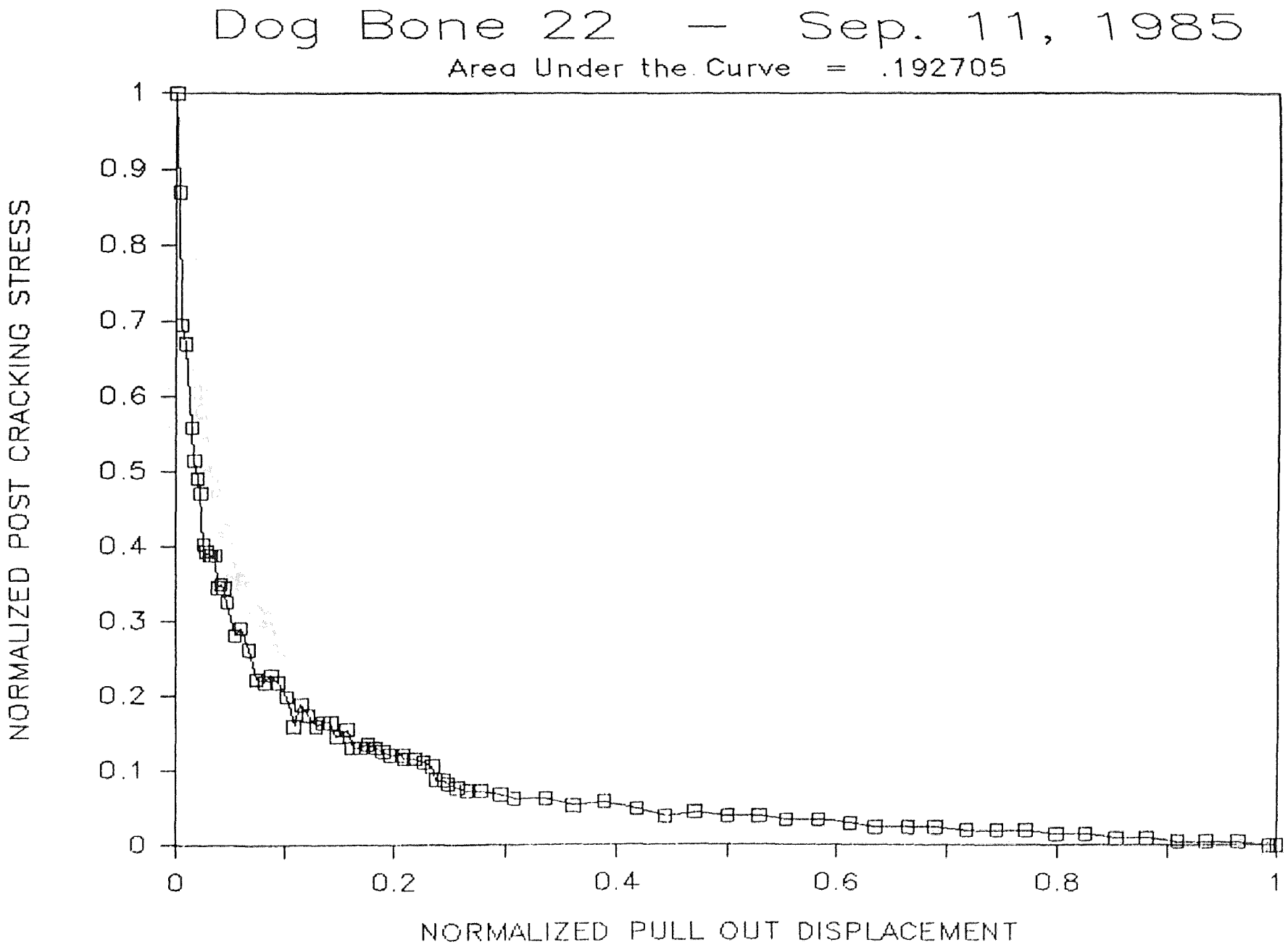
Dog Bone 22 — Sep. 11, 1985
Area Under the Curve = .192705
NORMALIZED POST CRACKING STRESS
NORMALIZED PULL OUT DISPLACEMENT
0
0.1
0.2
0.3
0.4
0.5
0.6
0.7
0.8
0.9
1
0
0.2
0.4
0.6
0.8
1

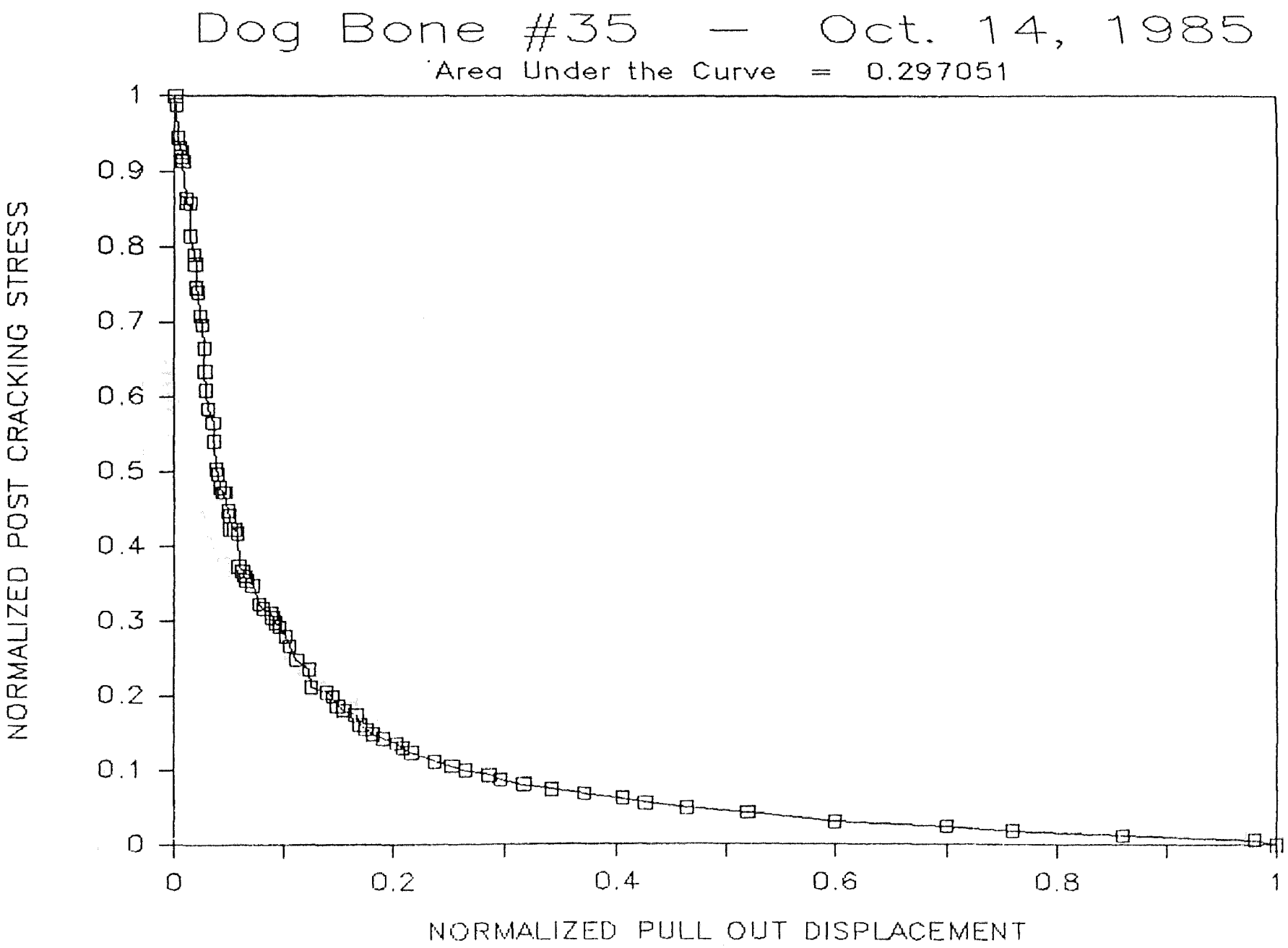
Dog Bone #35 — Oct. 14, 1985
Area Under the Curve = 0.297051
NORMALIZED POST CRACKING STRESS
1
0.9
0.8
0.7
0.6
0.5
0.4
0.3
0.2
0.1
0
0
0.2
0.4
0.6
0.8
1
NORMALIZED PULL OUT DISPLACEMENT

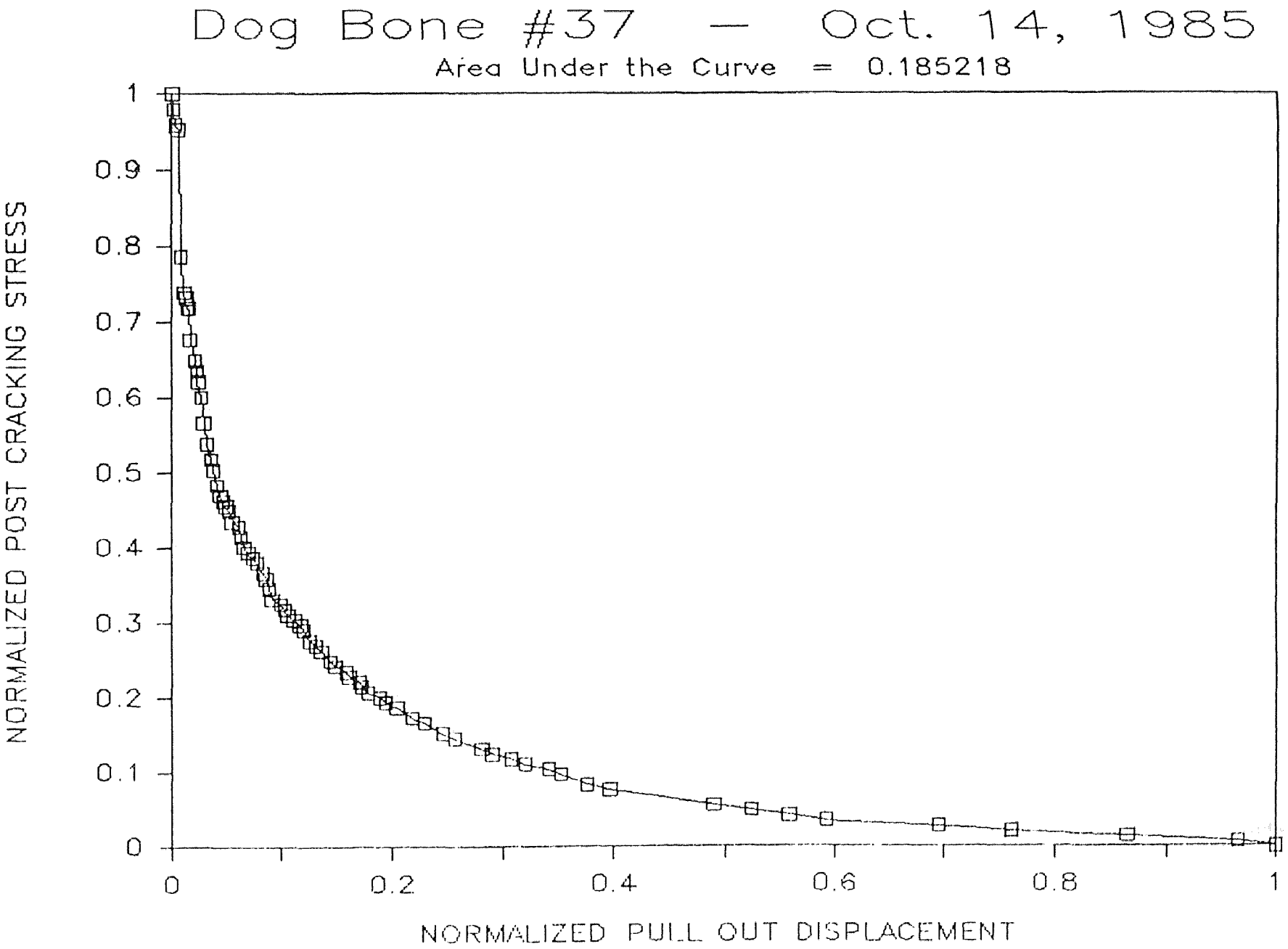
Dog Bone #37 — Oct. 14, 1985
Area Under the Curve = 0.185218
NORMALIZED POST CRACKING STRESS
1
0.9
0.8
0.7
0.6
0.5
0.4
0.3
0.2
0.1
0
0
0.2
0.4
0.6
0.8
1
NORMALIZED PULL OUT DISPLACEMENT

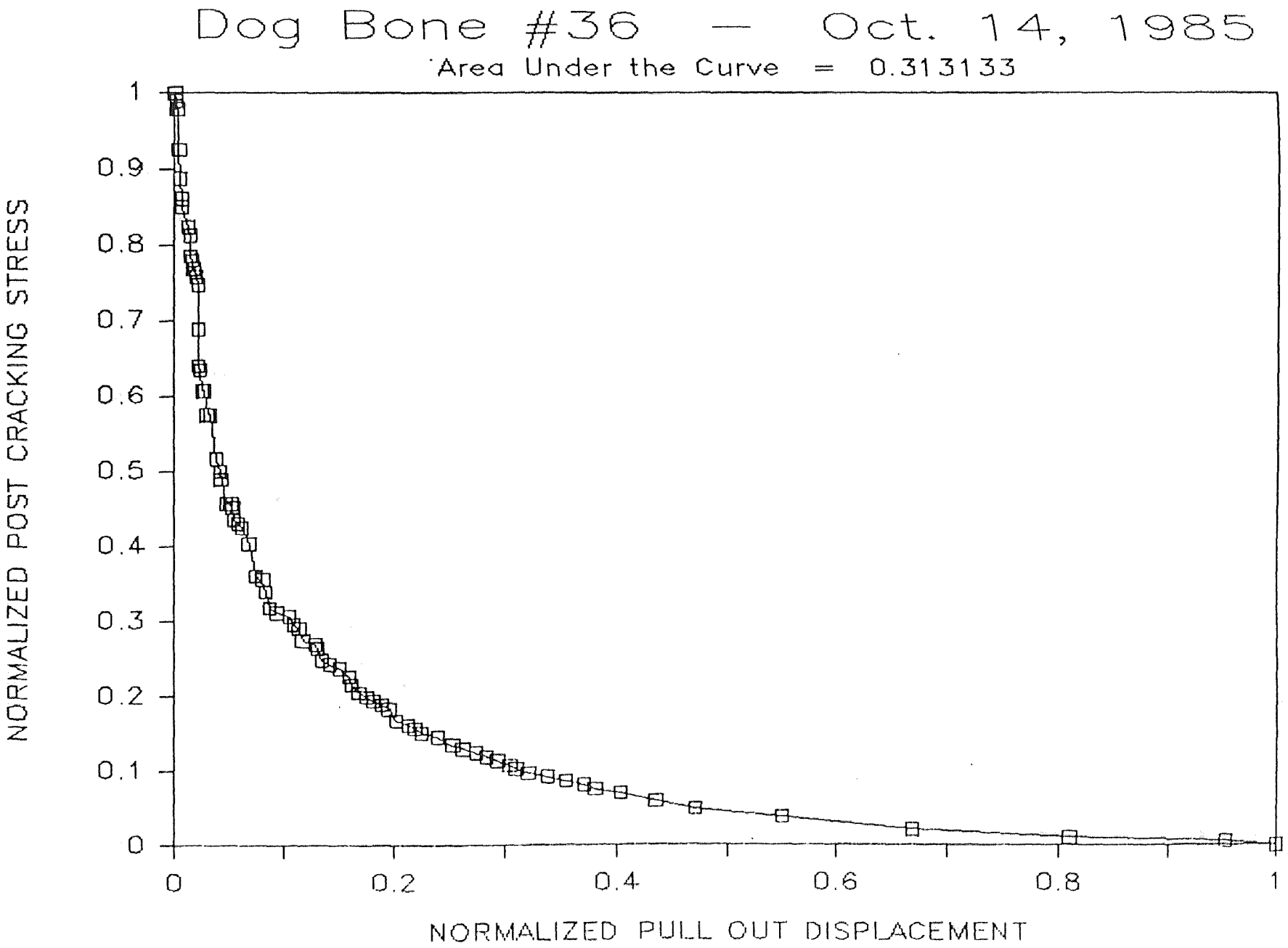
Dog Bone #36 — Oct. 14, 1985
Area Under the Curve = 0.313133
NORMALIZED POST CRACKING STRESS
NORMALIZED PULL OUT DISPLACEMENT
0
0.1
0.2
0.3
0.4
0.5
0.6
0.7
0.8
0.9
1
0
0.2
0.4
0.6
0.8
1

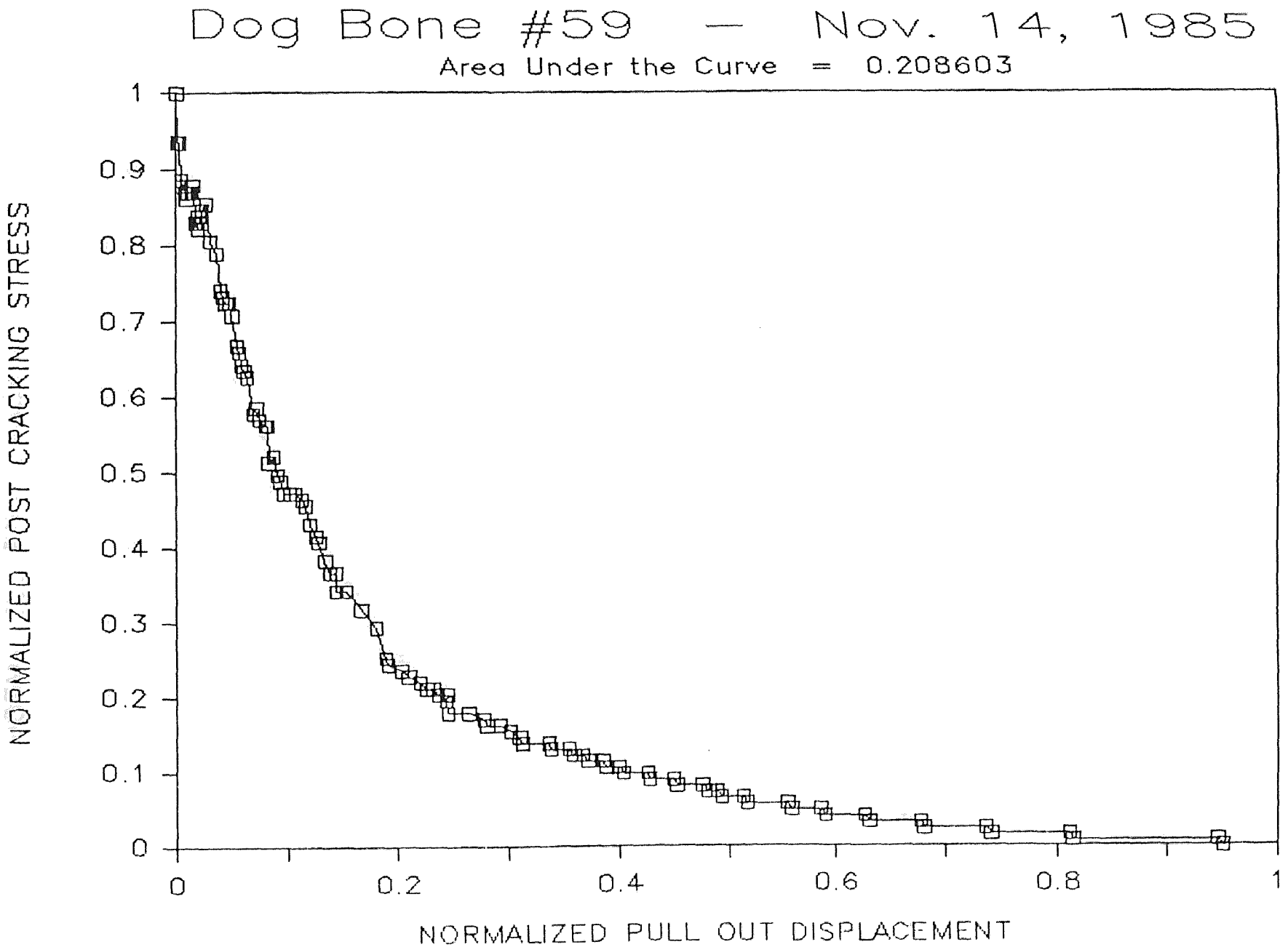
Dog Bone #59 — Nov. 14, 1985
Area Under the Curve = 0.208603
NORMALIZED POST CRACKING STRESS
NORMALIZED PULL OUT DISPLACEMENT
0
0.1
0.2
0.3
0.4
0.5
0.6
0.7
0.8
0.9
1
0
0.2
0.4
0.6
0.8
1

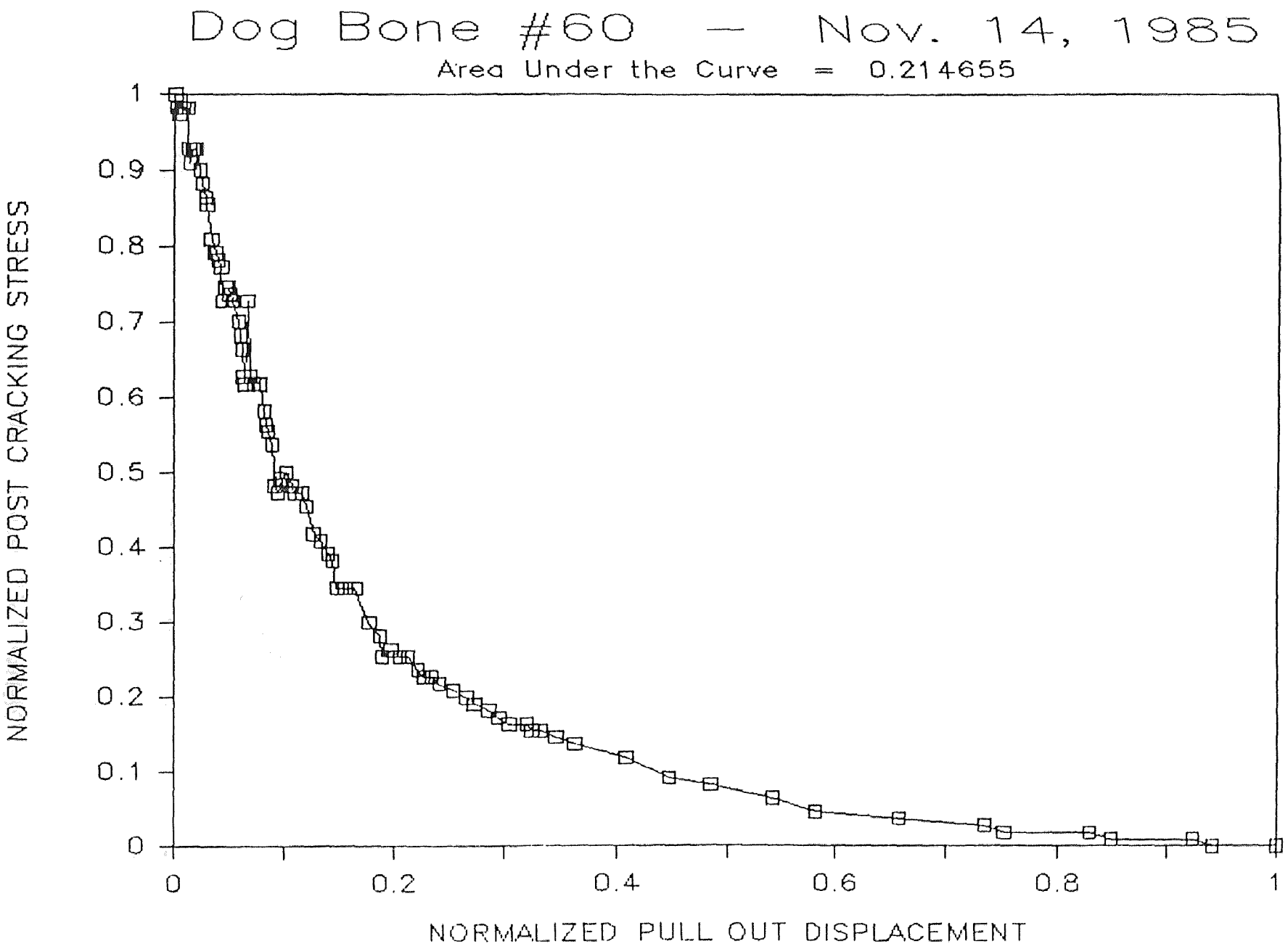
Dog Bone #60 — Nov. 14, 1985
Area Under the Curve = 0.214655
NORMALIZED POST CRACKING STRESS
1
0.9
0.8
0.7
0.6
0.5
0.4
0.3
0.2
0.1
0
0
0.2
0.4
0.6
0.8
1
NORMALIZED PULL OUT DISPLACEMENT

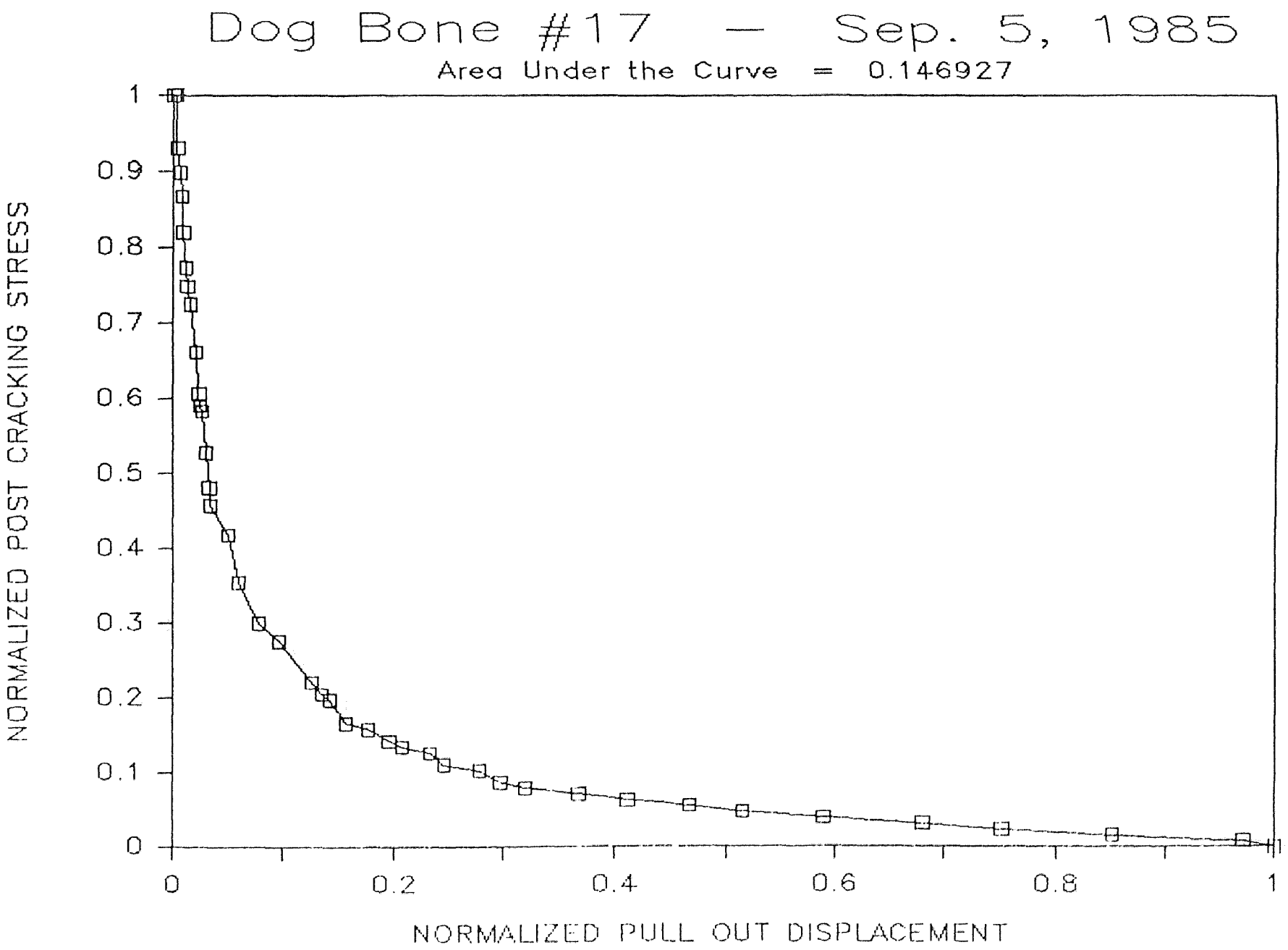
Dog Bone #17 — Sep. 5, 1985
Area Under the Curve = 0.146927
NORMALIZED POST CRACKING STRESS
NORMALIZED PULL OUT DISPLACEMENT
0
0.1
0.2
0.3
0.4
0.5
0.6
0.7
0.8
0.9
1
0
0.2
0.4
0.6
0.8
1

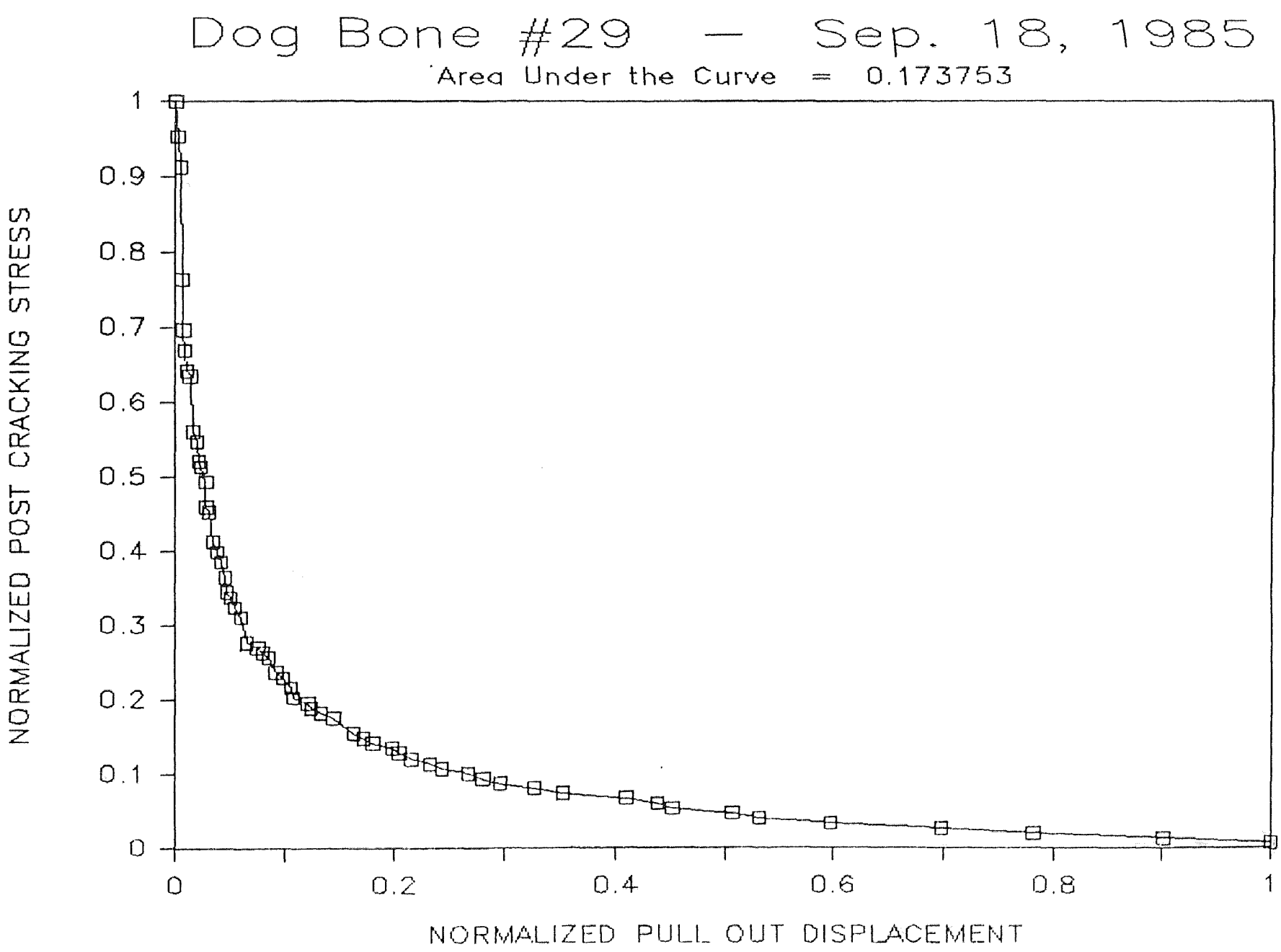
Dog Bone #29 — Sep. 18, 1985
Area Under the Curve = 0.173753
NORMALIZED POST CRACKING STRESS
NORMALIZED PULL OUT DISPLACEMENT
0
0.1
0.2
0.3
0.4
0.5
0.6
0.7
0.8
0.9
1
0
0.2
0.4
0.6
0.8
1

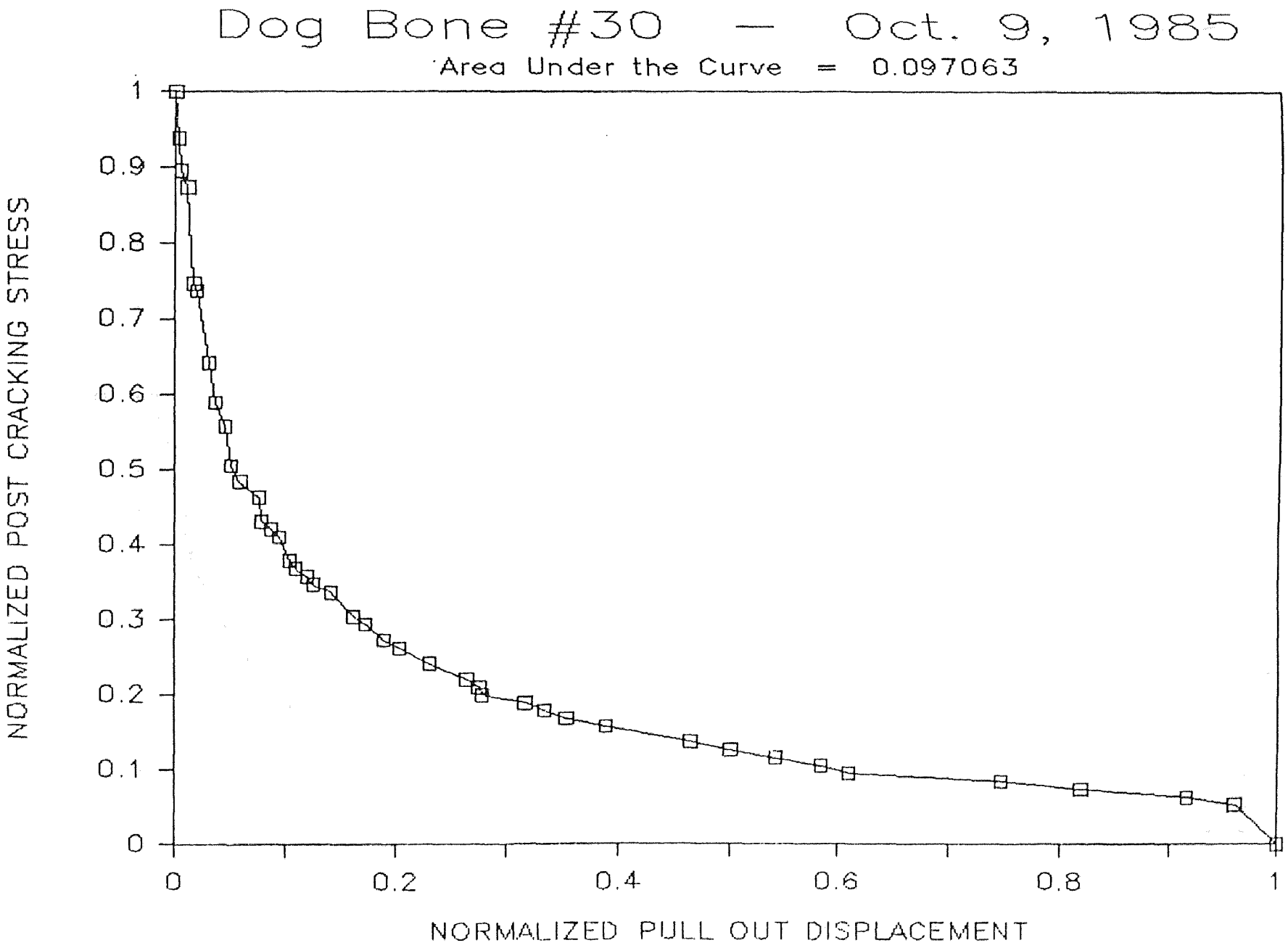
Dog Bone #30 — Oct. 9, 1985
Area Under the Curve = 0.097063
NORMALIZED POST CRACKING STRESS
NORMALIZED PULL OUT DISPLACEMENT
0
0.1
0.2
0.3
0.4
0.5
0.6
0.7
0.8
0.9
1
0
0.2
0.4
0.6
0.8
1

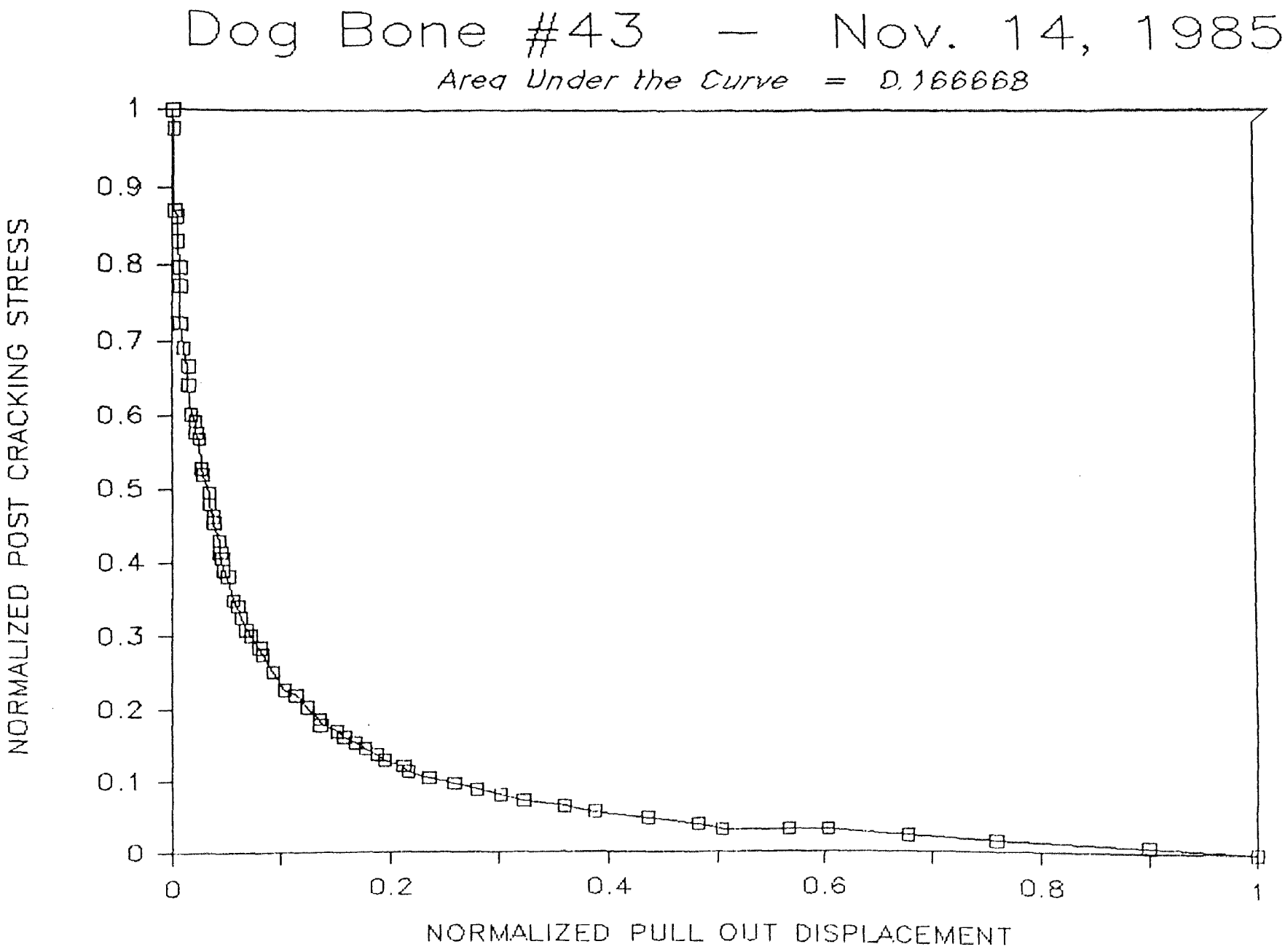
Dog Bone #43 — Nov. 14, 1985
Area Under the Curve = 0.166668
NORMALIZED POST CRACKING STRESS
NORMALIZED PULL OUT DISPLACEMENT
0
0.1
0.2
0.3
0.4
0.5
0.6
0.7
0.8
0.9
1
0
0.2
0.4
0.6
0.8
1

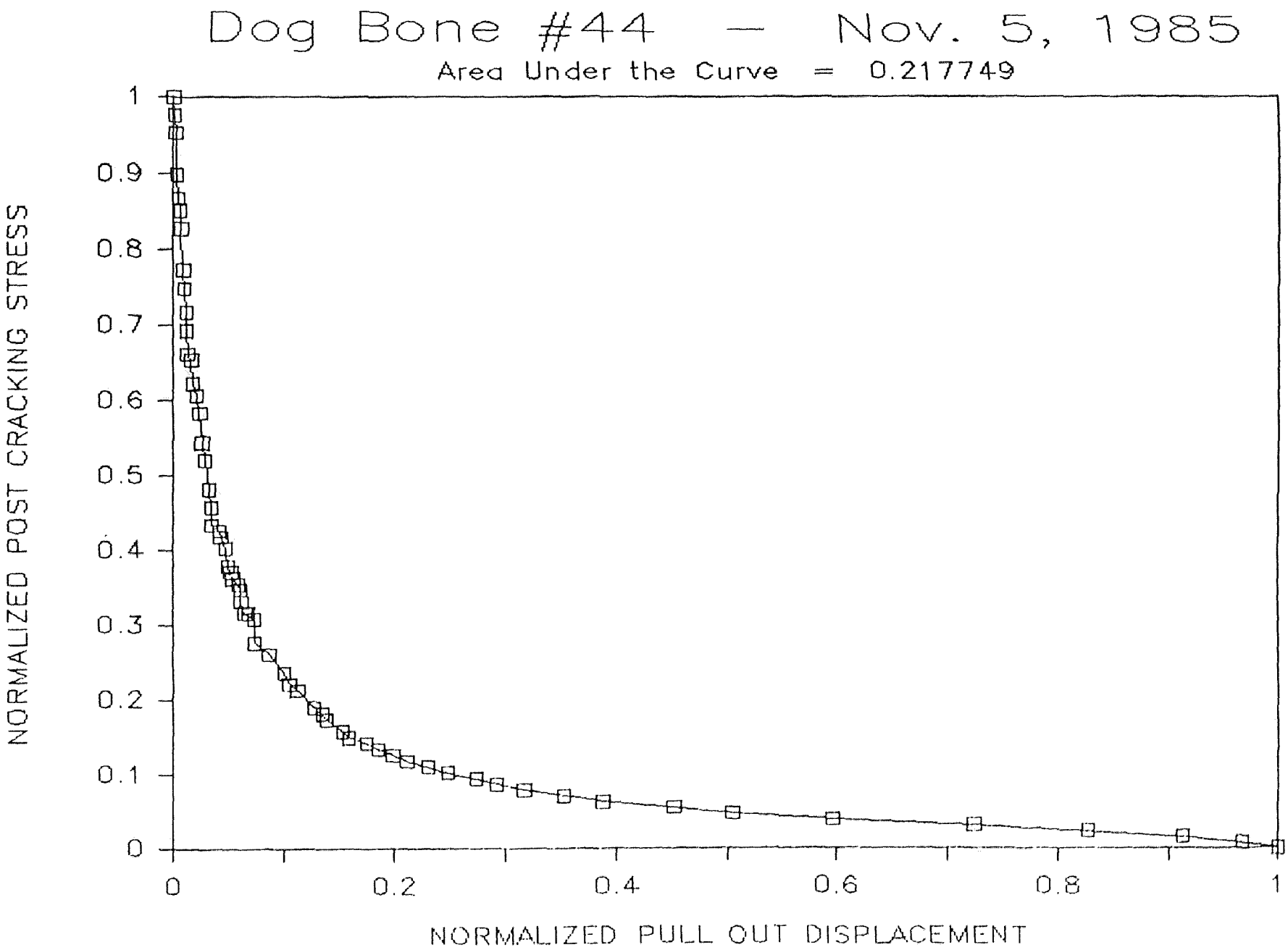
Dog Bone #44 — Nov. 5, 1985
Area Under the Curve = 0.217749
NORMALIZED POST CRACKING STRESS
NORMALIZED PULL OUT DISPLACEMENT
0
0.1
0.2
0.3
0.4
0.5
0.6
0.7
0.8
0.9
1
0
0.2
0.4
0.6
0.8
1

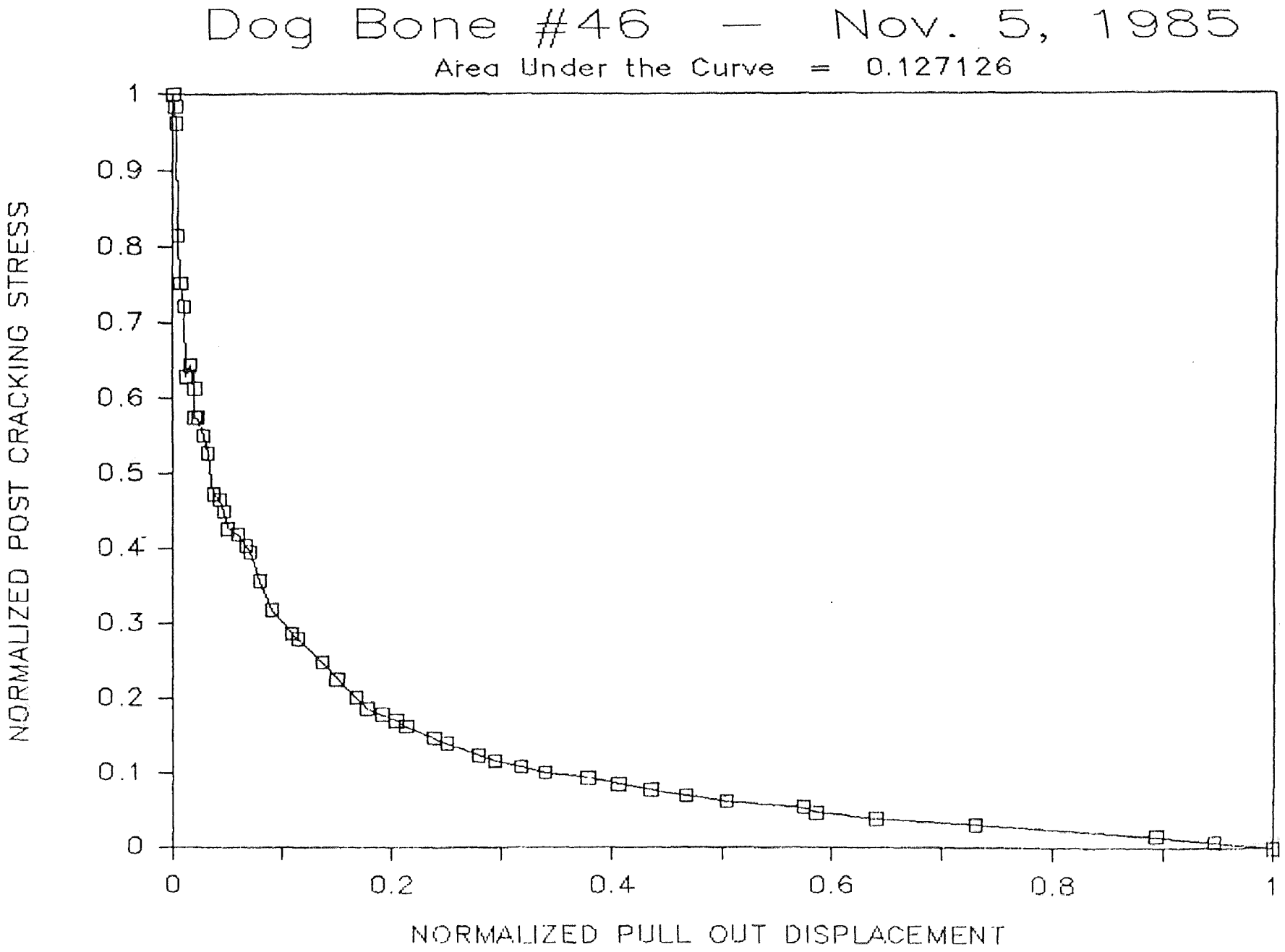
Dog Bone #46 — Nov. 5, 1985
Area Under the Curve = 0.127126
NORMALIZED POST CRACKING STRESS
1
0.9
0.8
0.7
0.6
0.5
0.4
0.3
0.2
0.1
0
0
0.2
0.4
0.6
0.8
1
NORMALIZED PULL OUT DISPLACEMENT

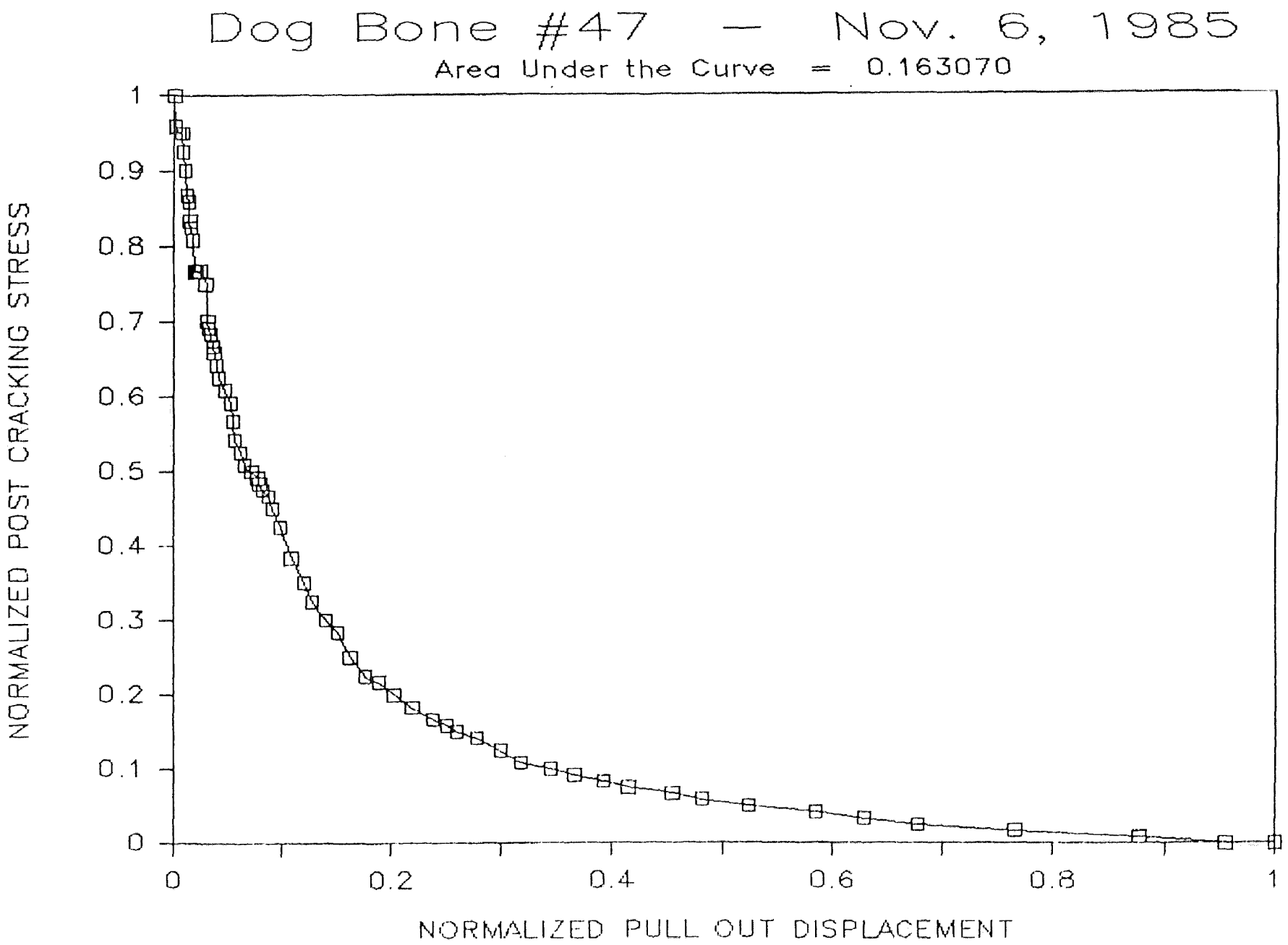
Dog Bone #47 — Nov. 6, 1985
Area Under the Curve = 0.163070
NORMALIZED POST CRACKING STRESS
NORMALIZED PULL OUT DISPLACEMENT
0
0.1
0.2
0.3
0.4
0.5
0.6
0.7
0.8
0.9
1
0
0.2
0.4
0.6
0.8
1

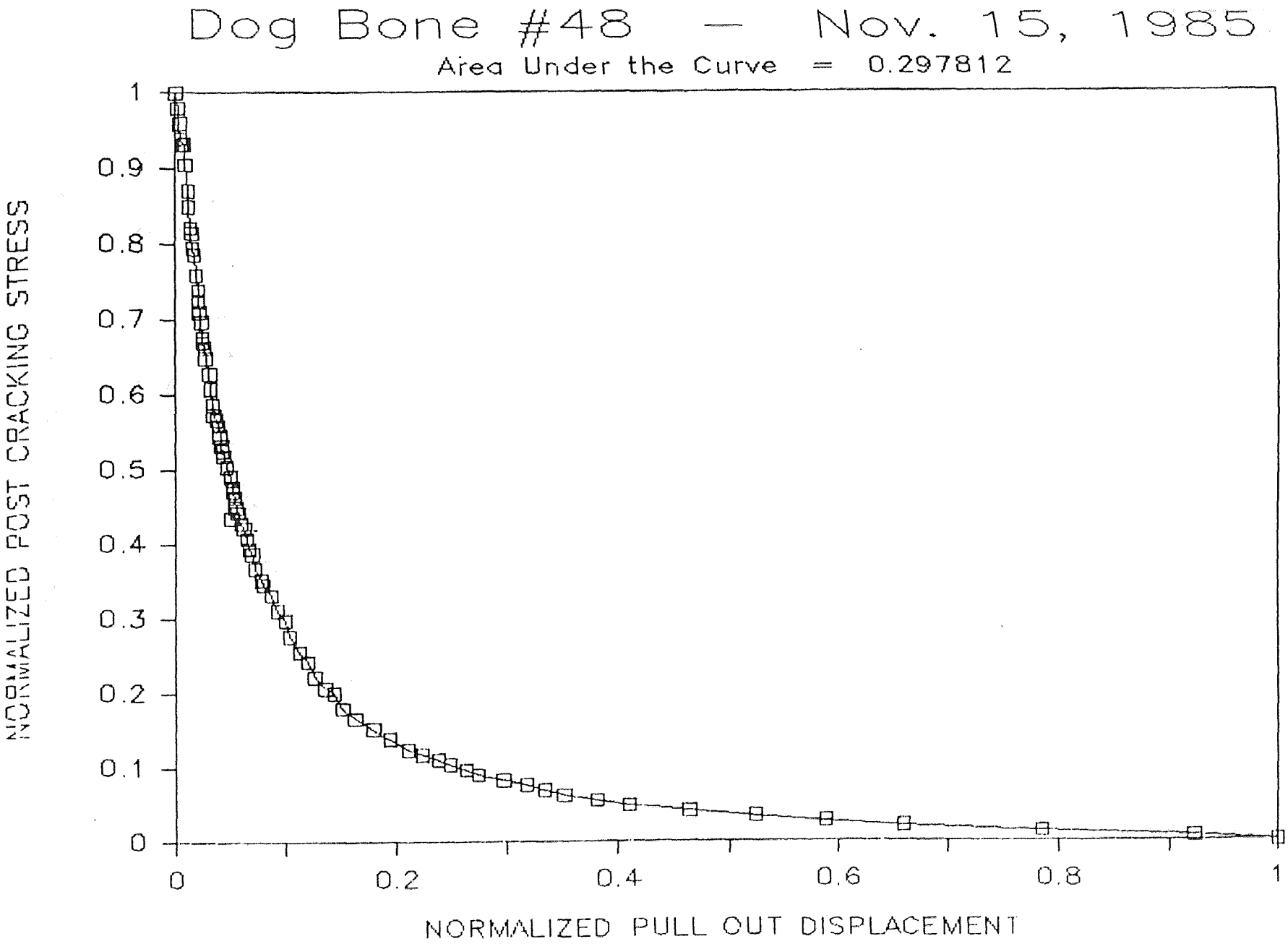
Dog Bone #48 — Nov. 15, 1985
Area Under the Curve = 0.297812
NORMALIZED POST CRACKING STRESS
1
0.9
0.8
0.7
0.6
0.5
0.4
0.3
0.2
0.1
0
0
0.2
0.4
0.6
0.8
1
NORMALIZED PULL OUT DISPLACEMENT

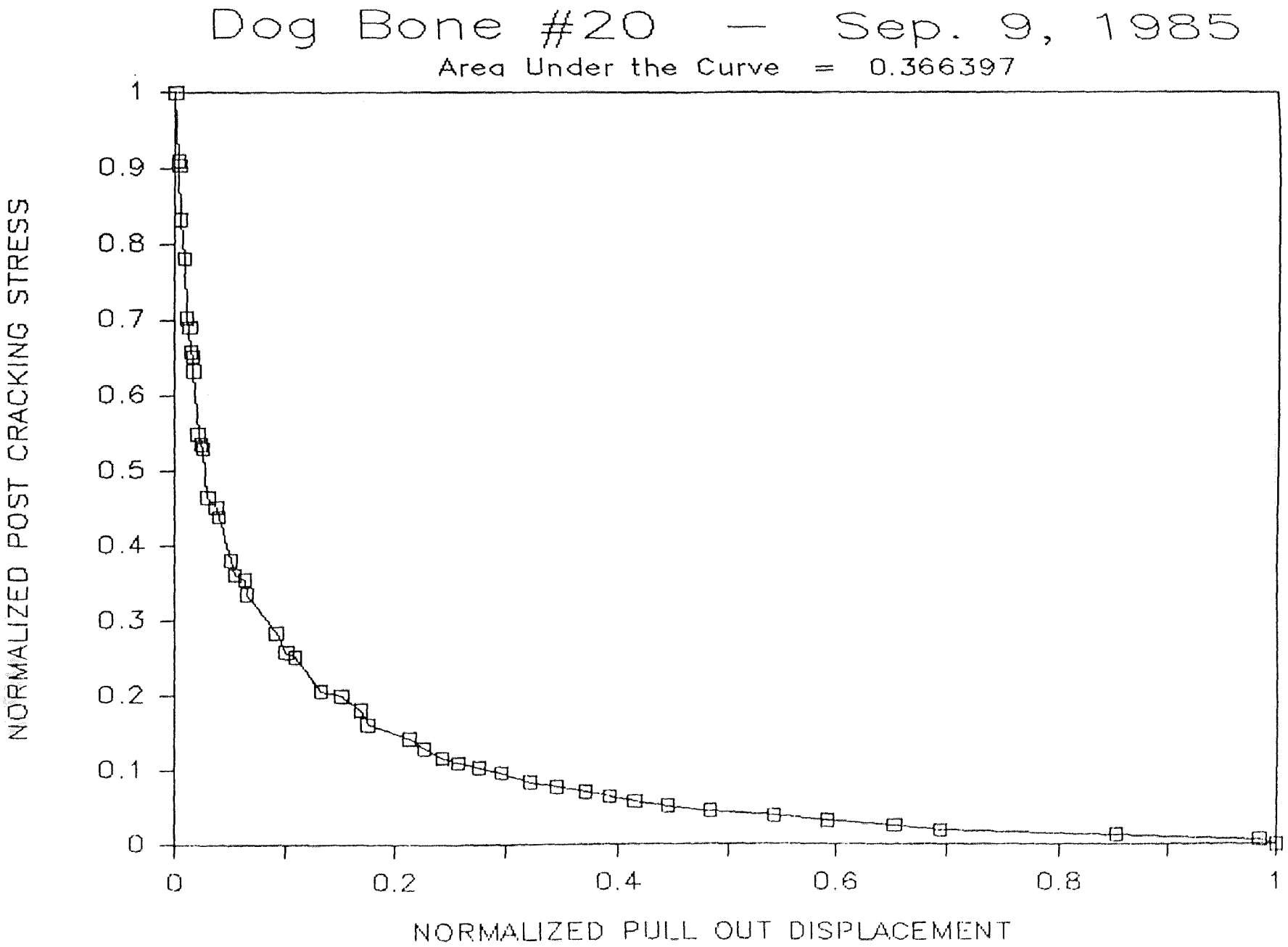
Dog Bone #20 — Sep. 9, 1985
Area Under the Curve = 0.366397
NORMALIZED POST CRACKING STRESS
NORMALIZED PULL OUT DISPLACEMENT
0
0.1
0.2
0.3
0.4
0.5
0.6
0.7
0.8
0.9
1
0
0.2
0.4
0.6
0.8
1

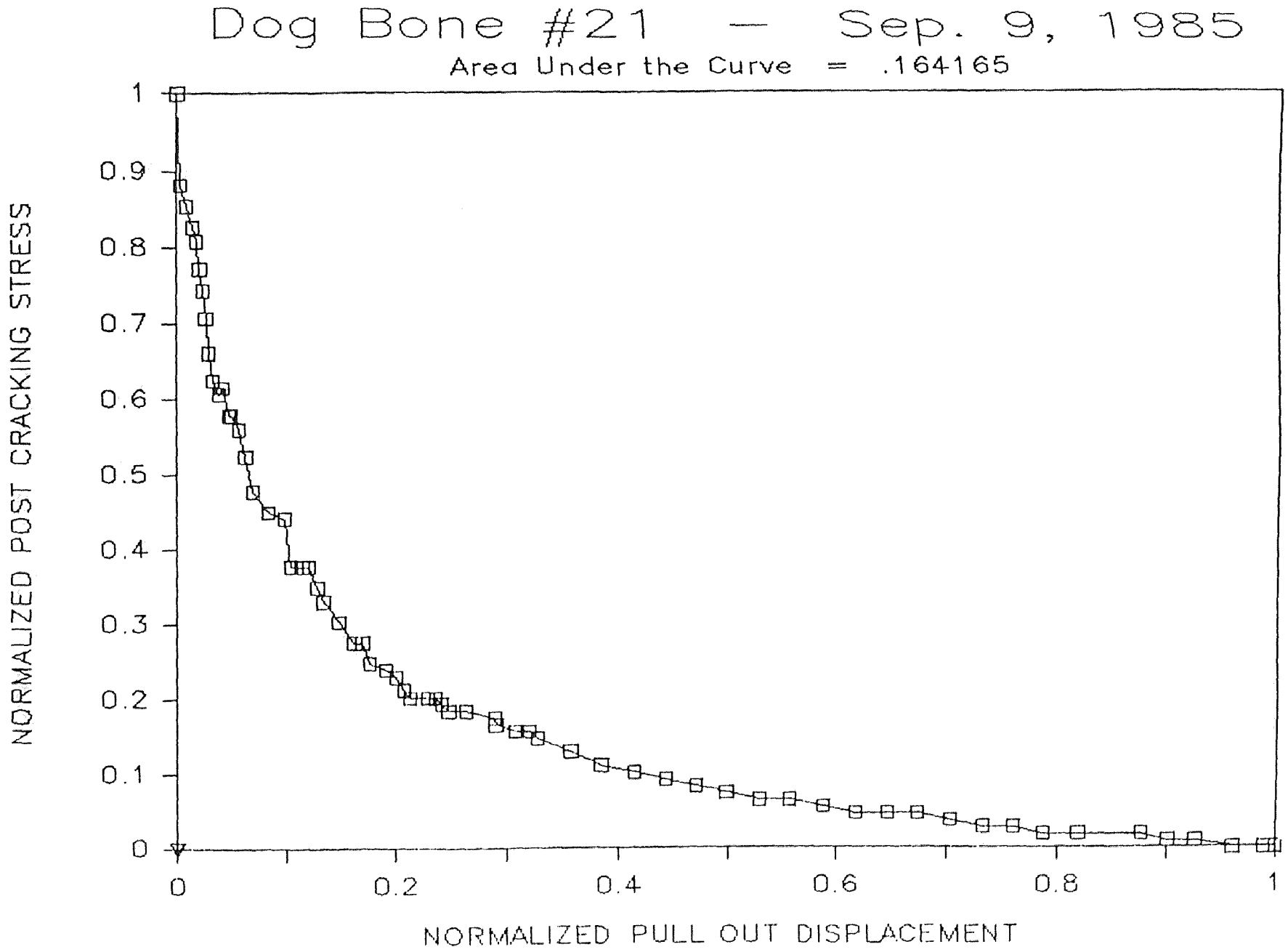
Dog Bone #21 — Sep. 9, 1985
Area Under the Curve = .164165
NORMALIZED POST CRACKING STRESS
1
0.9
0.8
0.7
0.6
0.5
0.4
0.3
0.2
0.1
0
0
0.2
0.4
0.6
0.8
1
NORMALIZED PULL OUT DISPLACEMENT

Dog Bone #33 — Oct. 11, 1985

Area Under the Curve = 0.187360

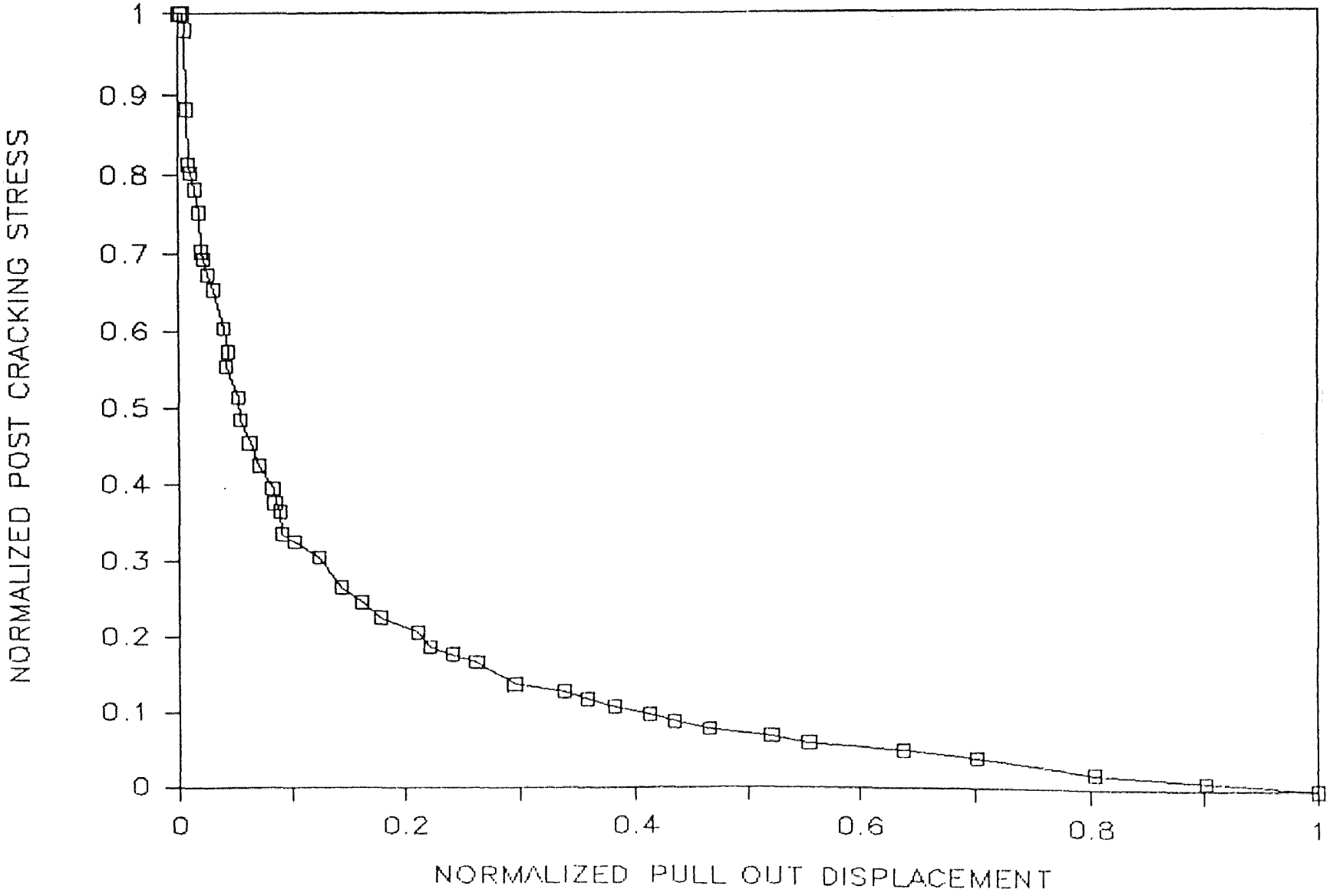

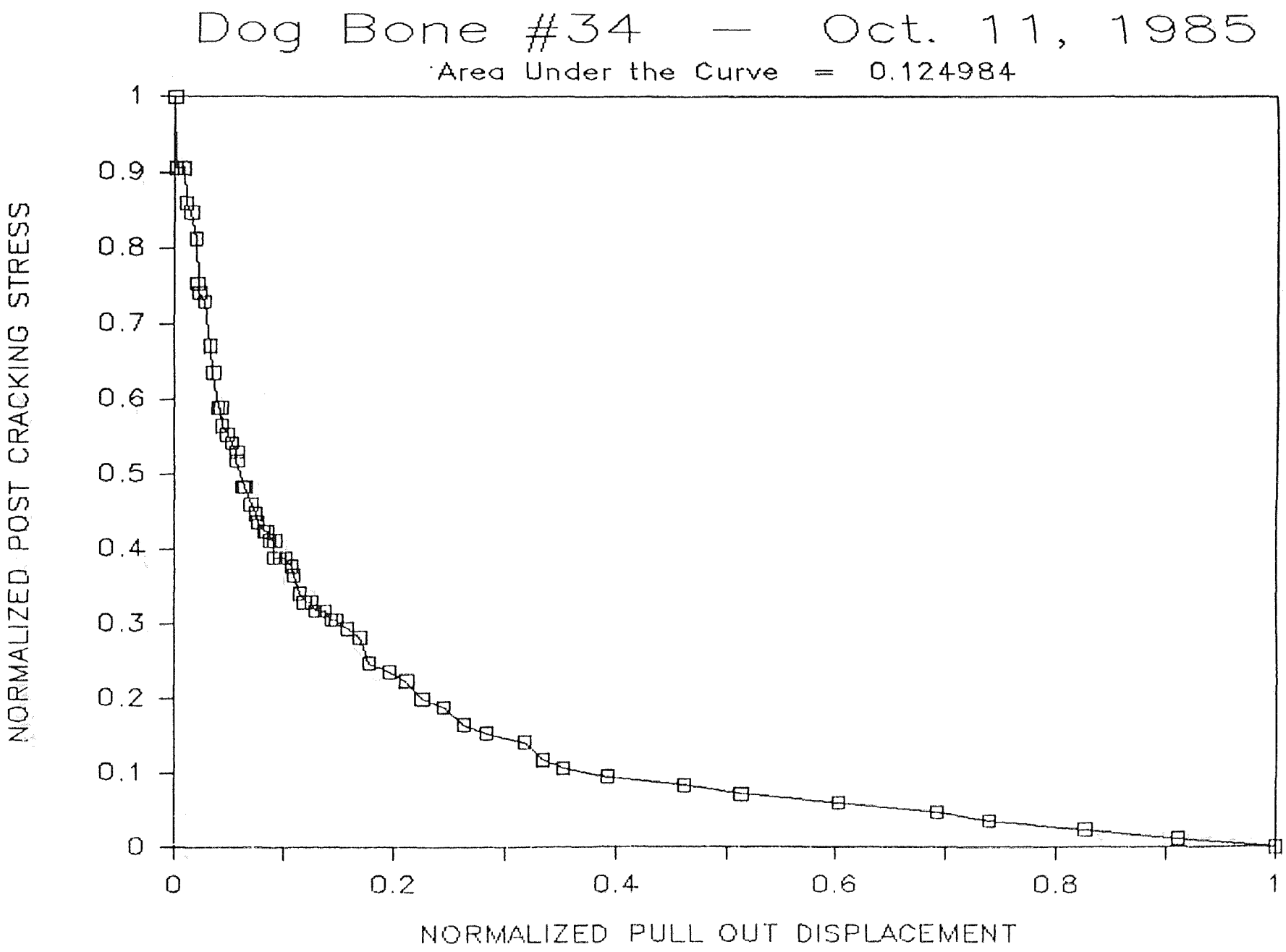
Dog Bone #34 — Oct. 11, 1985
Area Under the Curve = 0.124984
NORMALIZED POST CRACKING STRESS
NORMALIZED PULL OUT DISPLACEMENT
0
0.1
0.2
0.3
0.4
0.5
0.6
0.7
0.8
0.9
1
0
0.2
0.4
0.6
0.8
1

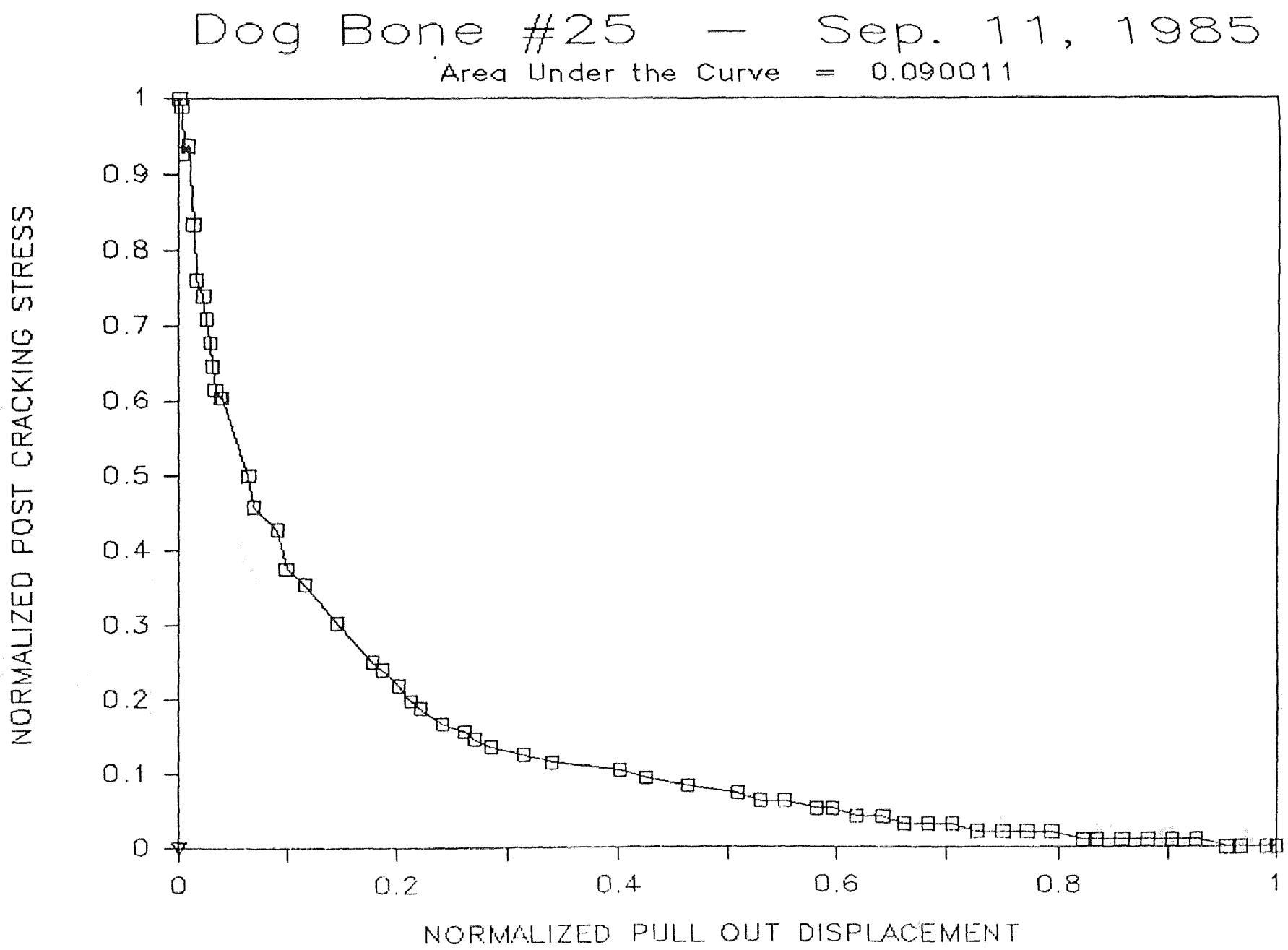
Dog Bone #25 — Sep. 11, 1985
Area Under the Curve = 0.090011
NORMALIZED POST CRACKING STRESS
1
0.9
0.8
0.7
0.6
0.5
0.4
0.3
0.2
0.1
0
0
0.2
0.4
0.6
0.8
1
NORMALIZED PULL OUT DISPLACEMENT

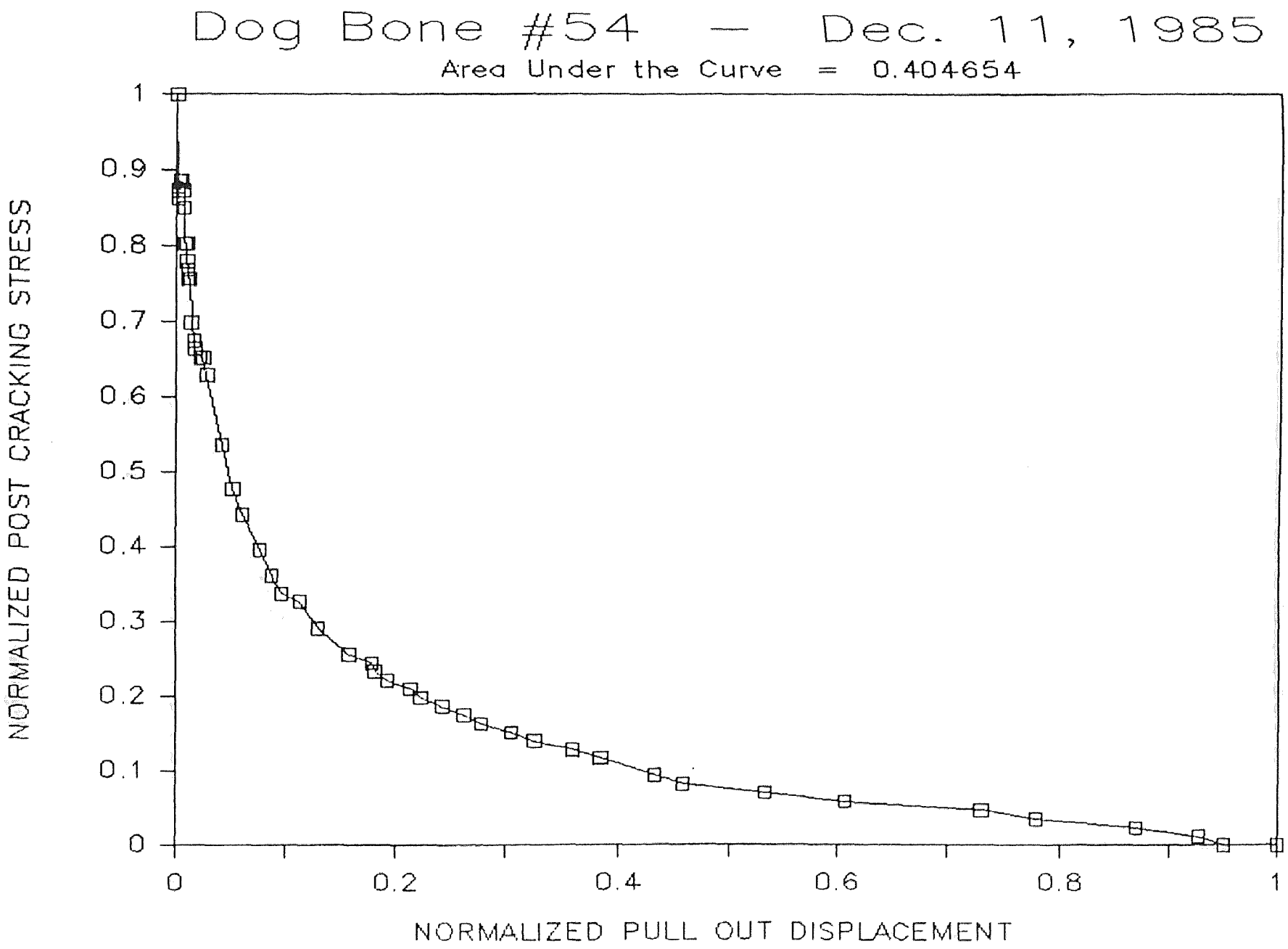
Dog Bone #54 — Dec. 11, 1985
Area Under the Curve = 0.404654
NORMALIZED POST CRACKING STRESS
NORMALIZED PULL OUT DISPLACEMENT
0
0.1
0.2
0.3
0.4
0.5
0.6
0.7
0.8
0.9
1
0
0.2
0.4
0.6
0.8
1

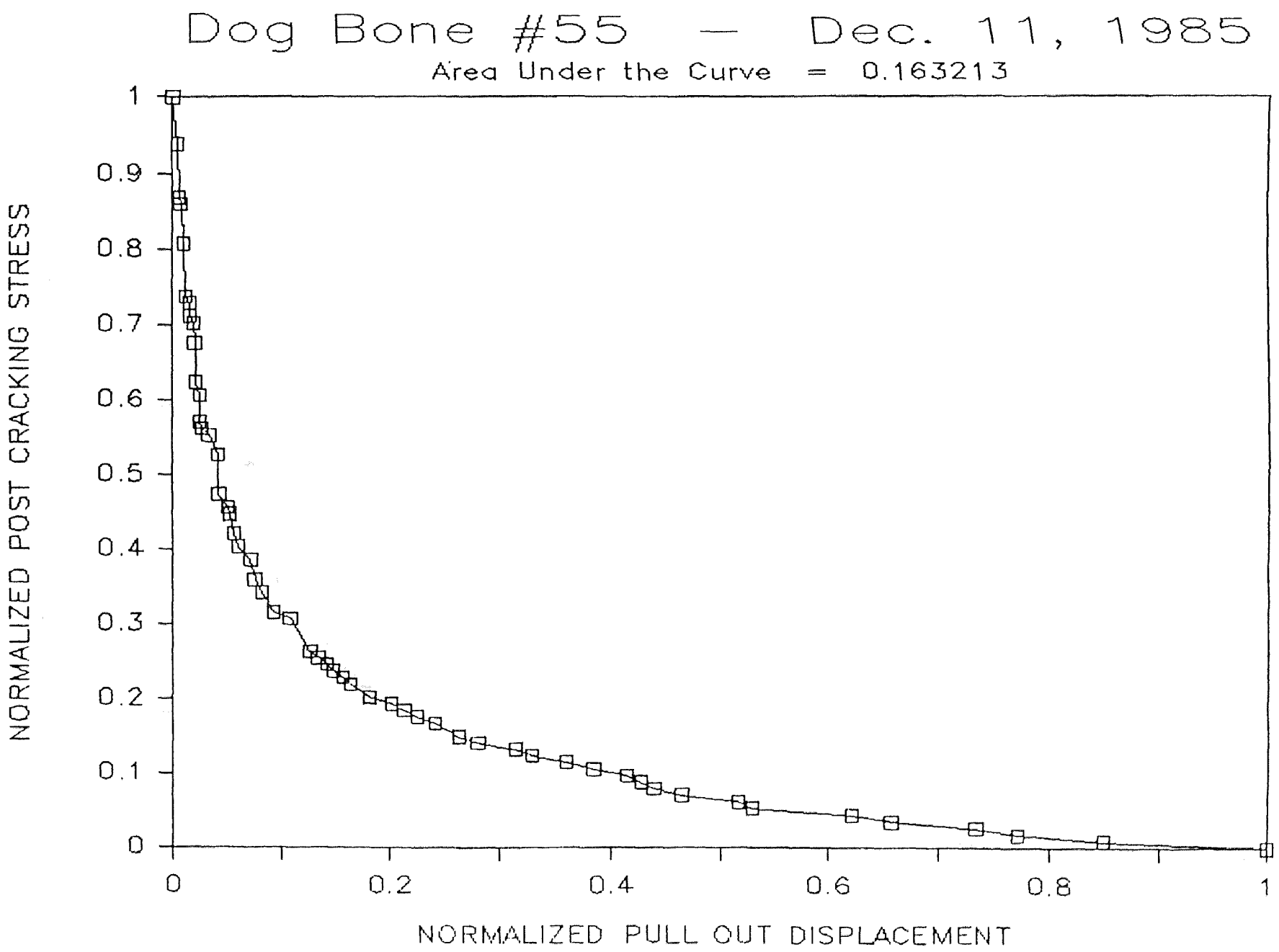
Dog Bone #55 — Dec. 11, 1985
Area Under the Curve = 0.163213
NORMALIZED POST CRACKING STRESS
NORMALIZED PULL OUT DISPLACEMENT
0
0.1
0.2
0.3
0.4
0.5
0.6
0.7
0.8
0.9
1
0
0.2
0.4
0.6
0.8
1

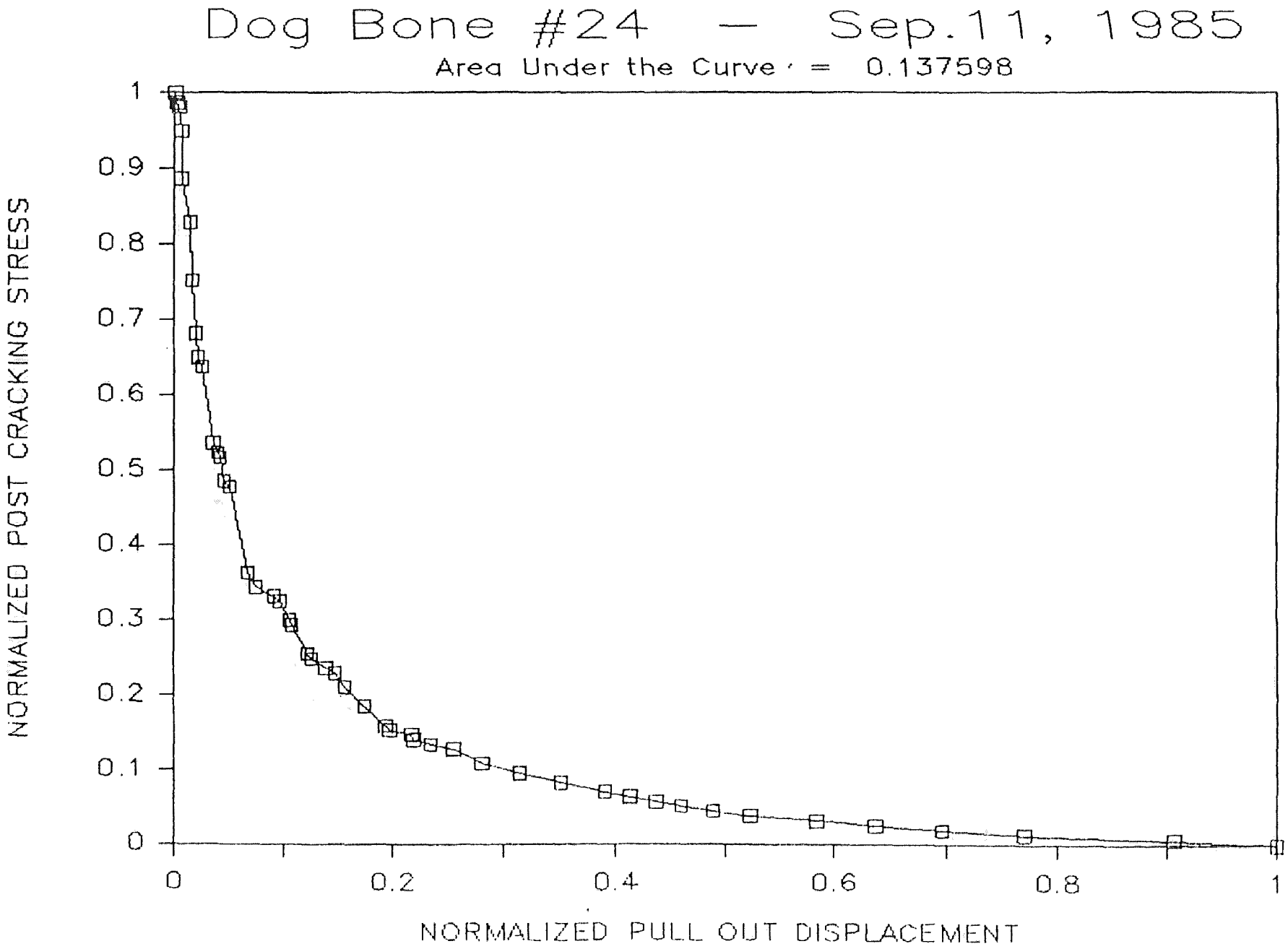
Dog Bone #24 — Sep.11, 1985
Area Under the Curve = 0.137598
NORMALIZED POST CRACKING STRESS
NORMALIZED PULL OUT DISPLACEMENT
0
0.1
0.2
0.3
0.4
0.5
0.6
0.7
0.8
0.9
1
0
0.2
0.4
0.6
0.8
1

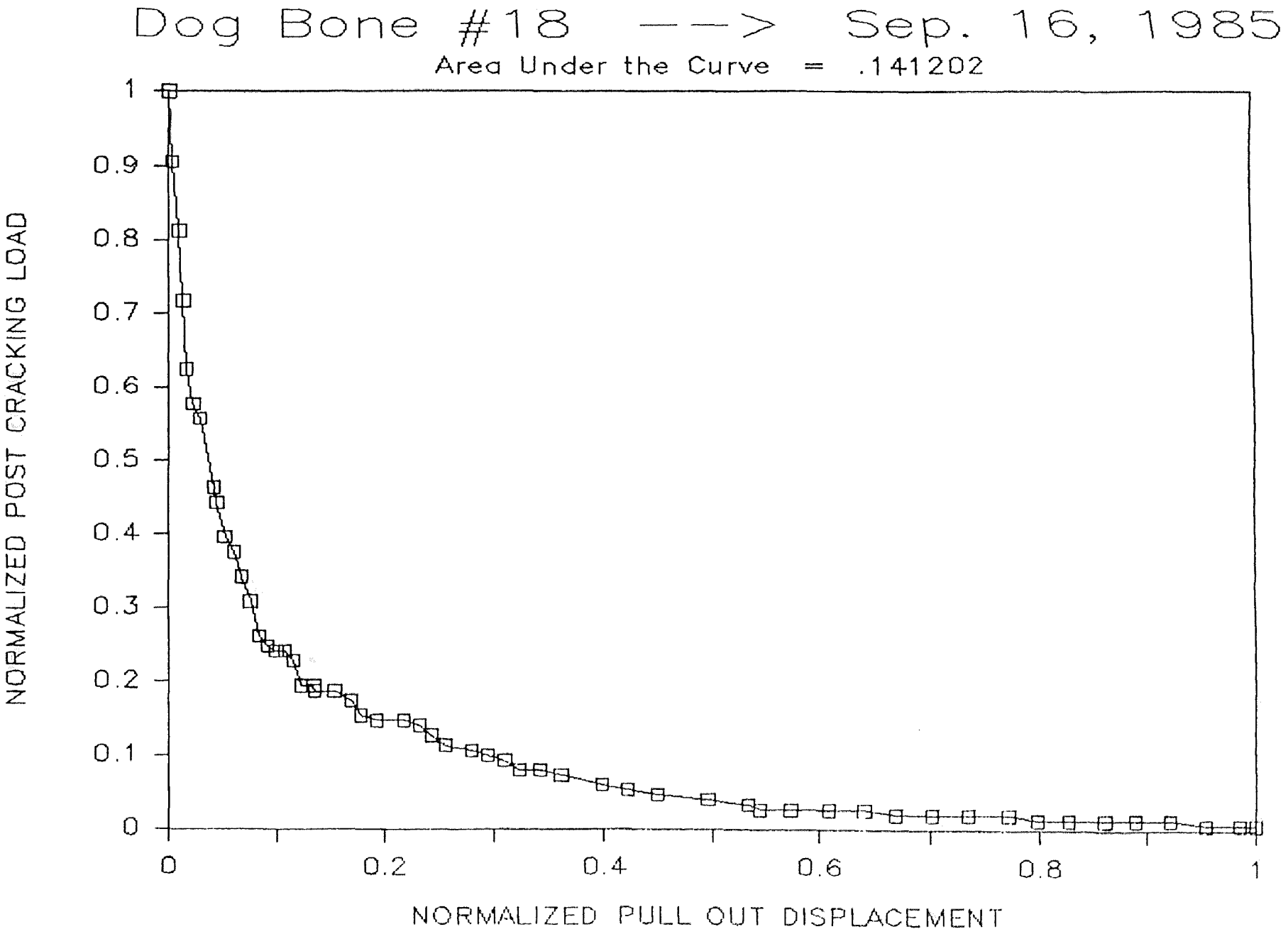
Dog Bone #18 ---> Sep. 16, 1985
Area Under the Curve = .141202
NORMALIZED POST CRACKING LOAD
1
0.9
0.8
0.7
0.6
0.5
0.4
0.3
0.2
0.1
0
0
0.2
0.4
0.6
0.8
1
NORMALIZED PULL OUT DISPLACEMENT

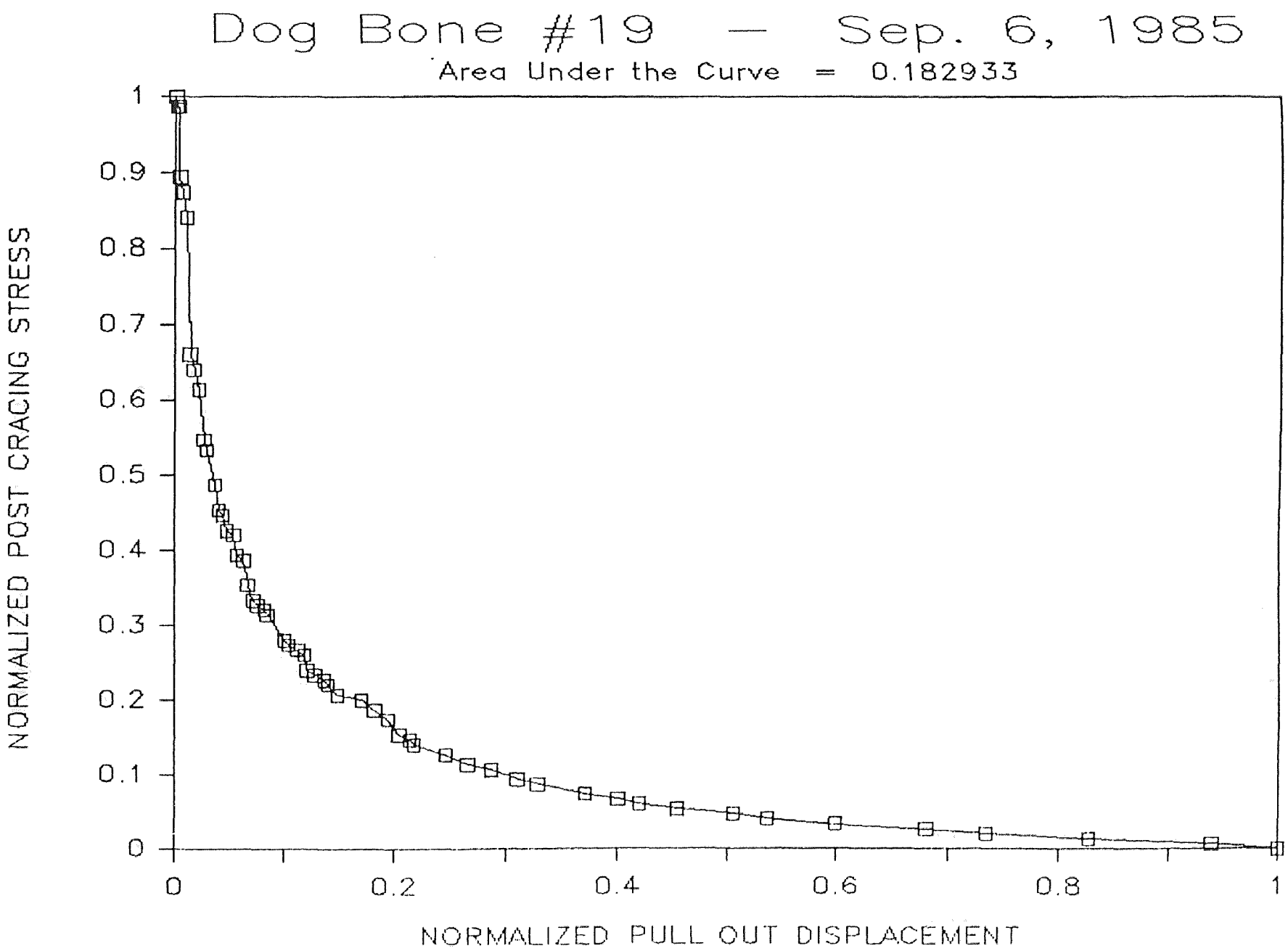
Dog Bone #19 — Sep. 6, 1985
Area Under the Curve = 0.182933
NORMALIZED POST CRACING STRESS
NORMALIZED PULL OUT DISPLACEMENT
0
0.1
0.2
0.3
0.4
0.5
0.6
0.7
0.8
0.9
1
0
0.2
0.4
0.6
0.8
1

Dog Bone #26 — Oct. 3, 1985

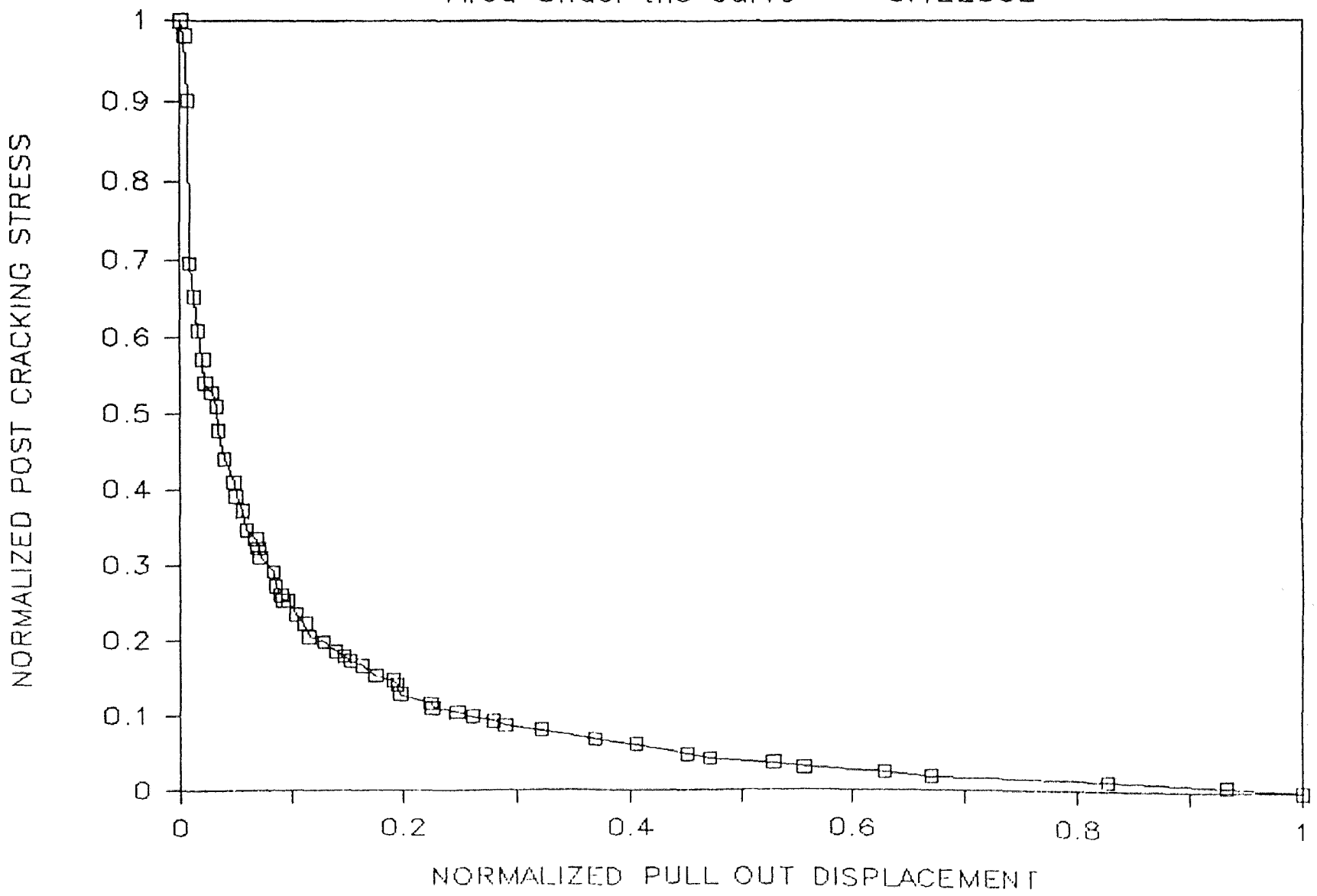

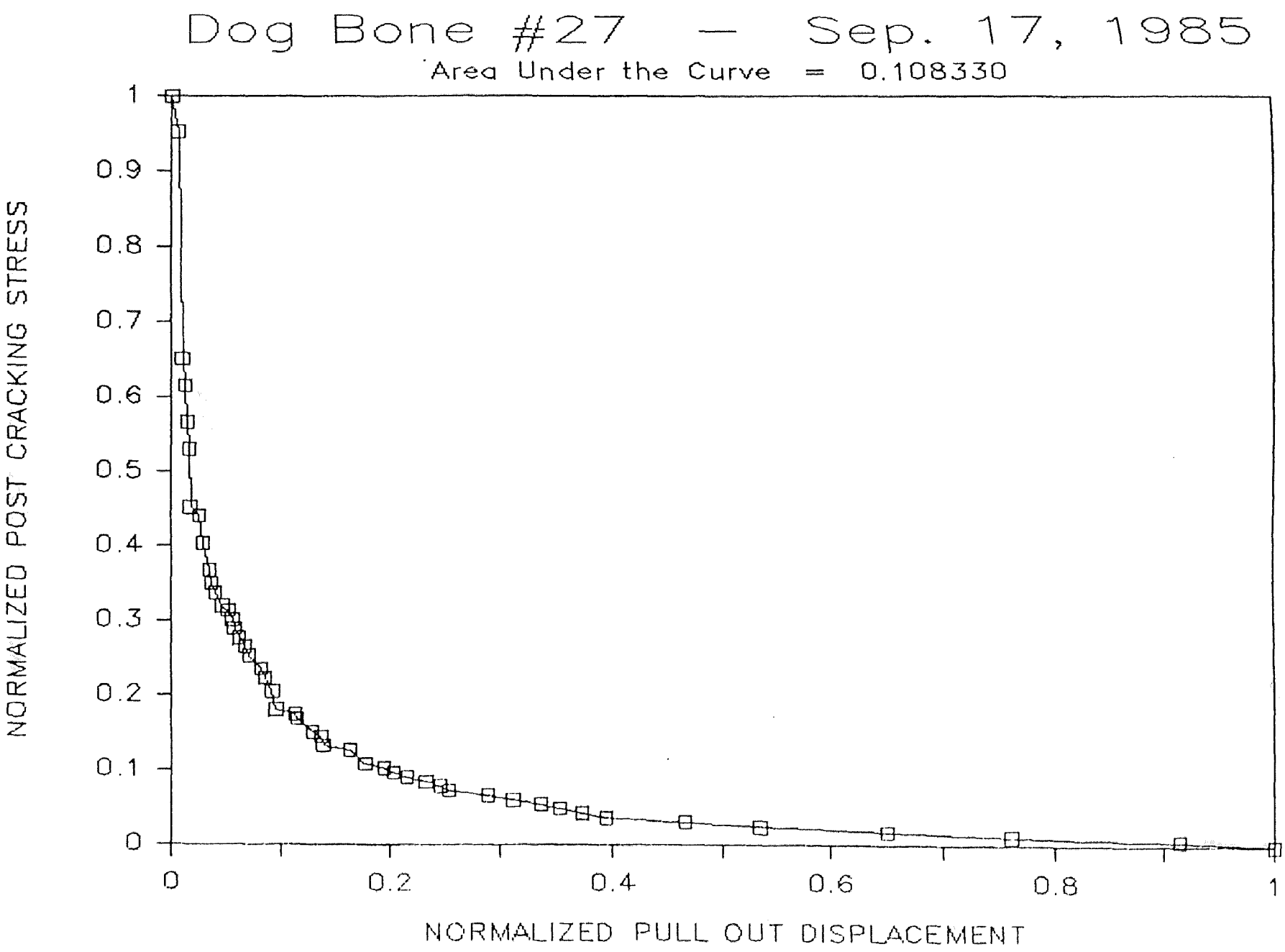
Dog Bone #27 — Sep. 17, 1985
Area Under the Curve = 0.108330
NORMALIZED POST CRACKING STRESS
1
0.9
0.8
0.7
0.6
0.5
0.4
0.3
0.2
0.1
0
0
0.2
0.4
0.6
0.8
1
NORMALIZED PULL OUT DISPLACEMENT

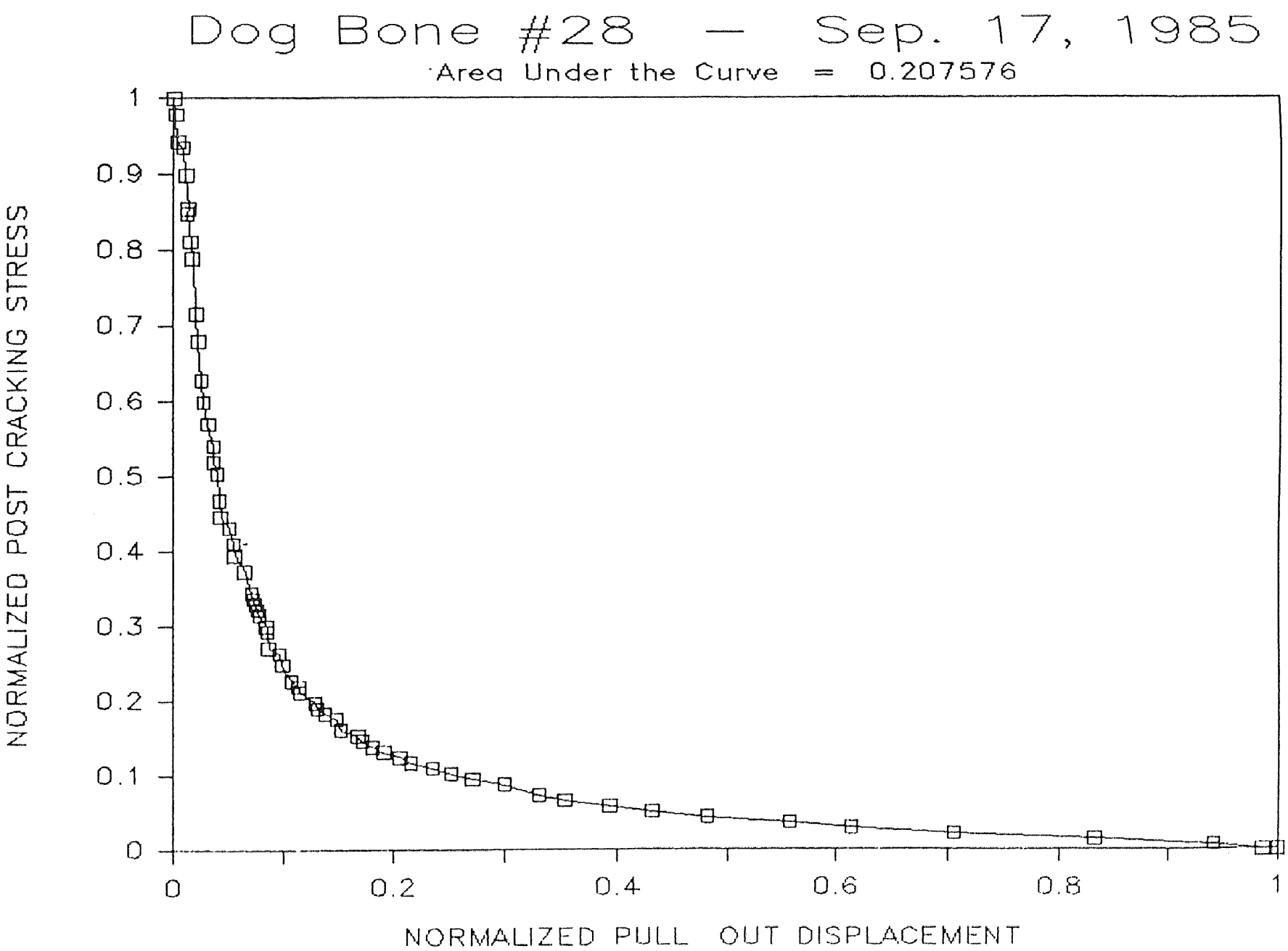
Dog Bone #28 — Sep. 17, 1985
Area Under the Curve = 0.207576
NORMALIZED POST CRACKING STRESS
1
0.9
0.8
0.7
0.6
0.5
0.4
0.3
0.2
0.1
0
0
0.2
0.4
0.6
0.8
1
NORMALIZED PULL OUT DISPLACEMENT

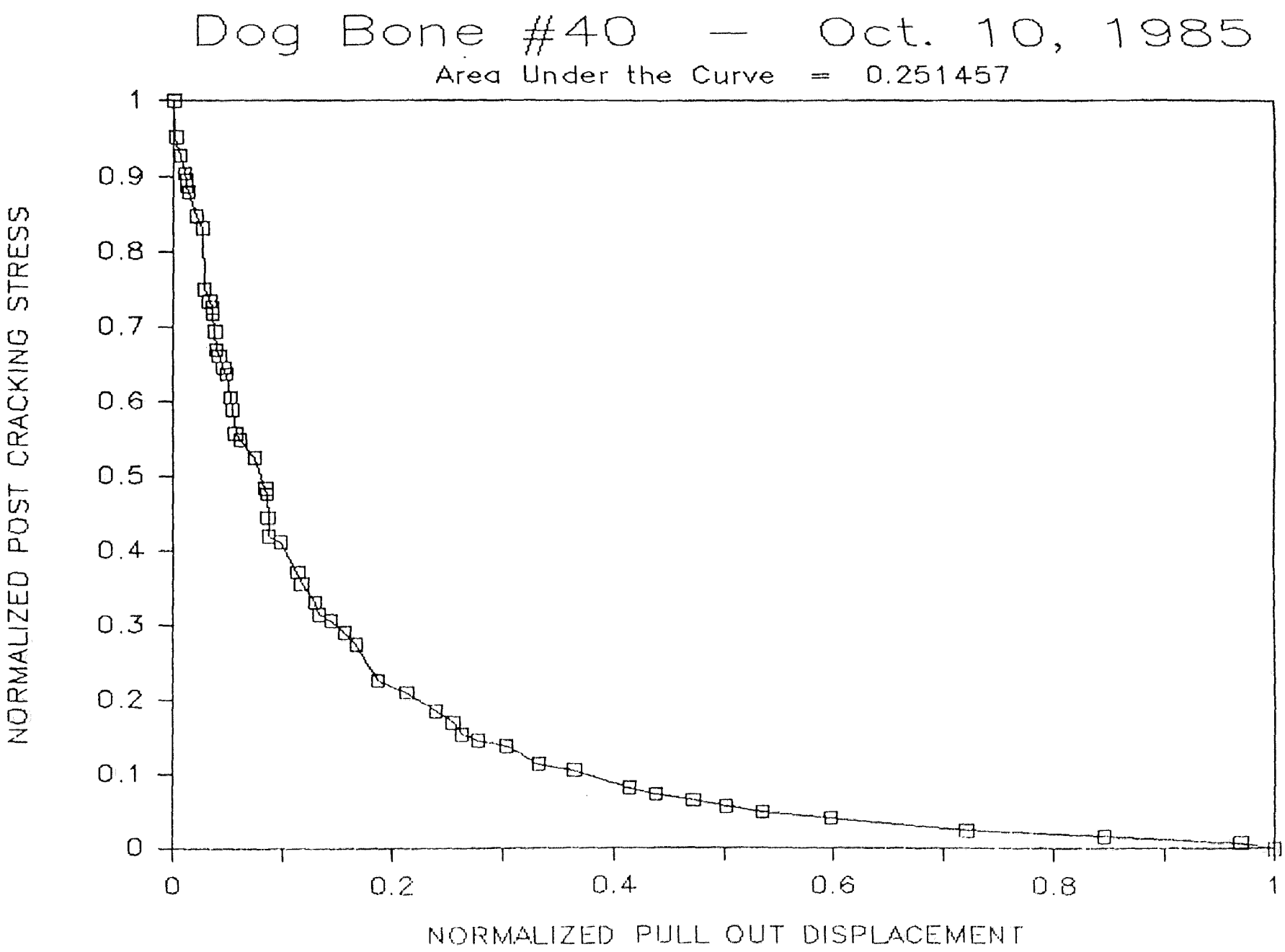
Dog Bone #40 — Oct. 10, 1985
Area Under the Curve = 0.251457
NORMALIZED POST CRACKING STRESS
1
0.9
0.8
0.7
0.6
0.5
0.4
0.3
0.2
0.1
0
0
0.2
0.4
0.6
0.8
1
NORMALIZED PULL OUT DISPLACEMENT

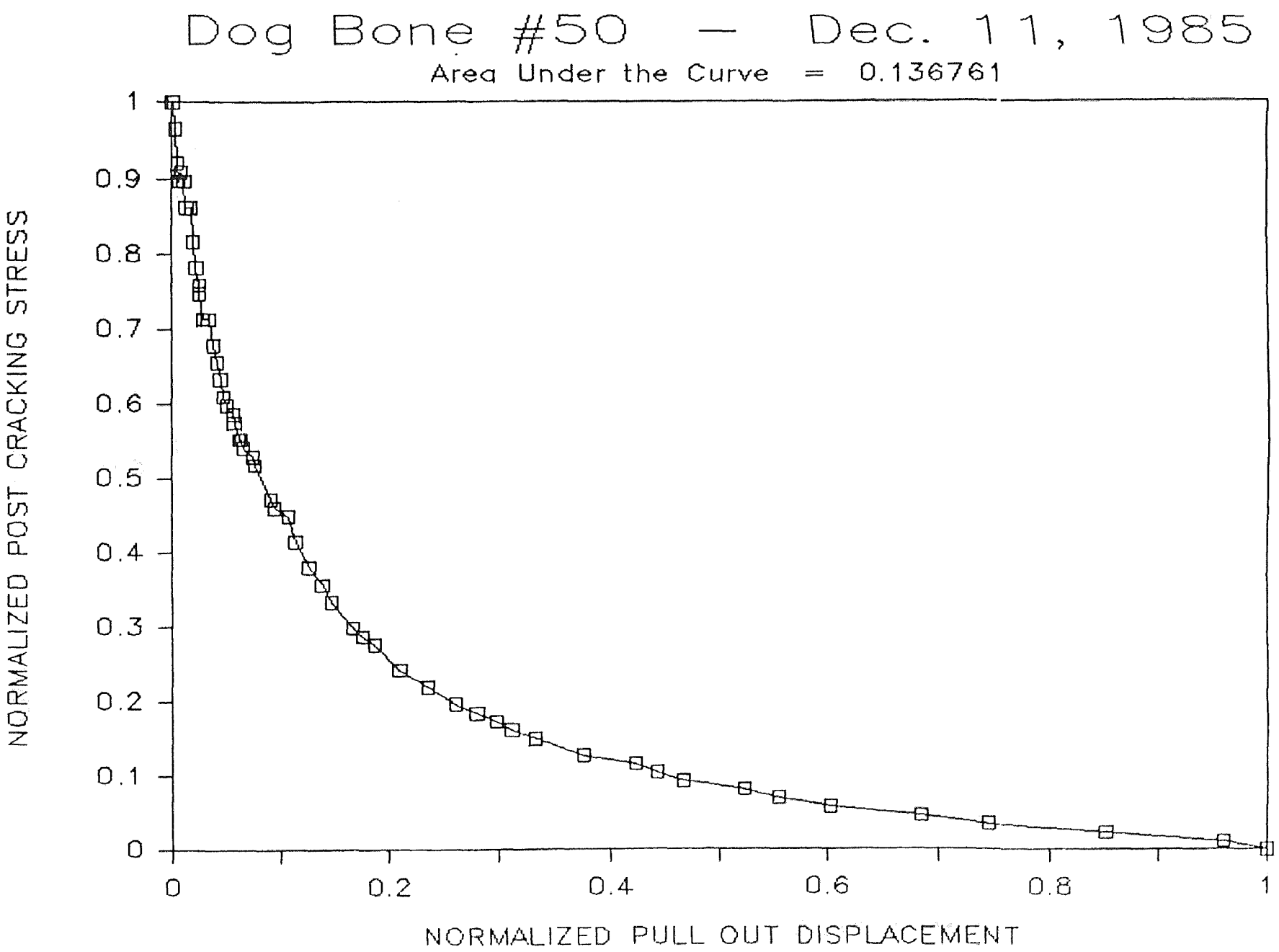
Dog Bone #50 — Dec. 11, 1985
Area Under the Curve = 0.136761
NORMALIZED POST CRACKING STRESS
1
0.9
0.8
0.7
0.6
0.5
0.4
0.3
0.2
0.1
0
0
0.2
0.4
0.6
0.8
1
NORMALIZED PULL OUT DISPLACEMENT

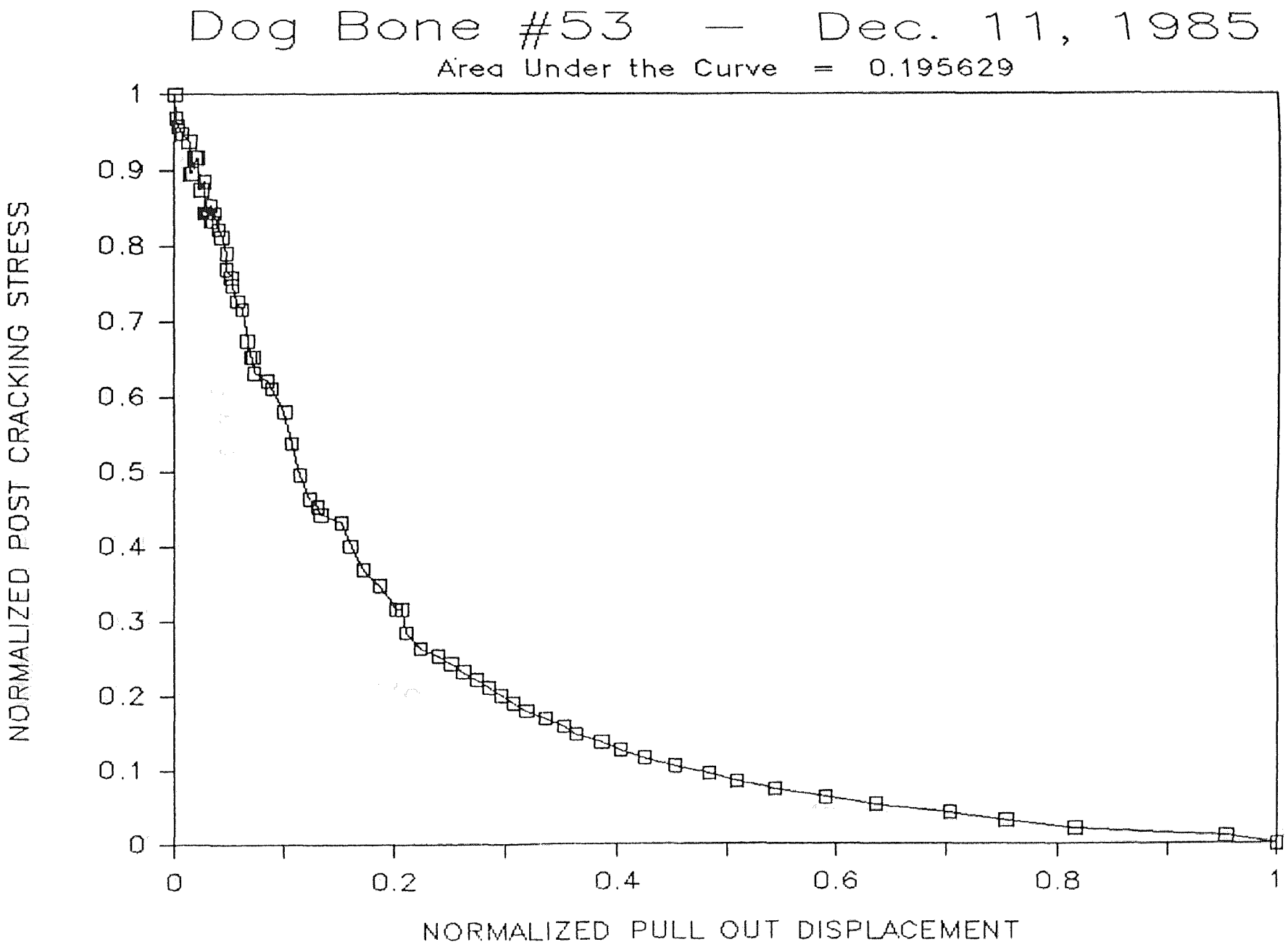
Dog Bone #53 — Dec. 11, 1985
Area Under the Curve = 0.195629
NORMALIZED POST CRACKING STRESS
NORMALIZED PULL OUT DISPLACEMENT
0
0.1
0.2
0.3
0.4
0.5
0.6
0.7
0.8
0.9
1
0
0.2
0.4
0.6
0.8
1

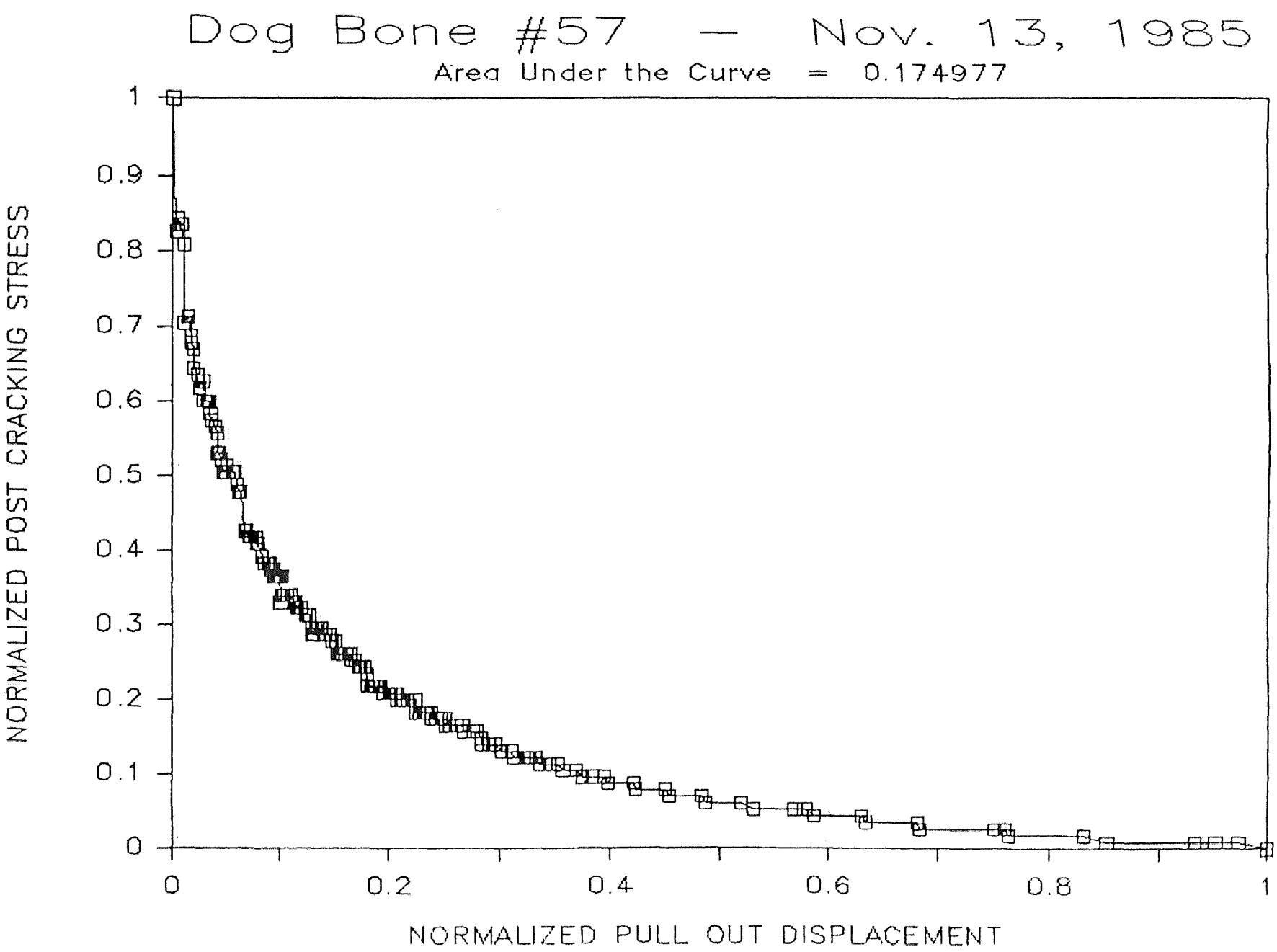
Dog Bone #57 — Nov. 13, 1985
Area Under the Curve = 0.174977
NORMALIZED POST CRACKING STRESS
NORMALIZED PULL OUT DISPLACEMENT
0
0.1
0.2
0.3
0.4
0.5
0.6
0.7
0.8
0.9
1
0
0.2
0.4
0.6
0.8
1

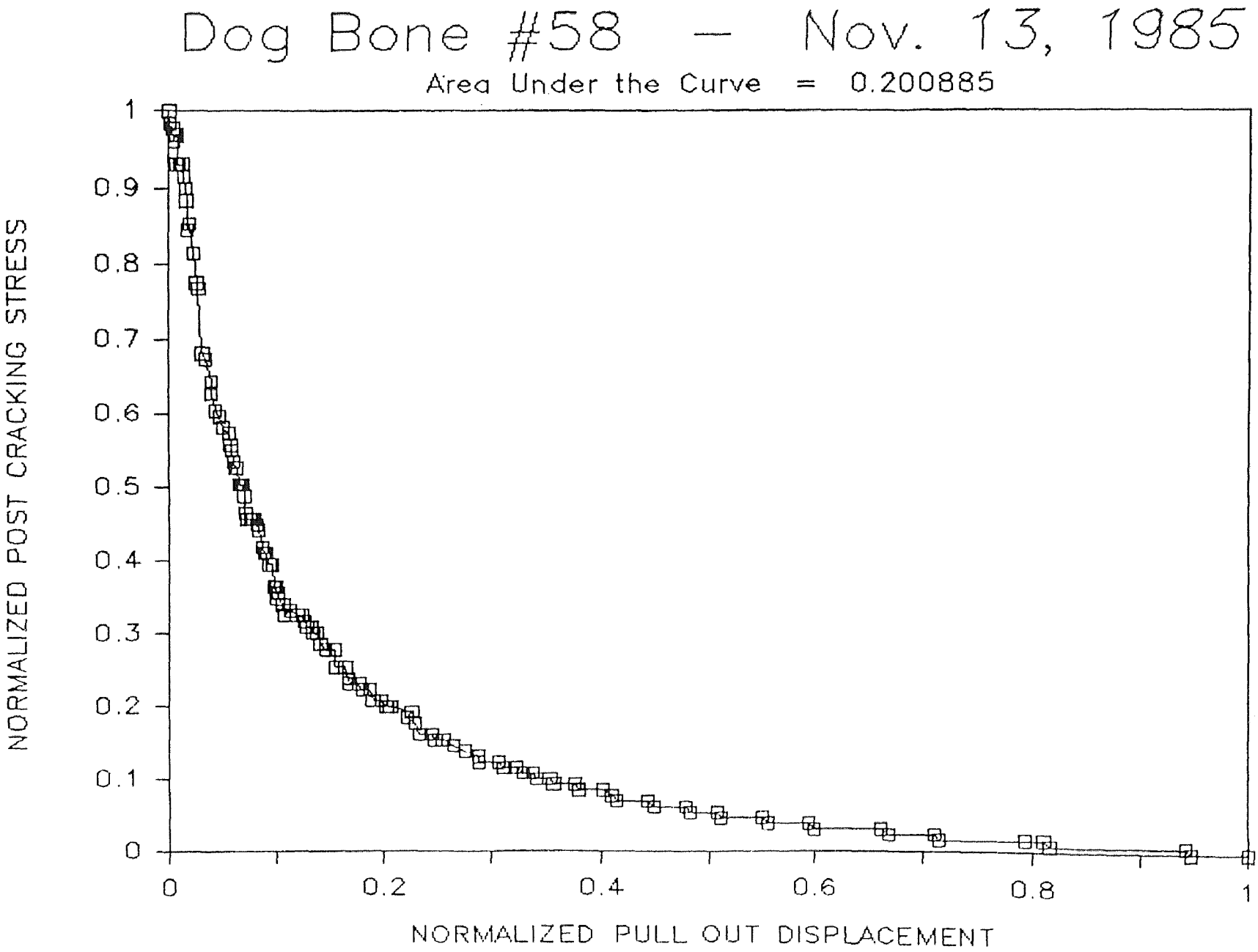
Dog Bone #58 — Nov. 13, 1985
Area Under the Curve = 0.200885
NORMALIZED POST CRACKING STRESS
1
0.9
0.8
0.7
0.6
0.5
0.4
0.3
0.2
0.1
0
0
0.2
0.4
0.6
0.8
1
NORMALIZED PULL OUT DISPLACEMENT

Dog Bone #31 — Oct. 10, 1985

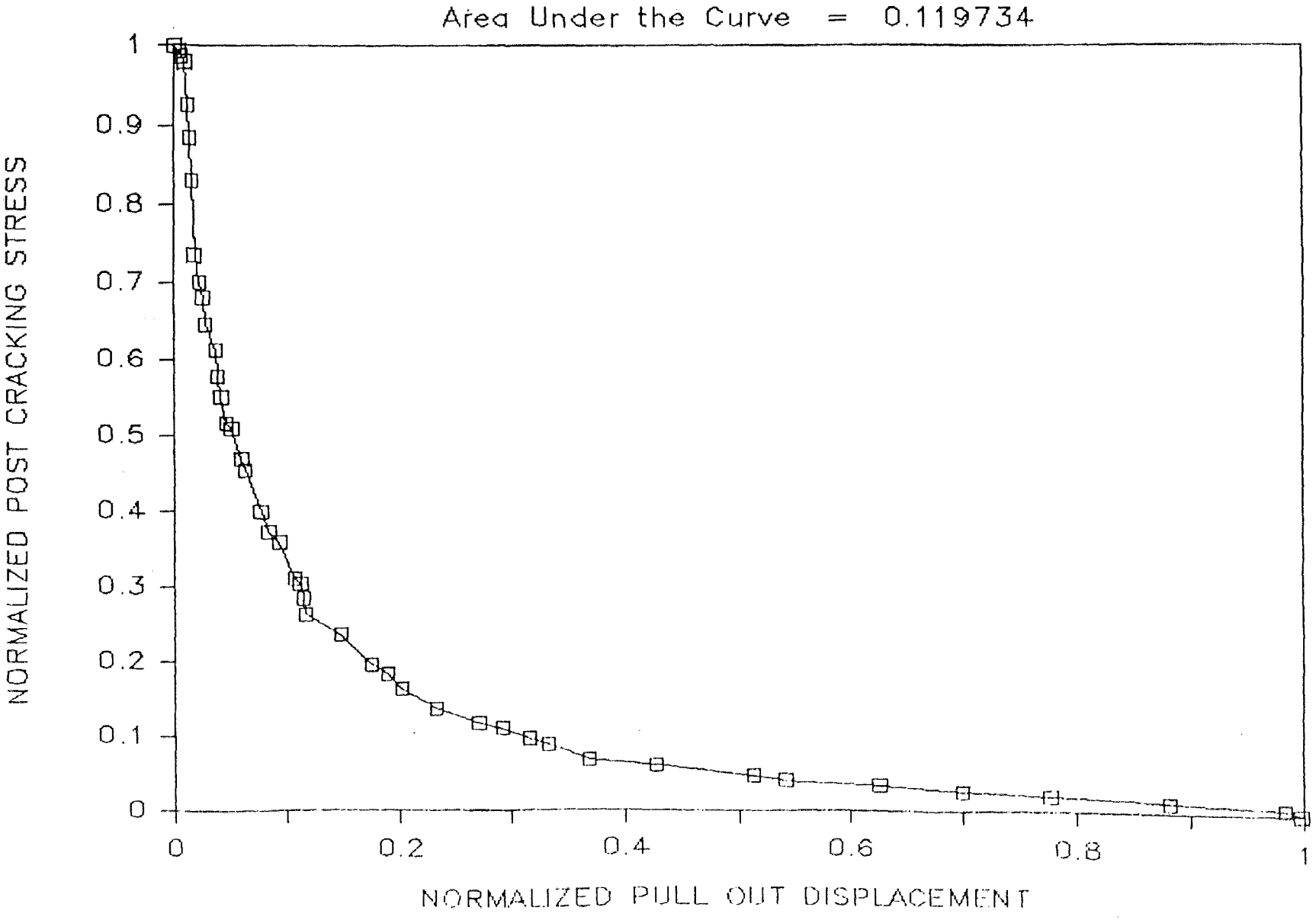

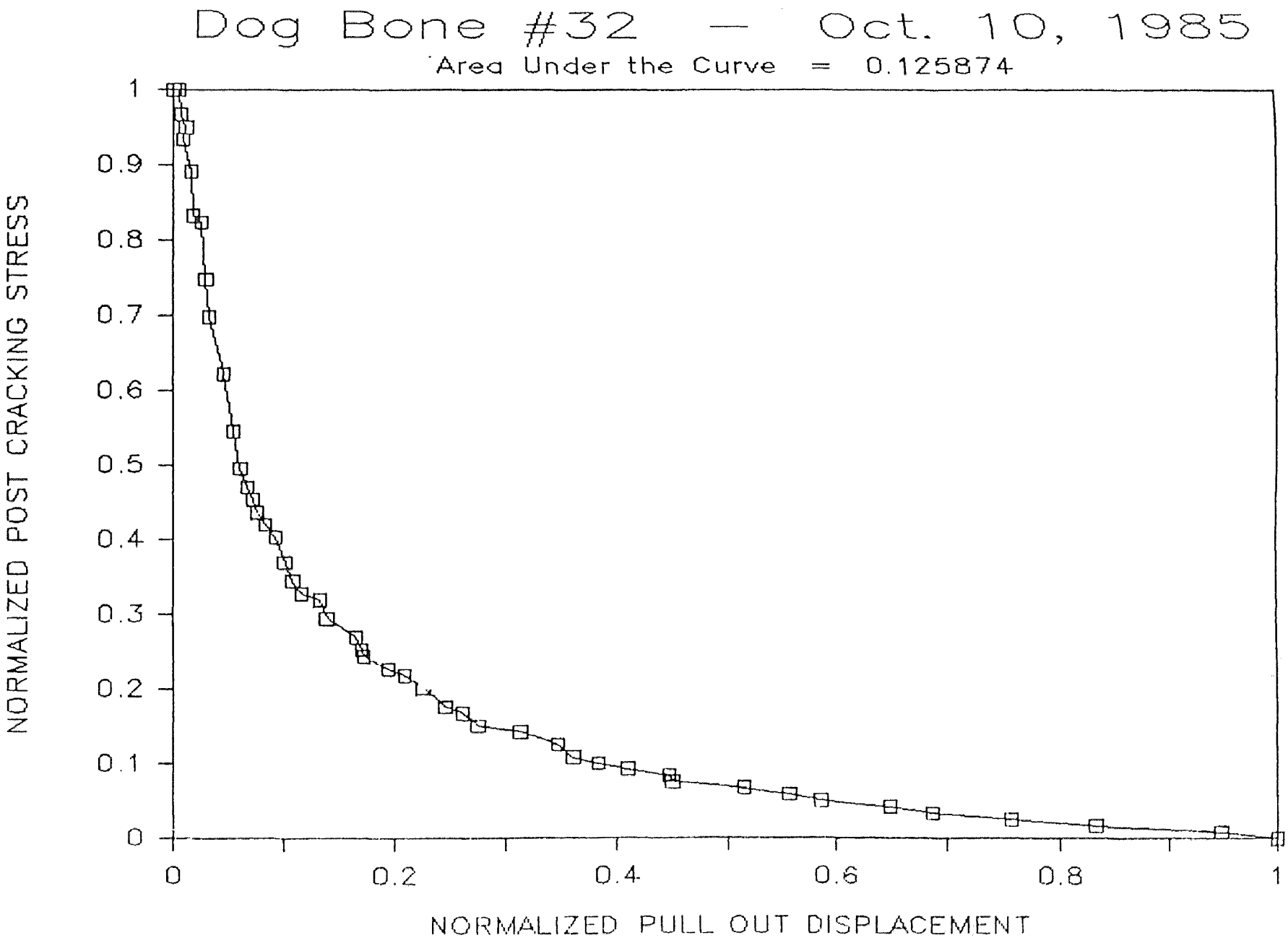
Dog Bone #32 — Oct. 10, 1985
Area Under the Curve = 0.125874
NORMALIZED POST CRACKING STRESS
NORMALIZED PULL OUT DISPLACEMENT
0
0.1
0.2
0.3
0.4
0.5
0.6
0.7
0.8
0.9
1
0
0.2
0.4
0.6
0.8
1

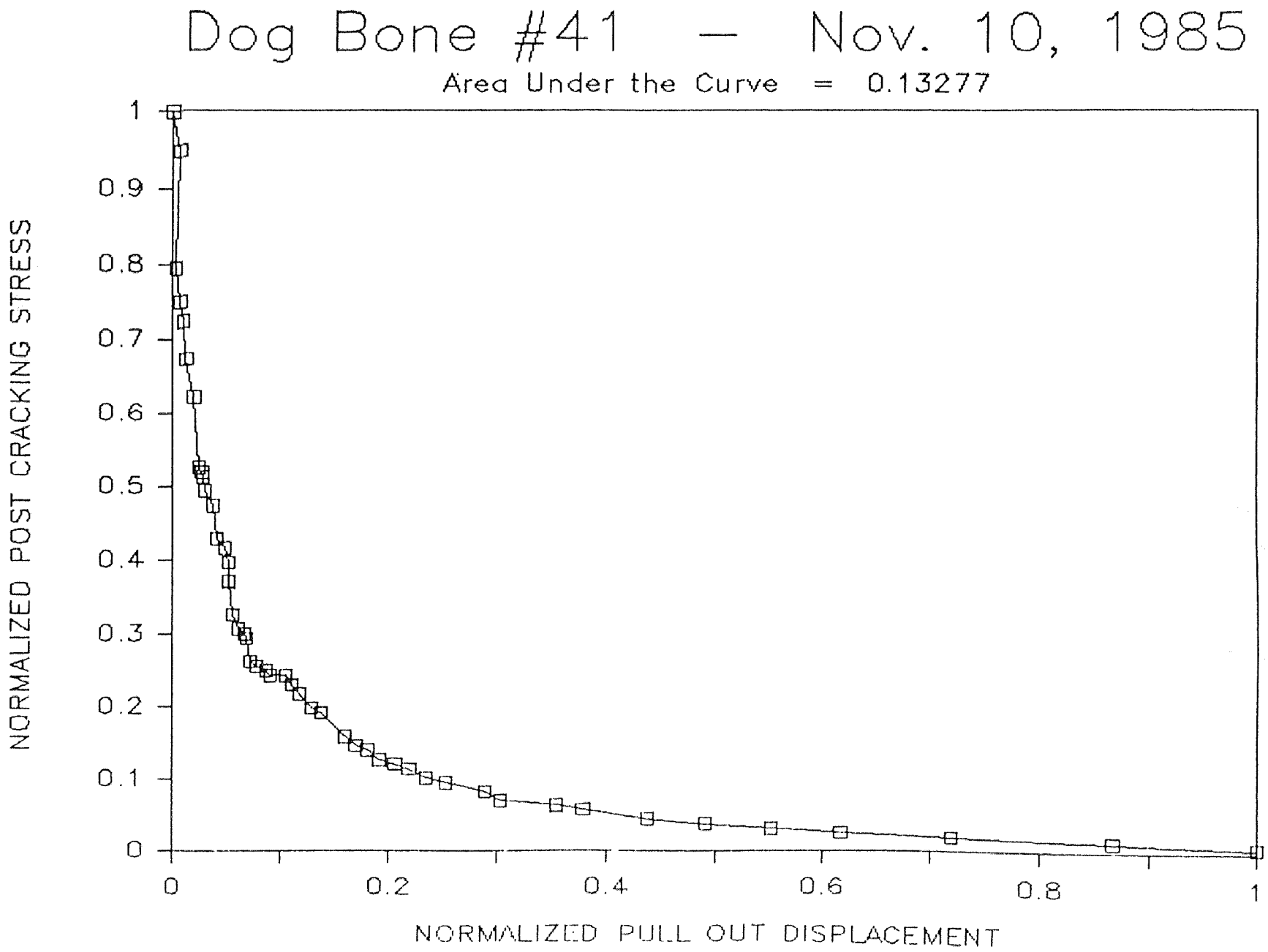
Dog Bone #41 — Nov. 10, 1985
Area Under the Curve = 0.13277
NORMALIZED POST CRACKING STRESS
NORMALIZED PULL OUT DISPLACEMENT
0
0.1
0.2
0.3
0.4
0.5
0.6
0.7
0.8
0.9
1
0
0.2
0.4
0.6
0.8
1

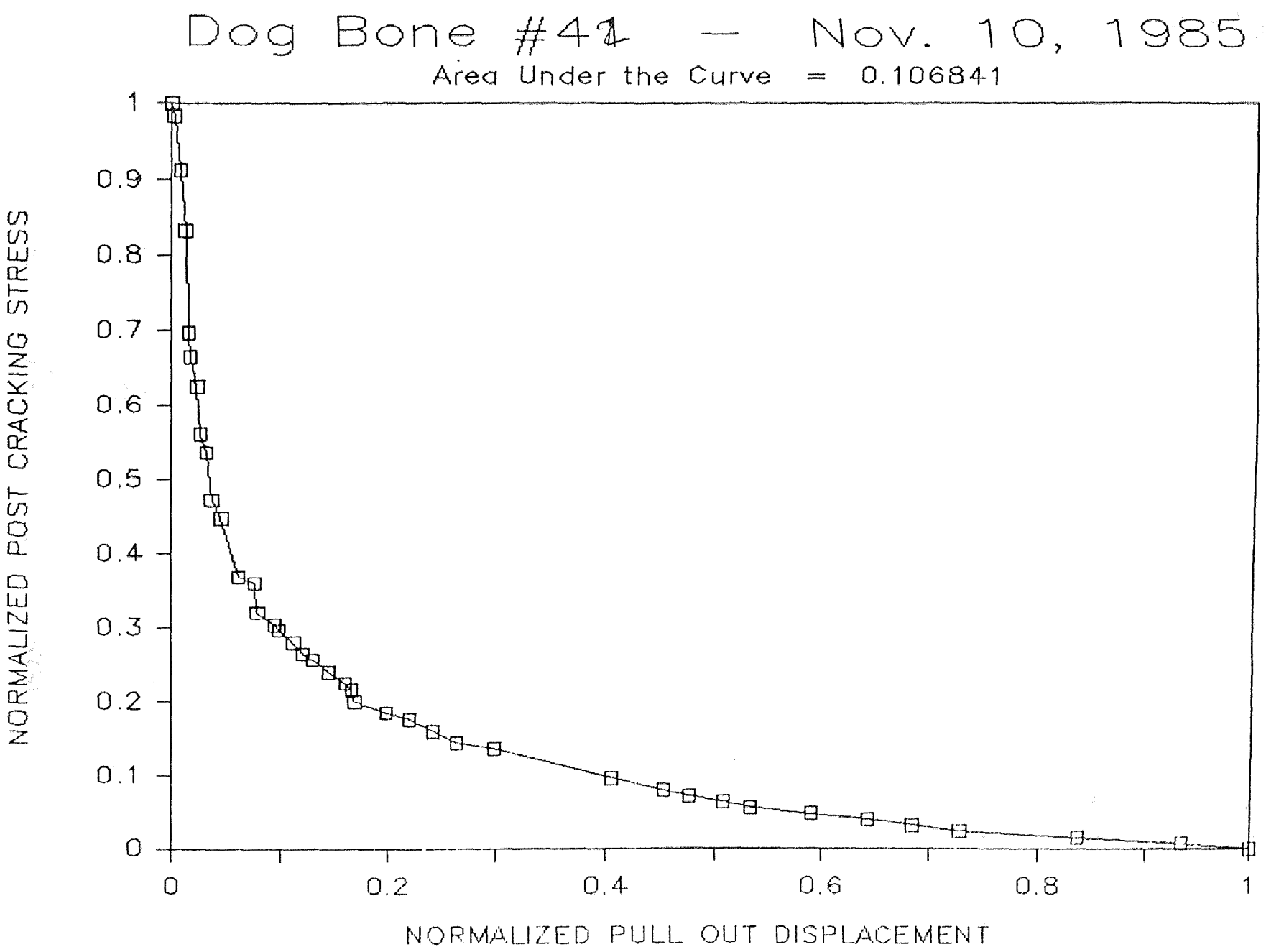
Dog Bone #41 — Nov. 10, 1985
Area Under the Curve = 0.106841
NORMALIZED POST CRACKING STRESS
NORMALIZED PULL OUT DISPLACEMENT
0
0.1
0.2
0.3
0.4
0.5
0.6
0.7
0.8
0.9
1
0
0.2
0.4
0.6
0.8
1

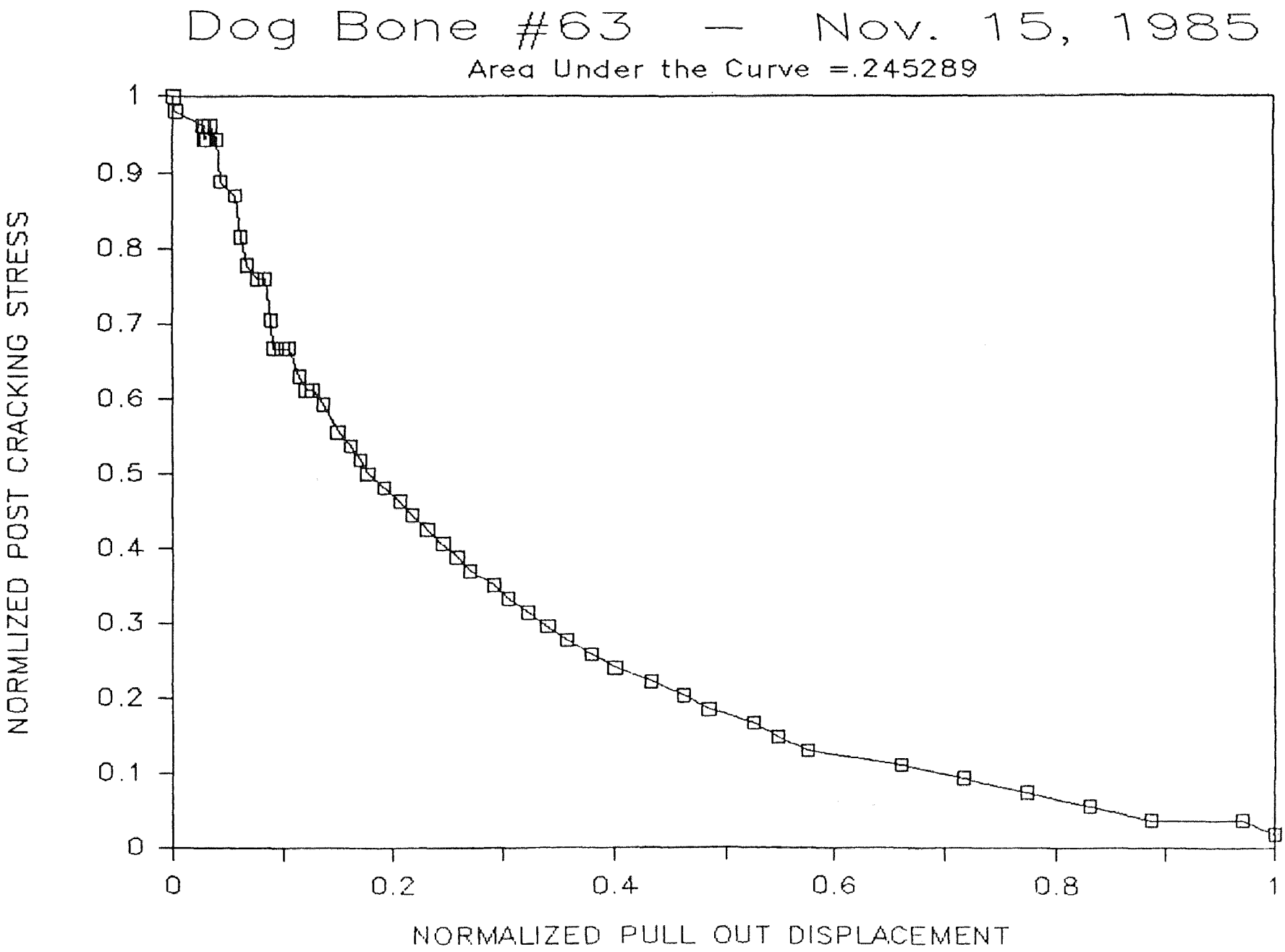
Dog Bone #63 — Nov. 15, 1985
Area Under the Curve =.245289
NORMLIZED POST CRACKING STRESS
1
0.9
0.8
0.7
0.6
0.5
0.4
0.3
0.2
0.1
0
0
0.2
0.4
0.6
0.8
1
NORMALIZED PULL OUT DISPLACEMENT

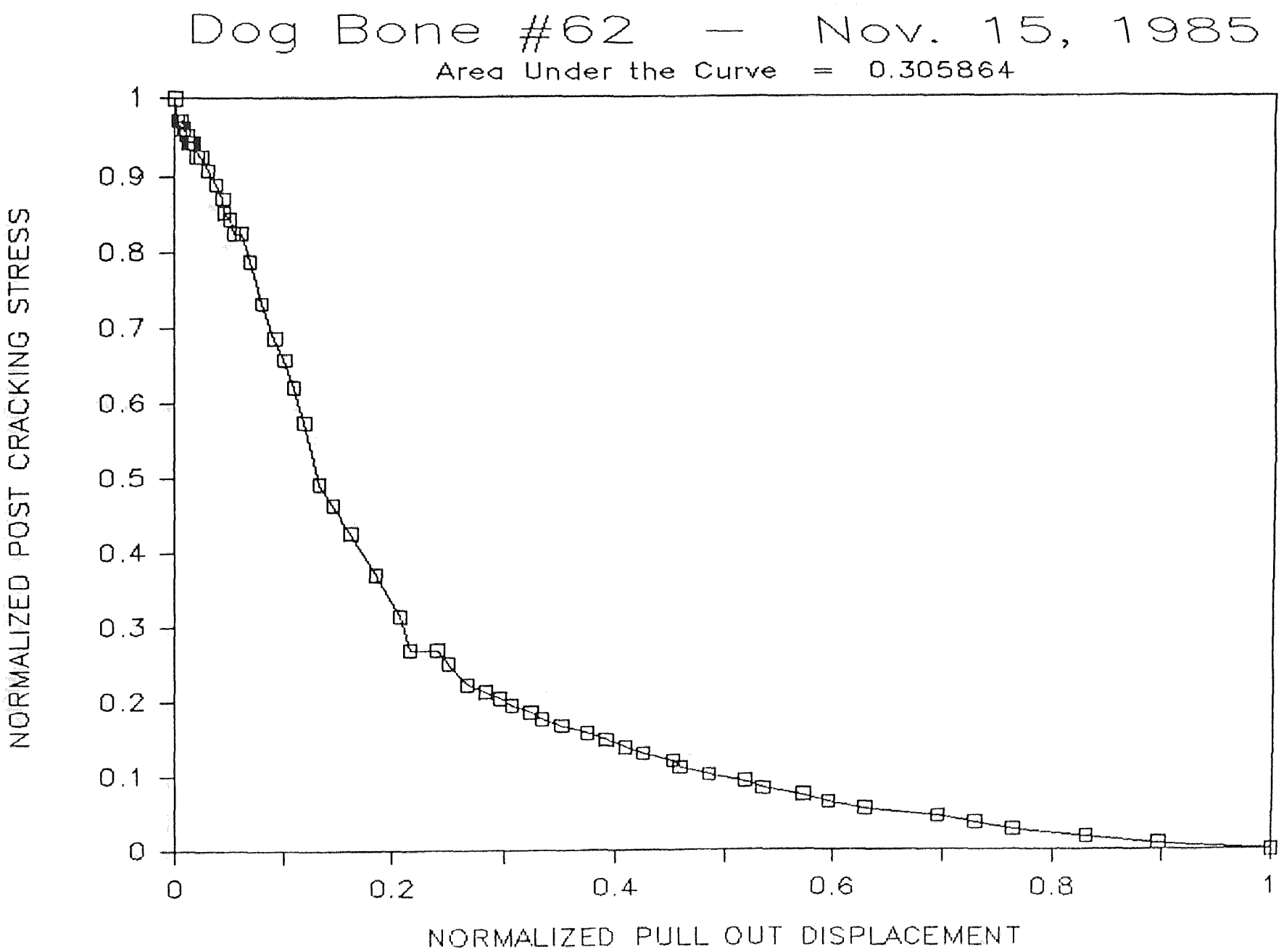
Dog Bone #62 — Nov. 15, 1985
Area Under the Curve = 0.305864
NORMALIZED POST CRACKING STRESS
NORMALIZED PULL OUT DISPLACEMENT
0
0.1
0.2
0.3
0.4
0.5
0.6
0.7
0.8
0.9
1
0
0.2
0.4
0.6
0.8
1

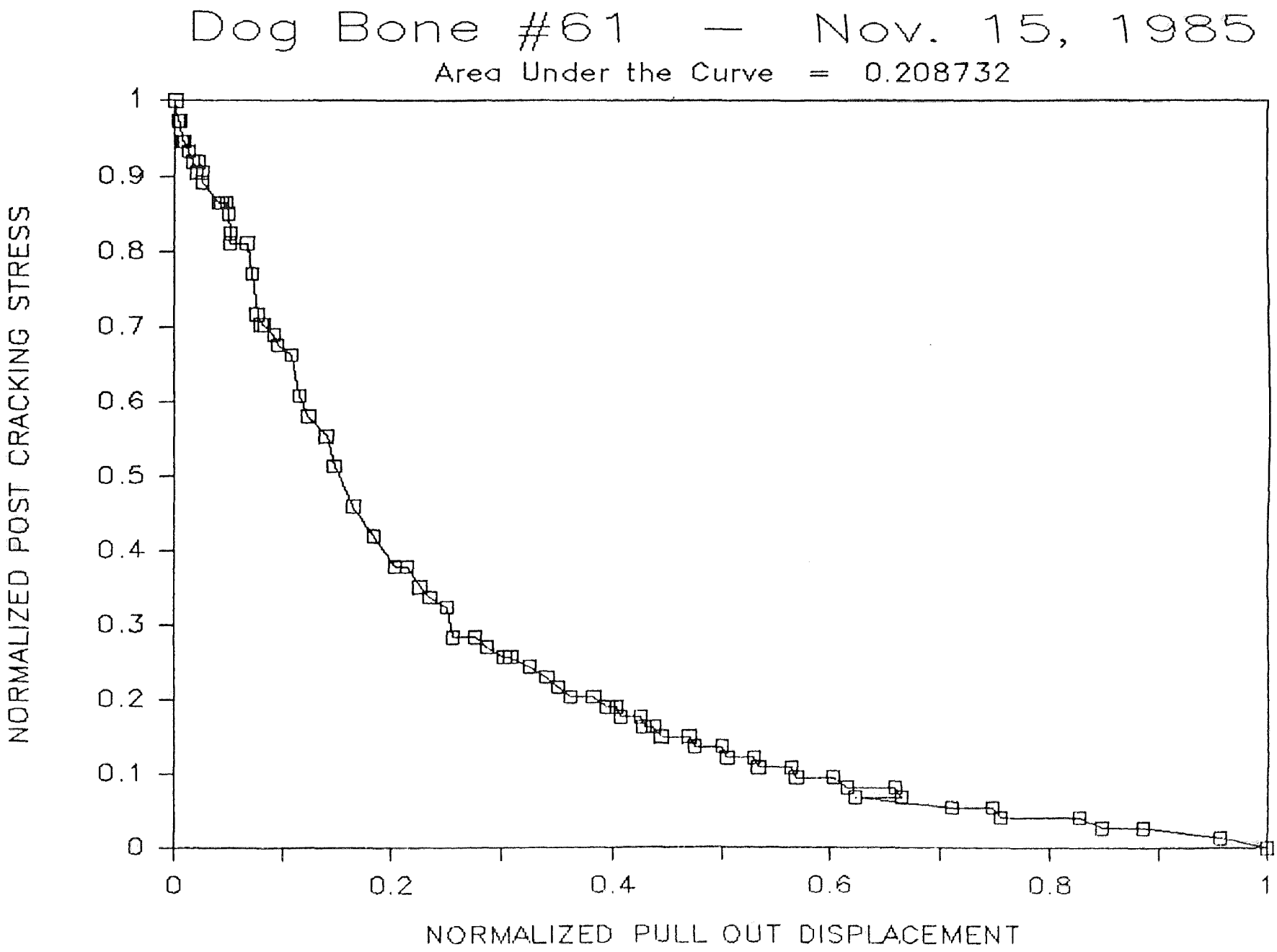
Dog Bone #61 — Nov. 15, 1985
Area Under the Curve = 0.208732
NORMALIZED POST CRACKING STRESS
NORMALIZED PULL OUT DISPLACEMENT
0
0.1
0.2
0.3
0.4
0.5
0.6
0.7
0.8
0.9
1
0
0.2
0.4
0.6
0.8
1

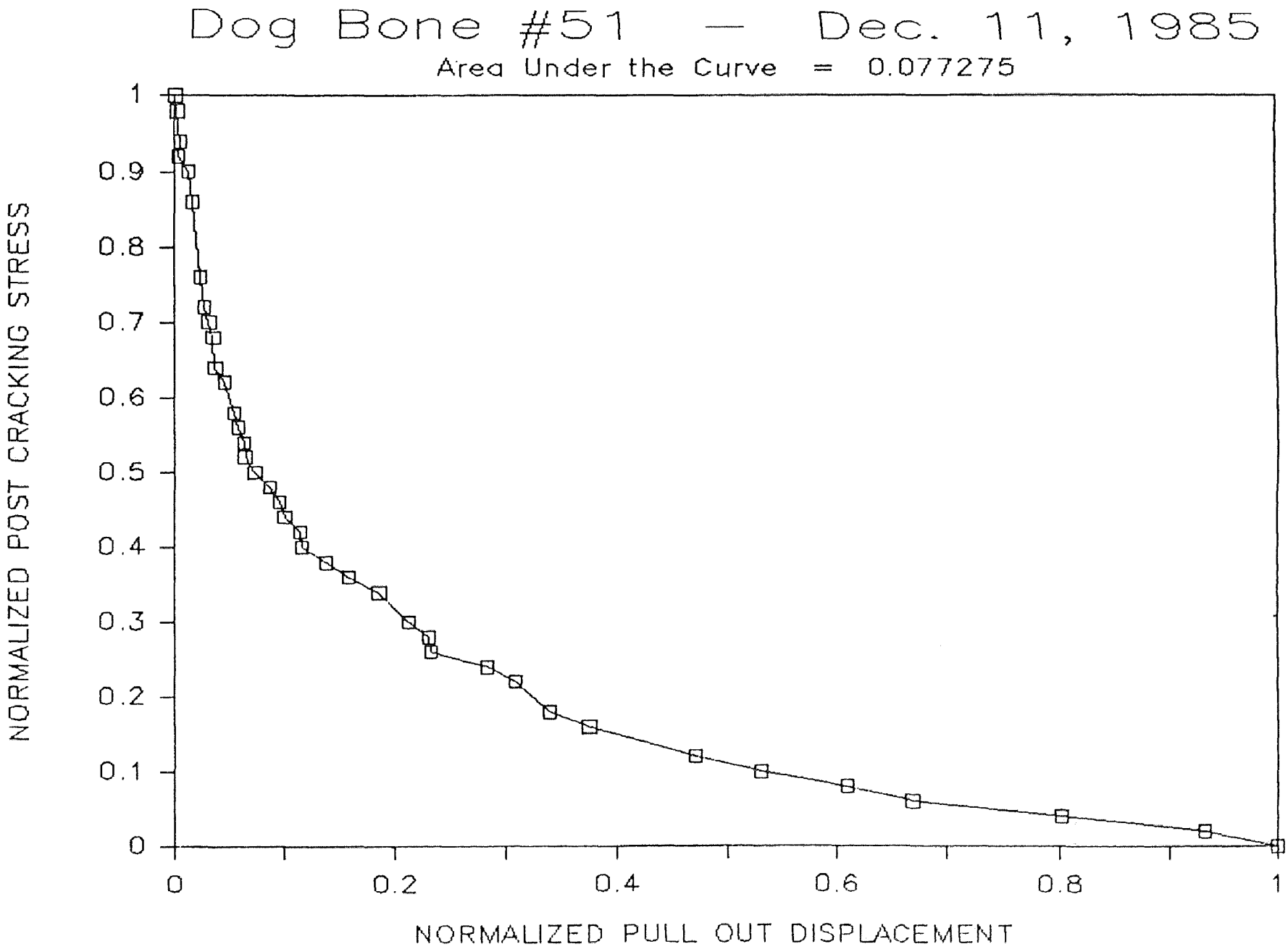
Dog Bone #51 — Dec. 11, 1985
Area Under the Curve = 0.077275
NORMALIZED POST CRACKING STRESS
NORMALIZED PULL OUT DISPLACEMENT
0
0.1
0.2
0.3
0.4
0.5
0.6
0.7
0.8
0.9
1
0
0.2
0.4
0.6
0.8
1

Dog Bone #52 — Dec. 11, 1985

Area Under the Curve = 0.061805

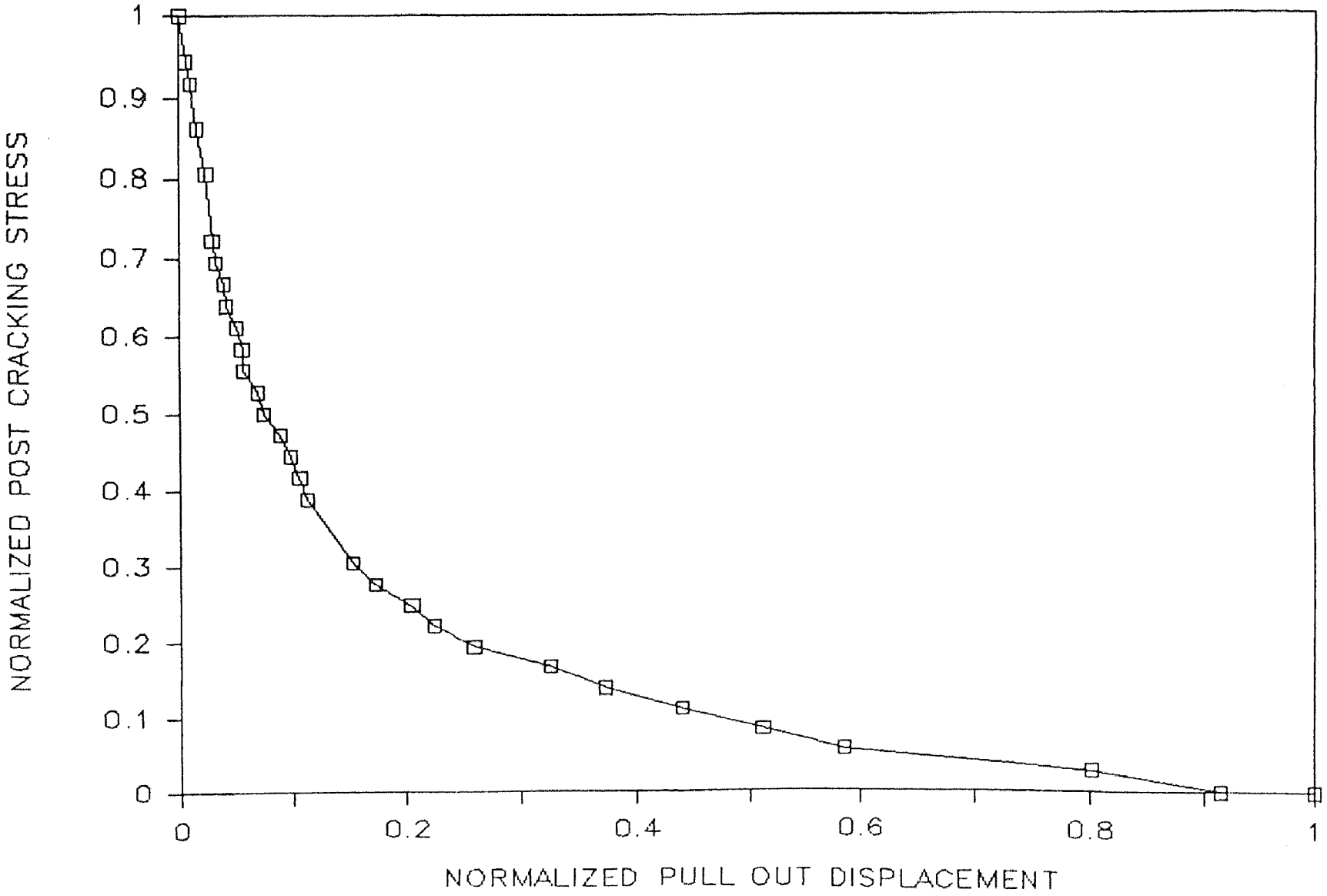

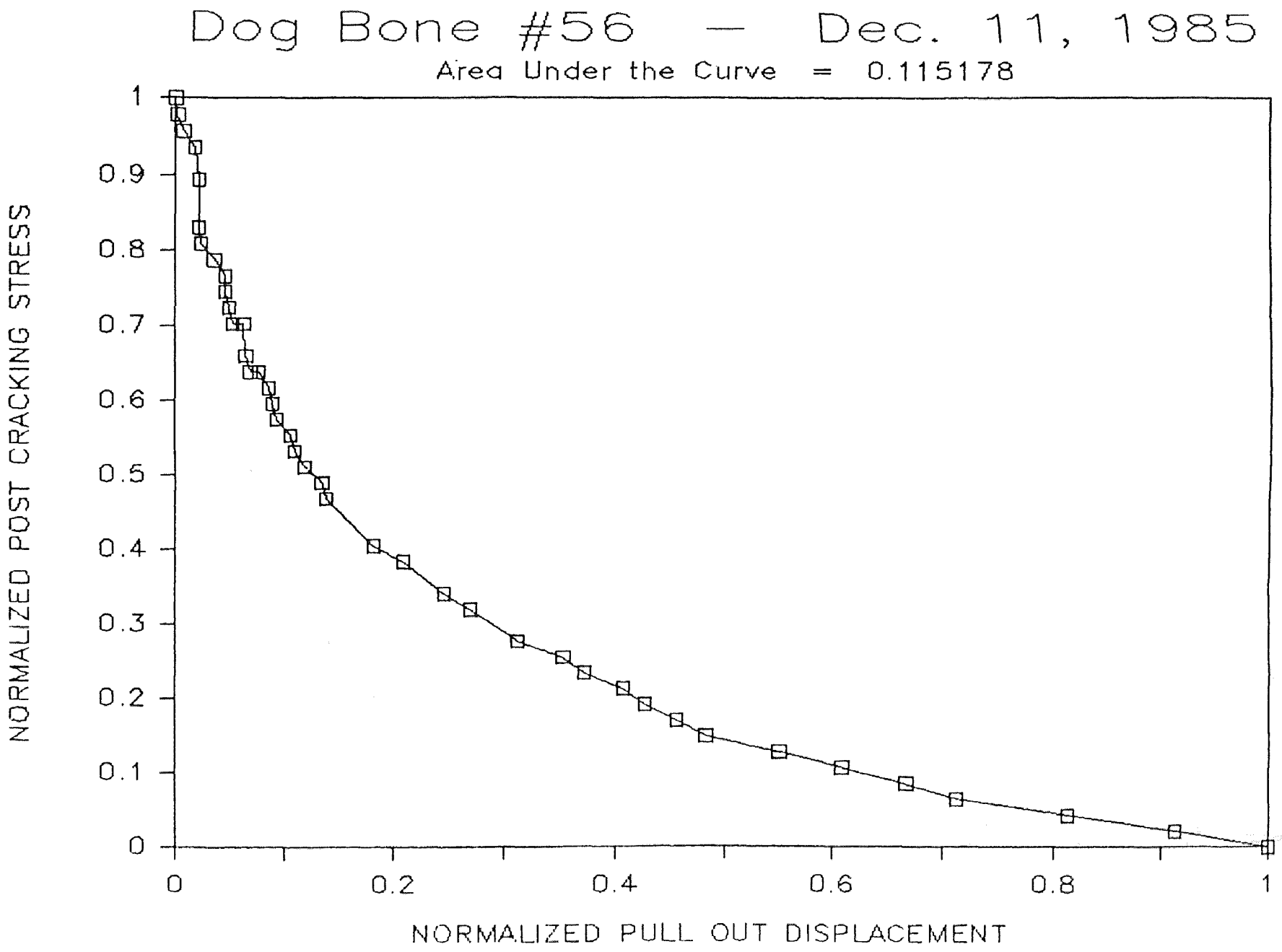
Dog Bone #56 — Dec. 11, 1985
Area Under the Curve = 0.115178
NORMALIZED POST CRACKING STRESS
NORMALIZED PULL OUT DISPLACEMENT
0
0.1
0.2
0.3
0.4
0.5
0.6
0.7
0.8
0.9
1
0
0.2
0.4
0.6
0.8
1

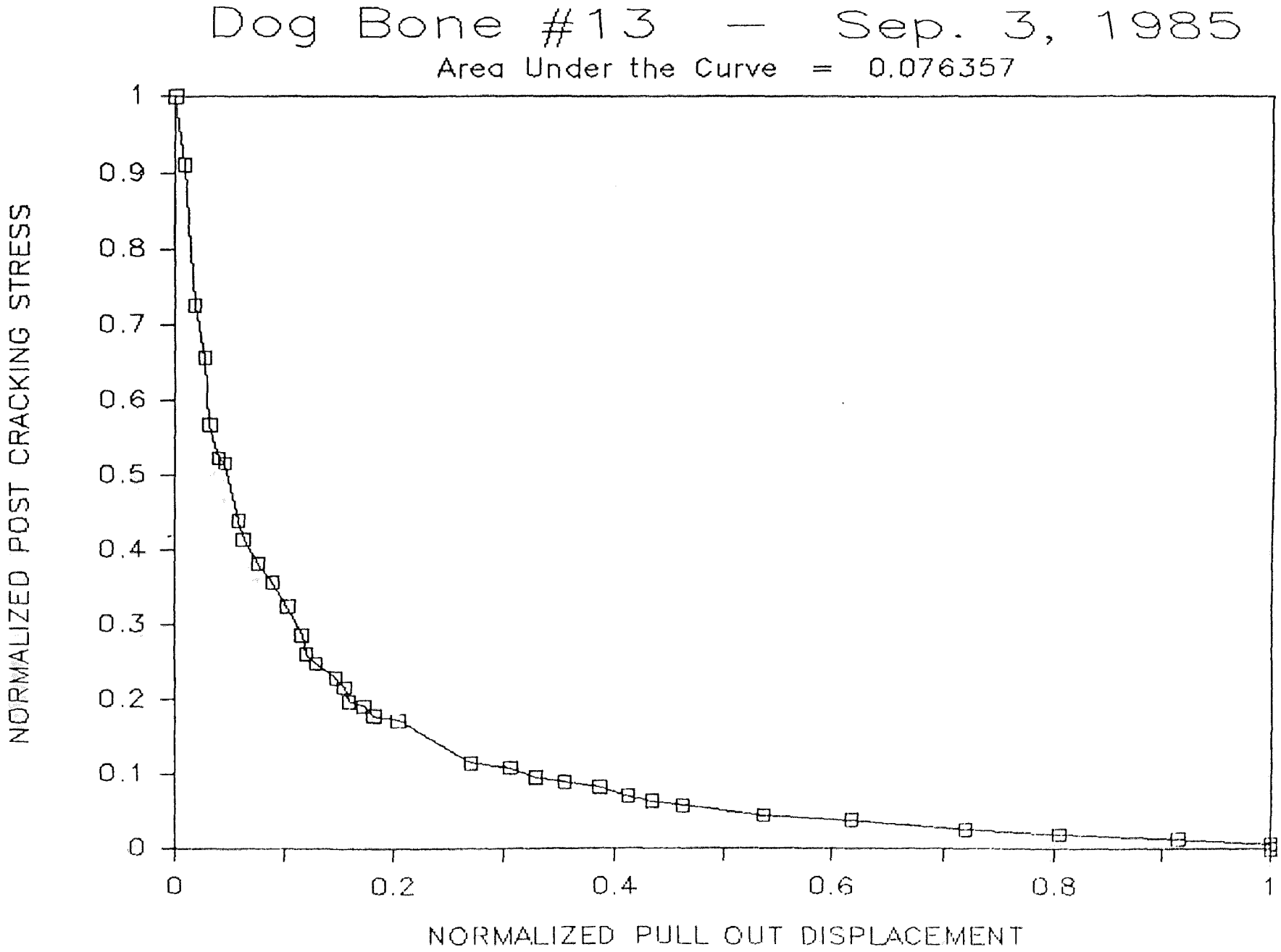
Dog Bone #13 — Sep. 3, 1985
Area Under the Curve = 0.076357
NORMALIZED POST CRACKING STRESS
1
0.9
0.8
0.7
0.6
0.5
0.4
0.3
0.2
0.1
0
0
0.2
0.4
0.6
0.8
1
NORMALIZED PULL OUT DISPLACEMENT

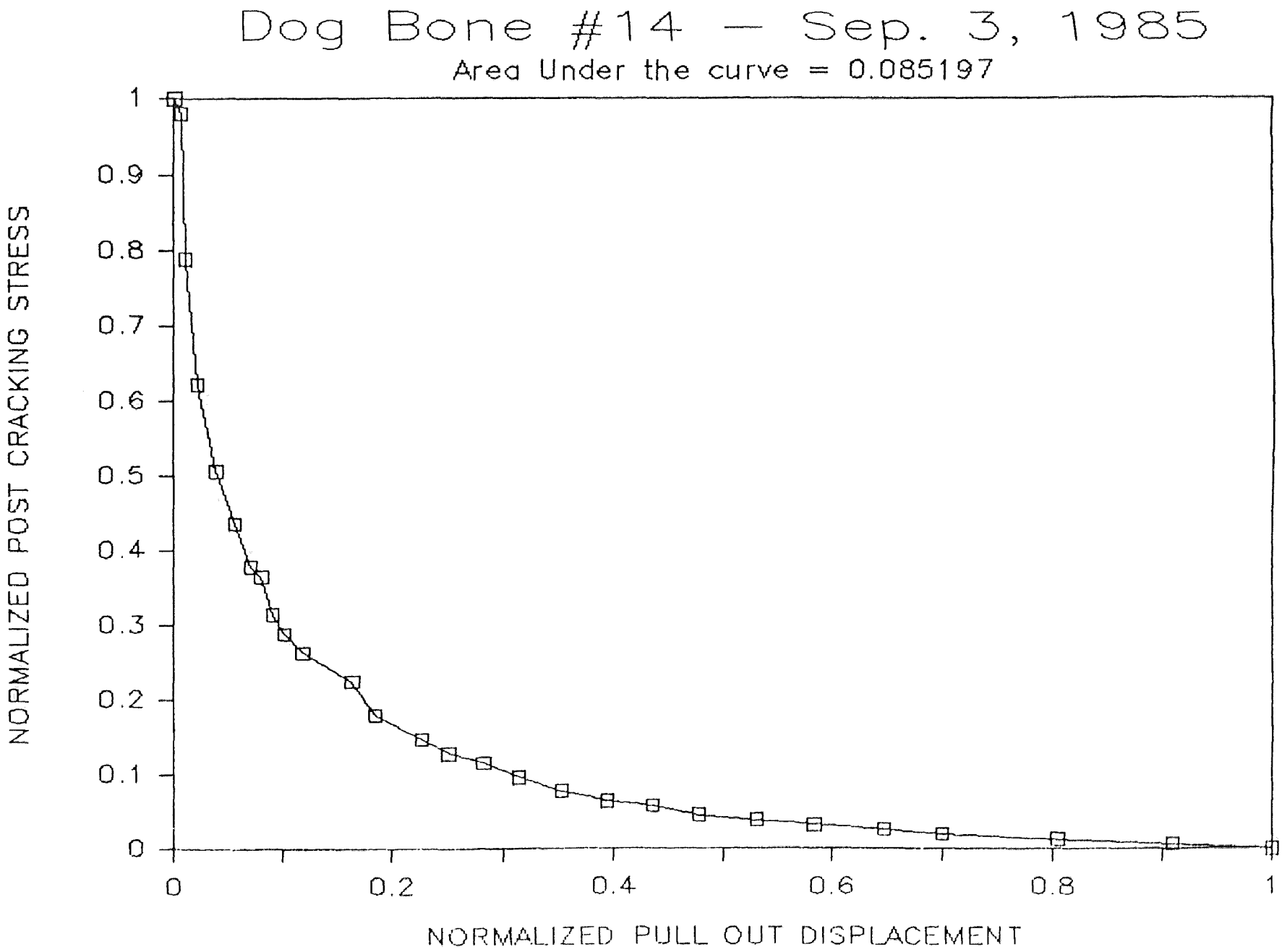
Dog Bone #14 — Sep. 3, 1985
Area Under the curve = 0.085197
NORMALIZED POST CRACKING STRESS
1
0.9
0.8
0.7
0.6
0.5
0.4
0.3
0.2
0.1
0
0
0.2
0.4
0.6
0.8
1
NORMALIZED PULL OUT DISPLACEMENT

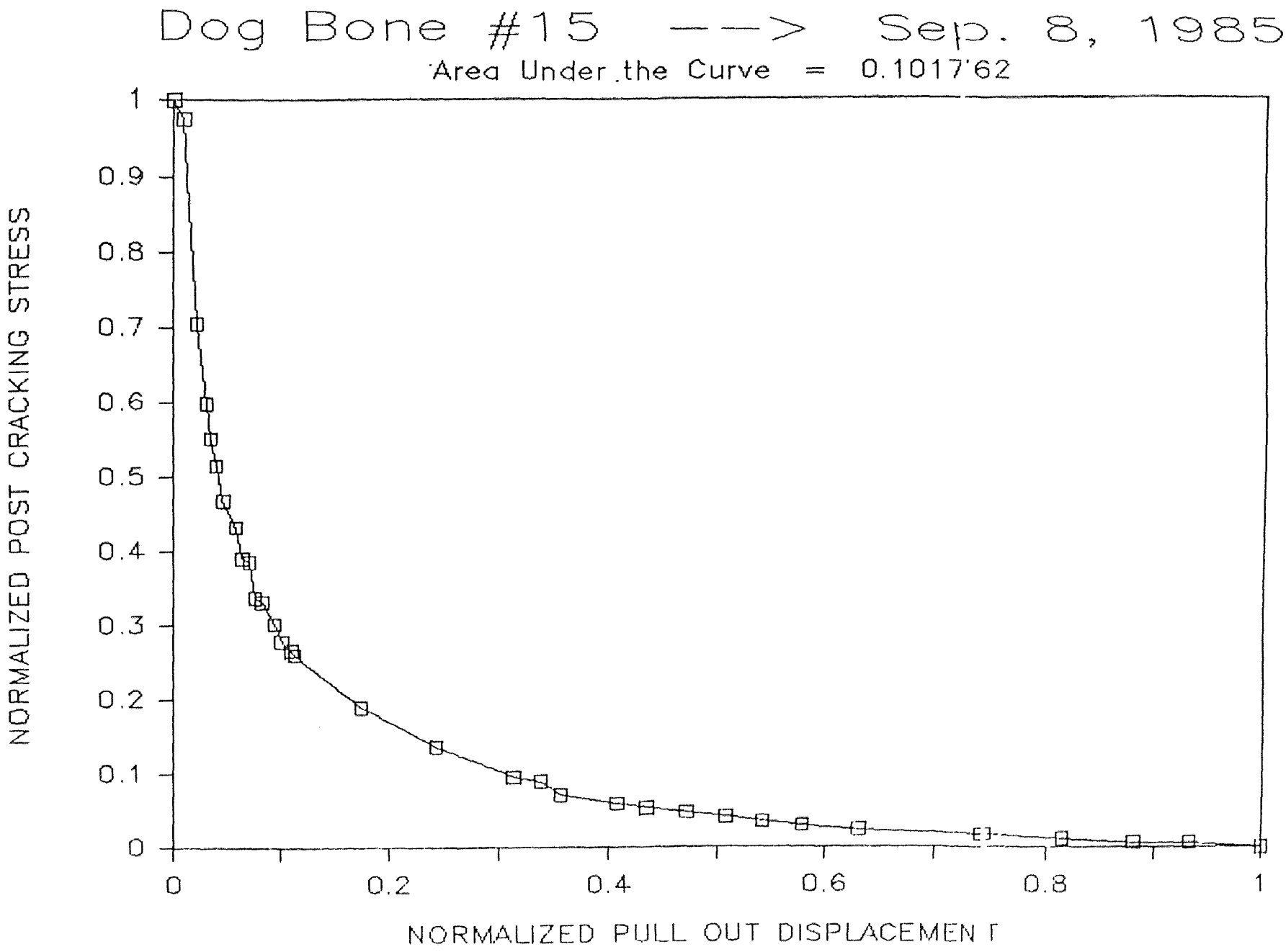
Dog Bone #15 ---> Sep. 8, 1985
Area Under the Curve = 0.101762
NORMALIZED POST CRACKING STRESS
1
0.9
0.8
0.7
0.6
0.5
0.4
0.3
0.2
0.1
0
0
0.2
0.4
0.6
0.8
1
NORMALIZED PULL OUT DISPLACEMENT

APPENDIX D

UNLOADING LOAD DISPLACEMENT RELATIONSHIP

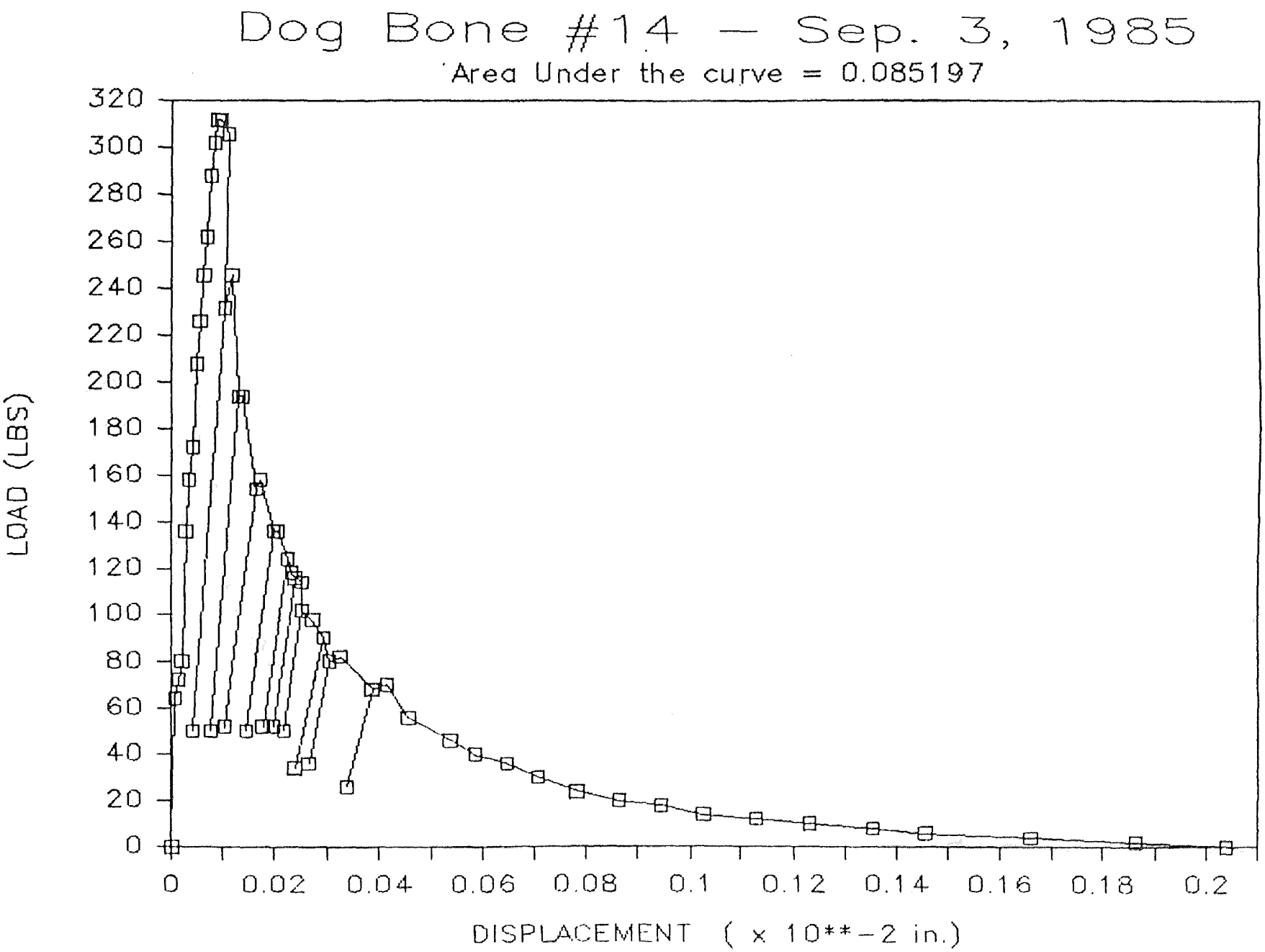
Dog Bone #14 — Sep. 3, 1985
Area Under the curve = 0.085197
LOAD (LBS)
320
300
280
260
240
220
200
180
160
140
120
100
80
60
40
20
0
0
0.02
0.04
0.06
0.08
0.1
0.12
0.14
0.16
0.18
0.2
DISPLACEMENT (x 10**-2 in.)

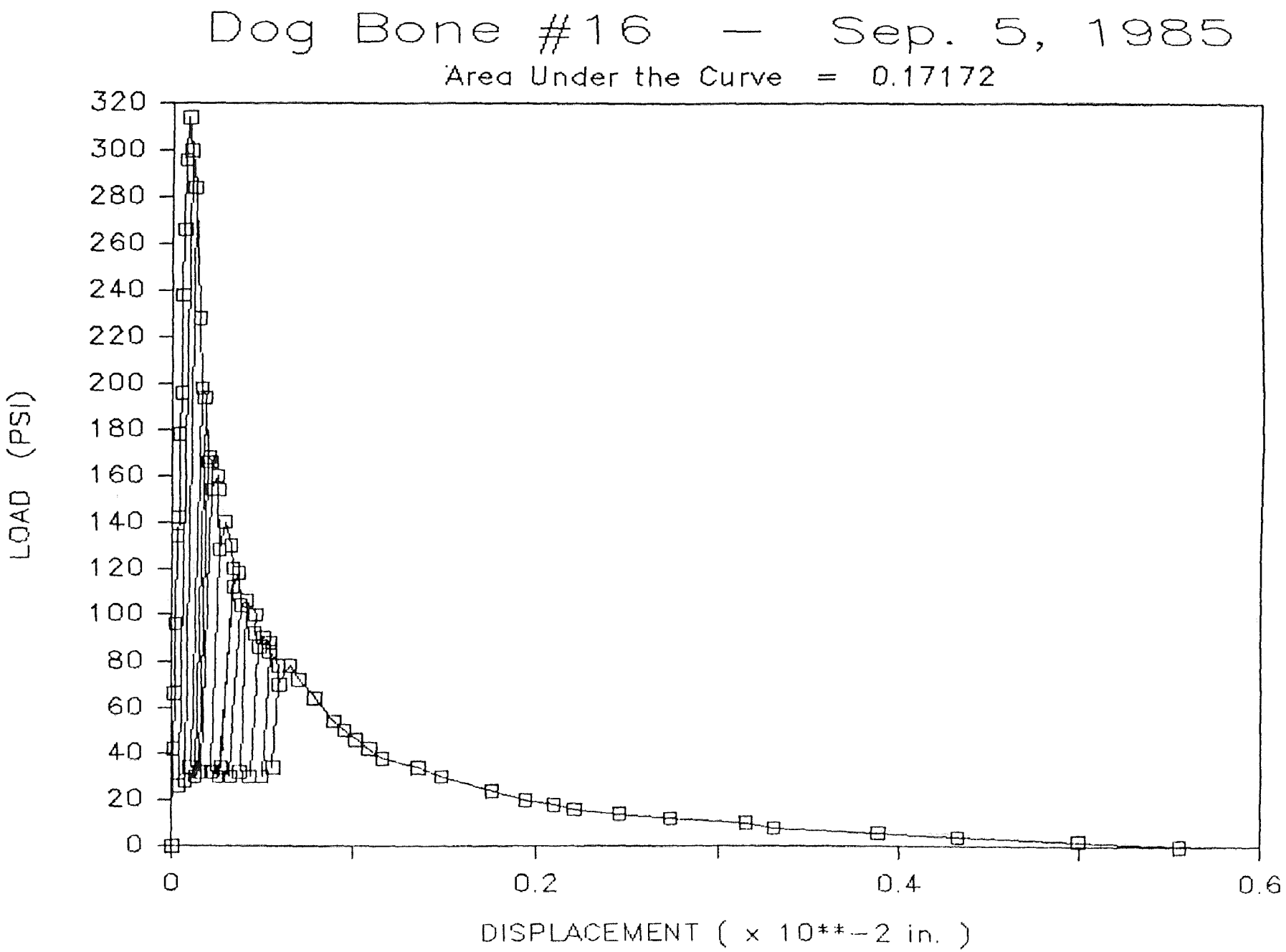
Dog Bone #16 — Sep. 5, 1985
Area Under the Curve = 0.17172
LOAD (PSI)
320
300
280
260
240
220
200
180
160
140
120
100
80
60
40
20
0
0
0.2
0.4
0.6
DISPLACEMENT (x 10**-2 in.)

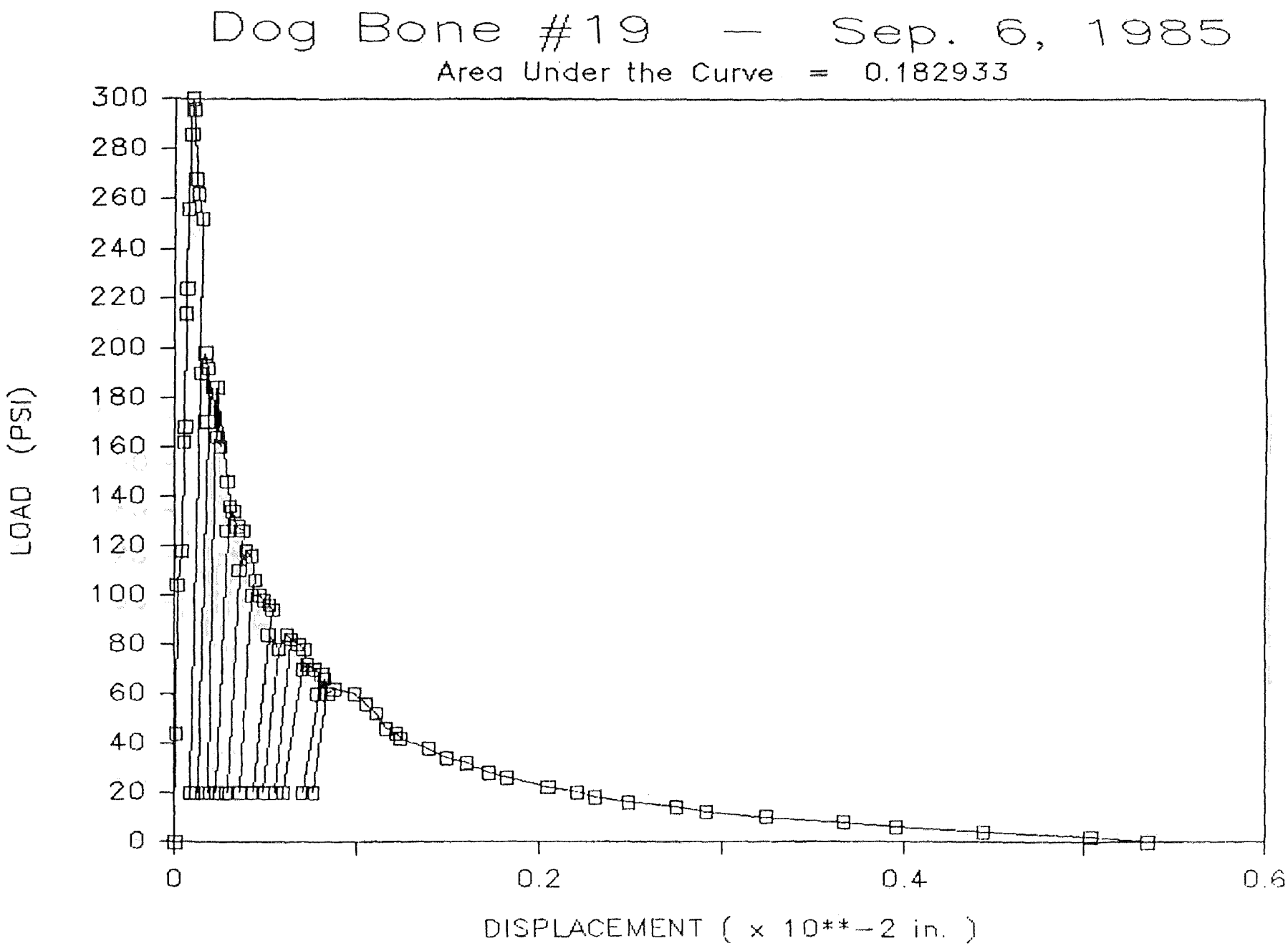
Dog Bone #19 — Sep. 6, 1985
Area Under the Curve = 0.182933
LOAD (PSI)
300
280
260
240
220
200
180
160
140
120
100
80
60
40
20
0
0
0.2
0.4
0.6
DISPLACEMENT (x 10**-2 in.)

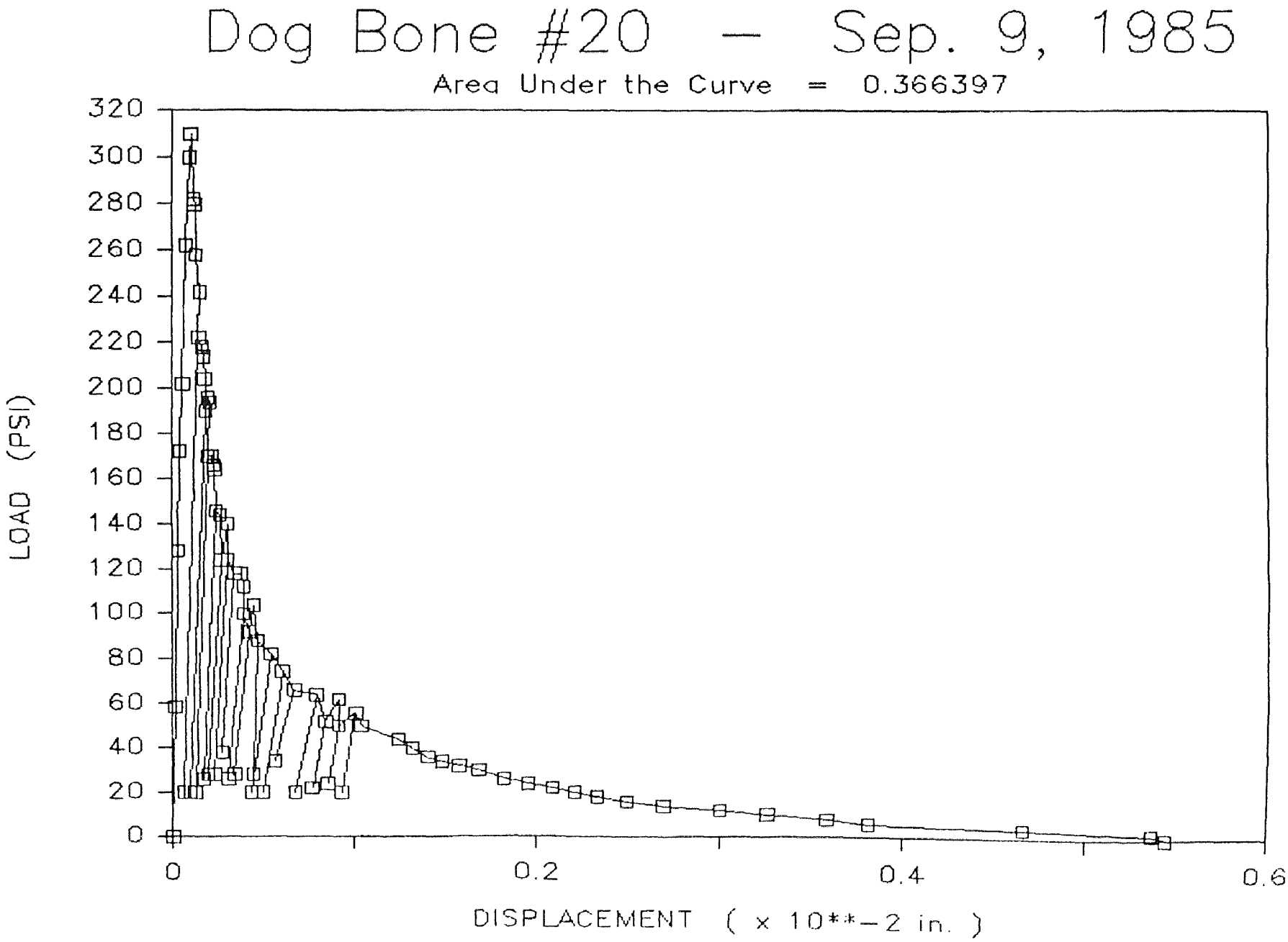
Dog Bone #20 — Sep. 9, 1985
Area Under the Curve = 0.366397
LOAD (PSI)
320
300
280
260
240
220
200
180
160
140
120
100
80
60
40
20
0
0
0.2
0.4
0.6
DISPLACEMENT (x 10**-2 in.)

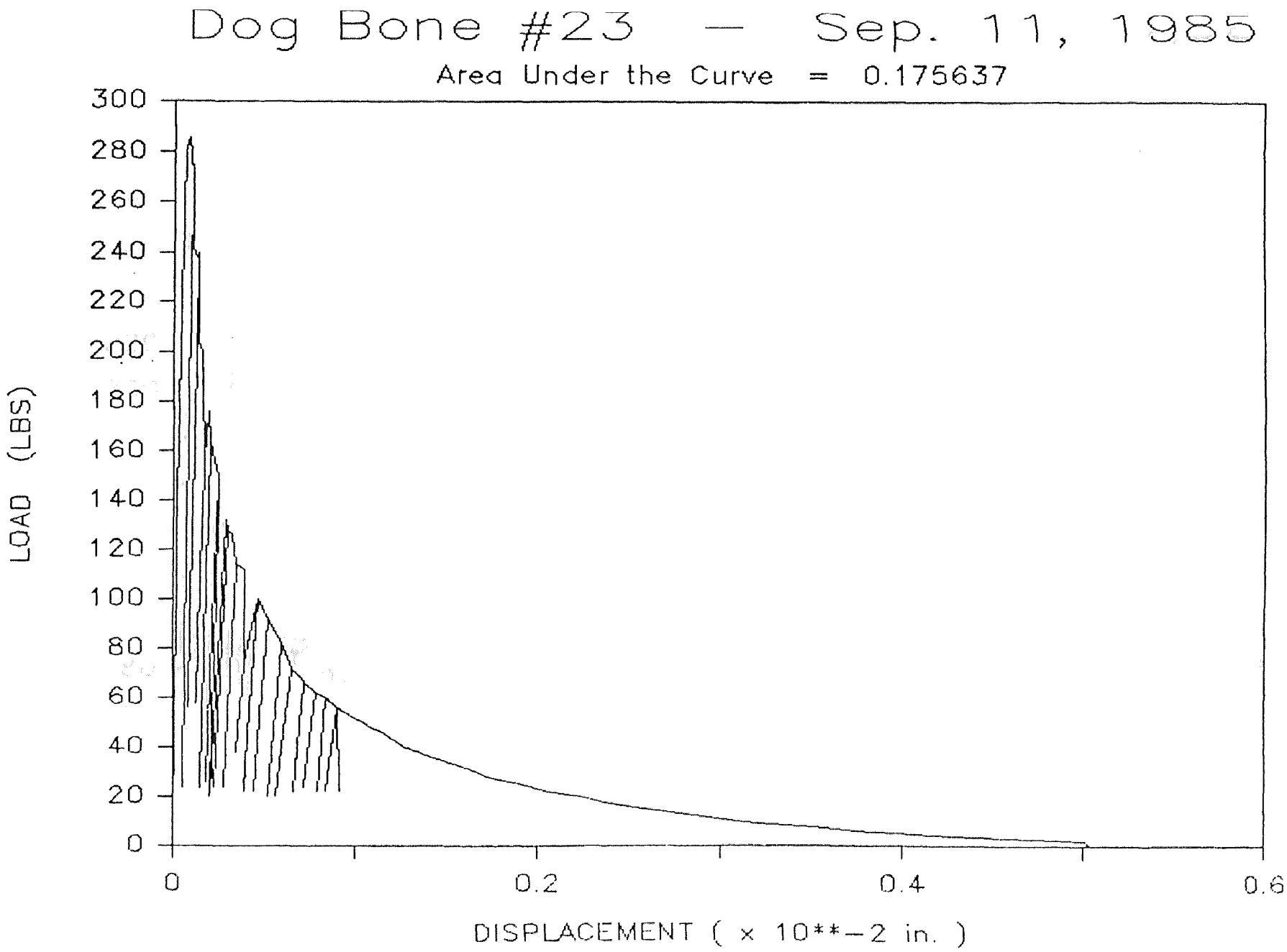
Dog Bone #23 — Sep. 11, 1985
Area Under the Curve = 0.175637
LOAD (LBS)
300
280
260
240
220
200
180
160
140
120
100
80
60
40
20
0
0
0.2
0.4
0.6
DISPLACEMENT (x 10**-2 in.)

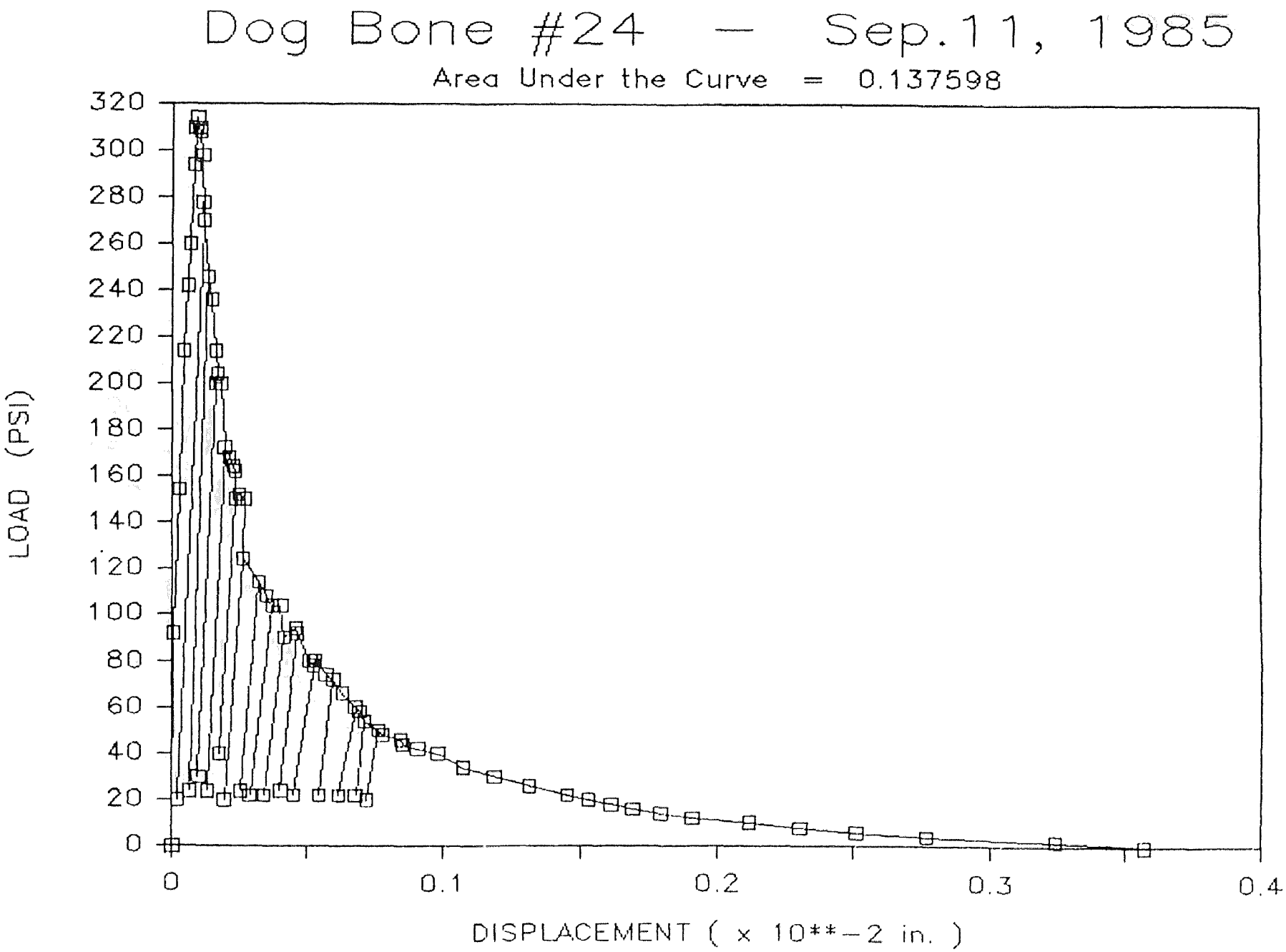
Dog Bone #24 — Sep.11, 1985
Area Under the Curve = 0.137598
LOAD (PSI)
320
300
280
260
240
220
200
180
160
140
120
100
80
60
40
20
0
0
0.1
0.2
0.3
0.4
DISPLACEMENT (x 10**-2 in.)

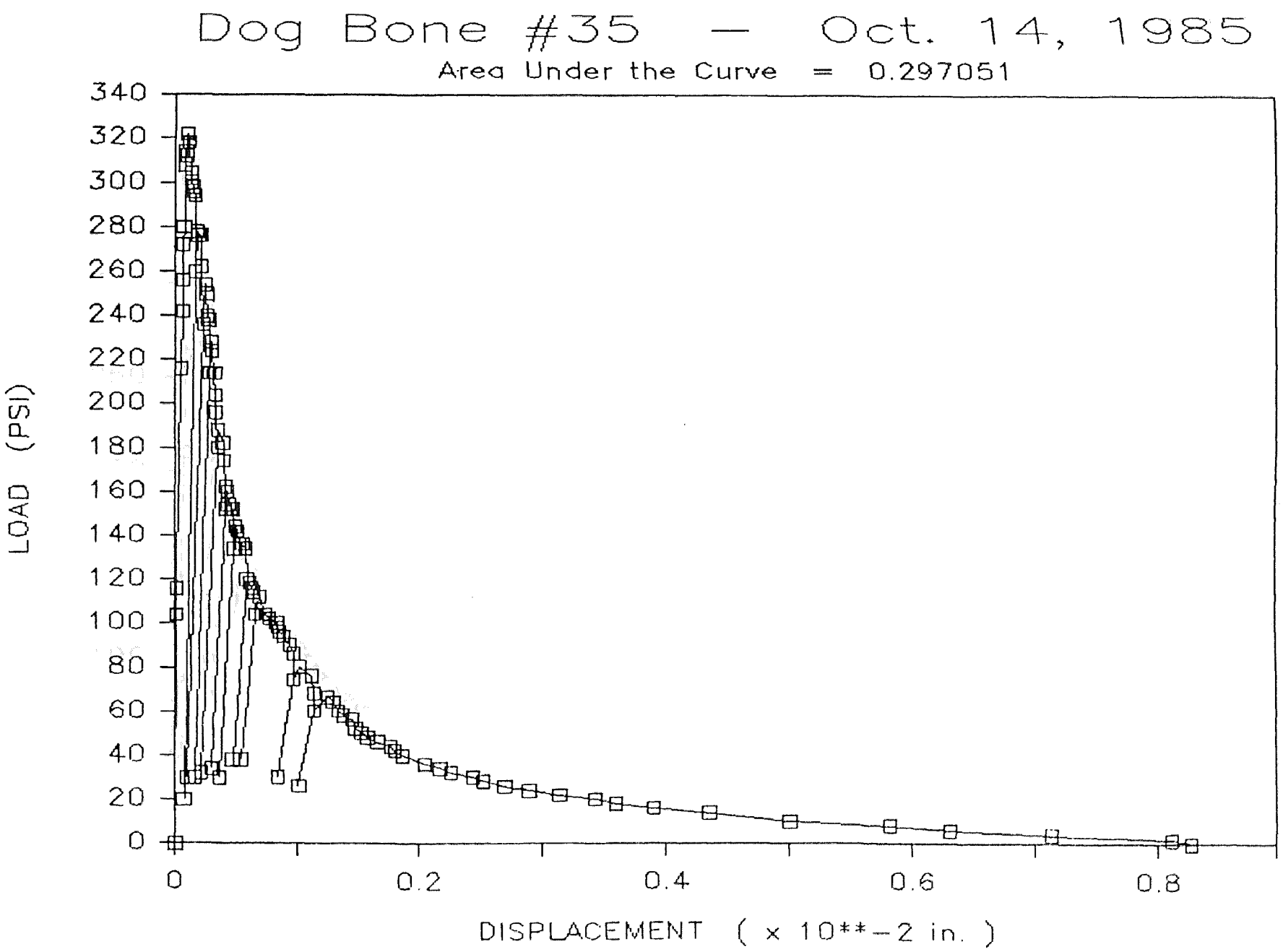
Dog Bone #35 — Oct. 14, 1985
Area Under the Curve = 0.297051
LOAD (PSI)
340
320
300
280
260
240
220
200
180
160
140
120
100
80
60
40
20
0
0
0.2
0.4
0.6
0.8
DISPLACEMENT (x 10**-2 in.)

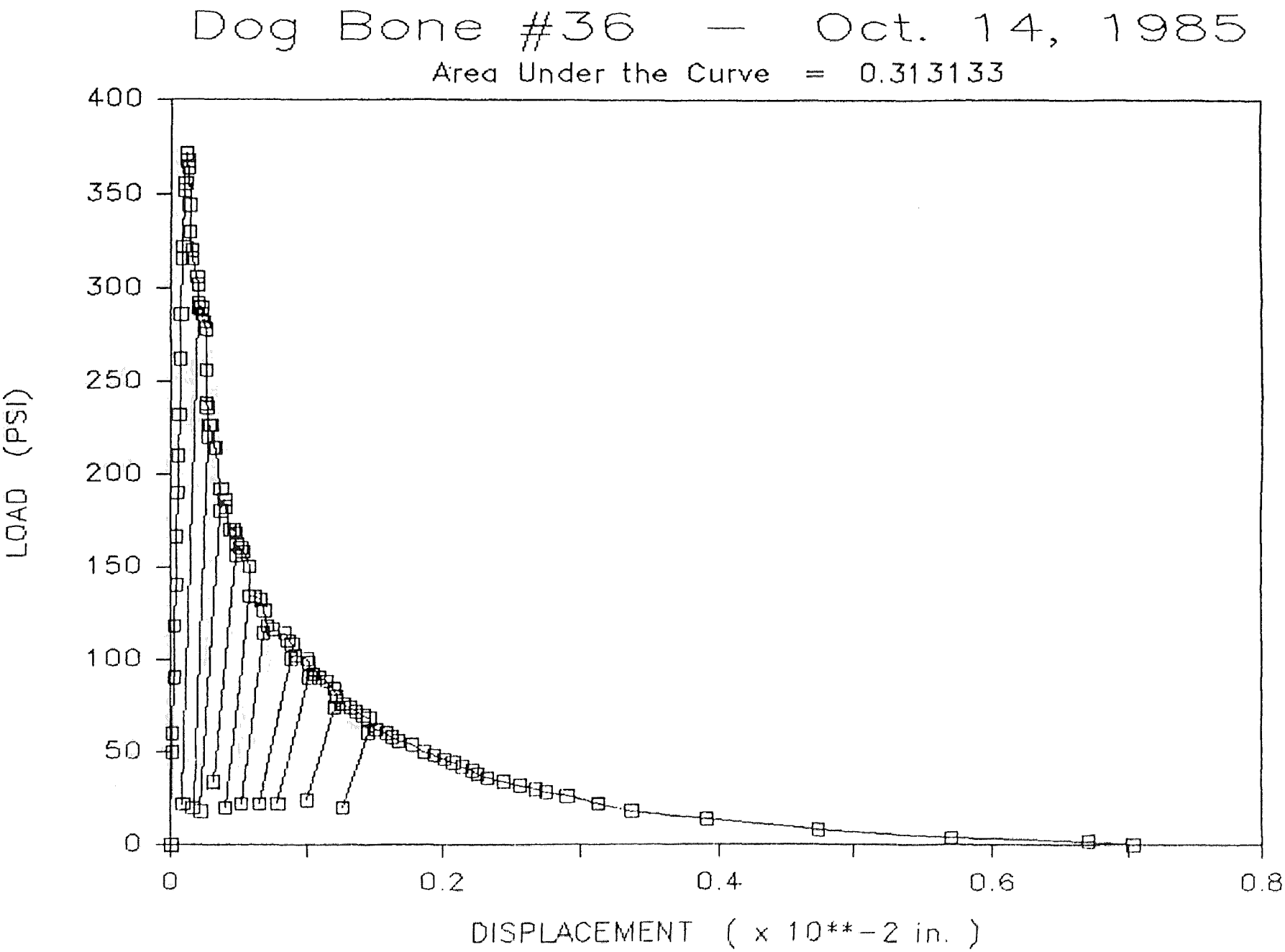
Dog Bone #36 — Oct. 14, 1985
Area Under the Curve = 0.313133
400
350
300
250
200
150
100
50
0
LOAD (PSI)
0
0.2
0.4
0.6
0.8
DISPLACEMENT (x 10**-2 in.)

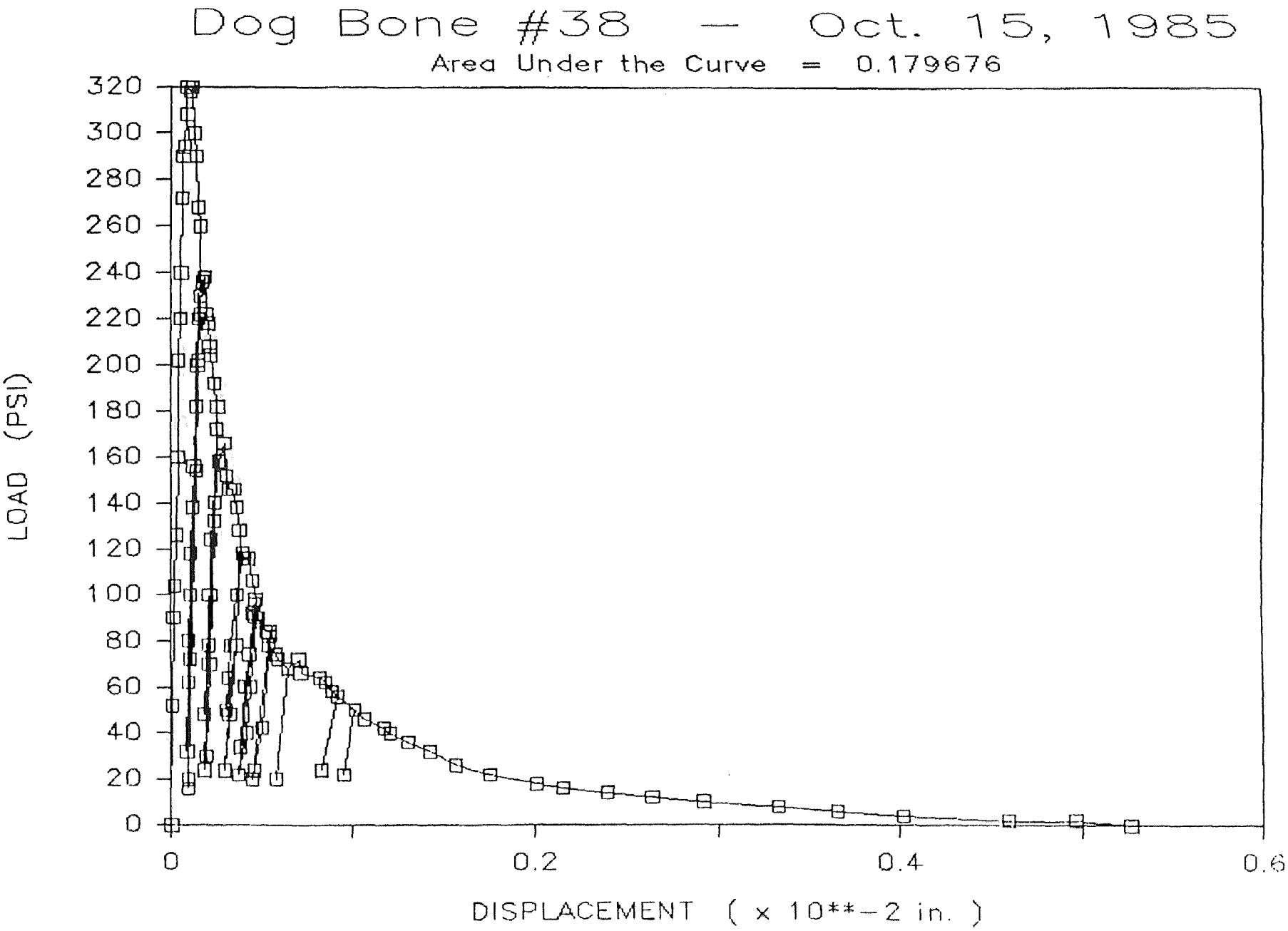
Dog Bone #38 — Oct. 15, 1985
Area Under the Curve = 0.179676
LOAD (PSI)
320
300
280
260
240
220
200
180
160
140
120
100
80
60
40
20
0
0
0.2
0.4
0.6
DISPLACEMENT (x 10**-2 in.)

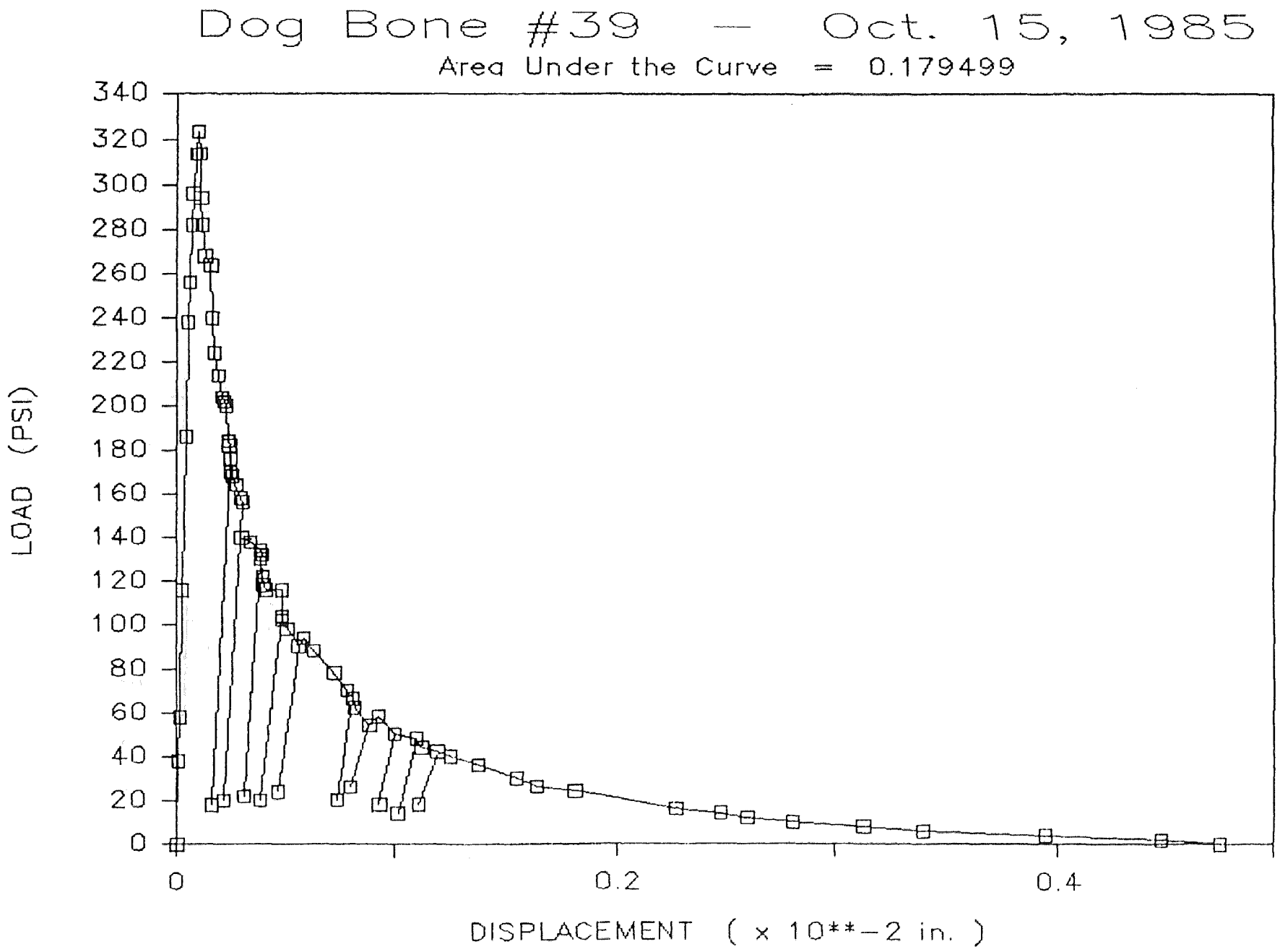
Dog Bone #39 — Oct. 15, 1985
Area Under the Curve = 0.179499
LOAD (PSI)
340
320
300
280
260
240
220
200
180
160
140
120
100
80
60
40
20
0
0
0.2
0.4
DISPLACEMENT (x 10**-2 in.)

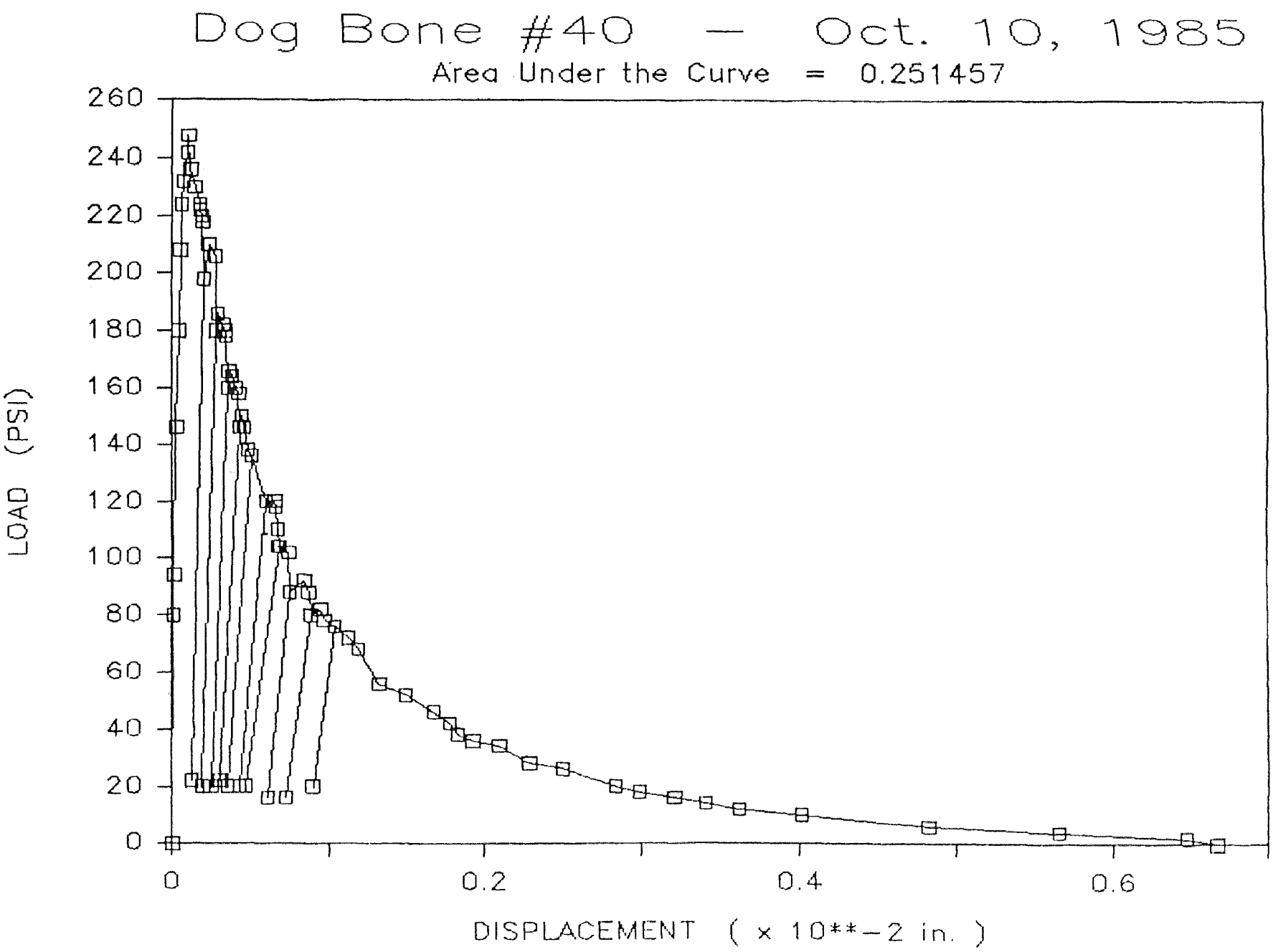
Dog Bone #40 — Oct. 10, 1985
Area Under the Curve = 0.251457
LOAD (PSI)
260
240
220
200
180
160
140
120
100
80
60
40
20
0
0
0.2
0.4
0.6
DISPLACEMENT (x 10**-2 in.)

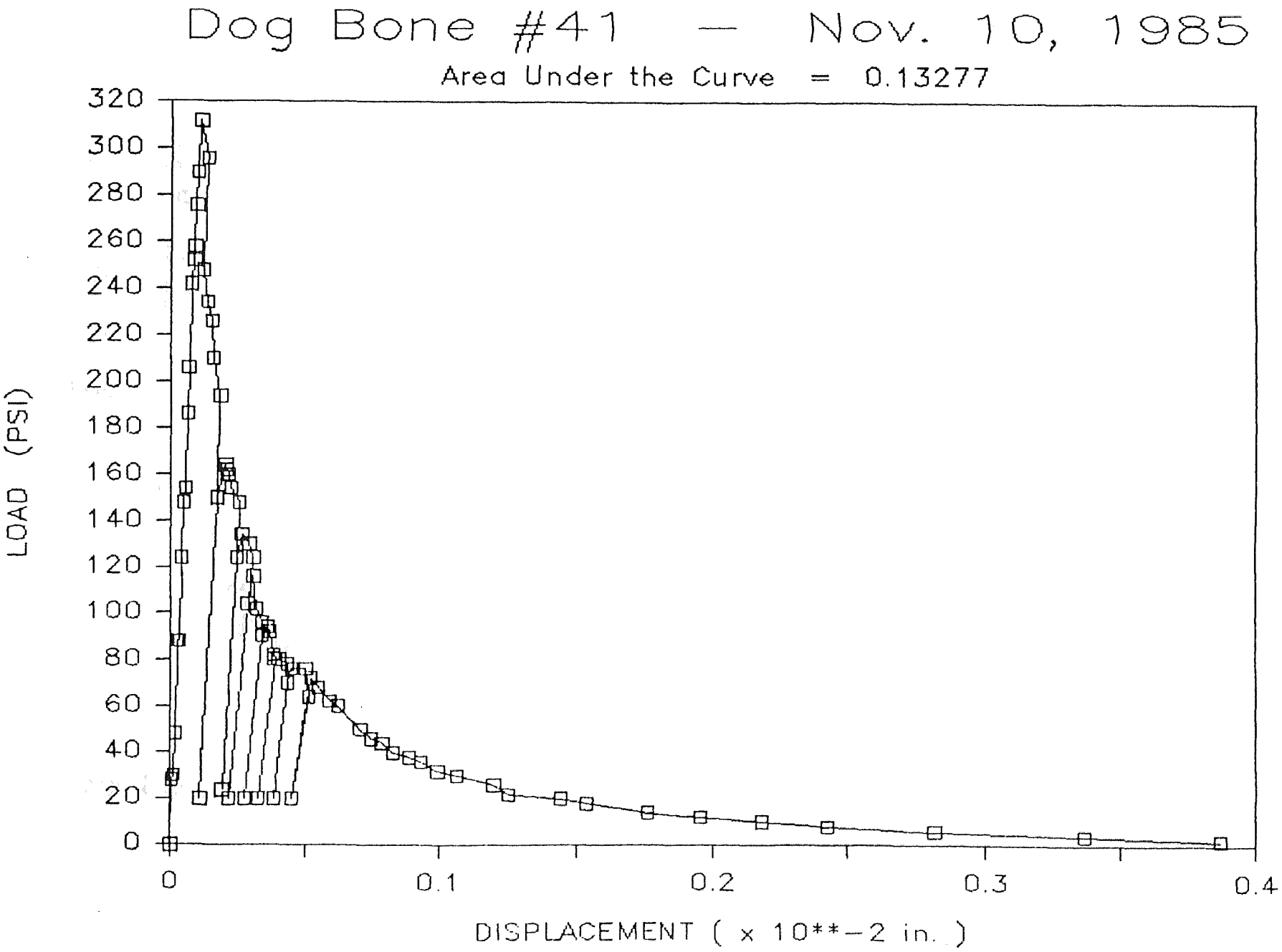
Dog Bone #41 — Nov. 10, 1985
Area Under the Curve = 0.13277
LOAD (PSI)
320
300
280
260
240
220
200
180
160
140
120
100
80
60
40
20
0
0
0.1
0.2
0.3
0.4
DISPLACEMENT (x 10**-2 in.)

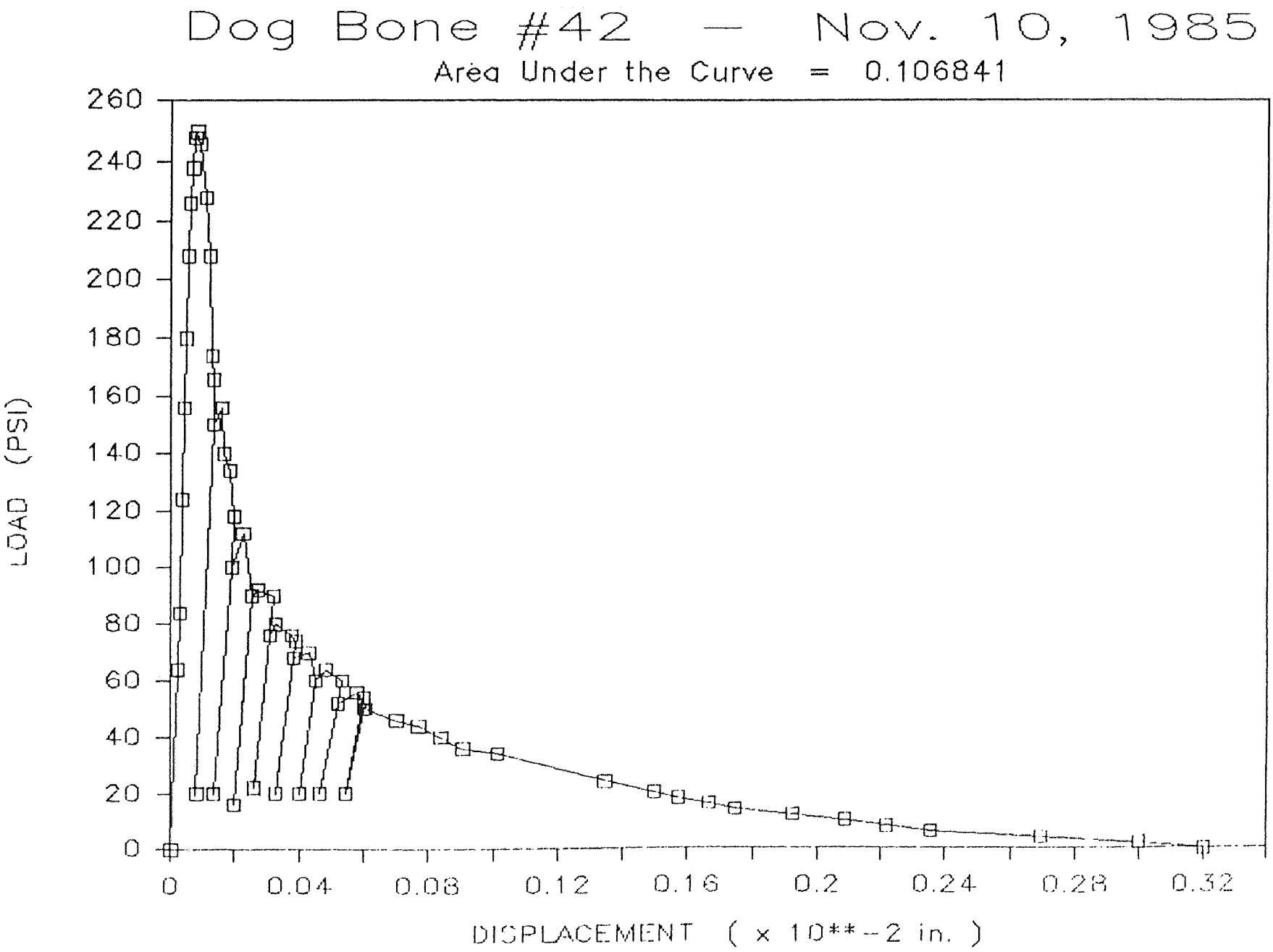
Dog Bone #42 — Nov. 10, 1985
Area Under the Curve = 0.106841
LOAD (PSI)
260
240
220
200
180
160
140
120
100
80
60
40
20
0
0
0.04
0.08
0.12
0.16
0.2
0.24
0.28
0.32
DISPLACEMENT (x 10**-2 in.)

Dog Bone #43 — Nov. 14, 1985

Area Under the Curve = 0.166668

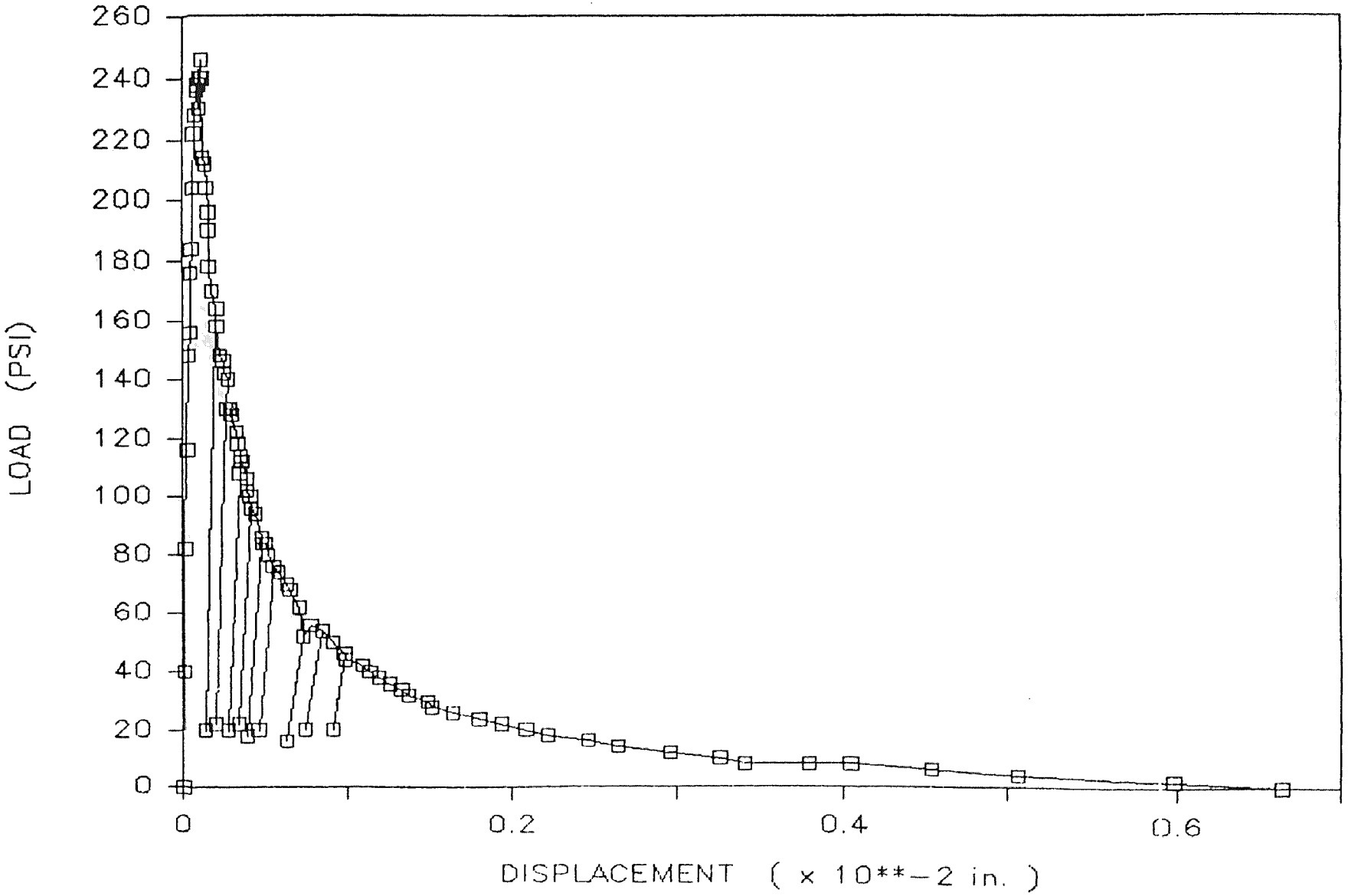

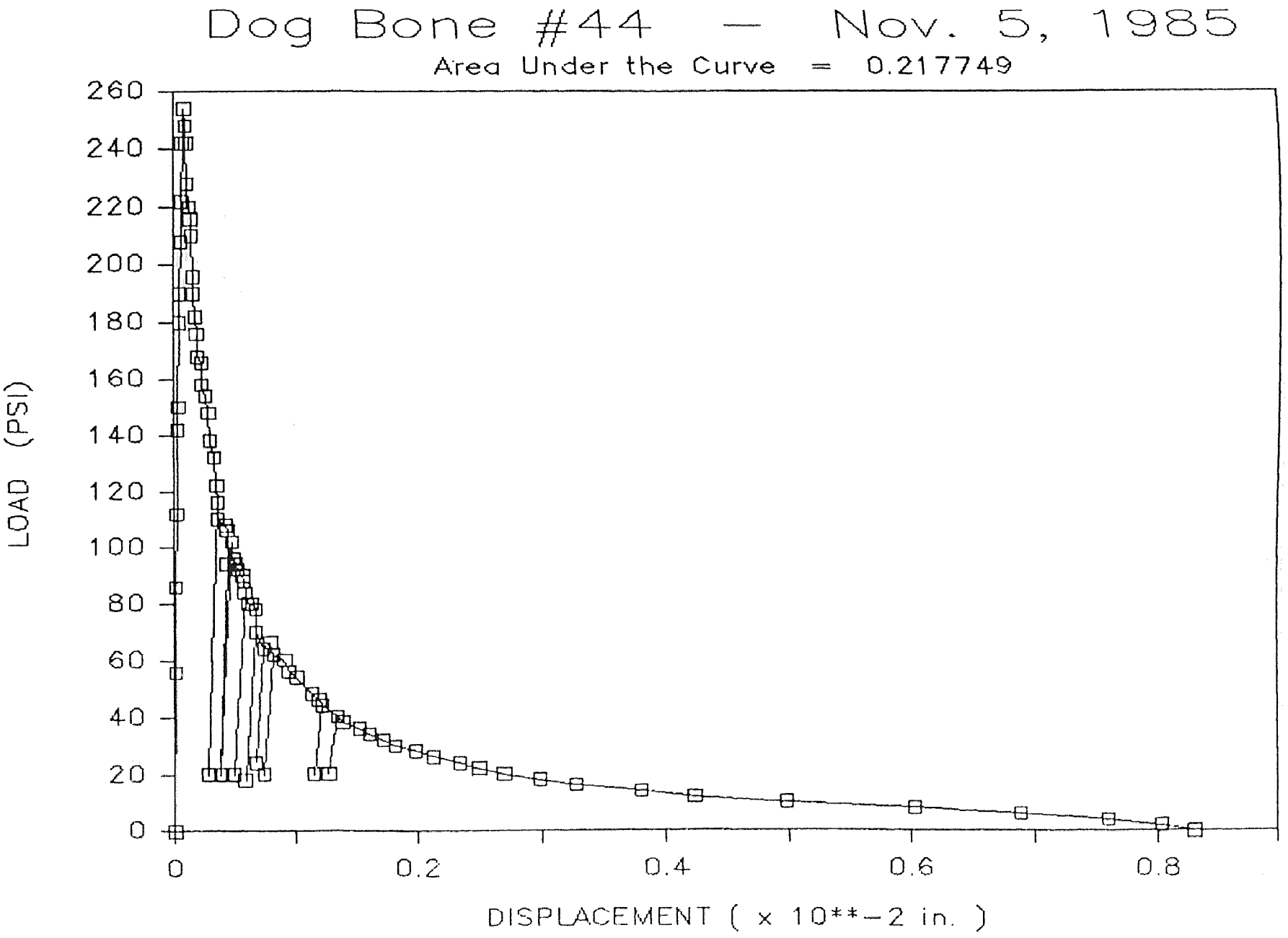
Dog Bone #44 — Nov. 5, 1985
Area Under the Curve = 0.217749
LOAD (PSI)
260
240
220
200
180
160
140
120
100
80
60
40
20
0
0
0.2
0.4
0.6
0.8
DISPLACEMENT (x 10**-2 in.)

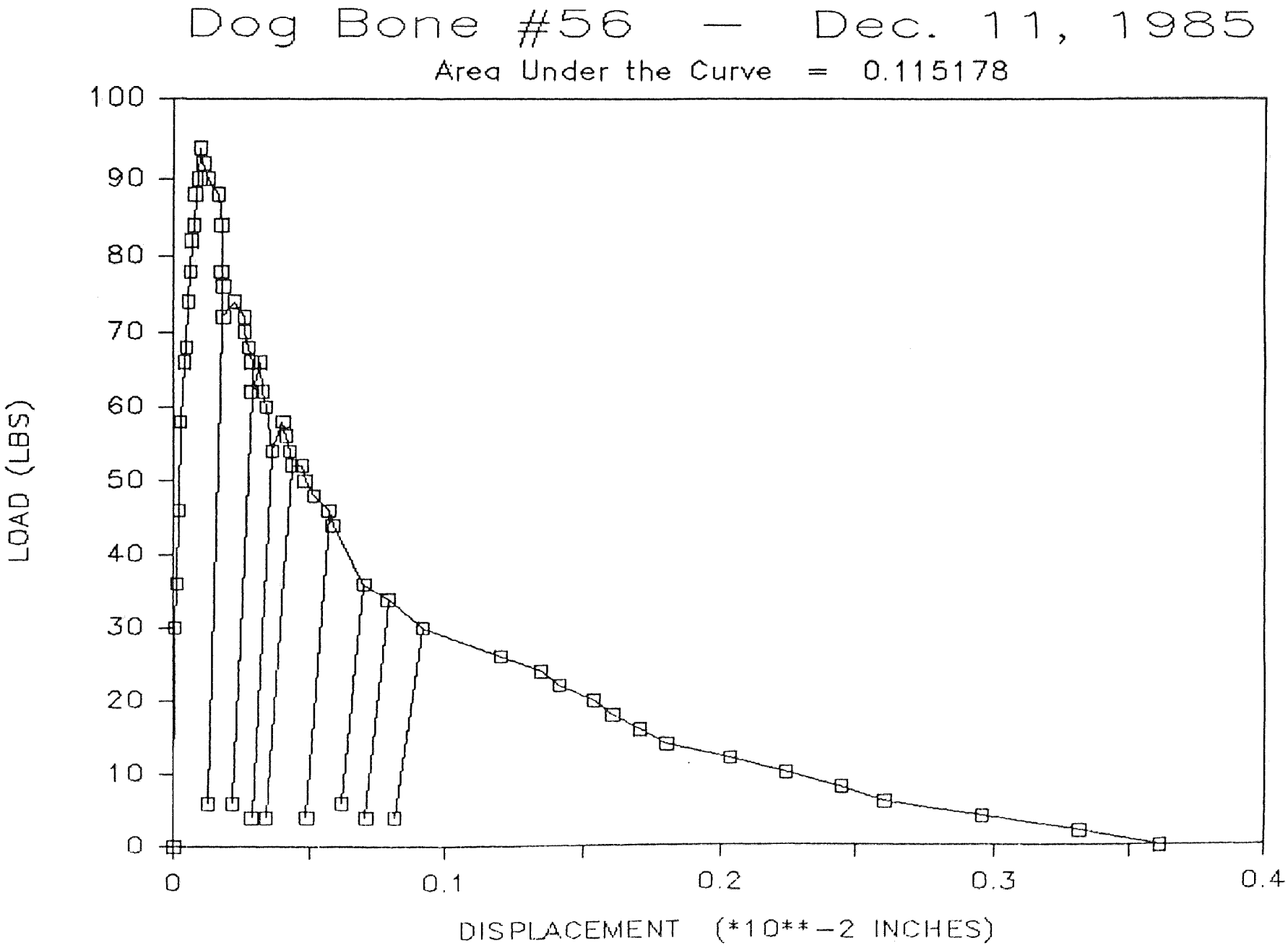
Dog Bone #56 — Dec. 11, 1985
Area Under the Curve = 0.115178
LOAD (LBS)
100
90
80
70
60
50
40
30
20
10
0
0
0.1
0.2
0.3
0.4
DISPLACEMENT (*10**-2 INCHES)

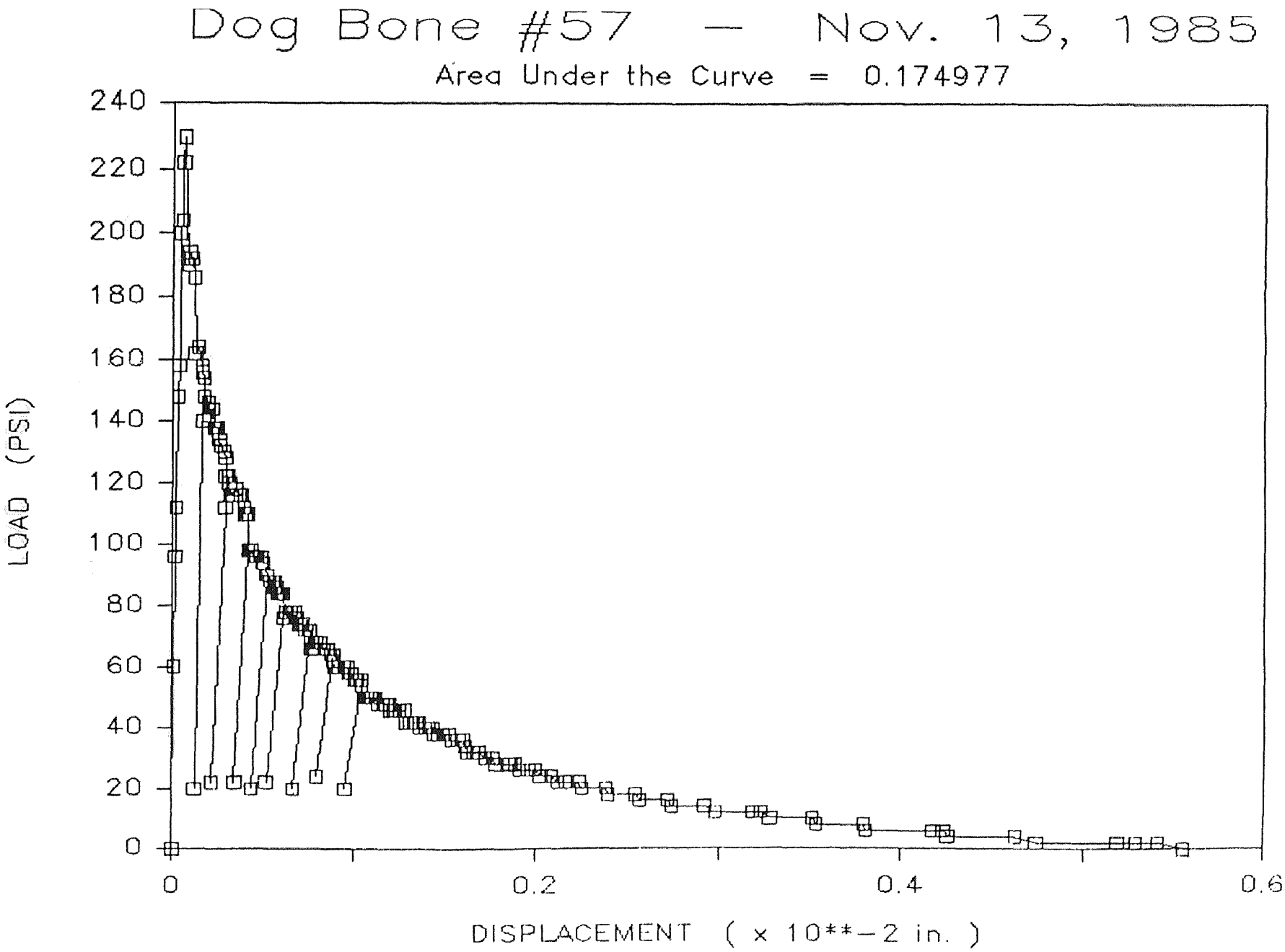
Dog Bone #57 — Nov. 13, 1985
Area Under the Curve = 0.174977
LOAD (PSI)
240
220
200
180
160
140
120
100
80
60
40
20
0
0
0.2
0.4
0.6
DISPLACEMENT (x 10**-2 in.)

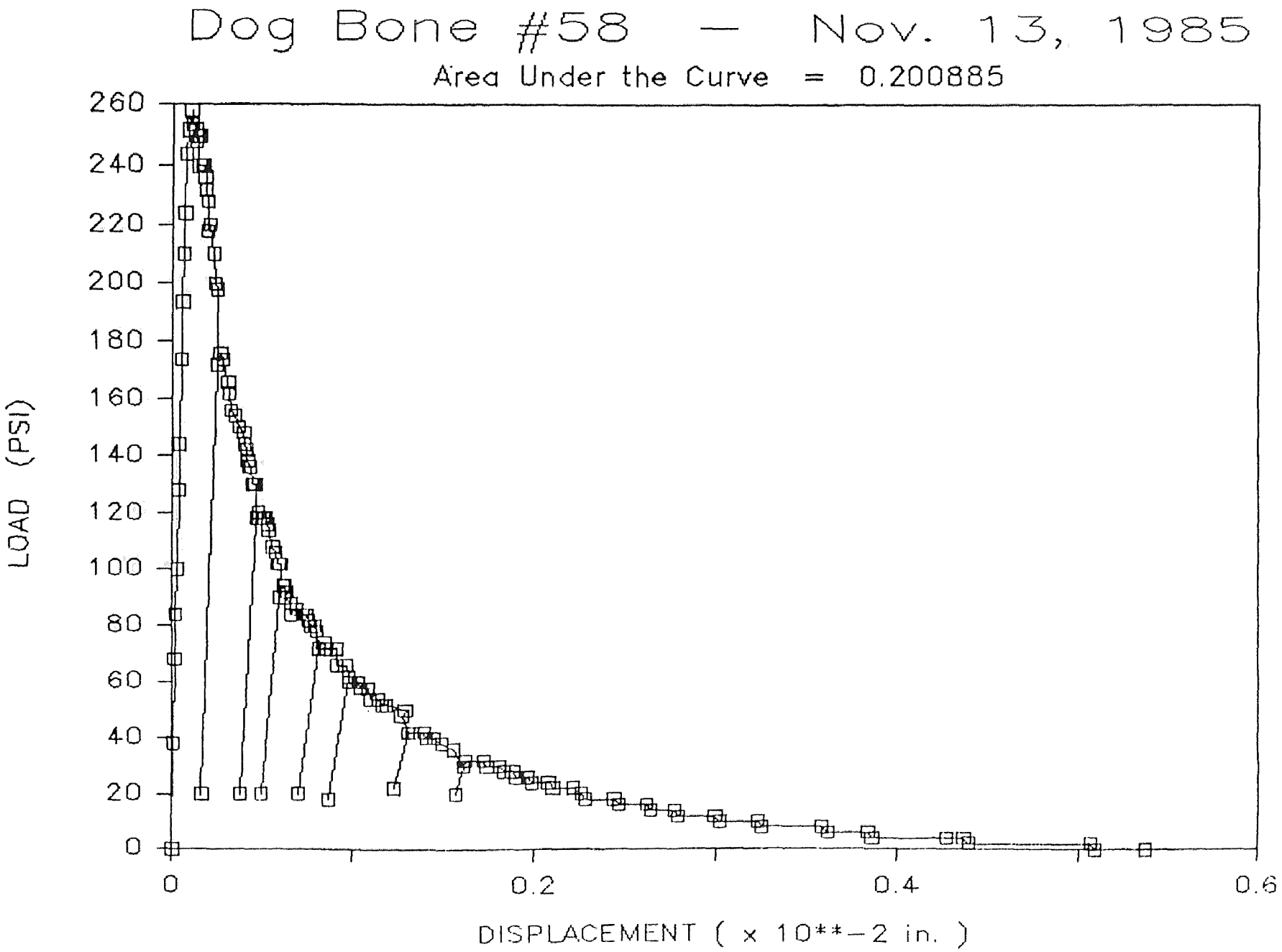
Dog Bone #58 — Nov. 13, 1985
Area Under the Curve = 0.200885
LOAD (PSI)
260
240
220
200
180
160
140
120
100
80
60
40
20
0
0
0.2
0.4
0.6
DISPLACEMENT (x 10**-2 in.)

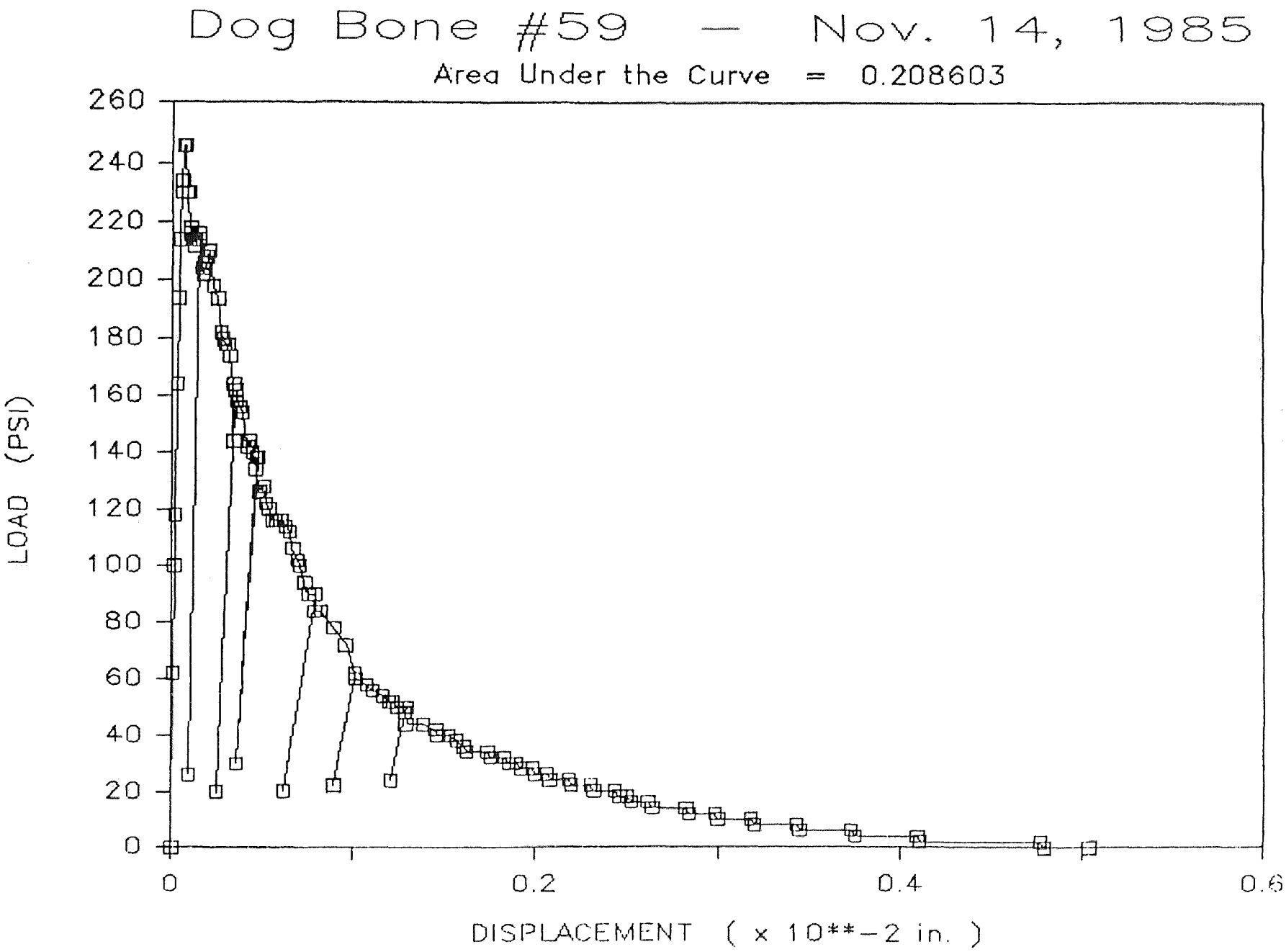
Dog Bone #59 — Nov. 14, 1985
Area Under the Curve = 0.208603
LOAD (PSI)
260
240
220
200
180
160
140
120
100
80
60
40
20
0
0
0.2
0.4
0.6
DISPLACEMENT (x 10**-2 in.)

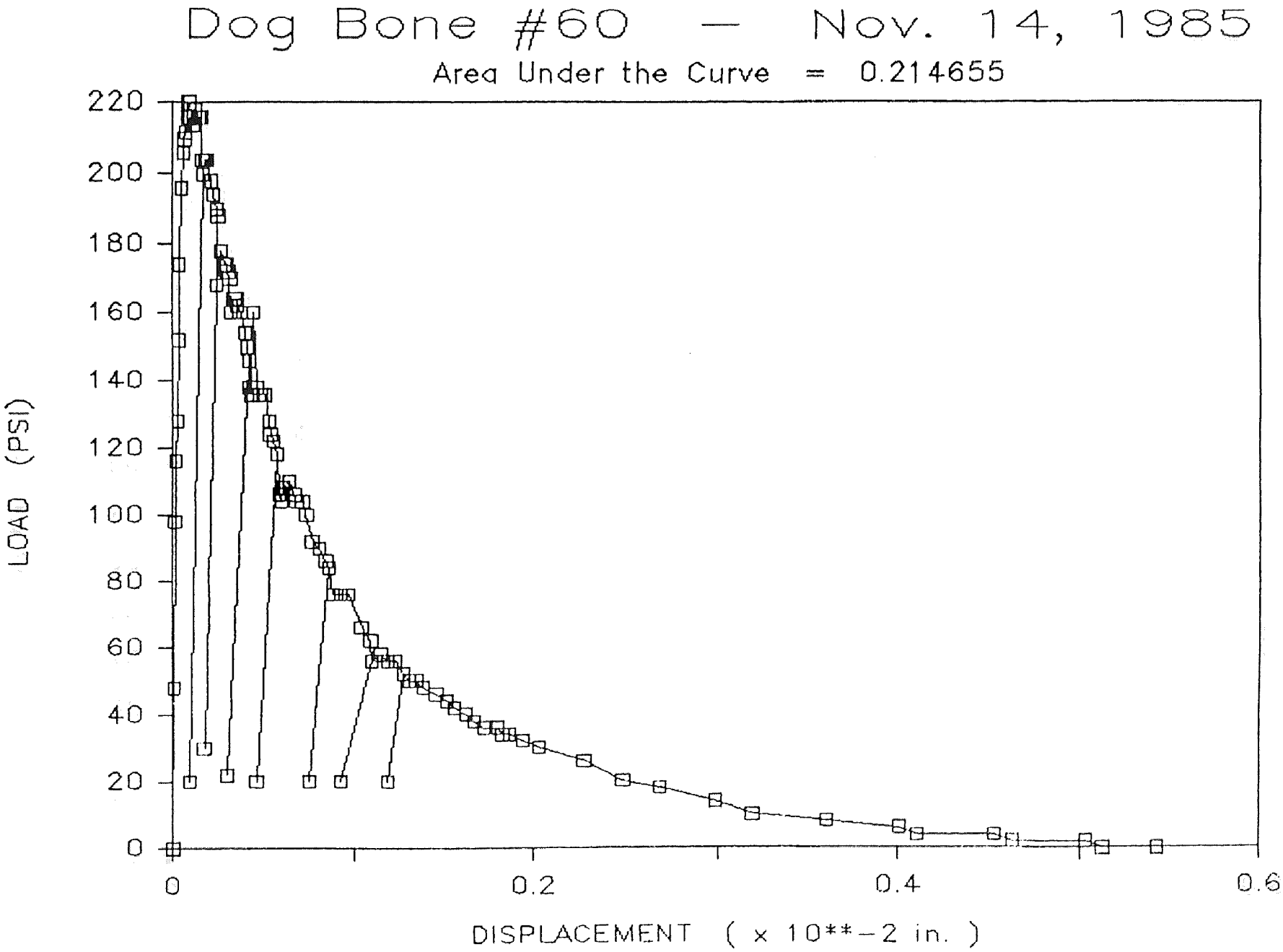
Dog Bone #60 — Nov. 14, 1985
Area Under the Curve = 0.214655
LOAD (PSI)
220
200
180
160
140
120
100
80
60
40
20
0
0
0.2
0.4
0.6
DISPLACEMENT (x 10**-2 in.)

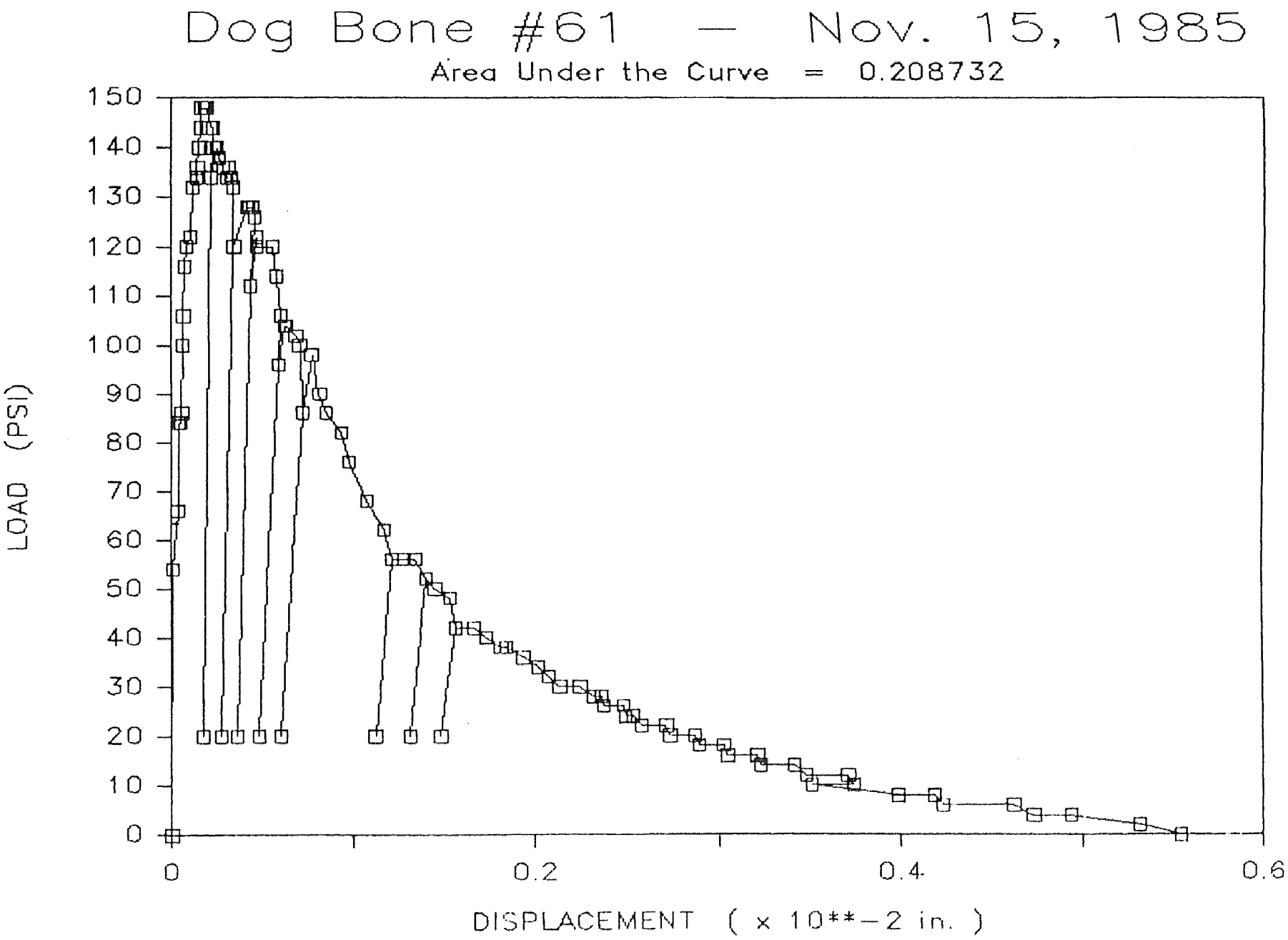
Dog Bone #61 — Nov. 15, 1985
Area Under the Curve = 0.208732
LOAD (PSI)
150
140
130
120
110
100
90
80
70
60
50
40
30
20
10
0
0
0.2
0.4
0.6
DISPLACEMENT (x 10**-2 in.)

APPENDIX E

ELASTIC YOUNG'S MODULUS IN POST-CRACKING ZONE

DOG—BONE—#14

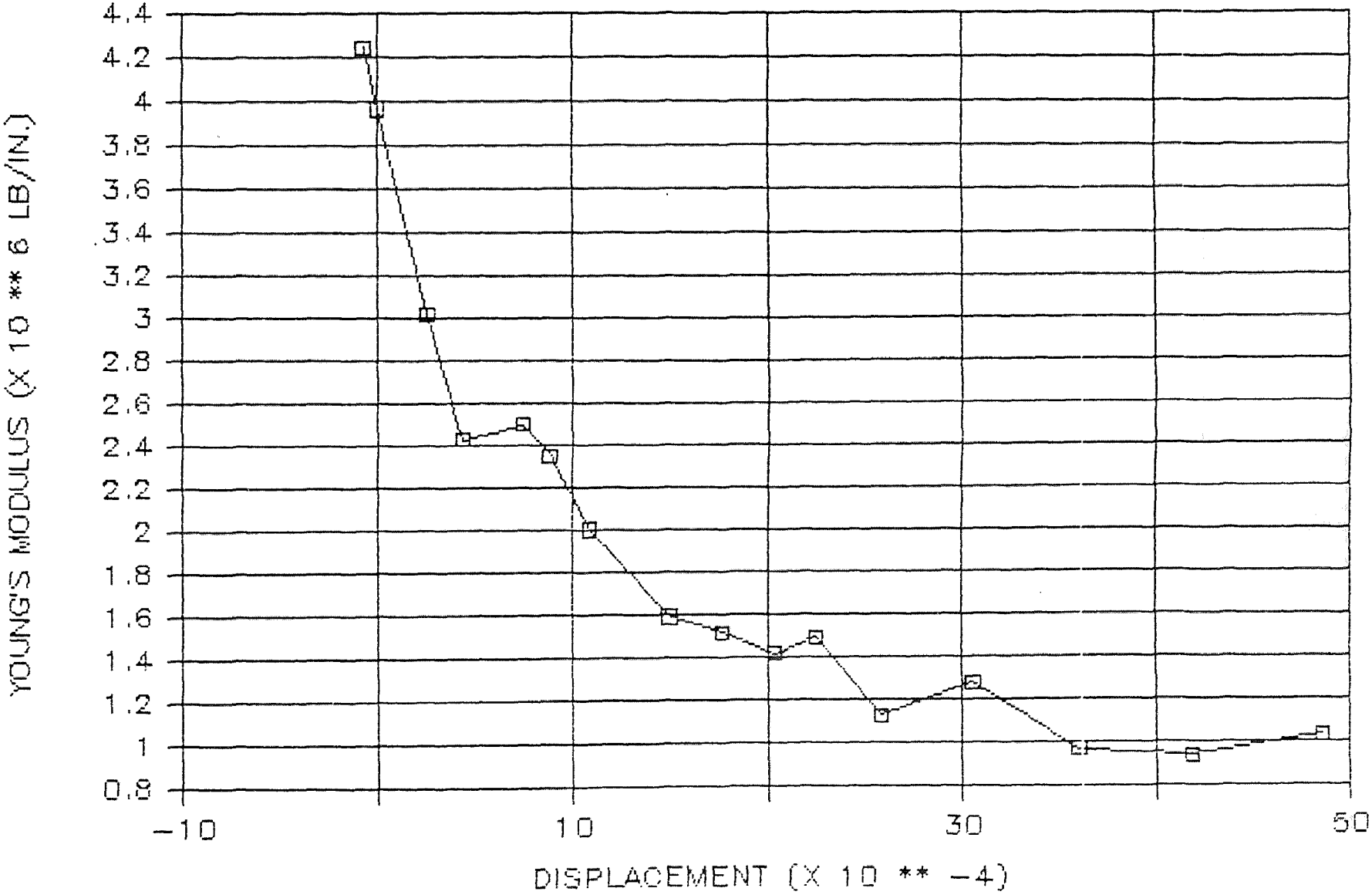
4.4
4.2
4
3.8
3.6
3.4
3.2
3
2.8
2.6
2.4
2.2
2
1.8
1.6
1.4
1.2
1
0.8
YOUNG'S MODULUS (X 10 ** 6 LB/IN.)
-10
10
30
50
DISPLACEMENT (X 10 ** -4)

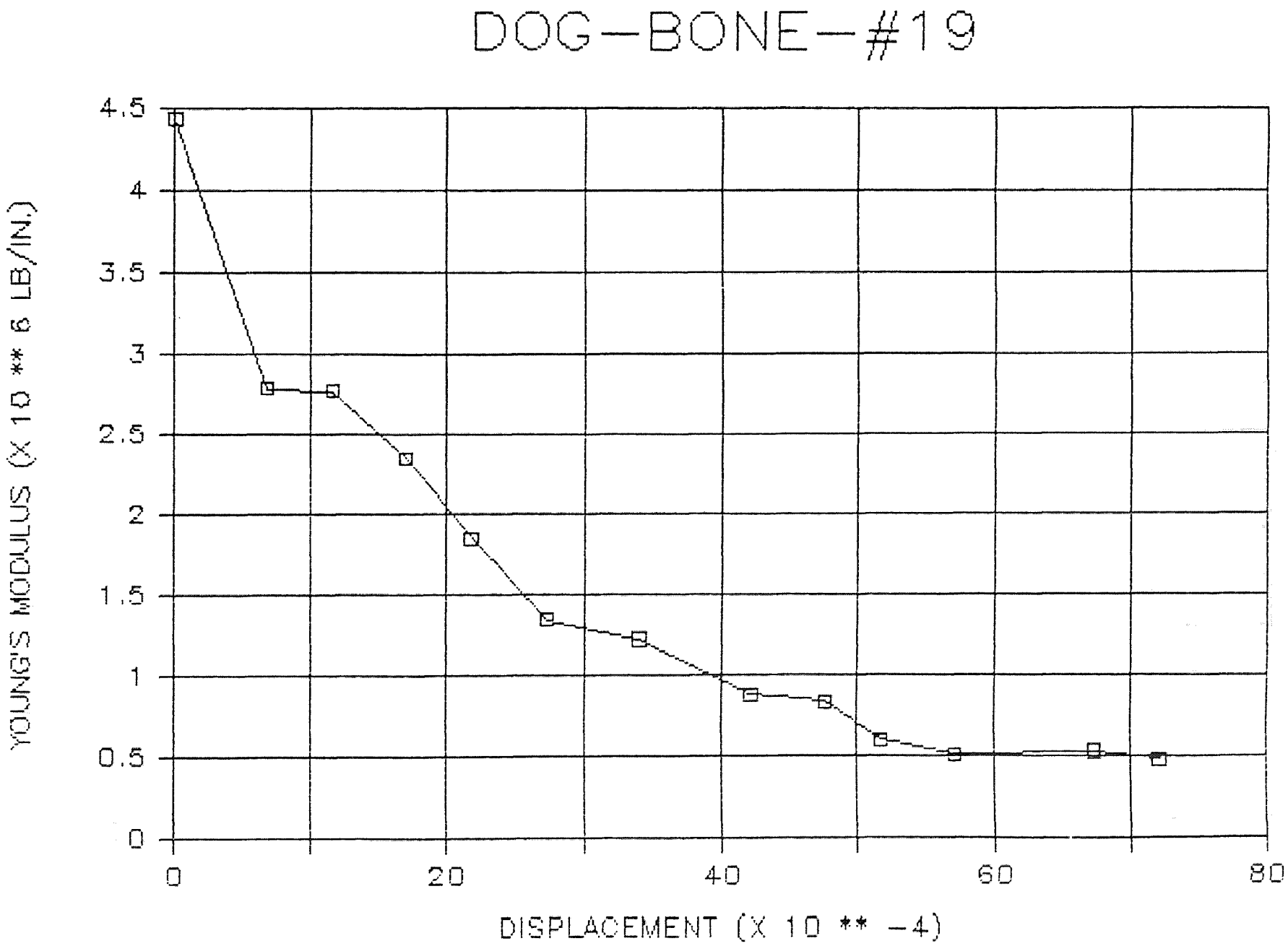
DOG-BONE-#19
YOUNG'S MODULUS (X 10 ** 6 LB/IN.)
4.5
4
3.5
3
2.5
2
1.5
1
0.5
0
0
20
40
60
80
DISPLACEMENT (X 10 ** -4)

DOG-BONE-#20

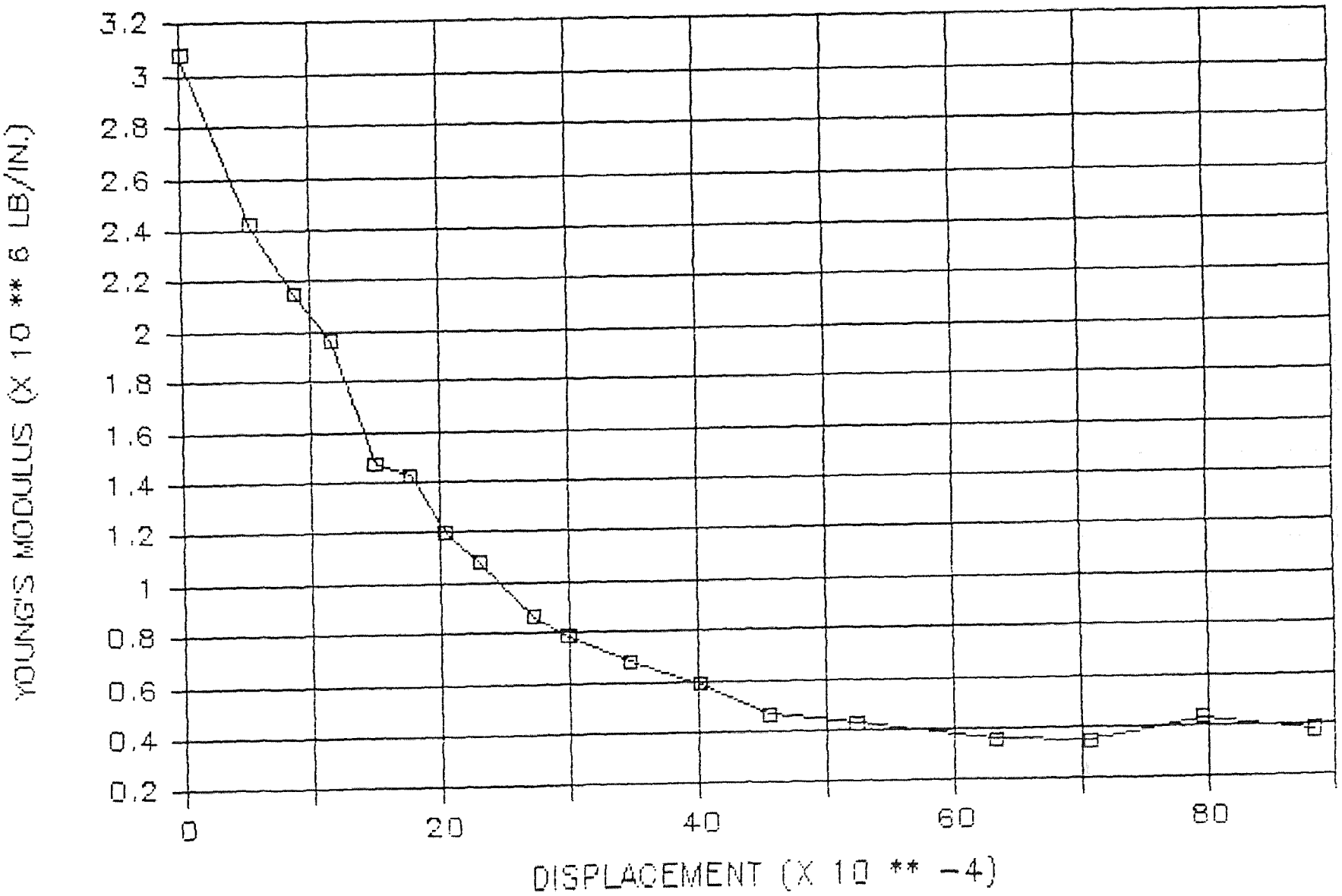
YOUNG'S MODULUS (X 10 ** 6 LB/IN.)
3.2
3
2.8
2.6
2.4
2.2
2
1.8
1.6
1.4
1.2
1
0.8
0.6
0.4
0.2
0
20
40
60
80
DISPLACEMENT (X 10 ** -4)

DOG-BONE-#23

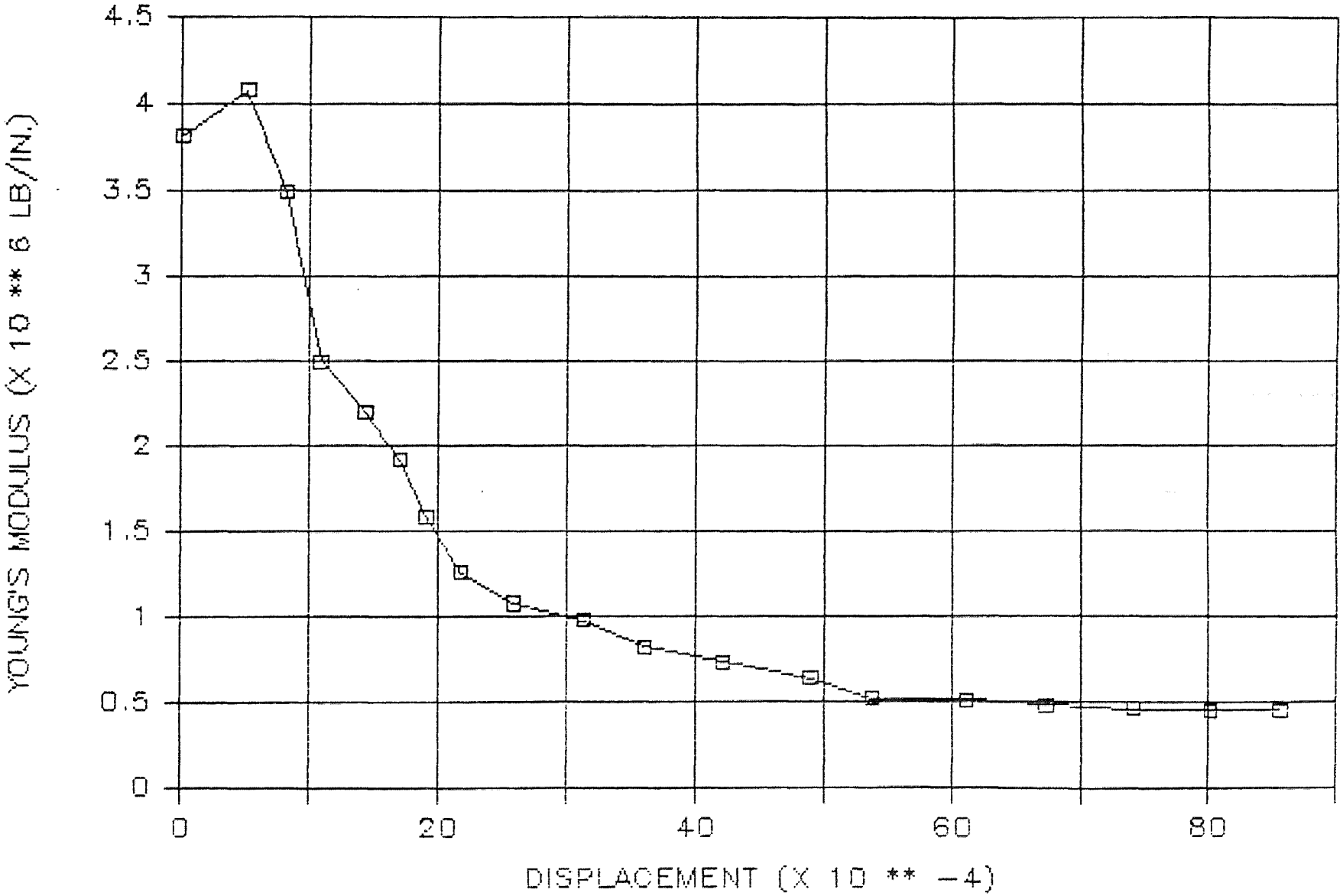
4.5
4
3.5
3
2.5
2
1.5
1
0.5
0
YOUNG'S MODULUS (X 10 ** 6 LB/IN.)
0
20
40
60
80
DISPLACEMENT (X 10 ** -4)

DOG—BONE—#35

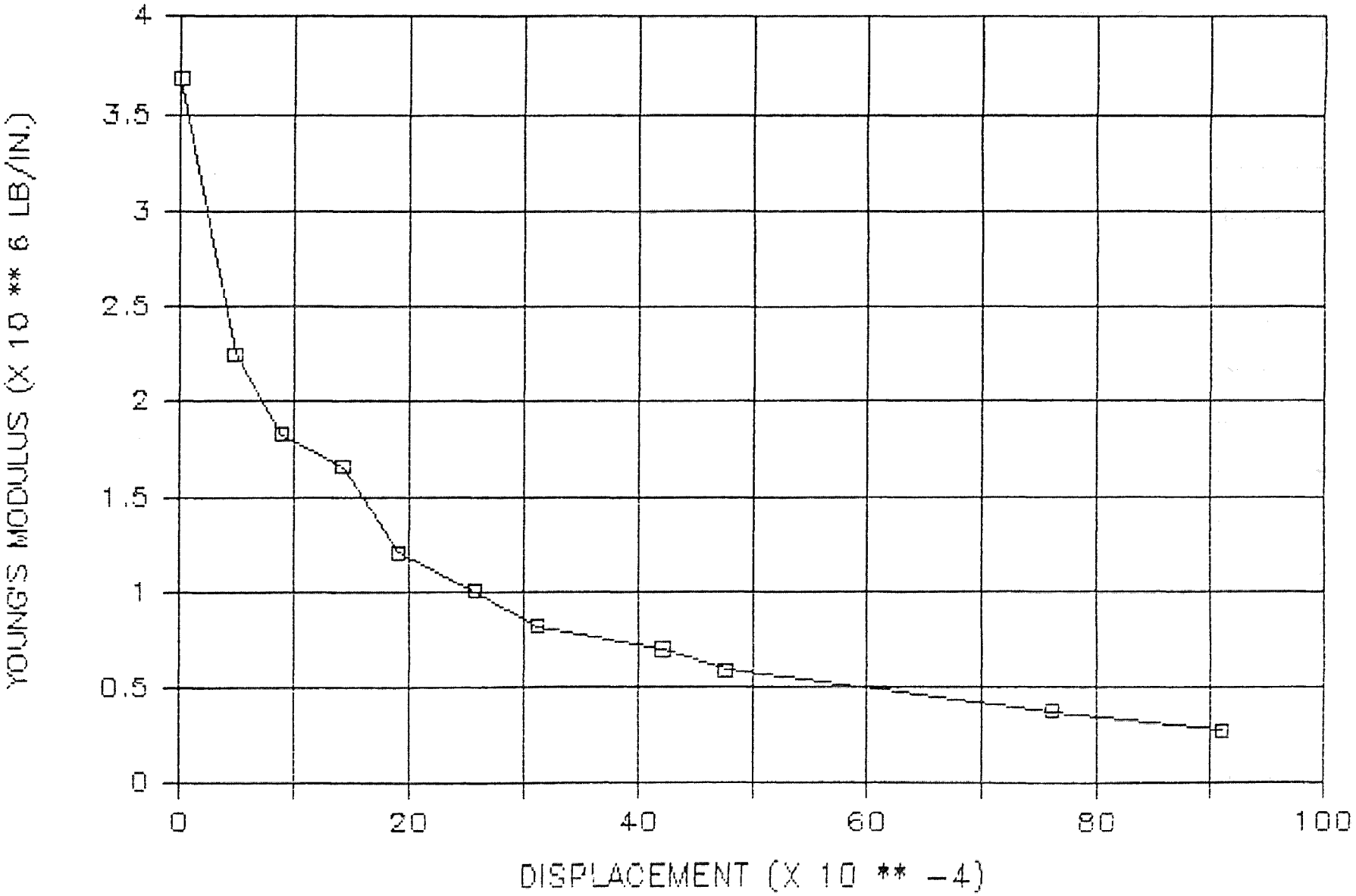
YOUNG'S MODULUS (X 10 ** 6 LB/IN.)
4
3.5
3
2.5
2
1.5
1
0.5
0
0
20
40
60
80
100
DISPLACEMENT (X 10 ** -4)

DOG—BONE—#36

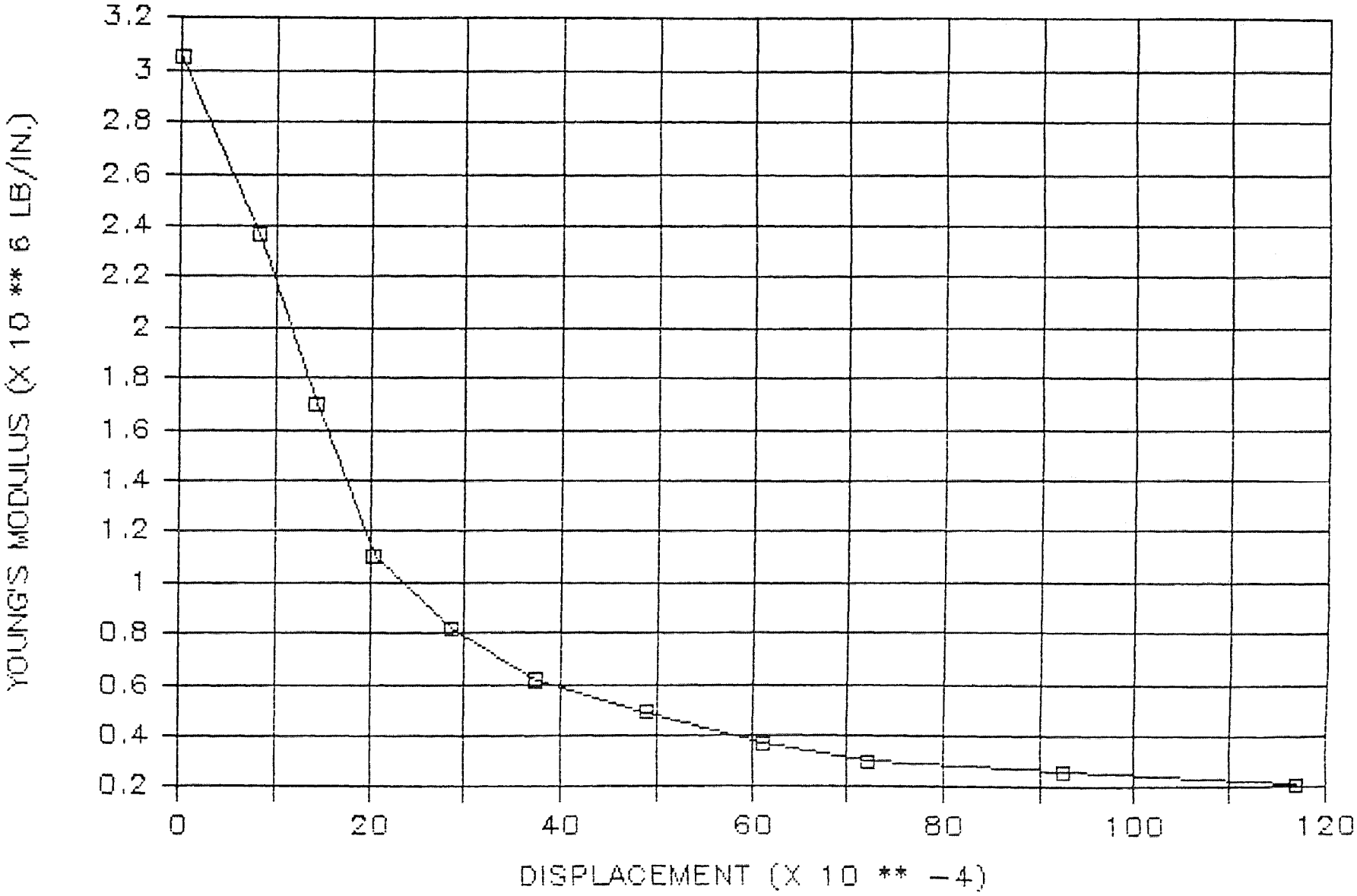
YOUNGS MODULUS (X 10 ** 6 LB/IN.)
3.2
3
2.8
2.6
2.4
2.2
2
1.8
1.6
1.4
1.2
1
0.8
0.6
0.4
0.2
0
20
40
60
80
100
120
DISPLACEMENT (X 10 ** -4)

DOG—BONE—#14

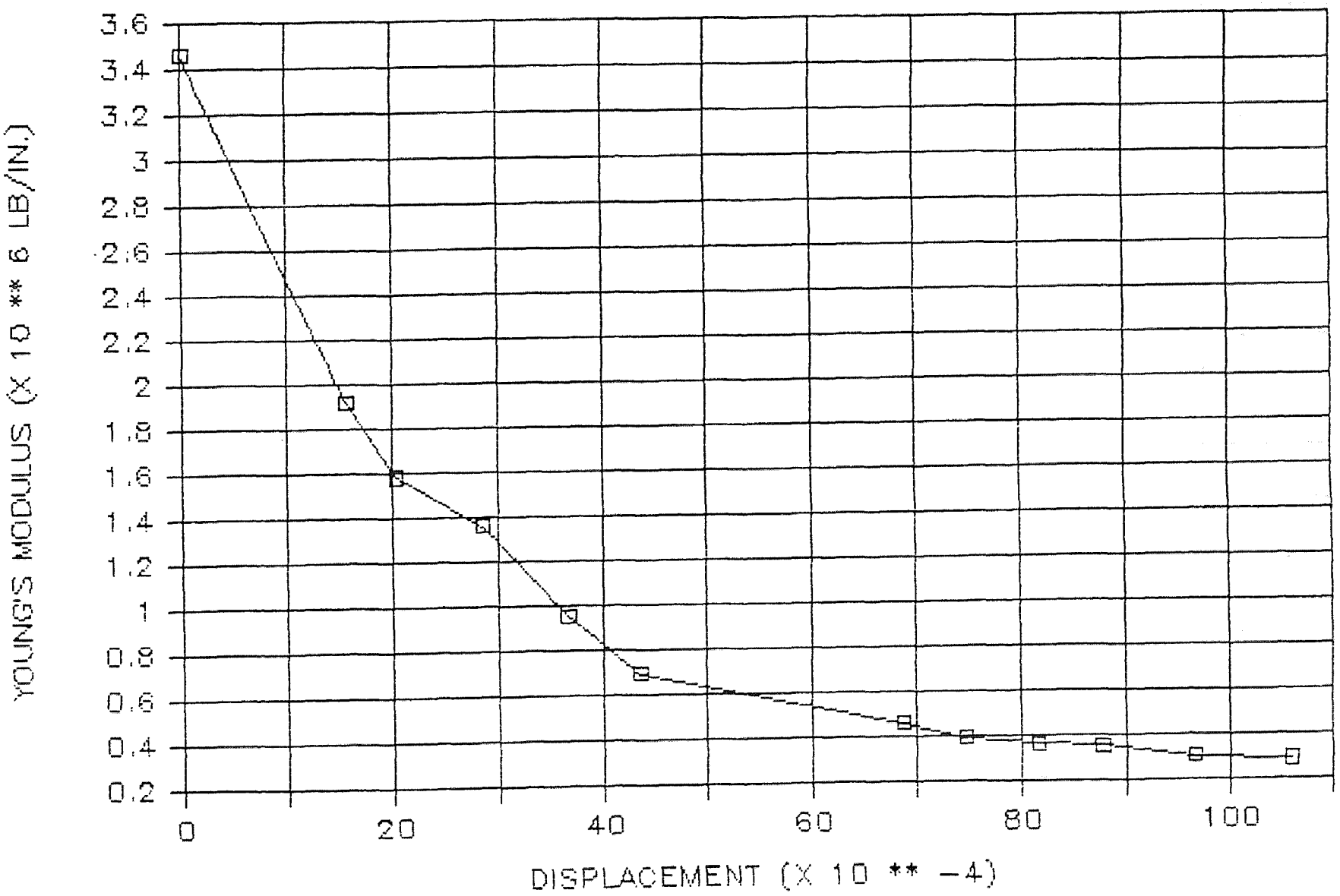
YOUNG'S MODULUS (X 10 ** 6 LB/IN.)
3.6
3.4
3.2
3
2.8
2.6
2.4
2.2
2
1.8
1.6
1.4
1.2
1
0.8
0.6
0.4
0.2
0
20
40
60
80
100
DISPLACEMENT (X 10 ** -4)

DOG—BONE—#40

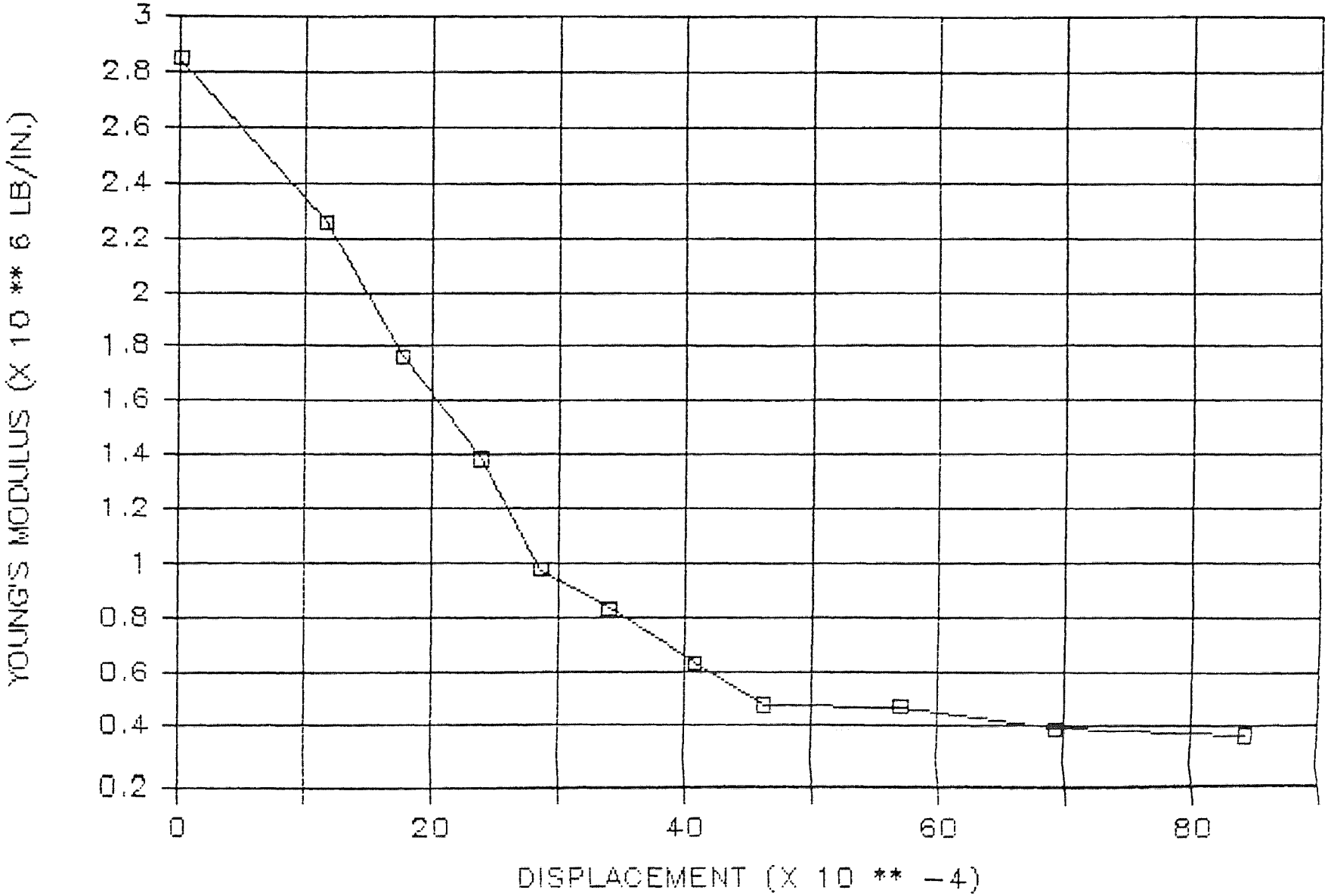
YOUNG'S MODULUS (X 10 ** 6 LB/IN.)
3
2.8
2.6
2.4
2.2
2
1.8
1.6
1.4
1.2
1
0.8
0.6
0.4
0.2
0
20
40
60
80
DISPLACEMENT (X 10 ** -4)

DOG—BONE—#41

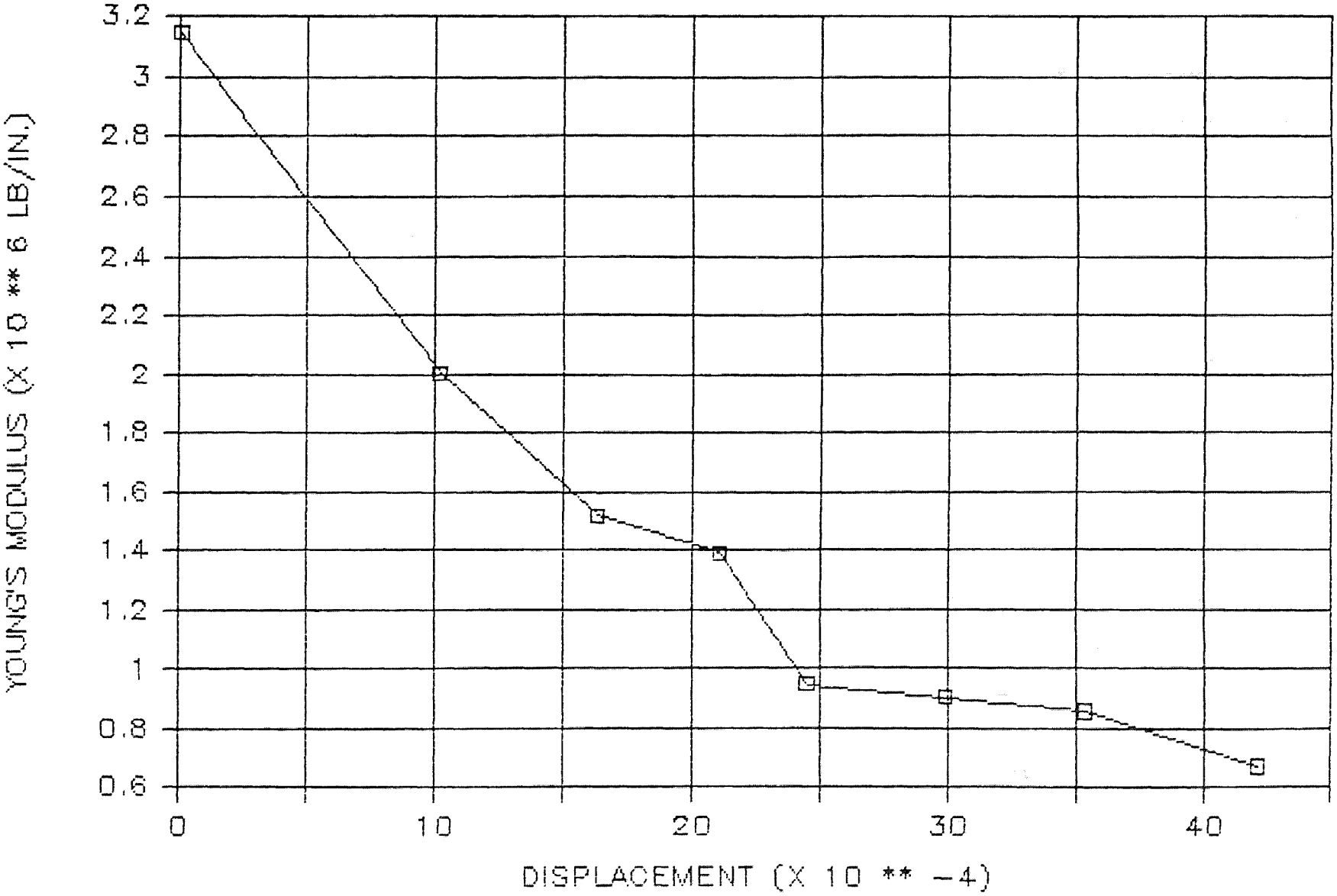
YOUNG'S MODULUS (X 10 ** 6 LB/IN.)
3.2
3
2.8
2.6
2.4
2.2
2
1.8
1.6
1.4
1.2
1
0.8
0.6
0
10
20
30
40
DISPLACEMENT (X 10 ** -4)

DOG-BONE-#42

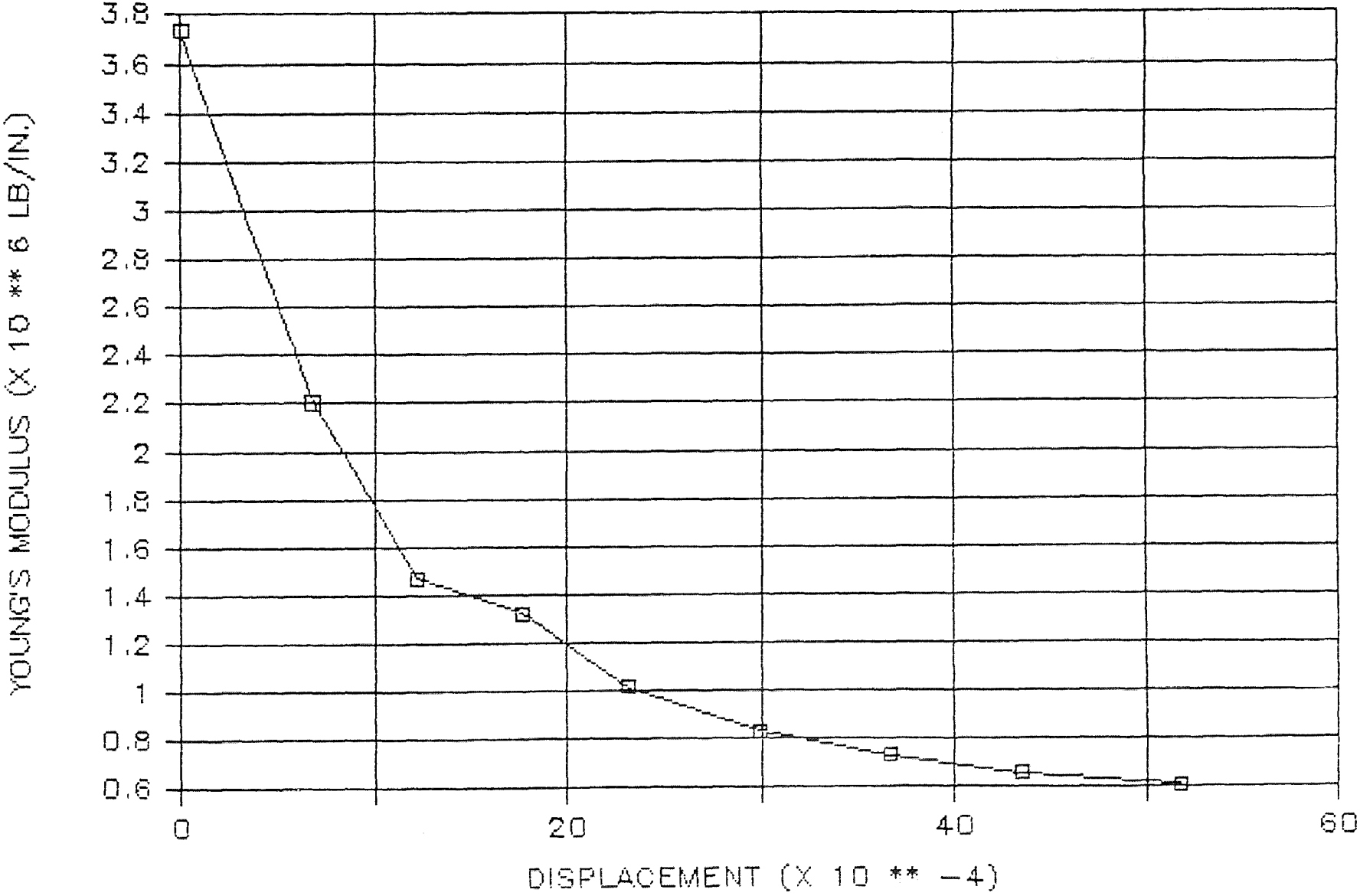
YOUNGS MODULUS (X 10 ** 6 LB/IN.)
3.8
3.6
3.4
3.2
3
2.8
2.6
2.4
2.2
2
1.8
1.6
1.4
1.2
1
0.8
0.6
0
20
40
60
DISPLACEMENT (X 10 ** -4)

DOG—BONE—#43

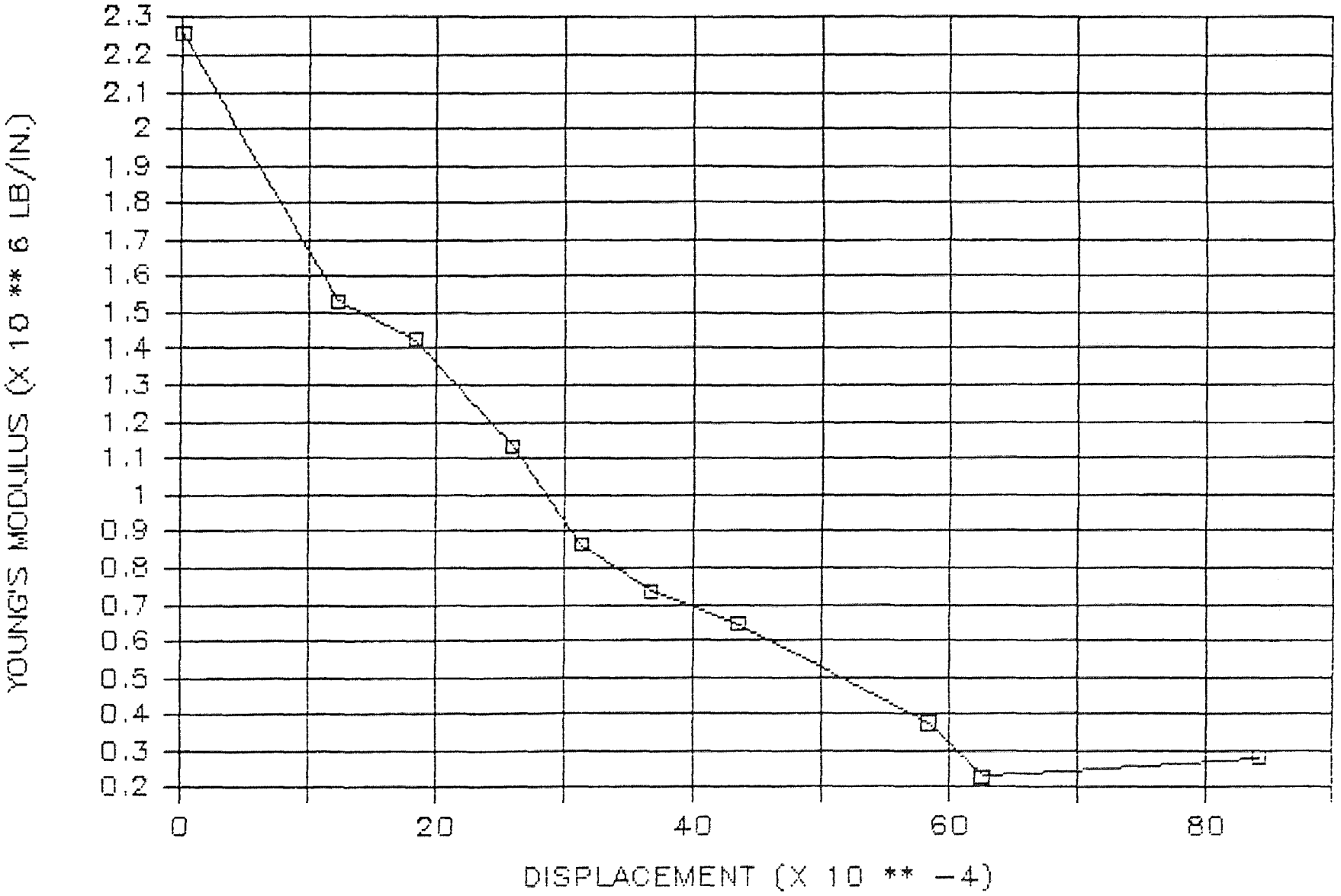
YOUNG'S MODULUS (X 10 ** 6 LB/IN.)
2.3
2.2
2.1
2
1.9
1.8
1.7
1.6
1.5
1.4
1.3
1.2
1.1
1
0.9
0.8
0.7
0.6
0.5
0.4
0.3
0.2
0
20
40
60
80
DISPLACEMENT (X 10 ** -4)

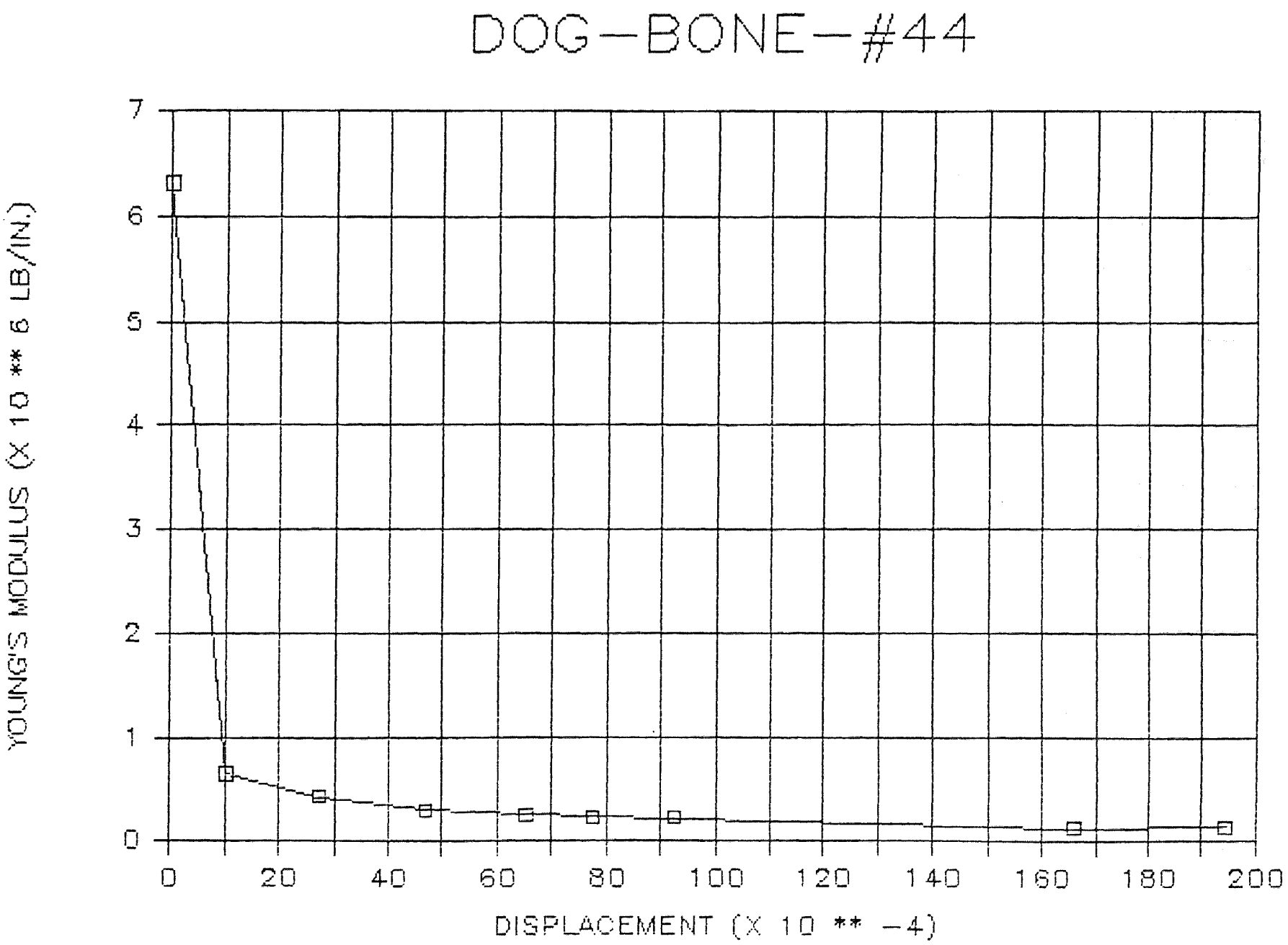
DOG-BONE-#44
YOUNG'S MODULUS (X 10 ** 6 LB/IN.)
7
6
5
4
3
2
1
0
0
20
40
60
80
100
120
140
160
180
200
DISPLACEMENT (X 10 ** -4)

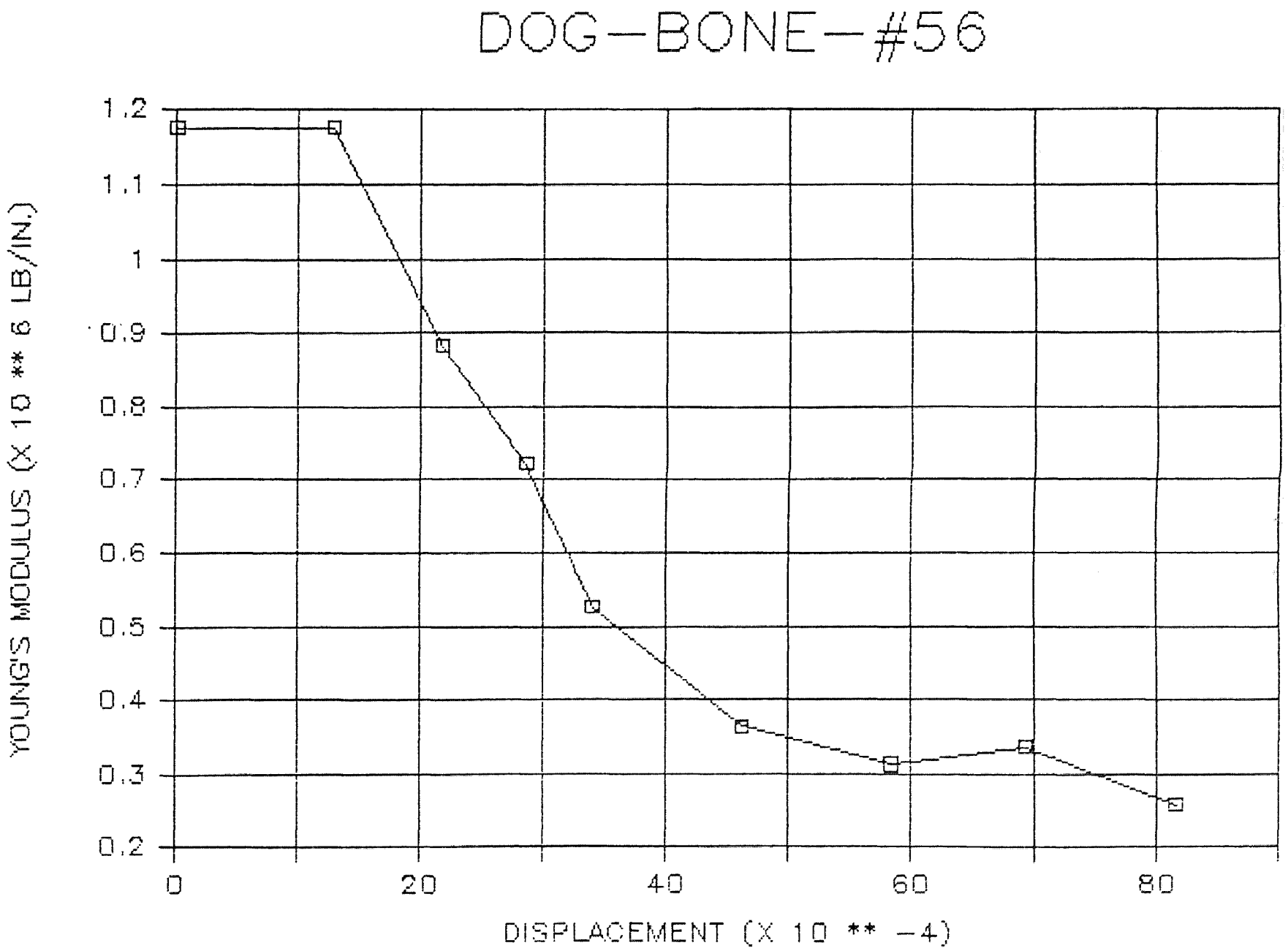
DOG-BONE-#56
YOUNG'S MODULUS (X 10 ** 6 LB/IN.)
1.2
1.1
1
0.9
0.8
0.7
0.6
0.5
0.4
0.3
0.2
0
20
40
60
80
DISPLACEMENT (X 10 ** -4)

DOG-BONE-#57

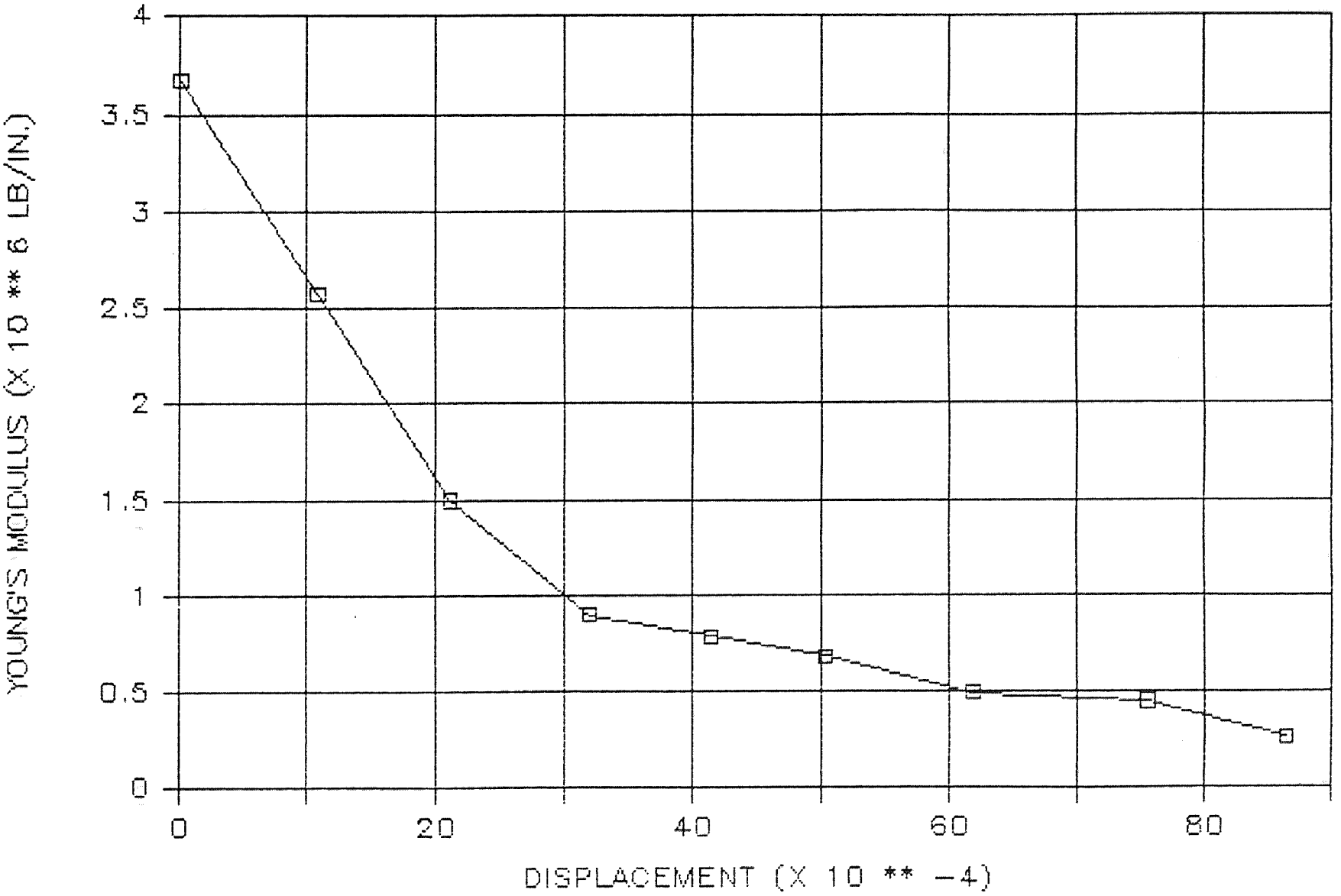
YOUNG'S MODULUS (X 10 ** 6 LB/IN.)
4
3.5
3
2.5
2
1.5
1
0.5
0
0
20
40
60
80
DISPLACEMENT (X 10 ** -4)

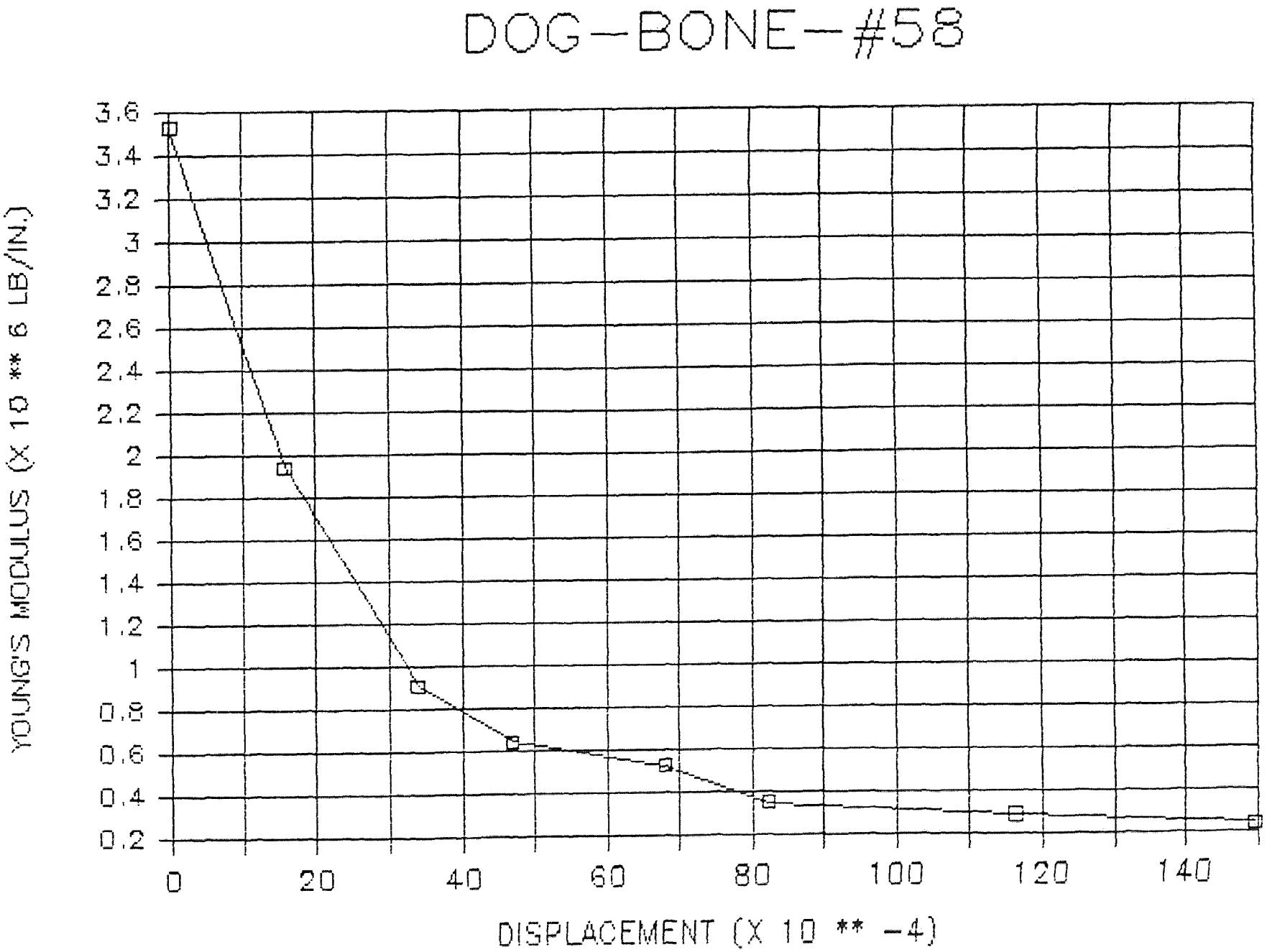
DOG-BONE-#58
YOUNG'S MODULUS (X 10 ** 6 LB/IN.)
3.6
3.4
3.2
3
2.8
2.6
2.4
2.2
2
1.8
1.6
1.4
1.2
1
0.8
0.6
0.4
0.2
0
20
40
60
80
100
120
140
DISPLACEMENT (X 10 ** -4)

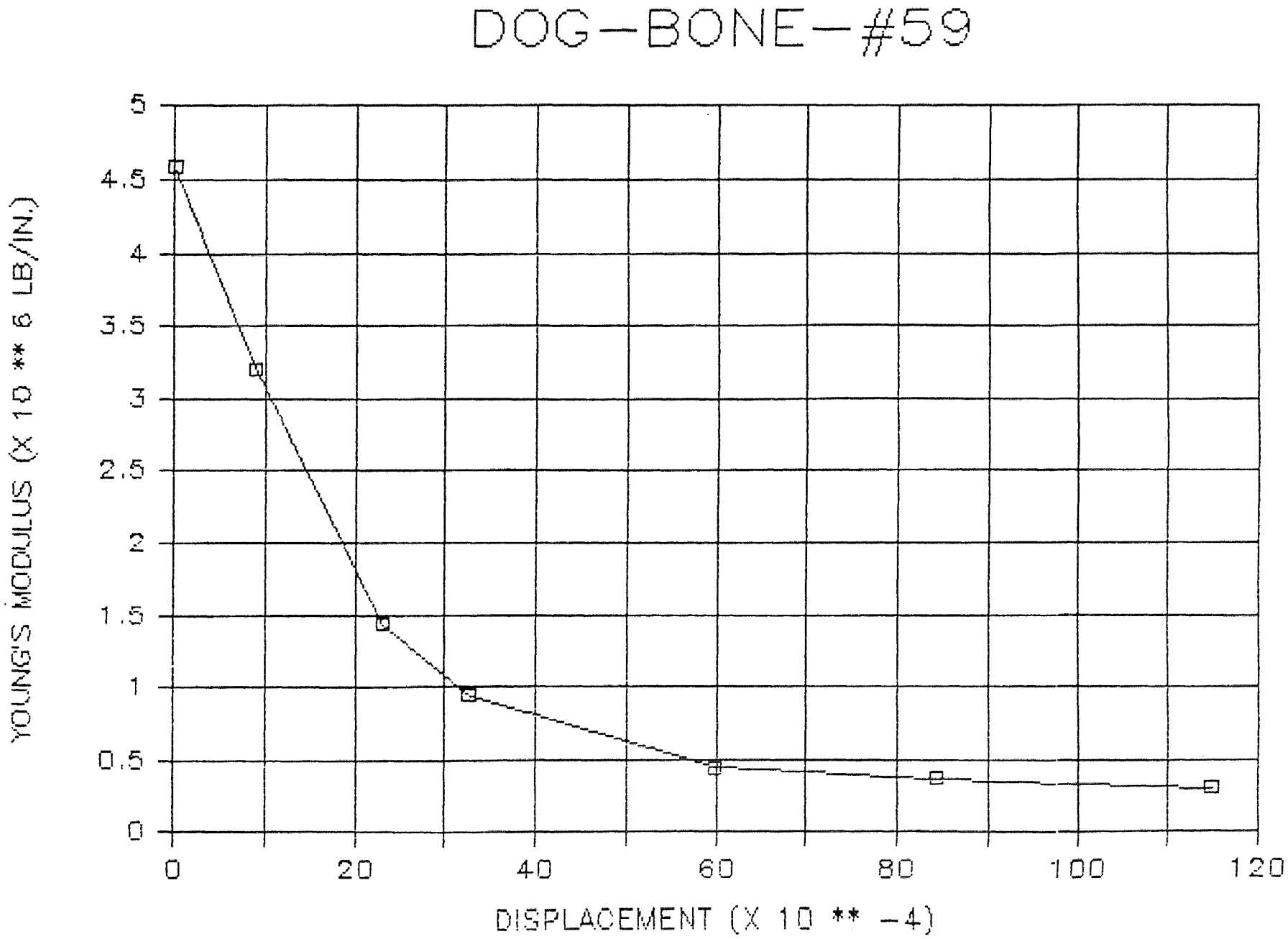
DOG-BONE-#59
YOUNG'S MODULUS (X 10 ** 6 LB/IN.)
5
4.5
4
3.5
3
2.5
2
1.5
1
0.5
0
0
20
40
60
80
100
120
DISPLACEMENT (X 10 ** -4)

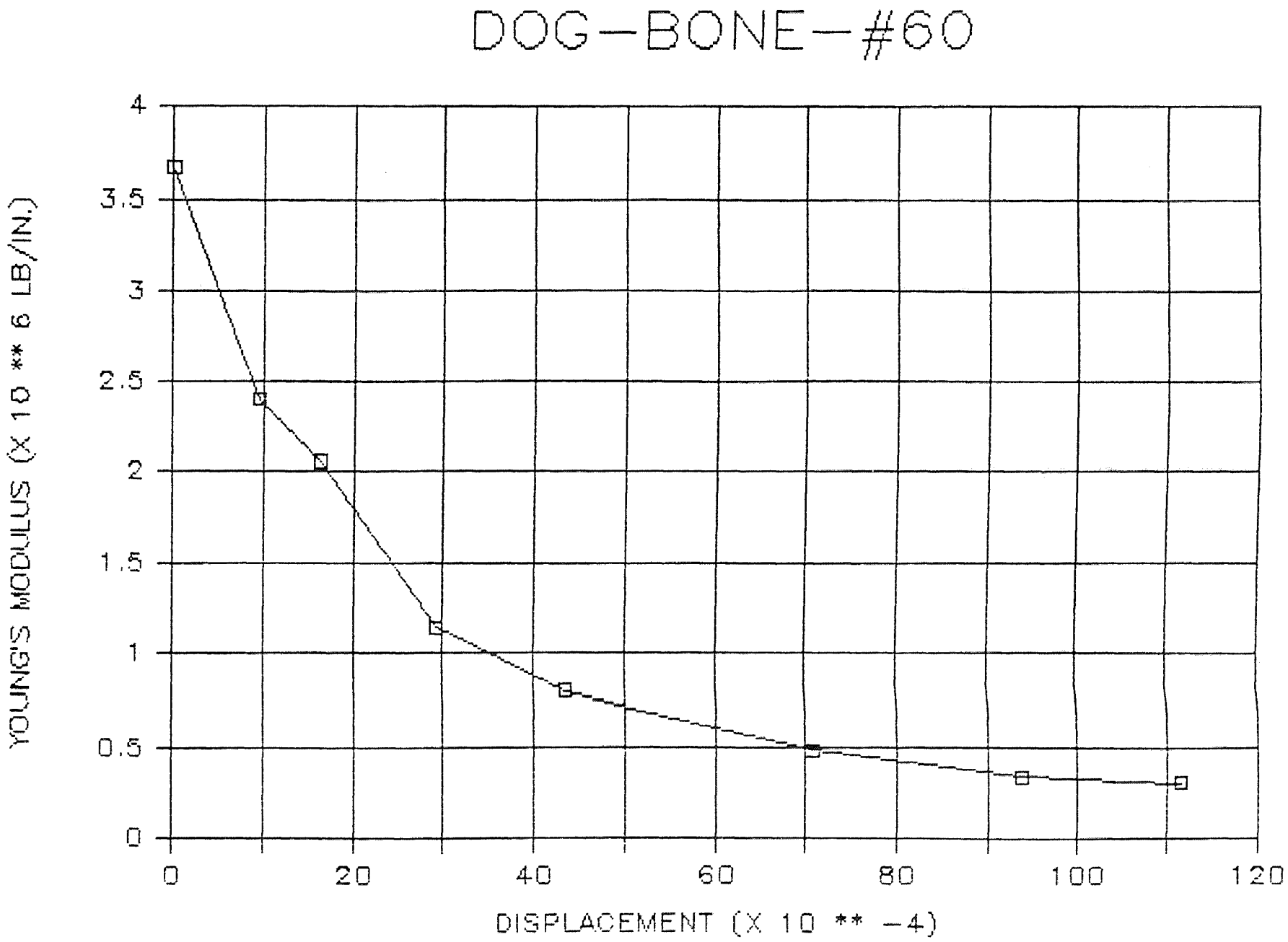
DOG-BONE-#60
YOUNG'S MODULUS (X 10 ** 6 LB/IN.)
4
3.5
3
2.5
2
1.5
1
0.5
0
0
20
40
60
80
100
120
DISPLACEMENT (X 10 ** -4)

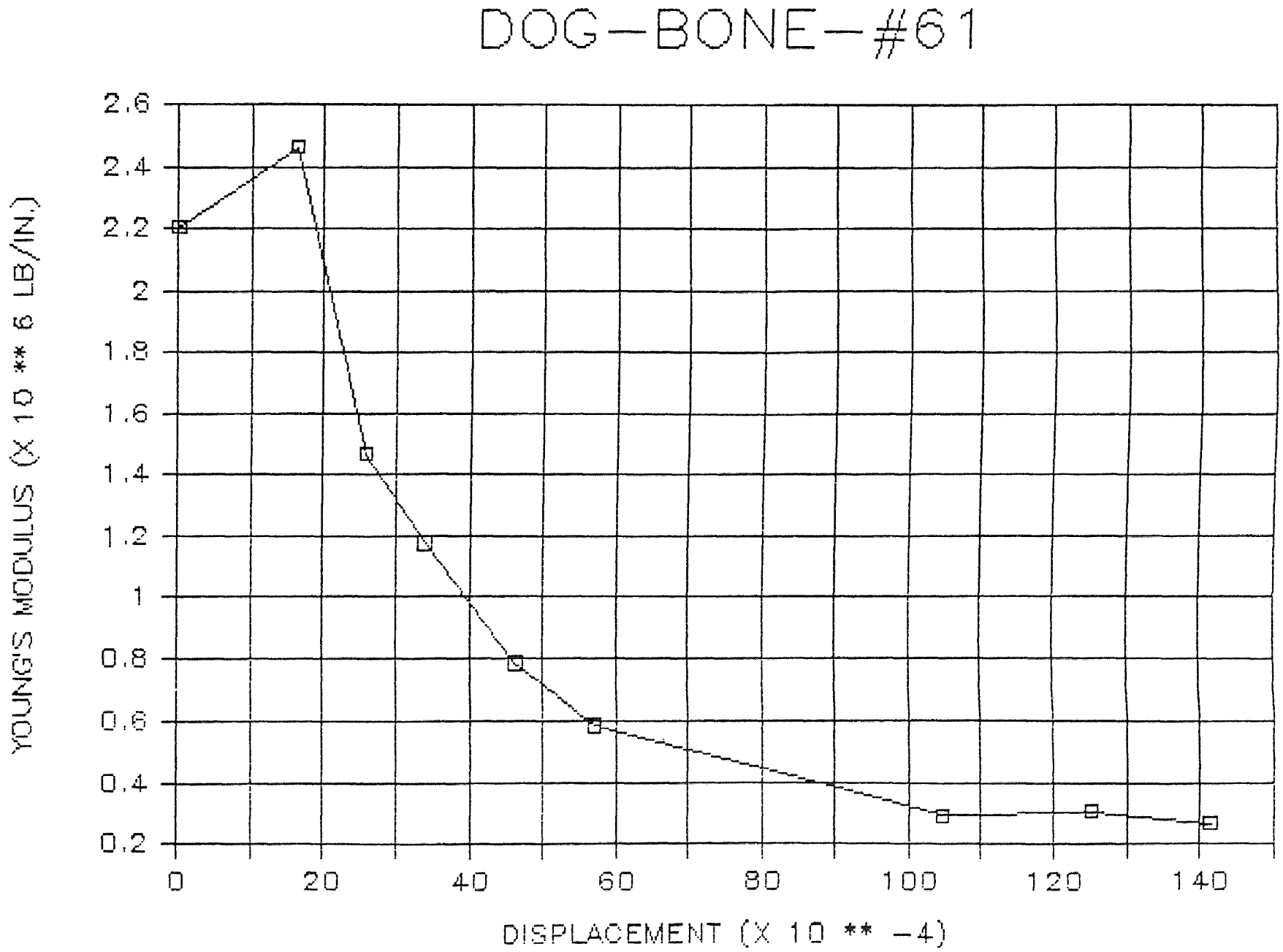
DOG-BONE-#61
YOUNGS MODULUS (X 10 ** 6 LB/IN.)
2.6
2.4
2.2
2
1.8
1.6
1.4
1.2
1
0.8
0.6
0.4
0.2
0
20
40
60
80
100
120
140
DISPLACEMENT (X 10 ** -4)